

**An archaeogenomic approach to the  
population history of Southwest Asia and  
the Aegean from the Neolithic to the  
Bronze Age**

**Dissertation**

**zur Erlangung des akademischen Grades eines**

**„doctor rerum naturalium“ (Dr. rer. nat.)**

**vorgelegt dem Rat der Fakultät für Biowissenschaften**

**der Friedrich-Schiller-Universität Jena**

**von MSc (Res) Eirini Skourtanioti**

**geboren am 18.05.1989 in Athen, Griechenland**

**Gutachter:**

1. Prof. Dr. Johannes Krause, Max Planck Institute for Evolutionary Anthropology
2. Ass. Prof. Dr. Choongwon Jeong, Seoul National University
3. Prof. Mehmet Somel, Middle East Technical University

**Tag der entlichen Verteidigung:** *13 July 2022*

# Table of Contents

<b>1</b>	<b>INTRODUCTION.....</b>	<b>1</b>
1.1	FROM GENETICS TO PALEO- AND ARCHAEOGENOMICS: A METHODOLOGICAL OVERVIEW .....	1
1.1.1	<i>Early applications of genetics to questions about the human past.....</i>	<i>1</i>
1.1.2	<i>Ancient DNA research: from the shadow to the spotlight.....</i>	<i>3</i>
1.2	A NEW HISTORY OF THE HUMAN PAST: 2010-PRESENT.....	7
1.2.1	<i>Archaeogenomic insights into the West Eurasian Neolithic and Bronze Age .....</i>	<i>9</i>
1.3	ARCHAEOLOGICAL AND ARCHAEOGENETIC BACKGROUND OF THE AEGEAN AND SOUTHWEST ASIAN PREHISTORY (NEOLITHIC-BRONZE AGE).....	12
1.3.1	<i>Remarks on terms of archaeological chronology.....</i>	<i>12</i>
1.3.2	<i>From Anatolia to the Aegean and the Caucasus: the Neolithic period.....</i>	<i>12</i>
1.3.3	<i>The Syro-Anatolian Chalcolithic and Bronze Age .....</i>	<i>16</i>
1.3.4	<i>The Aegean Bronze Age .....</i>	<i>19</i>
<b>2</b>	<b>OBJECTIVES OF THE THESIS .....</b>	<b>22</b>
<b>3</b>	<b>OVERVIEW OF MANUSCRIPTS AND AUTHOR CONTRIBUTIONS.....</b>	<b>24</b>
3.1	MANUSCRIPT A.....	24
3.2	MANUSCRIPT B.....	27
<b>4</b>	<b>MANUSCRIPT A.....</b>	<b>30</b>
<b>5</b>	<b>MANUSCRIPT B.....</b>	<b>74</b>
<b>6</b>	<b>DISCUSSION.....</b>	<b>100</b>
6.1	THE ROLE OF ADNA IN RECORDING HISTORY.....	100
6.2	CONTEXTUALIZATION OF ARCHAEOGENETIC INFERENCES FOR POPULATION MIGRATIONS AND HUMAN MOBILITY .....	101
6.2.1	<i>Migration during the Neolithic within Southwest Asia and the Aegean.....</i>	<i>101</i>
6.2.2	<i>The role of human mobility in the Near Eastern early-state and territorial-state societies .....</i>	<i>104</i>
6.2.3	<i>Disentangling the interplay of ‘eastern’ and ‘steppe’ ancestries in the Bronze Age Aegean .....</i>	<i>106</i>

6.3	A GLIMPSE AT PAST SOCIAL PRACTICES FROM ADNA.....	107
6.4	SAMPLING LIMITATIONS AND FUTURE PERSPECTIVES .....	109
<b>7</b>	<b>SUMMARY.....</b>	<b>112</b>
7.1	SUMMARY (ENGLISH) .....	112
7.2	ZUSAMMENFASSUNG (DEUTSCH) .....	114
<b>8</b>	<b>REFERENCES .....</b>	<b>117</b>
<b>9</b>	<b>EIGENSTÄNDIGKEITSERKLÄRUNG.....</b>	<b>142</b>
<b>10</b>	<b>ACKNOWLEDGMENTS .....</b>	<b>143</b>
<b>11</b>	<b>APPENDIX.....</b>	<b>145</b>
11.1	CANDIDATE-SPECIFIC CONTRIBUTIONS TO MANUSCRIPTS .....	145
11.1.1	<i>Manuscript A</i> .....	145
11.1.2	<i>Manuscript B</i> .....	146
11.2	TABLE 1. STAGES OF CULTURAL EVOLUTION IN ANATOLIA FROM THE NEOLITHIC TO THE BRONZE AGE .....	147
11.4	SUPPLEMENTARY MATERIAL FOR MANUSCRIPT A .....	149
11.5	SUPPLEMENTARY MATERIAL FOR MANUSCRIPT B .....	191

# 1 Introduction

This thesis is a contribution to an emerging corpus of research aspiring to record and illuminate aspects of the human history through the study of ancient genomes. Widely known today as archaeogenetics or archaeogenomics -to emphasize the scalar of the analyzed data- this field started from pioneering research almost four decades ago, managed to overcome technical limitations and is now enjoying a tremendous blossom. Characteristically, as of 2018 it was mentioned that ‘the time lag between data production and publication is longer than the time it takes to double the data in the field’ (Reich, 2018). Apart from indicative of the fast pace of the average data production, this remark might also announce a new formative period for the field’s scope. Irrespectively of that, as plainly defined by its composite name, archaeogenomics stands on the intersection of two disciplines, genetics and anthropology/archaeology, the foundations of which go back to the end of the nineteenth century. On the one hand, this new research area is advancing by harnessing fundamental principles of evolutionary genetics and building a new quantitative ‘language’ to decipher human past. On the other hand, it inherently incorporates archaeological explanations derived from the study of material culture that witnesses technological innovations, economic and political transformations, shifts in ideology and social interconnectedness across time and space (Gokcumen and Frachetti, 2020).

Southwest Asia and the Aegean have been among the first areas to experience what the early twentieth century archaeologist V. Gordon Childe characterized as ‘Neolithic and Urban Revolutions’. As such, the relevance and resonance of this thesis, which has principally been an endeavor for the successful recovery and analysis of ancient human DNA from these areas, comes in function with the theoretical and methodological archaeological background that frames the studied material. Considering this intrinsic feature of ‘duality’ of archaeogenetic studies like the present, the following introductory section aspires to explain how genes narrate human past, and to present the main archaeological features of these areas from the Neolithic to the Bronze Age.

## 1.1 From genetics to paleo- and archaeogenomics: a methodological overview

### 1.1.1 *Early applications of genetics to questions about the human past*

Since the discovery and formulation of the laws of heredity by Mendel in 1895, forty years had to pass until his results were finally revisited and started to be understood and accepted. While this hiatus has been disputed by some contemporary historians, it seems to hold that, besides Thomas H. Morgan’s work on *Drosophila*, the study of heredity gradually became intellectually isolated from other vital fields of biological research at the time, such as embryology (Morange, 2020). Even though the detachment of these two disciplines might sound problematic with today’s research standards, it had proven critical for the development of genetics (Falk, 1995; Morange, 2020). With a secondary or minimal interest in the chemical

nature and underlying molecular mechanisms, the study of the genes became more relevant to mathematicians and physicists who considered genes as discrete inheritable units, thus, the ‘atoms’ of biology, and the mutations as transmutations of elements (Morange, 2020). Within this context, it comes without surprise that by the 1930’s, some of the most fundamental principles of population genetics were already formulated; the mathematicians Ronald A. Fisher, John B. S. Haldane, Godfrey H. Hardy, the biologist Sewall Wright and the medical doctor Wilhelm Weinberg - to name some of the most influential – reconciled genetics and heredity laws with the idea of natural selection proposed by Charles Darwin.

Advances in biochemistry and X-ray crystallography during the 1940’s and 1950’s, culminated with the model of the double-stranded structure of the Deoxyribonucleic acid (DNA) by James D. Watson, Francis Crick, Rosalind Franklin and Maurice Wilkins. With the apparent implications of this finding on the DNA replication mechanism, the molecular basis of mutation, and the subsequent formulation of the central dogma of molecular biology, a synthetic dimension of mendelian genetics and Darwinian evolution also emerged: molecular biology became a source of quantitative and objective information about evolutionary history. By the early 60’s, researchers would use molecular data (both DNA and proteins) to understand human origins and our evolutionary relationship with our distant relatives, the apes (Goodman, 1963; Wilson and Sarich, 1969; King and Wilson, 1975), or the population structure within and between modern human populations (Cavalli-Sforza, 1966).

In 1987, following this growing research body of molecular human evolution, a group from California published the mitochondrial DNA restriction maps of 147 individuals from five geographic populations (Cann et al., 1987). The team showed that by using this maternally inherited and non-recombining DNA marker, state-of-the-art phylogenetic methods and a constant mutation rate, it was possible to trace the common ancestor of all the 147 lineages to a woman who lived in Africa ca. 200,000 years ago. The finding had a tremendous appeal, especially because of its implications on the long-standing debate of ‘multiregional’ and ‘out-of-Africa’ hypotheses of human evolution, whereby the former was refuted. Most critically though, its significance lied on the fact that it encouraged a generation of geneticists, anthropologists, and archaeologists to turn towards genetics as a powerful tool in order to elucidate key questions about the origins and evolution of our species.

In 1994, a study led by Luigi L. Cavalli-Sforza was published. ‘The history and Geography of Human Genes’ (Cavalli-Sforza et al., 1994), was a synthesis of three decades of research on human variation and its structure across the populations. Despite the limited tools and technologies that were available at that time, Cavalli-Sforza leveraged human genetic information from blood groups that was relatively abundant (ABO, MNS, Rh, etc.), developed methods to analyze those datasets, and introduced the application of principal components analysis (PCA) as a tool to summarize and visualize allele-frequency differences. The wide use of the aforementioned methods by population geneticists nowadays speaks for the pioneering spirit of Cavalli-Sforza’s research. However, his vision went beyond quantitative and qualitative methods in human genetic variation. Cavalli-Sforza used PCA-based allele frequency maps with the goal to superimpose genetic geography on top of prehistorical and historical evidence. He interpreted genetic gradients as evidence of demic expansion, or ‘demic

diffusion' (Ammerman and Cavalli-Sforza, 2014), that occurred in the past but were discernible in modern populations. For example, he would interpret the European gradient with Near Eastern epicenter in PC1 as evidence of the agriculturalist expansion, and a perpendicular gradient from North Europe to South Europe in PC2, as evidence of the Indo-European Kurgan culture expansion in Europe.

These ground-breaking methods and interpretations soon received criticism (Sokal et al., 1999). In spite of that, the study also added supportive evidence to a finding that was becoming a consensus among studies of worldwide human genetic variation. Contrary to dominant notions of human populations being divided into homogeneous groups or races, these allele-frequency studies seemed to be showing quite the opposite. Indeed, with the inclusion of highly-variable nuclear microsatellite loci (Bacaër, 2011; Rosenberg et al., 2002), it could be corroborated that up to 95% of genetic variation is embedded among the individuals of the same population, and a mere ca. 5% is due to differences among these major population grouping (Bacaër, 2011; Rosenberg et al., 2002). By the early 2000's, the increasing research body of mitochondrial and Y-chromosome DNA, blood groups, protein polymorphisms, microsatellite loci, created an arena for the study of human genotypes as an interplay of past human migrations, new mutations, natural selection, and assortative mating. Along with this perspective, a number of problems became obvious. The mitochondrial study in 1987 (Cann et al., 1987) was soon consolidated in the collective imagination as the 'Mitochondrial Eve', a possibly misleading term, as it created the impression that we would learn all about our evolutionary history by tracking the maternal or the paternal lineages (Reich, 2018). In addition, critique over the limitations of Cavalli-Sforza's synthetic maps solidified in 2008, when simulated data showed that the (sinusoidal) waves could be mathematical artifacts arising when PCA is applied to spatial data (Novembre and Stephens, 2008). In other words, genetic isolation by geographic distance could be behind the pattern of the expansion waves, and even though Neolithic expansion could explain the observed gradient across Europe, this could only be one of the possible explanations.

In conclusion, the aforementioned examples signal the importance to rethink evolutionary models considering that the story narrated by an entire genome -which is a mosaic of multitudes of ancestors- might considerably differ from the mitochondria. Moreover, the fact that nowadays genes roughly mirror geography (Novembre et al., 2008) does not imply a linear population process across time and geographical space. These two aspects highlight that direct access to genome-wide information from the past is imperative for painting a nuanced picture of our complex evolution as species and populations. The following section describes the developments that enabled, defined and expanded the scope of the ancient DNA studies, the so-called 'ancient DNA revolution'.

### *1.1.2 Ancient DNA research: from the shadow to the spotlight*

In 2001, after thirteen years of collective effort, the International Human Genome Sequencing Consortium released the first draft assembly of human genome (Lander et al., 2001). Today, twenty years later, the publication of the patent-free genetic blueprint of a human being is still considered a reference for the world's largest collaborative biological project; and

the subsequent progress on our understanding of human genome architecture, the genetic basis of disease, gene expression, and common and rare variation have revolutionized disciplines such as molecular medicine and human evolution. Sanger sequencing (chain termination DNA sequencing) was the implemented technology during the Human Genome Project, but it took only a few years until next-generation sequencing (NGS) technology became available in 2005. With NGS - a high-throughput methodology that massively parallels the sequencing of millions of DNA fragments - the sequencing of the entire human genome is now a matter of a day and the cost goes down to ca. 1,000\$, i.e., a hundred thousand times less the first draft. Marking the advent of the “-omics” era (high-throughput production of biomolecular data), it turned out that NGS triggered the development of the ancient genomics as well. However, to understand how and why NGS signified the blossom of ancient DNA research, it is important to consider the inherent problems related to the post-mortem degradation of ancient DNA molecules.

Ancient DNA (aDNA) refers to DNA recovered from organisms that died from decades to many thousand years ago. The lower temporal boundary is set by the oldest specimen from which DNA is recovered. Until recently, the oldest ancient DNA came from a ca. 800,000-year-old horse bone (Orlando et al., 2013), but this record has been now surpassed by the isolation of DNA from two mammoths in the Siberian permafrost that were older than one million years (van der Valk et al., 2021). In biochemical terms, aDNA also refers to the state of degradation that DNA molecules undergo post-mortem, with the initial action of endogenous enzymes followed by hydrolytic and oxidative reactions – depurinations and deaminations, respectively – as well as microbial digestion (Hofreiter et al., 2001; Lindahl, 1993; Lindahl and Andersson, 1972; Lindahl and Nyberg, 1972). These phenomena determine aDNA as typically short fragments with single-strand breaks (Pääbo and Wilson, 1991), and cytosine deaminations leading to uracils that are usually accumulated at the single-strand overhangs (Briggs et al., 2007; Dabney et al., 2013b; Brotherton et al., 2007). However, the degree of aDNA’s degradation depends also on other factors such as the type of tissue, the soil acidity, environmental humidity, temperature, and time since deposition (Lindahl and Nyberg, 1974; Sawyer et al., 2012; Weiß et al., 2016; Kendall et al., 2018).

Although insights into some of the biochemical features of aDNA existed since the 70’s, most of these features were still unknown at the time of the first successful attempts to isolate fragments of aDNA. These aDNA studies were published almost simultaneously from two different groups. The first extracted DNA from a superficial leg tissue of an ancient Egyptian mummy (Pääbo, 1985), while the second obtained it from the dried muscle tissue of an extinct zebra subspecies (Higuchi et al., 1984). To overcome the low copy number, both teams used bacterial cloning. This method soon gave place to the new powerful method of Polymerase Chain Reaction (PCR), which also revealed cloning artefacts during quagga’s previous DNA isolation (Pääbo and Wilson, 1988; Saiki et al., 1988). However, PCR would come with a limitation: it typically targets relatively long fragments, while the ancient endogenous fragments would range from 40 to 500 bp (Pääbo, 1989). Contamination present in the sample or introduced during the experimental procedure -and thereby amplified with the PCR- was a fundamental issue for the authenticity of the results; and it persisted for almost three decades despite the attempts to establish rigorous criteria for conducting aDNA research (clean room



for all pre-amplification steps, negative and positive controls etc.) and understand the contamination process (Cooper and Poinar, 2000; Pääbo, 1989; Pääbo et al., 2004; Gilbert et al., 2006).

The introduction of NGS technology finally dismantled this burden of constraints. It was not only the scaling of the sequencing throughput, but the step before the sequencing, the preparation of the genomic library. During the library preparation, the entire aDNA fragment becomes the insert, and universal adaptors are ligated at both ends. In this way, the characteristic damage patterns mentioned above could be revealed and described in detail. Then, by leveraging information from the immense amount of sequenced reads that map to the reference genome, it became possible to develop statistical tools that estimate contamination based on the mitochondrial or male X-chromosome heterozygosity (Fu et al., 2013; Korneliussen et al., 2014; Renaud et al., 2015), the actual pattern of damage distribution across an ancient fragment (Peyrégne and Peter, 2020), or the breakdown of linkage disequilibrium (LD) patterns occurring from the mixing of two or more DNA sources (Nakatsuka et al., 2020). At the same time, a general overview of the aDNA preservation becomes accessible through the collection of all sequenced reads that represent the metagenomic content of the sample from which DNA was extracted. Metagenomic information is critical when evaluating the necessary sequencing effort in order to recover sufficient whole-genome or genome-wide information, but also for understanding post-mortem DNA degradation by environmental microorganisms. Furthermore, metagenomic analysis enables the simultaneous study of the host organism/individual, its microbiome and the pathogens from which it was contaminated at the time of death (e.g., Schuenemann et al., 2018; Spyrou et al., 2018).

Alongside the development of the in-silico methods for the robust quality control of aDNA sequences, sampling and wet-lab protocols have also greatly improved throughout the years (Shapiro et al., 2019). In the first place, detailed guidelines for preventing and minimizing contamination during excavation, sample collection and subsequent handling (Llamas et al., 2017) have become popular within the community of geneticists, archaeologists and anthropologists. Then, aDNA extraction protocols have become standardized. Essentially, these protocols now combine available commercial kits for short DNA fragments (silica column based) with adjustments during various steps, such as sample pretreatment and lysis that depend on the starting material, and the restrictions with respect to the sample invasion (Dabney et al., 2013a; Mann et al., 2018; Boessenkool et al., 2017; Dabney and Meyer, 2019; Harney et al., 2021a; Gamba et al., 2016). Following the successful DNA extraction, optimization of library preparation protocols has achieved the partial or complete enzymatic repair of the deamination-induced aDNA damage (Rohland et al., 2015; Briggs et al., 2010), and the recovery of single-stranded and double-stranded fragments with strand breaks that cannot be incorporated into the genomic library with conventional protocols (Gansauge et al., 2017; Gansauge and Meyer, 2013). Lately, the various improvements on the different wet-lab steps have been combined together in a lysate-to-indexed-library protocol, allowing automation on liquid-handling systems, and thereby greatly reducing the time and cost of sample processing (Gansauge et al., 2020; Rohland et al., 2018).

Another technological breakthrough has been the development of enrichment methods that use probes designed as complementary to a reference genome of interest, or specific DNA sequences from the reference (Burbano et al., 2010; Maricic et al., 2010; Fu et al., 2013; Carpenter et al., 2013). The target sequences can be ‘captured’ by those probes and get amplified, while the remaining genetic material is washed away. In this way, entire mitochondrial genomes and large parts of nuclear genome or genome-wide data have been recovered from samples with 1% of endogenous DNA or less.

While nowadays it is possible to gain valuable insights from DNA recovered from mummified tissue (Salo et al., 1994), hair (Rasmussen et al., 2010), palaeofeces and coprolites (Hagan et al., 2020; Kuch and Poinar, 2012), plants (Willerslev et al., 2007; Willerslev et al., 2003), dental calculus (Warinner et al., 2015), animal skins and textiles (Anava et al., 2020; O’Sullivan et al., 2016), parchments (Teasdale et al., 2015) and sediment (Slon et al., 2017), skeletal elements are the most abundant and better preserved sample sources of aDNA. Efforts in order to determine the variation in aDNA preservation among skeletal elements led to an important finding: the petrous portion of the inner ear on the temporal bone preserves aDNA exceptionally well (Gamba et al., 2014; Pinhasi et al., 2015). This finding had a great impact, as it made possible to explore areas beyond the temperate and cold zones of high altitude that would typically produce the majority of aDNA data (Slatkin and Racimo, 2016).

Finally, it is necessary to mention the development of computational tools for genome analysis i.e., population structure, divergence of populations, admixture, effective population sizes, etc. Many of these methods are widely applied today in aDNA analysis for testing scenarios in population history. However, they were essentially developed or improved thanks to large-scale modern human genome projects such as the HapMap Project (Gibbs et al., 2003), 1000 Genomes Project (Auton et al., 2015), the Human Genome Diversity Project and the Simons Genome Diversity Project (Mallick et al., 2016). These projects aimed to build a global reference of human genetic variation and to elucidate human demography and selection. Demographic methods (split times, populations sizes) are broadly based on Markovian sequential coalescent (McVean and Cardin, 2005), or the allele frequency spectrum (AFS) calculated from the entire genome (Excoffier et al., 2013). Local ancestry deconvolution methods are haplotype-based methods relying on phased data [e.g., ChromoPainter and fineSTRUCTURE (Lawson et al., 2012)]. All of them are extremely powerful, but typically require high-coverage whole genomes or accurate diploid genotype calls at a dense set of markers, which are usually very challenging to obtain from ancient (human) remains. Alternatively, other methods harness allele-frequency differences and summarize patterns of genetic distance in low-dimensional space (e.g., Principal Component Analysis, Multi-Dimensional Scaling), model populations as  $n$  admixture components [i.e., ADMIXTURE (Alexander et al., 2009)], or calculate allele-frequency correlations to gather evidence about admixture and direction of gene-flow [i.e., ADMIXTOOLS (Durand et al., 2011; Patterson et al., 2012)]. Such methods can use genome-wide data (i.e., Single Nucleotide Polymorphisms - SNPs) as input, which means that genomes can be either genotyped *in silico*, or the DNA sample is genotyped/enriched at those SNPs. In principle though, the power of these methods relies on the proper ascertainment of the SNPs, that is, how the SNPs are chosen with respect

to the question that is addressed. For the inference of human population history, the main target SNPs are those that are ancestrally variable among populations. In this respect, from the millions of human polymorphisms representing common variation in the form of SNPs, those that are not under selection and are evenly dispersed across the genome (no linkage) are preferred. For example, the Affymetrix Human Origins (HO) contains 629,000 SNPs in total, classified in eleven different sets of SNPs, each of which is ascertained on a different population (Patterson et al., 2012). Currently, more than 3,500 modern individuals have been genotyped on this SNP array, thereby providing a rich reference database. In addition, an initial set of probes for DNA enrichment through capture was designed on the basis of the HO SNPs (390K) (Haak et al., 2015). It was lately expanded to over a million of nuclear markers (1240K) (Mathieson et al., 2015), and since then it has been widely applied in aDNA studies. Critically, the performance of the SNP arrays has been tested in the framework of F/D-statistics from ADMIXTOOLS, showing that inferences regarding admixture and directionality of gene-flow were possible with a few thousand SNPs (Patterson et al., 2012).

To a great extent, the manuscripts presented in this thesis have become possible thanks to the aforementioned developments in lab protocols and computational methods for data validation and genetic analysis. And so it applies to many other aDNA studies. As a matter of fact, the fast pace of these developments came as a response to the astonishing insights and potential that became obvious from the first aDNA applications.

## **1.2 A new history of the human past: 2010-present**

The first ancient human nuclear and mitochondrial genomes were published in 2010, and concerned archaic (Green et al., 2010; Krause et al., 2010; Reich et al., 2010) and ancient modern human lineages (Rasmussen et al., 2010). By comparing a draft Neanderthal genome composed of data from three individuals from Vindija Cave in Croatia (>38,000ya) with present-day humans from across the world, Green and colleagues showed that non-African populations are on average ca. 4% genetically closer to Neanderthals than the African ones. This finding could only be explained as interbreeding between Neanderthals and anatomically modern humans (AMH), likely in the Middle East, where their ranges were known to overlap. Even though traces of interbreeding were not recorded on the AMH mitochondrial genomes and the fossils, later studies confirmed this finding (Vernot and Akey, 2014; Sankararaman et al., 2014). Furthermore, Reich and colleagues were able to genetically define a distinct archaic lineage, the Denisovans -named after the cave in the Altai mountains-, otherwise only represented by a distal manual phalanx and a tooth. Episodes of admixture with modern humans were detected for Denisovans as well, however, these were mostly confined to present-day Australasian populations. The extent of the complex biological interactions of our species with these archaic human groups was substantially refined over the following years, and showed that the earliest AMH populations in Europe also carried signatures of recent admixture with Neanderthals (Hajdinjak et al., 2021; Fu et al., 2014), and interbreeding also occurred between Neanderthals and Denisovans (Slon et al., 2017). Finally, the elaborate mapping of the adaptive

introgression in human populations made possible to determine factors for both increased and reduced risk for Covid19 related to Neanderthal admixture (Zeberg and Pääbo, 2020; Zeberg and Pääbo, 2021).

With respect to the genetic history of AMH lineages, correlation of genomic information from geographical and temporally distant human remains gradually synthesized the landscape of long-range migrations. For example, following the publication of the 4,000-year-old extinct Palaeo-Eskimo (Rasmussen et al., 2010), which provided evidence of an early expansion to the Americas that did not contribute to present-day native Americans, other studies elucidated critical aspects of the peopling of the Americas (i.e., divergence times from East Asians and within America, number of founding events and the source populations etc.) (Raghavan et al., 2014a; Raghavan et al., 2014b; Rasmussen et al., 2014; Skoglund et al., 2015).

Within Eurasia, the genome of a 45,000-year-old individual - “Ust’Ishim”- showed a basal phylogenetic position with respect to West and East Eurasians. Not so far away, a 24,000-year-old individual – “Mal’ta” – had contributed to both West Eurasians and Native Americans at different proportions (Lazaridis et al., 2014; Raghavan et al., 2014b). This lineage persisted through the Last Glacial Maximum (LGM) to the 18,000-year-old individual ‘Afontovo Gora’, which shared additional genetic drift with Native Americans, this suggesting that the gene pool of their ancestors was formed after the LGM (Fu et al., 2016; Raghavan et al., 2014b; Skoglund and Mathieson, 2018). The joint analysis of 50 genomes from across Western Eurasia showed that, starting from 37,000 BP, all the hunter-gatherer lineages represented in the dataset shared some affinity to the present-day Europeans (Fu et al., 2016). However, after the LGM, one of these lineages prevailed in Western and Central Europe, while in the subsequent warming period (ca. 14,000 BP) another previously unknown lineage spread across Europe from Italy to Britain displacing much of the previously present lineages (Fu et al., 2016; Olalde and Posth, 2020). Named as ‘Villabruna’ after the type sample where this ancestry was described, and later as Western European hunter-gatherers (‘WEHG’ or ‘WHG’), this group showed affinity to both present-day European and Southwest Asians. Its pre-expansion geographic distribution remains unknown, but it extends to the east into southcentral Anatolia where it was encountered in an admixed form on a 15,000 yo hunter-gatherer (Feldman et al., 2019). Besides these widespread ancestries, others related to the hunter-gatherers of Scandinavia and Eastern Europe (abbreviated as ‘SHG’ and ‘EEHG’, respectively) have been formed at latest by the Early Holocene (Haak et al., 2010; Mathieson et al., 2015; Mittnik et al., 2018; Skoglund et al., 2014). In Southwest Asia, the Early Holocene hunter-gatherer populations from the Levant (present-day Jordan and Israel) were genetically distinct from those in the Zagros Mountain of Iran and the Caucasus (Broushaki et al., 2016; Jones et al., 2015; Lazaridis et al., 2016). However, they were found to share a basal ancestry -modeled as an early sprout before the diversification of all other non-African populations- that did not contribute to the European hunter gatherers (Lazaridis et al., 2014; Lazaridis et al., 2016; Jones et al., 2015).

At present, more than 200 hunter-gatherers’ genomes from across West Eurasia dated between 40,000 and 5,000 BP have been recovered (Olalde and Posth, 2020). Their overall genetic diversity -measured with heterozygosity- is lower than the one observed among modern populations inhabiting the same geographical range (Skoglund and Mathieson, 2018). In other

words, the present-day east-to-west gradient of genetic diversity cannot be linearly related to the successive founder events that took place during the colonization of Eurasia by AMH. Instead, in order to understand such patterns, we have to turn towards the last millennia of genetic history.

### *1.2.1 Archaeogenomic insights into the West Eurasian Neolithic and Bronze Age*

For most of Eurasia, and particularly Europe and Southwest Asia, the temporal range from ca. 10 to 5 millennia BP was marked by the Neolithic, a transformative period on human history. Neolithic is a term that was coined in 1865 by John Lubbock as the last period within the Stone Age. The Stone Age was the oldest within the three-age system (Stone, Bronze and Iron Age) that was proposed some years earlier by C. J. Thomson as a way to chronologically classify prehistoric artifacts in museum collections. This periodization is currently of little relevance for prehistorical chronological frameworks in some regions (e.g., Americas, sub-Saharan Africa). However, it became an established schema in the study of European and Southwest Asian (Near Eastern) prehistory, and beyond. The Neolithic signaled a change from hunting and gathering practices -that evolved throughout more than two million years- to new subsistence practices involving plant and animal domestication, and in most of the cases sedentarism. This transition was gradual, happened independently in many regions across the world and spread to nearby areas, hence ‘Neolithization’. The earliest evidence of farming communities comes from Southwest Asia, namely the ‘Fertile Crescent’; an extended area that spreads over the territory of present-day Jordan, Israel, Lebanon, Syria, Southern Turkey, Iraq, Iran, Egypt and Cyprus. The earliest stages of Neolithization are placed in the Levant and Northern Mesopotamia at ca. 12,000 BP, and lacked the use of pottery (Pre-pottery Neolithic). With the collection and study of archaeological data from Western Anatolia, the Aegean and the Balkans, a consensus is proposed over the last decades: the Neolithic reached Europe through Anatolia and the Aegean from the 9<sup>th</sup> millennium BP following a continental and a maritime (Mediterranean) route associated with the Linear Pottery and the Impressa/Cardial Pottery Cultures, respectively (Barnett, 2000; Bickle et al., 2013).

A traditional debate regarding the Neolithization concerns the underlying mechanism of the transition, whereby three main opposing theories have been formulated. The first postulates the transmission of technological knowledge from the Near Eastern farmers to the indigenous hunter-gatherer groups (‘Cultural Diffusion’ or ‘adoptionist’) (Edmonson, 1961). The second proposed the expansion of the farming communities (‘Demic Diffusion’ or ‘migrationist’) (Childe, 1925), while the third emphasized independent local innovations (‘indigenist’). The indigenist model has been disregarded for Europe, as most of the wild varieties of the domesticated plants and animals are found only in the Near East (Smith, 1995). The migrationist and adoptionist models represent the ends of a variegated spectrum of mechanisms, but they were not formulated as mutually exclusive (Ammerman and Cavalli-Sforza, 1973). In addition, integrative models such as elite dominance (Renfrew, 1987), leap-frog colonization (Zilhão, 1993; Arnaud, 1982), frontier mobility (Zvelebil and Lillie, 2000), or community infiltration (Neustupny, 1982) advocate for mechanisms of various grades and modes of genetic mixing and colonization.

The overlaying of aDNA information has greatly contributed to this question. First, within the Fertile Crescent and its northern fringes in Southcentral Anatolia, it was shown that there was principally genetic continuity between the local hunter-gatherers and the subsequent early farmers (Lazaridis et al., 2016; Feldman et al., 2019; Broushaki et al., 2016). The aDNA data from these studies came from within the geographic boundaries of the Neolithic formative area (Levant, Iran and Anatolia), and subtle genetic affinities between those distant Neolithic populations were described, indicating some degree of interconnectivity. Despite that, the main conclusion was that for some of the seminal centers of Neolithization, the farming practice emerged without much migration. Second, in Europe, the first aDNA evidence showed discontinuity between hunter-gatherers and early farmers. In addition, mitochondrial data pointed towards a near eastern origin of the latter (Bramanti et al., 2009; Fu et al., 2012; Haak et al., 2010). The first whole-genome data further corroborated this finding (Keller et al., 2012; Skoglund et al., 2012; Lazaridis et al., 2014). The most compelling evidence came in 2015, when genomes from Western Anatolia, Central, North and Western Europe were co-analyzed, revealing a common genetic origin of early European farmers (EEF) with those from Anatolia (Mathieson et al., 2015). Some EEF did exhibit slight differences though, which were quantified as small contribution of ancestry related to hunter-gatherers (WHG). Subsequent data further traced the concurrence of those two ancestries, and documented a resurgence of the WHG-ancestry during the Middle Neolithic (Haak et al., 2015; Lipson et al., 2017; Günther et al., 2015). Furthermore, the progressive filling of archaeogenomic gaps from East and Southeastern Europe, Southern France and Iberia hinted a complex picture with regional variation in admixture processes between farmers and the distinct hunter-gather populations (Mathieson et al., 2018; Mittnik et al., 2018; Rivollat et al., 2020; Villalba-Mouco et al., 2019; Valdiosera et al., 2018).

With a fast pace facilitated by technological advancements in sampling and hybridization enrichment, West Eurasia -and especially Europe- has become a stage for the application of large-scale archaeogenomic approaches. Over the last six years, whole-genome or genome-wide data from more than 2,500 ancient individuals has been produced, of which approximately 60% belonged to Neolithic or Bronze Age contexts. This increment of aDNA data has enabled detecting transformative large-scale prehistoric population movements, and understanding the granular specifics of such impactful events on a micro-scale, by exploring local gene-flow between neighbors (Gokcumen and Frachetti, 2020). For example, the complex biological interaction of hunter-gatherers and farmers in Europe had a profound demographic impact, reflected on the gene pool of modern Europeans. However, this can only partially explain their genetic makeup. Initially, an adequate model for Europeans was obtained with the inclusion of approximately 10% ancestry related to a basal lineage -named Ancestral North Eurasian (ANE) and represented by Mal'ta (Lazaridis et al., 2014; Raghavan et al., 2014b). It was soon revealed that behind this distal proxy lied a Bronze Age population represented by the so-called Yamnaya culture in the Eurasian Steppe. The Yamnaya culture, whose economy was based on sheep and cattle herding, emerged ca. 5,000 BP from previous cultures in the steppe and its periphery, and managed to successfully exploit the environment presumably through the adoption of innovations such as the wheel and the horse riding (Anthony, 2010;

Reich, 2018). The earliest presence of Yamnaya/steppe-related ancestry in Europe is documented in Central and Northern Europe, at the Late Neolithic-Early Bronze Age Corded-Ware archaeological horizon, named after the pottery impressions (Allentoft et al., 2015; Haak et al., 2010). These studies showed that the links between these cultures were associated with an extended westward migration, but also one eastward, essentially connecting Altai in Siberia with Scandinavia during the Early Bronze Age (Allentoft et al., 2015). However, recently the analysis of ancient horse genomes revealed that the westwards expansion was not facilitated by the domesticated horses that prevailed in Eurasia from ca. 2000 BCE (Librado et al., 2021). The route of the steppe-ancestry in Europe was since then refined through the study of other expansive archaeological horizons, such as the ‘Bell Beaker’, revealing a heterogenous demographic process whereby the expansion of this culture was not accompanied by admixture in some areas, while in other (e.g., Britain) it was (Olalde et al., 2018). Studies with a local focus have lent other nuances, such as long-lasting regression of farming and steppe ancestry, suggesting that populations were at dynamic admixture stages (Mittnik et al., 2019; Furtwängler et al., 2020). In addition, cross-disciplinary approaches combining ancestry profiles, reconstruction of familial relationships and assessment of individual mobility through stable isotope ratios, have managed to illuminate aspects of internal social organization, status inheritance and gender-biased mobility (Mittnik et al., 2018; Amorim et al., 2018; Martiniano et al., 2017; Olalde et al., 2019).

The present thesis is applying the aforementioned state-of-the-art methods and approaches on areas and archaeological periods within the West Eurasia which, at the time of this thesis, have been scarcely understood archaeogenetically. Southwest Asia and the Aegean have been among the first areas to witness the ‘Neolithic and Urban Revolutions’, but owing to sampling challenges -mainly due to poor aDNA preservation- the impact of these transformations on the population history has been only partially addressed. Manuscript A aims to reconstruct the genomic history of a large area within Southwest Asia, spanning from Anatolia to the Southern Caucasus and the Northern Levant. At the same time, diachronic genetic information is recovered from iconic archaeological sites, whose historical trajectory encapsulates critical transitions in subsistence practices and sociopolitical organization, and what is believed to have been multiethnic societies. Therefore, the scope of Manuscript A expands from supra-regional to local patterns of population interactions and individual mobility. Manuscript B follows the same approach on a geographically much narrower area, the Aegean. Despite that, the Aegean has harbored a lot of cultural diversity since the Neolithic, and therefore a focus is placed on understanding internal population dynamics and the expression of biological features on social practices, such as kin groups in collective burials.

The following section provides an overview of the archaeological research and theories formulated throughout more than a century regarding the developments on these areas. Along with the archaeogenetic information published over the last years, the following synthesis delineates the framework of the main questions addressed in the manuscripts.

### **1.3 Archaeological and archaeogenetic background of the Aegean and Southwest Asian prehistory (Neolithic-Bronze Age)**

#### *1.3.1 Remarks on terms of archaeological chronology*

The chronological framework applied on the areas in question is based on the Three-Age-System, which is a method of relative dating based on the presence of certain types of artifacts. For example, the chronological framework applied in Anatolian archaeology is a local variant of this system, but its transitional dates are mostly imported from outside the region (Schoop, 2011). Subsequently, some of the sub-period classifications do not always successfully reflect diverse subsistence models, technological and social complexity within Anatolia (Yakar, 2011) which is a large territory encompassing a lot of eco-geographical diversity. In the Aegean, the Bronze Age (ca. 3100-1050 BCE) has been divided according to three cultural designations that correspond to different regions within the Aegean: the ‘Minoan’ in Crete (after the mythical King of Minos at Knossos), the ‘Helladic’ in Mainland Greece (after the Greek word of ‘Greek’), and the ‘Cycladic’ (after the name of island complex on the Southcentral Aegean Sea). Further divisions (i.e., Early, Middle, Late) and subdivisions (e.g., Early Minoan IA) have been initially proposed for Crete (Evans, 1921; Evans, 1935), and Helladic and Cycladic chronologies broadly complemented this periodization system. However, subsequent discoveries have shown that material culture differences do not always fall within the boundaries of the proposed divisions, and that period/sub-period connotations between e.g., Minoan and Helladic were not always synchronous (Shelmerdine, 2008).

It is also important to mention the development of absolute dating methods, such as dendrochronology and radiocarbon ( $^{14}\text{C}$ ). The introduction of  $^{14}\text{C}$  at the late 1940’s and its subsequent technological improvements -such as the Acceleration Mass Spectrometry (AMS)-, the refinement of calibration curves, anti-contamination sampling and cleaning protocols, and the integration of Bayesian statistical frameworks (Ramsey, 2009) has helped researchers to establish reliable intra- and inter-site comparisons, maximizing the chronological resolution of cultural associations (e.g., Gkiasta et al., 2003; Manning, 1995). Nonetheless, caveats and controversies can arise with absolute chronologies owing to issues such as sample contamination, oscillations in the calibration curves, or marine reservoir effects.

Considering the central position that Anatolia occupies in this thesis, and the fact that it harbored some of the earliest Neolithic communities of Southwest Asia, an outlook of the stages of its cultural evolution from the Neolithic to the Bronze Age is presented in Table 1 (13.2 from the Appendix) after adaptation from Steadman and McMahon (2011).

#### *1.3.2 From Anatolia to the Aegean and the Caucasus: the Neolithic period*

The introduction of the term “Neolithic Revolution” in the early 20<sup>th</sup> century by Gordon Childe to designate a transformative cultural period in human societies had a profound impact to the course of prehistoric research. Initially, an emphasis was placed on the excavation of sites in the Fertile Crescent and in Southeastern Europe, the areas considered the formative zone of Neolithic and the origin of European Neolithic, respectively (Özdoğan, 2011). With considerably more data from across Anatolia collected over the last decades, this picture has



critically changed. A number of surveys and excavations conducted in Southeast and Central Anatolia (e.g., Göbelki Tepe, Pınarbaşı, Aşıklı Höyük and Boncuklu Höyük) have pushed the beginning of the Neolithic in these areas to earlier dates (ca. 8000-7000 BCE) and, despite their diversity in subsistence patterns, the process of Neolithization was more or less parallel to that of the Fertile Crescent (Özdoğan, 2011; Özdoğan, 1997). Subsequently, the formative area has now expanded to include highlands of the southeastern sections of Central Anatolia. By the end of the 8<sup>th</sup> millennium BCE, fully farming villages had developed in Central Anatolia and peak demographics are estimated to have reached by 6700-6500 BCE with 3,500-8,000 inhabitants in Çatalhöyük at the Konya Plain (Leppard, 2021; Cessford, 2005). Surprisingly, the earliest Neolithic strata do not appear in Western Anatolia before the 7<sup>th</sup> millennium BCE, almost 2,000 years later after the first PPN communities of Central Anatolia (Düring, 2010; Özdoğan, 2011). Even more remarkably, elements of the ‘Neolithic Package’ appear in the Aegean littoral and mainland Greece in synchronous deposits with those of Western Anatolia. The abrupt Neolithization in this area refutes the Wave-of-advance models of gradual and stepwise colonization (Krauß et al., 2018; Ammerman and Cavalli-Sforza, 1984). However, the interplay of demographics and acculturation of local foragers, the ecological factors that might have triggered this quasi-instantaneous spread during the 7<sup>th</sup> millennium, and the followed maritime routes remain contentious topics in archaeology. A westward large-scale movement from Central Anatolia as a response to the 8.2k climatic event has been postulated, and the coincidence of the two events has been further elaborated with the acquisition of more <sup>14</sup>C dates (Clare and Weninger, 2014; Clare et al., 2008; Weninger et al., 2014). Departures from this ‘Rapid Climate Change’ (RCC) model can be drawn within e.g., Western Anatolia, where evidence from regional climate proxies is more tenuous. Alternatively, a combined model of small-scale migration from Central Anatolia, whereby the hunter-gatherer knowledge about local environments assimilated with the expertise of incoming farmers, can be supported by artifact continuity among the Mesolithic sites of Ağaçalı and the Neolithic sites of the Fikirtepe horizon (Düring, 2016).

While the Bulgarian Early Neolithic displays clearly parallels with the neighboring Western Anatolian, implying a colonization through an inland route, it has been argued that the know-how introduced to Greece and the Aegean at the beginning of the Neolithic cannot be reduced to simple exchanges (Perlès, 2005). In addition, defining the ‘Neolithic package’ as a proxy for understanding the ‘how’, ‘from where’ and ‘to where’ of the Neolithization might not reach a consensus (Özdoğan, 2010; Perlès, 2005). By extension, the regional variation might equally enjoy explanations from multiple packages arriving at different times, to interaction of mobile groups relying on domesticates with mobile groups of hunter-gatherers-fishermen (Reingruber, 2011).

Currently, the <sup>14</sup>C record on the Aegean -although it might be subject to general biases such as uneven sampling and lacunas (Weninger et al., 2014)- provides the earliest dates for Neolithic at coastal sites in the South Aegean. While on the side of Western Anatolia these early dates are more tentatively ascribed to 6700 cal BCE (Reingruber, 2011; Thissen, 2010), in Crete, the absolute dates of the aceramic Neolithic levels under the Bronze Age Knossos (Evans, 1964) were recently reappraised with AMS, and are now securely placed before the

‘RCC’, from ca. 7000 to 6600 cal BCE (Douka et al., 2017; Efstathiou et al., 2004). The life span of the Knossos founder village is estimated to a short period paralleling the PPN in Cyprus, which is rooted in the 9<sup>th</sup> millennium BCE (Douka et al., 2017; Manning, 2014). An initial argument for intrusive movement of farmers in the island (e.g., Cherry, 1981) is further supported by more recent archaeobotanical and archeozoological evidence, attesting lack of comparable endemic wild species (Horwitz, 2013). To date, the exact origin of those settlers remains unknown. However, the early dating and the island’s geographical location has often favored interpretations integrating the Neolithization of Crete within the far-reaching coastal networks operating in the Eastern Mediterranean (i.e., South Anatolia and Northern Levant and Cyprus) since the Epipaleolithic and the Pre-Pottery periods (Horejs et al., 2015; Perlès, 2005; Reingruber, 2011; Broodbank, 2006; Simmons, 2014). Same scenario applies to other sites in Southern Greece, such as Franchthi in the Peloponnese. In general, the wide distribution of Melian obsidian in the Aegean since the Mesolithic points towards an established network of maritime connections (Perlès, 2003; Reingruber, 2011; Sampson et al., 2010; Milić, 2014).

Human DNA analysis has been applied to illuminate aspects of the Neolithic demography in the Eastern Mediterranean. The earliest studies using modern DNA as proxy of past mobility highlighted genetic connections between the Aegean and Anatolia (King et al., 2008; Paschou et al., 2014). However, correlating such genetic signals within specific past population events is more intricate with modern uniparental or genome-wide data alone. On the contrary, pre-Neolithic and Neolithic genetic data have revealed essential aspects of the demographic landscape across Anatolia and the Aegean. First, a time transect in Central Anatolia spanning from 13500 to 8500 BCE has shown genetic continuity between hunter-gatherers and the aceramic farmers, thereby aligning with archaeological evidence of a principally indigenous process of transition to farming (Feldman et al., 2019; Kılınç et al., 2016). However, a small portion of their gene pool traced back to populations related to the Early Holocene in Iran and Caucasus (Ganj Darej Neolithic from Neolithic Zagros, and hunter-gatherers from Kotias and Satsurbliya caves in Caucasus, abbreviated as ‘CHG’). This genetic signal cannot be considered transient or local, as it was found to persist on the Central Anatolian ceramic farmers of Tepecik-Çiftlik, almost two millennia later (Kılınç et al., 2016). Second, the late 7<sup>th</sup> millennium BCE populations from the Marmara region, in Western Anatolia, although genetically very similar to the Central Anatolian hunter-gatherers, exhibit some affinity to Neolithic populations from Southern Levant. This could be interpreted under a scenario in which gene-flow between Levant and Western Anatolia bypassed Central Anatolia, likely through Northern Levant and the southeastern Anatolian coast. Alternatively, this Levantine affinity might reflect older (e.g., Mesolithic) substructure within Anatolia. A more direct genetic link is proposed for the contemporaneous Early Neolithic genomes from Northern Greece and Marmara, which cluster together, excluding Central Anatolia (Hofmanova et al., 2016). Interestingly, these were also shown to maintain higher heterozygosity compared to Central Anatolia, a finding that challenges more simplistic scenarios of founding populations from Central Anatolia colonizing Western Anatolia and Northern Aegean (Kılınç et al., 2017).

The extent to which these differences reflect contributions from local hunter-gatherers is yet to be discovered. This particular genetic aspect remains poorly understood due to sample limitations. The Mesolithic genomes from Central Anatolia (AHG) and the Iron Gates in Romania were genetically linked either because -among other WHG lineages- Iron Gates HG were the most related to AHG, or due to a later gene-flow from Southeastern Europe to Anatolia (Feldman et al., 2019; Mathieson et al., 2018). It is currently unknown whether the Aegean Mesolithic gene pool was lying on a gradient of these two mixing ancestries, or harbored unique genetic diversity in this area. Remarkably, in contrast to the resurgence of ancestry related to European hunter gatherers (WHG) in Late Neolithic Europe, an increased affinity to CHG is observed in Late Neolithic and Chalcolithic Aegean (Mathieson et al., 2018; Omrak et al., 2016). Ancestry related to Early Holocene Iran and the Caucasus seems to have trans-versed a large area from Central Anatolia to the Aegean, but little is known about its pre-expansion geographic range, and/or whether areas to the east of Central Anatolia had acted as agents in this process.

From an archaeological perspective, the late appearance of Neolithic elements in North and Northeast Anatolia and the Caucasus around the 6<sup>th</sup> millennium BCE were likely associated with the transfer of commodities and knowhow rather than endemic movements (Özdoğan, 2014). In fact, the absence of older remains from Northcentral Anatolia has been attributed to a research hiatus (Düring, 2008; Özdoğan, 1996). However, it might reflect a later process of settling that was discouraged during the earliest stages of Neolithization because of the demanding nature of this mountainous and heavily forested area (Schoop, 2011; Schoop, 2005). In any case, in most regions of Anatolia, cultural traditions (mainly pottery) of the 6<sup>th</sup> millennium BCE -a period conventionally assigned to the Early Chalcolithic in Anatolia-, seem to emerge without breaks from the preceding Neolithic (Schoop, 2011).

In Southeastern Anatolia, the beginning of the Chalcolithic is associated with the late origin and proliferation of the North Mesopotamian Halaf tradition, at the end of the 7<sup>th</sup> millennium BCE. The Halaf tradition, which nowadays is recognized as rooted in the Neolithic, was a widespread type of painted pottery representing a notable change in pottery production and the symbolic complexity associated with it (Campbell, 2007). More recent data re-evaluation from Halafian sites suggest that those North Mesopotamian inhabitants followed semi-nomadic lifestyle, establishing seasonal campsites (Uerpmann, 1982; Seeden and Kaddour, 1983; Özbal, 2011; Akkermans, 1994). While this might hold to some extent for Southeastern Anatolia as well, the presence of numerous sites whose occupation stretches many hectares suggests otherwise (Özbal, 2011; and references therein). In addition, the assessment of the features of the local assemblages across Southeastern Anatolia resonates regional variability rather than superregional connections (Özbal, 2011).

Presence of Half painted ware has been documented further North, in Eastern Anatolia, at the site of Tilkitepe by Lake Van (Watson, 1982). The lower level of Tilkitepe represents the earliest evidence of settlement in Eastern Anatolia and suggests this area was part of a system of interactions oriented towards the upper Mesopotamia (Palumbi, 2011). An analogous artifact complex reminiscent of Halaf pottery traditions and architecture is represented in the Southern Caucasian 'Aratashen-Shulaveri-Shomutepe' Late Neolithic material culture

(Baudouin, 2019; Lyonnet et al., 2016; Nishiaki et al., 2015; Badalyan et al., 2010). However, the sporadic appearance of these features is reckoned as a result of occasional and intermediated interactions (Palumbi, 2007; Badalyan et al., 2004; Badalyan et al., 2007). In the Caucasus, the existence of archaeological sites since the Early Holocene was revealed by the 1990's, but the lack of paleoenvironmental data and radiocarbon dates hinder a comprehensive picture of the Mesolithic to the Early Neolithic transition and the 6<sup>th</sup> millennium BCE Neolithic of the Aratashen-Shulaveri-Shomutepe culture (Chataigner et al., 2014). However, besides the tenuous halafian influences, evidence indicates that the Neolithization of the Southern Caucasus, albeit unique in many aspects, did not develop detached from their neighbors. Firstly, the introduction of domesticated animal and plant species from northern Southwest Asia (i.e., southeastern Anatolia and the southwestern Caspian belt) (Chataigner et al., 2014). Secondly, the presence of obsidian of Armenian origin approximately 800 km to the south, at the North Mesopotamian site of Domuztepe (Frahm et al., 2016). Irrespective of whether obsidian traveled such long distances via human mobility or circulation networks, it poses Southern Caucasus as an active agent of innovations and their propagation, and not as a periphery of the North Mesopotamian world.

### *1.3.3 The Syro-Anatolian Chalcolithic and Bronze Age*

During the following millennia, these earlier connections in material culture attested between Northern Mesopotamia and Southeastern Anatolia, and extending to the Caucasus, culminated in interregional connections that encompassed areas of unprecedented scope (Parker, 2010). These far-reaching networks sprung from Southern Mesopotamia, and are related to the Ubaid and Uruk periods that succeeded each other. The Ubaid period spanning from 6500 to 3800 BCE (Carter and Philip, 2010), is associated with the production and proliferation of certain types of pottery and artifacts. Features of the Ubaid 'culture' were adopted by the Northern Mesopotamian Halaf during the late 6<sup>th</sup> millennium BCE, until the Northern Ubaid emerged under the impulse of new values issued by its southern neighbour (Forest, 2005). Besides the dissemination of ceramic styles that might carry encoded cultural messages regarding shared ideology and identity, Ubaid represents a transformative period characterized by the evolution from groups of farming villages to chiefdoms and ultimately the state-level polities (Forest, 2005; Parker, 2010; Henrickson and Thuesen, 1989). Subsequently, the "Ubaid Expansion" has been the subject of intensive research, and interpretations have been sought into proposals of migration, colonization or acculturation and peaceful appropriation (Stein and Özbal, 2007; Breniquet, 1987; Hole, 2000; Thuessen, 2000). However, even though Ubaid pottery is known to have reached beyond Northern Mesopotamia -as north as the Taurus mountains of Southeastern Anatolia- there is little recovered evidence on architecture and associated finds (Özbal, 2011) that would determinatively rule out any of these theories. Yet, a few sites from this period in Northern Mesopotamia, as well as west and north of it, have yielded architectural elements that show large parallels with Ubaid proper tripartite structures [e.g., Değirmentepe in Upper Euphrates (Gürdil, 2010; Stein and Özbal, 2007), Tepe Gawra and to some extent Kenan Tepe in Northern Mesopotamia (Parker, 2010)]. These tripartite buildings were probably related to large families, and the profound nature of the family structure suggests that this feature was introduced with people rather than by imitation (Frangipane, 2015a). At the same time, an holistic study of the Kenan Tepe assemblage

supports that the architecture was conditioned to local ecological conditions and that various products (e.g., obsidian and pottery) reached its inhabitants through different networks, while most of the Ubaid-styled pottery was produced locally (Campbell and Healey, 2016; Parker, 2010).

The nature of population interactions within the Greater Mesopotamia and its adjacent areas becomes a dominant theme when it comes to the next Mesopotamian expansion that took place during the 4<sup>th</sup> millennium BCE Middle and the Late Uruk periods ('Middle and Late Uruk expansion') (Algaze et al., 1989; Rothman, 1993; Schwartz, 1988). Named after the Sumerian city of Uruk, this period experienced the emergence of urbanism in Southern Mesopotamia. After ca. 3600 BCE, Uruk pottery started to appear from Southeastern Anatolia and the Northern Levant to the eastern Anatolian highlands. But in contrast to the preceding 'Ubaid Expansion', the 'Uruk Expansion' was accompanied by a large amount and variety of trading products, and therefore has been considered to reflect the expansion of a controlled trading system expedited from the south (Algaze, 2008; Rothman, 2011b). This view has been corroborated by a number of north Mesopotamian sites such as Hacinebi (Stein and Misir, 1993), Habuba Kabira (Stommenger, 1980) and Jebel Aruda (van Driel and van Driel-Murray, 1983) that have provided evidence of the existence of 'colonies', serving as trading outposts. However, the term 'colony' conceptually is shifted from the colonialist paradigm of contemporary history towards one in which indigenous and south Mesopotamians coexist for long periods engaging into symmetric exchanges (Stein, 2009). In other sites, recent analysis of artefactual assemblages has refuted the existence of any colony at all, and argues for rooted pottery traditions and local craftsmanship integrating Uruk features (e.g., Helwing, 1999).

One of the most compelling examples that lent critical nuances on what has been considered an expansionary phenomenon from the 'core' to the 'periphery' (Algaze, 2008; Algaze, 1993) comes from Arslantepe, one of the most extensively excavated sites in Eastern Anatolia. During the fourth millennium, Arslantepe experienced developments, structurally resembling those of Mesopotamia, which led to the development of a primary state system towards the end of the millennium (Frangipane, 2018; Frangipane, 2011; Frangipane, 2012b). However, the precocious early-state system at Arslantepe underwent a divergent trajectory defined by the local traditions of the Upper Euphrates, differences in the cult practices and the lack of urbanization (Frangipane, 2018). This indicates a more complex and deep process of socio-cultural transformation that reoriented the economic, political and cultural interests of indigenous elites towards Southern Mesopotamia. Moreover, evidence from the subsequent Late Chalcolithic-Early Bronze Age deposits on Arslantepe attests wide-range relations with pastoralists from the Northeastern Anatolia and South Caucasus (Palumbi, 2010). Pottery, sheep rearing and significant metallurgic developments point towards the incorporation of pastoral components into an economic system governed by central elites (Di Nocera, 2010; Frangipane, 2015a). However, at ca. 3000 BC, the early-state system at Arslantepe collapsed, and transhumant pastoralists occupied the site, giving rise to a period of profound instability characterised by meetings and clashes of various populations contending the site (Frangipane, 2012a; Frangipane, 2014; Frangipane, 2015b; Siracusano and Palumbi, 2014). These pastoralist populations have been associated with the 'Kura-Araxes culture' or 'Early Transcaucasian culture (ETC)', which is generally thought to have originated in the late 4<sup>th</sup> millennium BCE Southern Caucasus and expanded outwards around 3000-2900 BCE,

spreading westwards to Eastern Anatolia and the Northern and Southern Levant (Palumbi, 2017; Palumbi and Chataigner, 2014), and eastwards to Iran (Rothman, 2011a). To date, a handful of genomes recovered from human remains in Kura-Araxes contexts suggest those individuals belonged to the Early Bronze Age gene pool of Mountain Caucasus, and could be modelled as a combination of Western Chalcolithic Anatolia, Early Holocene Caucasus (CHG) and Chalcolithic Iran (Wang et al., 2019). It remains unknown whether this genetic profile disseminated further to the south of Caucasus with the expansion of ETC.

In conclusion, during the Chalcolithic and the Early Bronze Age, spheres of interactions developed, bridging large areas of the Near East and the Caucasus. Since the transition from the more egalitarian Halafian societies to centralized political, economic, and administrative systems issued in South Mesopotamia, there is abundant evidence of hybridisation of social practices and material culture across the Greater Mesopotamia. At the same time, Eastern Anatolia harboured interethnic societies of different social organisation and origin living side by side without engaging to inclusion or cultural mixing (Frangipane, 2015a). At the Northern Levant and Syro-Mesopotamia, urban centres continuously thrived during the Early Bronze Age of the 3<sup>rd</sup> millennium, whereas urban societies disappeared during the second half of the 3<sup>rd</sup> millennium at the Southern Levant, i.e., during the so-called intermediate Bronze Age. The onset of the Middle Bronze Age in Syro-Mesopotamia is associated with the emergence of the Amorite kingdoms, whereby the involvement of “Amorite” migrants from this region in the resurgence of urbanisation at the Southern Levant during the Middle Bronze Age is still under debate.

These developments led to the increasing nascent ‘internationalism’ of the Eastern Mediterranean basin and the entire Near East throughout the Middle and Late Bronze Age (ca. 2000-1200 BCE) and beyond, which is characterized by far-reaching contacts, an intensification of resource exploitation and management through connected sea and land routes (Akar, 2013; Feldman, 2006; Hodos, 2017). Our knowledge about these periods has been greatly enhanced by the discovery and decipherment large textual archives in this region (e.g., from Mari, Karum Kanis/Kültepe, Amarna, Ugarit to name but a few), and the large number of deciphered ancient Near Eastern languages. With the traveling of Old Assyrian merchants, writing appeared also in Anatolia, and it is established nowadays that the Near East hosted a large linguistic diversity, ranging from the Semitic Akkadian (Steadman and McMahan, 2011) to the early Indo-European branches in Anatolia, represented by the Luwian and Hittite. Therefore, the exchange and movement of traders, artisans, and representatives of kings, as well as the shifts in territorial control dynamics between kingdoms/empires are well documented (Beckman, 1996; Campbell, 1960; Michel, 2003).

In general, archaeological evidence points to cultural continuity in numerous sites between the Early Bronze and Middle Bronze Age Anatolia and the Northern Levant (Marro, 2007; D’Andrea, 2019; Pinnock, 2009), although substantial changes in the urban layout are observed (Matthiae, 2011). In addition, written records also inform us about an increasing ethnic fragmentation among various groups with diverse cultural background, which is reflected under the distinct names mentioned (e.g., the Amorites and the Hurrians) (Laneri and Schwartz, 2011; Nichols and Weber, 2006). Overall, the wide-ranging networks of social, cultural, and economic contacts have long been understood to involve increased levels of individual mobility across wide areas and possibly in a large scale. Recent approaches in

tracking human mobility through isotopic analysis (i.e., strontium and oxygen isotopes) are not numerous for the Near East Bronze Age (e.g., Buzon and Simonetti, 2013; Gregoricka, 2013; Yazıcıoğlu Santamaria, 2017), and suggest predominantly local populations. Moreover, over the last five years, archaeogenetic studies have documented transitions in the Central/Southern Levant that involve increasing gene flow from other areas from within the Near East (i.e., Anatolia and Iran), and report the presence of some individuals of distinct Caucasian genetic origins (Agranat-Tamir et al., 2020; Haber et al., 2017; Harney et al., 2018). However, the role of human mobility in Anatolia has been challenging question to address due to the scarcity of Middle and Late Bronze Age (LBA) burials especially.

#### 1.3.4 The Aegean Bronze Age

The Early Bronze Age Aegean is one of the most studied parts of the Mediterranean, largely because it is widely viewed as the context to scrutinize why and how the early urban, palatial societies emerged in Crete at the same level as other centers in the southern Levant (Broodbank, 2013). Despite the lack of radiocarbon dates from the end of the preceding Final Neolithic in Crete (contemporaneous to Middle-Late Chalcolithic in Anatolia), the start of the Early Bronze Age, not only in Crete but also in the Cyclades and the Southern Greek mainland, is placed towards the end of the fourth millennium BCE (Manning, 1995). At that time, the northern coast of the island was exposed to the developed maritime networks predominantly related to the Cycladic world. Even though the entire island complex of Cyclades encompasses a land mass orders of magnitude smaller than Crete, all the transformative stages in farming, social organization, symbolism and technology that led to the complex Aegean societies are evident in the Cycladic Final Neolithic and Bronze Age contexts (Renfrew, 1972). By the beginning of the Early Bronze Age, the Cyclades had all been probably settled, and towards the end of this period (ca. 2000 BCE), long-range links with the rest of the Aegean world - likely related to the movement of metals from its metal ores- were established (Broodbank, 2008). Besides the trade connections between Cyclades and the northern coasts of Crete, a cemetery of Cycladic funerary architecture at Hagia Photia, at the northeast of the island, suggests enclaves of Cycladic people during the Early Bronze Age (Day et al., 1998). At the same time, in the Southcentral Crete, monumental tholos (dome-shaped) tombs of multiple inhumations and pottery styles evidence cultural affinities with Anatolia and the Near East (Wilson, 2008; Cline, 2010). In general, monumental architecture, sealing systems, and the integration of the Aegean in Eastern Mediterranean networks of exchange, became common features across the Aegean by the Early Bronze Age II, reflecting the first ‘international spirit’ of the region (Renfrew, 1972). However, life disruption events seemed to have intercepted this path at least in the Greek mainland (ca. 2200 BCE -end of Early Helladic II). Despite the lack of high-resolution <sup>14</sup>C data from the Greek mainland (Manning, 1994), the approximate date of this disruption coincides with site destructions/abandonments in the Eastern Mediterranean from the Old Kingdom Egypt to the Akkadian Empire, which in turn have been associated to dramatic climate changes (Weiss, 2014; Weiss, 2017). However, such horizon of destruction is not evident in Crete, and soon the island experienced the emergence of the first palaces (Protopalatial Period/Middle Minoan). During that 150-year period, a number of approximately state-level polities appeared in Crete (mainly the central part), and were accompanied by

several other developments such as the Cretan Hieroglyphic script, an administrative sealing system and peak sanctuaries on hilltops (Manning and Knappett, 2008).

This quite rapid and dramatic transformation in Crete was initially explained as the result of radical influences from other cultures, especially the Egyptian (Evans, 1896). However, as new information became available, scholars have leaned towards a more internal process that was already in place during the Early Bronze Age (Early Minoan) (e.g., Cherry, 1983). Synthetic views have advocated that Crete was more proactive in establishing independent Mediterranean networks with Anatolia, the Levant, and Egypt, and strategically exploited the land for regional intensification (Manning and Knappett, 2008). The first ancient DNA analysis based on mitochondrial genomes suggested that, irrespectively of the extent of these external cultural influences, the ‘Minoan civilization’ developed from autochthonous populations (Hughey et al., 2013). A more recent study based on ancient genome-wide data, confirmed that populations from the Bronze Age period derived most of their ancestry from European-Anatolian Neolithic farmers, but also exhibited affinity related to populations from Iran and Caucasus (Lazaridis et al., 2017). The same affinity was also shown for contemporaneous individuals from Western Anatolia suggesting that this ‘eastern’ component could have reached the Aegean through Anatolia at latest by the Early/Middle Minoan period.

Although at these earliest stages Crete was fundamentally shaped by foreign settlement and contact, from the Middle Bronze Age onwards the island would take the initiative in reaching out to the wider Aegean world (Wilson, 2008). By the end of the Bronze Age, Cretans were participating in an international network that shipped goods over routes reaching from Mesopotamia to Italy and from Egypt to the Black Sea (Betancourt, 2008). In addition, the recovery of standard measures and weights suggests an agreed-upon system of exchange and that -considering the increased urbanization of the island- Cretan inhabitants might have enjoyed some kind of mobility (Younger and Rehak, 2008). Along with these commodities, the spread of Minoan artistic motifs in pottery and frescoes became evident from Miletos, Alalakh and Tell Kabri and Awaris/Tell el-Dab’a in the Anatolian and Levantine coasts to Egypt (Bietak and Marinatos, 1995; Niemeier and Niemeier, 2000; Niemeier and Niemeier, 2002). Whether these were painted by artists of Cretan origin or training remains difficult to prove.

Although the Minoan influences are apparent in the neighbouring Greek mainland, this region followed a different trajectory towards the formation of polities and a distinct culture commonly ascribed to ‘Mycenaean’ after the archetypal Greek Late Bronze Age site in Mycenae. Even though the ‘Mycenaean civilization’ thrived between 1700 and 1050 BCE (Late Helladic period), its roots can be traced in the preceding Middle Helladic period, some centuries after the life disruption at the end of the Early Helladic II. The combined information from residential and funerary architecture from this period offer valuable hints regarding the progressive emergence of lineage-based social differentiation, as it is evidently witnessed by the rich Shaft Graves and the presence of prestige good in the form of jewellery and weapons (Crowley, 2008; Cline, 2010; Wright, 2008). It is important to highlight that this political and cultural transformation was not uniform and concurrent throughout the central and southern mainland (Wright, 2008). The competition between rising elites during the Shaft Grave period led to regional conflicts, and culminated in the extinction of many local dominions on the Greek mainland. A first mainland military expedition to Crete during the 15<sup>th</sup> century has been



proposed (Wiener, 2015), but remains highly contested (Nafplioti, 2008; Miller, 2011). At the end of this conflict, the palatial period (Late Helladic IIIA-B) started with a smaller number of eminent polities. This turn to palace-dominated societies is also reflected in the administrative record inscribed on clay tablets with Linear B, an early form of the Greek (Chadwick, 1976). During this period, it is believed that the influence on Crete by the mainland centres was intensified and Cretan resources were systematically exploited with the help of turning centres like Knossos, and Chania into key posts for the administration of large parts of the island (Maran, 2005). Overall, the 'Mycenaeans' settled throughout most of the Greek mainland and the Aegean islands. Mycenaean products have been recovered in large numbers from sites on the Anatolian Aegean coast, Cyprus, the Levant and Egypt.

The origin of the 'Mycenaeans' has been intensely debated, as it is linked with the question of when the assumed ancestors of the later ethnic and linguistic group of the 'Greeks', who spoke an early branch of Indo-European languages arrived in Greece. Implying migration or even invasion, explanations have been commonly sought in transitional periods. Although climatic factors have been discussed as agents of the various destruction layers dating to the end of Early Helladic II, the occurrence of a cultural change was proposed and associated with the linguistic discontinuity in place names between a pre-Greek form (Indo-European or not) and the following Greek written in Linear B (Caskey, 1960; Haley and Blegen, 1928). Hence, combined together, this evidence corroborated the arrival of Indo-European speakers towards the end of the Early Helladic. Nevertheless, other theories have placed the event earlier at the end of the Neolithic/beginning of Bronze Age (Coleman, 2000) or even earlier, with the advent of agriculture (Renfrew, 1987). The former proposes a pre-Greek local language substrate and peaceful infiltration of Indo-European speakers from Anatolia ca. 3100 BCE. Besides the difference on the proposed origin of newcomers, this theory is generally concordant with the 'Kurgan hypothesis' which advocates successive migrations of early Indo-European speakers from the steppes and the Black Sea into the Balkans (Gimbutas et al., 1997).

Although no tool or method can absolutely settle this long-lasting debate, ancient DNA can place some constraints. Two recent studies have sampled a small number of individuals from across the Greek mainland and showed that both the individuals from Mycenaean contexts and those from Middle Helladic Northern Greece carry admixture signatures related to populations from the Eurasian Steppe (Clemente et al., 2021; Lazaridis et al., 2017). The absence of this component from the early phases of the Early Bronze Age (Early Helladic I-II) Euboea -an island at close reach from the mainland- may indicate that migration and admixture with populations from the north did not start before the Early Helladic II. In addition, if that was a gradual process starting north of the Aegean, it would presumably take time until the initially distinct gene pools homogenize across the entire mainland. Therefore, the timing and pace of introduction this 'northern' ancestry in the mainland, and subsequently whether, when and how it spread to the Aegean islands and beyond are poorly understood questions.

## 2 Objectives of the Thesis

The goal of this thesis is to address questions regarding human population dynamics, individual mobility and social practices in the Aegean and Southwest Asia, during an extended and critical period of human prehistory spanning from the Neolithic to the end of the Bronze Age (ca. 6000-1200/1050 BCE). More than a century of intensive archaeological research in this area has probed and mapped the scope of technological and societal advances that marked the transition to farming societies and later, the first state societies and palatial civilizations. While evidence of intercultural encounters and exchanges is abundant in the archaeological record, the biological trace of such interactions has been poorly understood.

The studies included in this dissertation, therefore, apply state-of-the-art archaeogenomic approaches for the reconstruction and analysis of genetic material from ancient human remains. Given the considerable challenges with the DNA preservation in the Eastern Mediterranean, certain methodological developments, namely the optimised bone sampling protocols and the DNA enrichment methods, have rendered possible the recovery of genome-wide data from a large number of individuals spanning large areas and successive time periods. Such spatially and temporally dense datasets enable the complement of the archaeological record, first, by providing a large-scale perspective of the biological interactions of the populations, and second, by illuminating the granular specifics of the population history within an archaeological site down to the level of individual life histories.

Within this broader objective of the thesis, the main questions addressed in each of the two manuscripts are formulated as follows.

### **Manuscript A:**

- Did the Late Neolithic/Early Chalcolithic populations from Central Anatolia, the Northern Levant and Southern Caucasus exhibit the same levels of genetic differentiation among each other as their hunter-gatherer and early farmer ancestors, or were they admixed? If so, what was the extent, direction and timing of this admixture?
- Was the emergence of the first state societies in Eastern Anatolia (Upper Euphrates) facilitated by the movement of people from Southern and Northern Mesopotamia? Were the subsequent events of socio-political conflict that led to the occupation of the same area by pastoral populations connected with the Caucasus marked by gene flow from the latter area?
- Were the Bronze Age populations across Anatolia genetically distinguishable and which admixture models could explain best such differences?
- Were the far-reaching contacts of the early globalised state societies in Eastern Mediterranean (2<sup>nd</sup> millennium BCE) expressed through co-mingling and co-existence of people from diverse areas and genetic origins?

### **Manuscript B:**

- How do the early farming populations from the island of Crete (Greece) genetically relate to those from Anatolia, Mainland Greece and the Levant? How can such

information integrate with current hypotheses regarding the origins of the first Neolithic settlers on the island?

- It has been observed that post-Neolithic, Aegean populations carried admixture signatures related to populations from the east (i.e., Caucasus/Iran). What admixture models best represent this genetic influx in terms of the real source populations, the degree and the mode of admixture (continuous or one-pulse like)? Do these demographic features differ between the Greek mainland, Crete and the other Aegean islands, which -despite interconnected- developed their unique cultural features and social organisation?
- Ancestry related to the Eurasian Steppe pastoralists reached Central Europe by ca. 2500 BCE, in Sicily by ca. 2200 BCE, and in Northern Greece latest by ca. 1900 BCE (recent finding by Clemente et al., 2021). How was this ancestry introduced and how was it distributed in the Greek mainland and the Aegean islands during the period when the Mycenaean culture flourished?
- Did the proposed increasing influence of the Greek mainland over Crete during the late Bronze Age (i.e., Minoan period for Crete) involve biological interaction between the populations on both sides?
- Were the members of collective burials genetically related and what do the reconstructed family pedigrees suggest about family structure and kin groups?
- Is there any evidence for isolated populations and/or intermarriage (consanguinity) and if so, is it more common in certain settings (i.e., cultural, eco-geographical)?

## 3 Overview of Manuscripts and Author Contributions

### 3.1 Manuscript A

#### “Genomic History of Neolithic to Bronze Age Anatolia, Northern Levant, and Southern Caucasus”

##### Authors

Eirini Skourtanioti, Yılmaz S. Erdal, Marcella Frangipane, Francesca Balossi Restelli, K. Aslihan Yener, Frances Pinnock, Paolo Matthiae, Rana Özbal, Ulf-Dietrich Schoop, Farhad Guliyev, Tufan Akhundov, Bertille Lyonnet, Emily L. Hammer, Selin E. Nugent, Marta Burri, Gunnar U. Neumann, Sandra Penske, Tara Ingman, Murat Akar, Rula Shafiq, Giulio Palumbi, Stefanie Eisenmann, Marta D’Andrea, Adam B. Rohrlach, Christina Warinner\*, Choongwon Jeong\*, Philipp W. Stockhammer\*, Wolfgang Haak\*, and Johannes Krause\*

\*Corresponding Authors

**Status:** Published

##### Reference

Skourtanioti, E., Erdal, Y. S., Frangipane, M., Balossi Restelli, F., Yener, K. A., Pinnock, F., Matthiae, P., Özbal, R., Schoop, U.-D., Guliyev, F., et al. 2020. Genomic History of Neolithic to Bronze Age Anatolia, Northern Levant, and Southern Caucasus. *Cell*, 181, 1158-1175.e28.

##### Summary

In **Manuscript A** we report genome-wide data from more than 100 ancient individuals recovered from genetically unexplored areas and/or periods of Southwestern Asia: Central, North and Eastern Anatolia, Northern Levant and South Caucasus, dated from the Late Neolithic to the Late Bronze Age.

The area of Southwestern Asia, commonly referred to in archaeology as the Near East, has been an influential region for the development of the first human civilisations. Studies of ancient population genomics during the last five years have shown that while the Early Neolithic populations within this area were genetically differentiated, in subsequent periods population structure seems to break down. The spatiotemporal scope of this population process had been poorly understood because -by the time of this publication- only few genomes from these later periods had been analysed. According to archaeology, cultural interregional interactions of Near Eastern populations following the Neolithic period evolved into a complex and deep process of socio-cultural transformation in which material and societal innovations issued in some areas would appear in some others either as abrupt introductions or as gradual local adaptations. Especially during the Bronze Age, a period when empires started to form,

cultural encounters globalised in the whole Eastern Mediterranean and therefore, the role of human mobility naturally emerges as a principal question.

The archaeogenomic dataset presented in Manuscript A covers a time transect spanning ca. four millennia of human history, and represents the largest so far assemblage of Near Eastern genomes published in one study, providing thereby novel genomic insights about the population history of the Near East.

We found that populations from Western Anatolia to the Southern Caucasus admixed during the Late Neolithic, and we could date the beginning of this population process at ca. 6,500 BCE. This timing correlates with the expansion of sedentary communities across Anatolia and the Southern Caucasus and suggests that the latter event was accompanied by gene exchange spanning a very large area, in contrast to the earlier transition from foraging to farming.

In subsequent millennia (Chalcolithic and Bronze Age periods), we found that populations from across Anatolia were genetically very similar and only very few of them exhibited evidence of subtle and transient gene flow from the Caucasus, despite the archaeological evidence for intense cultural contacts with neighbouring areas.

In contrast, in the Northern Levant we show that a genetic turnover took place during the state period and it is not related to admixture from nearby Anatolian populations, but rather to as-yet unsampled populations from Northern Mesopotamia.

We detected one genetically distinct individual in the Late Bronze Age Northern Levant that we could genetically determine as of Eastern Iranian/Central Asian origin, implying that individual mobility could cross the borders of the Eastern Mediterranean globalised societies.

Overall, we describe a largely homogeneous gene pool within which we could delineate different events of larger or local-scale human mobility. In addition, the geographically and temporally extensive sampling that we achieved in our study enabled us to integrate our findings with archaeological evidence, providing thereby a novel view on the research of the human history in the Near East.

### **Author Contributions**

Johannes Krause, Wolfgang Haak, Philipp W. Stockhammer, Choongwon Jeong, and Christina Warinner conceived the study. Choongwon Jeong, Wolfgang Haak, and Johannes Krause supervised the genetic work. Yılmaz S. Erdal, Marcella Frangipane, K. Aslihan Yener, Frances Pinnock, Paolo Matthiae, Rana Özbal, Farhad Guliyev, Tufan Akhundov, Bertille Lyonnet, Emily L. Hammer, Selin E. Nugent and Ulf-Dietrich Schoop provided archaeological material. Philipp W. Stockhammer, Yılmaz S. Erdal, Marcella Frangipane, Francesca Balossi Restelli, K. Aslihan Yener, Tara Ingman, Murat Akar, Rula Shafiq, Rana Özbal, Giulio Palumbi, Farhad Guliyev, Bertille Lyonnet, Emily L. Hammer, Ulf-Dietrich Schoop and Stefanie Eisenmann advised on the archaeological background and interpretation. Yılmaz Selim Erdal, Marcella Frangipane, Francesca Balossi Restelli, K. Aslihan Yener, Tara Ingman, Murat Akar, Rula Shafiq, Rana Özbal, Tufan Akhundov, Bertille Lyonnet, Ulf-Dietrich Schoop, Marta D'Andrea, and Eirini Skourtanioti wrote the archaeological and sample background section. Eirini Skourtanioti, Marta Burri, Gunnar U. Neumann, and Sandra Penske performed the

laboratory work. Eirini Skourtanioti performed the data analyses with Choongwon Jeong and Wolfgang Haak providing guidance. Adam B. Rohrlach performed analyses on the Y-chromosome markers and assignment of Y-haplogroups. Eirini Skourtanioti, Choongwon Jeong, and Wolfgang Haak wrote the manuscript with input from all co-authors.

**The candidate is:**

**First author**,  Co-first author,  Corresponding author,  Co-author

**Contribution of the authors to the publication**

<b>Author</b>	<b>Conceptual research design</b>	<b>Data analysis</b>	<b>Experimental work</b>	<b>Writing of the manuscript</b>	<b>Sample procurement</b>
Eirini Skourtanioti	10%	85%	65%	45%	0%
Johannes Krause	25%	0%	0%	5%	15%
Wolfgang Haak	20%	5%	0%	>15%	15%
Philipp W. Stockhammer	20%	0%	0%	5%	15%
Choongwon Jeong	15%	10%	0%	>15%	0%
Christina Warinner	10%	0%	0%	5%	5%
Other co-authors	0%	0%	0%	5%	50%
Lab Technicians <sup>1</sup>	0%	0%	35%	0%	0%

---

<sup>1</sup> Marta Burri, Gunnar U. Neumann, Sandra Penske

## 3.2 Manuscript B

### “Ancient DNA reveals admixture history and endogamy in the prehistoric Aegean”

#### Authors

Eirini Skourtanioti\*, Harald Ringbauer, Guido Alberto Gneccchi Ruscone, Raffaella Angelina Bianco, Marta Burri, Cécilia Freund, Anja Futwängler, Florian Knolle, Nuno Filipe Gomes Martins, Gunnar U. Neumann, Anthi Tiliakou, Anagnostis Agelarakis, Maria Andreadaki-Vlazaki, Philip Betancourt, Birgitta P. Hallager, Olivia A. Jones, Olga Kakavogianni, Athanasia Kanta, Panagiotis Karkanias, Efthymia Katakis, Konstantinos Kissas, Robert Koehl, Lynne Kvapil, Joseph Maran, Photini J. P. McGeorge, Alkestis Papadimitriou, Anastasia Papathanasiou, Lena Papazoglou-Manioudaki, Kostas Paschalidis, Naya Polychronakou-Sgouritsa, Sofia Preve, Eleni-Anna Prevedorou, Gypsy Price, Eftychia Protopapadaki, Tyede Schmidt-Schultz, Michael Schultz, Kim Shelton, Malcolm H. Wiener, Johannes Krause\*, Choongwon Jeong\*, Philipp W. Stockhammer\*

\*Corresponding Authors

**Status:** accepted at *Nature Ecology and Evolution* (by editor: September 2022, by production editor: November 2022; published: 16 January 2023). The version herein is the published which includes some additional work performed after the submission of the thesis for review.

#### Summary

As a bridge between Europe and the Near East, the Aegean is presented both as a region of significance for the spread of the Neolithic lifestyle across Europe, and a fragmented landscape that encapsulated advanced exchange networks since before the Neolithic. Throughout the subsequent Bronze Age period, the Aegean experienced the emergence of complex and sophisticated societies which -after a short but significant life disruption in mainland Greece- culminated to the formation of two prominent cultures. The Minoan culture in Crete and the Mycenaean in mainland Greece influenced each other and shared a legacy of mortuary practices, with collective burials as an expression and constitution of social belonging within local communities. Contrary to the immense archaeological importance of the region, the biological components associated with these cultural transformations in the Aegean since the Neolithic are currently poorly understood, mainly due to poor DNA preservation.

In **Manuscript B** we fill in this important gap of knowledge by generating and analyzing genome-wide data from 102 ancient individuals from the Greek mainland, Crete and other Aegean islands that date from the Neolithic to the Late Bronze Age. With a ca. three-fold increase in the number of individuals from previous publications, this dataset represents the largest assemblage of ancient Aegean genomes and the earliest Neolithic Aegean evidence coming from an island population. Using state-of-the art methods, we have been able to infer

a population history of multi-phased admixture and to shed light on social practices otherwise unattested at the archaeological context.

We find that the Neolithic population from Crete, presenting some of the earliest farmers in Europe, shared the same genetic profile as contemporary populations from the Greek mainland and Anatolia but exhibited lower genetic diversity, suggesting different population dynamics between the mainland and islands during the early phases of Neolithization.

The biological connection between the Aegean and Anatolian gene pools carried on during the Early Bronze Age suggesting that the progressive integration of Aegean societies within the exchange networks of the Eastern Mediterranean was accompanied by admixture of the Aegean populations with those from Anatolia.

Nevertheless, by the Late Bronze Age, we show that populations from the mainland carried additional admixture signatures related to the Bronze Age pastoralists from the Eurasian Steppe. We further elaborate how this process of population mixing differed from Central Europe, likely involving populations from Northern Balkans who -to date- remain understudied. After the Greek mainland, these signatures gradually also appear into Crete, thus providing a new angle for the long-debated hypothesis that Mycenaeans took over the control of the island from the 15<sup>th</sup> century onwards.

We also report the extraordinary finding of consanguinity at unparalleled levels for the aDNA record of prehistoric Europe and Southwest Asia. High levels of consanguineous endogamy -likely at the degree of first cousins- persisted for at least a millennium, pinpointing to a social practice that was shared mainly among island populations from different cultural contexts.

Finally, we reconstruct the pedigree of a Mycenaean infant burial and found that all infants were members of the same biological family. This is the first pedigree reconstructed archaeogenetically for the ancient Aegean, and at the same time the first aDNA study of an entire Mycenaean collective burial. After a century of archaeological efforts, we are now able to shed a novel light on the importance of biological kinship and its emplacement within the collective memory of a Mycenaean community.

### **Author Contributions**

Philipp W. Stockhammer, Choongwon Jeong, and Johannes Krause conceived, supervised and/or acquired funding for the study. Philipp W. Stockhammer, Maria Andreadaki-Vlazaki, Anagnostis Agelarakis, Philip Betancourt, Birgitta P. Hallager, Olivia A. Jones, Olga Kakavogianni, Athanasia Kanta, Konstantinos Kissas, Robert Koehl, Lynne Kvapil, Joseph Maran, Photini J. P. McGeorge, Anastasia Papathanasiou, Lena Papazoglou-Manioudaki, Kostas Paschalidis, Eleni-Anna Prevedorou, Gypsy Price, Eftychia Protopapadaki, Tyede Schmidt-Schultz, Michael Schultz, Naya Sgouritsa-Polychronakou, Kim Shelton and Malcolm H. Wiener assembled, studied the archaeological material and/or advised on the archaeological background and interpretation of the results. Raffaella Angelina Bianco, Marta Burri, Căcilia Freund, Anja Furtwängler, Florian Knolle, Nuno Filipe Gomes Martins, Gunnar U. Neumann and Anthi Tiliakou performed laboratory work. Eirini Skourtanioti coordinated the data analyses with guidance from Choongwon Jeong, and Eirini Skourtanioti, Guido Alberto



Gnecchi Ruscone and Harald Ringbauer analysed the data. Eirini Skourtanioti, Philipp W. Stockhammer and Choongwon Jeong wrote the manuscript with critical input from all the co-authors.

**The candidate is:**

**First author**,  Co-first author,  **Corresponding author**,  Co-author

**Contribution of the authors to the publication**

<b>Author</b>	<b>Conceptual research design</b>	<b>Data analysis</b>	<b>Experimental work</b>	<b>Writing of the manuscript</b>	<b>Sample procurement</b>
Eirini Skourtanioti	15%	85%	10%	60%	<5%
Philipp W. Stockhammer	40%	0%	0%	25%	>25%
Johannes Krause	30%	0%	0%	0%	15%
Choongwon Jeong	15%	10%	0%	10%	0%
Other co-authors	0%	5%	0%	5%	50%
Lab Technicians <sup>2</sup>	0%	0%	90%	0%	0%

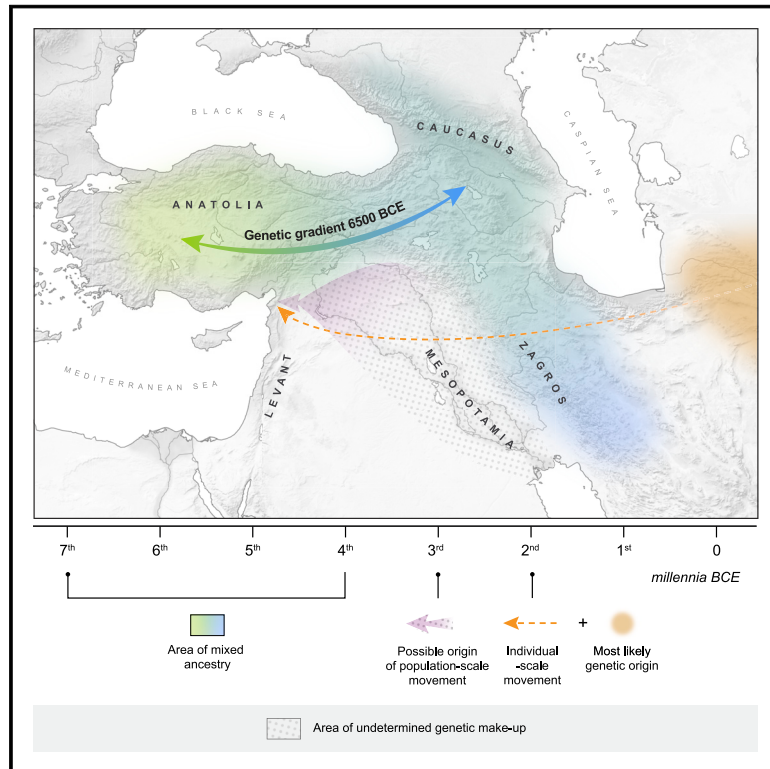
---

<sup>2</sup> Raffaella Angelina Bianco, Marta Burri, Cäcilia Freund, Anja Futwängler, Florian Knolle, Nuno Filipe Gomes Martins, Gunnar U. Neumann, Anthi Tiliakou

## 4 Manuscript A

# Genomic History of Neolithic to Bronze Age Anatolia, Northern Levant, and Southern Caucasus

## Graphical Abstract



## Authors

Eirini Skourtanioti, Yilmaz S. Erdal, Marcella Frangipane, ..., Philipp W. Stockhammer, Wolfgang Haak, Johannes Krause

## Correspondence

warinner@fas.harvard.edu (C.W.), cwjeong@snu.ac.kr (C.J.), philipp.stockhammer@lmu.de (P.W.S.), haak@shh.mpg.de (W.H.), krause@shh.mpg.de (J.K.)

## In Brief

Reconstruction of genomic history of the Near East in a time transect spanning from the Neolithic through the globalization events of the Middle and Late Bronze Ages.

## Highlights

- Genome-wide analysis of 110 ancient individuals from the Near East
- Gene pools of Anatolia and Caucasus were biologically connected ~6500 BCE
- Gene flow from neighboring populations in Northern Levant during 3<sup>rd</sup> millennium BCE
- One individual of likely Central Asian origin in 2<sup>nd</sup> millennium BCE Northern Levant



## Article

# Genomic History of Neolithic to Bronze Age Anatolia, Northern Levant, and Southern Caucasus

Eirini Skourtanioti,<sup>1</sup> Yilmaz S. Erdal,<sup>2</sup> Marcella Frangipane,<sup>3</sup> Francesca Balossi Restelli,<sup>3</sup> K. Aslihan Yener,<sup>4</sup> Frances Pinnock,<sup>3</sup> Paolo Matthiae,<sup>3</sup> Rana Özbal,<sup>5</sup> Ulf-Dietrich Schoop,<sup>6</sup> Farhad Guliyev,<sup>7</sup> Tufan Akhundov,<sup>7</sup> Bertille Lyonnet,<sup>8</sup> Emily L. Hammer,<sup>9</sup> Selin E. Nugent,<sup>10</sup> Marta Burri,<sup>1</sup> Gunnar U. Neumann,<sup>1</sup> Sandra Pense,<sup>1</sup> Tara Ingman,<sup>5</sup> Murat Akar,<sup>11</sup> Rula Shafiq,<sup>12</sup> Giulio Palumbi,<sup>13</sup> Stefanie Eisenmann,<sup>1</sup> Marta D'Andrea,<sup>3</sup> Adam B. Rohrlach,<sup>1,14</sup> Christina Warinner,<sup>1,15,\*</sup> Choongwon Jeong,<sup>1,16,\*</sup> Philipp W. Stockhammer,<sup>1,17,\*</sup> Wolfgang Haak,<sup>1,\*</sup> and Johannes Krause<sup>1,18,\*</sup>

<sup>1</sup>Department of Archaeogenetics, Max Planck Institute for the Science of Human History, Jena 07745, Germany

<sup>2</sup>Department of Anthropology, Hacettepe University, Ankara 06800, Turkey

<sup>3</sup>Department of Classics, Sapienza University of Rome, Rome 00185, Italy

<sup>4</sup>Institute for the Study of the Ancient World (ISAW), New York University, New York, NY 10028, USA

<sup>5</sup>Department of Archaeology and History of Art, Koç University, Istanbul 34450, Turkey

<sup>6</sup>School of History, Classics and Archaeology, University of Edinburgh, Edinburgh EH8 9AG, UK

<sup>7</sup>Institute of Archaeology and Ethnography, Azerbaijan National Academy of Sciences, Baku AZ1073, Azerbaijan

<sup>8</sup>PROCLAC/UMR Laboratory, French National Centre for Scientific Research, UMR 7192, Paris 75005, France

<sup>9</sup>Near Eastern Languages and Civilizations, University of Pennsylvania, Philadelphia, PA 19104, USA

<sup>10</sup>School of Anthropology and Museum Ethnography, University of Oxford, Oxford OX2 6PE, UK

<sup>11</sup>Department of Archaeology, Mustafa Kemal University, Alahan-Antakya, Hatay 31060, Turkey

<sup>12</sup>History Department, Ibn Haldun University, Istanbul 34494, Turkey

<sup>13</sup>Université Nice Sophia Antipolis, CEPAM (Cultures et Environnements. Préhistoire, Antiquité, Moyen Âge), CNRS-UMR 7264, Nice 06357, France

<sup>14</sup>ARC Centre of Excellence for the Mathematical and Statistical Frontiers, The University of Adelaide, Adelaide, SA 5005, Australia

<sup>15</sup>Department of Anthropology, Harvard University, Cambridge, MA 02138, USA

<sup>16</sup>School of Biological Sciences, Seoul National University, Seoul 08826, Republic of Korea

<sup>17</sup>Institute for Pre- and Protohistoric Archaeology and Archaeology of the Roman Provinces, Ludwig Maximilian University, Munich 80539, Germany

<sup>18</sup>Lead Contact

\*Correspondence: [warinner@fas.harvard.edu](mailto:warinner@fas.harvard.edu) (C.W.), [cwjeong@snu.ac.kr](mailto:cwjeong@snu.ac.kr) (C.J.), [philipp.stockhammer@lmu.de](mailto:philipp.stockhammer@lmu.de) (P.W.S.), [haak@shh.mpg.de](mailto:haak@shh.mpg.de) (W.H.), [krause@shh.mpg.de](mailto:krause@shh.mpg.de) (J.K.)

<https://doi.org/10.1016/j.cell.2020.04.044>

## SUMMARY

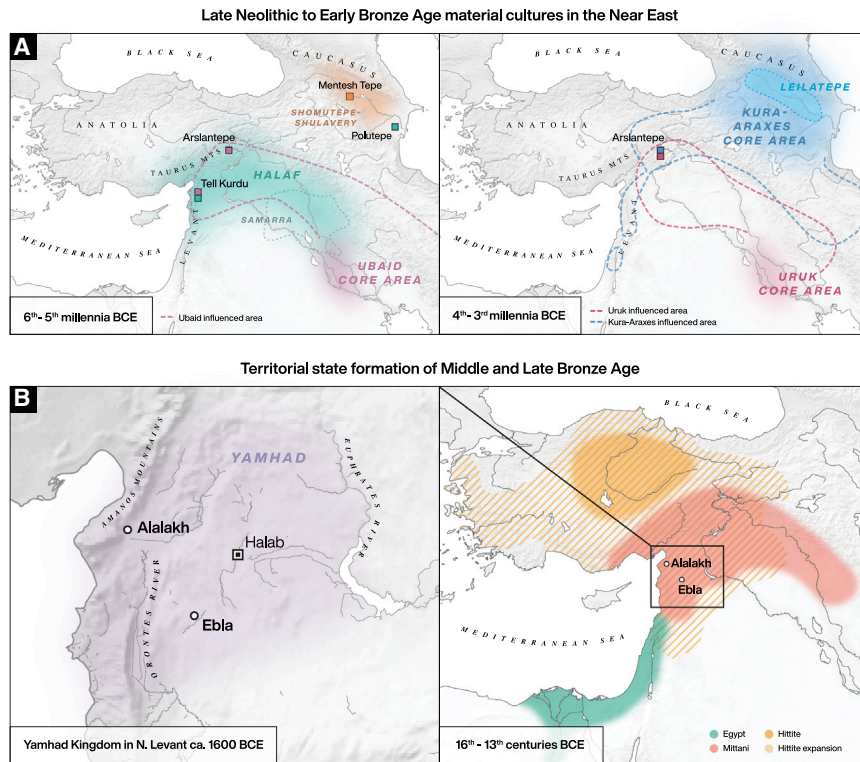
Here, we report genome-wide data analyses from 110 ancient Near Eastern individuals spanning the Late Neolithic to Late Bronze Age, a period characterized by intense interregional interactions for the Near East. We find that 6<sup>th</sup> millennium BCE populations of North/Central Anatolia and the Southern Caucasus shared mixed ancestry on a genetic cline that formed during the Neolithic between Western Anatolia and regions in today's Southern Caucasus/Zagros. During the Late Chalcolithic and/or the Early Bronze Age, more than half of the Northern Levantine gene pool was replaced, while in the rest of Anatolia and the Southern Caucasus, we document genetic continuity with only transient gene flow. Additionally, we reveal a genetically distinct individual within the Late Bronze Age Northern Levant. Overall, our study uncovers multiple scales of population dynamics through time, from extensive admixture during the Neolithic period to long-distance mobility within the globalized societies of the Late Bronze Age.

## INTRODUCTION

Since the beginnings of agriculture, the Near East has been an influential region in the formation of complex and early state-level societies and has drawn considerable research interest in archaeology since the 19<sup>th</sup> century (Killebrew and Steiner, 2014; McMahon and Steadman, 2012). Developments

in the field of ancient DNA (aDNA) over the last decade have shed light onto questions related to the process of Neolithization. Near Eastern farmers from South-Central Anatolia, the Southern Levant, and Northwestern Iran were descended from local foragers, and the transition from foraging to farming in these areas was shown to have been a biologically continuous process with only minor gene flow among them





**Figure 1. Cultural Developments and Territorial State Formation in Western Asia (Near East) from the 6<sup>th</sup> to the 2<sup>nd</sup> Millennium BCE**

(A) Approximate areas where important material cultures mentioned in the text developed between the 6<sup>th</sup> and 3<sup>rd</sup> millennia BCE. Approximate expansion range of these cultures outside of their proposed original land is given (dashed lines). Archaeological sites related to our study that have been influenced by these cultures are plotted in corresponding colors.

(B) Territorial shifts between Bronze Age kingdoms from the 16<sup>th</sup> to the 13<sup>th</sup> centuries BCE and location of studied sites Alalakh and Ebla. See also Figure S2.

(Broushaki et al., 2016; Feldman et al., 2019; Lazaridis et al., 2016).

Almost two millennia later, this situation had changed. In contrast to these Early Holocene populations, Chalcolithic/Eneolithic and Bronze Age populations from Western and Central Anatolia, the Southern Levant, Iran (Zagros), and the Caucasus show less genetic differentiation from each other, suggesting that these later periods were characterized by an extensive process of gene flow spanning a large area (Allentoft et al., 2015; de Barros Damgaard et al., 2018; Haber et al., 2017; Harnay et al., 2018; Jones et al., 2015; Lazaridis et al., 2016, 2017; Wang et al., 2019). However, the spatiotemporal scope of this process is poorly understood because of the lack of ancient genomes from areas that bridge these distant regions (i.e., Central and Eastern Anatolia) that, in turn, requires denser sampling. To date, the spatial distribution of features attributed to the “Neolithic package” across Anatolia suggests a heterogeneous multiple-event process that correlates with broader geographical zones (Özdoğan, 2014). However, whether population movement played a prominent role in the formation of these zones within Anatolia remains an open question.

Throughout Western Asia, archaeological evidence for the movement of peoples, material, and/or ideas is well documented (Figure 1). In the Southern Caucasus, archaeological research indicates relations with Northern Mesopotamia during the Late Neolithic (Halaf and Samarra cultures) (Badalyan et al., 2010; Nishiaki et al., 2015), and in Eastern Anatolia, a network of cultural connections marked by several expansive events, mostly related to the Mesopotamian world, is attested. These include an early intrusion of the South Mesopotamian Ubaid

culture into Upper Mesopotamia as far as the Taurus mountains of South-eastern Anatolia during the 5<sup>th</sup> millennium BCE (Frangipane, 2015a; Carter and Philip, 2010). It was followed, in the Southern Caucasus, by a strong influence at this time from Upper Mesopotamia during the late 5<sup>th</sup>–mid 4<sup>th</sup> millennium (Lyonnet, 2007; Lyonnet, 2012). From the middle to the end of the 4<sup>th</sup> millennium, another Southern Mesopotamian influence (the so-called “Middle and Late Uruk expansion”) reached Upper Mesopotamia and the upper stretches of the Euphrates and Tigris river valleys in Eastern Anatolia (Allen and Rothman, 2004). At the same time, during the second half of the 4<sup>th</sup> millennium BCE, the Kura-Araxes culture, which is generally thought to originate in the Southern Caucasus, expanded outward around 3000–2900 BCE, spreading westward to Eastern Anatolia and the Northern and Southern Levant (Palumbi, 2017; Palumbi and Chataigner, 2014) and eastward to Iran (Rothman, 2011). Evidence of these events comes from numerous excavations and is especially apparent in the long and extensively excavated sequence of occupations at Arslantepe in the Malatya plain of Eastern Anatolia. In the Northern Levant, material connections with Northern Mesopotamia start appearing in the 4<sup>th</sup> millennium BCE and have been attributed to either extensive cultural contacts or population movements.

The major question is, therefore: what was moving? Was this a movement of populations, material culture, ideas, or some combination? These earlier developments lead to the increasing “globalization” in the Eastern Mediterranean basin from the Middle Bronze Age (MBA) onward, which is characterized by an intensification of resource exploitation and management through connected sea and land routes (Akar, 2013; Feldman, 2006; Hodos, 2017). However, the role of human mobility is unclear and a challenging question to address due to the scarcity of Middle and Late Bronze Age (LBA) burials. In this regard, the site of Alalakh in the Amuq Valley (Turkey), with more than 300 burials dated to that period, represents an exceptional case for the application of aDNA studies.

Understanding the nature of this movement was the primary motivation behind this study. Here, we present a large-scale analysis of genome-wide data from key sites of prehistoric Anatolia, the Northern Levant, and the Southern Caucasian lowlands. Our goal was to reconstruct the genomic history of this part of the Near East by systematically sampling across this transition from the Neolithic to the interconnected societies of the MBA and LBA. Our new ancient genome-wide dataset consists of 110 individuals and encompasses four regional time transects in Central/North Anatolia, East Anatolia, the Southern Caucasian lowlands, and the Northern Levant, each spanning 2,000 to 4,000 years of Near Eastern prehistory. We find that mid-6<sup>th</sup> millennium populations from North/Central Anatolia and the Southern Caucasian lowlands were closely connected; they formed a genetic gradient (cline) that runs from Western Anatolia to the Southern Caucasus and Zagros in today's Northern Iran. This cline formed after an admixture event that biologically connected these two regions ca. 6500 BCE. Chalcolithic and Bronze Age populations across Anatolia also mostly descended from this genetic gradient. In the Northern Levant, by contrast, we identified a major genetic shift between the Chalcolithic and Bronze Age periods. During this transition, Northern Levantine populations experienced gene flow from new groups harboring ancestries related to both Zagros/Caucasus and the Southern Levant. This suggests a shift in social orientation, perhaps in response to the rise of urban centers in Mesopotamia, which to date remain genetically unsampled.

## RESULTS

### Sample Corpus and Data Compilation

We report genome-wide data from a targeted set of ~1.24 million ancestry-informative SNPs for 110 individuals from Anatolia, the Northern Levant, and the Southern Caucasian lowlands spanning ~4,000 years of prehistory. Nine of these individuals date to Late Neolithic/Early Chalcolithic ("LN/EC"; 6<sup>th</sup> millennium BCE) and come from three different geographic sectors: the Central/Northern Anatolian Boğazköy-Büyükaya, the Amuq Valley in Southern Anatolia/Northern Levant (Tell Kurdu), and the Southern Caucasian lowlands (Mentesh Tepe and Polutepe) (Figure 2A). The remaining 101 individuals date from the Late Chalcolithic to the Late Bronze Age ("LC-LBA"; 4<sup>th</sup>–2<sup>nd</sup> millennia BCE) and were collected from the following archaeological sites: Alalakh (modern Tell Atchana), Alkhantepe, Arslantepe, Ebla (modern Tell Mardikh), Çamlıbel Tarlası, İkiztepe, and Titriş Höyük (Figure 2A).

For in-depth population genetic analyses, we excluded a total of 16 individuals that did not meet quality requirements (e.g., SNP coverage, absence of damage patterns, contamination). All the remaining individuals showed damage patterns expected for ancient samples and had low contamination estimates ( $\leq 5\%$  for all but one, which has 10%). Overall, we performed genetic analyses on genome-wide data from 94 individuals, and 77 of these were accelerator mass spectrometry (AMS) radiocarbon dated (Figure 2B; Table S1). We grouped the individuals by archaeological site or area and archaeological period applying a nomenclature scheme that preserves this information (Figure 2C; STAR Methods). We also identified seven cases of 1<sup>st</sup> or 2<sup>nd</sup> degree relative pairs (Figure S1; Table S2) and restricted

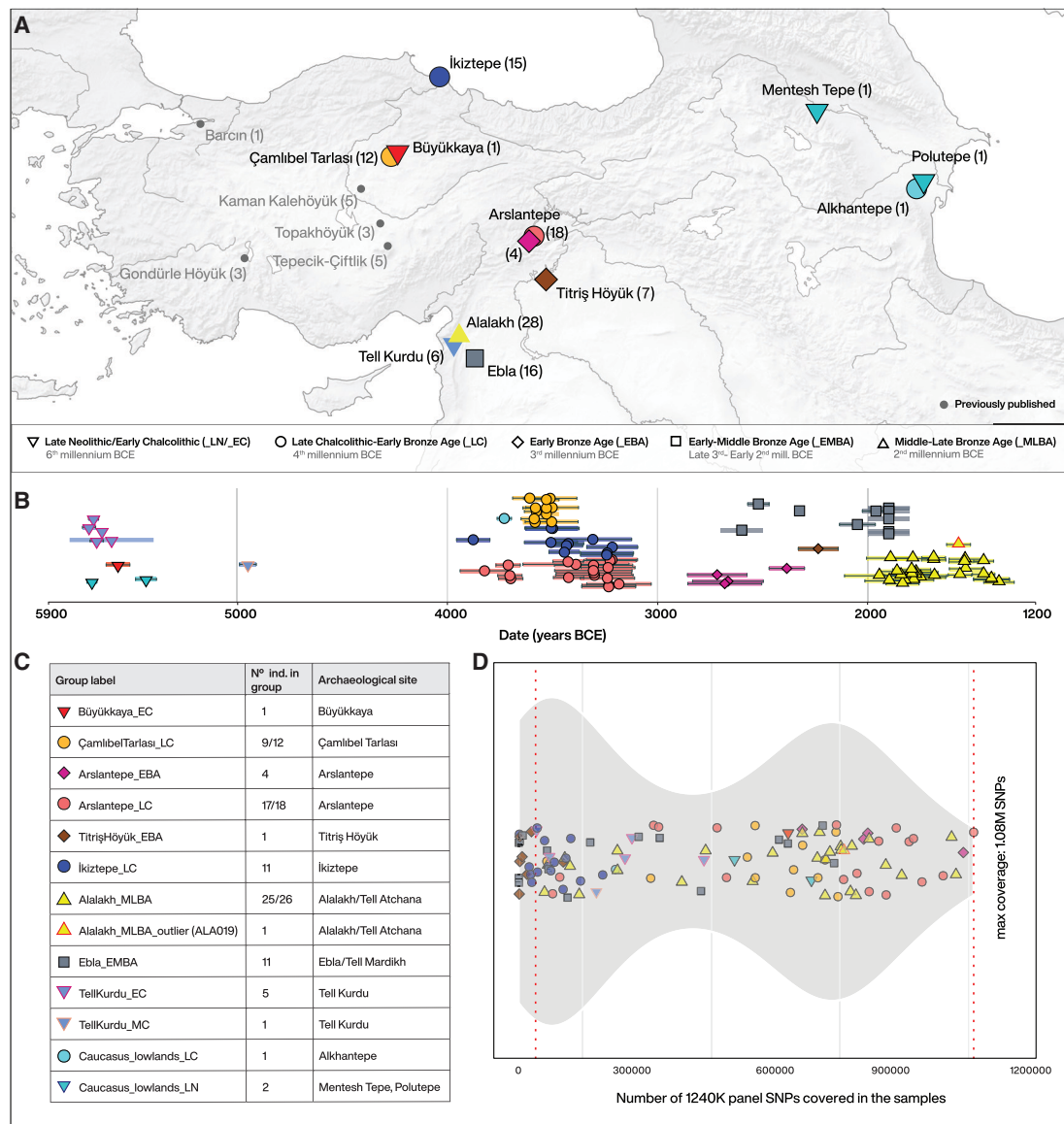
group-based genetic analyses for these groups ( $f$ -statistics,  $qpWave/qpAdm$ , and DATES) to 89 unrelated ( $\geq 3^{\text{rd}}$  degree) individuals (Figure 2C).

We merged our dataset with genetic data from ca. 800 previously published ancient individuals (Table S3; STAR Methods). Among these, 17 Anatolian individuals from the following archaeological sites overlap with our time transect and were co-analyzed with the Anatolian groups from our study: Tepecik-Çiftlik (Kılınç et al., 2016) ("Tepecik\_N"), Barcın (Mathieson et al., 2015) ("Barcın\_C"); Gondürle-Höyük (Lazaridis et al., 2017) ("GondürleHöyük\_EBA"), Topakhöyük (de Barros Damgaard et al., 2018) ("Topakhöyük\_EBA"), and Kaman-Kalehöyük (de Barros Damgaard et al., 2018) ("K.Kalehöyük\_MLBA") (Figure 2A).

### The Late Neolithic/Early Chalcolithic Genetic Structure in Anatolia, Northern Levant, and Caucasian Lowlands

So far, our knowledge of the gene pool of Neolithic Anatolia has been limited to individuals from Barcın and Menteşe in Western Anatolia (abbreviated here as "Barcın\_N") (Mathieson et al., 2015), Boncuklu from the Konya Plain in Central Anatolia (Feldman et al., 2019; Kılınç et al., 2016), and Tepecik-Çiftlik in Southern Anatolia (Kılınç et al., 2016). These individuals date from the 9<sup>th</sup> to the 7<sup>th</sup> millennium BCE and are succeeded by LN/EC individuals of this study. To overview the genetic structure in this Near Eastern region from the Neolithic to the Bronze Age, we first performed principal-component analysis (PCA) (Patterson et al., 2006; Price et al., 2006) of present-day West Eurasians populations and projected ancient individuals onto the top PCs (Figure 3A). Overall, LN/EC individuals are scattered along PC2 between Barcın\_N and ancient individuals from Iran/Caucasus (Figure 3B). TellKurdu\_EC are slightly shifted along PC1 toward Neolithic and Chalcolithic Levantine individuals. Büyükkaya\_EC is positioned further away from any Neolithic Anatolian reported to date and toward the direction of Neolithic and Chalcolithic Iranian individuals. Caucasus\_lowlands\_LN (two individuals from Polutepe and Mentesh Tepe) are positioned upward along PC2, between Büyükkaya\_EC and Chalcolithic Iran.

To formally test the qualitative differences observed in PCA, we compared the genetic affinity of LN/EC groups to earlier populations in Western Eurasia by computing  $f_4$ -statistics (Patterson et al., 2012) of the form  $f_4(Mbuti, p2; p3, X)$  (Figure 4). The statistic deviates from zero if a pair of Anatolian/Levantine/Caucasian groups ( $p3$  and  $X$ ) differ from each other in their genetic affinities to Epipaleolithic and Neolithic populations ( $p2$ ). We observe that Büyükkaya\_EC and Caucasus\_lowlands\_LN differ from Barcın\_N by sharing more alleles with Caucasus hunter-gatherers (CHG; Satsurlbia and Kotias Kilde caves) and Iran\_N (Ganj Dareh site in Zagros mountains) than with Barcın\_N (+2.2 to +5.5 SE), while sharing less alleles with hunter-gatherers from Western Europe (WHG) ( $\leq -4.3$  SE), Early European Farmers (EEF) ( $\leq -3.6$  SE), the Epipaleolithic Pınarbaşı individual from Anatolia ( $\leq -6.8$  SE), and with the Neolithic/Epipaleolithic Levant ( $-1.3$  to  $-9.4$  SE). By summarizing the  $f_4$ -statistics using  $qpAdm$  (Haak et al., 2015), we can adequately model both Büyükkaya\_EC and Caucasus\_lowlands\_LN as a two-way mixture of Barcın\_N and Iran\_N as source populations ( $p \geq 0.083$ ; 24%–31% from Iran\_N; Figure 4). Tepecik\_N, which occupies an intermediate



**Figure 2. Overview of Location, Ages, and Data Generation of Analyzed Individuals**

(A) Geographic location of archaeological sites with respective number of individuals with genetic data.

(B) Age of analyzed individuals in years BCE. Age is given as mean of the 2-sigma range of calibrated <sup>14</sup>C date (black horizontal lines) or mean of their proposed archaeological range when direct <sup>14</sup>C dates not available (colored thick lines).

(C) Grouping of individuals (after quality filtering) according to their location, time period and genetic profile. Number of individuals before and after removal of biological relatives is given when applicable.

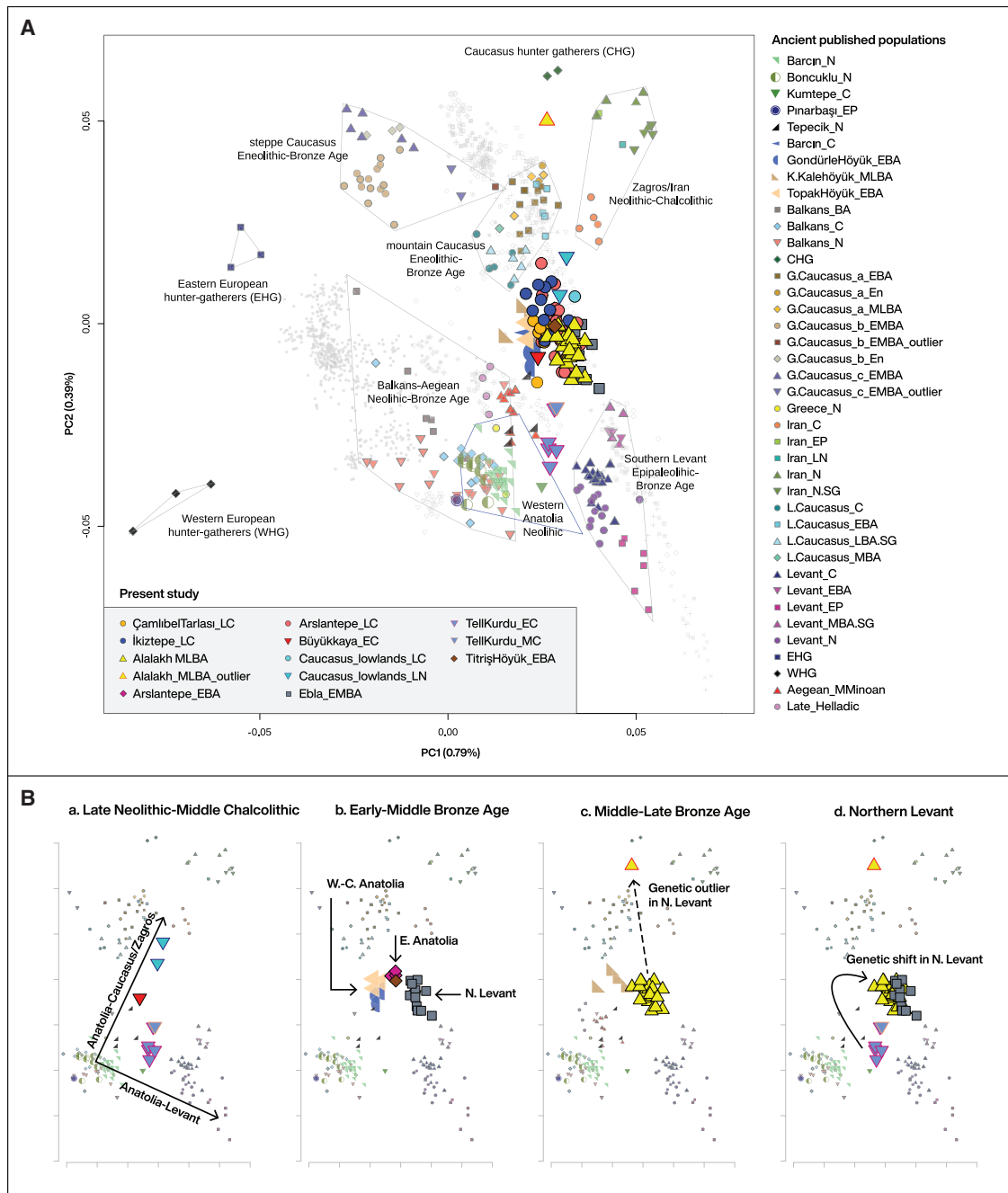
(D) Distribution of SNP coverage across individuals. Only individuals within a certain coverage range (marked with red dotted lines) were included in downstream analyses.

See also [Tables S1](#) and [S2](#) and [Figure S1](#).

position between Barcın\_N and Büyükkaya\_EC in the PCA, also fits the same model ( $p = 0.975$ ; 22% from Iran\_N). By replacing Iran\_N with CHG, we still obtain a good model fit for Büyükkaya\_EC ( $p \geq 0.825$ ; 24% from CHG), but not for Caucasus\_lowlands\_LN ( $p = 0.0001$ ).

Consistent with their positions on the PCA plot, TellKurdu\_EC does not fall on this cline of mixed Barcın\_N-Iran\_N ancestries but shows extra affinity with ancient Levantine populations.

Accordingly,  $f_4$ -statistics of the form  $f_4(Mbuti, Levant_N; X, TellKurdu_EC) \geq 3.3$  SE, show that TellKurdu\_EC has more affinity with the pre-pottery Neolithic Levantines (“Levant\_N”) than with any other Neolithic-Early Chalcolithic (“N-EC”) Anatolian population including an almost 1,000-year younger individual from the same area (TellKurdu\_MC). When compared to Barcın\_N, TellKurdu\_EC has significantly ( $< -4$  SE) less affinity with Mesolithic hunter-gatherers from Western, Eastern, and Southeastern Europe



**Figure 3. Principal-Component Analysis**

Principal-component analysis (PCA) was computed on the Human Origins (HO) SNP panel data of present-day West Eurasian populations (gray symbols) and ancient individuals were projected on them.

(A) PC1 and PC2 for ancient individuals from the present study and selected from previous publications.

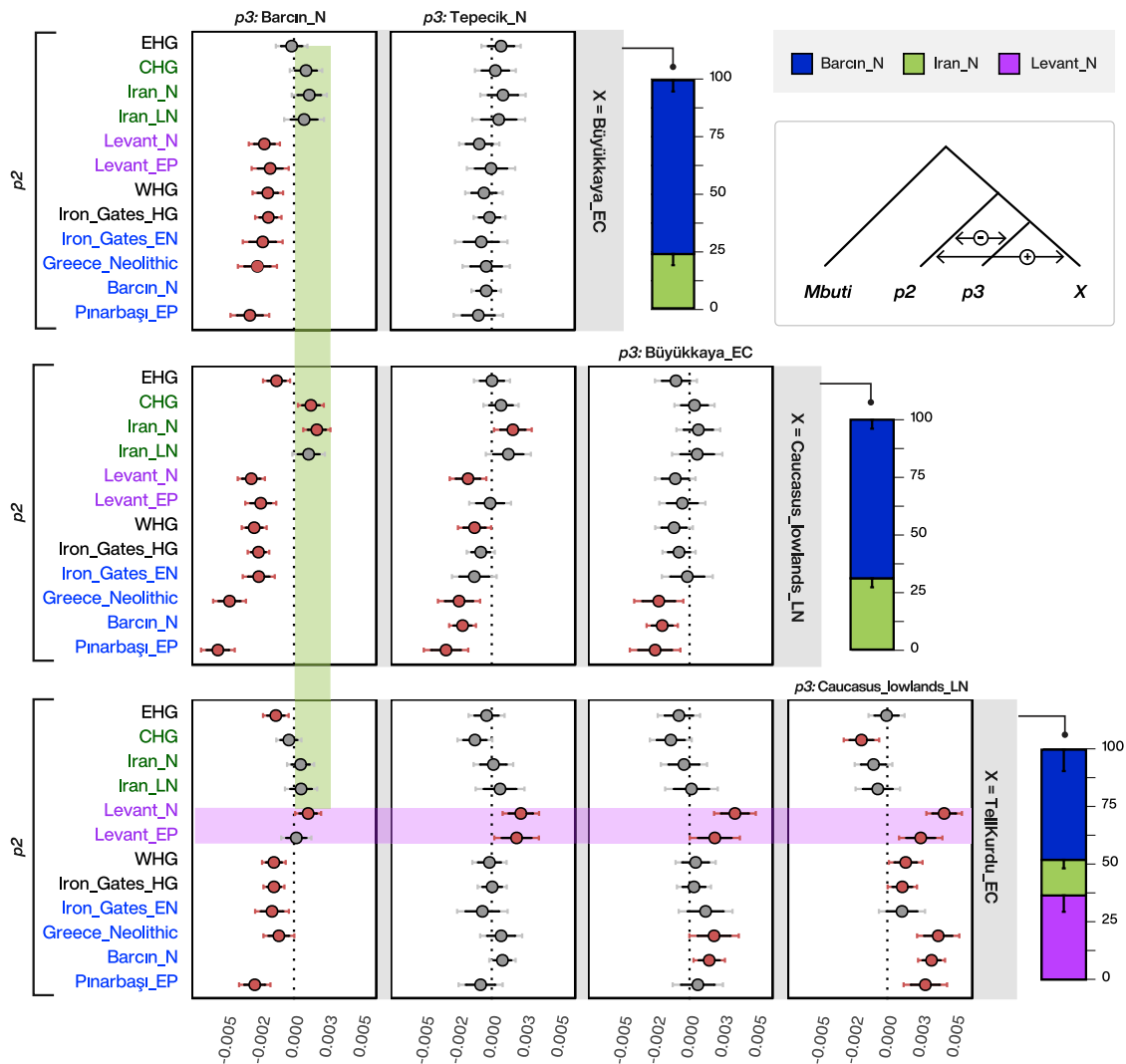
(B) PC1 and PC2 for individuals by archaeological time or geographic sector (a–d) with some of the important findings annotated.

(WHG, EHG, and Iron\_Gates, respectively). The admixture model with Barcın\_N+Iran\_N/CHG used above is not supported for TellKurdu\_EC ( $p < 1.47 \times 10^{-5}$ ). Instead, we can successfully model TellKurdu\_EC as a three-way mixture of Barcın\_N, Iran\_N (or CHG), and Levant\_N ( $p = 0.298$ ;  $15.5\% \pm 3.7\%$  from Iran\_N and  $36.6\% \pm 7.1\%$  from Levant\_N; Figure 4).

### Neolithic Admixture and a Common Genetic Profile of Chalcolithic and Bronze Age Groups

In contrast to the LN/EC individuals, LC-LBA individuals form a dense cloud in the West Eurasian PCA, roughly falling mid-way along the LN-EC cline that is delimited by ancient groups from Iran, the Caucasus, the Levant and Western Anatolia. We





**Figure 4. Genetic Affinity of Late Neolithic/Early Chalcolithic Populations with Early Holocene Populations from Iran, Caucasus, and Levant Measured with  $f_4$ -Statistics and Quantified with  $qpAdm$**

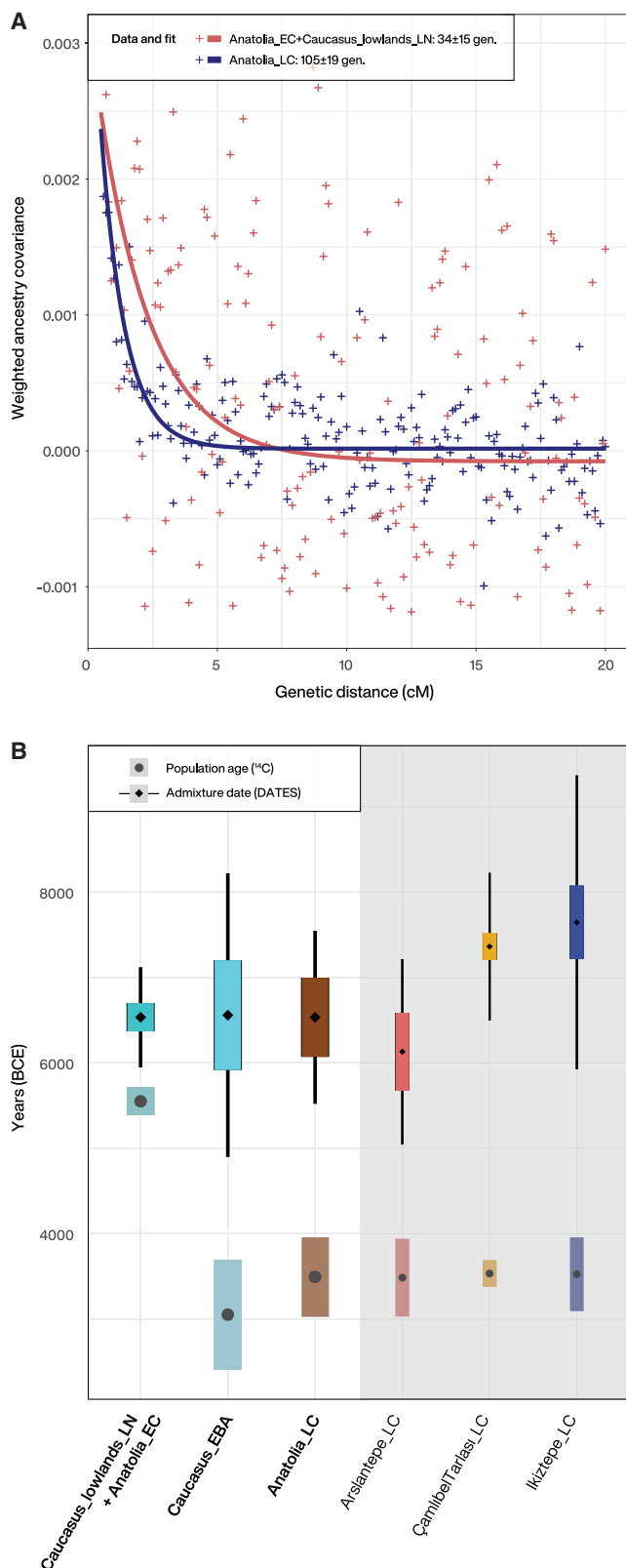
$f_4$ -statistic tests whether either  $p_3$  or  $X$  has excess affinity with  $p_2$  and becomes negative or positive accordingly, as shown in the simplified tree. SE for  $f_4$ -statistics are estimated by 5 cM block jackknifing and values that do not deviate from 0 in the  $\pm 3$  SE are represented in gray color. All three groups have more affinity with Iran compared to Barcin\_N (green bar), and TellKurdu\_EC has the more Levantine affinity compared to all (purple bar). These affinities are reflected in the inferred  $qpAdm$  models on the right. Ancestry proportions are plotted with  $\pm 1$  SE.

hypothesize that LC-LBA groups from Central/North and Eastern Anatolia may have descended from this older genetic structure and therefore share the same ancestry profile.

Consistent with PCA, outgroup- $f_3$  and  $f_4$ -statistics suggest a common genetic profile of the LC-LBA groups that is similar to that of the LN-EC cline. First, outgroup  $f_3$ (*Mbuti*; LC-LBA, *Test*), which measures the average shared genetic drift between LC-LBA and *Test* from their common outgroup *Mbuti* (Patterson et al., 2012), reached highest values when *Test* were Neolithic and Chalcolithic populations from Europe, Anatolia, and Northern Levant, such as Barcin\_N, TellKurdu\_EC, and Büyükaya\_EC (Table S4). Second, using Barcin\_N and additionally TellKurdu\_EC as local baselines, we computed  $f_4$ (*Mbuti*, *Test*; Barcin\_N/TellKurdu\_EC, *X*) to characterize the difference be-

tween Barcin\_N or TellKurdu\_EC and the LC-LBA groups (*X*) with respect to a set of ancient *Test* populations from West Eurasia (Table S5). Iran Neolithic and/or CHG consistently show excess affinity to LC-LBA when compared to TellKurdu\_EC and Barcin\_N. The Chalcolithic and Bronze Age populations from Iran (Iran\_C from the Seh Gabi site) and the Caucasus (Ailentoft et al., 2015; Lazaridis et al., 2016; Wang et al., 2019)—temporally closer to LC-LBA and located between Iran\_N/CHG and LC-LBA in the PCA—also occasionally only share more alleles with some of the LC-LBA groups when compared to Barcin.

We further explored the temporal aspect of the shared admixed profile of LC-LBA groups by estimating their admixture dates using the recently developed method, DATES (M. Chintalapati, N. Patterson, N. Alex, and P. Moorjani, personal



**Figure 5. Dating of Admixture in Anatolian and Caucasian Populations from the Late Neolithic to the Early Bronze Age**

(A) Decay of ancestry covariance estimated by DATES for Anatolia\_EC (Büyükkaya\_EC) and Caucasus\_lowlands\_LN grouped together and the three Late Chalcolithic populations Arslantepe\_LC, ÇamlıbelTarlasi\_LC, and İkiztepe grouped as “Anatolia\_LC.”

(B) Conversion of admixture dates into calendar dates (upper part of plot) after including both the age range for each population calculated from direct  $^{14}\text{C}$  dates (lower part of plot) and the  $\pm 1$  SE from DATES. Average population and admixture dates are shown with black dot. Average admixture date for the three populations with grouped individuals (bold letters) is 6500 years BCE. Admixture dates for individual populations from Anatolian\_LC span a wider time range.

communication) (STAR Methods). As we previously described, the LN-EC cline as varying proportions of Barcın\_N and Iran\_N/CHG ancestries, we selected both as source populations. However, given the small sample size of both Iran\_N and CHG and the large number of missing SNPs in Iran\_N, we also considered modern Caucasians (Armenians, Georgians, Azerbaijanis, Abkhazians, and Ingushians) as proxies of the second source population.

We focused on the three Late Chalcolithic groups with sufficiently large sample size and who are the earliest in time among the LC-LBA groups: ÇamlıbelTarlasi\_LC ( $n = 9$ ), İkiztepe\_LC ( $n = 11$ ), and Arslantepe\_LC ( $n = 17$ ). Taking individual estimates from all these individuals together (“Anatolia\_LC”), we obtain a robust admixture date estimate of  $105 \pm 19$  generations ago when we use Barcın\_N and modern Caucasians as proxies of the source gene pools (Figure 5A). Using a generation time of 28 years (Moorjani et al., 2016), this estimate equates to an admixture event  $\sim 3,000$  years before the time of the LC-LBA individuals, corresponding to  $\sim 6500$  years BCE (Figure 5B). We observe similar but noisier estimates from individual groups ÇamlıbelTarlasi\_LC, İkiztepe\_LC, and Arslantepe\_LC. Admixture dates estimated by two alternative methods, ALDER and rolloff (STAR Methods), overall matched our estimates with DATES (Figure S2).

Encouraged by these results, we extended the analysis to other ancient populations that are on the Early Chalcolithic cline, including Caucasus\_lowlands\_LN and Büyükkaya\_EC, published Early Bronze Age (EBA) individuals from the Caucasus (cluster a) (Wang et al., 2019; Lazaridis et al., 2016) (see Table S3 for group labels), as well as Iran\_C. For the Caucasus EBA individuals (“Caucasus\_a\_EBA”), dated to  $\sim 3,100$  years BCE, we obtain a similar admixture date of  $121 \pm 35$  generations. Importantly, the earlier two Caucasus\_lowlands\_LN and the one Büyükkaya\_EC individuals yielded more recent admixture dates of  $34 \pm 15$  generations before the age of the individuals ( $\sim 6500$  years BCE) (Figure 5A). The converted calendar date of  $\sim 6500$  years BCE matches the timing of the admixture event estimated from the Late Chalcolithic individuals (Figure 5B).

### Admixture Modeling of the Chalcolithic and Bronze Age Groups

Although we showed that it requires both Barcın\_N and Iran\_N-related ancestries to explain the ancestry composition of the LC-LBA groups, alternative combinations of ancient populations, which may be temporally and spatially more proximal to



than the Caucasus groups, although higher resolution data are necessary to compare them further.

Büyükkaya\_EC is the earliest individual in our dataset with a genetic profile similar to the LC-LBA groups within Anatolia. Therefore, we also tested a scenario in which the later LC-LBA groups had descended from the same gene pool without further external contribution.  $f_4(\text{Mbuti}_X; \text{Büyükkaya\_EC}, \text{LC-LBA})$  suggests that Büyükkaya\_EC shares more alleles with the European/Anatolian Farmers (e.g., Boncucklu, LBK, Barcın\_N) than LC-LBA groups do (Table S5). Likewise, most LC-LBA groups cannot be modeled in  $qpAdm$  as a sister group with Büyükkaya\_EC when Barcın\_N is included in the outgroups ( $p < 0.05$  for 1-way model for 11/12). Most LC-LBA groups are adequately modeled by adding the second ancestry of ancient Iran/Caucasus populations, while Alalakh\_MLBA and Ebla\_EMBA require a substantial contribution from ancient southern Levantine populations (Figure 6B).

Overall, the inference of the same admixture date drawn from both Late Neolithic and Late Chalcolithic populations combined with the  $qpAdm$  analyses suggest that the LC-LBA populations also derived from the Neolithic genetic cline but were substantially more homogenized than their predecessors (Figure 6A). Although the ancient groups from Iran are a better proxy for the eastern source than those from the Caucasus, we caution a naive literal interpretation of our results, as yet unsampled proxies from within Mesopotamia may represent true historical sources of this Iran/Caucasus-related ancestry.

### Genetic Turnover in the Bronze Age Northern Levant

The Northern Levant, represented by the sites Tell Kurdu, Ebla, and Alalakh, showcases the most noticeable genetic turnover among our four time transects. Within two millennia after the last Middle Chalcolithic Tell Kurdu individual (TellKurdu\_MC), the genetic profile of the populations in and around the Amuq valley (Alalakh\_MLBA and Ebla\_EMBA) changed to largely resemble contemporaneous Anatolians. However, the  $qpAdm$  modeling with Büyükkaya\_EC suggests that Alalakh\_MLBA and Ebla\_EMBA are still distinct from the other Anatolian groups with respect to their connection to the ancient Southern Levant. Their distinction is also captured by  $f_4$ -statistics whereby Ebla\_EMBA and Alalakh\_MLBA differ from the other LC-LBA groups with respect to their relation with older populations such as Barcın\_N and Caucasian groups (Figure S3). In addition, Barcın\_N/TellKurdu\_EC and/or ancient Caucasian groups cannot successfully model Ebla\_EMBA and Alalakh\_MLBA in  $qpAdm$  (Tables S6 and S7), suggesting that these sources do not represent good proxies of their true ancestries. Alternative models with the predecessor TellKurdu\_EC as a baseline ancestry and the geographically close Arslantepe\_LC as a potential proximal source did not improve the fit either ( $p \leq 1.3 \times 10^{-5}$ ; Table S8). However, admixture models become adequate by adding a southern Levantine population as the third source, with significant Levantine contributions: e.g., 27%–34% TellKurdu\_EC + 36%–38% G.Caucasus\_a\_En + 28%–38% Levant\_EBA ( $p \geq 0.492$ ).

Consistent with the extra gene flow after the time of TellKurdu\_EC, we obtain younger admixture dates in Alalakh\_MLBA than the other LC-LBA groups when we use either Anatolian or

Caucasian gene pools as sources:  $78 \pm 27$  generations (3880  $\pm$  746 years BCE) with Anatolia\_LC and  $44 \pm 8$  (3060  $\pm$  224 years BCE) with Caucasus\_a\_EBA. No exponential decay could be fitted when we used either Anatolia\_LC or Caucasus\_a\_EBA as one source and Levant\_C as a second.

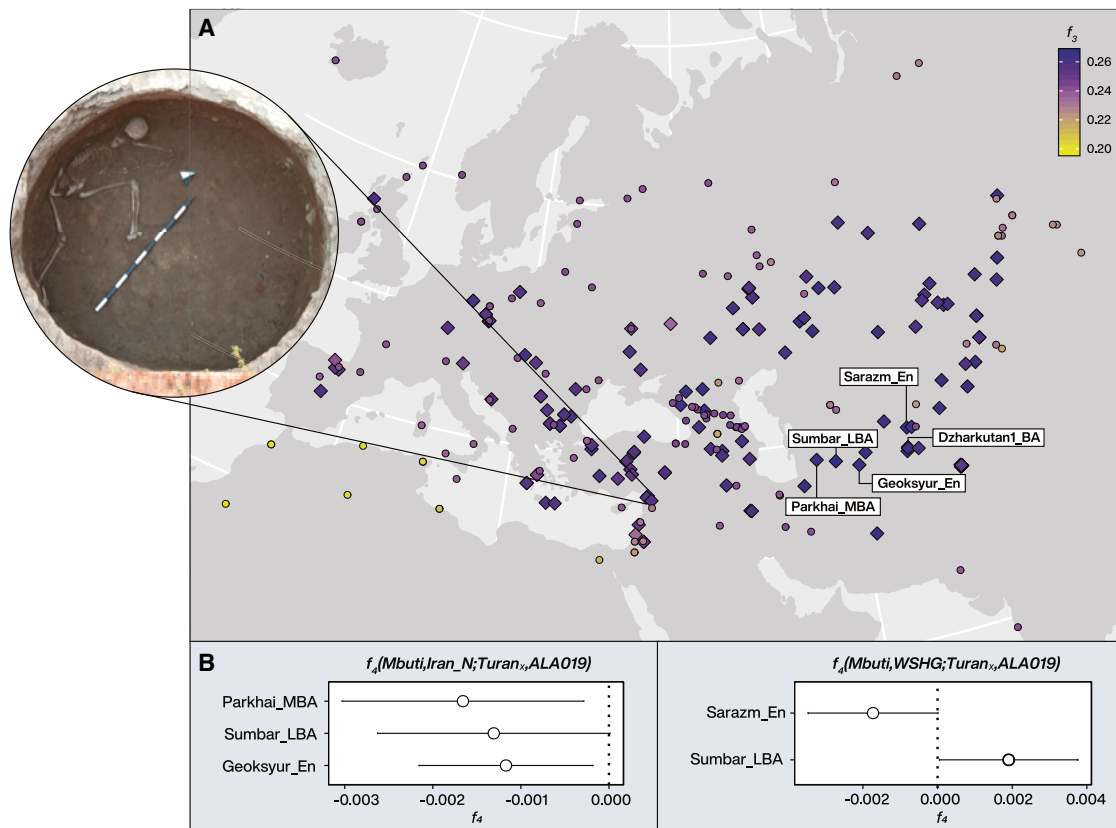
### Evidence for Individual Mobility in Alalakh

All genetic analyses of Alalakh\_MLBA were conducted at the exclusion of one female (ALA019) because of her outlier position in the PCA (Figure 3B). Discovered at the bottom of a well, the archaeological and anthropological context suggest that the skeletal remains of this woman, C14-dated to 1568–1511 cal BCE (AMS; 2-sigma), represent an irregular burial with evidence of several healed skeletal traumata (Figure 7; STAR Methods). We have ruled out the possibility of modern-day contamination based on the characteristic aDNA damage profile, low mitochondrial contamination and reproduction of the PCA coordinates after discarding all sequence reads without damage (STAR Methods). In the Eurasian PCA (Figure S4), ALA019 falls genetically closer to Chalcolithic and Bronze Age individuals from ancient Iran and Turan (present-day area of Iran, Turkmenistan, Uzbekistan, and Afghanistan) (Narasimhan et al., 2019). These populations represent a west-east genetic cline with varying proportions of ancestries related to Barcın\_N, Iran\_N and WSHG (hunter gatherers from Western Siberia). We confirmed the genetic affinity of ALA019 observed in the PCA with an  $outgroup-f_3$  test (Figure 7A). Other ancient populations from the Caucasus and the Western steppe also produced high affinity but  $f_4(\text{Mbuti}_X; \text{Turan}_x, \text{ALA019})$  suggest that ALA019 differs from other Turan individuals by occasionally sharing more or less alleles with either Iran\_N or WSHG (Figure 7B), which agrees with the presence of a genetic cline in this area. In the absence of ancient genomes from nearby regions such as Southern Mesopotamia, the most likely ancestral origin of this individual was somewhere in Eastern Iran or Central Asia.

## DISCUSSION

### Genetic Homogenization across Anatolia and the Southern Caucasus prior to the Bronze Age

Our study covers time transects of  $\sim 4,000$  years of Syro-Anatolian and  $\sim 2,000$  years of Southern Caucasian history, both starting from the 6<sup>th</sup> millennium BCE. In addition, our admixture date estimates allow us to infer a millennium further back in time to the Neolithic period. We describe a Late Neolithic/Early Chalcolithic (6<sup>th</sup> millennium BCE) genetic cline stretching from Western Anatolia (i.e., area around the Sea of Marmara) to the lowlands of the Southern Caucasus that was formed by an admixture process that started at the beginning of Late Neolithic ( $\sim 6500$  years BCE). The eastern end of this cline extends beyond the Zagros mountains with minute proportions of Anatolian (i.e., Western Anatolian-like) ancestry reaching as far as Chalcolithic and Bronze Age Central Asia (Narasimhan et al., 2019). To the south, Anatolian ancestry is present in the Southern Levantine Neolithic populations (Lazaridis et al., 2016), and to the north, in the Chalcolithic and Bronze Age populations from the Caucasus (mainly mountainous area) (Allentoft et al., 2015; Lazaridis



**Figure 7. Individual ALA019 from Alalakh Has High Genetic Affinity to the Ancient Contemporaneous Populations from Eastern Iran and Turan (Central Asia)**

(A) Shared genetic drift measured with outgroup  $f_3$ -statistics between ALA019 and ancient Eurasian (diamonds) and worldwide modern (circles) populations. The highest five values of the test are produced by populations from Turan which are labeled.

(B) Symmetry  $f_4$ -statistics show variable affinity to Iran\_N and WSHG among Turan<sub>x</sub> and ALA019. Horizontal bars represent  $\pm 3$  SE estimated by 5 cM jackknifing.

Photo of “Well Lady” (ALA019): Murat Akar, Alalakh Excavations Archive.

See also Figure S4.

et al., 2016; Wang et al., 2019), most likely as a result of the Late Neolithic admixture.

Evidence for genetic homogenization across larger geographic distances also comes from the uniparentally inherited Y chromosome lineages (Table S9). We observe the most common male lineages J1a, J2a, J2b, and G2a in all spatio-temporal groups of the region. Alongside the less frequent lineages H2 and T1a, these all form part of the genetic legacy that dates to the Neolithic or was already present in the region during the Upper Paleolithic (Wang et al., 2019; Lazaridis et al., 2016; Jones et al., 2015; Feldman et al., 2019; Broushaki et al., 2016). A few notable exceptions provide rather anecdotal but nonetheless important evidence for long distance mobility and extended Y-haplogroup diversity. For example, individual ART038 carries Y-haplotype R1b-V1636 (R1b1a2), which is a rare clade related to other early R1b-lineages, such as R1b-V88 that was found in low frequency in Neolithic Europe (e.g., Haak et al., 2015) and R1b-Z2103—the main Y-lineage that is associated with the spread of “steppe ancestry” across West Eurasia during the early Bronze Age. However, R1b-V1636 and R1b-Z2103 lineages split long before ( $\sim 17$  kya) and therefore

there is no direct evidence for an early incursion from the Pontic steppe during the main era of Arslantepe. Lineage L2-L595 found in ALA084 (Alalakh) has previously been reported in one individual from Chalcolithic Northern Iran (Narasimhan et al., 2019) and in three males from the Late Maykop phase in the North Caucasus (Wang et al., 2019). These three share ancestry from the common Anatolian/Iranian ancestry cline described here, which indicates a widespread distribution that also reached the southern margins of the steppe zone north of the Caucasus mountain range.

Dating the formation of the west-to-east cline during the 7<sup>th</sup> millennium BCE enables the contextualization of these genetic signals observed on both autosomal and uniparental markers with archaeological evidence of human mobility and changes in socio-cultural practices. The time around 6500–6400 years BCE marks a significant junction in the Anatolian Neolithic because it saw a sudden and massive expansion of sedentary communities into areas that had previously supported no or very few food-producing communities before (Brami, 2015; Düring, 2013). Subsequently, in the Southern Caucasus, the abrupt appearance of a Neolithic lifestyle and the introduction of

exogenous domesticated animal and plant species ca. 6000 BCE suggests some type of interaction with, and eventually intrusion of Neolithic populations from the neighboring regions, among which Southeastern Anatolia—along with Zagros and the Caspian belt—could be one of the most suitable candidates (Chataigner et al., 2014). Related to these events, the genetic structure of domesticated caprine populations within the Near East began to break down, and by the Chalcolithic period, goat herds across the region were found to harbor ancestries both from eastern and western Neolithic populations (Daly et al., 2018; Kadowaki et al., 2017). Although the exact timing of this admixture is not known, the parallel between human and livestock genetic histories suggests that livestock moved not only through trade networks but also together with people, as well as their material culture, ideas, and practices. This is indicated, for instance, by the circular Neolithic architecture of the Southern Caucasus (Baudouin, 2019; Lyonnet et al., 2016), which is reminiscent of the Halaf traditions, that were developing during the early 6<sup>th</sup> millennium in North Mesopotamia and along the Anatolian stretches of the Tigris and Euphrates river valleys.

In the subsequent millennia and until the Late Bronze Age, genetic continuity persisted in North-Central and Eastern Anatolia, which is supported by the genetic similarity of these later populations and the absence of new ancestry sources after the Neolithic period. This contradicts prior hypotheses for population change based on archaeological evidence of intense cultural interactions during this period. For example, the site of İkiztepe on the Turkish Black Sea Coast contains a material culture with strong Balkan affinities, and this has been argued to signify direct contact with populations across the Black Sea (e.g., Thisen, 1993), but these contacts do not seem to be accompanied by gene flow.

The site of Arslantepe provides another representative example. At the beginning of EBA, archaeological evidence at the site strongly suggests the presence of a disruptive socio-political conflict that led to the occupation of Arslantepe by pastoral populations with a connection to the Caucasus. In PCA and  $f_4$ -statistics, two individuals dating to this period show excess affinity with populations from the Caucasus and the Pontic steppe compared to their peers, while later Arslantepe\_EBA individuals do not share this Caucasian affinity (Table S10). This implies that the postulated demic interaction must have been transient and of small scale, although the small sample size from Arslantepe\_EBA ( $n = 4$ ) may not be sufficient to detect it. Subtle gene flow is consistent with recent findings from the site, suggesting that the EBA pastoralists occupying the site were more likely well-established local groups moving around the mountains rather than intrusive groups from the Caucasus (Frangipane, 2014).

The genetic landscape of Arslantepe also has important implications with respect to the interactions with the Mesopotamian world. Archaeological evidence indicates that in the 4<sup>th</sup> millennium BCE Mesopotamian populations established colonies in Southeastern Anatolia and Northern Syria (e.g., Habuba Kabira, Jebel Aruda, Hacinebi) during a period referred to as the Uruk Expansion (Algaze, 2005). However, the Uruk expansion was also a very complex and deep process of socio-cultural transformation that reoriented the economic, polit-

ical, and cultural interests of indigenous elites toward Southern Mesopotamia. Artifacts in Arslantepe reflect this complexity, and the genetic continuity shown here supports the notion that indigenous populations adopted these broader Uruk features and ideas without the transmission of genes.

### Population and Territorial State Dynamics in the Northern Levant

In contrast to the rest of Anatolia, the Northern Levant stands out as a region of the Near East with traceable post-Neolithic changes in the genetic structure. We found that the gene pools at Ebla and Alalakh can only be explained by more complex models that require additional contributions both from the Caucasus and Southern Levant. The inclusion of a source related to the Caucasus in our proposed model raises the question whether this turnover could be linked to the expansion of the Transcaucasian Kura-Araxes material culture to the Levant. This expansion is recorded in the region of the Northern Levant ca. 2800 BCE and could be associated with the movement/migration of people from Eastern Anatolia and the Southern Caucasian highlands (Greenberg and Palumbi, 2015; Greenberg et al., 2014). However, our results do not support this scenario for a number of reasons: (1) we do not find any substantial increase of Caucasus-related ancestry in the populations of the primary expansion area of Kura-Araxes (e.g., Eastern Anatolia), (2) populations from the highlands of the Southern Caucasus—including individuals from a Kura-Araxes context (“L.Caucasus\_EBA”)—as secondary source populations also fail, and (3) so do models with Arslantepe from Eastern Anatolia, a population located mid-way along the proposed expansion route from the Southern Caucasus to the Northern Levant.

Consequently, these interpretative caveats call for consideration of alternative historical scenarios, including scenarios of multiple gene-flow events that could have taken place in the intervening two millennia between the Tell Kurdu population and those of Bronze Age Ebla and Alalakh. However, written sources, archaeological, and paleoclimatic evidence suggest that a narrower time period—the end of the EBA—had been very critical with respect to political tensions and population mobility. It was during this period, for example, that Ebla was destroyed twice and re-established at the beginning of MBA. There are extensive textual references from the end of the EBA through the LBA referring to groups of people arriving into the area of the Amuq Valley. Although these groups were named, likely based on designations (e.g., Amorites, Hurrians), the formative context of their (cultural) identity and their geographic origins remain debated. One recent hypothesis (Weiss, 2014, 2017; Akar and Kara, 2020) associates the arrival of these groups with climate-forced population movement during the “4.2k BP event,” a Mega Drought that led to the abandonment of the entire Khabur river valley in Northern Mesopotamia and the search of nearby habitable areas.

Taking the above into consideration, we suggest that the ancestries we inferred for Alalakh and Ebla might best describe the genetic make-up of the EBA populations of unsampled Northern Mesopotamia. During the following MBA and LBA, we find no evidence of genetic disruption, even though shifts in territorial control dynamics between kingdoms/empires affected Ebla's and Alalakh's socio-cultural development (see STAR Methods).

Nevertheless, the case of the Alalakh individual with likely Central Asian origin is a finding that can be interpreted within the context of nascent internationalism of the Middle and Late Bronze Age Eastern Mediterranean societies. It calls for future research on the various societal features of this phenomenon and how these are reflected on the individual life histories.

### Conclusions

Overall, our large-scale genomic analysis reveals two major genetic events. First, during the Late Neolithic, gene pools across Anatolia and the Southern Caucasus mixed, resulting in an admixture cline. Second, during the Early Bronze Age, Northern Levant populations experienced gene flow in a process that likely involved yet to-be-sampled neighboring populations from Mesopotamia. Even though we could detect subtle and transient gene flow in Arslantepe, we acknowledge that disentangling questions related to local-scale population dynamics within the homogeneous Chalcolithic and Bronze Age Anatolian gene pool might be beyond the resolution of current analytical tools. Furthermore, while our sampling expands in number and geographic range on previous studies, the critical area of Mesopotamia remains unsampled; thus, although our picture of the genetic landscape of the Near East is highly suggestive, it remains incomplete. Nevertheless, the cumulative genetic dataset of Anatolia, the Southern Caucasus, and the Northern Levant between the Early and Late Bronze Age indicates that, following the genetic events of the Late Neolithic and Early Bronze Age, there was no intrusion of genetically distinct populations in this region. This conclusion is of great importance with respect to our understanding of the formation of complex Bronze Age socio-political entities.

### STAR★METHODS

Detailed methods are provided in the online version of this paper and include the following:

- **KEY RESOURCES TABLE**
- **RESOURCE AVAILABILITY**
  - Lead contact
  - Materials Availability
  - Data and Code Availability
- **EXPERIMENTAL MODEL AND SUBJECT DETAILS**
  - Description of **origin, archaeological and anthropological** context of analyzed individuals
  - Arslantepe, Turkey
  - Boğazköy-Büyükkaya, Turkey
  - Çamlıbel Tarlası, Turkey
  - İkiztepe, Turkey
  - Mentesh Tepe, Azerbaijan
  - Polutepe, Azerbaijan
  - Tell Atchana (Alalakh), Turkey
  - Tell Mardikh (Ebla), Syria
  - Tell Kurdu, Turkey
  - Titriş Höyük, Turkey
  - Abbreviations
  - Grouping of individuals and nomenclature
- **METHOD DETAILS**

- Direct AMS radiocarbon dating
- Preparation of aDNA
- Human genome enrichment, sequencing and haploid genotype sampling
- **QUANTIFICATION AND STATISTICAL ANALYSIS**
  - Quality control and test of kinship
  - PMDtools
  - Dataset
  - Sex determination and uniparental haplotypes
  - Principal component analysis
  - f-statistics
  - Modeling of ancestry proportions
  - Test of recent admixture
  - Visualizations

### SUPPLEMENTAL INFORMATION

Supplemental Information can be found online at <https://doi.org/10.1016/j.cell.2020.04.044>.

A video abstract is available at <https://doi.org/10.1016/j.cell.2020.04.044#mmc7>.

### ACKNOWLEDGMENTS

We thank G. Brandt, A. Wissgott, C. Freund, and R. Bianco (MPI-SHH) for support in laboratory work. We thank A. Mötsch for support in organization and sample management. We thank Michal Feldman, Stephen Clayton, Kay Prüfer, and the members of the population genetics group and the Max Planck-Harvard Research center for the Archaeoscience of the ancient Mediterranean (MHAAM) group in the Department of Archaeogenetics, MPI-SHH for their input and support. We thank Michelle O'Reilly and Hans Sell for graphics and video production support and Jason Ur for consultation on the manuscript. We thank the French-German National Agency for Research (ANR), the Centre national de la recherche scientifique (CNRS), and the French Ministry of Foreign Affairs for funding the excavation of Mentesh Tepe. We thank Jürgen Seeher and Andreas Schachner (Boğazköy Expedition of the German Archaeological Institute) for the permission to use samples from the site and for their support of this study. We thank Dr. Silvia Mogliazza for the analysis of the human skeletal remains from Tell Mardikh (Ebla). This study was funded by the Max Planck Society and the Max Planck-Harvard Research Center for the Archaeoscience of the Ancient Mediterranean.

### AUTHOR CONTRIBUTIONS

J.K., W.H., P.W.S., C.J., and C.W. conceived the study. C.J., W.H., and J.K. supervised the genetic work. Y.S.E., M.F., K.A.Y., F.P., P.M., R.Ö., F.G., T.A., B.L., E.L.H., S.E.N., and U.D.S. provided archaeological material. P.W.S., Y.S.E., M.F., F.B.R., K.A.Y., T.I., M.A., R.S., R.Ö., G.P., F.G., B.L., E.L.H., U.D.S., and S.E. advised on the archaeological background and interpretation. Y.S.E., M.F., F.B.R., K.A.Y., T.I., M.A., R.S., R.Ö., T.A., B.L., U.D.S., M.D'A., and E.S. wrote the archaeological and sample background section. E.S., M.B., G.N., and S.P. performed the laboratory work. E.S. performed the data analyses with C.J. and W.H. providing guidance. A.B.R. performed analyses on the Y chromosome markers and assignment of Y-haplogroups. E.S., C.J., and W.H. wrote the manuscript with input from all co-authors.

### DECLARATION OF INTERESTS

The authors declare no competing interests.

Received: November 29, 2019

Revised: March 18, 2020

Accepted: April 22, 2020

Published: May 28, 2020

## REFERENCES

- Akar, M. (2013). The Late Bronze Age Fortresses at Alalakh: Architecture and Identity in Mediterranean Exchange Systems. In *Across the Border: Late Bronze-Iron Age relations between Syria and Anatolia. Proceedings of a Symposium Held at the Research Center of Anatolian Studies, Koc University, Istanbul, May 31–June 1, 2010*, K.A. Yener, ed. (Peeters).
- Akar, M. (2017a). Late Middle Bronze Age International Connections: An Egyptian Style Kohl Pot from Alalakh. In *Questions, Approaches, and Dialogues in Eastern Mediterranean Archaeology Studies in Honor of Marie-Henriette and Charles Gates*, E. Kozal, M. Akar, Y. Heffron, Ç. Çilingiroğlu, T.E. Şerifoğlu, C. Çakırlar, S. Ünlüsoy, and E. Jean, eds. (Ugarit-Verlag).
- Akar, M. (2017b). Pointed Juglets as an International Trend in Late Bronze Ritual Practices: A View from Alalakh. In *Overturning Certainties in Near Eastern Archaeology: A Festschrift in Honor of K. Aslihan Yener*, Ç. Maner, M.T. Horowitz, and A.S. Gilbert, eds. (Brill).
- Akar, M. (2019). Excavation Results. In *Tell Atchana, Alalakh: The Late Bronze II City. 2006–2010 Excavation Seasons*, K.A. Yener, M. Akar, and M.T. Horowitz, eds. (Koç University Press).
- Akar, M., and Kara, D. (2020). The formation of collective, political and cultural memory in the Middle Bronze Age: foundation and termination rituals at Toprakkhisar Höyük. *Anatolian Studies*. <https://doi.org/10.1017/S0066154619000139>.
- Akhundov, T. (2007). Sites de migrants venus du Proche-Orient en Transcaucasie. In *Les cultures du Caucase (VIe–IIIe millénaires avant notre ère). Leurs relations avec le Proche-Orient*, B. Lyonnet, ed. (CNRS Editions/ERC).
- Akhundov, T.I. (2011). Archaeological Sites of the Mugan Steppe and Prerequisities for Agricultural Settlement in the South Caucasus in the Neolithic–Eneolithic. *Stratum* 2, 219–236.
- Akhundov, T.I. (2014). Алчантепе – Поселение начала бронзового века в Азербайджане. С. 78–92. Труды института истории материальной культуры № 10. С.78–92. Санкт-Петербург.
- Akhundov, T.I. (2018). The South Caucasus on the Threshold of the Metal Age. In *Context and Connection: Studies on the Archaeology of the Ancient Near East in Honour of Antonio Sagona*, A. Batmaz, G. Bedianashvili, A. Michalewicz, and A. Robinson, eds. (Peeters).
- Akhundov, T.I., Makhumudova, V.A., Hasanova, A.M., Ramazanly, G.K., and Rakhmanov, A.A. (2017). Памятники МуГанской степи и ПредПосылки расселения ранних земледельцев на Южном Кавказе в эпоху неолита–энеолита. *Stratum plus*. N2, 2011, Санкт-Петербург, Кишинёв, Одесса, Бучарест. СС. 219–236.
- Akkermans, P.M.M., and Schwartz, G.M. (2003). *The Archaeology of Syria: From Complex Hunter-Gatherers to Early Urban Societies (c. 16,000–300 BC)* (Cambridge University Press).
- Algaze, G. (2005). *The Uruk World System: the Dynamics of Expansion of Early Mesopotamian Civilization* (University of Chicago Press).
- Algaze, G., Goldberg, P., Honça, D., Matney, T., Misir, A., Rosen, A., Schlee, D., and Somers, L. (1995). Titiş Höyük, a small EBA urban center in south-eastern Anatolia: the 1994 season. *Anatolica* 21, 13–64.
- Algaze, G., Kelly, J., Matney, T., and Schlee, D. (1996). Late EBA urban structure at Titiş Höyük, southeastern Turkey: the 1995 season. *Anatolica* 22, 129–139.
- Algaze, G., Dinckan, G., Hartenberger, B., Matney, T., Pournelle, J., Rainville, L., Rosen, S., Rupley, E., Schlee, D., and Vallet, R. (2001). Research at Titiş Höyük in southeastern Turkey: the 1999 season. *Anatolica* 27, 23–106.
- U.B. Alkım, H. Alkım, and Ö. Bilgi, eds. (1988). *The First and Second Season's Excavations (1974–1975)* (Türk Tarih Kurumu Basımevi).
- Allen, M., and Rothman, M. (2004). Uruk, Mesopotamia & Its Neighbors: Cross-Cultural Interactions in the Era of State Formation. *American Antiquity* 69, 152.
- Allentoft, M.E., Sikora, M., Sjögren, K.G., Rasmussen, S., Rasmussen, M., Stenderup, J., Damgaard, P.B., Schroeder, H., Ahlström, T., Vinner, L., et al. (2015). Population genomics of Bronze Age Eurasia. *Nature* 522, 167–172.
- Badalyan, R., Harutyunyan, A., Chataigner, C., Le Mort, F., Chabot, J., Brochier, J.-E., Balasescu, A., Radu, V., and Hovsepian, R. (2010). The settlement of Aknashen-Khatunarkh, a Neolithic site in the Ararat plain (Armenia): excavation results 2004–2009. *TÜBA-AR* 13, 187–220.
- Baffi Guardata, F. (1988). Les Sépultures d'Ebla à l'âge du Bronze Moyen. In *Wirtschaft und Gesellschaft von Ebla. Akten der Internationalen Tagung Heidelbergl 4.–7. November 1986*, H. Waetzold and H. Hauptmann, eds. (Akten der internationalen Tagung).
- Baffi Guardata, F. (2000). Les Tombes du Bronze Moyen dans le Secteur des Fortifications à Ebla. In *Proceedings of the 1st International Congress on the Archaeology of the Ancient Near East, Rome, May 18th–23rd 1998*, P. Matthiae, A. Enea, L. Peyronel, and F. Pinnock, eds. (Sapienza University of Rome).
- Balossi Restelli, F., Alvaro, C., Erdal, Y.S., Bartosiewicz, L., Frangipane, M., Liberotti, G., and Sador, L. (2012). Late Chalcolithic 3–4 Developments in the Upper Euphrates Malatya Plain, Rome. *Sapienza Università di Roma* 27, 235–259.
- Barnes, E. (2012). *Atlas of Developmental Field Anomalies of the Human Skeleton: A Paleopathology Perspective* (John Wiley & Sons, Inc.).
- Bartl, P.V., and Bonatz, D. (2013). Across Assyria's Northern Frontier: Tell Fekheriye at the End of the Late Bronze Age. In *Across the Border*, K.A. Yener, ed. (Peeters).
- Bartosiewicz, L., and Gillis, R. (2011). Preliminary report on the animal remains from Çamlıbel Tarlası, Central Anatolia. *Archaeol. Anz.* 2011, 76–79.
- Baudouin, E. (2019). Rethinking architectural techniques of the Southern Caucasus in the 6th millennium BC: A re-examination of former data and new insights. *Paéorient* 45, 115–150.
- Bilgi, Ö. (2000). İkiztepe Kazıları. In *Türkiye Arkeolojisi ve İstanbul Üniversitesi (1932–1999)*, Ö. Bilgi, ed. (Başak Matbaacılık ve Tanıtım Hizmetleri Ltd. Şti).
- Bilgi, Ö. (2004). İkiztepe Mezarlık Kazıları ve Ölü Gömme Gelenekleri 2000–2002 Dönemleri. *Anadolu Araştırmaları* 17, 25–50.
- Brami, M.N. (2015). A graphical simulation of the 2,000-year lag in Neolithic occupation between Central Anatolia and the Aegean basin. *Archaeol. Anthropol. Sci.* 7, 319–327.
- Breniquet, C. (1996). La disparition de la culture de Halaf. Les origines de la culture d'Obeid dans le Nord de la Mésopotamie (Éditions Recherche sur les Civilisations).
- Brothwell, D.R. (1981). *Digging up Bones: the Excavation, Treatment and Study of Human Skeletal Remains* (Cornell University Press).
- Broushaki, F., Thomas, M.G., Link, V., López, S., van Dorp, L., Kirsanow, K., Hofmanová, Z., Diekmann, Y., Cassidy, L.M., Diez-Del-Molino, D., et al. (2016). Early Neolithic genomes from the eastern Fertile Crescent. *Science* 353, 499–503.
- Bryce, T. (2005). *The Kingdom of the Hittites* (Oxford University Press).
- Haas, J., Buikstra, J.E., Ubelaker, D.H., and Aftandilian, D.; Field Museum of Natural History (1994). Standards for Data Collection from Human Skeletal Remains: Proceedings of a Seminar at the Field Museum of Natural History, Organized by Jonathan Haas (Arkansas Archaeological Survey).
- Bulu, M. (2016). An Intact Palace Kitchen Context from Middle Bronze Age Alalakh: Organization and Function. In *Proceedings of the 9th International Congress on the Archaeology of the Ancient Near East*, O. Kaelin, R. Stucky, and A. Jamieson, eds. (Harrassowitz Verlag).
- Bulu, M. (2017). A Syro-Cilician Pitcher from a Middle Bronze Age Kitchen at Tell Atchana, Alalakh. In *Overturning Certainties in Near Eastern Archaeology: A Festschrift in Honor of K. Aslihan Yener*, Ç. Maner, M.T. Horowitz, and A. Gilbert, eds. (Brill).
- Byers, S. (2011). *Introduction to Forensic Anthropology* (Pearson).
- Calcagnile, L., Quarta, G., and D'Elia, M. (2013). Just at That Time: 14C Determinations and Analyses from EB IVA Layers. In *Ebla and Its Landscape. Early State Formation in the Ancient Near East*, P. Matthiae and N. Marchetti, eds. (Left Coast Press).



- Carter, R.A., and Philip, G. (2010). Beyond the Ubaid. Transformation and Integration in the Late Prehistoric Societies of the Middle East (Chicago University press).
- Chataigner, C., Badalyan, R., and Arimura, M. (2014). The Neolithic of the Caucasus (Oxford University Press).
- Conti, A.M., and Persiani, C. (1993). When worlds collide. Cultural developments in Eastern Anatolia in the Early Bronze Age. In *Between the Rivers and over the Mountains*, M. Frangipane, H. Hauptmann, M. Liverani, P. Matthiae, and M. Mellink, eds. (Università Sapienza di Roma).
- Courcier, A., Jalilov, B., Aliyev, I., Guliyev, F., Jansen, M., Lyonnet, B., Mukhtarov, N., and Museibli, N. (2016). The Ancient Metallurgy in Azerbaijan from the End of the Neolithic to the Early Bronze Age (6th-3rd Millennium BCE): an Overview in the Light of New Discoveries and Recent Archaeometallurgical Research. In *From Bright Ores to Shiny Metals*. Festschrift for A. Hauptmann, G. Körlin, M. Prange, T. Stöllner, and U. Yalçin, eds. (Deutsches Bergbaumuseum).
- D'Andrea, M. (2018). The Early Bronze IVB pottery from Tell Mardikh/Ebla. Chrono-typological and technological data for framing the site within the regional context. *Levant*, 1–29.
- D'Andrea, M. (2019). The EB-MB Transition at Ebla. A State-of-the-Art Overview in the Light of the 2004–2008 Discoveries at Tell Mardikh. In *Pearls of the Past. Studies on Near Eastern Art and Archaeology in Honour of Frances Pinnock*, M. D'Andrea, M.G. Micale, D. Nadali, S. Pizzimenti, and A. Vacca, eds. (Zaphon).
- D'Andrea, M. (2014–2015). Early Bronze IVB at Ebla. Stratigraphy, Chronology, and Material Culture of the Late Early Syrian Town and Their Meaning in the Regional Context. In *Studies on the Archaeology of Ebla after 50 Years of Discoveries*, P. Matthiae, M. Abdulkarim, F. Pinnock, and M. Alkhalid, eds. (Annales Archéologiques Arabes Syriennes).
- Daley, T., and Smith, A.D. (2013). Predicting the molecular complexity of sequencing libraries. *Nat. Methods* 10, 325–327.
- Daly, K.G., Maisano Delser, P., Mullin, V.E., Scheu, A., Mattiangeli, V., Teasdale, M.D., Hare, A.J., Burger, J., Verdugo, M.P., Collins, M.J., et al. (2018). Ancient goat genomes reveal mosaic domestication in the Fertile Crescent. *Science* 367, 85–88.
- de Barros Damgaard, P., Martiniano, R., Kamm, J., Moreno-Mayar, J.V., Kroonen, G., Peyrot, M., Barjamovic, G., Rasmussen, S., Zacho, C., Baimukhanov, N., et al. (2018). The first horse herders and the impact of early Bronze Age steppe expansions into Asia. *Science* 360, aar7711.
- Düring, B. (2013). Breaking the bond: investigating the Neolithic expansion in Asia Minor in the seventh millennium BC. *J. World Prehist.* 26, 75–100.
- Eisenmann, S., Bánffy, E., van Dommelen, P., Hofmann, K.P., Maran, J., Lazaridis, I., Mittnik, A., McCormick, M., Krause, J., Reich, D., and Stockhammer, P.W. (2018). Reconciling material cultures in archaeology with genetic data: The nomenclature of clusters emerging from archaeogenomic analysis. *Sci. Rep.* 8, 13003–3.
- Erdal, Ö.D. (2012a). A Possible Massacre at Early Bronze Age Tiriti Höyük, Anatolia. *Int. J. Osteoarchaeol.* 22, 1–21.
- Erdal, Y.S. (2012b). The Population Replacement at Arslantepe: Reflections on the Human Remains. *Origini: Preistoria E Protostoria Delle Civiltà Antiche* 34, 301–316.
- Feldman, M.H. (2006). *Diplomacy by Design* (The University of Chicago Press).
- Feldman, M., Fernández-Domínguez, E., Reynolds, L., Baird, D., Pearson, J., Hershkovitz, I., May, H., Goring-Morris, N., Benz, M., Gresky, J., et al. (2019). Late Pleistocene human genome suggests a local origin for the first farmers of central Anatolia. *Nat. Commun.* 10, 1218.
- Frangipane, M. (2012a). The Collapse of the 4th Millennium Centralised System at Arslantepe and the Far-Reaching Changes in 3rd Millennium Societies. *Origini: Preistoria E Protostoria Delle Civiltà Antiche* 34, 237–260.
- Frangipane, M. (2012b). Fourth Millennium Arslantepe: The Development of a Centralised Society without Urbanisation. *Origini: Preistoria E Protostoria Delle Civiltà Antiche* 34, 19–40.
- Frangipane, M. (2014). After collapse: Continuity and Disruption in the settlement by Kura-Araxes-linked pastoral groups at Arslantepe-Malatya (Turkey). *New data. Paéorient* 40, 169–182.
- Frangipane, M. (2015a). Different types of multiethnic societies and different patterns of development and change in the prehistoric Near East. *Proc. Natl. Acad. Sci. USA* 112, 9182–9189.
- Frangipane, M. (2015b). Upper Euphrates Societies and Non-Sedentary Communities Linked to the Kura-Araxes World. Dynamics of Interaction, as seen from Arslantepe. In *International Symposium on East Anatolia-South Caucasus Cultures: Proceedings II*, M. Isikli and B. Can, eds. (Cambridge Scholars Publishing).
- Frangipane, M. (2018). Different Trajectories in State Formation in Greater Mesopotamia: A View from Arslantepe (Turkey). *J. Archaeol. Res.* 26, 3–63.
- Frangipane, M., Di Nocera, G.M., Hauptmann, A., Morbidelli, P., Palmieri, A., Sadori, L., Schultz, M., and Schmidt-Schultz, T. (2001). New Symbols of a New Power in a “Royal” Tomb from 3 000 BC Arslantepe, Malatya (Turkey). *Paéorient* 27, 105–139.
- Fu, Q., Hajdinjak, M., Moldovan, O.T., Constantin, S., Mallick, S., Skoglund, P., Patterson, N., Rohland, N., Lazaridis, I., Nickel, B., et al. (2015). An early modern human from Romania with a recent Neanderthal ancestor. *Nature* 524, 216–219.
- Fu, Q., Posth, C., Hajdinjak, M., Petr, M., Mallick, S., Fernandes, D., Furtwängler, A., Haak, W., Meyer, M., Mittnik, A., et al. (2016). The genetic history of Ice Age Europe. *Nature* 534, 200–205.
- Gamba, C., Jones, E.R., Teasdale, M.D., McLaughlin, R.L., Gonzalez-Fortes, G., Mattiangeli, V., Domboróczy, L., Kövári, I., Pap, I., Anders, A., et al. (2014). Genome flux and stasis in a five millennium transect of European prehistory. *Nat. Commun.* 5, 5257.
- González-Fortes, G., Jones, E.R., Lightfoot, E., Bonsall, C., Lazar, C., Grandal-d'Anglade, A., Garralda, M.D., Drak, L., Siska, V., Simalcsik, A., et al. (2017). Paleogenomic Evidence for Multi-generational Mixing between Neolithic Farmers and Mesolithic Hunter-Gatherers in the Lower Danube Basin. *Curr. Biol.* 27, 1801–1810.
- Greenberg, R., and Palumbi, G. (2015). Corridors and Colonies: Comparing Fourth–Third Millennium BC Interactions in Southeast Anatolia and the Levant. In *The Cambridge Prehistory of the Bronze and Iron Age Mediterranean*, A.B. Knapp and P. van Dommelen, eds. (Cambridge University Press).
- Greenberg, R., Shimelmitz, R., and Iserlis, M. (2014). New evidence for the Anatolian origins of ‘Khirbet Kerak Ware people’ at Tel Bet Yerah (Israel), ca 2800 BC. *Paéorient* 40, 183–201.
- Günther, T., Valdiosera, C., Malmström, H., Ureña, I., Rodriguez-Varela, R., Sverrisdóttir, Ó.O., Daskalaki, E.A., Skoglund, P., Naidoo, T., Svensson, E.M., et al. (2015). Ancient genomes link early farmers from Atapuerca in Spain to modern-day Basques. *Proc. Natl. Acad. Sci. USA* 112, 11917–11922.
- Haak, W., Lazaridis, I., Patterson, N., Rohland, N., Mallick, S., Llamas, B., Brandt, G., Nordenfelt, S., Harney, E., Stewardson, K., et al. (2015). Massive migration from the steppe was a source for Indo-European languages in Europe. *Nature* 522, 207–211.
- Haber, M., Doumet-Serhal, C., Scheib, C., Xue, Y., Danecek, P., Mezzavilla, M., Youhanna, S., Martiniano, R., Prado-Martinez, J., Szpak, M., et al. (2017). Continuity and Admixture in the Last Five Millennia of Levantine History from Ancient Canaanite and Present-Day Lebanese Genome Sequences. *Am. J. Hum. Genet.* 101, 274–282.
- Harney, É., May, H., Shalem, D., Rohland, N., Mallick, S., Lazaridis, I., Sarig, R., Stewardson, K., Nordenfelt, S., Patterson, N., et al. (2018). Ancient DNA from Chalcolithic Israel reveals the role of population mixture in cultural transformation. *Nat. Commun.* 9, 3336.
- Heinz, M. (1992). *Tell Atchana Alalakh: die Schichten VII–XVII* (Kevelaer and Neukirchen-Vluyn, Butzon & Bercke and Neukirchener Verlag).
- Hillson, S. (2014). *Tooth Development in Human Evolution and Bioarchaeology* (Cambridge University Press).
- T. Hodos, ed. (2017). *The Routledge Handbook of Archaeology and Globalization* (Routledge).

- Hofmanová, Z., Kreutzer, S., Hellenthal, G., Sell, C., Diekmann, Y., Díez-Del-Molino, D., van Dorp, L., López, S., Kousathanas, A., Link, V., et al. (2016). Early farmers from across Europe directly descended from Neolithic Aegeans. *Proc. Natl. Acad. Sci. USA* *113*, 6886–6891.
- Horowitz, M.T. (2015). The Evolution of Plain Ware Ceramics at the Regional Capital of Alalakh in the 2nd Millennium BC. In *Plain Pottery Traditions of the Eastern Mediterranean and Near East: Production, Use, and Social Significance*, C. Glatz, ed. (Left Coast Press).
- Horowitz, M.T. (2019). The Local Ceramics of Late Bronze II Alalakh. In *Tell Atchana, Alalakh, K.A. Yener, M. Akar, and M.T. Horowitz, eds. (Koç University Press)*.
- Ingman, T. (2020). Mortuary Practices and GIS Modeling at Tell Atchana, Alalakh. In *Alalakh and Its Neighbors: Proceedings of the 15th Anniversary Symposium at the New Hatay Archaeology Museum, June 10–12, 2015*, K.A. Yener, ed. (Peeters).
- Ingman, T. (2017). The Extramural Cemetery at Tell Atchana, Ancient Alalakh and GIS Modeling. In *Overturning Certainties in Near Eastern Archaeology: A Festschrift in Honor of K. Aslihan Yener, Ç. Maner, M.T. Horowitz, and A. Gilbert, eds. (Brill)*.
- Irvine, B.T. (2017). An Isotopic Analysis of Dietary Habits in Early Bronze Age Anatolia (Freie Universität Berlin).
- Jeong, C., Wilkin, S., Amgalantugs, T., Bouwman, A.S., Taylor, W.T.T., Hagan, R.W., Bromage, S., Tsolmon, S., Trachsel, C., Grossmann, J., et al. (2018). Bronze Age population dynamics and the rise of dairy pastoralism on the eastern Eurasian steppe. *Proc. Natl. Acad. Sci. USA* *115*, E11248.
- Jeong, C., Balanovsky, O., Lukianova, E., Kahbatkyzy, N., Flegontov, P., Zaporozhchenko, V., Immel, A., Wang, C.-C., Ixan, O., Khussainova, E., et al. (2019). The genetic history of admixture across inner Eurasia. *Nat. Ecol. Evol.* *3*, 966–976.
- Jones, E.R., Gonzalez-Fortes, G., Connell, S., Siska, V., Eriksson, A., Martiniano, R., McLaughlin, R.L., Gallego Llorente, M., Cassidy, L.M., Gamba, C., et al. (2015). Upper Palaeolithic genomes reveal deep roots of modern Eurasians. *Nat. Commun.* *6*, 8912.
- Jónsson, H., Ginolhac, A., Schubert, M., Johnson, P.L., and Orlando, L. (2013). mapDamage2.0: fast approximate Bayesian estimates of ancient DNA damage parameters. *Bioinformatics* *29*, 1682–1684.
- Kadowaki, S., Ohnishi, K., Arai, S., Guliyev, F., and Nishiaki, Y. (2017). Mitochondrial DNA Analysis of Ancient Domestic Goats in the Southern Caucasus: A Preliminary Result from Neolithic Settlements at Göytepe and Hacı Elamxanlı Tepe. *Int. J. Osteoarchaeol.* *27*, 245–260.
- Kearse, M., Moir, R., Wilson, A., Stones-Havas, S., Cheung, M., Sturrock, S., Buxton, S., Cooper, A., Markowitz, S., Duran, C., et al. (2012). Geneious Basic: an integrated and extendable desktop software platform for the organization and analysis of sequence data. *Bioinformatics* *28*, 1647–1649.
- Kennett, D.J., Plog, S., George, R.J., Culleton, B.J., Watson, A.S., Skoglund, P., Rohland, N., Mallick, S., Stewardson, K., Kistler, L., et al. (2017). Archaeogenomic evidence reveals prehistoric matrilineal dynasty. *Nat. Commun.* *8*, 14115.
- Kılınc, G.M., Omrak, A., Özer, F., Günther, T., Büyükkarakaya, A.M., Bıçakçı, E., Baird, D., Dönertaş, H.M., Ghalichi, A., Yaka, R., et al. (2016). The Demographic Development of the First Farmers in Anatolia. *Curr. Biol.* *26*, 2659–2666.
- Killebrew, A.E., and Steiner, M. (2014). *The Oxford Handbook of the Archaeology of the Levant c. 8000–332 BCE* (Oxford University Press).
- Klengel, H. (1992). *Syria: 3000 to 300 B.C. A Handbook of Political History* (Akademie Verlag).
- Kloss-Brandstätter, A., Pacher, D., Schönherr, S., Weissensteiner, H., Binna, R., Specht, G., and Kronenberg, F. (2011). HaploGrep: a fast and reliable algorithm for automatic classification of mitochondrial DNA haplogroups. *Hum. Mutat.* *32*, 25–32.
- Korneliusson, T.S., Albrechtsen, A., and Nielsen, R. (2014). ANGSD: Analysis of Next Generation Sequencing Data. *BMC Bioinformatics* *15*, 356.
- Kwong, Y., Rao, N., and Latief, K. (2011). MDCT findings in Baastrup disease: disease or normal feature of the aging spine? *AJR Am. J. Roentgenol.* *196*, 1156–1159.
- Laneri, N. (2002). The Discovery of a Funerary Ritual: Inanna/Ishtar and Her Descent to the Nether World in Tiriş Höyük, Turkey. *East and West* *52*, 9–51.
- Laneri, N. (2007). Burial practices at Tiriş Höyük, Turkey: an interpretation. *J. Near East. Stud.* *66*, 241–266.
- Lauinger, J. (2015). *Following the Man of Yamhad: Settlement and Territory at Old Babylonian Alalakh* (Brill).
- Lazaridis, I., Patterson, N., Mitnik, A., Renaud, G., Mallick, S., Kirsanow, K., Sudmant, P.H., Schraiber, J.G., Castellano, S., Lipson, M., et al. (2014). Ancient human genomes suggest three ancestral populations for present-day Europeans. *Nature* *513*, 409–413.
- Lazaridis, I., Nadel, D., Rollefson, G., Merrett, D.C., Rohland, N., Mallick, S., Fernandes, D., Novak, M., Gamarra, B., Sirak, K., et al. (2016). Genomic insights into the origin of farming in the ancient Near East. *Nature* *536*, 419–424.
- Lazaridis, I., Mitnik, A., Patterson, N., Mallick, S., Rohland, N., Pfrengle, S., Furtwängler, A., Peltzer, A., Posth, C., Vasilakis, A., et al. (2017). Genetic origins of the Minoans and Mycenaeans. *Nature* *548*, 214–218.
- Li, H., and Durbin, R. (2009). Fast and accurate short read alignment with Burrows-Wheeler transform. *Bioinformatics* *25*, 1754–1760.
- Li, H., Handsaker, B., Wysoker, A., Fennell, T., Ruan, J., Homer, N., Marth, G., Abecasis, G., and Durbin, R.; 1000 Genome Project Data Processing Subgroup (2009). The Sequence Alignment/Map format and SAMtools. *Bioinformatics* *25*, 2078–2079.
- Lipson, M., Szécsényi-Nagy, A., Mallick, S., Pósa, A., Stégmár, B., Keerl, V., Rohland, N., Stewardson, K., Ferry, M., Michel, M., et al. (2017). Parallel palaeogenomic transects reveal complex genetic history of early European farmers. *Nature* *551*, 368–372.
- Loh, P.-R., Lipson, M., Patterson, N., Moorjani, P., Pickrell, J.K., Reich, D., and Berger, B. (2013). Inferring admixture histories of human populations using linkage disequilibrium. *Genetics* *193*, 1233–1254.
- Lyonnet, B. (2007). La culture de Maikop, la Transcaucasie, l'Anatolie orientale et le Proche-Orient: relations et chronologie. In *Les cultures du Caucase (Vieille millénaire av. n.è.). Leurs relations avec le Proche-Orient*, B. Lyonnet, ed. (CNRS-éditions, ERC).
- Lyonnet, B. (2012). Mentesh Tepe Pottery. *Archäologische Mitteilungen aus Iran und Turan* *44*, 97–108.
- Lyonnet, B. (2014). The Early Bronze Age in Azerbaijan in the light of recent discoveries. *Paëorient* *40*, 115–130.
- Lyonnet, B. (2016). A Grave with a Wooden Wagon in Transcaucasia (Azerbaijan). Its Relations with Central Asia. In *V. Sarianidi Memorial Volume, Transaction of Margiana Archaeological Expedition, N.A. Dubova, P.M. Kozhin, M.F. Kosarev, M.A. Mamedov, R.G. Muradov, R.M. Sataev, and A.A. Tishkin, eds. (Staryj Sad)*.
- Lyonnet, B. (2017). Mentesh Tepe 2012–2014. The Pottery. In *The Kura Projects. New Research on the Later Prehistory of the Southern Caucasus*, B. Helwing, T. Aliyev, B. Lyonnet, F. Guliyev, S. Hansenand, and G. Mirtskhulava, eds. (D. Reimer).
- Lyonnet, B., Akundov, T., Almamedov, K., Bouquet, L., Courcier, A., Jellilov, B., Huseynov, F., Loute, S., Makharadze, Z., and Reynard, S. (2008). Late Chalcolithic Kurgans in Transcaucasia. The cemetery of Soyuk Bulaq (Azerbaijan). *Archäologische Mitteilungen aus Iran und Turan* *40*, 27–44.
- Lyonnet, B., Guliyev, F., Bouquet, L., Bruley-Chabot, G., Samzun, A., Pecqueur, L., Jovenet, E., Baudouin, E., Fontugne, M., Raymond, P., et al. (2016). Mentesh Tepe, an early settlement of the Shomu-Shulaveri Culture in Azerbaijan. *Quat. Int.* *395*, 170–183.
- Mann, R., and Hunt, D. (2005). *Photographic Regional Atlas of Bone Disease: A Guide to Pathologic and Normal Variation in the Human Skeleton* (Charles C. Thomas).
- Manuelli, F. (2013). Arslantepe, Late Bronze Age. Hittite influence and local traditions in an Eastern Anatolian community (Sapienza Università di Roma).

- Marchetti, N. (2013). Working for the Elites. The Pottery Assemblage of Building. In *Ebla and Its Landscape. Early State Formation in the Ancient Near East*, P. Matthiae and N. Marchetti, eds. (Left Coast Press), p. 4.
- Marchetti, N., and Nigro, L. (1995–1996). Handicraft Production, Secondary Food Transformation and Storage in the Public Building P4 at EB IVA Ebla. *Berytus* 42, 9–36.
- Marsh, B. (2010). Geoarchaeology of the human landscape at Boğazköy-Hattuša. *Archaeol. Anz.* 2010, 201–207.
- Martiniano, R., Cassidy, L.M., Ó'Maoldúin, R., McLaughlin, R., Silva, N.M., Manco, L., Fidalgo, D., Pereira, T., Coelho, M.J., Serra, M., et al. (2017). The population genomics of archaeological transition in west Iberia: Investigation of ancient substructure using imputation and haplotype-based methods. *PLoS Genet.* 13, e1006852.
- Mathieson, I., Lazaridis, I., Rohland, N., Mallick, S., Patterson, N., Roodenberg, S.A., Harney, E., Stewardson, K., Fernandes, D., Novak, M., et al. (2015). Genome-wide patterns of selection in 230 ancient Eurasians. *Nature* 528, 499–503.
- Mathieson, I., Alpaslan-Roodenberg, S., Posth, C., Szécsényi-Nagy, A., Rohland, N., Mallick, S., Olalde, I., Broomandkoshbacht, N., Candilio, F., Cheronet, O., et al. (2018). The genomic history of southeastern Europe. *Nature* 555, 197–203.
- Matney, T., and Algaze, G. (1995). Urban Development at Mid-Late Early Bronze Age Tiriş Höyük in Southeastern Anatolia. *Bull. Am. Schools Orient. Res.* 299–300, 33–52.
- Matney, T., Algaze, G., and Pittman, H. (1997). Excavations at Tiriş Höyük in southeastern Turkey: a preliminary report of the 1996 season. *Anatolica* 23, 61–84.
- Matney, T., Algaze, G., and Rosen, S. (1999). Early Bronze Age urban structure at Tiriş Höyük, southeastern Turkey: the 1998 season. *Anatolica* 25, 185–201.
- Matney, T., Algaze, G., Dulik, M.C., Erdal, Ö.D., Erdal, Y.S., Gökçümen, O., Lorenz, J., and Mergen, H. (2012). Understanding Early Bronze Age Social Structure Through Mortuary Remains: A Pilot aDNA Study From Tiriş Höyük, Southeastern Turkey. *Int. J. Osteoarchaeol.* 22, 338–351.
- Matthiae, P. (1993a). L'aire sacrée d'Ishtar à Ébla: résultats des fouilles de 1990-1992. *Comptes rendus de l'Académie des Inscriptions et Belles-Lettres* 137, 613–662.
- Matthiae, P. (1993b). On this Side of the Euphrates. A Note on the Urban Origins in Inner Syria. In *Between the Rivers and Over the Mountains. Archaeologica, Anatolica et Mesopotamica Alba Palmieri Dedicata*, M. Frangipane, H. Hauptmann, M. Liverani, P. Matthiae, and M. Mellink, eds. (Universita di Roma-La Sapienza).
- Matthiae, P. (2002). About the Formation of Old Syrian Architectural Tradition. In *Papers on the Archaeology and History of Mesopotamia and Syria presented to David Oates in Honour of his 75th Birthday*, L. al-Gailani Werr, J. Curtis, H. Martin, A. McMahon, J. Oates, and J. Reade, eds. (NABU).
- Matthiae, P. (2006). Un grand temple de l'époque des Archives dans l'Ebla protosyrienne: Fouilles à Tell Mardikh 2004-2005. *Comptes rendus des séances de l'Académie des Inscriptions et Belles-Lettres* 150, 447–493.
- Matthiae, P. (2007). Nouvelles fouilles à Ébla en 2006. Le Temple du Rocher et ses successeurs protosyriens et paléosyriens. *Comptes rendus des séances de l'Académie des Inscriptions et Belles-Lettres* 151, 481–525.
- Matthiae, P. (2009a). Crisis and Collapse: Similarity and Diversity in the Three Destructions of Ebla from EB IVA to MB II. *Scienze dell'Antichità* 15, 165–204.
- Matthiae, P. (2009b). Temples et reines de l'Ébla Protosyrienne: Résultats de fouilles à Tell Mardikh en 2007 et 2008. *Comptes rendus des séances de l'Académie des Inscriptions et Belles-Lettres* 153, 747–791.
- Matthiae, P. (2010). Ebla la città del trono. *Archeologia e storia*, (Torino, Piccola Biblioteca Einaudi), p. 492.
- Matthiae, P. (2011). Fouilles à Tell Mardikh-Ébla en 2009-2010: les débuts de l'exploration de la citadelle paléosyrienne. *Comptes rendus des séances de l'Académie des Inscriptions et Belles-Lettres* 155, 735–773.
- Matthiae, P. (2013a). About the Formation of Old Syrian Architectural Tradition. In *Studies on the History and Archaeology of Ebla 1980-2010*, F. Pinnock, ed. (Harrassowitz Verlag).
- Matthiae, P. (2013b). A Long Journey. Fifty Years of Research on the Bronze Age at Tell Mardikh. In *Ebla and Its Landscape. Early State Formation in the Ancient Near East*, P. Matthiae and N. Marchetti, eds. (Left Coast Press).
- Matthiae, P. (2020). The Problem of Ebla Destruction at the End of EB IVB: Stratigraphic Evidence, Radiocarbon Datings, Historical Events. In *New Horizons in the Study of the Early Bronze III and Early Bronze IV of the Levant*, S. Richard, ed. (Eisenbrauns).
- Mazzoni, S. (1991). Ebla e la formazione della cultura urbana in Siria. *Parola Passata* 46, 163–194.
- McColl, H., Racimo, F., Vinner, L., Demeter, F., Gakuhari, T., Moreno-Mayar, J.V., van Driem, G., Gram Wilken, U., Seguin-Orlando, A., de la Fuente Castro, C., et al. (2018). The prehistoric peopling of Southeast Asia. *Science* 361, 88–92.
- McMahon, G., and Steadman, S. (2012). *The Oxford Handbook of Ancient Anatolia (10,000–323 BCE)* (Oxford University Press).
- Meyer, M., Kircher, M., Gansauge, M.-T., Li, H., Racimo, F., Mallick, S., Schraiber, J.G., Jay, F., Prüfer, K., de Filippo, C., et al. (2012). A high-coverage genome sequence from an archaic Denisovan individual. *Science* 338, 222–226.
- Mittnik, A., Wang, C.-C., Pfrengle, S., Daubaras, M., Zariņa, G., Hallgren, F., Allmāe, R., Khartanovich, V., Moiseyev, V., Törv, M., et al. (2018). The genetic prehistory of the Baltic Sea region. *Nat. Commun.* 9, 442.
- Mondal, M., Casals, F., Xu, T., Dall'Olio, G.M., Pybus, M., Netea, M.G., Comas, D., Laayouni, H., Li, Q., Majumder, P.P., and Bertranpetit, J. (2016). Genomic analysis of Andamanese provides insights into ancient human migration into Asia and adaptation. *Nat. Genet.* 48, 1066–1070.
- Monroy Kuhn, J.M., Jakobsson, M., and Günther, T. (2018). Estimating genetic kin relationships in prehistoric populations. *PLoS ONE* 13, e0195491.
- Montesanto, M. (2020). The 12th Century BC at Alalakh: New Ceramic Evidence for Local Development and Foreign Contact. In *Alalakh and its Neighbors: Proceedings of the 15th Anniversary Symposium at the New Hatay Archaeology Museum*, June 10–12, 2015, K.A. Yener, ed. (Peeters).
- Moorjani, P., Patterson, N., Hirschhorn, J.N., Keinan, A., Hao, L., Atzmon, G., Burns, E., Ostrer, H., Price, A.L., and Reich, D. (2011). The history of African gene flow into Southern Europeans, Levantines, and Jews. *PLoS Genet.* 7, e1001373.
- Moorjani, P., Sankararaman, S., Fu, Q., Przeworski, M., Patterson, N., and Reich, D. (2016). A genetic method for dating ancient genomes provides a direct estimate of human generation interval in the last 45,000 years. *Proc. Natl. Acad. Sci. USA* 113, 5652–5657.
- Morgan, M., Pagès, H., Obenchain, V., and Hayden, N. (2019). Rsamtools: Binary alignment (BAM), FASTA, variant call (BCF), and tabix file import. R package version 1.34.1 ed.. <http://bioconductor.org/packages/Rsamtools>.
- Narasimhan, V.M., Patterson, N., Moorjani, P., Rohland, N., Bernardos, R., Mallick, S., Lazaridis, I., Nakatsuka, N., Olalde, I., Lipson, M., et al. (2019). The formation of human populations in South and Central Asia. *Science* 365, eaat7487.
- Nigro, L. (2002). The Middle Bronze Age Horizon of Northern Inner Syria on the Basis of the Stratified Assemblages of Tell Mardikh and Hama. In *Céramique de l'âge du Bronze en Syrie I. La Syrie du Sud et la Vallée de l'Oronte*, M. Al-Maqdissi, V. Matojan, and C. Nicolle, eds. (Bibliothèque Archéologique et Historique).
- Nishiaki, Y., Guliyev, F., and Kadowaki, S. (2015). Chronological Contexts of the Earliest Pottery Neolithic in the South Caucasus: Radiocarbon Dates for Goytepe and Hacı Elamxanlı Tepe, Azerbaijan. *Am. J. Archaeol.* 119, 279–294.
- Olalde, I., Schroeder, H., Sandoval-Velasco, M., Vinner, L., Lobón, I., Ramirez, O., Civit, S., García Borja, P., Salazar-García, D.C., Talamo, S., et al. (2015). A Common Genetic Origin for Early Farmers from Mediterranean Cardial and Central European LBK Cultures. *Mol. Biol. Evol.* 32, 3132–3142.

- Olalde, I., Brace, S., Allentoft, M.E., Armit, I., Kristiansen, K., Booth, T., Rohland, N., Mallick, S., Szécsényi-Nagy, A., Mittnik, A., et al. (2018). The Beaker phenomenon and the genomic transformation of northwest Europe. *Nature* 555, 190–196.
- Olalde, I., Mallick, S., Patterson, N., Rohland, N., Villalba-Mouco, V., Silva, M., Dulias, K., Edwards, C.J., Gandini, F., Pala, M., et al. (2019). The genomic history of the Iberian Peninsula over the past 8000 years. *Science* 363, 1230–1234.
- Özbal, R., Gerritsen, F., Diebold, B., Healey, E., Aydın, N., Loyette, M., Nardulli, F., Reese, D., Ekstrom, H., Sholts, S., et al. (2004). Tell Kurdu Excavations 2001. *Anatolica* 30, 37–107.
- Özbal, R.F. (2006). Households, Daily Practice and Cultural Appropriation at Sixth Millennium Tell Kurdu. PhD Thesis (Northwestern University).
- Özdemir, K., and Erdal, Y.S. (2012). Element Analizleri ile Erken Tunç Çağı İki-tepe Toplumunun Yaşadığı Ekolojik Ortam ve Besin Kaynaklarının Belirlenmesi Üzerine Bir Deneme. In *Türkiye’de Arkeometrinin Ulu Çınarları*. Prof. Dr. Ay Melek Özer ve Prof. Dr. Şahinde Demirci’ye Armağan, A.A. Akyol and K. Özdemir, eds. (Homer Kitapevi).
- Özdoğan, M. (2014). A new look at the introduction of the Neolithic way of life in Southeastern Europe. Changing paradigms of the expansion of the Neolithic way of life. *Documenta Praehistorica* 41, 33.
- Palumbi, G. (2011). The Arslantepe Royal Tomb and the “manipulation” of the Kurgan ideology in Eastern Anatolia at the beginning of the third millennium. In *Ancestral Landscapes: Burial Mounds in the Copper and Bronze Ages*. Proceedings of the International Conference held in Udine, May 15th–18th, 2008, E. Borgna and S. Müller Celka, eds. (Travaux de la Maison de l’Orient méditerranéen), pp. 47–59.
- Palumbi, G. (2017). Push or Pull Factors? The Kura-Araxes ‘Expansion’ from a Different Perspective: the Upper Euphrates Valley. In *At the Northern Frontier of Near Eastern Archaeology: Recent Research on Caucasia and Anatolia in the Bronze Age*, Humboldt Kolleg Conference Proceedings Venice 8–11 January 2013, Subartu XXXVIII, E. Rova and M. Tonussi, eds. (Turnhout), pp. 113–132.
- Palumbi, G., and Chataigner, C. (2014). The Kura-Araxes Culture from the Caucasus to Iran, Anatolia and the Levant: Between unity and diversity. *Paéorient* 40, 247–260.
- Papadopoulou, I., and Bogaard, A. (2012). A preliminary study of the charred macrobotanical assemblage from Çamlıbel Tarlası, north-central Anatolia. *Archaeol. Anz.* 2012, 123–132.
- Patterson, N., Price, A.L., and Reich, D. (2006). Population structure and eigenanalysis. *PLoS Genet.* 2, e190.
- Patterson, N., Moorjani, P., Luo, Y., Mallick, S., Rohland, N., Zhan, Y., Genschoreck, T., Webster, T., and Reich, D. (2012). Ancient admixture in human history. *Genetics* 192, 1065–1093.
- Pecqueur, L., and Jovenet, E. (2017). La sépulture 342 de Mentesh Tepe (Azerbaïdjan): un exemple de chaîne opératoire funéraire complexe au Néolithique. Etude préliminaire. In *The Kura Projects. New Research in the Later Prehistory of Southern Caucasus*, B. Helwing, T. Aliyev, B. Lyonnet, F. Guliyev, S. Hansen, and G. Mirtskhulava, eds. (D. Reimer).
- Pecqueur, L., Decaix, A., and Lyonnet, B. (2017). Un kourgane de la phase Martkopi à Mentesh Tepe (Période des Premiers Kourganés, Bronze ancien). In *The Kura Projects. New Research in the Later Prehistory of Southern Caucasus*, B. Helwing, T. Aliyev, B. Lyonnet, F. Guliyev, S. Hansen, and G. Mirtskhulava, eds. (D. Reimer).
- Peltzer, A., Jäger, G., Herbig, A., Seitz, A., Knip, C., Krause, J., and Nieselt, K. (2016). EAGER: efficient ancient genome reconstruction. *Genome Biol.* 17, 60.
- Pickard, C., Schoop, U.-D., Dalton, A., Sayle, K.L., Channell, I., Calvey, K., Thomas, J.-L., Bartosiewicz, L., and Bonsall, C. (2016). Diet at Late Chalcolithic Çamlıbel Tarlası, north-central Anatolia: an isotopic perspective. *J. Archaeol. Sci.* 5, 296–306.
- Pickard, C., Schoop, U.-D., Bartosiewicz, L., Gillis, R., and Sayle, K.L. (2017). Animal keeping in Chalcolithic North-Central Anatolia: What can stable isotope analysis add? *Archaeol. Anthropol. Sci.* 9, 1349–1362.
- Pickrell, J.K., Patterson, N., Barbieri, C., Berthold, F., Gerlach, L., Güldemann, T., Kure, B., Mpoloka, S.W., Nakagawa, H., Naumann, C., et al. (2012). The genetic prehistory of southern Africa. *Nat. Commun.* 3, 1143.
- Pinhasi, R., Fernandes, D., Sirak, K., Novak, M., Connell, S., Alpaslan-Roodenberg, S., Gerritsen, F., Moiseyev, V., Gromov, A., Raczyk, P., et al. (2015). Optimal Ancient DNA Yields from the Inner Ear Part of the Human Petrous Bone. *PLoS ONE* 10, e0129102.
- Pinnock, F. (2009). EB IVB-MB I in Northern Syria: Crisis and Change of a Mature Urban Civilisation. In *The Levant in Transition. Proceedings of a Conference Held at the British Museum on 20–21 April 2004*, P.J. Parr, ed. (The Palestine Exploration Fund).
- Poulmarc’h, M., Pecqueur, L., and Jailov, B. (2014). An Overview of Funerary Practices in the Southern Caucasus. *Paéorient* 40, 231–246.
- Price, A.L., Patterson, N.J., Plenge, R.M., Weinblatt, M.E., Shadick, N.A., and Reich, D. (2006). Principal components analysis corrects for stratification in genome-wide association studies. *Nat. Genet.* 38, 904–909.
- Prüfer, K., de Filippo, C., Grote, S., Mafessoni, F., Korlević, P., Hajdinjak, M., Vernot, B., Skov, L., Hsieh, P., Peyrégne, S., et al. (2017). A high-coverage Neandertal genome from Vindija Cave in Croatia. *Science* 358, 655–658.
- Pucci, M. (2020). Drinking in Iron Age Atchana. In *Alalakh and its Neighbors: Proceedings of the 15th Anniversary Symposium at the New Hatay Archaeology Museum, June 10–12, 2015*, K.A. Yener and T. Ingman, eds. (Peeters).
- Raghavan, M., Skoglund, P., Graf, K.E., Metspalu, M., Albrechtsen, A., Moltke, I., Rasmussen, S., Stafford, T.W., Jr., Orlando, L., Metspalu, E., et al. (2014). Upper Palaeolithic Siberian genome reveals dual ancestry of Native Americans. *Nature* 505, 87–91.
- Rasmussen, M., Anzick, S.L., Waters, M.R., Skoglund, P., DeGiorgio, M., Stafford, T.W., Jr., Rasmussen, S., Moltke, I., Albrechtsen, A., Doyle, S.M., et al. (2014). The genome of a Late Pleistocene human from a Clovis burial site in western Montana. *Nature* 506, 225–229.
- Reimer, P.J., Bard, E., Bayliss, A., Beck, J.W., Blackwell, P.G., Bronk Ramsey, C., Buck, C.E., Cheng, H., Edwards, R.L., Friedrich, M., et al. (2013). IntCal13 and Marine13 Radiocarbon Age Calibration Curves 0–50,000 Years cal BP. *Radiocarbon* 55, 1869–1887.
- Renaud, G., Slon, V., Duggan, A.T., and Kelso, J. (2015). Schmutzi: estimation of contamination and endogenous mitochondrial consensus calling for ancient DNA. *Genome Biol.* 16, 224.
- Roaf, M. (1998). *Bildatlas der Weltkulturen, Mesopotamien* (Bechtermünz Verlag).
- Roberts, C., and Manchester, K. (1995). *The Archaeology of Disease* (Alan Sutton Publishing Limited).
- Rohland, N., Harney, E., Mallick, S., Nordenfelt, S., and Reich, D. (2015). Partial uracil-DNA-glycosylase treatment for screening of ancient DNA. *Philos. Trans. R. Soc. Lond. B Biol. Sci.* 370, 20130624.
- Rothman, M. (2011). Migration and Resettlement: Godin Period IV. In *On the High Road*, H. Gopnik and M. Rothman, eds. (Mazda Publishers/ROM).
- Rothschild, B. (2002). Porotic hyperostosis as a marker of health and nutritional conditions. *Am. J. Hum. Biol.* 14, 417–418, discussion 418–420.
- Sagona, A. (2017). Encounters beyond the Caucasus: The Kura-Araxes Culture and the Early Bronze Age (3500–2400 BC). *The Archaeology of the Caucasus: From Earliest Settlements to the Iron Age* (Cambridge University Press).
- Scandone Matthiae, G. (2002). *Materiali e Studi Archeologici di Ebla 3. Gli avori egittizzanti del Palazzo Settentrionale* (Sapienza University of Rome).
- Schaefer, M., Black, S., and Scheuer, L. (2009). *Juvenile Osteology: a Laboratory and Field Manual* (Academic).
- Schoop, U.-D. (2005). Early Chalcolithic in North-Central Anatolia: The evidence from Boğazköy-Büyükkaya. *TÜBA-AR* 8, 15–37.
- Schoop, U.-D. (2011). The Chalcolithic on the Plateau. In *The Oxford Handbook of Ancient Anatolia (10,000–323 BCE)*, S.R. Steadman and G. McMahon, eds. (Oxford University Press).
- Schoop, U.-D. (2015). Çamlıbel Tarlası: Late Chalcolithic settlement and economy in the Budaközü Valley (north-central Anatolia). In *The Archaeology of*

- Anatolia I. Recent Discoveries (2011–2014), S.R. Steadman and G. McMahon, eds. (Cambridge Scholars Publishing).
- Schoop, U.-D. (2018). Die Besiedlung des Oberen Plateaus vom Chalkolithikum bis in die althethitische Zeit. In *Büyükkaya II. Bauwerke und Befunde der Grabungskampagnen 1952–1955 und 1993–1998*, J. Seeher, ed. (Walter de Gruyter GmbH).
- Schoop, U.-D., Grave, P., Kealhofer, L., and Jacobsen, G. (2009). Radiocarbon dates from Chalcolithic Çamlıbel Tarlası. *Archaeol. Anz.* 2009, 66–67.
- Schoop, U.-D., Pickard, C., and Bonsall, C. (2012). Radiocarbon dating chalcolithic Büyükkaya. *Archaeol. Anz.* 2012, 115–120.
- Schubert, M., Lindgreen, S., and Orlando, L. (2016). AdapterRemoval v2: rapid adapter trimming, identification, and read merging. *BMC Res. Notes* 9, 88.
- Schultz, M. (2003). Light Microscopic Analysis in Skeletal Paleopathology. In *Identification of Pathological Conditions in Human Skeletal Remains*, Second Edition, D. Ortner, ed. (Academic Press).
- Scott, G., and Irish, J. (2017). Human Tooth Crown and Root Morphology: The Arizona State University Dental Anthropology System (Cambridge University Press).
- Seguin-Orlando, A., Korneliusen, T.S., Sikora, M., Malaspinas, A.-S., Manica, A., Moltke, I., Albrechtsen, A., Ko, A., Margaryan, A., Moiseyev, V., et al. (2014). Paleogenomics. Genomic structure in Europeans dating back at least 36,200 years. *Science* 346, 1113–1118.
- Shafiq, R. (2020). Come and Hear My Story: The ‘Well-Lady’ of Alalakh. In *Alalakh and its Neighbors: Proceedings of the 15th Anniversary Symposium at the New Hatay Archaeology Museum, June 10–12, 2015*, K.A. Yener and T. Ingman, eds. (Peeters).
- Siracusano, G., and Palumbi, G. (2014). “Who’d be happy, let him be so: nothing’s sure about tomorrow. Discarded bones in an Early Bronze I élite area at Arslantepe (Malatya, Turkey): remains of banquets?” In *Proceedings of the 8th International Congress on the Archaeology of the Ancient Near East 30 April–4 May 2012, University of Warsaw, Vol. 3*, P. Bieliński, M. Gawlikowski, R. Koliński, D. Ławecka, A. Sołtyśiak, and Z. Wygnańska, eds. (Harrassowitz Verlag).
- Skoglund, P., Northoff, B.H., Shunkov, M.V., Derevianko, A.P., Pääbo, S., Krause, J., and Jakobsson, M. (2014). Separating endogenous ancient DNA from modern day contamination in a Siberian Neandertal. *Proc. Natl. Acad. Sci. USA* 111, 2229–2234.
- Skoglund, P., Posth, C., Sirak, K., Spriggs, M., Valentin, F., Bedford, S., Clark, G.R., Reepmeyer, C., Petchey, F., Fernandes, D., et al. (2016). Genomic insights into the peopling of the Southwest Pacific. *Nature* 538, 510–513.
- Skoglund, P., Thompson, J.C., Prendergast, M.E., Mitnick, A., Sirak, K., Hajdinjak, M., Salie, T., Rohland, N., Mallick, S., Peltzer, A., et al. (2017). Reconstructing Prehistoric African Population Structure. *Cell* 171, 59–71.
- Thissen, L. (1993). New Insights in Balkan-Anatolian Connections in the Late Chalcolithic: Old Evidence from the Turkish Black Sea Littoral. *Anatol. Stud.* 43, 207–237.
- Thomas, J.-L. (2011). Preliminary observations on the human skeletal remains from Çamlıbel Tarlası. *Archaeol. Anz.* 2011, 73–76.
- Thomas, J.-L. (2012). Human remains from a 6th millennium B.C. infant burial found at Boğazköy-Büyükkaya, Turkey. *Archaeol. Anz.* 2012, 121–123.
- Thomas, J.-L. (2017). Late Chalcolithic skeletal remains and associated mortuary practices from Çamlıbel Tarlası in Central Anatolia. In *Children, Death and Burial: Archaeological Discourses*, E.M. Murphy and M. Le Roy, eds. (Oxbow).
- Vacca, A. (2015). Before the Royal Palace G. The Stratigraphic and Pottery Sequence of the West Unit of the Central Complex: The Building G5. *Studia Eblaitica* 7, 1–32.
- Vacca, A. (2014–2015). Recherches sur les périodes pré-et proto-palatale d’Ébla au Bronze ancien III-IVA1. In *Studies on the History and Archaeology of Ebla after 50 Years of Discoveries*, Damas, P. Matthiae, M. Abdulkarim, F. Pinnock, and M. Alkhalid, eds. (Les annales archéologiques arabes syriennes).
- von Dassow, E. (2005). Archives of Alalakh IV in Archaeological Context. *Bull. Am. Schools Orient. Res.* 338, 1–69.
- von Dassow, E. (2008). State and Society in the Late Bronze Age: Alalakh Under the Mittani Empire (CDL Press).
- von den Driesch, A., and Nadja, P. (2004). Vor- und frühgeschichtliche Nutztierhaltung und Jagd auf Büyükkaya in Boğazköy-Ḫattuša, Zentralanatolien (Mainz : P. von Zabern).
- Vyas, D.N., Al-Meer, A., and Mulligan, C.J. (2017). Testing support for the northern and southern dispersal routes out of Africa: an analysis of Levantine and southern Arabian populations. *Am. J. Phys. Anthropol.* 164, 736–749.
- Waldron, T. (2001). *Shadows in the Soil: Human Bones and Archaeology* (Tempus Publishing).
- Wang, C.C., Reinhold, S., Kalmykov, A., Wissgott, A., Brandt, G., Jeong, C., Cheronet, O., Ferry, M., Harney, E., Keating, D., et al. (2019). Ancient human genome-wide data from a 3000-year interval in the Caucasus corresponds with eco-geographic regions. *Nat. Commun.* 10, 590.
- Weiss, H. (2014). The northern Levant during the intermediate Bronze Age: altered trajectories. In *The Oxford Handbook of the Archaeology of the Levant: c. 8000–332 BCE*, A.E. Killebrew, ed. (Oxford University Press).
- Weiss, H. (2017). 4.2 ka BP megadrought and the Akkadian collapse. In *Megadrought and Collapse: From Early Agriculture to Angkor*, H. Weiss, ed. (Oxford University Press).
- Welton, M.L. (2010). Mobility and Social Organization on the Ancient Anatolian Black Sea Coast: An Archaeological, Spatial and Isotopic Investigation of the Cemetery at İkiztepe (University of Toronto).
- Wittke, A.-M. (2010). The Hittite Empire, ‘Ḫattuša’, in the 13th cent. BC. In *Historical Atlas of the Ancient World*, C. Salazar, ed. (Brill).
- Woolley, C.L. (1939). Excavations at Atchana-Alalakh, 1938. *Ant. J.* 19, 1–37.
- Woolley, C.L. (1955). *Alalakh: An Account of the Excavations at Tell Atchana in the Hatay, 1937–1949* (Oxford University Press).
- K.A. Yener, ed. (2005). *The Amuq Valley Regional Projects, Volume 1: Surveys in the Plain of Antioch and Orontes Delta, Turkey, 1995–2002* (Oriental Institute of the University of Chicago).
- K.A. Yener, ed. (2010). *The Amuq Valley Regional Projects: Excavations in the Plain of Antioch: Tell Atchana, Ancient Alalakh* (Koç University).
- Yener, K.A. (2011). Hittite Metals at the Frontier: A Three-Spiked Battle Ax from Alalakh. In *Metallurgy: Understanding How, Learning Why: Studies in Honor of James D. Muhly, P. Betancourt and S.C. Ferrence*, eds. (INSTAP Academic Press).
- Yener, K.A. (2013a). New Excavations at Alalakh: The 14th–12th Centuries BC. In *Across the Border: Late Bronze–Iron Age Relations Between Syria and Anatolia. Proceedings of a Symposium Held at the Research Center of Anatolian Studies, Koc University, Istanbul, May 31–June 1, 2010*, K.A. Yener, ed. (Peeters).
- Yener, K.A. (2013b). A Plaster Encased Multiple Burial at Alalakh: Cist Tomb 3017. *Amilla: The Quest for Excellence. Studies in Honor of Günter Kopcke on the Occasion of his 75 Birthday* (INSTAP Academic Press).
- Yener, K.A. (2015a). Material Evidence of Cult and Ritual at Tell Atchana, Ancient Alalakh: Deities of the Transitional Middle-Late Bronze Period. In *From the Treasures of Syria: Essays on Art and Archaeology in Honour of Stefania Mazzoni, P. Ciafardini and D. Giannesi*, eds. (Netherlands Institute for the Near East).
- Yener, K.A. (2015b). A Monumental Middle Bronze Age Apsidal Building at Alalakh. In *NOSTOI: Indigenous Culture, Migration + Integration in the Aegean Islands + Western Anatolian During the Late Bronze + Early Iron Ages, N.C. Stampolidis, Ç. Maner, and K. Kopanias*, eds. (Koç University Press).
- Yener, K.A., and Yazıcıoğlu, G.B. (2010). Excavation Results. In *The Amuq Valley Regional Projects: Excavations in the Plain of Antioch: Tell Atchana, Ancient Alalakh*, K.A. Yener, ed. (Koç University Press).
- K.A. Yener, M. Akar, and M.T. Horowitz, eds. (2019). *Tell Atchana, Alalakh: The Late Bronze II City. 2006–2010 Excavation Seasons* (Koç University Press).

**STAR★METHODS**

**KEY RESOURCES TABLE**

REAGENT or RESOURCE	SOURCE	IDENTIFIER
Biological Samples		
Ancient skeletal element	This study	ALA001
Ancient skeletal element	This study	ALA002
Ancient skeletal element	This study	ALA004
Ancient skeletal element	This study	ALA008
Ancient skeletal element	This study	ALA009
Ancient skeletal element	This study	ALA011
Ancient skeletal element	This study	ALA013
Ancient skeletal element	This study	ALA014
Ancient skeletal element	This study	ALA015
Ancient skeletal element	This study	ALA016
Ancient skeletal element	This study	ALA017
Ancient skeletal element	This study	ALA018
Ancient skeletal element	This study	ALA019
Ancient skeletal element	This study	ALA020
Ancient skeletal element	This study	ALA023
Ancient skeletal element	This study	ALA024
Ancient skeletal element	This study	ALA025
Ancient skeletal element	This study	ALA026
Ancient skeletal element	This study	ALA028
Ancient skeletal element	This study	ALA029
Ancient skeletal element	This study	ALA030
Ancient skeletal element	This study	ALA034
Ancient skeletal element	This study	ALA035
Ancient skeletal element	This study	ALA037
Ancient skeletal element	This study	ALA038
Ancient skeletal element	This study	ALA039
Ancient skeletal element	This study	ALA084
Ancient skeletal element	This study	ALA095
Ancient skeletal element	This study	ALX002
Ancient skeletal element	This study	ART001
Ancient skeletal element	This study	ART004
Ancient skeletal element	This study	ART005
Ancient skeletal element	This study	ART009
Ancient skeletal element	This study	ART010
Ancient skeletal element	This study	ART011
Ancient skeletal element	This study	ART012
Ancient skeletal element	This study	ART014
Ancient skeletal element	This study	ART015
Ancient skeletal element	This study	ART017
Ancient skeletal element	This study	ART018
Ancient skeletal element	This study	ART019
Ancient skeletal element	This study	ART020
Ancient skeletal element	This study	ART022

(Continued on next page)

*Continued*

REAGENT or RESOURCE	SOURCE	IDENTIFIER
Ancient skeletal element	This study	ART023
Ancient skeletal element	This study	ART024
Ancient skeletal element	This study	ART026
Ancient skeletal element	This study	ART027
Ancient skeletal element	This study	ART032
Ancient skeletal element	This study	ART038
Ancient skeletal element	This study	ART039
Ancient skeletal element	This study	ART042
Ancient skeletal element	This study	CBT001
Ancient skeletal element	This study	CBT002
Ancient skeletal element	This study	CBT003
Ancient skeletal element	This study	CBT004
Ancient skeletal element	This study	CBT005
Ancient skeletal element	This study	CBT010
Ancient skeletal element	This study	CBT011
Ancient skeletal element	This study	CBT013
Ancient skeletal element	This study	CBT014
Ancient skeletal element	This study	CBT015
Ancient skeletal element	This study	CBT016
Ancient skeletal element	This study	CBT017
Ancient skeletal element	This study	CBT018
Ancient skeletal element	This study	ETM001
Ancient skeletal element	This study	ETM003
Ancient skeletal element	This study	ETM004
Ancient skeletal element	This study	ETM005
Ancient skeletal element	This study	ETM006
Ancient skeletal element	This study	ETM010
Ancient skeletal element	This study	ETM012
Ancient skeletal element	This study	ETM014
Ancient skeletal element	This study	ETM015
Ancient skeletal element	This study	ETM016
Ancient skeletal element	This study	ETM017
Ancient skeletal element	This study	ETM018
Ancient skeletal element	This study	ETM021
Ancient skeletal element	This study	ETM023
Ancient skeletal element	This study	ETM025
Ancient skeletal element	This study	ETM026
Ancient skeletal element	This study	IKI002
Ancient skeletal element	This study	IKI006
Ancient skeletal element	This study	IKI009
Ancient skeletal element	This study	IKI012
Ancient skeletal element	This study	IKI016
Ancient skeletal element	This study	IKI017
Ancient skeletal element	This study	IKI019
Ancient skeletal element	This study	IKI020
Ancient skeletal element	This study	IKI024
Ancient skeletal element	This study	IKI030
Ancient skeletal element	This study	IKI032

(Continued on next page)

**Continued**

REAGENT or RESOURCE	SOURCE	IDENTIFIER
Ancient skeletal element	This study	IKI034
Ancient skeletal element	This study	IKI036
Ancient skeletal element	This study	IKI037
Ancient skeletal element	This study	IKI038
Ancient skeletal element	This study	KRD001
Ancient skeletal element	This study	KRD002
Ancient skeletal element	This study	KRD003
Ancient skeletal element	This study	KRD004
Ancient skeletal element	This study	KRD005
Ancient skeletal element	This study	KRD006
Ancient skeletal element	This study	MTT001
Ancient skeletal element	This study	POT002
Ancient skeletal element	This study	TIT003
Ancient skeletal element	This study	TIT012
Ancient skeletal element	This study	TIT014
Ancient skeletal element	This study	TIT015
Ancient skeletal element	This study	TIT019
Ancient skeletal element	This study	TIT021
Ancient skeletal element	This study	TIT025
<b>Chemicals, Peptides, and Recombinant Proteins</b>		
0.5 M EDTA pH 8.0	Life Technologies	Cat# AM9261
1 M Tris-HCl pH 8.0	Thermo Fisher Scientific	Cat# 15568025
10x Buffer Tango	Life Technologies	Cat# BY5
1x Tris-EDTA pH 8.0	AppliChem	Cat# A8569,0500
20% SDS	Serva	Cat# 39575.01
3M Sodium Acetate (pH 5.2)	Sigma Aldrich	Cat# S7899
5M NaCl	Sigma Aldrich	Cat# S5150
ATP 100 mM	Thermo Fisher Scientific	Cat# R0441
BSA 20mg/mL	New England Biolabs	Cat# B9000
Bst DNA Polymerase2.0, large frag.	New England Biolabs	Cat# M0537
D1000 Reagents	Agilent Technologies	Cat# 5067-5583
D1000 ScreenTapes	Agilent Technologies	Cat# 5067-5582
Denhardt's solution	Sigma Aldrich	Cat# D9905
dNTP Mix	Thermo Fisher Scientific	Cat# R1121
Dynabeads MyOne Streptavidin T1	Thermo Fisher Scientific	Cat# 65602
Ethanol	Merck	Cat# 1009832511
GeneAmp 10x PCR Gold Buffer	Thermo Fisher Scientific	Cat# 4379874
GeneRuler Ultra Low Range DNA Ladder	Life Technologies	Cat# SM1211
Guanidine hydrochloride	Sigma Aldrich	Cat# G3272
Herculase II Fusion DNA Polymerase	Agilent Technologies	Cat# 600679
Human Cot-I DNA	Thermo Fisher Scientific	Cat#15279011
Isopropanol	Merck	Cat# 1070222511
PEG-8000	Promega	Cat# V3011
PfuTurbo Cx Hotstart DNA Polymerase	Agilent Technologies	Cat# 600412
Proteinase K	Sigma Aldrich	Cat# P2308
Salmon sperm DNA	Thermo Fisher Scientific	Cat# 15632-011
Sera-Mag Magnetic Speed-beads Carboxylate-Modified (1 mm, 3EDAC/PA5)	GE LifeScience	Cat# 65152105050250

(Continued on next page)



**Continued**

REAGENT or RESOURCE	SOURCE	IDENTIFIER
Sodiumhydroxide Pellets	Fisher Scientific	Cat# 10306200
SSC Buffer (20x)	Thermo Fisher Scientific	Cat# AM9770
T4 DNA Polymerase	New England Biolabs	Cat# M0203
T4 Polynucleotide Kinase	New England Biolabs	Cat# M0201
Tween-20	Sigma Aldrich	Cat# P9416
Uracil Glycosylase inhibitor (UGI)	New England Biolabs	Cat# M0281
USER enzyme	New England Biolabs	Cat# M5505
Water	Sigma Aldrich	Cat# 34877
<b>Critical Commercial Assays</b>		
High Pure Viral Nucleic Acid Large Volume Kit	Roche	Cat# 5114403001
HiSeq 4000 SBS Kit (50/75 cycles)	Illumina	Cat# FC-410-1001/2
DyNAmo Flash SYBR Green qPCR Kit	Thermo Fisher Scientific	Cat# F415L
MinElute PCR Purification Kit	QIAGEN	Cat# 28006
NextSeq 500/550 High Output Kit v2 (150 cycles)	Illumina	Cat# FC-404-2002
Oligo aCGH/Chip-on-Chip Hybridization Kit	Agilent Technologies	Cat# 5188-5220
Quick Ligation Kit	New England Biolabs	Cat# M2200L
<b>Deposited Data</b>		
Raw and analyzed data (European nucleotide archive)	This study	ENA: PRJEB37213
Haploid genotype data for 1240K panel (Edmond Data Repository of the Max Planck Society)	This study	<a href="https://nam03.safelinks.protection.outlook.com/?url=https%3A%2F%2Fedmond.mpg.de%2Fimeji%2Fcollection%2Fzj1HseOUbd1OaEo&amp;data=02%7C01%7Ctarpin%40cell.com%7C9e00ef7c44fa29cf808d7f0cd4e15%7C9274ee3f94254109a27f9fb15c10675d%7C0%7C0%7C637242637306430495&amp;sdata=sua73V0iRT5WUYnKdCdVszof7MzyI5bA3LkT%2FM6tQv0%3D&amp;reserved=0">https://nam03.safelinks.protection.outlook.com/?url=https%3A%2F%2Fedmond.mpg.de%2Fimeji%2Fcollection%2Fzj1HseOUbd1OaEo&amp;data=02%7C01%7Ctarpin%40cell.com%7C9e00ef7c44fa29cf808d7f0cd4e15%7C9274ee3f94254109a27f9fb15c10675d%7C0%7C0%7C637242637306430495&amp;sdata=sua73V0iRT5WUYnKdCdVszof7MzyI5bA3LkT%2FM6tQv0%3D&amp;reserved=0</a>
<b>Software and Algorithms</b>		
AdapterRemoval v2.2.0	Schubert et al., 2016	<a href="https://github.com/MikkelSchubert/adapterremoval">https://github.com/MikkelSchubert/adapterremoval</a>
ADMIXTOOLS v5.1	Patterson et al., 2012; Loh et al., 2013	<a href="https://github.com/DReichLab/AdmixTools">https://github.com/DReichLab/AdmixTools</a>
ALDER v1.03	Loh et al., 2013	<a href="http://cb.csail.mit.edu/cb/alder/">http://cb.csail.mit.edu/cb/alder/</a>
ANGSD v0.910	Korneliusson et al., 2014	<a href="http://www.popgen.dk/angsd/index.php/ANGSD">http://www.popgen.dk/angsd/index.php/ANGSD</a>
bamUtil v1.0.13	<a href="https://github.com/statgen/bamUtil">https://github.com/statgen/bamUtil</a>	<a href="https://github.com/statgen/bamUtil">https://github.com/statgen/bamUtil</a>
BWA v0.7.12	Li and Durbin, 2009	<a href="http://bio-bwa.sourceforge.net/">http://bio-bwa.sourceforge.net/</a>
CircularMapper v1.93.5	Peltzer et al., 2016	<a href="https://github.com/apeltzer/CircularMapper">https://github.com/apeltzer/CircularMapper</a>
DATES	M. Chintalapati, N. Patterson, N. Alex, and P. Moorjani, personal communication	<a href="https://github.com/priyamoorjani/DATES">https://github.com/priyamoorjani/DATES</a>
DeDup v0.12.2	Peltzer et al., 2016	<a href="https://github.com/apeltzer/DeDup">https://github.com/apeltzer/DeDup</a>
EIGENSOFT v6.0.1	Patterson et al., 2006; Price et al., 2006	<a href="https://github.com/DReichLab/EIG">https://github.com/DReichLab/EIG</a>

(Continued on next page)

**Continued**

REAGENT or RESOURCE	SOURCE	IDENTIFIER
Geneious	Kearse et al., 2012	<a href="https://www.geneious.com">https://www.geneious.com</a>
haplogrep	Kloss-Brandstätter et al., 2011	<a href="https://haplogrep.i-med.ac.at">https://haplogrep.i-med.ac.at</a>
mapDamage v2.0.6	Jónsson et al., 2013	<a href="https://github.com/ginolhac/mapDamage">https://github.com/ginolhac/mapDamage</a>
pileupCaller	<a href="https://github.com/stschiff/sequenceTools">https://github.com/stschiff/sequenceTools</a>	<a href="https://github.com/stschiff/sequenceTools">https://github.com/stschiff/sequenceTools</a>
PMDtools	Skoglund et al., 2014	<a href="https://github.com/pontusssk/PMDtools">https://github.com/pontusssk/PMDtools</a>
preseq v2.0	Daley and Smith, 2013	<a href="https://github.com/smithlabcode/preseq">https://github.com/smithlabcode/preseq</a>
READ	Monroy Kuhn et al., 2018	<a href="https://bitbucket.org/tguenther/read/src/default/">https://bitbucket.org/tguenther/read/src/default/</a>
Rsamtools	Morgan et al., 2019	<a href="http://bioconductor.org/packages/release/bioc/html/Rsamtools.html">http://bioconductor.org/packages/release/bioc/html/Rsamtools.html</a>
SAMtools v1.3	Li et al., 2009	<a href="http://www.htslib.org/doc/samtools.html">http://www.htslib.org/doc/samtools.html</a>
Schmutzi	Peltzer et al., 2016	<a href="https://github.com/greanod/schmutzi">https://github.com/greanod/schmutzi</a>

**RESOURCE AVAILABILITY****Lead contact**

Further information and requests for resources and reagents should be addressed to and will be fulfilled by the Lead Contact, Johannes Krause ([krause@shh.mpg.de](mailto:krause@shh.mpg.de)).

**Materials Availability**

This study did not generate new unique reagents.

**Data and Code Availability**

The accession number for the aligned sequence data (BAM format) reported in this paper is European Nucleotide Archive (ENA): PRJEB37213. Haploid genotype data for the 1240K panel is available in eigenstrat format via the Edmond Data Repository of the Max Planck Society (<https://edmond.mpdl.mpg.de/imeji/collection/zdj1HseOUbd1OaEo>).

**EXPERIMENTAL MODEL AND SUBJECT DETAILS****Description of origin, archaeological and anthropological context of analyzed individuals**

Alkhantepe, Azerbaijan

39.3607139°N, 48.4613556°E

Excavation: Mughan Neolithic-Eneolithic expedition of the Institute of Archaeology and Ethnography of Azerbaijan National Academy of Sciences, 2006-2017, directed by Tufan Isaak oglu Akhundov

The site of Alkhantepe is situated on a plain without visible water ways, 4 km north of the Uchtepe village, in the Jalilabad district of Azerbaijan. It is a narrow belt of the eastern part of the Mughan steppe limited by the spurs of Brovary Range from the west and the Caspian Sea from the east. Presently, the topography of the site is flat with its north-eastern part slightly refracting and lowering. The surface of the settlement has been surveyed for many years and samples of ceramic vessels and stone objects have been found. Test trenches and expanded excavations show that the area occupied by the ancient settlement was about 4 ha in size and the thickness of cultural layers is up to 3 m. Materials recovered from the surface surveys as well as the excavation of cultural layers are identical and give the opportunity to relate this settlement to the Leilatepe tradition.

The cultural layers below the modern-day surface of the site consisted of seven construction horizons which can be divided into two distinct units. As it became clear in the process of excavation, the upper 1.2 m. cultural layer was formed in ancient times due to an earthquake which resulted in a period of abandonment (at least of the excavated parts of the site). Settlement activity resumed shortly afterward. Judging from the material evidence, this new settlement equally represents a new stage in the history of the site with distinct features in architecture and building techniques.

In contrast to the preceding time when adobe was widely used, buildings of the younger settlement stage were light constructions of rectangular form made of reeds and poles covered with clay and with a hearth in the middle.

For the first stage of settlement, excavations revealed round and rectangular mud-huts with subsoil walls and walls constructed from adobe, altars, different household hearths and production furnaces, pits, and partition walls of adobe. The burials of the settlement's inhabitants were found on different levels among these constructions. The burials included individuals of all age groups, from new-borns and teenagers to adults. Only one exception was observed: babies were buried in ceramic vessels.

Survey and excavation uncovered a rich archaeological material consisting mainly of ceramics of Leilatepe tradition that is also represented by tools and objects of stone and bone. Additionally, metal objects, metallic slag and tools of metallic production were found (Akhundov, 2014, 2018).

One individual from Alkhantepe was analyzed for aDNA and is included in genetic analyses.

- ■ ALX002 (Alkhantepe Burial N2) is the individual from a burial that was revealed in a distance from the eastern wall in the south square of the excavated area at a depth of 1,48 m. The remains of this individual were buried in a shallow oval pit and they, as well as the pit, were poorly preserved. However, judging from the preserved remains, the deceased was put into the pit in a crouched position, lying on his/her left side with the head placed on a north-east orientation. A lead ring with unclosed ends, made of round wire, was found lying on the shin's bone. Dating of human tooth: 3776-3661 cal BCE (4950 ± 23 BP, MAMS-40330)

### Arslantepe, Turkey

38.381944°N, 38.361111°E

Excavation: Sapienza University of Rome, 1961-present, directed by Marcella Frangipane

The site of Arslantepe is a 4.5 ha mound located in the highland fertile Malatya plain of Eastern Anatolia, 12 km from the western bank of the Euphrates river. From the point of view of Mesopotamian archaeology, the site is at a geographical and cultural border zone, in the northern highlands outside Mesopotamia proper and along pathways that potentially connect the alluvium of the Euphrates with different worlds, from the Caucasus to the Pontic regions and Central Anatolia. The uninterrupted and extensive excavation of the site since 1961 brought to light a four millennia long occupation starting around 4700 BCE, but possibly even earlier, as testified by the presence of Neolithic and Chalcolithic pottery on the surface of the mound. Among this are Ubaid ceramics and we know that the Malatya plain was directly involved by the expansion of Mesopotamian Ubaid culture, also by the Ubaid presence at the neighboring site of Değirmentepe. The finding of Halaf period ceramics suggests that this contact was strong in Neolithic phases too. During the fourth millennium, Arslantepe undergoes developments that structurally resemble those of Mesopotamia, even though it shows its own peculiarities, with a clear and steady growth in economic and social development, which brings the site to develop a primary state system toward the end of the millennium, parallel to that of Mesopotamia, but with features of its own (Frangipane, 2018). In the earlier phases of this period (Arslantepe Period VII, 3900-3400 BCE) contacts with Central Anatolia are also evidenced, but material culture shows that the strongest relations of the site are with the south-west toward the Amuq and Quoeiq (Balossi Restelli et al., 2012). The moment of proper state development (Arslantepe Period VI A, 3400-3200 BCE) is revealed by the foundation of a precocious palace complex with a sophisticated bureaucracy and control over the economy of the populations, which shows an increase in contacts with Mesopotamia proper, but also with other mountainous regions of North-Central and North-Eastern Anatolia and the Caucasus (Frangipane, 2012b). The contacts with the north-eastern regions further increase at the collapse of this early state system, when pastoral groups that were already living in the area and moving along the mountains with their flocks of sheep and goats briefly settle at the site, by building huts and fences for animals directly on the ruins of the palace (period VI B1, 3200-3100 BCE), giving rise to a period of profound instability characterized by meetings and clashes of various populations contending the site. In the course of their seasonal occupations, the pastoral groups of Period VIB1 also built more durable structures, among which a large mud-brick communal building, probably used a reception hall for meetings and feasting (Frangipane, 2012a, 2014, 2015b; Siracusano and Palumbi, 2014). This is a period of unrest and fast changes: Following the less permanent occupation of Period VI B1, an imposing fortification wall was built on the top of the mound, surrounding a large open area and with a series of rooms adjoining it on the interior (period VIB2, early phase). In this phase, only the remains of post-holes, probably belonging to temporary huts and fences, were found outside the wall, and the dates obtained from charcoals and seeds from the rooms adjoining the wall indicate an approximate date of about 3100 BCE. In a second phase of Period VIB2, a village of farmers was extensively brought to light along the slope, outside the fortification wall that was not in use anymore, and was dated between 3000 and 2850 BCE. The frequent overlapping of the C14 dates from all these periods, as well as the features of the archaeological evidence suggest that all the events occurred at Arslantepe from the destruction and collapse of the Palace to the establishment of the VIB2 village of farmers seem to have succeeded one another in a very fast and dramatic way, in the course of a short period of time.

Occupation at Arslantepe continues uninterrupted throughout the whole 3<sup>rd</sup> millennium with an initial return to mobility (VI C, 2750-2500 BCE), followed by the presence of competing small polities in the whole plain, of which Arslantepe was probably one of the largest (VI D, 2500-2000 BCE) (Frangipane, 2012a; Conti and Persiani, 1993). This was a period of greater stability and an apparent decrease in external contacts, as material culture shows a remarkable continuity for several centuries.

During the 2<sup>nd</sup> millennium the site comes under Hittite influence (first with the Hittite reign and then the Empire) (Manuelli, 2013) and will eventually become capital of a Neo-Hittite reign at the collapse of the Empire. Arslantepe is eventually abandoned after the Assyrian king Sargon II conquers and destroys the site in 712 BCE.

Human remains at Arslantepe have been found both as burials and as scattered human remains within pits and fills of buildings. Period VII is the one with the most finds, predominantly formed by burials related to domestic occupation, thus dug under the floors of houses. Buried individuals are mostly infants and adult women (Erdal and Balossi Restelli, in press). Rarely sparse human bones are found, but are probably due to disturbances of burials that must have taken place already in antiquity. In the latest level of occu-

pation in Period VII a burial ground has also been identified, outside a Temple structure, where possibly special burials were positioned: 2 infant jar burials were identified, one infant stone cist and an adult inhumation.

The following VI A period is the period in which Arslantepe becomes the center of a primary state system, testified by a monumental palatial complex. No burials belonging to this phase have been found, but in one of the two temples of the complex (Temple A) a human skull was lying on the floor at the center of the building together with the skull of a wild pig. Both must have been part of a ritual practice, taking place in the room.

Yet different is the situation of human bones found in Period VI B1, when most remains are partial skeletons, found in pits or scattered within fills covering the collapsed palace ruins, thus not proper burials.

In the following VI B2 village of Early Bronze Age very interestingly the practice of burying infants under the house floors appears to have disappeared. An interesting group of human bones have been however found in a pit cut into the floor of the open space inside the fortification wall in the early phase of the period. These belong to a minimum number of 16 partial individuals not in anatomical connection, mostly male and adults, found in this pit together with some animal bones (Erdal, 2012b).

To a period in between the end of VI B1 and the beginning of VI B2 belongs the so-called 'royal tomb' (Frangipane et al., 2001), an imposing cist grave built at the bottom of a large pit, which was very atypical for the local culture. It was an extremely rich tomb containing an adult man with plenty of funerary gifts among which 65 metal objects, and with a complex funerary practice including the possible sacrifice of 4 adolescents (almost all female) on the stone slabs covering the cist (Palumbi, 2011; Frangipane et al., 2001). Ceramic materials in the tomb are perfectly in keeping with what was found in the early phase of Period VI B2, as well as in the communal building of Period VI B1, that is a mixture of local light-colored wares with Reserved Slip decoration in the Uruk tradition and Red-Black handmade ware of Caucasian and Anatolian inspiration.

The rest of the Early Bronze Age period sees rare human remains, and only one of a male burial from the vicinities of the domestic area has been included in this work.

Twenty-two individuals from Arslantepe produced genome-wide data and are included in genetic analyses.

- ART001 (H156 S138) is a female in pit burial from Period VI D2. Evidence of epicondylitis was observed on both humeri. The remains also exhibit evidence of severe osteoarthritis. Dating of human bone: 2470-2301 cal BCE (3908 ± 26 BP, MAMS-33533).
- ■ ART004 (H238 S156) is an old male in a pit dug under and sealed by the floor of a house. Period VII. Dating of human bone: 3758-3642 cal BCE (4906 ± 26 BP, MAMS-33534)
- ■ ART005 (H250 S169) is an old female buried in a domestic area of the settlement from Period VII. The relation with the overlying architecture is not preserved. A red slipped and burnished beaker were held in her hands and traces of red ochre were found on and next to the knees. Evidence for the following pathological conditions was present on the remains: osteoporosis, hyperostosis frontalis interna, severe osteoarthritis on joints, severe osteoarthritis on cervical and lumbar vertebra, dental diseases such as dental caries, periapical abscess, periodontitis, dental calculus, and linear enamel hypoplasia. Dating of human bone: 3770-3654 cal BCE (4934 ± 27 BP, MAMS-33535).
- ■ ART009 (H326) is an adult male represented by a skull and disarticulated bones found on the floor of a dwelling from Period VI B2, together with other bones from at least two individuals. No pathology was found on the preserved bones. Dating of human bone: 2834-2497 cal BCE (4069 ± 20 BP, MAMS-33536)
- ■ ART010 (H327 S220-2) is a ca. 7-year-old child represented by a skull and disarticulated long bones found on the floor of a dwelling from Period VI B2, together with other bones from at least two individuals. The cranium exhibits evidence of a possible perimortem trauma on left parietal bone and infectious lesions on the endocranial surface of the occipital. Linear enamel hypoplasia was observed on the permanent upper central incisors and the deciduous canines display evidence of non-alimentary use. Dating of human bone: 2857-2505 cal BCE (4095 ± 26 BP, MAMS-33537)
- ■ ART011 (S220-1) is a ca. 30-year-old female represented by a skull and disarticulated long bones found on the floor of a dwelling from Period VI B2, together with other bones from ART009 and ART010. No pathology was found on preserved cranial bones. Dating: 2839-2581 cal BCE (4103 ± 26 BP, MAMS-33538)
- ■ ART012 (H331) is a young adult female represented by a skull found on the floor of central room of Temple A (palatial complex of Period VI A) lying next to the skull of a wild pig. No pathology was found on this skull. Dating of human bone: 3338-3031 cal BCE (4479 ± 27 BP, MAMS-33539)

S216 is a simple pit containing a collective burial of human remains belonging to a minimum of 16 individuals. The pit is partly sealed by a VI B2 floor surface and cuts VI B1 levels of occupation of Arslantepe. There are also bone fragments of animals. This pit is not a burial type that is encountered in this period in Anatolia or neighboring areas. The human remains in this secondary burial consist of unarticulated cranial and post-cranial bones. Some small bones such as metacarpals, metatarsals and phalanges are also present but they are very few compared to the long bones and crania. Bioarchaeological studies of the human remains suggest that there are at least 13 adult crania. Moreover, three sub-adults are also present among the human remains. A total of eight out of the 13 adult crania have signs of perimortem blunt forced traumas (Erdal, 2012b). Petrous bones from the following eleven individuals were analyzed for DNA:

- ■ ART014 (S216 Cr2) is the cranium of a male individual. Dating of human bone: 3492-3119 cal BCE (4573 ± 27 BP, MAMS-33540)
- ■ ART015 (S216 Cr3) is the cranium of a male individual with a perimortem and two healed traumas. Dating of human bone: 3369-3110 cal BCE (4557 ± 25 BP, MAMS-33541)
- ■ ART017 (S216 Cr8) is the cranium of a male individual. No pathology was observed. Dating of human bone: 3351-3103 cal BCE (4516 ± 25 BP, MAMS-33542)
- ■ ART018 (S216 Cr9) is the cranium of a male individual. No pathology was observed. Dating of human bone: 3491-3122 cal BCE (4573 ± 25 BP, MAMS-33543)
- ■ ART019 (S216 Cr10) is the cranium of a male individual. No pathology was observed. Dating of human bone: 3499-3355 cal BCE (4623 ± 24 BP, MAMS-33544)
- ■ ART020 (S216 Cr11) is the cranium of an individual with one healed and one unhealed trauma on the left parietal bone. Dating of human bone: 3362-3105 cal BCE (4536 ± 25, BP MAMS-33545)
- ■ ART022 (S216 Cr13) is the cranium of an individual with one perimortem trauma on the right parieto-temporal region. Dental diseases were also detected. Dating of human bone: 3642-3137 cal BCE (4681 ± 75 BP, MAMS-33546)
- ■ ART023 (S216 Cr14) is the cranium of a male individual with one healed trauma on the right parietal and one perimortem trauma on the left parietal. Dating of human bone: 3486-3117 cal BCE (4563 ± 25 BP, MAMS-33547)
- ■ ART024 (S216 Temp1) is an isolated temporal bone of a male individual. Dating of human bone: 3497-3352 cal BCE (4614 ± 24 BP, MAMS-33548)
- ■ ART026 (S216 Temp3) is an isolated temporal bone of a female individual. Dating of human bone: 3340-3096 cal BCE (4491 ± 26 BP, MAMS-33549)
- ■ ART027 (S216 Temp4), temporal bones of a male individual. Dating of human bone: 3365-3108 cal BCE (4546 ± 25 BP, MAMS-33550)
- ■ ART032 (A1335 rP4 B) is represented by sparse human bones found under the floor of entrance of a communal building from Period VI B1. Dating of human bone: 3484-3124 cal BCE (4568 ± 21 BP, MAMS-34110)
- ■ ART038 [S150 (H221)] is a young female from Period VI B1/VI B2 lying on top of stone slabs closing the Royal tomb. Probably sacrificed. Dating of human bone: 3361-3105 cal BCE (4534 ± 27 BP, MAMS-34112)
- ■ ART039 [C7-D7 (H378)] is represented by a disturbed mandible stratigraphically contemporary to the burial ground of the end of Period VII. Dating of human tooth: 3762-3646 cal BCE (4916 ± 27 BP, MAMS-34116)
- ■ ART042 [S254 (H382)] is an infant in a jar burial from burial ground belonging to the end of Period VII. Dating of human bone: 3941-3708 cal BCE (5014 ± 29 BP, MAMS-34119)

### Boğazköy-Büyükaya, Turkey

40.022056°N, 34.620611°E

Excavation: Boğazköy Expedition of the German Archaeological Institute (Istanbul Section), 1996-1998, directed by Jürgen Seeher

The settlement on the rock massif Büyükaya (Çorum Province), within the boundaries of the later Hittite capital Hattuša, is, so far, the oldest known settlement in North-Central Turkey (Schoop, 2005, 2018). A small hamlet-sized village was situated on the uppermost plateau of Büyükaya, high above the later city area, from where it overlooked the southern end of the Budaközü Valley. Although detailed information about the palaeo-environment of the area is lacking, this area must have been covered by forest in the past and offered few of the open spaces which are more typical for other parts of Anatolia.

Later use of the location is responsible for the fragmentary preservation of the site. Covering an area of ca. 300 sqm at the southern end of the plateau, a number of floors, hearths and storage pits were found which indicated the (probably short-lived) existence of a few small wooden structures above a fill consisting of burnt *pisé* material. At the western limit of the site, the segment of a narrow ditch was found. A single grave, belonging to a young child, was found beneath a strip of flooring, not far from one of the hearths.

Very few small finds were recovered, including a number of sickle blades made from local flint, a few heavy stone pounders and a series of fragments of polished marble bracelets. The pastoral economy relied predominantly on the exploitation of cattle, sheep and goats (von den Driesch and Nadja, 2004).

The pottery of this small settlement displays the dark-faced, burnished surfaces which are typical for the Anatolian north of this time. A small number of sherds are decorated in stab-and-drag technique or painted on a white slip. Although the assemblage is certainly representative of a discrete cultural entity which has not yet discovered elsewhere, there are clear morphological links toward contemporary Early Chalcolithic societies further to the west (Eskişehir area) and the south (Cappadocia/the Central Anatolian Plain).

Two radiocarbon dates, taken from human bone (see below) and from charcoal recovered from one of the pits, indicate a chronological position of the settlement within the second quarter of the 6<sup>th</sup> millennium BC (Schoop et al., 2012).

The single individual from Boğazköy-Büyükaya produced genome-wide data and is included in genetic analyses.

- ■ CBT018 (Grave 347/410-315) is an infant aged 6-12 months (Thomas, 2012; Schoop et al., 2012) buried in a pit grave without any goods. The skeleton was found in contracted body position. In all probability, this grave represents an intramural

burial below a house floor. Dating of human bone: 5626-5515 cal BCE (6635 ± 30 BP, SUERC-36800 [GU25423]).

### Çamlıbel Tarlası, Turkey

40.019745°N, 34.586129°E

Excavation: Boğazköy Expedition of the German Archaeological Institute (Istanbul Section) / University of Edinburgh, 2007-2009, directed by Ulf-Dietrich Schoop

Çamlıbel Tarlası is a small settlement situated on a low plateau within a narrow lateral valley branching off the southern end of the main Budaközü Valley (Çorum Province), approximately 2.5 km west of the earlier site on Büyükkaya (Schoop, 2015). The site was the location of a small hamlet which never comprised more than three to five contemporary houses. There are three distinctive and relatively short periods of permanent human presence at Çamlıbel Tarlası. In between these habitation phases, the site continued to be visited on a seasonal bases, probably by the same community, as shown by the remnants of continued agricultural and other activities during these times.

One attracting factor of the location appears to have been the presence of copper ore outcrops further into the valley. Within the settlement, fragments of copper ore, slag and crucibles show metallurgical as well as other pyrotechnical activities such as the production of enstatite (artificial steatite), quicklime and charcoal-burning. Beginning environmental degradation in the surroundings may have been a consequence of these fuel-intensive activities (Marsh, 2010).

Houses had walls constructed from stamped *pisé* on stone bases. Many had domed bread ovens in their interiors, standing on floors made from stamped earth or lime plaster. One ÇBT III building (S3 “Burnt House”) clearly had a special, probably ritualistic purpose. Notable finds include a casting mold for ring-shaped figurines, enstatite micro-beads, Cappadocian obsidian and blades made from exotic flint. The pastoral economy showed an emphasis on cattle and pig-raising, with evidence of secondary product use for cattle and caprines (Bartosiewicz and Gillis, 2011). The plant-based economy suggests the working of small, intensively tended agricultural plots, with a high importance of legumes (Papadopoulou and Bogaard, 2012).

A total of 17 graves were retrieved during excavations. The majority belonged to infants and children (Thomas, 2011, 2017). Most of the stratigraphically attributable graves belong to ÇBT II and a small number to ÇBT III. Two adults seem to have been buried at times when the site was uninhabited. Babies and younger children (up to two years) were found in large pottery containers, within which their bones were not usually encountered in articulated arrangement. Elder children and adults, by contrast, were buried in narrow pits, as intact skeletons in contracted body position. With the possible exception of Graves 4 and 13, none of the burials contained any grave goods. Most children were encountered in exterior spaces, in close proximity to the house walls. Deviating from this scheme, three graves (2, 16 and 17) were found below the floors of two separate structures. Remarkably, DNA analysis has shown these three individuals to be siblings (see Figure S1). Human remains and a large set of animal bones were subjected to stable-isotope analysis (Pickard et al., 2016, 2017).

Radiocarbon analysis conducted on plant seeds and human bone show a short chronological span of the whole sequence of 70 to 140 years toward the middle of the 4<sup>th</sup> millennium BCE (3676/3535 to 3634/3508 cal BCE cal; 17 samples) (Schoop et al., 2009). Çamlıbel Tarlası and the nearby site of Yanıkaya constitute a variant of a larger cultural entity whose best-known representative is the Late Chalcolithic settlement at the base of Alişar Höyük (Schoop, 2011).

Twelve individuals from Çamlıbel Tarlası produced genome-wide genetic data and are included in genetic analyses.

- ■ CBT001 (Grave 1, ÇBT 204-1103) is a 9-15 months-old infant in a jar burial in juxtaposition to the west wall of building S9 (ÇBT II), under a strip of external flooring. Dating of human bone: 3632-3378 cal BCE (4725 ± 20 BP, MAMS-41627).
- ■ CBT002 (Grave 2, ÇBT 327-921) is a 9-15 months-old infant in an intramural jar burial within one of two immediately juxtaposed pits under ÇBT II building S11. The outlines of the neighboring empty pit were marked and visible on the surface of the floor. Traces of red ochre were found on some of the bones. This grave also contained a few bones of a second individual, a second trimester fetus. Dating of human bone: 3652-3525 cal BCE (4809 ± 30 BP, MAMS-41630).
- ■ CBT003 (Grave 3, ÇBT 80-1086) is a 2-4 years-old infant, probably buried in contracted body position. The burial was fragmentary and came from a disturbed ÇBT II-III context but is possibly associated with the “Burnt House” S3 (ÇBT III). No grave goods were found.
- ■ CBT004 (Grave 4, ÇBT 406-3224) is a 8-10 years-old infant buried in a pit grave from a ÇBT II/III context. The skeleton was recovered in an extremely contracted body position. Copper staining on the upward-facing mandible and disturbance of vertebrae suggest that the grave was re-opened and that a metallic artifact was recovered at some point after the burial. Dating of human bone: 3636-3521 cal BCE (4765 ± 20 BP, MAMS-41628).
- ■ CBT005 (Grave 5, ÇBT 464-4072) is a 6-8 years-old child in a pit grave with the skeleton in contracted body position. This grave was found close to a major ÇBT IV building (S6), dug into virgin soil and covered by topsoil (context ÇBT I-IV). Dating of human bone: 3630- 3377 cal BCE (4713 ± 21 BP, MAMS-41629).
- ■ CBT010 (Grave 10, ÇBT 923-5423) is a 2<sup>nd</sup>-3<sup>rd</sup> trimester fetus in a jar burial cut into bedrock, associated with a fragmentary ÇBT III building above.
- ■ CBT011 (Grave 11, ÇBT 970-6074) is a 7-9 years-old child buried in a pit grave with the skeleton in contracted body position. The grave was in an external area, in juxtaposition to the southeast wall of building S21 (ÇBT II).

- ■ CBT013 (Grave 13, ÇBT 950-6118) is a 6-8 years-old child buried in a pit grave with the skeleton in contracted body position. The burial was found under an auxiliary structure to the building S21 (ÇBT II). A bent copper perforator was found underneath the skull bones. Dating of human bone: 3643-3526 cal BCE (4796 ± 23 BP, MAMS-41631).
- ■ CBT014 (Grave 14, ÇBT 971-6144) is a 4-5 years-old child buried in a pit grave with the skeleton in contracted body position. The burial was found in an external area close to the building S29 (ÇBT II). Dating of human bone: 3640-3385 cal BCE (4767 ± 28 BP, MAMS-41632).
- ■ CBT015 (Grave 15, ÇBT 978-6140) is a fetus - 3 months-old infant in a jar burial below the building S21 (ÇBT II). Dating of human bone: 3643-3522 cal BCE (4787 ± 28 BP, MAMS-41633).
- CBT016 (Grave 16, ÇBT 894-5819) is a 1.5-2.5 years-old infant in a jar burial below the east room of the building S25 (ÇBT II). The location of the grave was marked by a circle of stones set in the floor. This grave also contained a rib from a second individual, a fetus. Dating of human bone: 3692-3527 cal BCE (4828 ± 29 BP, MAMS-41634).
- ■ CBT017 (Grave 17, ÇBT 1010-5876) is a 12-15 months-old infant whose skeletal remains were poorly preserved. The burial was possibly a pit grave found under a strip of flooring under the west room of building S25 (ÇBT II).

### İkiztepe, Turkey

41.6136944°N, 35.8711361°E

Excavation: Istanbul University, from 1974 to 2012, directed by late U. Bahadır Alkım and Önder Bilgi

İkiztepe is a prehistoric site in the Black Sea Region in Anatolia, Turkey. The site is located 7 km west of modern town of Bafra in Samsun province, on a hilly area, 9 km north of actual seashore of Black Sea (Bilgi, 2004; Özdemir and Erdal, 2012). İkiztepe means twin mounds in Turkish, however it actually consists of four mounds (I-IV). All these mounds were settled from the Early Chalcolithic period up to the Early Hittite period. A total of 700 simple pit graves, dated to the Late Chalcolithic period and belonging to the dwellers of Mound III, were excavated in the extramural graveyard in Mound I (Bilgi, 2004). Human remains, which are extremely well preserved in terms of bone and collagen contents, are housed in the Hacettepe University Skeletal Biology Laboratory (Husbio-L).

İkiztepe is surrounded by modern Bafra plain formed by the alluvial deposits of Kızılırmak and some lagoons on the sea shore (Alkım et al., 1988). It is suggested that the settlement was located on the edge of the Black Sea during the time it was settled (Bilgi, 2000). Kızılırmak, 7 km to the east of the site at the present time, was running close to the settlement. The lifestyle of İkiztepe people was dependent on agriculture. However, the studies on animal remains and human mobility suggest that pastoral lifestyle might have also been important for these people (Welton, 2010). Dietary habits of the people were mainly based on the terrestrial C3 food sources (Irvine, 2017). Sulfur and nitrogen isotopes do not support a nutrition model that is composed of seafood and freshwater food sources.

Almost all the individuals at İkiztepe were excavated in simple pit burials without a standard tendency concerning the direction of the bodies. Except for the other Anatolian Late Chalcolithic and Early Bronze Age settlements, İkiztepe individuals were buried in supine position with the arms parallel to the body. Plenty of metal objects such as spearhead, dagger, harpoon, hook, spiral, ring and bracelet were found together with burials (Bilgi, 2004). Metal objects were produced by arsenical copper alloy. However, golden and silver rings, earrings, amulets, and pendants were also found. The number of grave goods tends to increase with the age of individuals. Moreover, there are some important differences between genders: males were buried mostly with weapons such as spearheads and quadruple spirals, on the other hand, females were buried with jewellery, pottery and daggers.

A total of eleven individuals from İkiztepe produced genome-wide data and are included in genetic analyses.

- ■ IKI002 (IT SK528) is a 50 to 60-year-old female in a primary simple pit burial. The individual was buried in supine position with the legs extended and the arms parallel to the body. The skeleton was well preserved except from some missing long bones (right and left ulna and tibia, right radius). Grave goods include a stone necklace and a spearhead. The remains displayed evidence of a possible dermoid cyst on the skull, a healed fracture on a rib, moderate osteoporosis, moderate osteoarthritis on the vertebra and caries on upper third molar. Small amount of dental calculus and mild were also observed. Dating of human tooth: 3338-3095 cal BCE (4488 ± 22 BP, MAMS-40673)
- ■ IKI009 (IT SK552) is a 18 to 28-year-old female in a primary simple pit burial. The individual was buried in supine position, extending southeast to northwest with the legs extended, the arms parallel to the body, and the skull facing left. The left arm, the pelvis and both femur bones are missing. Among the grave goods three spearheads were found. The remains display evidence of infection on the maxillary sinus (sinusitis), mild porotic hyperostosis, small amount of calculus and enamel hypoplasia on the anterior teeth. Dating of human tooth: 3366-3115 cal BCE (4552 ± 22 BP, MAMS-40674)
- ■ IKI012 (IT SK567) is a 25 to 46-year-old female in supine position, extending east to west with the legs extended, the right arm on the abdominal cavity, the left arm on the chest, and the skull facing right. The preservation of the skeleton was very good. Grave goods included a spearhead. The remains exhibit presence of two healed depression traumas on the skull, mild osteoarthritis on thoracic vertebra. Small amount of calculus and enamel hypoplasia on anterior teeth were also observed. Dating of human tooth: 3368-3118 cal BCE (4557 ± 22 BP, MAMS-40675)

- ■ IKI016 (IT SK581) is a 45 to 70-year-old female in supine position, extending west to east with the legs extended, the arms parallel to the body, and the skull facing left. All bones are present. Grave goods include two daggers, a spearhead, a bowl, two gold earrings, a frit necklace and a lead pendant. The remains exhibit presence of an unhealed fracture on a rib, mild osteoarthritis on joints and vertebra, Schmorl's nodes on thoracic and lumbar vertebra, and small amount calculus. Dating of human tooth: 3518-3371 cal BCE ( $4671 \pm 22$  BP, MAMS-40676)
- ■ IKI017 (IT SK593) is a 63 to 70-year-old female in supine position, extending southeast to northwest with the legs extended and the arms parallel to the body. The skeleton is well preserved except from some missing long bones (right forearm, right tibia). A spearhead and earrings are among the grave goods. The remains exhibit presence of moderate osteoarthritis on the joints and the lumbar vertebra, caries on the upper second molar, small amount of calculus, enamel hypoplasia on both anterior and posterior dentition and moderate periodontitis. Dating of human tooth: 3494-3124 cal BCE ( $4580 \pm 26$  BP, MAMS-40677)
- ■ IKI024 (IT SK635) is a 25 to 35-year-old male, in supine position. All bones are complete and well preserved. The remains of this individual exhibit a number of pathologies: a healed fracture on left radius, a healed fracture on fifth metacarpal, periostitis on anterior surfaces of tibia and fibula, moderately developed porotic hyperostosis, severe osteoarthritis on the distal end of left ulna possibly because of the fracture on left radius, mild osteoarthritis on thoracic and lumbar vertebra, three dental caries on both upper and lower posterior dentition, small amount of calculus, linear enamel hypoplasia on the upper anterior dentition, periapical abscess on the lower third molar and mild periodontitis. Dating of human tooth: 3958-3799 cal BCE ( $5080 \pm 27$  BP, MAMS-40678)
- ■ IKI030 (IT SK652) is a 45 to 60-year-old female, in supine position. The skeleton is complete and well preserved. The remains of this individual exhibit a number of pathologies: a healing fracture on a rib, infection on the internal surface of a rib, severe osteoporosis, mildly developed osteoarthritis on thoracic and lumbar vertebra, antemortem loss of upper second molar, 4 dental caries on posterior dentition, moderate calculus, periapical abscess on upper first molars and severe periodontitis. Dating of human tooth: 3512-3357 cal BCE ( $4536 \pm 26$  BP, MAMS-40679)
- ■ IKI034 (IT SK665) is a 14 to 15-year-old child in supine position, extending west to east. The state of the skeleton's preservation was fair. No grave goods were found. The remains exhibit evidence of a healed depression trauma on skull, small amount of dental calculus on the anterior dentition and linear enamel hypoplasia on both anterior and posterior dentitions. Dating of human tooth: 3500-3352 cal BCE ( $4623 \pm 26$  BP, MAMS-40680)
- ■ IKI036 (IT SK668) is a 30 to 40-year-old female in supine position, extending west to east with the skull facing right. The skeleton was well preserved except from distal ends of tibia and feet which were missing. Grave goods consist of a frit necklace and a ring. The remains exhibit the following pathologies: a healed depression trauma on skull, mildly developed osteoarthritis on lumbar vertebra, nine dental caries on both upper and lower posterior dentitions, small amount of dental calculus and linear enamel hypoplasia on all teeth. Dating of human tooth: 3627-3374 cal BCE ( $4700 \pm 26$  BP, MAMS-40681)
- ■ IKI037 (IT SK675) is a 35 to 40-year-old male, extending south to north, scattered. The skeleton was found complete. Grave goods include a spearhead and a frit necklace. The following pathologies were detected on the remains: three healed depression traumas on skull, both healed and unhealed fractures on carpals and phalanges, healed green stick fractures on three ribs, small sized auditory exostoses on both ear holes, mild osteoarthritis on carpals and metacarpals, Schmorl's nodes on thoracic and lumbar vertebra, two dental caries on upper posterior dentition, small amount of calculus, linear enamel hypoplasia on both upper and lower anterior teeth. Dating of human tooth: 3635-3382 cal BCE ( $4748 \pm 29$  BP, MAMS-40682)
- ■ IKI038 (IT SK677) is a 45 to 50-year-old female in supine position, extending south to north. The preservation state of the remains was very good. No grave goods were found. The remains exhibit multiple healed and unhealed fractures on ribs, a small sized button osteoma on frontal, mildly developed osteoarthritis on joints, thoracic and lumbar vertebra. Dating of human tooth: 3633-3381 cal BCE ( $4738 \pm 26$  BP, MAMS-40683)

### Mentesh Tepe, Azerbaijan

40.9418889°N, 45.8327778°E

Excavation: French Ministry of Foreign Affairs, CNRS and French-German ANR, 2008-2015, directed by Bertille Lyonnet and Farhad Guliyev

The small mound of Mentesh Tepe on the lower fan of the Zeyem Chaj – an affluent of the left bank of the Kura River, originally probably covered 0.5 ha but had been totally destroyed recently or lays beneath modern houses. Remains of its lower/main occupations were preserved under the surface. Three main periods interrupted by gaps of several centuries have been identified. The earliest (period I) is related to the Late Neolithic Shomu-Shulaveri Culture (SSC) with circular architecture both above ground and partly dug into it, and is dated by radiocarbon dates between ca. 5770-5600 BCE (Lyonnet et al., 2016). However, being on the most eastern edge of the SSC, it also presents some specific features, and relations with areas further east in the Mil'-Karabagh Steppe have been underlined (Lyonnet, 2017). This period provided several infant burials and an exceptional collective grave most probably dug into an abandoned circular house with 30 individuals of mixed ages and sexes in primary position, with no evidence of trauma, enamel hypoplasia or other pathology indicating a violent episode or starvation (Pecqueur and Jovenet, 2017). After a long abandonment, a very light reoccupation probably by mobile groups is dated to ca. 4600 BCE (period II). It was



followed ca. 4350–4100 BCE by an important settlement (period III) with a totally new rectangular, and possibly tripartite, architecture. This with several other features in the material culture point at relations with the eastern areas of the Mugan Steppe and with Northern Mesopotamia (Lyonnet, 2012). Copper-based metallurgy shows a quick development (Courcier et al., 2016). This period at Mentesh clearly announces the further development and tighter relations between Southern Caucasus (Leilatepe culture) and Northern Mesopotamia (LC2-3) in the first half of the 4<sup>th</sup> millennium BCE (Akhundov, 2007; Lyonnet, 2007). Not very far from Mentesh, on the right bank of the Kura River, the same team excavated kurgans at Soyug Bulaq dating to this first half of the 4<sup>th</sup> millennium, with one rather richly furnished with a copper knife, a stone scepter, lapis, gold and silver-copper beads. These kurgans are clearly related on the one hand to those of Sé Girdan on the south of Lake Urmia and on the other to those of the Maykop culture (Lyonnet et al., 2008), as well as to the Leilatepe culture.

Mentesh Tepe was abandoned during all this period and later only used for burials (period IV). A first kurgan was built for collective/successive inhumations (at least 39 individuals) and used during the early phase of the Kura-Araxes culture in the second half of the 3<sup>rd</sup> millennium BC. The kurgan was put to fire at the end, leaving the human bones in a very bad state of preservation (Lyonnet, 2014; Poulmarc'h et al., 2014). The site was possibly short-term occupied after that, until a second kurgan was built ca. 2500–2400 BCE, containing three individuals and a four-wheel cart. Its rather rich material – gold and carnelian beads and ring, an imported shell ring, spirals of tin-bronze, a silver small casket and a good amount of pottery – relate it to the Martkopi phase of the so-called Early Kurgan Culture (Pecqueur et al., 2017), a period when long distance connections develop (Lyonnet, 2016).

Extensive genetic characterization of the Late Neolithic population of Mentesh Tepe is being conducted by CNRS UMR 7206/MNHN USM 104. Here, we analyzed one individual from the Late Neolithic collective burial of Mentesh Tepe which produced genome-wide data and was included in the genetic analyses.

- ■ MTT001 (Grave 342 20 7, 12; Individual 1) is an immature individual aged between 10 and 14 years buried in the Late Neolithic collective grave. The skeleton, the last to be buried of a group of 30 individuals, was found lying face down with the legs twisted. In this collective grave, the imbrication of some of the skeletons tend to point at simultaneous inhumations, while a layer of sediment covers others indicating a possible lapse of time between them. The good bone preservation and their excavation by a group of anthropologists provided many details. They show a not natural distribution of sexes (more women than men) and ages (no infant less than one year, many immatures (65%)). For more details see Pecqueur and Jovenet (2017). Dating of human bone: 7010 ± 45 BP (Sac A 41508/Gif-13016); dating of human tooth: 5717–5670 cal BCE (6802 ± 23 BP, MAMS-40333)

### Polutepe, Azerbaijan

39.5186111°N, 48.6500000°E

Excavation: Mughan Neolithic-Eneolithic expedition of the Institute of Archaeology and Ethnography of Azerbaijan National Academy of Sciences, 2006–2017, directed by Tufan Isaak oglu Akhundov

The site of Polutepe is situated on the south coast of Injachay river, on the territory of Uchtepe village, in the Jalilabad district of Azerbaijan. It is a narrow belt (zone) of the eastern part of the Mughan steppe limited by the spurs of Brovary Range to the west and the Caspian Sea to the east. Presently, the settlement is represented by a 6-ha ashy hill of up to 6 m high. Its central part is occupied by the modern cemetery of Uchtepe village. Extensive excavations have revealed cultural layers of 7 m thick. The upper layer of the site's deposits is 1 m thick and is represented by the remains of a Medieval settlement related to the IX–XI centuries CE. It is saturated with a large number of simple and glazed ceramics characteristic of the above-mentioned time.

The lower 6 m layer of cultural deposits of the settlement belongs to the Neolithic period. It contains various remains of Neolithic material culture characteristic of other Neolithic settlements of this region and which were defined by us as “Mughan Neolithic” culture. A large number of remains of ceramic utensils, bone and stone tools and other objects, burials of Neolithic inhabitants of this settlement, remains of different constructions from adobe and kilns for baking of ceramics were revealed in the different construction horizons of this layer. The greatest part of the excavated area represents a productive sector of the settlement and the revealed constructions are mainly represented by the remains of different round-planned, oval and rectangular barriers.

The unearthed burials of the settlement's inhabitants included individuals of mixed sex and all age groups, from babies to old adults aged several dozen years. The burial rituals had been performed in shallow pits on different plots among the constructions. The deceased were placed in crouched position of different degrees. Often, they were covered by red ochre and were decorated with beads that were furnished by ceramic bowl. The lower horizons of the cultural layers revealed a cult hearth and more than two dozen small stylised female clay figures.

In the stretch between the Medieval and Neolithic layers ruins and separate findings of ceramics belonging to Kura-Araxes culture and different stages of the Middle Bronze Age have been revealed as well (Akhundov, 2011; Akhundov et al., 2017).

One individual from Polutepe was analyzed for aDNA and is included in genetic analyses.

- ■ POT002 (Polutepe Burial N2) is an infant buried in a pit in a crouched position and the head orientated to the north-west. The burial was unearthed at 2.4 m depth from the Neolithic layer (approximately 10 m below the earth). The remains of the infant were very poorly preserved. Dating of human tooth: 5508–5376 cal BCE (6491 ± 26 BP, MAMS-40331)

**Tell Atchana (Alalakh), Turkey**

36.23778°N, 36.38472°E

Excavation: Trustees of the British Museum, 1937-1939 and 1946-1949, directed by Sir Leonard Woolley; Turkish Ministry of Culture and Tourism, 2003-present, directed by Kutlu Aslıhan Yener

Tell Atchana is located at the southward bend of the Orontes River in the Amuq Valley in the modern state of Hatay, Turkey (Yener, 2005, 2010). The latest chronology (see Yener, 2013a; Yener et al. 2019) puts the foundation of the site in the terminal Early Bronze Age or the earliest Middle Bronze Age (ca. 2200-2000 BCE) and the abandonment of the city in the Late Bronze Age at ca. 1300 BCE, with an Iron Age re-occupation constituting Level O (ca. 1190-750 BCE). Three hundred and forty-two burials have been documented to date, although 151 of these were excavated in the initial excavations in the 1930s and 1940s, conducted by Sir Leonard Woolley (Woolley, 1955), and the skeletal remains were not preserved. The remaining 180 graves have been discovered since 2003 as part of the renewed excavations directed by K. Aslıhan Yener. Of these, 134 were found in an extramural cemetery just outside the city fortification wall in Area 3 on the northeast slope of the mound (Akar, 2017a; Ingman, 2017; Yener and Yazıcıoğlu, 2010), while the remaining 57 were within the city in various locations, e.g., in abandoned buildings, in courtyards, etc., 26 of which were found in 2015-2019 in Area 4 in what seems to be a designated cemetery area. The overwhelming majority of the graves are single, simple pit burials, although multiple burials, cist graves, pot burials, secondary burials, and cremations have also been found in smaller numbers, as well as two constructed tombs, the Plastered Tomb in the extramural cemetery and the Shaft Grave in the Level VII (Middle Bronze II) palace (Woolley, 1939, 1955). The preservation of the burials varies widely, with those in the extramural cemetery often badly preserved and heavily disturbed, due to proximity to topsoil, slope wash, and other post-depositional processes (Akar, 2017a; Ingman, 2017) and those which are within the city walls typically much better preserved. Types and numbers of grave goods also varies with burial context, with grave goods being much rarer in the extramural cemetery, typically consisting of one or two ceramic vessels and perhaps a single piece of jewelry (typically either a metal pin or a beaded bracelet/necklace) (Ingman, 2017). In the burials within the city, though, grave goods generally are much more numerous and varied (Ingman, 2020).

Little is known about the city's early history, given the very small areas exposed to date, but the material culture recovered belongs largely to the Northwest Syrian so-called Amorite horizon, including especially Syro-Cilician Ware ceramics (Bulu, 2016, 2017; Heinz, 1992; Woolley, 1955). Sometime during this period, Alalakh and Mukish became subservient to the Amorite kingdom of Yamhad, based in Aleppo, and the kings of Alalakh had close familial ties to the kings of Yamhad (Klengel, 1992; Lauinger, 2015). Most of our understanding of Middle Bronze Age Alalakh comes from the end of the period, in Period 7, where a large palace with an archive and an attached temple, as well as a tripartite city gate, the city's fortification wall, and another potential temple have been found (Woolley, 1955; Yener, 2015a, 2015b). This period marks the first real evidence of a nascent internationalism at Alalakh (Akar, 2017a), and it ends with a large-scale fire that burned the Royal Precinct (Klengel, 1992; Woolley, 1955), often attributed to the Hittite king Hattušili I in the course of his campaigns into Syria against Yamhad (Bryce, 2005). Although the precise date of the Period 7 destruction has not yet been fixed, it marks a shift in material culture and is therefore taken as the end of the Middle Bronze age at the site, ca. 1650 BCE.

The succeeding Late Bronze I, consisting of Periods 6-4 at Tell Atchana, can generally be described as having a Hurrian/Mitannian character. This period is unclear not only at Tell Atchana, but also across Syria more generally: the destruction of Aleppo and the kingdom of Yamhad by the Hittites, accomplished shortly after the destruction of Alalakh, was followed by their destruction of Babylon (Bryce, 2005; Klengel, 1992), ending the Amorite kingdoms and apparently causing no small amount of chaos in the region (Akkermans and Schwartz, 2003). By the early fifteenth century BCE, however, the kingdom of Mitanni, based at Washukanni in the Upper Khabur (identified as Tell el Fekheriye) (Bartl and Bonatz, 2013) had emerged from the territories once controlled by Yamhad (Akkermans and Schwartz, 2003), and Alalakh became a vassal to this new regional power. This period is most well-documented in Period 4 at the site, which is characterized by a palace with archives documenting a Hurrian-style class system and many Hurrian names (von Dassow, 2008), a temple, and other administrative buildings, such as Woolley's Level IV Castle (Woolley, 1955). The material culture of Late Bronze I shows affinities with the Hurrian world to the east, such as Nuzi Ware (Woolley, 1955; Yener et al., 2019), as well as strong contacts with other, more far-flung regions, such as Cyprus (Woolley, 1955; Yener et al., 2019). This period, like Period 7, ends with a site-wide burning ca. 1400 BCE that may be associated with Tudhaliya II (Akar, 2019).

Late Bronze II, Periods 3-1, represents the last stages of Mitanni vassalhood (Period 3) and the take-over of the city by the Hittites and its incorporation into their empire (Periods 2-1) (Yener, 2013a; Yener et al., 2019). The major construction in this period were the Northern and Southern Fortresses in Period 2 (Akar, 2013, 2019), which blend characteristics of Egyptian and Hittite defensive architecture. The scale of the construction projects, the unusual building techniques, and the hints of possible Hittite administration from this period, in the form of grain distribution tablets from probable late Period 3/early Period 2 contexts (von Dassow, 2005), all suggest that Hittite Great King Suppiluliuma I took over the site, installing a vassal to rule as governor [perhaps the Tudhaliya depicted on the basalt orthostat found by Woolley in the Level Ib temple; (Woolley, 1955) and that either the king or his governor initiated the Fortresses' construction (Yener et al., 2019). The arrival of the Hittites is also visible in the material culture of the site at this time, with the introduction of several types of North Central Anatolian (NCA) ceramics, typical of the Hittite homeland (Akar, 2017b; Horowitz, 2015, 2019), as well as Hittite seals and sealings (Woolley, 1955), and a Hittite-style shaft hole axe (Yener, 2011). Contacts with the Aegean world apparently increased, judging from the large quantities of Mycenaean wares found in these periods, and the Mitannian Nuzi Ware developed into a local style termed Atchana Ware which also continues to be found in great numbers (Yener et al., 2019). The Late Bronze II occupation ends ca. 1300 BCE, when the city was abandoned, except for the temple and perhaps several

buildings around it, which continued in use into the mid-13th century BCE (Yener, 2013a; Yener et al., 2019). Early Iron Age ceramics date partial architectural remains to the mid-twelfth century BCE, testifying to a small-scale re-settlement in this period (Montesanto, 2020; Pucci, 2020; Yener, 2013a). Another structure dating to Iron II has also recently been identified above the Northern Fortress, demonstrating that small-scale occupation continued, at least sporadically, at Tell Atchana, even while the main settlement moved to Tell Tayinat, the Iron Age capital of the area, only 713 m away (Yener, 2013a).

A total of 26 individuals from Alalakh produced genome-wide data and are included in genetic analyses.

- ■ ALA001 (Square 45.71, Locus 03-3017, Pail 257, Skeleton 04-9), Burial 4 in the Plastered Tomb (Yener, 2013b) in the Area 3 extramural cemetery, is the adult man (auricular age estimation of 40-45 years old) (Haas et al., 1994) in the bottom layer of this tomb. The remains exhibit the presence of Diffuse Idiopathic Skeletal Hyperostosis (DISH), a joint disease characterized by the formation of new bone in the shape of flowing melted wax found on the right side of thoracic vertebrae 4-10. DISH etiology is unclear, but it is believed to be related to obesity and diabetes (Waldron, 2001). Several of the joints and vertebrae exhibit signs of degenerative joint disease in the form of marginal osteophytes and enthesophytes (Waldron, 2001). Examination of the dentition exhibited two episodes of dental enamel hypoplasia correlating to the ages of 1.9/2.1 years and 4.5/4.7 years old, thus indicating two health disturbances that occurred during childhood growth periods (Hillson, 2014). A piece of plaster had been inserted into his mouth. His head was propped up with an s-curve jar, and in the area of his torso and pelvis were found seven bronze pins and a silver toggle pin. Eight gold appliques stamped with rosettes were around his head and chest, and a gold foil was to the left of his head. A Cypriot Base Ring I jug was along the southeast wall of the tomb and another was near his right forearm; two spindle bottles (one Red Lustrous Wheelmade Ware and one locally made in Red Burnished Ware) were found, one placed in the south corner of the tomb and one at his left elbow; a Syrian Brown-Grey Burnished Ware cylindrical cup was in crook of his right arm and another was found just above his left elbow; and, a Red Slipped narrow-necked jug was along the southwest wall of the tomb. An amber pendant was found on his legs, along with a bone spindle whorl, several pieces of chert, and beads of carnelian, bone, faience, and glass were also discovered with the body. Two haunches of beef had been placed near his left arm and left femur, and a caprid molar was also found with his remains, indicating that food had been deposited with him. This is the single richest assemblage of grave goods ever found with an individual at Tell Atchana. Dating of human bone: 1496-1325 cal BCE (3151 ± 24 BP, MAMS-33675).
- ■ ALA002 (Square 45.71, Locus 03-3017, Pail 246, Skeleton 04-8), Burial 2 in the Plastered Tomb (Yener, 2013b) in the Area 3 extramural cemetery, is the young adult male (age estimation of 19-21 years based on the different degrees of epiphyseal plates fusion) (Schaefer et al., 2009) in the top layer of this tomb. The orbital bones exhibit *cribra orbitalia*, along with porotic hyperostosis on both parietal bones located medially along the coronal suture, indicating the body's response to a pathological condition (Rothschild, 2002). Both humeri have the non-metric trait of Septal Aperture (Barnes, 2012). A vertical bone had been placed inside his mouth. Six bronze pins were found around his torso, along with a bone needle. Several gold appliques stamped with rosettes (one with red pigment preserved on the stamped side) were found near his head, and he was wearing an *in situ* necklace of alternating gold, carnelian, and vitreous white beads. Additional beads of the same materials were also found with this individual. A gold ring was found *in situ* on his left thumb. Several clay pellets and pieces of chert, as well as two lumps of vitrified material (one placed under his chin), were also found with this individual. Dating of human bone: 1496-1401 cal BCE (3158 ± 22 BP, MAMS-33676).
- ■ ALA004 (Square 45.72, Locus 03-3002, Pail 40, Skeleton 04-25) is an adult male (age estimated as 40-45 years old) (Haas et al., 1994) found in a bone scatter that likely represents a disturbed primary burial in the Area 3 extramural cemetery. The remains are half complete and mixed with other individuals' remains. Both fibulae and the right tibia all exhibit well-healed Periostitis (indicating an episode of infection or trauma) along the medial shafts (Mann and Hunt, 2005). Marginal osteophytes and enthesopathy are found on the pelvis and left shoulder (Waldron, 2001), a condition that is typical of old age. The skull exhibits a well-healed trauma located on the left side of the frontal bone (Byers, 2011). No grave goods were recovered. Dating of human bone: 1895-1752 cal BCE (3507 ± 23 BP, MAMS-33677).
- ■ ALA008 (Square 45.44, Locus 133, AT 17652) is represented by an adult skull (with features indicating a male, age estimation of 25-35 years) (Haas et al., 1994) and several finger bones, although the simple pit grave continued into the east baulk, in the Area 3 extramural cemetery. No grave goods were found. Dating of human bone: 1881-1700 cal BCE (3473 ± 23 BP, MAMS-33678).
- ■ ALA011 (Square 45.44, Locus 146, AT 18960) is a child (3.5-4 years old) (Schaefer et al., 2009) buried in a simple pit grave inside a casemate within the Area 3 fortification wall (Ingman, 2017; unpublished data). Only the legs and feet were within the square, as the grave extended into the north baulk. A Simple Fine Ware shoulder goblet was found in the baulk near the child's pelvis. Dating of human bone: 1741-1624 cal BCE (3382 ± 23 BP, MAMS-33680).
- ■ ALA013 (Square 45.44, Locus 152, AT 19260) is an infant (dental age of 1.5-2 years old) (Schaefer et al., 2009) found in the Area 3 extramural cemetery. Age estimation based on skeletal long bone growth gave an age of 6-8 months (Schaefer et al., 2009), thus indicating that the child had stunted growth of around 1 year. The upper first molars exhibit the dental morphology feature of Carabelli's cusp (Scott and Irish, 2017). A bronze ring and a silver ring, two beaded necklaces, a Simple Ware biconical cup (at the left elbow), a Simple Ware globular juglet (at the left side of the pelvis), a Simple Ware short-neck jar

- (at the left elbow), and a piece of lead wire were found. Dating of human bone: 1878-1693 cal BCE (3457 ± 24 BP, MAMS-33681).
- ■ ALA014 (Square 45.45, Loci 8 and 9, AT 8836) is an adult (age estimation of 35-55 years) (Haas et al., 1994) found in a simple pit grave in the Area 3 extramural cemetery. There were no grave goods. Dating of human bone: 1743-1630 cal BCE (3392 ± 23 BP, MAMS-33682).
  - ■ ALA015 (Square 45.45, Loci 18 and 19, AT 15741) is an adult found in the Area 3 extramural cemetery in a simple pit grave. A shell pendant was found in the grave. Dating of human bone: 2014-1781 BCE (3566 ± 26 BP, MAMS-33683).
  - ■ ALA016 (Square 32.54, Locus 85, AT 17541) is an adult female (age estimation of 65-75 years old) (Haas et al., 1994) buried in a simple pit grave in a temporarily abandoned building in the Royal Precinct below a subsequent floor. The skeletal remains exhibit evidence of degenerative joint disease (osteoarthritis - OA) found on the majority of the joints, such as knees and hand phalanges, with eburnation (Waldron, 2001). Vertebrae joints exhibited fusion, in addition to OA, with the cervical 7 and thoracic 1-4 all fused. There is the rare presence of adventitious bursa on lumbar 4 and 5 (Kwong et al., 2011). The frontal bone exhibited *hyperostosis frontalis interna* on the ventral surface (Roberts and Manchester, 1995). Examination of the dentition showed two episodes of dental enamel hypoplasia correlating to the ages of 2.8/3.1 years and 4.2/4.9 years old (Hillson, 2014), thus indicating two health disturbances that had occurred during childhood growth periods. A bronze pin was next to the skull, and several bone and vitreous beads were in the area of the neck. Dating of human bone: 1617-1506 cal BCE (3566 ± 26 BP, MAMS-33683).
  - ■ ALA017 (Square 32.57, Loci 160 and 164, AT 10070) is a young adult female (dental age of 17-25 years old) (Brothwell, 1981) buried in a simple pit burial dug into a street in the Royal Precinct. Only the top of the skull was found within the excavation area, as the rest of the burial extended into the east baulk. The nuchal crest is score 4, as a male (Haas et al., 1994), thus indicating the use of the neck muscles for carrying heavy material, possibly on the head. The upper first molars exhibit the dental morphology feature of Carabelli's cusp (Scott and Irish, 2017). The skull and the deposit above it were both burnt, likely as a result of a post-deposition burning episode unrelated to the burial. Three Grey Burnished Ware vessels (a narrow-necked jug, a long-necked globular juglet, and an omphalos bowl) were grouped above the head, and a conch shell pendant was also recovered from the burial. Dating of human bone: 1614-1466 cal BCE (3264 ± 23 BP, MAMS-33685).
  - ■ ALA018 (Square 42.29, Locus 44, AT 19127) is a child (dental aged at 4.5-5.5 years) buried in a simple pit grave in an accumulation fill not far outside the Royal Precinct. Skeletal growth gave the age estimation of 3.5-4 years (Schaefer et al., 2009), thus indicating a stunted growth by around 1 year. Examination of the dentition exhibited two episodes of dental enamel hypoplasia correlating to the ages of 1.5/1.7 years and 2.0/2.3 years old (Hillson, 2014), thus indicating two health disturbances during childhood growth periods. A string of vitreous beads was around the neck, a Nuzi Ware goblet was behind the feet, and an astragalus was also found in the grave. Dating of human bone: 1497-1326 cal BCE (3154 ± 26 BP, MAMS-33686).
  - ■ ALA019 (Square 32.57, Locus 247, AT 15878) is an adult female aged 40-45 years old (Haas et al., 1994) found at the bottom of a very deep well [hence, dubbed "the Well Lady"; (Shafiq, 2020)]. The remains exhibit presence of osteoarthritis with eburnation (OA) on the cervical vertebrae between C1 and C2 (Waldron, 2001), along with the rare presence of adventitious bursa (Kwong et al., 2011) on lumbar 3 and 4. The individual shows evidence of healed trauma on the frontal bone of the skull (Byers, 2011) and two healed fractured ribs (Shafiq, 2020). Enthesophytes were found on both calcaneal bones (Waldron, 2001). The upper lateral incisors exhibit the dental morphology feature of shoveling, score 5 (Scott and Irish, 2017). Her dentition exhibited multiple episodes of dental enamel hypoplasia, starting from 1.3 years old up to 4.6 years old, with a total of twelve childhood growth disturbances (correlating to the ages of 1.3/1.5, 1.7/1.8, 1.9/2.0, 2.0/2.3, 2.6/2.8, 2.7/3.0, 2.8/3.1, 3.1/3.4, 3.5/3.7, 3.7/4.2, and 4.0/4.4-4.6 years old) (Hillson, 2014). She was discovered facedown with her limbs splayed, indicating that she had been carelessly thrown into the well while it was still in use (probably for domestic/craft purposes or for animals). As this individual's deposition was the result of misadventure, rather than deliberate burial, there are no accompanying grave goods. Dating of human bone: 1625-1511 BCE (3298 ± 23 BP, MAMS-33687).
  - ■ ALA020 (Square 44.86, Loci 18 and 22, AT 15460) is a young adult female (age estimation of 25-35 years old) (Haas et al., 1994) buried in a simple pit grave dug into a debris layer in Area 2, although bones of another individual, a male, based on the pelvic features, were mixed into the debris. The frontal bones exhibit *cribra orbitalia*, indicating a stressful health condition at the time of death (Rothschild, 2002). The dentition exhibits dental enamel hypoplasia occurred at the ages of 1.7/1.8 and 2.2/2.4-2.7 (Hillson, 2014). No grave goods were found. Dating of human bone: 1502-1395 BCE (3167 ± 29 BP, MAMS-33688).
  - ■ ALA023 (Square 45.44, Locus 65, AT 6029) is a child (dental age of 6.5-7 years) (Schaefer et al., 2009) in a simple pit grave -part of a cluster of three burials in the Area 3 extramural cemetery (with ALA025 and Locus 67)- whose skull was placed directly over that of ALA025. The skull exhibits the non-metric feature of Apical Bone on the occipital bone (Barnes, 2012). A lead ring was found in the fill above the remains. Dating of human bone: 1921-1763 BCE (3520 ± 25 BP, MAMS-38610).
  - ■ ALA024 (Square 45.44, Locus 68, AT 6572) is a child (2-3 years old) (Schaefer et al., 2009) in a simple pit grave in the Area 3 extramural cemetery. A Simple Ware short-neck jar was found above her head. Dating of human bone: 2111-1779 BCE (3586 ± 39 BP, MAMS-33690).
  - ■ ALA025 (Square 45.44, Locus 66, AT 6032) is an adolescent female aged 13-14 years old in a simple pit grave directly under ALA023 in the Area 3 extramural cemetery. The skeletal growth of long bones gives an age of 11 years old (Schaefer et al., 2009), indicating stunted growth of two years. The frontal bones exhibit *cribra orbitalia* (Rothschild, 2002) in the healing process

at the time of death. Dentition exhibit two health disturbances, with dental enamel hypoplasia at the ages of 3.3/3.4 and 4.3/4.8 years (Hillson, 2014). A Simple Fine Ware short-neck jar was placed on her crossed arms. Dating of human bone: 1877-1686 BCE (3443 ± 25 BP, MAMS-33691).

- ■ ALA026 (Square 45.44, Locus 70, AT 6931) is a child aged 3.5-4 years in a simple pit burial in the Area 3 extramural cemetery. However, the skeletal age gives 2.5 years (Schaefer et al., 2009), indicating in stunted growth of 1 year. A Syrian Brown-Grey Burnished Ware piriform juglet was placed near the mandible. Dating of human bone: 1744-1628 BCE (3390 ± 25 BP, MAMS-33692).
- ■ ALA028 (Square 45.44, Locus 73, AT 7395) is an adult female aged 30-40 years old (Haas et al., 1994) represented by disarticulated remains in simple pit grave in the Area 3 extramural cemetery. This grave was directly above the pit grave of ALA029, with the pelvis of ALA028 resting on the skull of ALA029. This burial likely represents a primary burial that was disturbed; the disturbed remains were collected and then reburied. No grave goods were found. Dating of human bone: 1877-1666 BCE (3440 ± 26 BP, MAMS-33693).
- ■ ALA029 (Square 45.44, Locus 79, AT 7695) is an adult female aged 20-30 years old (Haas et al., 1994) represented by the skull in a simple pit grave directly below ALA028. The skull was partially crushed by the pelvis of ALA028, which rested directly on top of it. Although the majority of the bones were in anatomical position, the grave was clearly reopened/disturbed in antiquity, as both femurs had been turned upside-down. This may have occurred at the same time as ALA028's burial. A Simple Ware short-neck jar was under her chin, a Syrian Brown-Grey Burnished Ware piriform juglet was behind her skull, and a toggle pin was found during screening. Dating of human bone: 1880-1695 BCE (3465 ± 26 BP, MAMS-33694).
- ■ ALA030 (Square 45.44, Locus 105, AT 10669) is an adult female, aged 30-35 years old (Haas et al., 1994), who seems to have been killed during the destruction of the building next to the fortification wall in Area 3. The remains indicate a rather small-sized female, with a collapsed vertebra body of L1 (Waldron, 2001) on the left side of the vertebral body, a possible case of carrying heavy weights, along with bone growth on lower thoracic T11 and T12. The left shoulder exhibit a condition of *osteochondritis dissecans*, a joint pathology (Waldron, 2001). Both humeri exhibit the non-metric trait of Septal Aperture (Barnes, 2012). The upper incisors show the dental morphology feature of shoveling (Scott and Irish, 2017). Evidence of six health disturbances during the growth period are visible as dental enamel hypoplasia at the ages of 1.3/1.5, 1.7/2.0, 1.9/2.1, 2.6/2.8, 2.8/3.1, and 3.2/3.3 years (Hillson, 2014). Found in a burnt room context, she was discovered on her back with her arms pulled up to her chin and her legs disappearing into the west baulk. Because this individual met with her death, and was subsequently buried, by misadventure, there were no grave goods. Dating of human bone: 1612-1457 BCE (3256 ± 25 BP, MAMS-33695).
- ■ ALA034 (Square 45.45, Locus 6, AT 8830) is an adult female aged between 25-35 years old (Haas et al., 1994) whose simple pit grave in the Area 3 extramural cemetery remains mostly within the west baulk. No grave goods were found. Dating of human bone: 1874-1666 BCE (3436 ± 24 BP, MAMS-33696).
- ■ ALA035 (Square 45.45, Locus 7, AT 7940) is an adult male aged between 25-35 years old (Haas et al., 1994) whose remains were found in the Area 3 extramural cemetery in a simple pit containing the dense and highly disarticulated remains of three other adults (two males and one female). ALA035 appears to have been a primary burial, and the remains of the three other adults were likely redeposited with this individual after having been disturbed. The lower limbs, femur, and tibia exhibit *periostitis* along the shafts (Mann and Hunt, 2005), and joint disease of the scapula was also identified (Waldron, 2001). There is one line of dental enamel hypoplasia at the age of 1.9/2.1 years old (Hillson, 2014). No grave goods were found. Dating of human bone: 1948-1774 BCE (3542 ± 24 BP, MAMS-33697).
- ■ ALA037 (Square 45.45, Loci 30 and 31, AT 11452) is a concentration of bones containing the disturbed remains of multiple individuals in the Area 3 extramural cemetery. The long bones are oriented northeast-southwest, parallel to the slope of the mound in this area, which may be the result of post-depositional slope wash or deliberate secondary repositioning. Given the high degree of disturbance in this area generally due to post-depositional processes (Ingman, 2017), the former is perhaps more likely. No grave goods were found. Dating of human bone: 1882-1701 BCE (3477 ± 24 BP, MAMS-33698).
- ■ ALA038 (Square 45.71, Locus 03-3017, Pail 236, Skeleton 09-07), Burial 1 in the Plastered Tomb (Yener, 2013b) in the Area 3 extramural cemetery is an adult female (aged 35-45 years old) (Haas et al., 1994) in the top layer of this grave and the final individual deposited in the tomb. Both humeri exhibit the non-metric trait of Septal Aperture (Barnes, 2012). Although, this burial was disturbed, probably due to its proximity to the topsoil, in the area of her head and torso were found several bronze pins, as well as beads made of gold, metal, amber, and stone. Two Simple Ware bottle jugs were placed with her, one atop her torso and one along her left femur, and two Simple Ware globular pitchers were found, one near her skull and one at her right hip. A Simple Ware lamp was under the right side of her pelvis. A cattle humerus and a sheep haunch were above the right side of her pelvis, indicating that food offerings were deposited with this individual. Dating of human bone: 1613-1461 cal BCE (3260 ± 24 BP, MAMS-33699).
- ■ ALA039 (Square 44.85, Locus 15, AT 14466) is represented by a skull of an adult female aged 50-60 years old (Haas et al., 1994) and was placed upright with a human pelvis (presumably belonging to the same individual, but this is uncertain) next to it. These remains were found in a simple pit dug into an accumulation layer with *tandirs* and trash pits in Area 2. The skull shows evidence of blunt trauma located on the right parietal bone in a circular shape, with the bones fractured ventrally. There are no radiating fracture lines and no signs of healing, termed *perimortem*. The fracture size measures 16.2 × 15.3 mm with a depth inside the bone of 2.5 mm, suggesting that this was most probably the cause of death, indicating a violent death (Byers, 2011).

Under the skull was a chunk of iron oxide. This is likely a secondary burial, given the iron oxide and the non-random positioning of the skull, but it could also have been disturbed from an unpreserved (or as-yet-undiscovered) grave. Dating of human bone: 1448-1303 BCE (3125 ± 24 BP, MAMS-33700).

- ■ ALA084 (Square 45.72, Locus 03-3065, Skeleton 04-19) is an adult female aged 25-30 years (Haas et al., 1994), buried in a simple pit grave in the Area 3 extramural cemetery. The ventral surface of the occipital, parietal, and frontal bones all exhibit meningeal reaction, indicating a case of infection or trauma (Schultz, 2003), and porotic hyperostosis was also observed (Rothschild, 2002). No grave goods were found. Dating of human tooth: 2006-1777 BCE (3556 ± 25 BP, MAMS-41108).
- ■ ALA095 (45.72, L03-3013/3016, pail 54) is represented by a tooth that was part of a heap of bones and teeth from a minimum of three individuals (2 mature and 1 immature) lying on top of a single pit grave of an adult male from the Area 3 extramural cemetery. No grave goods were found. Dating of human tooth: 1913-1756 BCE (3516 ± 25 BP, MAMS-41109)

### Tell Mardikh (Ebla), Syria

35.798°N, 36.798°E

Excavation: Italian Expedition of the Sapienza University of Rome (Missione Archeologica Italiana in Siria - MAIS), 1964-2010, directed by Paolo Matthiae

Tell Mardikh, ancient Ebla is an archaeological site located in the Idlib Governorate, 56 km southwest of Aleppo, on the limestone plateau of Northern Syria. The excavations revealed a long occupation sequence, spanning from at least Early Bronze Age III until the Iron Age, with later occupation or frequentation in the Hellenistic/Roman, Byzantine, and Crusader Periods (for an overview, see Matthiae, 2010).

Although stray archaeological materials dating from the Chalcolithic period were found at Ebla, the earliest settlement uncovered thus far at Tell Mardikh dates from Early Bronze III (ca. 2750/2700-2550 BCE) and is represented by the remains of non-residential structures with facilities for crop storage uncovered on the Acropolis Italian Expedition of the Sapienza University of Rome (Matthiae, 1993b; Mazzoni, 1991; Vacca, 2015). This evidence documents a formative phase of urbanisation that puts the developmental trajectory of Ebla in line with the development of other archaeological site in western inland Syria, such as Hama and Qatna, and with neighboring regional areas, such as the Middle Euphrates Valley and the Jazirah (Vacca, 2015).

The process toward increasing social, economic, and political complexity continued during the initial stage of Early Bronze IVA (ca. 2550-2450 BC) (Vacca, 2014-2015, 2015). It culminated, in the developed phase of the Early Bronze IVA (ca. 2450-2300 BCE), in the formation of an archaic state ruled by Ebla (Matthiae, 2013b), documented by the archives of cuneiform tablets discovered in the destruction layer of the Royal Palace B dating from this period. It is estimated that the territory controlled by Ebla extended from around Hama, to the south, to Karkemish, to the north. At this time, Ebla had diplomatic and commercial relationships with equivalent kingdoms located along the Euphrates River Valley, in Upper Syria and in Upper Mesopotamia, as well as with Byblos and with Egypt. A fierce destruction put an end to this flourishing phase (Matthiae, 2009a), which is placed in the interval between 2367 and 2297 cal BCE by the average weight of available radiometric determinations (Calcagnile et al., 2013).

After this dramatic event, during Early Bronze IVB (ca. 2300-2000 BCE) Ebla lived a stage of initial crisis and following reorganization during the initial and central stages of the period, respectively, followed by a phase of new growth, represented by the reappearance of public, monumental architecture at the site, during the late phase of the period, during the 21st century BCE (D'Andrea, 2014-2015; Matthiae, 2006, 2007, 2009b). At this time, Ebla had commercial relations with the Ur III Dynasty in southern Mesopotamia. Another destruction put an end to this phase of the settlement (Matthiae, 2009a, 2020) followed by a short squatters' reoccupation (Matthiae, 2020; D'Andrea, 2014-2015, 2018) and by a substantial reconstruction of the city of the Middle Bronze Age at the onset of the 2<sup>nd</sup> millennium BCE, when an Amorite dynasty seized power.

It seems more and more possible that some of the cultural developments of the Middle Bronze Age (ca. 2000-1600 BCE) started earlier, during Early Bronze IVB and elements of continuity between Early Bronze IV and the Middle Bronze Age have been noticed in material culture, architecture, iconography, and royal ideology (D'Andrea, 2019; Matthiae, 2002, 2013a; Pinnock, 2009). However, the reconstruction of the Middle Bronze Age city was marked by substantial changes in the urban layout. The new 2<sup>nd</sup> millennium BCE city comprised the massive earthen rampart fortifications with four city-gates and several forts and fortresses; a Royal Citadel with a royal palace and dynastic temple on the Acropolis (Matthiae, 2011), encircled by an inner fortification; and a belt of temples, sanctuaries, and palaces around the Acropolis uncovered on the north, west and south sides.

Epigraphic data allowed determining that the new Middle Bronze Age city was the seat of Amorite leaders since the beginning. From circa 1800 BCE, Ebla was subjugated by the kingdom of Yamhad, centered on Aleppo, but remained a major regional center, with a flourishing and sophisticated urban culture, as testified, for example, by the jewelry and metalwork found in the Royal Hypogea or the bone and ivory Egyptianizing inlays discovered in the Northern Palace (Scandone Matthiae, 2002), as well as with far-reaching interregional relations. A third, final, destruction brought also the Middle Bronze Age settlement of Ebla to an end; from a bi-lingual Hittite-Hurrian text called Song of Release, it seems that the site was destroyed by a coalition of Hittites and Hurrians led by an otherwise unknown personage called Pizikarra of Nineveh (Matthiae, 2009a).

After this major destruction, the site never recovered as a regional center, although it was continuously occupied during the Late Bronze Age (ca. 1600-1200 BCE), as demonstrated by the archaeological investigations on the Acropolis (Matthiae, 2011). The site was occupied by a rural village during Iron Age I-III (ca. 1200-535 BCE), and was the seat of a palace during the Persian/Hellenistic

Period (ca. 535-55 BCE). Subsequently, it was occupied by a monastic community during the Roman/Byzantine Period (ca. 55 BCE-AD 600), and, after this, it was never permanently settled again; at the time of the First Crusade, at the end of the 11<sup>th</sup> century AD, the troops of Godfrey of Bouillon shortly stopped at the site on their way to Jerusalem (Matthiae, 2010).

A total of eleven individuals from Ebla produced genome-wide data and were included in genetic analyses.

- ■ ETM001 (individual from TM.82/79.G.400, Dep K (A+B) or Tomb D1) (Baffi Guardata, 1988) is a 5 to 7-year-old child represented by a fragmentary skull and a few fragmentary skeletal remains in a multiple pit burial. The pit was cut through the layers associated with the EB IVA Palace G and is dated to the Middle Bronze I (ca. 2000-1800 BCE). Funerary goods included 19 pottery vessels, a bronze bracelet, and animal bones (Baffi Guardata, 1988).
- ■ ETM004 (TM.98.V.538, D.7417, Skull A) is a child aged between 6 and 12 years whose remains were identified by a skull in a pit burial with multiple mixed disarticulated inhumations (e.g., ETM005 and ETM006). The burial is dated to the Middle Bronze Age I (ca. 2000-1800 BCE). Funerary goods were represented by 16 pottery vessels, either complete or almost complete.
- ■ ETM005 (TM.98.V.538, D.7417, Skull B; same burial as ETM004) is an adult aged between 30 and 40 years identified by the skull. Dental pathologies were observed.
- ■ ETM006 (TM.98.V.538, D.7417, Skull C; same burial as ETM004) is an adult aged between 30 and 40 years identified by the skull. Dental pathologies were observed.
- ■ ETM010 (TM.98.CC.113, D.7278) is a macroscopically possible male individual, aged between 30 and 40 years in a pit grave from the Early Bronze III Period (ca. 2700-2500 BCE). The skeletal remains were fragmentary and disarticulated. Dental pathologies and osteological conditions at the lower limbs were observed.
- ■ ETM012 (TM.91.P.853/2) is an infant aged 6-12 months, possibly buried in a jar. The skeletal remains were found in room L.5021 of Building P4 (for the archaeological context and pottery assemblage of the building) (see Matthiae, 1993a, 2013; Marchetti and Nigro, 1995-1996), a workshop area, lying on the floor of the room, along with a large amount of pottery sherds, suggesting that this might have originally been a jar burial. In spite of the fragmented condition of the burial, almost the complete skeleton of the infant was recovered. No evidence of pathologies was present and no associated funerary goods were found. Dating of human bone: 2572-2470 cal BCE (3997 ± 25 BP, MAMS-41114)
- ■ ETM014 (TM.95.V.491, D.6371) is an individual aged between 30 and 35 years in a poorly preserved pit burial (Baffi Guardata, 2000). The skeletal remains were also very fragmentary. Caries were observed on one of the preserved teeth. The tomb was identified in the area of the Middle Bronze Age I (ca. 2000-1800 BCE) rampart; funerary goods were represented by a single combed jar (Baffi Guardata, 2000).
- ■ ETM016 (TM.95.V.497, D.6384) is a male individual aged 20-30 years, buried in a crouched position in a pit that dates to the Late or terminal Middle Bronze IB (ca. 1850 BCE). The pit burial was possibly originally lined with mud bricks. The complete skeleton was preserved (Baffi Guardata, 2000) and did not display any evidence of pathologies. Funerary goods included five pottery vessels: a miniature cup in Cooking Ware fabric, a cooking pot, a combed jar, a miniature trefoil-mouthed juglet, and a carinated bowl (Baffi Guardata, 2000). Dating of human bone: 2026-1896 cal BCE (3605 ± 25 BP, MAMS-41116)
- ■ ETM018 (TM.98.AA.310, D.7363) is a macroscopically possible male individual, older than 45 years who was identified by an incomplete skull. He was buried with at least two more individuals in a pit burial that was covered by mud bricks and was dated to the Middle Bronze I (ca. 2000-1800 BCE). His dental condition is consistent with the age at death. Funerary goods included a fragmentary clay figurine, a shell, and eight pottery vessels: a jar, two collared jars/bowls, a piriform jar, an ovoid jar, and three carinated bowls. Presence of animal bones was associated with the burial. Dating of human tooth: (2135-1964 cal BCE, 3667 ± 26 BP, MAMS-41635)
- ■ ETM023 (TM.82.G.438, D. μ TM.83.G.438) is an individual aged 15-18 years that was found in pit seemingly intruding into the Early Bronze IVA layers of Palace G. The skeletal remains of this individual were incomplete and exhibited visible signs of burning. The skull was recovered complete. The chronology is not determined, although the anthropological report refers to an EB IVA date for the bones (ca. 2350/2300 BCE).
- ■ ETM026 (TM.83.G, D.3620 or D.22 in Baffi Guardata [2000]) is a male individual aged 25-30 years, in a primary crouched burial. The pit burial is dated to the Middle Bronze I (2000-1800 BCE), possibly to its earliest phase (Nigro, 2002). The skeletal remains were well preserved, though incomplete and fragmentary. The dentition displayed evidence of tartar and enamel hypoplasia. Funerary goods include a jar with double-everted rim and a cooking pot (Baffi Guardata, 1988) and the skull of an ovine was associated with the human bones (Baffi Guardata, 1988)

### Tell Kurdu, Turkey

36.329405°N, 36.444255°E

Excavation: University of Chicago, Oriental Institute, 1995-2001, directed by Kutlu Aslıhan Yener. The site of Tell Kurdu is located in the Amuq Plain in the Turkish province of Hatay in southern Turkey (Özbal et al., 2004). The roughly triangularly shaped Amuq Plain measures about 35 × 40 km and is covered with fertile agricultural soils. The plain is surrounded on all sides by upland ranges including the Amanus Mountains, Kurt Dağ, Jebel Zahwiye and Jebel al-Aqra and is fed by three rivers: the Kara Su, the Afrin and the Orontes. The mound of Tell Kurdu, located centrally in the plain, was occupied in the 6<sup>th</sup> and the 5<sup>th</sup> millennia BCE and is the

largest prehistoric site known in the valley. The 6<sup>th</sup> millennium levels at the site correspond to the Amuq C Phase contemporaneous with the North Mesopotamian Halaf Period, while the 5<sup>th</sup> millennium levels correspond to the Amuq E Phase, which based on the Northern Mesopotamian chronological periods equates with the Ubaid Period. All of the six burials from Tell Kurdu analyzed for this project come from the 2001 excavations which were concentrated on the north of the mound (Özbal, 2006). Excavations here yielded a neighborhood of densely packed small structures separated by streets and alleys that date to the Amuq C Phase of the 6<sup>th</sup> millennium BCE. Based on stratigraphy, one of the burials analyzed (KRD001) was securely dated within the architectural phase while most of the other burials in this study including KRD003, KRD004, KRD005, KRD006 were stratigraphically unclear and were assumed to date to just after the architecture had been abandoned. However, the radiocarbon dates suggest that they fall squarely within the main architectural phase or were buried very briefly following abandonment. Even though it essentially came from the same area, KRD002 dates to about a millennium later when this part of the mound functioned as a cemetery during the Amuq E Phase. The main occupation in this phase was concentrated on the southern parts of the mound. The age descriptions and sex designations for the burials described below come from an unpublished study by Lorentz and supersede those published in (Özbal et al., 2004).

A total of six individuals from Tell Kurdu produced genome-wide data and are included in the genetic analyses.

- ■ KRD001 (TK\_12:81) is an adolescent aged 10-12 years. The burial was securely dated to the Amuq C Phase related to the main architectural phase. No burial gifts were found associated with the skeleton which was discovered in a tightly flexed position. The inhumation was found cut into the lowest excavated floor of Room R06 and sealed by an overlying floor. Dating of human bone: 5710-5662 cal BCE (6783 ± 23 BP, MAMS-40663).
- ■ KRD002 (TK\_24:3) is a relatively well-preserved mature adult. The burial included one small Amuq E Phase painted cup which was placed not far from the individual's head. Unlike other burials which are typically found in simple pits, this one was placed in a rectangular mudbrick box of which the bottom row of bricks was preserved. Dating of human bone: 4991-4911 cal BCE (6044 ± 22 BP, MAMS-40664).
- ■ KRD003 (TK\_22:2) is a mature adult placed in a simple pit in a tightly flexed position. The burial included a small painted necked-jar placed near the head as well as a Dark Faced Burnished globular jar discovered by the feet. Dating of human bone: 5661-5630 cal BCE (6739 ± 23 BP, MAMS-40665).
- ■ KRD004 (TK\_25:80) is an adult male placed in a pit in a tightly flexed position. A small Dark Faced Burnished necked-jar was discovered by the head. A partial cattle mandible had been left just over the neck of the jar. Dating of human bone: 5703-5639 cal BCE (6766 ± 25 BP, MAMS-40666).
- ■ KRD005 (TK\_25:89) is an infant buried in a flexed position. A small unpainted vessel was directly by the infant's head. The burial's stratigraphic relationship to the architecture is not clear but it was placed in room R45 either when the room was in use or shortly after abandonment. Dating of human bone 5739-5676 cal BCE (6738 ± 24 BP, MAMS-40667).
- ■ KRD006 (TK\_26:12) is an infant placed in a large bowl. Near the infant and possibly associated with the burial, excavations yielded a small painted miniature vessel, which based on decoration and style must be considered Amuq C in date. Given the location of the burial inside room R54 and the motifs on the nearby vessel, we expect this burial to be contemporaneous with the others analyzed here (with the exception of KRD002) and that it dates to approximately 5700 cal BCE.

### Titriş Höyük, Turkey

37.4759306°N, 38.6783333°E

Excavation: University of California San Diego 1991-1999, directed by Guillermo Algaze

Titriş Höyük, situated in the lower Euphrates basin, is located 45 km north of Şanlıurfa, Turkey (Matney and Algaze, 1995). On the basis of C14 dating, three culture levels were identified at the site; Early EBA (ca. 2900–2600 BCE), Mid EBA (ca. 2600/2500–2400/2300 BCE) and Late EBA (ca. 2300–2200/2100 BCE) (Algaze et al., 1995, 1996, 2001; Matney et al., 1997, 1999). Spread over a 43-hectare area, Titriş Höyük has an acropolis in the center, the Lower Town surrounding the acropolis, and the Outer Town which consists of sparsely scattered suburban areas (Matney and Algaze, 1995).

The settlement expanded from the acropolis to the Lower Town during the Early EBA. In the Mid EBA, the Lower Town developed further and spread toward the Outer Town. There is an extramural cemetery dating to this period 400 m. west of the settlement. The settlement had undergone significant changes with the Late EBA; the houses in Outer Town were abandoned and the city was surrounded by a large fortification wall. Titriş Höyük people who started to live behind this wall in the Late EBA stopped using the extramural cemetery and began to bury their dead in housing areas, beneath the floors of rooms or courtyards (Laneri, 2007).

Since the excavations in the Early EBA level were limited to a small area, only one cist grave could be unearthed. On the other hand, there are 50 and 67 graves dating to Mid and Late EBA respectively. These graves consist of simple pits, stone cists and pithoi. Multiple burials were found in both Mid and Late EBA graves. While some individuals were articulated, some others completely lost their articulation. The skeletal remains which have no articulation, are represented only by skull and a few postcranial bones. It is stated that all the bones except skulls were removed to make room for the last deceased (Laneri, 2007; Matney et al., 2012). For this reason, the preservation condition of Titriş Höyük skeletal remains is not good and the individuals are represented only by fragments. Pots in various forms, bronze pins, bronze/silver earrings and rings, necklaces of stone beads are among the grave goods of both Mid and Late EBA graves. However, unlike Mid EBA graves, daggers and spearheads were found in Late EBA graves (Laneri, 2007).



The most remarkable burial among Titiş Höyük graves is the burial made on a plaster basin. Chemical analyses carried out with the samples taken from these plastered platforms found in most of the Late EBA houses demonstrate that these platforms might have been used in wine processing. The circular and slightly concave plastered platform, 140 cm in diameter, consist of a floor where small and medium-sized limestone is combined with muddy plaster at the bottom, pebbles in the middle and a thick limestone powder which was also used for the floor of the houses at the top (Laneri, 2002; Matney and Algaze, 1995). Skeletal remains belonging to minimum 19 individuals were found on one of these platforms during the 1998 excavation season (three subadults, three adult females, 13 adult males). At this unique burial, while postcranial bones were piled up at the center of the plaster basin, the crania were placed on the top of the postcranial bones at the edges without a unity of direction. 13 of the 16 adult individuals have perimortem traumas caused by an axe, dagger and spearhead on their skulls. Based on the presence of skeletal remains of each age and sex groups in this grave and the high frequency of perimortem traumata on the skulls, it was concluded that these individuals were victims of a possible massacre (Erdal, 2012a).

One individual from Titiş Höyük produced genome-wide data and is included in genetic analyses.

- ■ TIT021 (TH80084) is one of the 16 skulls on the plaster basin. Since it is a secondary burial, its relationship with scattered postcranial bones could not be established. Considering the morphological structure of the skull, the individual was estimated to be male. According to the ectocranial suture closure, it is estimated that the individual is a middle adult aged 35–40 years. There are two healed depressed traumas on the skull. In addition, two perimortem traumas were identified, one caused by a penetrating or a sharp object and the other by a sharp object. Due to the lack of healing marks around these penetrating and sharp force traumas on the left side of the skull, it was determined that the individual died as a result of these traumas. Dating of human tooth: 2331–2143 cal BCE (3799 ± 25 BP, MAMS-40684)

### Abbreviations

E = Early, M = Middle, L = Late, EP = Epipaleolithic, N = Neolithic, C = Chalcolithic, BA = Bronze Age, Eneolithic = En.

### Grouping of individuals and nomenclature

For the purpose of this study, we mainly used as group designation the name of the archaeological site and the archaeological period (Eisenmann et al., 2018). We caution here that period-based cultural divisions such as “Chalcolithic” and “Neolithic” vary from region to region and must be considered artificial boundaries instead of absolute chronological markers. For example, 6<sup>th</sup> millennium BCE is considered Early Chalcolithic in Anatolia and Late Neolithic in Southern Caucasus. Tell Kurdu, albeit located in Northern Levant, is a site that displays a mixture of both Anatolian and North Mesopotamian elements with regards to its architecture and material culture. Therefore, its 6<sup>th</sup> millennium BCE levels are more usually referred to as Early Chalcolithic based on the Anatolian chronological designations.

Sites for which samples covered more than one archaeological period were Arslantepe and Tell Kurdu. Given the temporal distribution of the samples at Arslantepe (Figure 2B), we grouped together all individuals from the Late Chalcolithic and the very beginning of Early Bronze Age as “Arslantepe\_LC” and those from Early Bronze age as “Arslantepe\_EBA.”

Genetic information (PCA-based) was also taken into consideration for outlying individuals (i.e., Alalakh\_MLBA\_outlier). Also, in order to maintain information about intragroup variability, we measured with  $f_4$ -statistics whether any individuals systematically shared more alleles with other populations compared to other individuals from the group.

Exception to the archaeological site-period nomenclature were the two Neolithic sites in the Southern Caucasian lowlands (Mentesh Tepe and Polutepe), each represented by only one individual (MTT001 and POT002 respectively). We grouped these two individuals as Caucasus\_lowlands\_LN (in agreement with  $f_4$ -statistics suggesting no breaks in their cladality). For consistency, we refer to the Chalcolithic site of Alkhantepe (ALX002) as Caucasus\_lowlands\_LC. Accordingly, published individuals/groups from Anatolia were renamed applying the same scheme, i.e., name of archaeological site “underscore” archaeological period.

For other ancient groups relevant to our study we applied a nomenclature system of area and archaeological time period (ex Levant\_EBA) provided that this does not contradict genetic evidence. Especially, for the area of Caucasus where genetic characterization has been carried on a big number of ancient individuals (Allentoft et al., 2015; Lazaridis et al., 2016; Wang et al., 2019), we used a combined nomenclature of ecogeographical area, archaeological time and genetic clustering. All new group labels are given in Table S3.

### METHOD DETAILS

#### Direct AMS radiocarbon dating

All individuals with newly-reported genetic data and without direct dating previously performed on them were dated at the radiocarbon dating facility of the Klaus-Tschira-Archäometrie-Zentrum at the CEZ Archaeometry gGmbH, Mannheim, Germany using a MICADAS-AMS and ~1gr of bone material. With a few exceptions, we dated a sample from the same skeletal element that was sampled for the DNA extraction. Collagen was extracted from the bone samples, purified by ultrafiltration (fraction > 30kD) and freeze-dried. Collagen was combusted to CO<sub>2</sub> in an Elemental Analyzer (EA) and CO<sub>2</sub> was converted catalytically to graphite. <sup>14</sup>C

ages were normalized to  $\delta^{13}\text{C} = -25\text{‰}$  and were given in BP (before present) meaning years before 1950. The calibration was done using the dataset INTCAL13 (Reimer et al., 2013) and the software SwissCal 1.0 (L. Wacker, ETH-Zürich).

### Preparation of aDNA

We extracted DNA and prepared next generation sequencing libraries from 174 samples in a dedicated aDNA facility in Jena following established protocols for DNA extraction and library preparation.

Prior to sampling of petrous bones, we carefully wiped the bone surface with 10% bleach and water and then UV-irradiated the surface for 30 min. Sampling targeted the inner-ear portion of the petrous bone (Pinhasi et al., 2015), but the method varied based on the preservation conditions of the sample and/or the destructive constraints as follows:

- Well preserved samples without constraints in destructive sampling: a bone wedge was cut out around the region of the cochlea using an electric saw (K-POWERgrip EWL 4941), removed the surface and ground it to fine bone powder.
- Poorly preserved samples: cutting in the middle with a jeweler's saw and drilling bone powder (K-POWERgrip EWL 4941) from one side directly at the osseous labyrinth.
- Minimally invasive method: removal of surface layer and drilling from outside targeting the area of the inner ear.

After UV-irradiation step (30 min) teeth were cut at the cemento-enamel junction and then sampled by drilling from the inner pulp chamber of the crown. Whenever this sampling method could not yield a minimum of 50 mg of bone powder, we complemented with bone powder drilled from the pulp of the root.

We used 50–100 mg of bone powder for the DNA extraction. First, we incubated the bone powder in a lysis buffer containing 0.45 M EDTA, pH 8.0 and 0.25 mg/ml Proteinase K with overnight rotation at 37°C. After centrifugation, we transferred the supernatant to a new 15 ml tube containing 10.4 mL of binding buffer of 5 M Guanidine hydrochloride (Sigma-Aldrich), 40% Isopropanol (Merck) and 400  $\mu\text{L}$  of 3 M Sodium Acetate pH 5.2 (Sigma-Aldrich). We spun the mix through a silica column (High Pure Viral Nucleic Acid Large Volume Kit; Roche) at 1,500 rpm for 8 min. We dry-spun the column with centrifugation at 14,000 rpm for 2 min and washed the DNA bound to the column twice with 450  $\mu\text{L}$  of wash buffer (High Pure Viral Nucleic Acid Large Volume Kit; Roche) and spinning at 8,000 *rcf.* for 1 min. After two dry-spin steps of 30 s, we incubated the columns for 3 min with 50  $\mu\text{L}$  Tris-EDTA elution buffer (High Pure Viral Nucleic Acid Large Volume Kit; Roche) containing 0.05% of Tween 20% (Sigma-Aldrich) and spun for 2 min at 14,000 rpm. We repeated this elution step, and collected the 100  $\mu\text{L}$  of eluted DNA in a LoBind collection tube (Eppendorf). All DNA extracts were stored at  $-20^\circ\text{C}$ . At every extraction experiment we included one blank control (extraction buffer) and bone powder of cave bear as a positive control.

We prepared double-stranded libraries from 25  $\mu\text{L}$  of DNA extract using the partial Uracil-DNA-glycosylase (UDG) protocol, which removes most of the deaminated cytosines – aDNA damage occurring post-mortem – but maintains some molecules with terminal damage (Rohland et al., 2015). We performed the partial UDG-treatment by adding 25  $\mu\text{L}$  of mastermix consisting of 0.07 USER enzyme, 0.2 mg/ml BSA, 1.2 mM ATP (all NEB), 0.1 mM dNTP mix (Thermo Fisher Scientific), 1.2X Buffer Tango (Life Technologies), and finally incubating for 30 min at 37°C and 1 min at 12°C. We then added 0.13 U UGI (Uracil Glycosylase inhibitor) and repeated the incubation step. For the blunt-end repair of the double-stranded molecules we added 0.5 U T4 Polynucleotide Kinase, 0.08 U T4 DNA Polymerase (both NEB), and incubated for 20 min at 25°C for 20 min and then 10 min at 10°C. We purified the product with a standard MinElute PCR purification Kit (QIAGEN) eluting in 18  $\mu\text{L}$  of EB containing 0.05% of Tween (EBT). The ligation of Illumina adaptors was carried out with 1X Quick Ligase Buffer (NEB) and (0.25  $\mu\text{M}$  adaptor mix) in a total reaction volume of 40  $\mu\text{L}$  and 1  $\mu\text{L}$  of 0.125 U Quick Ligase followed by an incubation at 22°C for 10 min and another MinElute purification step. The fill-in of the ligated adaptors included 1X isothermal buffer, 0.4 U/ $\mu\text{L}$  Bst-polymerase (NEB), 0.125 mM dNTP mix and an incubation at 37°C for 30 min followed by 10 min at 80°C. A negative library control ( $\text{H}_2\text{O}$ ) was taken along at every experiment.

We evaluated the success of library preparation by quantifying the number of unique molecules in an aliquot from each library with qPCR performed on a LightCycler 96 (Roche) installed outside the clean room and using IS7/IS8 primers and the DyNAmo SYBP Green qPCR kit (Thermo Fisher Scientific). We assigned unique combinations of two 8bp-long indices at every library and attached them with an amplification reaction using *Pfu-Turbo Cx Hotstart DNA Polymerase* (Agilent Technologies) and 10 cycles of 30 s at 58°C and 1 min at 72°C followed by an elongation step at 72°C for 10 min. We purified the amplified product with a MinElute kit (QIAGEN) and then eluted in 50  $\mu\text{L}$  EBT. We re-quantified an aliquot from every indexed library with qPCR using IS5/IS6 primers and we reamplified to  $10^{13}$  copies with Herculase II Fusion Polymerase following the manufacturer's protocol. After another purification step with final elution at 50  $\mu\text{L}$  of EBT, we measured an aliquot at an Agilent 4200 TapeStation in order to check fragment length and concentration.

### Human genome enrichment, sequencing and haploid genotype sampling

We pooled libraries equimolarly to 10nm and submit them for sequencing in one of the in-house sequencing platforms HiSeq 4000 or NextSeq500 using a paired-end (PE 2x50) or a single-read (SR 75) kit. After initial shotgun sequencing of 5–10 million reads (or 10–20 for PE sequencing) and demultiplexing, all libraries were processed through EAGER (Peltzer et al., 2016), a modular pipeline that streamlines the raw sequence data from FastQC and quality filtering to mapping and duplicate removal and outputs important quality information such as complexity of libraries, percentage of endogenous DNA damage, and fragment length. Sequencing adapters

were clipped with AdapterRemoval (v2.2.0) (Schubert et al., 2016) and merged (paired-end sequencing) while all fragments shorter than 30 bp were discarded. Mapping was performed with BWA (v0.7.12) (Li and Durbin, 2009) with a quality filter of q30 against the hs37d5 sequence reference. For the removal of PCR duplicates we used dedup (v0.12.2) (Peltzer et al., 2016), which considers both beginning and end of the merged reads with the same orientation. C to T and G to A mis-incorporations were evaluated with the tool mapdamage (v2.0.6) (Jónsson et al., 2013). Libraries that passed the thresholds of quality control (> 0.1% of endogenous DNA, > ~5% C to T mis-incorporation at terminal 5' base) were subjected to an in-solution hybridization enrichment that targets at 1,233,3013 genome-wide and ancestry-informative SNPs ("1240K SNP capture") (Mathieson et al., 2015). Libraries were not pooled prior to this enrichment experiment. Whenever the mitochondrial reads from either the shotgun sequencing or the 1240K capture were not sufficient for the reconstruction of the whole mitochondrial genome, the call of mitochondrial haplotypes and the estimation of mitochondrial contamination, we carried out another in-solution enrichment which targets at the whole mitochondrial DNA ("mito capture") (Fu et al., 2015). Captured libraries were sequenced at the order of 20 million reads (or 40 million for PE) and were streamlined through EAGER with the same parameters as for shotgun sequencing data. We ran preseq (v2.0) (Daley and Smith, 2013) on 1240K data, a tool that uses a histogram of targeted sites and the number of unique and duplicated reads in order to compute an extrapolation of the library complexity for bigger sequencing experiments. Subsequently, we deeper-sequenced the captured libraries to maximize the use of each library's complexity. We merged bam files across libraries from the same individual and re-ran dedup. We generated masked versions of the bam files in which we masked the ends of the reads until the nucleotide with mis-incorporation frequency  $\leq 1\%$  using trimBam ([https://genome.sph.umich.edu/wiki/BamUtil:\\_trimBam](https://genome.sph.umich.edu/wiki/BamUtil:_trimBam)). To minimize the reference bias in low-coverage data, after generating the pileup (with -q30 and -Q30 filters), we extracted haploid genotypes with the tool pileupCaller (<https://github.com/stschiff/sequenceTools/tree/master/src/SequenceTools>), which randomly chooses a single read at every SNP position and generates pseudo-diploid genotypes. We performed the random calling both on the original and the masked bam files of each library. For the final genotypes we kept the transitions from the masked and the transversions from the original bam files.

## QUANTIFICATION AND STATISTICAL ANALYSIS

### Quality control and test of kinship

We only included individuals with  $\geq 40,000$  SNPs of the potential 1240K SNPs covered for downstream population genetics analysis. We estimated contamination on these individuals based on the mitochondrial heterozygosity (Renaud et al., 2015) and on the heterozygosity at the polymorphic sites on the X chromosome on the males with ANGSD (Korneliussen et al., 2014).

Samples from same individual or samples from genetically related individuals are relatively common cases when working with bone material from archaeological sites. To test for biological kinship, we estimated the pairwise mismatch rate (pmr) (Kennett et al., 2017) among all possible pairs of individuals from within an archaeological site by counting the number of SNPs for which the two individuals had a mismatch on genotype (0-2 or 2-0) and dividing with the total number of overlapping SNPs (SNPs without missing data in either individual).

It is known that two genomic libraries produced from the same individual or two identical twins (coefficient of relatedness  $r = 1$ ) will exhibit a pmr which should be half of that of a pair of unrelated individuals ( $r = 0$ ) and the pmr will be a linear function of  $r$  (Jeong et al., 2018). Assuming no inbreeding within the population, the pmr of unrelated individuals (UI) can be empirically estimated by the distribution of pmr of multiple individuals. When we detected pairs with IT pmr, we cross-checked with the archaeological context whether these can be attributed to cases of samples from the same individual and, subsequently we merged the data under the name of one individual. For pairs with  $IT < pmr < UI$  we calculated the coefficient of relatedness  $r$  as  $(UI - pmr) / IT$ . For statistically robust estimates of the coefficient we used READ (Monroy Kuhn et al., 2018) which computes pmr in non-overlapping windows of 1 Mbps and also calculates standard errors.

### PMDtools

We used PMDtools (Skoglund et al., 2014), a statistical framework for the evaluation and isolation of aDNA reads based on their damage profile, on the one genetic outlier individual from Alalakh. To reduce reference bias, we provided a reference masked for 1240K SNP positions.

### Dataset

We merged our final dataset with publicly available datasets of ancient and modern individuals (de Barros Damgaard et al., 2018; Feldman et al., 2019; Fu et al., 2016; Gamba et al., 2014; González-Fortes et al., 2017; Günther et al., 2015; Haber et al., 2017; Harney et al., 2018; Hofmanová et al., 2016; Jeong et al., 2019; Jones et al., 2015; Lazaridis et al., 2014, 2016, 2017; Lipson et al., 2017; Martiniano et al., 2017; Mathieson et al., 2018; McColl et al., 2018; Meyer et al., 2012; Mittnik et al., 2018; Mondal et al., 2016; Olalde et al., 2015, 2018, 2019; Pickrell et al., 2012; Prüfer et al., 2017; Raghavan et al., 2014; Rasmussen et al., 2014; Seguin-Orlando et al., 2014; Skoglund et al., 2016, 2017; Vyas et al., 2017; Narasimhan et al., 2019) (see Table S3). We also merged with datasets of worldwide modern populations genotyped on the Human Origins array by keeping the intersection of SNPs. Both 1240K and HO datasets were restricted to the autosomal portion.

### Sex determination and uniparental haplotypes

We used “samtools depth” from the samtools (v1.3) (Li et al., 2009) providing the bed file with the 1240K SNPs to calculate the coverage on X, Y and autosomal chromosomes. We normalized X and Y coverage by the autosomal coverage (X-rate and Y-rate respectively). For females without contamination we expect X-rate  $\approx 1$  and Y-rate  $\approx 0$ . Accordingly, for uncontaminated males we expect both X-rate and Y-rate to be  $\approx 0.5$ .

In order to determine the Y haplogroups of the male individuals, we first used pileups from the bam files Rsamtools package (Morgan et al., 2019) and called the Y chromosome SNPs from reads with mapping and base qualities  $\geq 30$ . We manually assigned Y chromosome haplogroups by manually inspecting the derived SNPs in the pileups included in the ISOGG SNP index (v.14.07) (last downloaded 7 January 2019) (Table S9).

The mitochondrial consensus sequences were inferred from the mito-capture data using Schmutzi (Renaud et al., 2015) and mapping with CircularMapper (Peltzer et al., 2016) against the rCRS with mapping quality filter of  $q30$  and consensus quality score  $Q30$ . The mitochondrial haplotypes of the consensus sequences ( $\geq 5X$  coverage) were assigned by Haplogrep (Kloss-Brandstätter et al., 2011) after visual inspection of bam pileup in Geneious (v11.0.4) (Kearse et al., 2012) (Table S9).

### Principal component analysis

We performed principal component analysis on two subsets of the Human Origins Dataset: (a) 171 West Eurasian populations (2,343 individuals), and (b) 85 West Asian and East Mediterranean populations (1,221 individuals) using the smartpca program of EIGENSOFT (v6.01) (Patterson et al., 2006; Price et al., 2006) with default parameters and the options lsqproject: YES, numoutlieriter: 0, to project ancient individuals onto the first two components.

### f-statistics

We computed outgroup  $f_3$ -statistics using the program qp3Pop from the package ADMIXTOOLS (v5.1) (Patterson et al., 2012) and looked for evidence of maximized shared drift. We also computed  $f_4$ -statistics using qpDstat from the same package that provide evidence of gene flow based on allele frequency sharing. We applied default parameters and the options f4mode: YES.

### Modeling of ancestry proportions

We used the programs *qpWave* and *qpAdm* (version 810) from ADMIXTOOLS to model the studied populations (targets) as a combination of ancestry proportions from putative selected source populations (references). This method does not require explicit knowledge about the phylogeny of the populations but harnesses the fact that if the target is related to a set of right populations (outgroups) through the references (left populations) and the references relate asymmetrically to the outgroup populations, then the target can be modeled as a combination of the references and the admixture proportions can be estimated by solving a matrix of  $f_4$ -statistics (Haak et al., 2015). Therefore, the choice of outgroups and references is of major importance. We used a set of outgroups that represents past and modern global genetic variation (Mbuti.DG, Ami.DG, Mixe.DG, Kostenki14, EHG, Villabruna, Levant\_EP) and provides a good resolution for distinguishing populations from Iran, Levant Caucasus and Anatolia. Prior to the ancestry modeling we used *qpWave* to test whether our outgroup choice can distinguish the tested references.

### Test of recent admixture

We tested for signal of recent admixture events applying the recently developed method DATES (<https://github.com/priyamoorjani/DATES>) (M. Chintalapati, N. Patterson, N. Alex, and P. Moorjani, personal communication) with the following parameters: binsize = 0.001, and fit of decay curve from 0.0045 (lovalfit) to 1 (maxdist) distance bins (all in Morgan units). DATES is based on the algorithm of the rolloff program, which is specifically designed to test admixture in low-coverage ancient genome data where genotypes are typically haploid and missing rate is high (Narasimhan et al., 2019). For each individual in the admixed target population, it first estimates the global admixture proportion by simply fitting the genotype vector of the target individual as a linear combination of the allele frequency vectors of the two source populations. Then it calculates the genotype residual by subtracting the expected genotype value, a weighted mean of source allele frequency and the corresponding global admixture proportion, from the target genotype. Finally, it multiplies the allele frequency difference between the two sources to the genotype residual to correct for the arbitrariness of the allele coding as zero or one. The weighted genotype residual performs a crude estimate of local ancestry (i.e., whether a genomic segment descends from the first or the second source), and thus the correlation between a pair of SNPs within a single individual is expected to exponentially decay as a function of the genetic distance between SNPs and the number of generations since admixture. For each genetic distance bin, DATES calculates a correlation of the weighted genotype residual across all SNP pairs within that bin and estimates admixture date in a single individual by fitting the exponential decay curve against the genetic distance. It can also easily accumulate information across target individuals without information loss, by simply using all SNP pairs from all individuals to calculate the correlation coefficient in each distance bin. Estimated times are given in generations assuming 28 years per generation (Moorjani et al., 2016). Compared to admixture LD methods such as ALDER (Loh et al., 2013) and Rolloff (Moorjani et al., 2011; Patterson et al., 2012), which require a minimum number of samples and coverage of the target population in order to estimate LD with precision, DATES can perform on a single sample from the admixed population. We further tested results where DATES detected a signal of admixture by computing two-reference weighted LD and decay fit with ALDER (v1.03) and rolloff (<https://github.com/DReichLab/AdmixTools/blob/master/src/rolloff.c>) from ADMIXTOOLS. Since ALDER allows only a small fraction of missingness

for a SNP position across the individuals of the target population, grouping individuals with variable coverage decreases the resolution of the analysis. Therefore, we performed ALDER on all possible pairs of individuals within the target population, excluding individuals with less than  $\sim 10\%$  coverage and parameters `binsize = 0.0005`, `mindist = 0.005` (all in Morgan units), `mincount = 2`, `checkmap = NO` and `use_naive_algo = NO`. For `rolloffp` we used parameter `binsize = 0.0005`, fitted the exponential curve using data between 0.005 and 0.5 distance bins (all in Morgan units). The exponential fit was performed using the `nls` function in R. Standard errors were calculated using a leave-one-chromosome-out approach.

### Visualizations

We produced all graphs in Rstudio (*v1.1.383*) and Adobe Illustrator CC 2020 (24.0.2). Maps were created in QGIS using the Natural Earth dataset. We produced all graphs in Rstudio (*v1.1.383*) and Adobe Illustrator CC 2020 (24.0.2). Maps were created in QGIS using the Natural Earth dataset. We consulted [Breniquet \(1996\)](#); [Greenberg and Palumbi \(2015\)](#); [Roaf \(1998\)](#); [Sagona \(2017\)](#), [Carter and Philip \(2010\)](#) and [Wittke \(2010\)](#) for the creation of maps in [Figure 1](#).

## **5 Manuscript B**

# Ancient DNA reveals admixture history and endogamy in the prehistoric Aegean

Received: 15 May 2022

Accepted: 11 November 2022

Published online: 16 January 2023

 Check for updates

A list of authors and their affiliations appears at the end of the paper

The Neolithic and Bronze Ages were highly transformative periods for the genetic history of Europe but for the Aegean—a region fundamental to Europe’s prehistory—the biological dimensions of cultural transitions have been elucidated only to a limited extent so far. We have analysed newly generated genome-wide data from 102 ancient individuals from Crete, the Greek mainland and the Aegean Islands, spanning from the Neolithic to the Iron Age. We found that the early farmers from Crete shared the same ancestry as other contemporaneous Neolithic Aegeans. In contrast, the end of the Neolithic period and the following Early Bronze Age were marked by ‘eastern’ gene flow, which was predominantly of Anatolian origin in Crete. Confirming previous findings for additional Central/Eastern European ancestry in the Greek mainland by the Middle Bronze Age, we additionally show that such genetic signatures appeared in Crete gradually from the seventeenth to twelfth centuries BC, a period when the influence of the mainland over the island intensified. Biological and cultural connectedness within the Aegean is also supported by the finding of consanguineous endogamy practiced at high frequencies, unprecedented in the global ancient DNA record. Our results highlight the potential of archaeogenomic approaches in the Aegean for unravelling the interplay of genetic admixture, marital and other cultural practices.

The Aegean has long been recognized as a region of major importance for understanding transregional societal transformations between Europe and the Near East. Already during the seventh millennium BC, the first farming communities emerged in the Aegean, whereby the earliest evidence was unearthed on the island of Crete—that is, the oldest occupation level below the later palace of Knossos<sup>1</sup>—but the origins of these populations remain ambiguous. The next major transformation in Aegean prehistory took place during the Early Bronze Age (EBA; about 3100–2000 BC). Complex societies emerged, characterized by sophisticated architecture, metallurgy, sealing systems and the integration of the Aegean in the Bronze Age Eastern Mediterranean networks of exchange. During the late third millennium BC, the Greek mainland witnessed a severe societal breakdown (at the end of Early Helladic II) with lasting impact until the later Middle Helladic period of the early second millennium<sup>2,3</sup>. This disruption has been attributed to various factors, among them dramatic climatic changes<sup>2,4,5</sup> and the arrival of

new groups<sup>6–8</sup>. Crete does not seem to have suffered a comparable period of decline<sup>9,10</sup>. With the emergence of the first palaces during the nineteenth century BC in the Middle Minoan period, the island’s societies transformed into a hitherto unknown sophistication in art, architecture and social practices.

Only a few centuries later, during the late Middle Bronze Age (MBA; Middle Helladic for the mainland), the first rich shaft graves of local elites appeared in southern mainland Greece, often displaying Minoan influences<sup>11</sup>. The competition between rising elites during the Shaft Grave period led to regional conflicts and culminated in the decline of many local dominions on the Greek mainland and possibly a first mainland military expedition to Crete during the fifteenth century<sup>12</sup>. At the end of this conflict, the palatial period (Late Helladic IIIA–B) started with a few eminent polities centred in Mycenae, Tiryns, Pylos, Athens, Hagios Vasileios in Laconia, Thebes, Orchomenos and Dimini—to name only the most prominent ones<sup>13–15</sup>. During this time,

✉ e-mail: [eirini\\_skourtanioti@eva.mpg.de](mailto:eirini_skourtanioti@eva.mpg.de); [krause@eva.mpg.de](mailto:krause@eva.mpg.de); [pajuccw@gmail.com](mailto:pajuccw@gmail.com); [philipp.stockhammer@lmu.de](mailto:philipp.stockhammer@lmu.de)

the influence on Crete by mainland centres intensified and Cretan resources were systematically exploited with the help of turning key palatial centres and cities like Knossos, Hagia Triada and Chania into outposts for the administration of large parts of the island<sup>16</sup>. So far, past human migrations in the Aegean were primarily reconstructed on the basis of archaeological and textual evidence but bioarchaeological studies have been adding new information during recent decades<sup>17–22</sup>.

Biomolecular approaches based on ancient DNA (aDNA) have been introduced in prehistoric Aegean research during the last decade. The first aDNA study analysed mitochondrial genomes<sup>23</sup>, emphasizing autochthonous developments rather than migration from outside Crete. Subsequent studies generated nuclear aDNA data and showed a common gene pool for the Aegean Neolithic populations, indicating that the southern Greek mainland differed from the northern in its higher genetic affinity to early Holocene populations from the Iran/Caucasus<sup>24,25</sup>. Others reported the presence of this ‘eastern’ (Iran/Caucasus-associated) genetic component in both Bronze Age (BA) Cretan (Minoan) and southern Greek mainland (Mycenaean) populations<sup>26</sup>. However, the last carried additional ancestry linked to the Western Eurasian Steppe herders (WES)<sup>27,28</sup> or Armenia. Recently, Clemente and colleagues expanded the sampling scope of the BA Aegean to the northern mainland and the Aegean Islands corroborating the previous findings but also reporting higher WES-related ancestry in MBA individuals from northern Greece<sup>29</sup>.

Recent archaeogenetic studies outside the Aegean have engaged into integrating biological information as elements of the past social organization and structures<sup>30–33</sup>, whereby it is necessary to acknowledge that relational identities are not determined only through biological kinship<sup>34</sup>. Most approaches to past kinship in the Aegean were based on morphometric and non-metric analyses<sup>17,19,35</sup> and first PCR-based studies were unsuccessful<sup>36</sup>. However, the potential of this line of evidence from the Aegean BA is outstanding due to the richness of collective burials as an expression and constitution of social belonging within local communities<sup>37</sup>.

## Results

### The archaeogenetic dataset

Here, we generated new genome-wide data from 102 prehistoric individuals from Aegean Neolithic ( $n = 6$ ), BA ( $n = 95$ ), as well as Iron Age contexts (IA;  $n = 1$ ) (Fig. 1 and Supplementary Note 1), thereby achieving a fourfold increase in sample size from previously published datasets. This sample, owing to the geographical and temporal distribution, enables us to address complex features of admixture history and other biological aspects interwoven into these prehistoric societies (for example, marital practices). Nea Styra on the island of Euboea and Lazarides on the island of Aegina add to the post-Neolithic sites included that date to the time before the debated disruption around 2200 BC (the end of Early Helladic II on the Greek mainland). The remaining individuals from the mainland and the islands are attributed to the Mycenaean culture of the Late Bronze Age (LBA) (Aidonia, Glyka Nera, Lazarides, Koukounaries, Mygdalia and Tiryns). Most of the data come from Crete (66 of 102 individuals), in a time transect that covers early phases of the Neolithic (Aposelemis; late seventh to early sixth millennia BC) and the BA (Hagios Charalambos—Early-Middle Minoan; Chania, Aposelemis and Krousonas—Late Minoan). With the exception of Aposelemis and XANO35 from Chania (about 1700–1450 BC), all other Late Minoan individuals date between about 1400 and 1100 BC (LMII–III). All the analysed skeletal remains from Nea Styra, Mygdalia, BA Aposelemis, Krousonas, Aidonia and Hagios Charalambos belonged to the same within-site collective burial context; for the latter, *Yersinia pestis* and *Salmonella enterica* were also recently detected<sup>38</sup>. Extracted aDNA was immortalized into genomic libraries, part of which were enriched for 1,233,013 ancestry-informative single nucleotide polymorphisms (SNPs) (1240K) (Methods) and sequencing data were evaluated for aDNA preservation and contamination (Supplementary Tables 1 and 2).

In our inferences for the Aegean individuals, we re-appraised all previously published contemporaneous individuals from this area<sup>24–26,29</sup> (Fig. 1). We also radiocarbon dated 43 of the skeletal remains that yielded genome-wide data (Supplementary Table 3; Methods).

### Transregional genetic entanglements of Aegean populations

To visualize genetic ancestry variation, we first performed a principal component analysis (PCA) on modern West Eurasian populations and projected onto the first two PCs the ancient individuals from the Aegean and nearby regions (Fig. 2). The six individuals from Neolithic Aposelemis cluster with other early European and Anatolian/Aegean farmers, suggesting that the gene pool of Neolithic Crete was linked to the broader Aegean during that period. After around two millennia, the EBA and MBA individuals show a substantial change in their PC coordinates, shifted along PC2 towards Early Holocene Iran/Caucasus and the descending Chalcolithic and BA Anatolians/BA Caucasians. This shift does not seem uniform, as the five individuals from Nea Styra, who were buried together in the same shaft grave, show substantial genetic variation. Finally, the LBA individuals deviate from these earlier BA individuals towards BA Central and Eastern Europe, suggesting multiphased genetic shifts in the Aegean since the Neolithic.

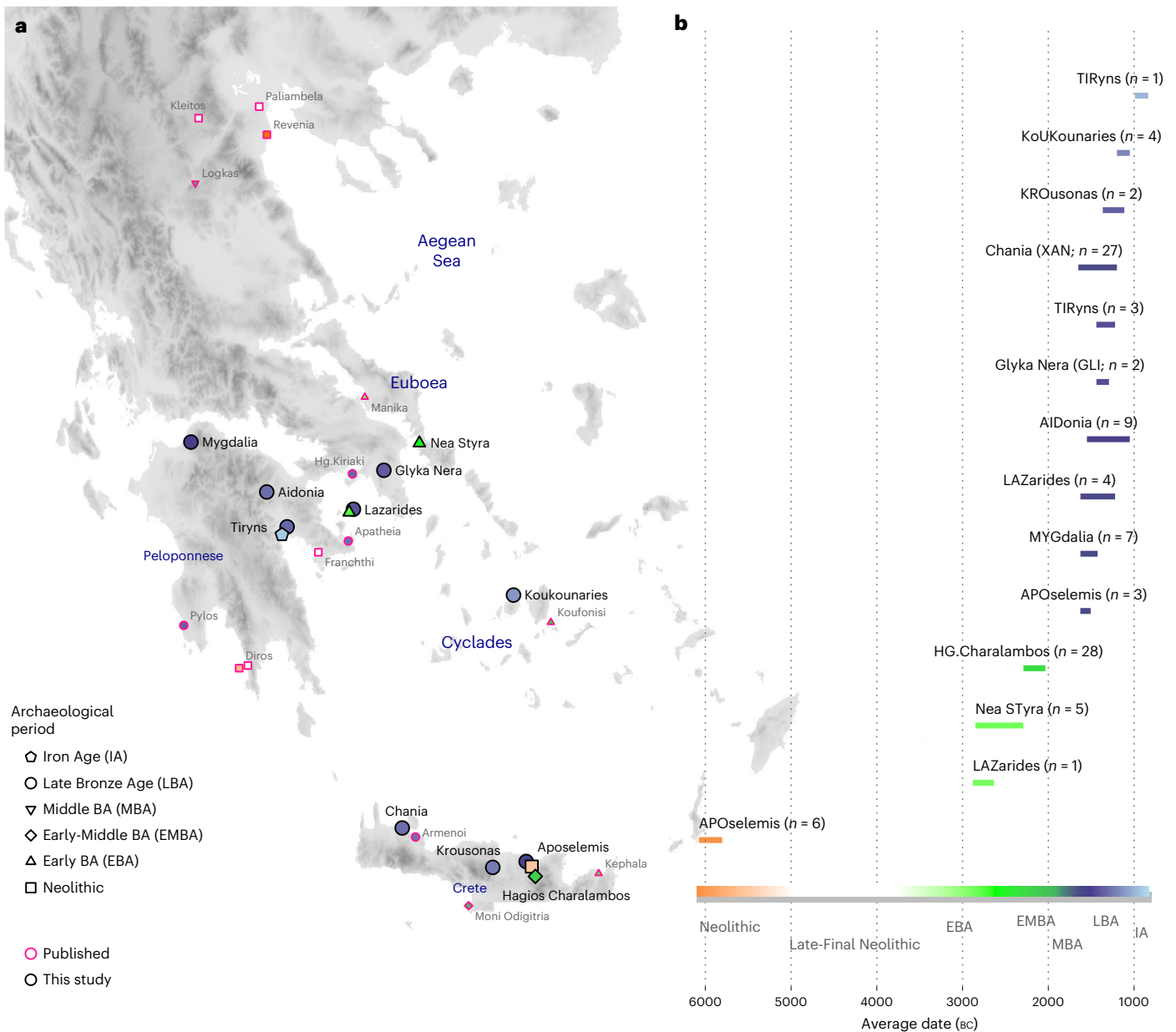
To formally test whether the remarks from the PCA are consistent with diachronic gene-flow events, we used  $f_4$ -statistics of the form  $f_4(\text{Mbuti, Test; Anatolian farmers, Aegean})$  (Methods; Supplementary Note 2) that contrast the various Aegean groups with the Anatolian farmers east of the Aegean (Supplementary Table 4). Affinities with far-eastern groups like Neolithic Iran are traced for Neolithic Aposelemis (or APO004) but only reach significance levels ( $\geq 3$  s.e. or  $Z \geq 3$ ) on the EBA group from Nea Styra and then prevail for most of the later Aegean BA groups. However, the LBA ones additionally share alleles with contemporaneous or earlier (Mesolithic) populations from Central and Eastern Europe (for example, Eastern European hunter-gatherers: EEHG, Germany ‘Corded\_Ware’, ‘Russia\_Samara\_EBA\_Yamnaya’ and ‘Russia\_North\_Caucasus’). In addition, evidence of admixture from these groups was confirmed with admixture  $f_3$  test (Supplementary Table 5 and Supplementary Note 2).

### Neolithic to Early/Middle Bronze Age

Informed by the  $f$ -statistics, we explored formal admixture models using the software qpAdm (Methods; Supplementary Note 2). First, we tested a no-admixture model, which treated every individual as a sister group of Neolithic western Anatolia (‘W. Anatolia\_N’) and then models by adding sequentially Neolithic Iran (‘W. Iran\_N’) and EEHG (Fig. 3). Substantial EEHG coefficients were fitted only on LBA and the two MBA individuals from the northern mainland ranging from around 5% to 25%, which explains why for some of them the simpler Anatolia + Iran Neolithic model was also adequate. Notably, Iran/Caucasus-related genetic influx was inferred in published individuals from the later Neolithic phases on the mainland (I2318, I709 and I3920; Peloponnese, around the fifth millennium BC)—but not earlier—as well as most of the EBA individuals from Euboea, Aegina and Koufonisia. Overall, the genetic heterogeneity among the Late Neolithic (LN) to EBA is not correlated with time alone, since within the Nea Styra grave male individuals carried substantially varying proportions of Iranian-related ancestry. By applying DATES on the LN and EBA individuals from the mainland and the islands (Methods), we obtained an average admixture date of around  $4300 \pm 250$  BC (Supplementary Table 6), which is slightly younger when estimated from the Nea Styra individuals alone (about  $3900 \pm 460$  BC). This variance in admixture dates also corroborates ongoing biological admixing with incoming individuals from the east of the Aegean following the establishment of the first Neolithic Aegean communities.

We further evaluated genetic heterogeneity with cladality tests using qpWave (Extended Data Fig. 1). Our results confirmed that various pairs within EBA Euboea, Aegina and Koufonisia were not cladal





**Fig. 1 | Location and dates of individuals with newly generated aDNA data.**

**a**, Geographical distribution of archaeological sites mentioned in the study annotated by period. Sites with smaller symbols of light outline refer to the published datasets that are co-analysed and follow the same symbol/colour scheme. Data obtained from the same site but different periods, are annotated

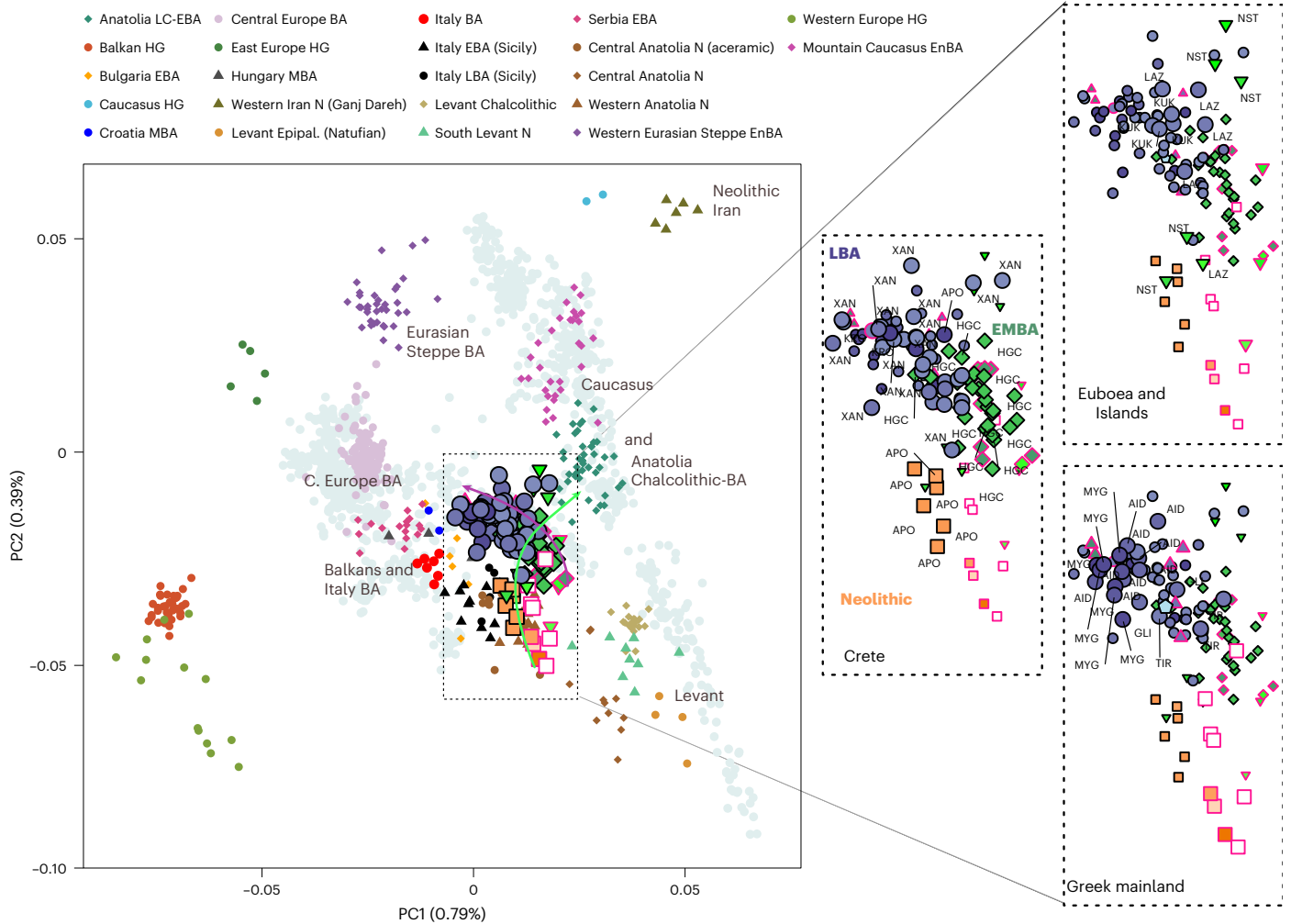
with jittering points. **b**, The number of individuals analysed and their date range based on archaeological chronology or radiocarbon dating. Site names are abbreviated in three-letter capitalized identifiers as indicated in the labels. E, Early; M, Middle; L, Late. See also Supplementary Tables 2 and 3.

to each other with respect to a set of reference populations (model  $P < 0.05$ ), highlighting substantial genetic variation among coeval groups. In stark contrast, in Early Middle Bronze Age (EMBA) Crete the rate of non-cladal pairs (25 of 741) was the one expected for true models of cladal pairs to be rejected with a cutoff of 5% given a uniform distribution of the  $P$  values.

To increase the resolution of admixture inferences, we repeated qpAdm in groups of individuals 'Crete Aposelemis N' ( $n = 6$ ), 'S. Mainland-Islands LN-EBA' ( $n = 13$ ) and 'Crete EMBA' ( $n = 29$ ) following a 'competing' approach described in previous studies (Methods and Supplementary Information 2). For Aposelemis, the one-way model from Neolithic western Anatolia was adequate when aceramic farmers from central Anatolia (Boncuklu site) were included in the reference populations but the one-way model with the latter as a source failed

even without adding western Neolithic Anatolia to the references ( $P = 9.32 \times 10^{-5}$ ) (Supplementary Note 2).

Subsequently, we modelled the differences of the two descending 'S. Mainland LN-EBA' and 'Crete EMBA' groups from the earlier Aegean farmers with two-way models from these local farmers and various southwest Asian populations (Supplementary Table 7). Most of the two-way models including Neolithic Aposelemis were not rejected, indicating a decreased resolution owing to the low SNP coverage and small group size of Aposelemis. On the contrary, when models included 'W. Anatolia N' as a local source instead, only the one with an additional 28% contribution from the Eneolithic/BA Southern Caucasus was feasible for 'S. Mainland-Islands LN-EBA' (Fig. 3b). Accordingly, for 'Crete EMBA', the additional ancestry was better modelled with Late Chalcolithic/Early Bronze Age (LC-EBA) Anatolia (highest  $P = 4.9 \times 10^{-3}$ ); however



**Fig. 2 | West Eurasian PCA (grey background points) with projection of ancient Aegean and other ancient relevant populations (coloured points).** The arrows indicate the two major observed genetic shifts: from the Neolithic (N) to the EBA and from the MBA to the LBA. A zoom-in of coordinates for the

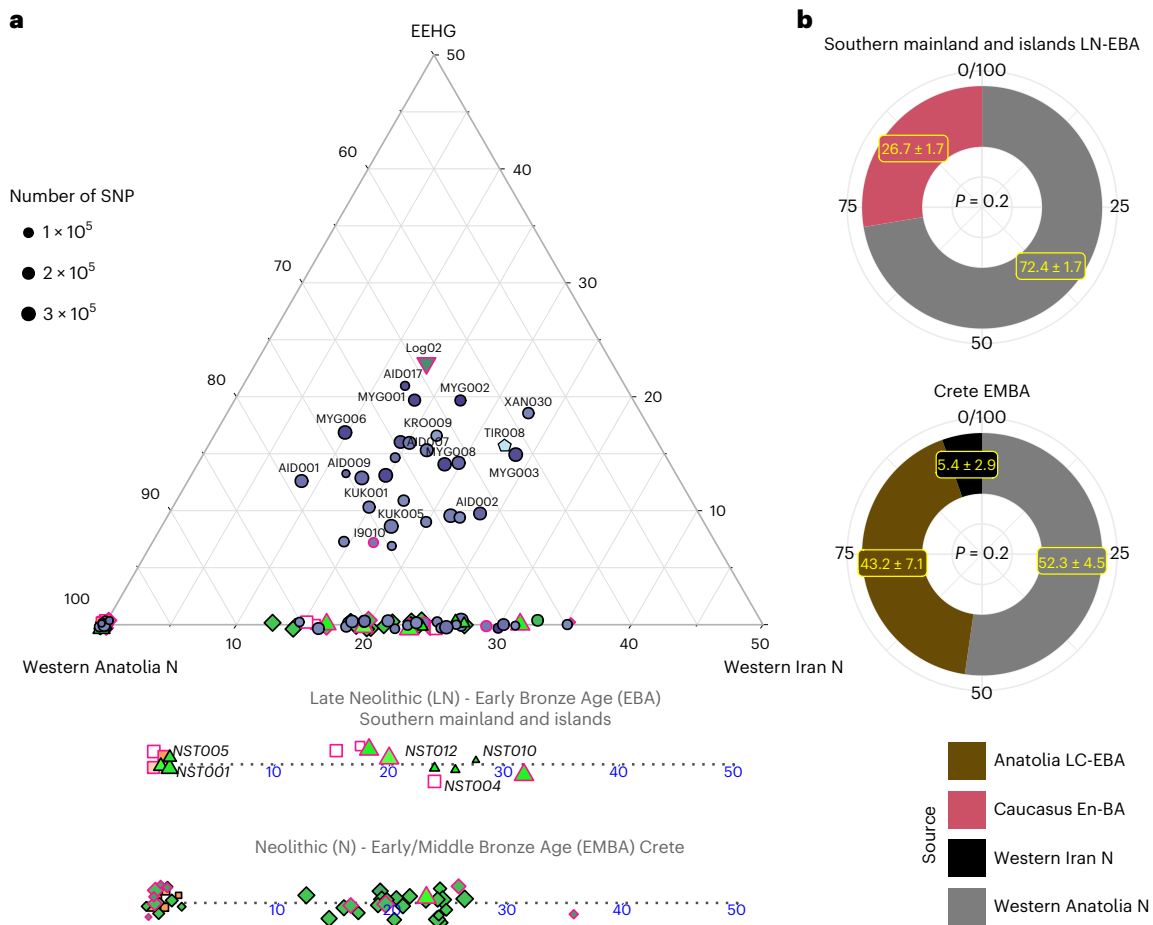
Aegean samples is given and is subdivided by region (right). In every panel, the coordinates of the counterparts are plotted in the background in faded colours. The three-letter identifier of every individual is plotted as well. HG, hunter-gatherers; Epipal., Epipalaeolithic.

this model only became adequate as a three-way with an additional minute component (5%) from ‘W. Iran N’ (Fig. 3b).

### Mobility in the Middle/Late Bronze Age Aegean

For the LBA groups and the IA individual, we explored models of mixture from the corresponding ascending group (‘S. Mainland-Islands LN-EBA’ and ‘Crete EMBA’) and several European populations dated between around 3500 and 1000 BC (Supplementary Table 8). Informed by the previous analyses, we restricted the possible second sources to populations such as the EBA herders from the Pontic-Caspian Steppe (here grouped under ‘W. Eurasian Steppe En-BA’ and typically representing WES) and those shown to share a close genetic affinity with them. We first tested these models on ‘Site\_Period’ groups, only if the cladality test (qpWave) agreed with grouping them as a homogeneous cluster (Supplementary Figs. 1 and 3a). Within the larger group from Chania, departures from cladality ( $P < 0.05$ ) were more frequent (~10%) and were predominantly driven from specific individuals lying at the two ends of the EBA-LBA cline in the PCA (Extended Data Fig. 2b). To explore how these reflect significant differences in the admixture modelling, we analysed the group from Chania into the following three subgroups: ‘Chania LBA (XAN030)’, ‘Chania LBA (a)’ (XAN014, XAN028, XAN034) and ‘Chania LBA (b)’ (all the others) (Supplementary Table 8).

We found various sources ranging from East Europe, to Central and South Europe adequately fitting most models for the LBA Aegean groups. The smaller and heterogeneous sample of BA Bulgarian individuals or BA Sicily did not fit. Models with Serbia (EBA), Croatia (MBA) and Italy (EMBA) were adequate most of the time, while those with ‘W. Eurasian Steppe En-BA’ (En, Eneolithic) or some Central European source (for example, Germany LN-EBA ‘Corded Ware’) were adequate for all groups at the  $P \geq 0.01$  cutoff. Therefore, at the moment it is not possible to more closely identify the region(s) from where this genetic affinity was derived. Among the groups of the southern mainland, the estimated coefficients of the WES-related ancestry are overlapping ( $\pm 1$  s.e.) and average to 22.3% (Fig. 4a) but were substantially lower than for Logkas in the northern mainland ( $43\text{--}55\% \pm 4\%$ ). No significant differences were noted for IA Tiryns ( $\pm 1$  s.e.), indicating—albeit with limited evidence—genetic continuity after the end of the BA at least for this site. Similar coefficient ranges as in the southern mainland are observed for the nearby islands and the Cyclades, although the model for the one individual from Salamis shows no WES-related ancestry. In sharp contrast, in Crete, WES-related coefficients vary from 0% to about 40% clustering in three groups with significantly different coefficients. Among the individuals with minimal/no WES ancestry are the earliest, dating to the late seventeenth or sixteenth century BC Aposelemis, whereas the youngest (Krousonas, Armenoi; twelfth



**Fig. 3 | Admixture modelling with qpAdm per individual and group. a**, Ternary plot for a three-way admixture model of Aegean individuals using the distal sources of ceramic farmers from Western Anatolia, Western Iranian farmers from Ganj Dareh and the EEHG, all dating to about 6000 BC. Because qpAdm is based on allele frequency differences, modelling of individual targets has a lower resolution especially when the SNP coverage is low. A few of the Late-Final Neolithic (LN) and EBA individuals show additional ancestry related to Neolithic Western Iran. To better visualize the fluctuation or Iranian-like coefficients among the LN-E/MBA individuals, the Anatolian–Iranian axis is also provided separately for Crete and the mainland islands. Fitting models were chosen with a cutoff of  $P \geq 0.01$ , with only four individuals falling in the lower range

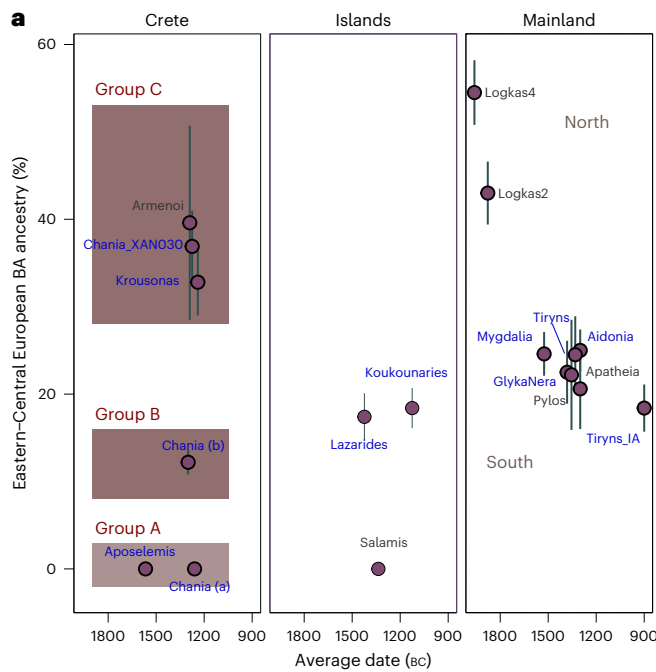
( $0.01 \leq P < 0.05$ ). **b**, Allele frequencies are averaged among all LN-EBA individuals from the southern mainland and all EMBA Cretan individuals and modelled using proximal in time and space source populations. For the former, a source proxy from the Eneolithic/BA Caucasus fits better than Anatolia, whereas the opposite holds for Crete. However, for the latter, the model becomes adequate with the inclusion of additional low contribution from Neolithic Iran. *P* values and standard errors of mean were calculated by the qpAdm program applying a likelihood ratio test and the 5 cM block jackknifing method, respectively. No correction for multiple testing has been made. See also Extended Data Fig. 1 and Supplementary Tables 4–7.

century BC) harbour some of the highest amounts. However, within the ancient city of Chania, individuals spanning a short period of about three centuries display the entire range, a pattern consistent with an early phase of mixing between divergent populations.

To better understand these remarkable ancestry patterns in LBA Crete, we tested competing admixture models by interchanging the candidate second sources in which we now included ‘Mainland MLBA’ that consisted of all the individuals from the third panel of Fig. 4a (both southern and northern). For a comparison, we also tested the same models on the grouped targets ‘Islands LBA’ (Euboea, Aegina, Salamis and Cyclades), ‘S. Mainland’ and ‘N. Mainland’—being aware that such artificial subdivisions of landscapes might not reflect past categorizations. The results are summarized in Fig. 4b. Interchanging the sources resulted in the rejection of some previously adequate sources (for example, ‘Italy BA’ for ‘Islands LBA’). Overall, proximal sources like EBA Serbia, MBA Croatia and BA Italy failed to model both mainland and island groups ( $P \leq 5.80 \times 10^{-3}$ ), whereas models with Central or Eastern European sources remained adequate. However, two-way models with all of the above sources as well as ‘Mainland MLBA’

fit the allele frequencies of all the LBA individuals from Crete (‘Crete LBA’). This also applied when we modelled the two clusters from LBA Crete separately (Fig. 4a and Supplementary Table 9) but for the Crete LBA (group C) with high WES ancestry (individuals XAN030, KRO008, KRO009 and published Armenoi), just one source from ‘Mainland MLBA’ became adequate.

**Insights into sex bias, biological kinship and marital practices** Studies have shown that in some regions of Europe—like the Iberian Peninsula, Central Europe and Britain—the large-scale gene flow associated with the Eurasian Steppe during the BA resulted in the prevalence of the Y chromosome R1a and R1b haplogroups<sup>28</sup> or even involved male-biased admixture<sup>33,39,40</sup>. For the Aegean, we also estimated a significantly lower WES-ancestry proportion on the X chromosomes of the male individuals compared to most of the autosomes, which is consistent with male-biased admixture (Extended Data Fig. 3). However, only four out of the 30 male individuals dating post-sixteenth century BC (LBA and IA) carry the R1b1a1b Y haplogroup. The remaining—as well as the EBA/MBA ones—attest to the high prevalence of Y haplogroups J and G/G2



**Fig. 4 | Proximal two-way qpAdm models for the MLBA groups. a**, Estimated mean coefficient (coeff.) ( $\pm 1$  s.e.) of additional ancestry (WES-related) using as proxy a BA Central European population ('Germany LN-EBA Corded Ware'). For every group we assumed local ancestry in the models using the ascending population from the corresponding area (that is, EMBA Crete, LN-EBA southern Greek mainland and islands or LN northern mainland (for Logkas). Newly reported LBA groups are annotated in blue letters. Before we applied the modelling on every 'Site\_Period' group, we performed a test of cladality among all individuals which suggested substructure within the LBA site of Chania in Crete and resulted in three analysis groups. Overall, individuals from LBA Crete are distributed in three groups of non-overlapping WES-related ancestry estimations (A, B and C).

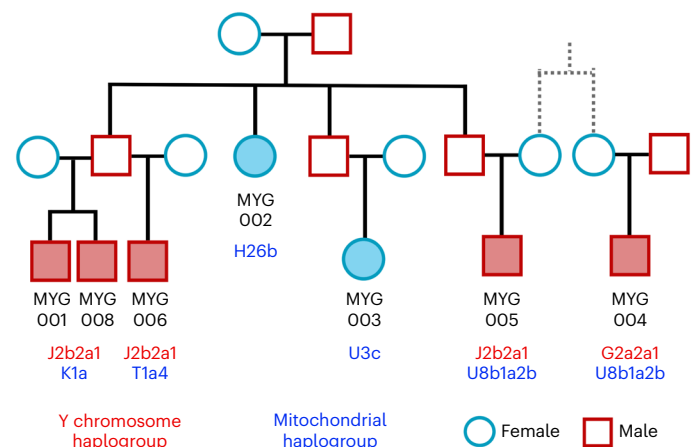
Target	Source 2 (rotating)	P value	Coeff. 1	Coeff. 2	s.e.	P value (no rotation)
Islands LBA	Croatia MBA	$9.7 \times 10^{-4}$	0.62	0.38	0.04	$5.5 \times 10^{-6}$
Islands LBA	Germany 'Corded Ware'	$3.6 \times 10^{-1}$	0.81	0.19	0.02	
Islands LBA	Italy BA (WES)	$2.3 \times 10^{-3}$	0.56	0.44	0.05	$5.7 \times 10^{-2}$
Islands LBA	Serbia EBA	$1.3 \times 10^{-5}$	0.72	0.28	0.03	$1.0 \times 10^{-3}$
Islands LBA	W. Eurasian Steppe EnBA	$3.3 \times 10^{-1}$	0.84	0.16	0.02	
Mainland LBA	Croatia MBA	$5.8 \times 10^{-3}$	0.51	0.49	0.04	$2.8 \times 10^{-3}$
Mainland LBA	Germany 'Corded Ware'	$3.6 \times 10^{-1}$	0.76	0.24	0.01	
Mainland LBA	Italy BA (WES)	$1.3 \times 10^{-5}$	0.43	0.57	0.06	$2.1 \times 10^{-3}$
Mainland LBA	Serbia EBA	$1.9 \times 10^{-10}$	0.64	0.36	0.03	$1.3 \times 10^{-4}$
Mainland LBA	W. Eurasian Steppe EnBA	$8.9 \times 10^{-2}$	0.8	0.2	0.01	
Mainland MBA	Croatia MBA	$1.3 \times 10^{-1}$	0.05	0.95	0.07	
Mainland MBA	Germany 'Corded Ware'	$1.7 \times 10^{-1}$	0.53	0.47	0.03	
Mainland MBA	Italy BA (WES)	$4.7 \times 10^{-3}$	-0.15*	1.15*	0.10	$2.5 \times 10^{-1}$
Mainland MBA	Serbia EBA	$4.8 \times 10^{-10}$	0.3	0.7	0.05	$9.6 \times 10^{-4}$
Mainland MBA	W. Eurasian Steppe EnBA	$2.4 \times 10^{-4}$	0.63	0.37	0.03	$6.8 \times 10^{-5}$
Crete LBA	Croatia MBA	$6.5 \times 10^{-1}$	0.76	0.23	0.03	
Crete LBA	Germany 'Corded Ware'	$5.0 \times 10^{-1}$	0.89	0.11	0.01	
Crete LBA	Italy BA (WES)	$3.4 \times 10^{-1}$	0.74	0.26	0.03	
Crete LBA	Serbia EBA	$2.0 \times 10^{-1}$	0.82	0.18	0.02	
Crete LBA	W. Eurasian Steppe EnBA	$8.0 \times 10^{-2}$	0.9	0.1	0.01	
Crete LBA	Mainland MLBA	$3.8 \times 10^{-1}$	0.61	0.39	0.04	

Models are supported with  $P \geq 0.05$ , with the exception of Tiryns\_IA and Pylos with  $P = 0.02$  and  $0.04$ , respectively. **b**, Modelling results using the approach of rotating competing sources 2 in the right populations set (R1) (Supplementary Note 2) for Crete, the mainland and the islands. Low  $P$  values ( $< 0.01$ ) indicate poor fit of the tested model and are annotated in red. For these models, the  $P$  values are compared with the model fit without rotation of the sources. The gradual shift in Crete can be explained with admixture from the mainland but other proximal sources fit equally well.  $P$  values and standard errors of mean were calculated by the qpAdm program applying a likelihood ratio test and the 5 cM block jackknifing method, respectively. No correction for multiple testing has been made. See also Extended Data Fig. 2 and Supplementary Tables 8 and 9.

(39 and 10 out of 59, respectively; Supplementary Table 2). These were already present in Early Holocene Iran/Caucasus and among Anatolian and European farmers<sup>41-45</sup> and very common in the Chalcolithic Anatolia and the Levant as well<sup>42,46,47</sup>, further highlighting the importance of the contacts between the Aegean and southwest Asian populations since the Early Neolithic.

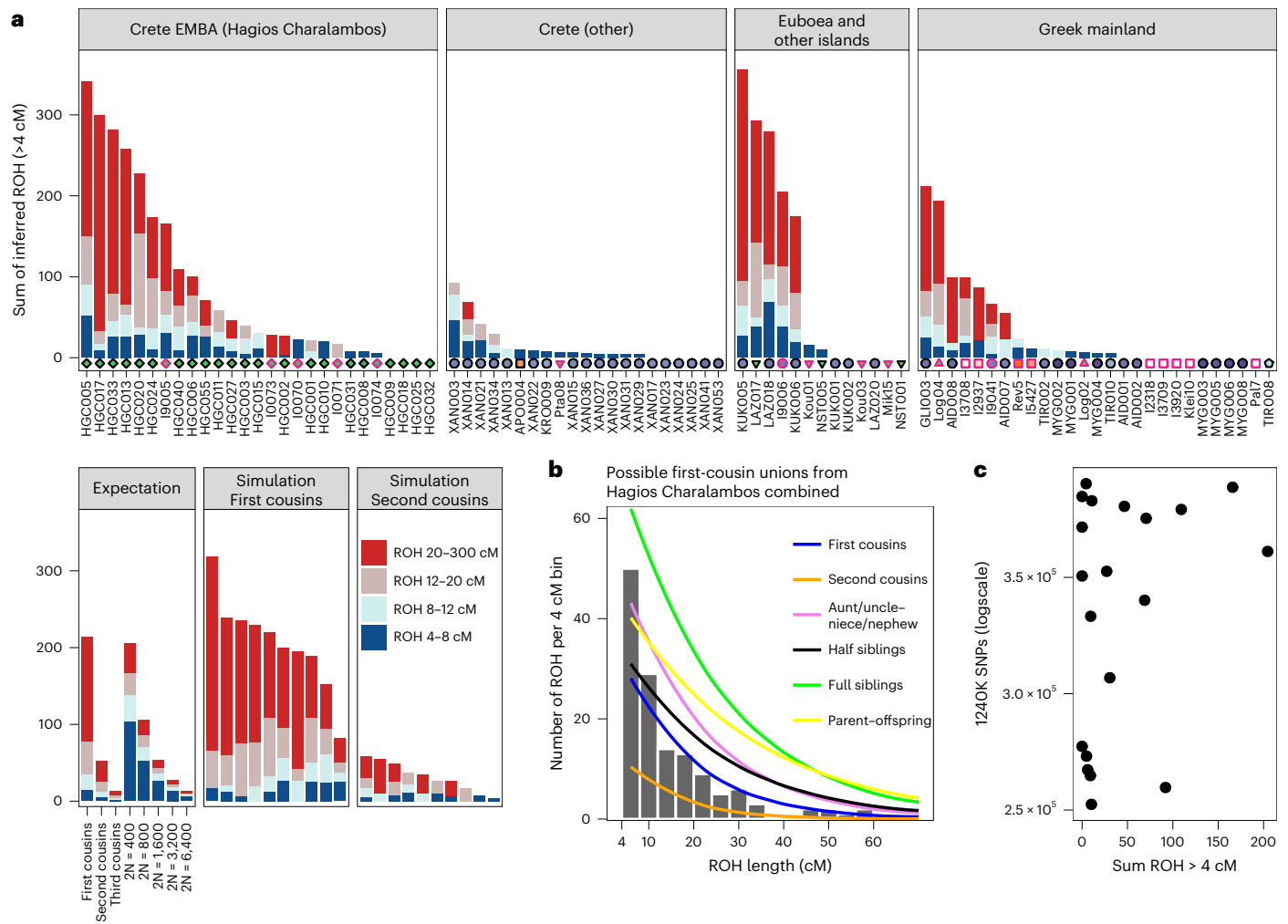
Biological relatedness and its representation in prehistoric collective burials has been poorly understood in the Aegean. Here, we present the first evidence for representation of biologically kin groups from a collective intramural infant grave dating to the LBA—a type of burial which existed since the Neolithic Aegean but became more common since the MBA<sup>48,49</sup>. Located within the Mycenaean (LBA) settlement in Mygdalia, a small cist grave was the primary inhumation of at least eight perinatal infants and one of the six child burials under the houses of the settlement (Supplementary Note 1). By estimating the degree of relatedness among seven of these infants (Methods; Extended Data Fig. 4 and Supplementary Note 3) and assigning the uniparental haplogroups (Supplementary Table 2), the relationship of the infants could be resolved in a single extended family tree whereby the six infants were the children and grandchildren of one couple (Fig. 5). The seventh individual (MYG004) was not a direct offspring of this family but related to MYG005 in the third degree through the maternal line, plausibly as first cousins.

Additional evidence of biological relatedness comes from Aidonia, where pairs of first- to third-degree relatives were determined among individuals buried within the three chamber tombs and the ossuary of Hagios Charalambos at the Lasithi plateau (Supplementary Note 1 and Extended Data Fig. 4). The individuals studied from



**Fig. 5 | Reconstruction of the family tree for the infants from the burial in Mygdalia (MYG; solid colour shapes).** The most parsimonious relationship between MYG004 and MYG005 is given. See also Extended Data Fig. 4.

Hagios Charalambos represent a secondary deposition of intermingled skeletons but were all unearthed from a particular section of the cave (Supplementary Note 1). Besides some pairs of close relatives (first to second degree), many pairs represent distant relatives. In addition to this high frequency of distant genetic relatedness, we also report extraordinarily high levels of consanguinity (~50% of the 27 individuals) estimated from the runs of homozygosity (ROH) by performing



**Fig. 6 | Runs of homozygosity estimated with hapROH. a**, Inferred ROH per ancient Aegean individual. Results are plotted by area and the archaeological period/date of each individual is provided following the same symbol/colour scheme introduced in Fig. 1. Simulations and expectations for given parental relationships and demographic scenarios are given. For many individuals the ROH length distribution matches close-kin unions (first and second cousins).

**b**, Combined histogram of ROH length from all close-union offspring cases from the ossuary of Hagios Charalambos at the Lasithi plateau in Crete, compared to expected densities for certain parental relationships. See also Figs. 5 and 6. **c**, Scatterplot of lower coverage samples (250,000–400,000 SNPs) with total length of inferred ROH indicates that hapROH can reliably estimate long ROH at lower thresholds (Methods).

hapROH on the genotyping data<sup>50</sup> (Fig. 6a; Methods). The individual ROH histograms matched more with the expectations for parents being related to the degree of first cousins, half-siblings and aunt/uncle-nephew/niece (Extended Data Fig. 5). However, given the stochastic nature of genetic recombination and the often-compromised coverage of ancient samples, one individual's genome might only noisily match the expectations. Therefore, we combined the possible first-cousin unions cases and the cumulative histogram this produced favoured the parental relationship of first cousins against other scenarios (Fig. 6b and Extended Data Fig. 6). Coupling the evidence for frequent distant relatives and cousin-cousin unions suggests that those individuals formed a small endogamous community that regularly practiced first-cousin intermarriages.

Intriguingly, endogamy is not a unique feature of Hagios Charalambos. We applied the method on another 61 Aegean individuals from all the periods that met recommended SNP coverage thresholds. In total, we found that ~30% of the individuals have most of their ROH in the bin of the longest ROH blocks, consistent with being offspring of parents related to a degree equivalent to first and second cousins (Fig. 6a). Offspring of close-kin unions were identified from the Neolithic through the LBA but due to the uneven sampling no conclusions can be drawn

regarding temporal trends. Consanguinity was also present in higher frequency in the smaller islands of Salamis, Lazarides, Koukounaries and Koufonisia (50%) but overall it seemed common throughout the Aegean. The observed high frequency of endogamy diachronically points to a rather common social practice in the prehistoric Aegean that is so far unattested in the rest of the global aDNA record<sup>50</sup>.

Finally, we observe a lowered genetic diversity among the Neolithic Aposelemis individuals, measured by a substantially reduced rate of mismatching alleles between pairs of samples (median  $P_0 \approx 0.22$ ) (Extended Data Fig. 4; Methods). This signal can be due to several reasons. First, a lower  $P_0$  would be consistent with Aposelemis being a small endogamous community; however the absence of any long ROH in APO004, the single individual with sufficient coverage to infer long ROH, does not support this hypothesis. Second, the lowered pairwise diversity could represent multiple pairs of second-degree relatives. However, to fit all pairs into a single consistent pedigree would require that all six individuals are half-siblings from either the maternal or the paternal side, with the exception of a single pair of full siblings (APO004–APO028). Due to the low SNP coverage in all the individuals, uniparental markers can neither rule out nor confirm such a pedigree but its high specificity places it as a less likely scenario.

Finally, long-term reduction of population size (bottlenecks) can cause lower population heterozygosity and such a signal has been previously reported for instance in hunter-gatherer groups and Cardial Neolithic Iberians<sup>51,52</sup>. Individuals from such drifted populations are expected to exhibit shorter ROH (4–8 cM), which are currently not detectable in low-coverage individuals such as APO004. Further supporting this scenario, the inferred heterozygosity ( $h$ ) within the Aposelemis individuals was also reduced (mean  $h \approx 0.1$ ) and close to the expectation when assuming that the average pairwise diversity ( $P_0 \approx 0.2$ ) represents the diversity of the population and not pairs of close relatives. Summarizing, the current evidence is most consistent with the scenario of the Aposelemis early farmers descending from a small-sized population.

## Discussion

Our large-scale archaeogenomic approach provides new evidence regarding the role of human mobility in Aegean prehistory. The unprecedented finding of high frequency of consanguinity reveals a cultural practice otherwise unattested in the archaeological record.

First, our analyses on the Neolithic cemetery of Aposelemis, post-dating the earliest levels at Knossos by about 1,000 years, suggest an Anatolian origin of the first Neolithic settlers, consistent with architectural, palaeobotanical and lithic evidence<sup>53</sup> and recent evaluation of wild and domestic fauna at those earliest levels that also suggest animal husbandry<sup>54</sup>. While a similar genetic connection was observed for coeval mainland populations<sup>24,25</sup>, the genetic impact of Mesolithic and Neolithic populations from the other Aegean Islands, remain unknown but the evidence of a pre-Neolithic island horizon of a seafaring tradition<sup>55</sup> forces us to further elucidate the role of hunter-gatherers in the uptake of Neolithic subsistence practices in future studies. Thus, the reduced heterozygosity of the Aposelemis population might be interpreted as a coalescence of a small population of Anatolian farmers who settled the island in the early seventh millennium BC and remained biologically isolated for a period of time or as mobile small-sized populations arriving from nearby islands or a combination of both.

Subsequently, our findings indicate that the genetic landscape of Crete changed substantially since the early sixth millennium BC, marked by an influx of Anatolian populations inferred with our qpAdm modelling and admixture dating. Interestingly, eastern gene flow is also evident in other parts of Greece (Euboea, Aegina and Cyclades) since the LN but seems more episodic and oriented to populations from the Caucasus. In addition, although Y haplogroups are unresolved, male exogamy should be discussed as a plausible contributing factor to the heterogeneous genetic profiles among the male individuals from Nea Styra, in line with evidence from biodistance on a neighbouring site<sup>35</sup>. Overall, while a more even sampling would be critical, current data seem to support that the eastern gene flow was not symmetric across the Aegean.

The disruption of life that is manifested in the Aegean and the Balkans via settlement dislocation during the late third millennium BC could be related to a breakdown of social structures and/or climatic challenges<sup>56</sup>. The finding of ‘northern’ ancestry in the MBA and LBA populations from the Greek mainland, does not support a large-scale population displacement but the north–south gradient indicates the directionality of this migration and population mingling. Some putatively proximal sources like ‘Serbia EBA’ or ‘Bulgaria BA’ failed to model this ‘incoming’ ancestry in many groups and R1b Y haplogroups were rather infrequent among LBA Aegean groups, all of which points to different migration dynamics in the BA Balkans and Greece, compared to other parts of Central and Western Europe.

A more direct demographic connection can be proposed regarding the LBA Cretan and Greek mainland populations. Following an horizon of destructions targeting palatial centres and elite symbols in Crete (Late Minoan IB)<sup>57</sup>, material culture, funerary architecture and burial practices are believed to express innovations with features traditionally ascribed to the Mycenaean culture. On these grounds, an invasion of the island by people from the Greek mainland (around fifteenth century BC)

has been proposed but remains highly contested<sup>12,58–60</sup>. While unable to settle this debate decisively, the genetic analyses demonstrate that Cretan populations at larger port cities biologically mixed with populations coming to the island during the course of a few centuries. The presence of individuals with some of the highest WES-related ancestry proportions within LBA Aegean (Crete LBA group C), despite fitting with a scenario that the Greek mainland was the only source of incoming people, it could also suggest that populations from more distant areas (for example, Italy) contributed to the Crete LBA transition, a possibility that is supported in the material culture as well<sup>61–63</sup>.

All different migrations proposed here (to Crete during the Neolithic and EBA, to the Greek mainland before the LBA and from the mainland to Crete during the LBA) differ in their bioarchaeological evidence, which, therefore, must not be seen as a simple proof of an archaeological hypothesis but as an additional perspective enabling us to unravel the complexity of past mobilities.

Finally, the evidence for consanguinity adds another layer regarding human mobility and social practices. Since the fundamental work by ref. 64, the phenomenon of cross-cousin unions has been much debated in anthropology, whereby in present-day societies, the evidence for cross-cousin unions is diverse, ranging from a common practice via toleration up to prohibition<sup>65</sup>. Different social, economic and ecological arguments have been brought forward as underlying reasons, for example, geographic isolation, endemic pathogen stress, integrity of inherited land and so on<sup>66</sup>. A combination of several factors combined with subsistence-specific needs (for example, olive cultivation forcing local constancy) might have shaped this practice in the Aegean. However, small population size was probably not a major reason in the Aegean as the reduced short-range ROH shown in our analyses is consistent with larger population sizes. Moreover, cross-cousin unions were practiced in different geographic contexts—on islands of different sizes as well as the Greek mainland and are not evident at some places during the second millennium (for example, Chania). Future studies need to further elucidate the factors that were responsible for the emergence, continuity and disappearance of marital practices. So far, the importance of cross-cousin unions in the prehistoric Aegean is unique among the currently available data for prehistoric endogamy, which is otherwise rarely evidenced<sup>50,67–69</sup>. This might indicate different standpoints with respect to marital practices of rural versus urban societies and/or that those were amenable to cultural influences and changed over time. Studying the interplay between past mortuary practices and social structure—including marital or residence rules—from an integrative bioarchaeological perspective has just become possible and future studies will help to refine our understanding of past social belonging.

## Methods

No statistical methods were applied for the determination of sample size and randomization.

The overall burial record from the Aegean Bronze Age is a corpus which underwent specific selection criteria in the past and has been subject to specific modes of preservation and excavation since then (for example, only individuals with a certain status and/or age were buried in a way that allows their study at present). The corpus of samples analysed in this study represents a broad variety of burial contexts (for example, shaft graves/collective graves, single graves, primary and secondary burials) through time and none of the burials would be termed ‘elite’ or ‘outstanding’ in its respective archaeological/historical context. There is also no sampling bias with respect to sex, age or locality of the burials and diverse cultural settings were included (for example, individuals from urban centres like Tiryns and Chania and remote hamlets like Mygdalia).

## Preparation of aDNA analysis

For the purpose of this study, we sampled 385 skeletal elements originally assigned to 357 ancient individuals. Teeth and petrous bones

made >95% of the sample corpus but when these elements were missing other parts such as tibia and femora were chosen. All sampling took place in a dedicated aDNA laboratory of MPI-SHH in Jena, following the laboratory's archived protocols <https://doi.org/10.17504/protocols.io.bqebmtan> and <https://doi.org/10.17504/protocols.io.bdyvi7w6>, the latter being an adaptation of a published protocol<sup>70</sup>. The aDNA extraction from most of the bone powder samples was performed with a modified silica-based protocol<sup>71</sup>. A detailed description of the steps is given in <https://doi.org/10.17504/protocols.io.baksicwe>. Genomic libraries were prepared from these extracts according to a double-stranded (ds) library protocol<sup>72</sup> with an initial step of partial UDG treatment<sup>73</sup> (<https://doi.org/10.17504/protocols.io.bmh6k39e>), followed by Illumina dual indexing (<https://doi.org/10.17504/protocols.io.bakticwn>). For a portion of the samples, we used an extraction-to-indexed library protocol supported by an automated liquid-handling system<sup>74,75</sup> which constructs libraries from single-stranded (ss) molecules. From every extract, at least one of the produced libraries was initially sequenced at a low depth (5–10 million reads) on an Illumina HiSeq400 platform with a setup of 50 cycles and paired-end or 75 cycles and single-read sequencing. Raw FastQC files were processed through EAGER pipeline<sup>76</sup> for removal of adaptors (AdapterRemoval v.2.2.0; ref. 77), mapping against the human reference hs37d5 with the Burrows–Wheeler aligner (BWA; v.0.7.12; ref. 78) with mapping quality and length filters of 30, and removal of PCR duplicates with dedup (v.0.12.2; ref. 76). Resulting information about library complexity and percentage of endogenous DNA was combined with mapDamage (v.2.0.6; ref. 79) estimates to evaluate the profile of endogenous aDNA preservation (Supplementary Table 1). Overall, our initial screening revealed that human aDNA preservation was very low to moderate (0.1–10% human endogenous DNA). Therefore, only aDNA enrichment methods are an economically viable strategy that allows one to generate data from a large number of individuals. Here, we chose to minimize batch effects and consistently generated in-solution hybridization enrichment data, consisting of ~1.2 million ancestry-informative positions (1240K capture)<sup>28,43,80,81</sup> from all samples with 0.1% human endogenous DNA or more. We note that a small proportion of the sampled libraries exhibited high DNA preservation (nine samples with >10% and up to ~40% endogenous content), which would make sequencing of the whole human genome cost-efficient and doing so could address additional research questions (for example, about rare variants). Only part of the immortalized libraries was used to produce enrichment data. The remaining libraries are permanently stored at the MPI-SHH/EVA laboratory facilities and future studies can use this resource to generate whole-genome data from these libraries.

Following the 1240K enrichment, the selected libraries were sequenced at standard ~20 million reads. For the evaluation of the post-1240K capture data, we rerun EAGER and mapDamage with the same settings. We also used the bed file of 1240K SNP positions to estimate on-target endogenous before-and-after 1240K capture and evaluate the performance of the protocol. We used Preseq (v.2.0; ref. 82) with the parameters <lc\_extrap -s 1e5 -e 1e9> to predict the unique reads yielded in larger sequencing experiments. For libraries with low complexity, whenever that was possible, we opted for preparation of multiple libraries from the same extract. Additional sequencing data from the same library or multiple libraries from one DNA extract or same individual that were produced with the same protocols were processed equally and all data were merged at the level of bam files with Samtools (v.1.3) and dedup was run again. We authenticated aDNA using three different methods on the bam files that estimate modern DNA contamination on ancient samples. We analysed single-stranded, no-UDG-treated libraries with AuthenticT (v.1.0.0; ref. 83) that relies on the distribution of damage-induced deamination across the length of the ancient molecules. We run the module for contamination estimate on males from ANGSD<sup>84</sup>, which relies on heterozygosity on polymorphic SNPs on the X chromosome. We previously trimmed bam files for terminal damage with trimBam ([https://genome.sph.umich.edu/wiki/BamUtil\\_trimBam](https://genome.sph.umich.edu/wiki/BamUtil_trimBam)) and reported the method 1 estimation. Finally, we analysed all libraries with schmutzi<sup>85</sup> after mapping mitochondrial reads with CircularMapper (v.1.93.5) and removing duplicates<sup>76</sup> and downsampling to 30,000 reads. Run modules contDeam and schmutzi estimated endogenous deamination, called an endogenous consensus and, based on this, computed the contamination rate. Ratios of mitochondrial/nuclear DNA that are very high (>200) can be unreliable for mitochondrial contamination estimates<sup>86</sup>. Therefore, when applicable, we relied on other methods and/or the behaviour of such samples in population genetic analyses.

The genetic sex was determined from a scatterplot of coverage on X and Y chromosomes normalized for autosomal coverage, which provided an unambiguous distinction between males and females and also matched the macroscopic estimations for adult individuals in all but a few exceptions (Supplementary Note 1).

We extracted genotypes from the pileups of original and trimmed bam files of ds libraries using the tool pileupCaller (<https://github.com/stschiff/sequenceTools/tree/master/src/SequenceTools>) and the option randomHaploid, which randomly chooses an allele to represent the genotype at a given SNP position. For the final genotype file, we kept transitions from the masked version and transversions from the original version. We genotyped the pileups from ss-library bams by activating the option singleStrandMode in pileupCaller which filters out forward-mapping reads with a C-T polymorphism and reverse-mapping reads with a G-A polymorphism, thereby effectively removing bias due to damage. Because of the differences in data production between ds and ss libraries, when applicable, we merged such libraries on the genotype level by randomly choosing a non-missing genotype at every position. Individuals with <20,000 SNPs, ≥10% contamination estimate or absence of such estimate were excluded from subsequent analyses. For selected individuals, we run pileupCaller with the option -randomDiploid and calculated within individual heterozygosity as number of ht sites/number of all sites.

We merged our final dataset with the release of publicly available genotype datasets of ancient and modern individuals (v.5.0.0) (<https://reich.hms.harvard.edu/allen-ancient-dna-resource-aadr-downloadable-genotypes-present-day-and-ancient-dna-data>), to which we added the recently published aDNA data from Italy<sup>87</sup> and based our inferences on a subset of the published data older than 2,000 years from across Eurasia. For the merging with the worldwide modern populations on the Human Origins array (~0.5 million SNPs) we kept the intersection of SNPs between the two panels. For downstream analyses we restricted all data to the 22 autosomes.

We assigned mitochondrial haplogroups and haplotypes from the consensus sequence (q30) generated by schmutzi and the software Haplogrep (v.2.1.25; ref. 88) applying a quality threshold of 0.65. To assign Y haplogroups, we filtered the pileup from the trimmed bams for ISOGG SNPs and for every such SNP we calculated its record of being either ancestral or derived. Then, via manual inspection we checked whether the presence of diagnostic SNPs for a given haplogroup followed a root-to-tip trajectory or whether there were spurious jumps in the phylogeny because of damage. For libraries with low coverage on mitochondrial and Y chromosome DNA, we additionally performed whole-genome and SNP enrichments, respectively, according to established protocols<sup>81,89</sup>. A summary of genetic sex, contamination estimates, SNP coverage and Y/mito-haplogroup assignments is given in Supplementary Table 2.

### Analysis of population structure

We performed PCA using the smartpca program from the EIGENSOFT (v.6.01) package<sup>90</sup>. To avoid bias in the calculation of PCs introduced by high rates of missingness on aDNA, we computed the PCA on 84 modern West Eurasian populations (1,264 individuals genotyped on the Illumina Affymetix Human Origins array) and projected ancient individuals with the option lsproject.

### Admixture analysis with ADMIXTOOLS

We estimated  $f$ -statistics using the package ADMIXTOOLS (v.5.1; ref. 91). Depending on their formulation,  $f$ -statistics can provide a measure of genetic drift or test for hypotheses of admixture and allele sharing excess. While outgroup  $f_3$ -test of the form (Mbuti; X, Test)—for X and Test non-African populations—produces high values when X and Test share common drift,  $f_4$ (Mbuti, Y; X, Test) tests whether X and Y or Test and Y share more alleles than expected from the null hypothesis (X and Test cladal to Y). Therefore,  $f_4$ -statistics under given settings can provide useful hints for admixture and the possible sources. In addition, computation of  $f_4$ -statistics comes with a framework for block jackknife estimation of Z-scores, which we use for annotation of significant results ( $|Z| \geq 3$ ). We also run admixture  $f_3$ (A; B, C) that tests whether the allele frequencies of population A are intermediate between B and C, with negative value indicating admixture. Using the information from the  $f$ -statistics results we built a framework for running tools qpWave and qpAdm from the same package. A detailed description of the machinery behind these tools is provided in ref. 28. In brief, the method harnesses information about allele frequency differences calculated by multiple  $f_4$ -statistics that relate a set of reference (right) populations with a set of targets (left) populations. Specifically, qpWave is used to estimate the minimum number of independent gene pools that explain a set of targets from the references. In practice, if two targets are related with the references as one gene pool, then they are cladal (undistinguishable) to the resolution of the references. In qpAdm, which is a derivative of qpWave, this principle is leveraged to model a target population as a mixture of contributions from  $n$  source populations. The fit of the full model and the nested simpler models are evaluated and  $P < 0.05$  or 0.01 is generally interpreted as an inadequate explanation of the data. Admixture coefficients outside of the [0,1] range are also evidence of a poor fit of the full model. For the comparison of admixture coefficients from different chromosomes, we computed  $Z = (\text{coefficient}_A - \text{coefficient}_X) / \sqrt{(\text{s.e.}_A^2 + \text{s.e.}_X^2)}$ , where A was any of the 22 autosomes, X the sex chromosome X, s.e. the jackknife standard deviation from the qpAdm and applied a significance threshold of  $Z \geq 3$ .

To further discern differences in ancestries and their admixture coefficients by exploring source populations that potentially serve as proxies of the real sources in terms of time, space as well as the archaeological evidence, we applied a ‘competing’ approach described in previous studies<sup>92,93</sup>. In this approach, candidate source populations are interchanged between the reference (right) and source (left) populations in the qpAdm setting. If the one placed in the right population is a better proxy for the real source than the one tested in the left ones, the model is expected to fit poorly the data (low  $P$  value).

### Admixture dating

We used the software DATES (v.753) (<https://github.com/priyamoorejani/DATES>) to test for exponential decay of local ancestry in a source population given two admixing sources. The decay rate is informative about the time since admixture; thus, the method can effectively date recent admixture events. A detailed explanation of the method is provided<sup>47,94,95</sup>. We run the method with standard parameters: in Morgan units binsize = 0.001 and fit of decay curve from 0.0045 (lovalfit) to 1 (maxdist) distance bins.

### Analysis of biological relatedness

For detection of closely related individuals, we applied the method READ<sup>96</sup>. In this approach, the coefficient of relatedness [0,1] between two individuals is estimated from their rate of mismatching allele ( $P_0$ ) normalized with the pairwise allele differences among unrelated individuals within the population ( $\alpha$ ), which is by default calculated as the median from the provided dataset. In this way, the method corrects for SNP ascertainment, marker density, genetic drift and inbreeding. An important implication from this formula is that for given  $\alpha$ , the  $P_0$  for two identical individuals will be  $\alpha/2$  and hence aDNA data from

samples belonging to the same individual can be easily detected. The method also calculates  $P_0$  on non-overlapping windows of the genome and computes standard errors.

To detect relatives at a more distant degree, we run lcMLkin<sup>97</sup> on the masked versions of bam files with the options -l phred and -g best. This method uses a maximum likelihood framework to infer identical by descent (IBD) on low-coverage DNA sequencing data from genotype likelihoods computed with bcftools. The coefficient of relatedness  $r$  is then calculated as  $k_{1/2} + k_2$ , with  $k_1$  and  $k_2$  the probabilities to share one or both alleles IBD, respectively. The method can also distinguish between parent–offspring ( $k_0 = 0$ ) and siblings ( $k_0 \geq 0$ , depending on recombination rate) and in theory infer relatedness as distant as fifth degree. However, in low-quality data such as aDNA discrepancies from the expected  $k_0$ ,  $k_1$ ,  $k_2$  values are common especially for comparisons relying on <10,000 SNPs<sup>31</sup>.

To resolve pedigrees that differ in the IBD probabilities (for example, half-siblings or double first cousins), we performed gene imputations with GenImp (v.1.3; ref. 98) and assessed matching and opposing homozygotes (Supplementary Note 3).

### Analysis of ROH

We inferred ROH using hapROH (v.1.0; ref. 50) (<https://github.com/hringbauer/hapROH>), a method designed to analyse low-coverage aDNA data by leveraging linkage disequilibrium from a panel of modern haplotype references. On 1240K data of at least 0.3× coverage, the method can successfully recover ROH longer than 4 cM. In cases of close parental relatedness, which produce long ROH in the offspring, the method can be efficient for detecting very long ROHs at an even lower coverage. Here, we called ROH in 65 of the Aegean samples (including previously published) with >250,000 SNPs. We simulated individual ROH for a given degree of parental relatedness using the software pedsim (<https://github.com/williamslab/ped-sim>) as described in Supplementary Section 4, hapROH. We used the embedded functions of the program for plotting the ROH as bars, individual or combined histograms and karyotypes.

### Direct AMS radiocarbon dating

Skeletal samples from 38 individuals were submitted to the radiocarbon dating facility of the Klaus-Tschira-Archäometrie-Zentrum at the CEZ Archaeometry gGmbH, Mannheim, Germany, which uses a MICADAS-AMS platform. The same sample from which DNA was extracted was preferred. Collagen was extracted from the bone samples, purified by ultrafiltration (fraction >30 kD) and freeze-dried. Collagen was combusted to CO<sub>2</sub> in an elemental analyser and CO<sub>2</sub> was converted catalytically to graphite. The <sup>14</sup>C ages were normalized to  $\delta^{13}\text{C} = -25\%$  and were given in BP (before present, meaning years before 1950). The calibration was done using the datasets IntCal13 (ref. 99) and IntCal20 and the software SwissCal 1.0.

### Visualizations

We produced all graphs and maps with Rstudio (v.1.1.383), python (v.3.7) and Inkscape (v.0.92.4).

### Reporting summary

Further information on research design is available in the Nature Portfolio Reporting Summary linked to this article.

### Data availability

The raw (FASTQ) and aligned sequence data (BAM format; after MAPQ 30, length filter 30bp and removal of duplicates) reported in this paper can be accessed through the European Nucleotide Archive under the project name: PRJEB56216. Haploid genotype data for the 1240K panel are available in eigenstrat format ([https://figshare.com/projects/Genotype\\_data\\_for\\_103\\_individuals\\_from\\_study\\_Ancient\\_DNA\\_reveals\\_admixture\\_history\\_and\\_endogamy\\_in\\_the\\_prehistoric\\_Aegean/156152](https://figshare.com/projects/Genotype_data_for_103_individuals_from_study_Ancient_DNA_reveals_admixture_history_and_endogamy_in_the_prehistoric_Aegean/156152)).



## Code availability

No new code and method were developed. Details on the settings for admixture modelling and dating are provided in Supplementary Note 2.

## References

- Evans, J. D. Excavations in the Neolithic settlement of Knossos, 1957–60. Part I. *Annu. Br. Sch. Athens* **59**, 132–240 (1964).
- Maran, J. *Kulturwandel auf dem griechischen Festland und den Kykladen im späten 3. Jahrtausend v. Chr.* (Habelt, 1998).
- Wiersma, C. & Voutsaki, S. (eds) *Social Change in Aegean Prehistory* (Oxbow Books, 2017).
- Weiss, H. The genesis and collapse of third millennium north Mesopotamian civilization. *Science* **261**, 995–1004 (1993).
- Weiss, H. in *The Oxford Handbook of the Archaeology of the Levant: c. 8000–332 BCE* (ed. Killebrew, A. E.) 367–387 (Oxford Univ. Press, 2014).
- Blegen, C. W. The Coming of the Greeks: II. The geographical distribution of prehistoric remains in Greece. *Am. J. Archaeol.* **32**, 146–154 (1928).
- Caskey, J. L. The early Helladic period in the Argolid. *J. Am. Sch. Classical Stud. Athens* **29**, 285–303 (1960).
- Forsén, J. *The Twilight of the Early Helladics: A Study of the Disturbances in East-Central and Southern Greece Towards the end of the Early Bronze Age* (Univ. Gothenburg, 1992).
- Brogan, T. M. “Minding the gap”: reexamining the Early Cycladic III “gap” from the perspective of Crete. A regional approach to relative chronology, networks, and complexity in the Late Prepalatial period. *J. Archaeol.* **117**, 555–567 (2013).
- Schoep, I., Tomkins, P. & Driessen, J. M. (eds) *Back to the Beginning: Reassessing Social and Political Complexity on Crete During the Early and Middle Bronze Age* (Oxbow Books, 2012).
- Voutsaki, S. in *Eliten in der Bronzezeit* (eds Aravantinos, V. L. et al.) 103–142 (Verl. des Römisch-Germanischen Zentralmuseums, 1999).
- Wiener, M. H. in *The Great Islands: Studies of Crete and Cyprus Presented to Gerald Cadogan* (eds MacDonald, C. F. et al.) 131–142 (Kapon Editions, 2015).
- Cline, E. H. (ed.) *The Oxford Handbook of the Bronze Age Aegean (ca. 3000–1000 BC)* (Oxford Univ. Press, 2010).
- Deger-Jalkotzy, S. & Hertel, D. *Das Mykenische Griechenland: Geschichte, Kultur, Stätten* (CH. Beck Wissen, 2018).
- Killen, J. T. & Voutsaki, S. (eds) *Economy and Politics in the Mycenaean Palace States* (Cambridge Philological Society, 2001).
- Maran, J. in *Ariadne's Threads. Connections between Crete and the Greek Mainland in late Minoan III (LM IIIA2 to LM IIIC)* (eds D'Agata, A. L. & Moody, J. A.) 415–431 (Scuola Archeologica Italiana di Atene, 2005).
- Moutafi, I. *Towards a Social Bioarchaeology of the Mycenaean Period: A Biocultural Analysis of Human Remains from the Voudeni Cemetery, Achaea, Greece* (Oxbow Books, 2021).
- Papathanasiou, A. *The Bioarchaeological Analysis of Neolithic Alepotrypa Cave, Greece* (BAR, 2001).
- Prevedorou, E.-A. *The Role of Kin Relations and Residential Mobility during the Transition from Final Neolithic to Early Bronze Age in Attica, Greece*. PhD thesis, Arizona State Univ. (2015).
- Schepartz, L. A., Fox, S. C. & Bourbou, C. *New Directions in the Skeletal Biology of Greece* (American School of Classical Studies at Athens, 2009).
- Triantaphyllou, S. *A Bioarchaeological Approach to Prehistoric Cemetery Populations from Central and Western Greek Macedonia* (Archaeopress, 2001).
- Tritsaroli, P. *Pratiques Funéraires en Grèce Centrale à la Période Byzantine: Analyse à Partir des Données Archéologiques et Biologiques* (Muséum National d'Histoire Naturelle, 2006).
- Hughey, J. R. et al. A European population in Minoan Bronze Age Crete. *Nat. Commun.* **4**, 1861 (2013).
- Hofmanová, Z. et al. Early farmers from across Europe directly descended from Neolithic Aegeans. *Proc. Natl Acad. Sci. USA* **113**, 6886–6891 (2016).
- Mathieson, I. et al. The genomic history of southeastern Europe. *Nature* **555**, 197–203 (2018).
- Lazaridis, I. et al. Genetic origins of the Minoans and Mycenaeans. *Nature* **548**, 214–218 (2017).
- Olalde, I. et al. The Beaker phenomenon and the genomic transformation of northwest Europe. *Nature* **555**, 190–196 (2018).
- Haak, W. et al. Massive migration from the steppe was a source for Indo-European languages in Europe. *Nature* **522**, 207–211 (2015).
- Clemente, F. et al. The genomic history of the Aegean palatial civilizations. *Cell* <https://doi.org/10.1016/j.cell.2021.03.039> (2021).
- Cassidy, L. M. et al. A dynastic elite in monumental Neolithic society. *Nature* **582**, 384–388 (2020).
- Mittrnik, A. et al. Kinship-based social inequality in Bronze Age Europe. *Science* **366**, 731 (2019).
- Yaka, R. et al. Variable kinship patterns in Neolithic Anatolia revealed by ancient genomes. *Curr. Biol.* **31**, 2455–2468 (2021).
- Olalde, I. et al. The genomic history of the Iberian Peninsula over the past 8000 years. *Science* **363**, 1230 (2019).
- Brück, J. Ancient DNA, kinship and relational identities in Bronze Age Britain. *Antiquity* **95**, 228–237 <https://doi.org/10.15184/aqy.2020.216> (2021).
- Prevedorou, E. & Stojanowski, C. M. Biological kinship, postmarital residence and the emergence of cemetery formalisation at prehistoric Marathon. *Int. J. Osteoarchaeol.* **27**, 580–597 (2017).
- Bouwman, A. S. et al. Kinship in Aegean prehistory? Ancient DNA in human bones from mainland Greece and Crete. *Annu. Br. Sch. Athens* **104**, 293–309 (2009).
- Boyd, M. J. in *Death Rituals, Social Order and the Archaeology of Immortality in the Ancient World. “Death Shall Have No Dominion”* (eds Renfrew, C. et al.) 200–220 (Cambridge Univ. Press, 2016).
- Neumann, G. U. et al. Ancient *Yersinia pestis* and *Salmonella enterica* genomes from Bronze Age Crete. *Curr. Biol.* **32**, 3641–3649 (2022).
- Martiniano, R. et al. The population genomics of archaeological transition in west Iberia: investigation of ancient substructure using imputation and haplotype-based methods. *PLoS Genet.* **13**, e1006852 (2017).
- Saag, L. Human genetics: lactase persistence in a battlefield. *Curr. Biol.* **30**, R1311–R1313 (2020).
- Jones, E. R. et al. Upper Palaeolithic genomes reveal deep roots of modern Eurasians. *Nat. Commun.* **6**, 8912 (2015).
- Lazaridis, I. et al. Genomic insights into the origin of farming in the ancient Near East. *Nature* **536**, 419–424 (2016).
- Mathieson, I. et al. Genome-wide patterns of selection in 230 ancient Eurasians. *Nature* **528**, 499–503 (2015).
- Rivollat, M. et al. Ancient genome-wide DNA from France highlights the complexity of interactions between Mesolithic hunter-gatherers and Neolithic farmers. *Sci. Adv.* **6**, eaaz5344 (2020).
- Lipson, M. et al. Parallel palaeogenomic transects reveal complex genetic history of early European farmers. *Nature* **551**, 368–372 (2017).
- de Barros Damgaard, P. et al. The first horse herders and the impact of early Bronze Age steppe expansions into Asia. *Science* <https://doi.org/10.1126/science.aar7711> (2018).
- Skourtanioti, E. et al. Genomic history of Neolithic to Bronze Age Anatolia, Northern Levant, and Southern Caucasus. *Cell* **181**, 1158–1175 (2020).
- Papazoglou-Manioudaki, L. & Paschalidis, C. in *Proc. 3rd Int. Interdisciplinary Colloquium: The Periphery of the Mycenaean World* (ed. Karantzali, E.) 437–487 (Ministry of Culture and Sports, 2021).

49. McGeorge, P. J. P. in *2èmes Rencontres d'Archéologie de l'IFEA: Le Mort dans la Ville Pratiques, Contextes et Impacts des Inhumations Intra-muros en Anatolie, du Début de l'Age du Bronze à l'Epoque Romaine* (ed. Henry, O.) 1–20 (IFEA-Ege yayinlari, 2011).
50. Ringbauer, H., Novembre, J. & Steinrücken, M. Parental relatedness through time revealed by runs of homozygosity in ancient DNA. *Nat. Commun.* **12**, 5425 (2021).
51. Valdiosera, C. et al. Four millennia of Iberian biomolecular prehistory illustrate the impact of prehistoric migrations at the far end of Eurasia. *Proc. Natl Acad. Sci. USA* **115**, 3428 (2018).
52. Ceballos, F. C. et al. Human inbreeding has decreased in time through the Holocene. *Curr. Biol.* **31**, 3925–3934 (2021).
53. Evans, J. D. in *Knossos, A Labyrinth of History: Papers Presented in Honour of Sinclair Hood* (eds Evely, D. et al.) 1–22 (British School at Athens, 1994).
54. Horwitz, L. K. in *The Neolithic Settlement of Knossos in Crete: New Evidence for the Early Occupation of Crete and the Aegean Islands* (eds Efstratiou, N. et al.) 171–192 (INSTAP Academic Press, 2013).
55. Efstratiou, N., Karetsou, A. & Ntinou, M. (eds) *The Neolithic Settlement of Knossos in Crete: New Evidence for the Early Occupation of Crete and the Aegean Islands* (INSTAP Academic Press, 2013).
56. Andreou, S. in *The Oxford Handbook of the Bronze Age Aegean (ca. 3000–1000 BC)* (ed. Cline, E. H.) 643–659 (Oxford Univ. Press, 2010).
57. Driessen, J. & Macdonald, C. F. *The Troubled island: Minoan Crete Before and After the Santorini Eruption* (Université de Liège, 1997).
58. Nafplioti, A. “Mycenaean” political domination of Knossos following the Late Minoan IB destructions on Crete: negative evidence from strontium isotope ratio analysis (87Sr/86Sr). *J. Archaeol. Sci.* **35**, 2307–2317 (2008).
59. Miller, M. *The Funerary Landscape at Knossos. A Diachronic Study of Minoan Burial Customs with Special Reference to the Warrior Graves* (BAR Publishing, 2011).
60. D'Agata, A. L., Girella, L., Papadopoulou, E. & Aquini, D. G. (eds) *One State, Many Worlds. Crete in the Late Minoan II-III A2 Early Period* (Edizioni Quasar, 2022).
61. Maran, J. & Stockhammer, P. W. Emulation in ceramic of a bronze bucket of the Kurd type from Tiryns. *ORIGINI* **44**, 93–110 (2020).
62. Miller, M. in *Local and Global Perspectives on Mobility in the Eastern Mediterranean* (ed. Aslaksen, O. C.) 111–133 (The Norwegian Institute at Athens, 2016).
63. Pålsson Hallager, B. Crete and Italy in the Late Bronze Age III Period. *Am. J. Archaeol.* **89**, 293–306 (1985).
64. Lévi-Strauss, C. *Les Structures Élémentaires de la Parenté* (Presses Universitaires de France, 1949).
65. Hamamy, H. et al. Consanguineous marriages, pearls and perils: Geneva International Consanguinity Workshop Report. *Genet. Med.* **13**, 841–847 (2011).
66. Ember, C. R., Gonzalez, B. & McCloskey, D. *Marriage and Family* (HRAF, 2021).
67. Alt, K. W. et al. Earliest evidence for social endogamy in the 9,000-year-old-population of Basta, Jordan. *PLoS ONE* **8**, e65649 (2013).
68. Freilich, S. et al. Reconstructing genetic histories and social organisation in Neolithic and Bronze Age Croatia. *Sci. Rep.* **11**, 16729 (2021).
69. Prowse, T. L. & Lovell, N. C. Concordance of cranial and dental morphological traits and evidence for endogamy in ancient Egypt. *Am. J. Phys. Anthropol.* **101**, 237–246 (1996).
70. Pinhasi, R. et al. Optimal ancient DNA yields from the inner ear part of the human petrous bone. *PLoS ONE* <https://doi.org/10.1371/journal.pone.0129102> (2015).
71. Dabney, J. et al. Complete mitochondrial genome sequence of a Middle Pleistocene cave bear reconstructed from ultrashort DNA fragments. *Proc. Natl Acad. Sci. USA* **110**, 15758 (2013).
72. Meyer, M. & Kircher, M. Illumina sequencing library preparation for highly multiplexed target capture and sequencing. *Cold Spring Harb. Protoc.* **2010**, pdb.prot5448 (2010).
73. Rohland, N., Harney, E., Mallick, S., Nordenfelt, S. & Reich, D. Partial uracil-DNA-glycosylase treatment for screening of ancient DNA. *Philos. Trans. R. Soc. Lond. B* **370**, 20130624–20130624 (2015).
74. Gansauge, M.-T. et al. Single-stranded DNA library preparation from highly degraded DNA using T4 DNA ligase. *Nucleic Acids Res.* **45**, e79–e79 (2017).
75. Rohland, N., Glocke, I., Aximu-Petri, A. & Meyer, M. Extraction of highly degraded DNA from ancient bones, teeth and sediments for high-throughput sequencing. *Nat. Protoc.* <https://doi.org/10.1038/s41596-018-0050-5> (2018).
76. Peltzer, A. et al. EAGER: efficient ancient genome reconstruction. *Genome Biol.* **17**, 60 (2016).
77. Schubert, M., Lindgreen, S. & Orlando, L. AdapterRemoval v2: rapid adapter trimming, identification, and read merging. *BMC Res. Notes* **9**, 88–88 (2016).
78. Li, H. & Durbin, R. Fast and accurate short read alignment with Burrows–Wheeler transform. *Bioinformatics* **25**, 1754–1760 (2009).
79. Jónsson, H., Ginolhac, A., Schubert, M., Johnson, P. & Orlando, L. mapDamage2.0: fast approximate Bayesian estimates of ancient DNA damage parameters. *Bioinformatics* **29**, 1682–1684 (2013).
80. Fu, Q. et al. DNA analysis of an early modern human from Tianyuan Cave China. *Proc. Natl. Acad. Sci. USA* **110**, 2223–2227 (2013).
81. Fu, Q. et al. An early modern human from Romania with a recent Neanderthal ancestor. *Nature* **524**, 216–219 (2015).
82. Daley, T. & Smith, A. D. Predicting the molecular complexity of sequencing libraries. *Nat. Methods* **10**, 325–327 (2013).
83. Peyrégne, S. & Peter, B. M. AuthenticCT: a model of ancient DNA damage to estimate the proportion of present-day DNA contamination. *Genome Biol.* **21**, 246 (2020).
84. Korneliusson, T. S., Albrechtsen, A. & Nielsen, R. ANGSD: analysis of next generation sequencing data. *BMC Bioinf.* **15**, 356 (2014).
85. Renaud, G., Slon, V., Duggan, A. T. & Kelso, J. Schmutzi: estimation of contamination and endogenous mitochondrial consensus calling for ancient DNA. *Genome Biol.* **16**, 224 (2015).
86. Furtwängler, A. et al. Ratio of mitochondrial to nuclear DNA affects contamination estimates in ancient DNA analysis. *Sci. Rep.* **8**, 14075 (2018).
87. Sauepe, T. et al. Ancient genomes reveal structural shifts after the arrival of Steppe-related ancestry in the Italian Peninsula. *Curr. Biol.* <https://doi.org/10.1016/j.cub.2021.04.022> (2021).
88. Weissensteiner, H. et al. HaploGrep 2: mitochondrial haplogroup classification in the era of high-throughput sequencing. *Nucleic Acids Res.* **44**, W58–W63 (2016).
89. Rohrlach, A. B. et al. Using Y-chromosome capture enrichment to resolve haplogroup H2 shows new evidence for a two-path Neolithic expansion to Western Europe. *Sci. Rep.* **11**, 15005 (2021).
90. Patterson, N., Price, A. L. & Reich, D. Population structure and eigenanalysis. *PLoS Genet.* **2**, e190 (2006).
91. Patterson, N. et al. Ancient admixture in human history. *Genetics* **192**, 1065 (2012).
92. Fernandes, D. M. et al. The spread of steppe and Iranian-related ancestry in the islands of the western Mediterranean. *Nat. Ecol. Evol.* **4**, 334–345 (2020).
93. Harney, É., Patterson, N., Reich, D. & Wakeley, J. Assessing the performance of qpAdm: a statistical tool for studying population admixture. *Genetics* <https://doi.org/10.1093/genetics/iyaa045> (2021).
94. Narasimhan, V. M. et al. The formation of human populations in South and Central Asia. *Science* **365**, eaat7487 (2019).

95. Chintalapati, M., Patterson, N. & Moorjani, P. The spatiotemporal patterns of major human admixture events during the European Holocene. *eLife* **11**, e77625 (2022).
96. Monroy Kuhn, J. M., Jakobsson, M. & Gunther, T. Estimating genetic kin relationships in prehistoric populations. *PLoS ONE* **13**, e0195491 (2018).
97. Lipatov, M., Sanjeev, K., Patro, R. & Veeramah, K. R. Maximum likelihood estimation of biological relatedness from low coverage sequencing data. Preprint at *bioRxiv* <https://doi.org/10.1101/023374> (2015).
98. Spiliopoulou, A., Colombo, M., Orchard, P., Agakov, F. & McKeigue, P. GenImp: fast imputation to large reference panels using genotype likelihoods from ultralow coverage sequencing. *Genetics* **206**, 91–104 (2017).
99. Reimer, P. J. et al. IntCal13 and Marine13 radiocarbon age calibration curves 0–50,000 years cal BP. *Radiocarbon* **55**, 1869–1887 (2013).

## Acknowledgements

We thank A. Mötsch for the support in the sample organization and management. We thank G. Brandt, A. Wissgott (MPI-Science of Human History; MPI-SHH) and the laboratory team from MPI-Evolutionary Anthropology for support in the laboratory work. We thank the members of the Max Planck-Harvard Research Center for the Archaeoscience of the ancient Mediterranean (MHAAM), the population genetics group from MPI-SHH/EVA, N. Patterson, M. Feldman, B. Rohrlach and K. Masy for their useful feedback. We warmly thank D. Michailidis and Z. Chalatsi from the Wiener Lab at the American School of Classical Studies at Athens for their support with sampling. We thank K. Prüfer for support in bioinformatics. We thank Arturo Cueva Temprana for support with the graphics. This study was funded by the Max Planck Society, the MHAAM, the National Research Foundation of Korea grant funded by the Korea government (2020R1C1C1003879) and the European Research Council (ERC) under the European Union's Horizon 2020 research innovation programme (ERC-2020-COG 101001951-MySocialBelng) as part of P. W. Stockhammer's ERC Consolidator Grant project 'MySocialBelng: Mycenaean Social Belonging from an Integrative Bioarchaeological Perspective'. We express our wholehearted gratitude to the late M. Kosma and the late D. Schilardi for their utmost contributions to Greek archaeology, as well as to years of research which contributed to making this study possible. They are both deeply missed.

## Author contributions

P.W.S., C.J., J.K. and E.S. conceived and supervised the study, and P.W.S., C.J. and J.K. acquired funding. P.W.S., A.A., M.A.-V., P.B., B.P.H., O.A.J., O.K., A.K., P.K., K.K., R.K., L.K., J.M., P.J.P.M., A. Papadimitriou, A. Papathanasiou, L.P.-M., K.P., N.P.-S., E.-A. Prevedorou, G.P., E. Protopapadaki, T.S.-S., M.S., K.S. and M.H.W. assembled, studied the archaeological material, supported sampling and/or advised on the archaeological background and interpretation of the results.

A.A., M.A.-V., P.B., B.P.H., O.A.J., A.K., E.K., R.K., L.K., J.M., P.J.P.M., A. Papathanasiou, L.P.-M., K.P., N.P.-S., S.P., E.-A. Prevedorou, G.P., E.P., M.S. and K.S. wrote the archaeological and sample background section. E.S., R.A.B., M.B., C.F., A.F., F.K., N.F.G.M., G.U.N. and A.T. performed laboratory work. E.S. and C.J. supervised the data analyses and E.S., H.R. and G.A.G.R. analysed the data. E.S., P.W.S., H.R. and C.J. wrote the manuscript with critical input from all co-authors.

## Funding

Open access funding provided by Max Planck Society.

## Competing interests

The authors declare no competing interests.

## Additional information

**Extended data** is available for this paper at <https://doi.org/10.1038/s41559-022-01952-3>.

**Supplementary information** The online version contains supplementary material available at <https://doi.org/10.1038/s41559-022-01952-3>.

**Correspondence and requests for materials** should be addressed to Eirini Skourtanioti, Johannes Krause, Choongwon Jeong or Philipp W. Stockhammer.


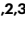





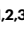

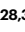


**Peer review information** *Nature Ecology & Evolution* thanks Sofia Voutsaki, Cristian Capelli and the other, anonymous, reviewer(s) for their contribution to the peer review of this work. Peer reviewer reports are available.

**Reprints and permissions information** is available at [www.nature.com/reprints](http://www.nature.com/reprints).

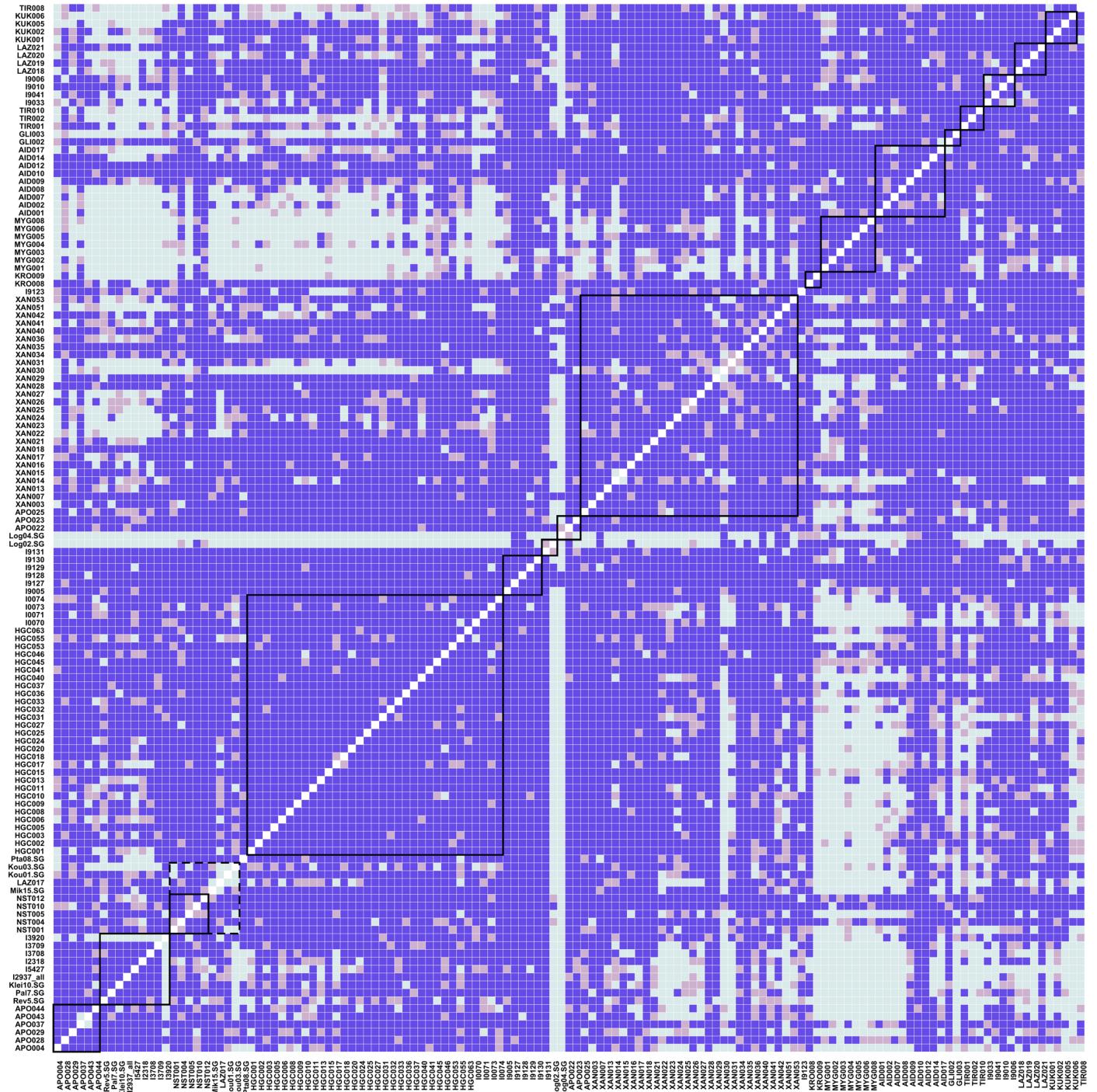
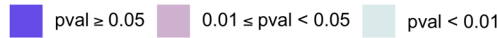
**Publisher's note** Springer Nature remains neutral with regard to jurisdictional claims in published maps and institutional affiliations.

**Open Access** This article is licensed under a Creative Commons Attribution 4.0 International License, which permits use, sharing, adaptation, distribution and reproduction in any medium or format, as long as you give appropriate credit to the original author(s) and the source, provide a link to the Creative Commons license, and indicate if changes were made. The images or other third party material in this article are included in the article's Creative Commons license, unless indicated otherwise in a credit line to the material. If material is not included in the article's Creative Commons license and your intended use is not permitted by statutory regulation or exceeds the permitted use, you will need to obtain permission directly from the copyright holder. To view a copy of this license, visit <http://creativecommons.org/licenses/by/4.0/>.

© The Author(s) 2023

**Eirini Skourtanioti** <sup>1,2,3,30</sup> , **Harald Ringbauer** <sup>1,2,4</sup>, **Guido Alberto Gnechchi Ruscone** <sup>1,2,3</sup>, **Raffaella Angelina Bianco**<sup>2,3</sup>, **Marta Burri**<sup>2,3</sup>, **Căcilia Freund**<sup>2,3</sup>, **Anja Furtwängler**<sup>1,2,3</sup>, **Nuno Filipe Gomes Martins**<sup>2,3</sup>, **Florian Knolle**<sup>2,3</sup>, **Gunnar U. Neumann** <sup>1,2,3</sup>, **Anthi Tiliakou**<sup>1,2,3</sup>, **Anagnostis Agelarakis**<sup>5</sup>, **Maria Andreadaki-Vlazaki**<sup>6</sup>, **Philip Betancourt**<sup>7</sup>, **Birgitta P. Hallager**<sup>8</sup>, **Olivia A. Jones** <sup>9</sup>, **Olga Kakavogianni**<sup>10</sup>, **Athanasia Kanta**<sup>11</sup>, **Panagiotis Karkanas**<sup>12</sup>, **Efthymia Katakis**<sup>6</sup>, **Konstantinos Kissas**<sup>13</sup>, **Robert Koehl**<sup>14</sup>, **Lynne Kvapil**<sup>15</sup>, **Joseph Maran**<sup>16</sup>, **Photini J. P. McGeorge**<sup>17</sup>, **Alkestis Papadimitriou**<sup>18</sup>, **Anastasia Papathanasiou**<sup>19</sup>, **Lena Papazoglou-Manioudaki**<sup>20</sup>, **Kostas Paschalidis**<sup>20</sup>, **Naya Polychronakou-Sgouritsa**<sup>21</sup>, **Sofia Preve**<sup>6</sup>, **Eleni-Anna Prevedorou**<sup>12,22</sup>, **Gypsy Price**<sup>23</sup>, **Eftychia Protopapadaki**<sup>6</sup>, **Tyede Schmidt-Schultz**<sup>24</sup>, **Michael Schultz**<sup>24,25</sup>, **Kim Shelton**<sup>26</sup>, **Malcolm H. Wiener**<sup>27</sup>, **Johannes Krause** <sup>1,2,3,30</sup> , **Choongwon Jeong** <sup>28,30</sup>  & **Philipp W. Stockhammer** <sup>1,2,3,29,30</sup> 

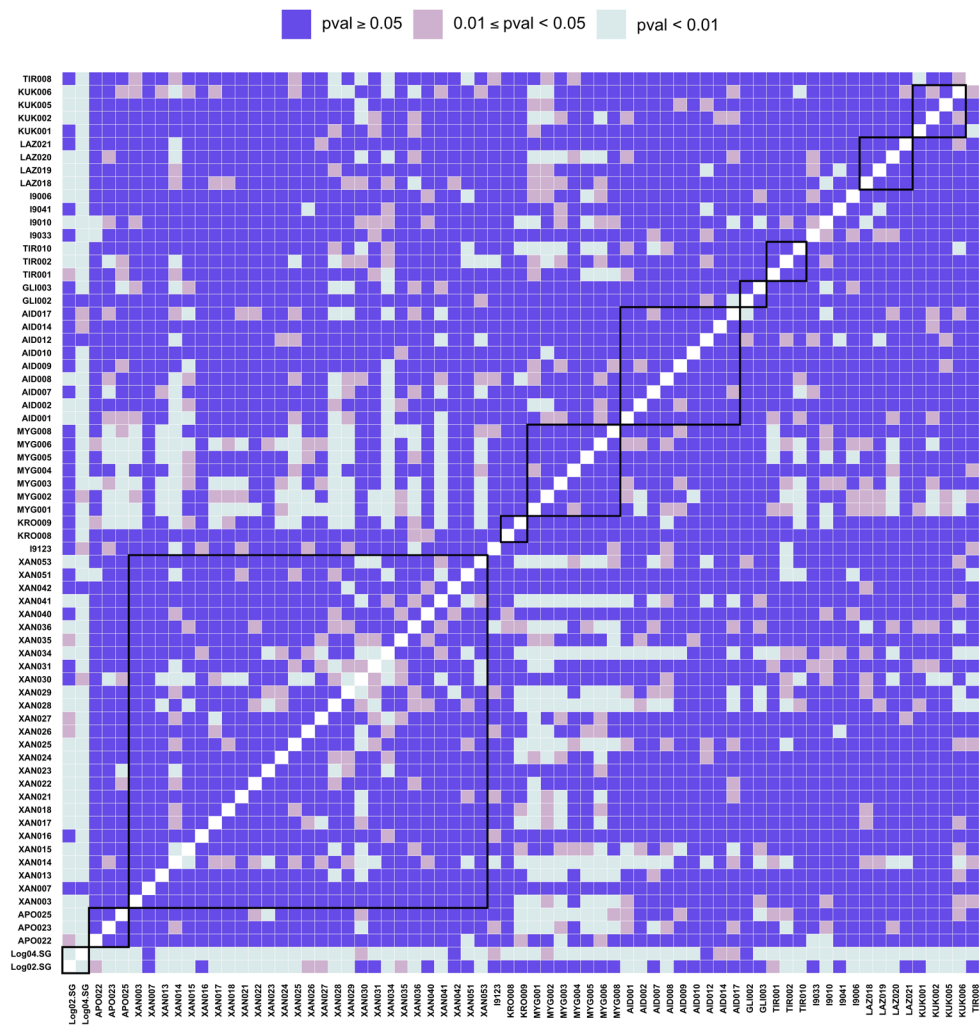
<sup>1</sup>Department of Archaeogenetics, Max Planck Institute for Evolutionary Anthropology, Leipzig, Germany. <sup>2</sup>Max Planck Harvard Research Center for the Archaeoscience of the Ancient Mediterranean (MHAAM), Leipzig, Germany. <sup>3</sup>Department of Archaeogenetics, Max Planck Institute for the Science of Human History, Jena, Germany. <sup>4</sup>Department of Human Evolutionary Biology, Harvard University, Cambridge, MA, USA. <sup>5</sup>Department of History, Adelphi University, New York, NY, USA. <sup>6</sup>Ephorate of Antiquities of Chania, Hellenic Ministry of Culture and Sports, Chania, Greece. <sup>7</sup>Institute for Aegean Prehistory, Temple University, Philadelphia, PA, USA. <sup>8</sup>Danish Institute at Athens, Athens, Greece. <sup>9</sup>Department of Sociology and Anthropology, West Virginia University, Morgantown, WV, USA. <sup>10</sup>Ephorate of Antiquities of East Attica, Hellenic Ministry of Culture and Sports, Athens, Greece. <sup>11</sup>Antiquities for the Heraklion Prefecture (Director Emerita), Hellenic Ministry of Culture and Sports, Heraklion, Greece. <sup>12</sup>Malcolm H. Wiener Laboratory for Archaeological Science, American School of Classical Studies at Athens, Athens, Greece. <sup>13</sup>Ephorate of Antiquities of Arcadia, Hellenic Ministry of Culture and Sports, Tripoli, Greece. <sup>14</sup>Classical and Oriental Studies, Hunter College, New York, NY, USA. <sup>15</sup>Department of History, Anthropology, and Classics, Butler University, Indianapolis, IN, USA. <sup>16</sup>Institute for Prehistory, Protohistory and Near Eastern Archaeology, University of Heidelberg, Heidelberg, Germany. <sup>17</sup>British School at Athens, Athens, Greece. <sup>18</sup>Ephorate of Antiquities of Argolida, Hellenic Ministry of Culture and Sports, Nafplio, Greece. <sup>19</sup>Ephorate of Palaeoanthropology and Speleology, Hellenic Ministry of Culture and Sports, Athens, Greece. <sup>20</sup>National Archaeological Museum, Athens, Greece. <sup>21</sup>Department of Archaeology and History of Art, University of Athens, Athens, Greece. <sup>22</sup>School of Human Evolution and Social Change, Arizona State University, Tempe, AZ, USA. <sup>23</sup>SEARCH, Inc., Cornelius, NC, USA. <sup>24</sup>Center of Anatomy, University of Göttingen, Göttingen, Germany. <sup>25</sup>Department of Biology, University of Hildesheim, Hildesheim, Germany. <sup>26</sup>Department of Ancient Greek and Roman Studies, University of California, Berkeley, CA, USA. <sup>27</sup>Institute for Aegean Prehistory, Greenwich, CT, USA. <sup>28</sup>School of Biological Sciences, Seoul National University, Seoul, Republic of Korea. <sup>29</sup>Institute for Pre- and Protohistoric Archaeology and Archaeology of the Roman Provinces, Ludwig Maximilian University, Munich, Germany. <sup>30</sup>These authors jointly supervised this work: Philipp W. Stockhammer, Choongwon Jeong, Johannes Krause, Eirini Skourtanioti. ✉e-mail: [eirini\\_skourtanioti@eva.mpg.de](mailto:eirini_skourtanioti@eva.mpg.de); [krause@eva.mpg.de](mailto:krause@eva.mpg.de); [pajuccw@gmail.com](mailto:pajuccw@gmail.com); [philipp.stockhammer@lmu.de](mailto:philipp.stockhammer@lmu.de)



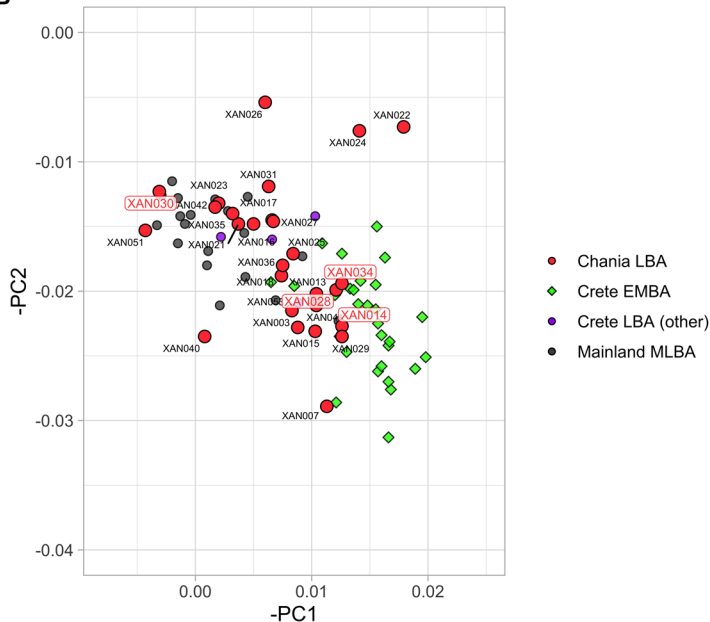
**Extended Data Fig. 1 | Heatmap of pairwise qpWave tests.** Low  $P$  values (conventionally  $< 0.05$ ) are interpreted as a poor fit of the model and as more than one stream of ancestries being needed to explain the pair. Solid-line squares annotate clusters of individuals that date to the same period and come from the same archaeological site. Dashed-line square annotates Early Bronze Age

(EBA) individuals from the islands of Euboea, Aegina and Koufonisia in Cyclades. Results are plotted in decreasing chronological order (Neolithic-Iron Age). We applied R11 (Supplementary Note 2) as a set of reference populations ('right pops').  $P$  values were calculated by the qpWave program applying a likelihood ratio test. No correction for multiple testing was performed.

A



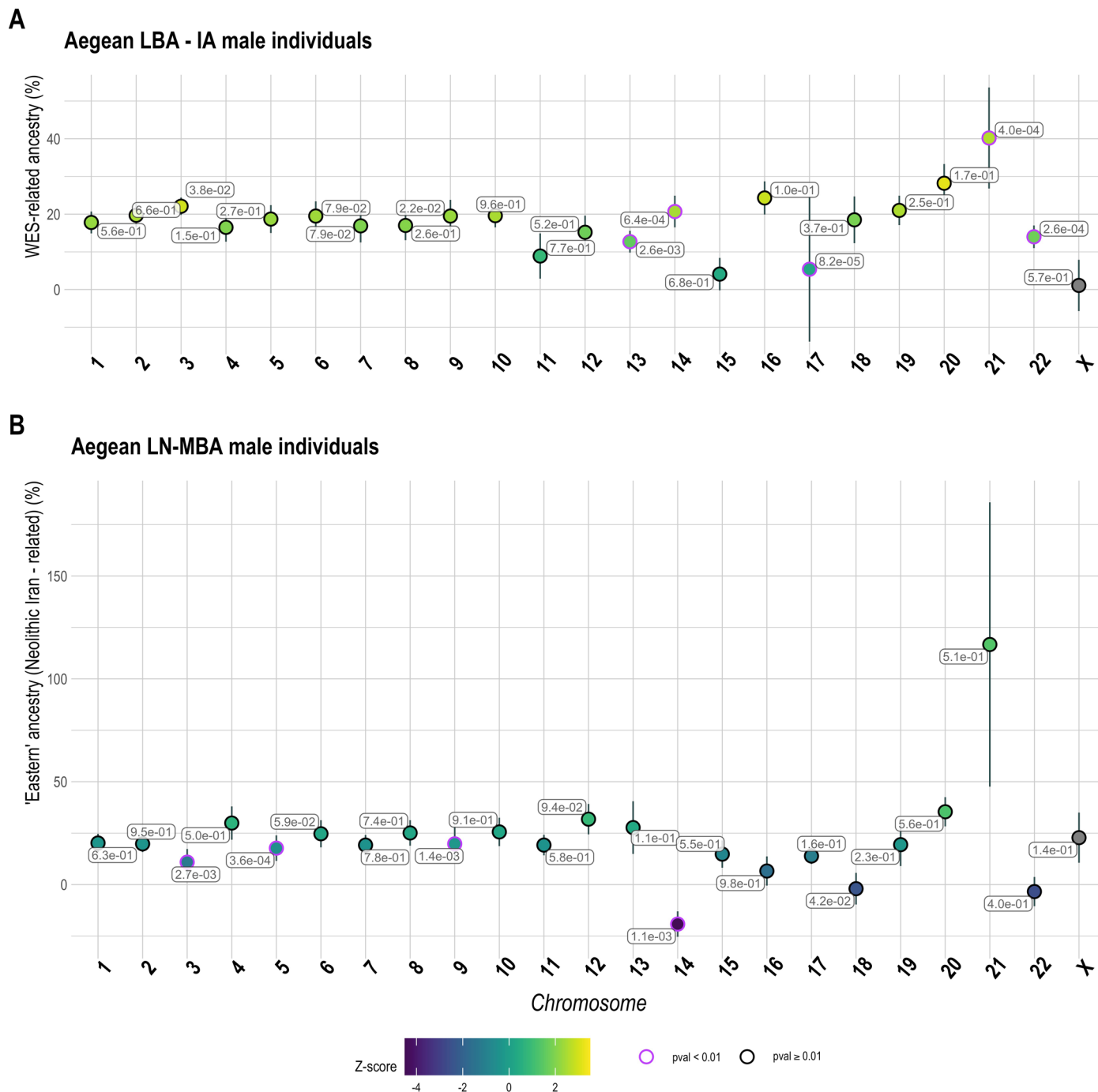
B



Extended Data Fig. 2 | See next page for caption.

**Extended Data Fig. 2 | Heatmap of pairwise qpWave tests and comparison with PCA coordinates.** **A.** Test of streams of ancestry necessary to explain a pair of individuals from a set of reference populations for the Middle/Late Bronze Age and one Iron Age individual from Tiryns. We repeated the analysis presented in Extended Data Fig. 1 by adding to the set of reference populations (R11) 'W. Eurasian Steppe En-BA'. This setting increased the rate of non-cladal pairs ( $P < 0.01$ ; at least two streams of ancestry) only among individuals from Chania (XAN)

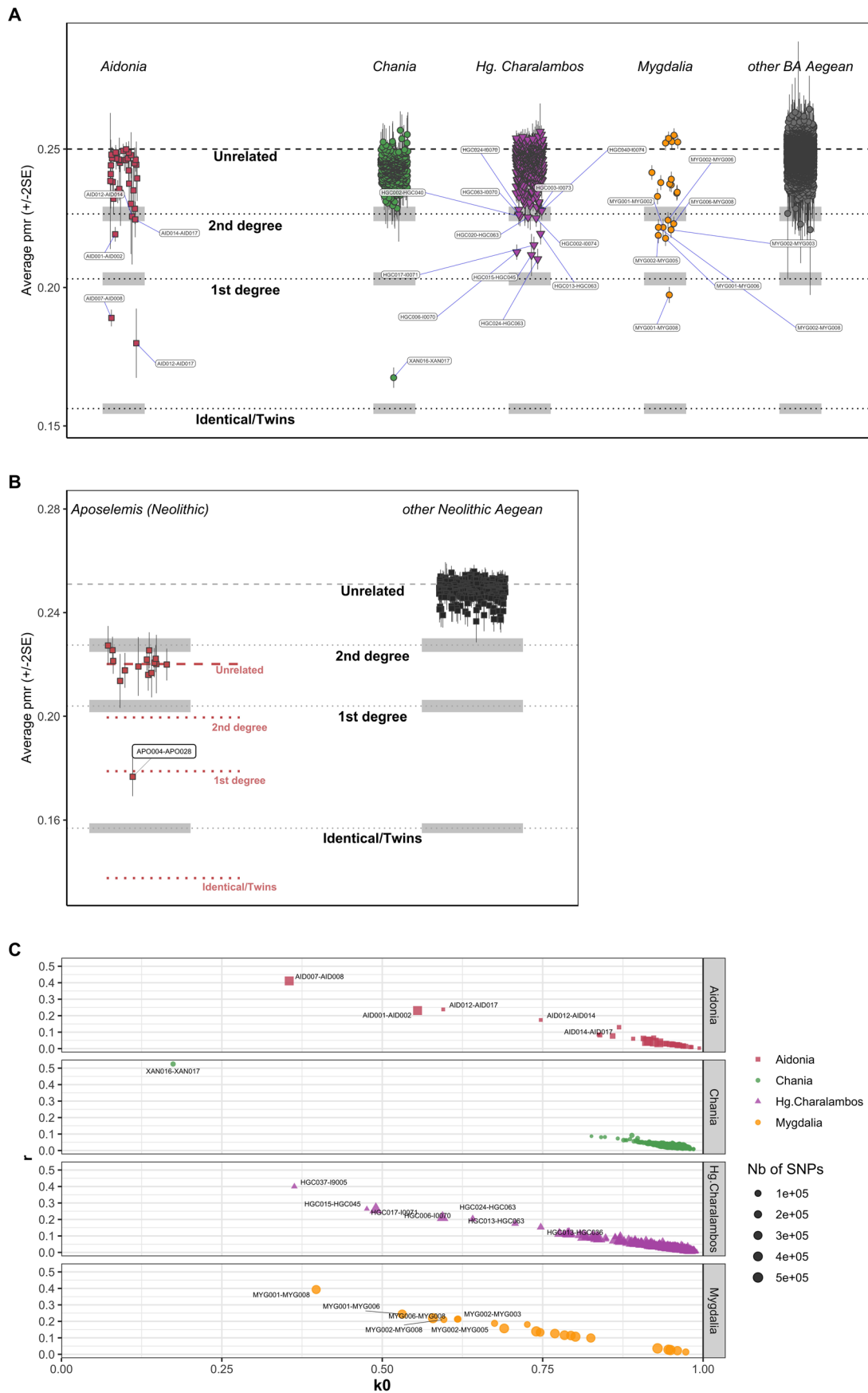
and led us to analyse Chania in three subgroups.  $P$  values were calculated by the qpWave program applying a likelihood ratio test. No correction for multiple testing was performed. **B.** The PC1-PC2 coordinates from the Western Eurasian PCA displaying XAN individuals with their IDs. Those analysed separately are annotated in red letters (XAN014, XAN028 and XAN034 were grouped together and XAN030 apart).



**Extended Data Fig. 3 | Estimated mean coefficients ( $\pm 1SE$ ) of additional post-Neolithic ancestries measured on all the autosomes separately, and the X chromosome of the Aegean male individuals grouped by period. A.** Positive coefficients from 'W. Eurasian Steppe En-BA' in LBA-IA males were fitted ( $P \geq 0.01$ ) for most autosomes as well as chromosome X. WES-related ancestry estimated from the X chromosome was substantially lower compared to the autosomes,

although only a few of these comparisons were significant ( $Z\text{-score} \geq 3$ ). B. The same analysis for the 'eastern' ancestry indicates no sex bias in admixture between the Late Neolithic and the Middle Bronze Age.  $P$  values and standard errors of mean were calculated by the qpAdm program applying a likelihood ratio test and the 5 cM block jackknifing method, respectively. No correction for multiple testing was performed.

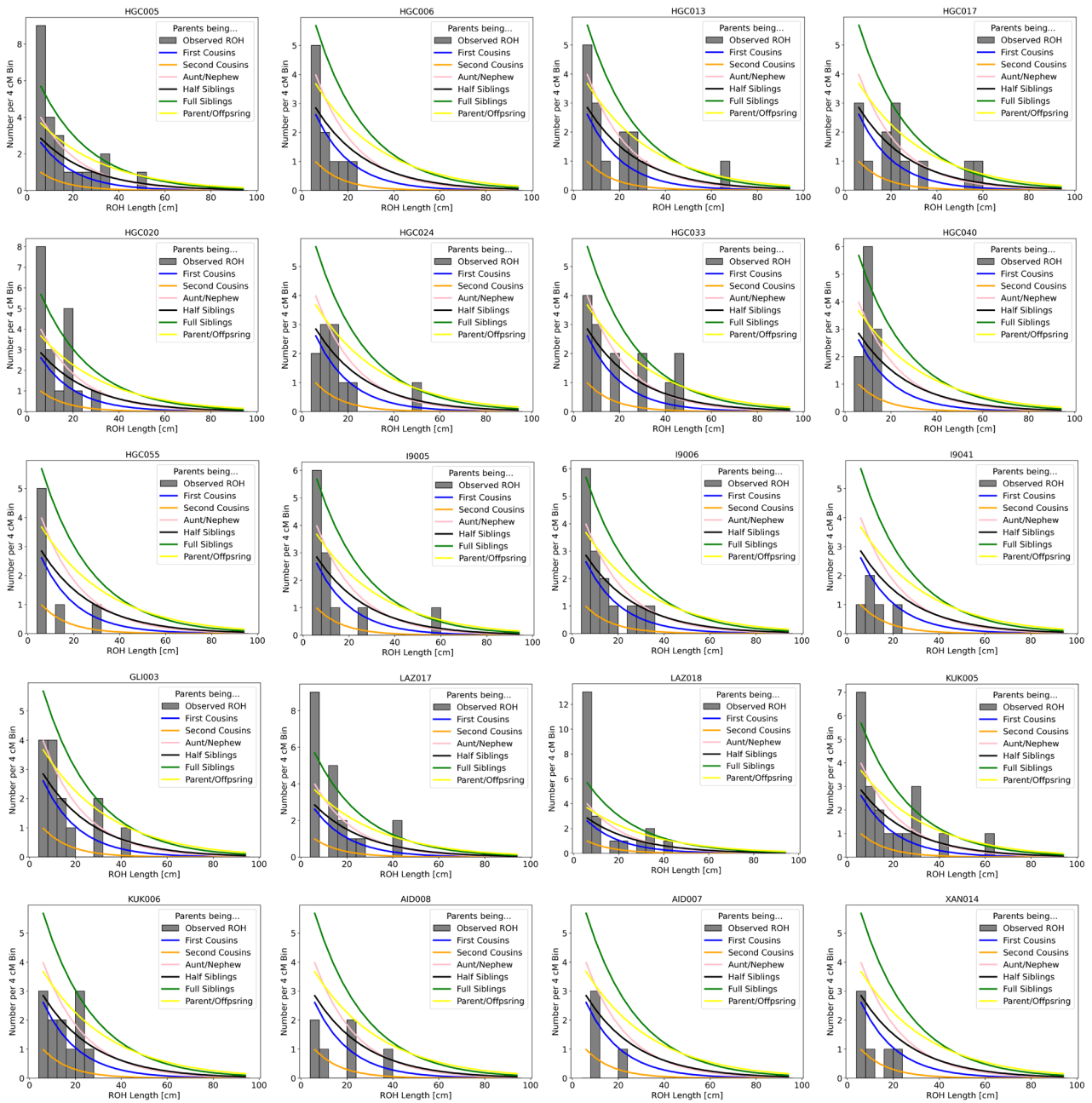




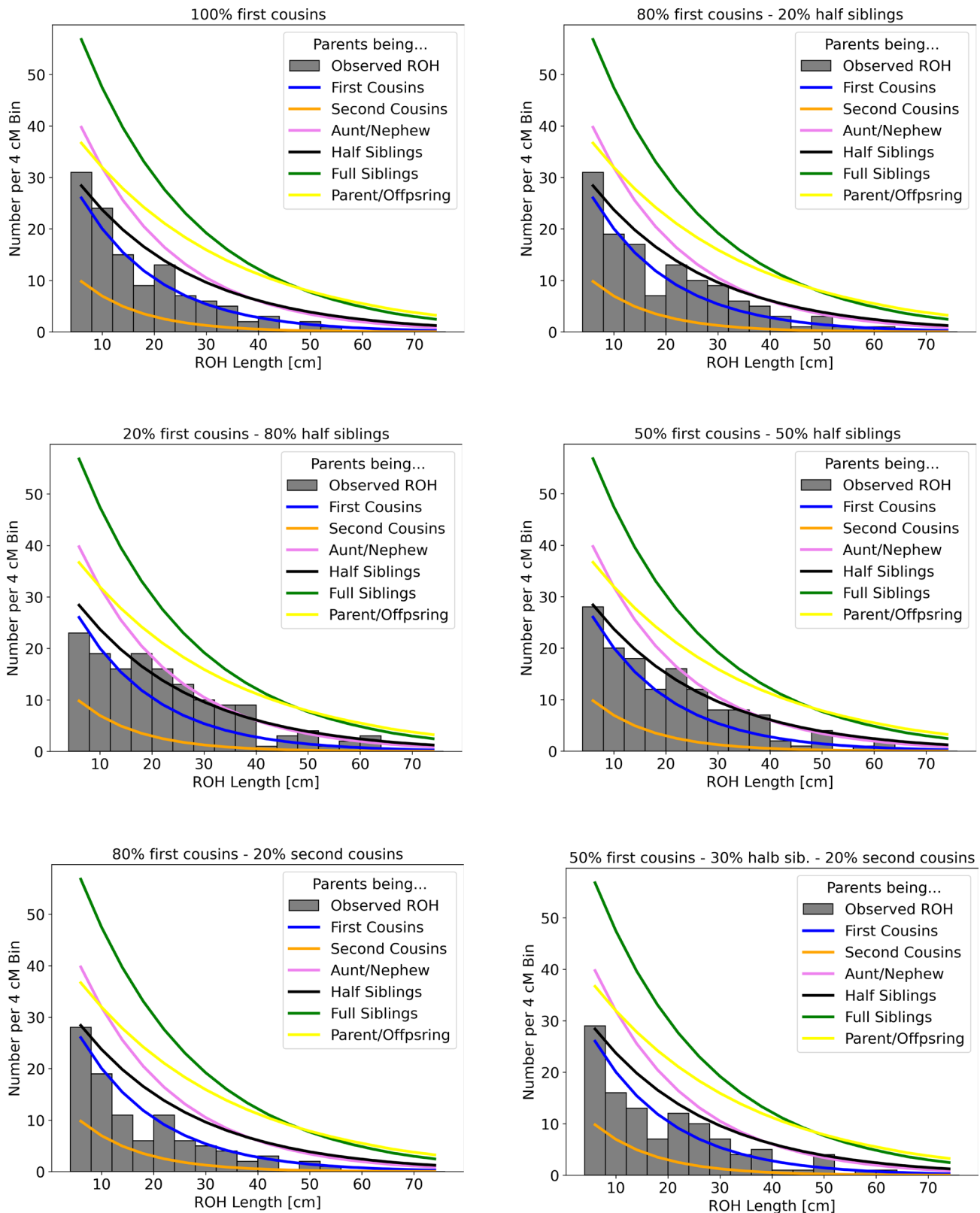
Extended Data Fig. 4 | See next page for caption.

**Extended Data Fig. 4 | Estimation of genetic relatedness with two different methods. A.** The pairwise differences ( $PO$ ) were computed with READ and are plotted as  $\pm 2SE$  of the mean. The dashed line indicates the median value calculated from all pairwise comparisons used for normalization (baseline of unrelatedness). Dotted lines show the cutoffs for the classification to second and first degrees and identical/twins. Confidence intervals were calculated by the software and are indicated in gray shadows. Results are provided separately for sites with related individuals. **B.** READ results for Neolithic Aposelemis in comparison to other Aegean Neolithic sites from the Greek mainland and

Western Anatolia (mean pairwise differences with  $\pm 2SE$ ) suggest that the baseline of unrelatedness might be lower for the Aposelemis population, and normalization of  $PO$  produces lower cutoffs for close relatives (light-red lines). In this scenario, APO004 and APO028 are second-degree relatives. Because SNP ascertainment influences  $PO$  values, only individuals enriched for 1240K, or *in silico* genotyped on these SNPs were included. **C.** IcMLkin analysis. Scatterplot of  $kO$  against  $r$  for sites displaying pairs of relatives. First and up to third-degree relatives from Mygdalia are distinguished by both methods, as well as several pairs from Hagios Charalambos and Chania.



**Extended Data Fig. 5 | ROH length distribution for individuals with evidence of consanguinity (cross-cousin unions).** The ROH histograms are plotted for every case separately along with the expected densities for given parental relationships.



**Extended Data Fig. 6 | Histogram of ROH after combining simulated close-kin offspring, and expected densities for certain parental relationships.** For the three parental relatedness scenarios (half-siblings, first cousins and second cousins), 1000 offspring were simulated with the software *pedsim* (Methods). For comparison with Fig. 6b, the histogram of every panel was created after

combining ten simulated individuals at different proportions. Histograms with all simulated first cousins, or 80% first cousins and 20% second cousins mostly closely match the histogram from the combined Hagios Charalambos individuals.

## Reporting Summary

Nature Portfolio wishes to improve the reproducibility of the work that we publish. This form provides structure for consistency and transparency in reporting. For further information on Nature Portfolio policies, see our [Editorial Policies](#) and the [Editorial Policy Checklist](#).

### Statistics

For all statistical analyses, confirm that the following items are present in the figure legend, table legend, main text, or Methods section.

n/a Confirmed

- The exact sample size ( $n$ ) for each experimental group/condition, given as a discrete number and unit of measurement
- A statement on whether measurements were taken from distinct samples or whether the same sample was measured repeatedly
- The statistical test(s) used AND whether they are one- or two-sided  
*Only common tests should be described solely by name; describe more complex techniques in the Methods section.*
- A description of all covariates tested
- A description of any assumptions or corrections, such as tests of normality and adjustment for multiple comparisons
- A full description of the statistical parameters including central tendency (e.g. means) or other basic estimates (e.g. regression coefficient) AND variation (e.g. standard deviation) or associated estimates of uncertainty (e.g. confidence intervals)
- For null hypothesis testing, the test statistic (e.g.  $F$ ,  $t$ ,  $r$ ) with confidence intervals, effect sizes, degrees of freedom and  $P$  value noted  
*Give  $P$  values as exact values whenever suitable.*
- For Bayesian analysis, information on the choice of priors and Markov chain Monte Carlo settings
- For hierarchical and complex designs, identification of the appropriate level for tests and full reporting of outcomes
- Estimates of effect sizes (e.g. Cohen's  $d$ , Pearson's  $r$ ), indicating how they were calculated

*Our web collection on [statistics for biologists](#) contains articles on many of the points above.*

### Software and code

Policy information about [availability of computer code](#)

Data collection No software was used for data collection (see section below).

Data analysis EAGER (v1.92.59), AdapterRemoval (v2.2.0), BWA (v0.7.12), samtools (v1.3), dedup (v0.12.2), mapDamage (v2.0.6), Preseq (v2.0), CircularMapper (v1.93.5), Schmutzi, AuthenticCT(v1.0.0), ANGSD (v0.910), trimBam, pileupCaller, EIGENSOFT(7.2.1), ADMIXTOOLS (v5.1), DATES (v753), hapROH (v1.0), READ, IcMLkin, GATK (v3.5), GenImp (v1.3), Haplogrep (v2.1.25)

For manuscripts utilizing custom algorithms or software that are central to the research but not yet described in published literature, software must be made available to editors and reviewers. We strongly encourage code deposition in a community repository (e.g. GitHub). See the Nature Portfolio [guidelines for submitting code & software](#) for further information.

### Data

Policy information about [availability of data](#)

All manuscripts must include a [data availability statement](#). This statement should provide the following information, where applicable:

- Accession codes, unique identifiers, or web links for publicly available datasets
- A description of any restrictions on data availability
- For clinical datasets or third party data, please ensure that the statement adheres to our [policy](#)

Sequencing data can be accessed through the European Nucleotide Archive (ENA) under project ID: PRJEB56216. Haploid genotype data for the 1240K panel in eigenstrat format will be also provided.

## Field-specific reporting

Please select the one below that is the best fit for your research. If you are not sure, read the appropriate sections before making your selection.

Life sciences  Behavioural & social sciences  Ecological, evolutionary & environmental sciences

For a reference copy of the document with all sections, see [nature.com/documents/nr-reporting-summary-flat.pdf](https://nature.com/documents/nr-reporting-summary-flat.pdf)

## Ecological, evolutionary & environmental sciences study design

All studies must disclose on these points even when the disclosure is negative.

Study description	This study employs ancient DNA laboratory protocols to produce genome-wide data from human skeletal remains and applies statistical tools from the field of population genetics to address questions regarding the population history such as admixture, genetic relatedness, demography and consanguinity.
Research sample	Human skeletal remains from the Aegean (present-day Greece) that were recovered from archaeological excavations.
Sampling strategy	The overall burial record from the Aegean Neolithic and Bronze Age is a corpus which underwent specific selection criteria in the past and has been subject to specific modes of preservation and excavation since then (e.g., only individuals with a certain status and/or age were buried in a way that allows their study at present). The corpus of samples analyzed in this study represents a broad variety of burial contexts (e.g., shaft graves/collective graves, single graves, primary and secondary burials) through time, and comes from areas with distinct features with respect to their archaeological history. The majority of the samples dates to the Bronze Age, an archaeological period at the core of our questions regarding the contacts of the populations with neighbouring regions and the social organization.
Data collection	Bone powder was sampled following minimally invasive methods for sampling of archaeological material. DNA was extracted converted into a genomic library with adaptors for sequencing on Illumina platforms.
Timing and spatial scale	Timing scale: Neolithic (ca. 6000 BC; n=6), Bronze Age (ca. 2800-1050 BC; n=95), Iron Age (ca. 900 BC; n=1) Spatial scale: Southern Greek mainland, Aegean islands and Crete.
Data exclusions	Processed samples for which a very low coverage of genetic markers was generated (e.g., $\leq 40,000$ SNPs), or modern DNA contamination was estimated high.
Reproducibility	Sequence data will be uploaded to the European Nucleotide Archive, and all parameters (e.g., mapping quality filters, genotyping methods, admixtools) are provided in the Method's section and Supplementary Note 2.
Randomization	No statistical methods were applied for the determination of sample size and randomization.
Blinding	Blinding was not relevant/possible for our study, since all the data come from archaeological samples.
Did the study involve field work?	<input type="checkbox"/> Yes <input checked="" type="checkbox"/> No

## Reporting for specific materials, systems and methods

We require information from authors about some types of materials, experimental systems and methods used in many studies. Here, indicate whether each material, system or method listed is relevant to your study. If you are not sure if a list item applies to your research, read the appropriate section before selecting a response.

### Materials & experimental systems

n/a	Involved in the study
<input checked="" type="checkbox"/>	<input type="checkbox"/> Antibodies
<input checked="" type="checkbox"/>	<input type="checkbox"/> Eukaryotic cell lines
<input type="checkbox"/>	<input checked="" type="checkbox"/> Palaeontology and archaeology
<input checked="" type="checkbox"/>	<input type="checkbox"/> Animals and other organisms
<input checked="" type="checkbox"/>	<input type="checkbox"/> Human research participants
<input checked="" type="checkbox"/>	<input type="checkbox"/> Clinical data
<input checked="" type="checkbox"/>	<input type="checkbox"/> Dual use research of concern

### Methods

n/a	Involved in the study
<input checked="" type="checkbox"/>	<input type="checkbox"/> ChIP-seq
<input checked="" type="checkbox"/>	<input type="checkbox"/> Flow cytometry
<input checked="" type="checkbox"/>	<input type="checkbox"/> MRI-based neuroimaging

## Palaeontology and Archaeology

Specimen provenance	Access to the material was granted through different applications: for every archaeological site a separate application was submitted to the Greek Ministry of Culture and Sports, and after its approval, skeletal samples and/or bone powder could be exported to Germany. All permits were issued in Greek and copies could be provided upon request.
---------------------	--

Specimen deposition	Samples in the form of small fragments (e.g., petrous bones, teeth) or bone powder (max. 200 mg) were exported and sent to the Max Planck Institute for the Science of Human History (MPI-SHH) Lab facility, in Jena, Germany.
Dating methods	Radiocarbon dating with Accelerator Mass Spectrometry on bone/tooth samples weighing up to 1g. Samples were sent to the Klaus-Tschira-Archäometrie-Zentrum at the CEZ Archaeometry gGmbH, in Mannheim, Germany and were analyzed on a MICADAS-AMS platform. Measurements were calibrated using the datasets IntCal13 and IntCal20 and the software SwissCal 1.0.
<input checked="" type="checkbox"/> Tick this box to confirm that the raw and calibrated dates are available in the paper or in Supplementary Information.	
Ethics oversight	No ethical approval/guidance was required. All the material was accessed after permission from the Greek Ministry of Culture and Sports and the agreement of the institutions/researchers who studied archaeologically the material and who also agreed to participate in this study.

Note that full information on the approval of the study protocol must also be provided in the manuscript.

## 6 Discussion

### 6.1 The role of aDNA in recording history

Over the last years, the introduction of aDNA analysis tools has demonstrated the great potential of the method to complement evidence derived from the study of the past through traditional approaches, or even illuminate previously unknown facades of it. In prehistoric contexts, our knowledge of the past cultures has been built piece by piece through the recovery of artifacts and burial practices, and their spatiotemporal correlation. It is important to bear in mind that this ‘traditional’ way of study of the past has not stayed monolithic through the years, but has enjoyed advancements in e.g., excavation methods, the implementation of mathematical models on archaeological data (e.g., demic or cultural diffusion), the integration of paleoenvironmental information, most of which essentially reflect turning points in theoretical interpretative frameworks in archaeology. One such has been the shift from the cultural-history phase to processual archaeology during the 60’s, which advocated for a biocultural approach. Bioarchaeology, initially defined as the study of animal remains and later the study of human remains from archaeological sites, was born from that new theoretical background (Buikstra and Beck, 2006). There is nowadays a growing corpus of bioarchaeological research that documents critical information from sex, health status, non-metric and genetic traits, to insights about social inequality, warfare and interpersonal violence. In addition, the more recent development of molecular methods for the measurement of isotope ratios on human bones and the comparison with environmental baselines has enabled the reconstruction of paleodiets and patterns of within-lifetime individual mobility.

The above methodological approaches apply to the study of historical contexts, even with a wider application, as the available material for study is more abundant and usually better preserved. The main difference regarding the study of these later periods lies on the reliance on the textual records, that include from deciphered administrative transactions of the early states, to legal documents and documents authored by past historians. Such literary sources can be very valuable; especially the latter often represents eye-witnessing of facts, but can also entail subjective point of views or fragmentary narrations. It is therefore critical for both historical and prehistorical periods to apply -when possible- scientific approaches.

Within the broad scope of the science of the human past, aDNA is becoming a standard tool for addressing diverse questions from human population genetics to plant and animal domestication, molecular identification of pathogenic microorganisms and microbiome composition. The potential of these approaches has recently expanded with the isolation and study of other informative biomolecules such as RNA and proteins, and the first insights from methylation maps (for a review of all these applications see Lindqvist, 2019). New nuances have been lent to well-documented historic events such the Justinianic plague and the Black Death epidemics through the reconstruction of the *Yersinia pestis* pathogen genomes recovered from human remains of different locations (Keller et al., 2019; Spyrou et al., 2019). More recently, a phylogenetically basal branch of the same pathogen was detected in Bronze Age individuals from across Eurasia (Andrades Valtueña et al., 2017). Although little is currently



known with respect to the virulence and the transmission vector of this early form of plague, the synchronous dissemination of the disease and the spread of people associated with Yamnaya culture in Europe might indicate some association (Reich, 2018). The realm of applications of aDNA as a means to delve into human history is nicely illustrated by a recent study that analyzed aDNA from the animal skins that were used to create the Dead Sea Scrolls, the religious manuscripts written by the people of Qumran between the 3<sup>rd</sup> and 2<sup>nd</sup> century BCE (Anava et al., 2020). The study identified skin pieces of cattle provenance which, considering the inhospitable local conditions for cattle, suggest that cow-made scrolls were brought and possibly written from outside. Consequently, through this side-evidence from animal DNA, it has been possible to propose a broader than a small sectarian Jewish community in the Iron Age.

On the other hand, analysis of aDNA directly from the human remains can provide more definitive evidence about migration, admixture, isolation, consanguineous endogamy, patri- or matrilinear social organization and patterns of genomic selection owing to environmental adaptation. The insights gained within prehistoric Eurasia through whole-genome and genome-wide analysis have been previously covered extensively. The manuscripts enclosed in this thesis fill-in important gaps in the human genomic history of Southwest Asia and the Aegean in Europe. These two neighboring regions have been interconnected throughout millennia of well-documented cultural exchange, and themes in archaeology and history often approach the region of the Aegean, the western section of Anatolia, Levant and the Egypt as one entity, the Eastern Mediterranean. Accordingly, the implication of the findings from these two large-scale genomic studies are discussed below jointly. Finally, a mention will be given to a follow-up tandem study, whereby combined isotopic and genomic data from Alalakh -a Bronze Age site presented in Manuscript A- map human mobility within the region of the Amuq Valley (Ingman et al., 2021)

## **6.2 Contextualization of archaeogenetic inferences for population migrations and human mobility**

### *6.2.1 Migration during the Neolithic within Southwest Asia and the Aegean*

The first archaeogenomic studies on Southwest Asia revealed high levels of genetic differentiation that persisted throughout the transition to the farming (Feldman et al., 2019; Kılınç et al., 2016; Lazaridis et al., 2016; Broushaki et al., 2016; Hofmanova et al., 2016; Mathieson et al., 2015). Although this small number of Early Holocene genomes leaves some seminal areas uncovered (e.g., Southeastern Anatolia and Northern Mesopotamia), succeeding populations from around three millennia later could be broadly explained as a mixture of those earlier Neolithic ancestral anchors from Anatolia, Southern Levant and Iran/Caucasus (de Barros Damgaard et al., 2018; Lazaridis et al., 2017; Lazaridis et al., 2016; Haber et al., 2017; Harney et al., 2018). Manuscript A engaged in disentangling the patterns of human mobility and population mixing from the Late Neolithic through the Late Bronze Age in the interconnected areas of Anatolia, the Southern Caucasus and the Northern Levant. The analyses

revealed persisting genetic homogeneity within Anatolia from the Early Chalcolithic onwards. However, the genomes from Anatolia to the Caucasus disclosed a robust temporal admixture signal that extended the Anatolian and Iranian/Caucasian-related ancestries from their earlier geographic distributions ca. 6500 BCE. The statistical resolution of the applied method of admixture dating might not have the power to distinguish between quasi-punctual mass migration over a constant contact over a larger period. However, the detection of the same average admixture date (ca. 6500 BCE) from Central and Northern Anatolia to the Caucasus suggest a broad-scale admixture event during the Late Neolithic period.

While this finding enjoys some interpretations from the existing literature, it also exposes some important missing links. Initially, an intrinsic problem arises from the currently limited knowledge regarding the ‘native’ ranges of the Anatolian, and the Iranian and Caucasian ‘ancestries’. Defined by Early Holocene genomes from these respective areas, little is known about the ancestral genetic make-up of the areas in-between, such as Eastern Anatolia and Mesopotamia. In addition, at these earlier periods, coexistence of various ancestries within a region is a possibility. An Anatolian-like lineage dating to the LGM has been identified in the Caucasus (Lazaridis et al., 2018). Although the populations representing this lineage might have retracted to the south or replaced by the Early Holocene hunter-gatherers (CHG), it should be also considered that their descendants persisted as north as e.g., the northeastern parts of Anatolia. Accordingly, the range of the (West) Iranian and Caucasian ancestries could extend to some sectors of Northern Mesopotamia. Considering the above knowledge gaps, it is currently challenging to disentangle the mode of population movement that resulted in the ca. 6500 BCE genetic cline by harnessing archaeogenetic data alone. On the other hand, by overlaying archaeological information, an interesting correlation emerges with respect to the abrupt introduction of Neolithic sites in Western Anatolia and the Aegean littoral, radiocarbon-dated to the early 7<sup>th</sup> millennium BCE. As previously explained, the extent of acculturation of local hunter-gatherers or the triggering of westward population movement by climatic events are contestable topics in archaeology. The contribution of Manuscript A on this regard was to extend the scope of population immigration and interactions to areas east of Central Anatolia. Because the admixture signal was inferred from the genomes of individuals from descending generations (ca. 5000-3000 BCE), it is reasonable to assume that the geographical origins of the first generations have been different. Subsequently, there are at least two general scenarios that can be proposed regarding the geographical aspects of the 6500 BCE mobility event. In the first scenario, admixture initially occurred within the formative zone of Neolithization and then populations carrying this new gene combination started to spread to other areas of Anatolia and the Caucasus. This scenario provides a convincing explanation about the co-presence of Anatolian, Levantine and Iranian-related genomic components on the 6<sup>th</sup> millennium BCE population at Tell Kurdu in Southeastern Anatolia, although the Levantine affinity could also be attributed to the Halafian connections that the site developed later. In the second scenario, admixture included populations beyond the strict geographical range of the Fertile Crescent and up to the Caucasus. This scenario enjoys support in the distinct local cultural features attested both in the Caucasus and Eastern Anatolia (Chataigner et al., 2014; Palumbi, 2011), the bidirectional exchange networks between Southeastern Anatolia and the Caucasus (Frahm

et al., 2016), and the simultaneous break-down of genetic structure of goat domesticates in Anatolia, Iran, Caucasus and the Levant (Daly et al., 2018). A weaker point in the latter scenario is the scarcity of settlement evidence from northern and eastern sectors of Anatolia dating to the 7<sup>th</sup> millennium BCE or before. However, this fact can be attributed to research lacunas (Düring, 2008; Özdoğan, 1996; Palumbi, 2011), and therefore future archaeological and aDNA data from these contexts would greatly contribute to deciphering the nature of the population entanglements in this area.

The introduction of the distinct ancestry related to Caucasus and Iran in Anatolia has rendered possible to track human mobility further beyond, in the Aegean. In Southern Greece, aDNA could be recovered from the Neolithic occupations at the caves Franchthi and Diros in the Peloponnese (Mathieson et al., 2018). In contrast to the European Neolithic populations, the genomes of those individuals required some contribution related to CHG. In the context of the analysis of the Neolithic individuals from Crete in Manuscript B, the aDNA data from these individuals were re-appraised. The new analyses suggest that the signal of CHG-related genetic component comes from the later individuals (5<sup>th</sup>-4<sup>th</sup> millennium BCE), and is dated to approximately thirty generations before the time of those individuals, hence during the early 6<sup>th</sup> millennium BCE. A similar signal has been reported between Early and Late Neolithic individuals from Northern Greece (Hofmanova et al., 2016). Taken together, a synthesis of current archaeological and genetic information could advocate that ‘eastern’ ancestry related to CHG/Neolithic Iran had reached Central Anatolia by mid-7<sup>th</sup> millennium BCE through large-scale immigrations (see also Kılınç et al., 2016); from there, it gradually disseminated to both sides of the Aegean Sea (Greece and Western Anatolia), where the distribution of elements of the ‘Neolithic package’ suggest multiple routes and expansion waves of the Neolithic way of life (Özdoğan, 2011; Özdoğan, 2014; Perlès, 2003; Perlès, 2005). Crete also witnessed the arrival of populations carrying this ‘eastern’ ancestry by the Early Bronze Age, or even earlier. In Manuscript B, genetic data from some of the island’s earliest farmers are presented. Buried in the late 7<sup>th</sup> millennium cemetery of Aposelemis, at the northern coast of the island, these individuals had barely any DNA preserved in their bones. Eventually, genome-wide data could be generated from six individuals which were shown to exhibit more genetic affinity to other Aegean genomes from the Eastern Mediterranean than from Central Anatolia. A more specific geographic origin could not be pinpointed at the moment, due to the low coverage of the data and the absence of contemporaneous genomes from the Anatolian littoral and Cyprus. However, the reduced genetic diversity -deduced as the most plausible interpretation of low rate of mismatching alleles among the Aposelemis individuals- indicates variegated population dynamics between Neolithization of the Greek mainland and the islands. In more specific, this genetic feature might indicate that the far-reaching coastal networks that resulted in the Neolithic settlement of Crete (Horejs et al., 2015; Perlès, 2005; Reingruber, 2011) were operated by small-sized founding populations.

### 6.2.2 *The role of human mobility in the Near Eastern early-state and territorial-state societies*

A central question of Manuscript A was whether and how small or large-scale mobility was an agent of the different networks of interregional cultural contacts that were consolidated during the Chalcolithic and Bronze Age in Anatolia and the Northern Levant. In the Southern Levant, where some of the oldest transitional farming communities have been attested (Davies and Charles, 1999), the stages of population interactions have been well documented over the last years. As it was recently shown, marked cultural changes identified towards the end of the Chalcolithic period in the Central/Southern Levant (ca. 5<sup>th</sup>-4<sup>th</sup> millennia BCE) had been accompanied -if not propelled- by populations related to Iran and Anatolia (Harney et al., 2018). Gene-flow in the area continued through the succeeding Bronze Age (Haber et al., 2017; Lazaridis et al., 2016), although it was proposed that these later populations were derived from a more genetically diverse local population than the one represented by the sampled Chalcolithic individuals (Harney et al., 2018). Manuscript A demonstrated that within the large territory of Anatolia, no influx from distinct gene pool(s) could be associated with the early-state formation in Eastern Anatolia (Frangipane, 2012b), or the shared artifactual features between Central/North Anatolia and the Balkans (Schoop, 2011). This finding gives prominence to indigenous sociocultural developments oriented towards external influences; a complex process that could be discerned only recently through the extension of excavations and the study of new artifacts from Eastern Anatolia (Frangipane, 2018). However, no conclusion about a general model of minimal role of immigration can be reached with respect to the Uruk and Ubaid 'expansions'. Instead, the findings from Manuscript A should encourage an endeavor for properly contextualized archaeogenomic evidence from across the Greater Mesopotamia.

With respect to the niches of interethnic societies within Eastern Anatolia suggested by the material culture, the association with archaeogenetic data is more tenuous. A subtle genetic affinity with Bronze Age pastoralists from the Caucasus was documented on some individuals from Arslantepe. Nevertheless, a correlation with a cultural 'identity' was not possible, as these individuals belonged to a secondary deposition of victims of interpersonal violence (Erdal, 2012). As a matter of fact, the co-presence of cultural groups with differences in subsistence and burial practices, does not need to be identifiable genetically, since the assumption that genes correspond to cultural groups and/or ethnicity can be erroneous. The Kura-Araxes cultural tradition expanded from Southern Caucasus to the south in Eastern Anatolia and Western Iran, through adaptation to new locations, until it got ultimately assimilated into a majority culture (Rothman, 2015). Therefore, understanding the nature of the biological/demographic interactions throughout this process entails the integration of future archaeogenomic data from contexts associated with Kura-Araxes spanning their entire geographic range.

The interactions of populations with diverse ethnic backgrounds becomes a dominant theme during the Middle and Bronze Ages Near Eastern societies, when ethnic identity is not only inferred from material culture, but also through ancient scripts that document in detail the movement of traders, artisans and administrative representatives. In Manuscript A, aDNA was

analyzed from individuals buried in two cities, Alalakh and Ebla, capitals of prominent kingdoms in the Northern Levant. The individuals from both sites were shown to bear a distinct composition of genes from their Anatolian neighbors and the preceding populations from the same area (i.e., Tell Kurdu). This composition could be genetically explained through complex models built from the available aDNA data. Eventually though, the co-interpretation with ancient textual records and paleoenvironmental data favored the scenario of population migration from Northern Mesopotamia.

Besides the novel archaeogenomic insights regarding human mobility at the scale of populations, Manuscript A revealed that in a total of almost forty individuals, all but one were shown to be genetically indistinguishable to the resolution of the methods and the reference data. Similar ratios or a ‘local’ majority and a small number of individuals with genetic origins identified to distant areas is the consensus for Bronze Age Southern Levant according to recent archaeogenetic studies (Agranat-Tamir et al., 2020; Haber et al., 2017; Haber et al., 2020). Therefore, from the current evidence it seems to hold that the early globalized societies of the Eastern Mediterranean were in their vast majority inhabited by people of local ancestry, whereas the presence of people from far-reaching areas -despite not uncommon- was more an occasional feature.

It is important to mention that ‘local’ ancestry cannot be defined in absolute terms. First, it reflects the current state of knowledge which depends on the access to diachronic and geographically dense genomic data. Second, the definition of genetic ancestry cannot be immutable in the study of human population history. This is because in many parts of the world -and especially West Eurasia- genetic structure starts to break down after the Bronze Age. Therefore, while broader ancestry profiles can be widespread, fine-scale structure might become visible only after assembling and co-analyzing large aDNA datasets, or via looking into other structural features of the genomes (e.g., distribution of local ancestry tracts). However, such quantitative and qualitative requirements are difficult to fulfil in areas such as the Eastern Mediterranean, where the aDNA preservation is typically poor. Moreover, considering that genes represent only one façade of ‘locality’, -the others being the local upbringing and the social integration- recent interdisciplinary studies have aspired to map human mobility by combining ancestry profiles with isotopic information (Frei et al., 2019; Ingman et al., 2021). In the study from Ingman and colleagues, we generated oxygen and strontium isotopes from up to 77 individuals from Alalakh, and we increased the genomic data reported in Manuscript A from 27 to 37 individuals. The two lines of evidence corroborated to a largely homogeneous gene pool and local upbringing of the Alalakh population. The five individuals that were raised outside of the Amuq Valley belonged to the same gene pool, suggesting an origin from within the Northern Levant. Interestingly, the individual with genetic origins related to Bronze Age Central Asia was also consistent with a local upbringing. However, due to a lack of biologically available strontium isotope ratios from the Central Asian areas, it is not currently possible to definitively rule out a childhood spent in these regions.

### 6.2.3 *Disentangling the interplay of ‘eastern’ and ‘steppe’ ancestries in the Bronze Age Aegean*

Across Europe, the transition to the Bronze Age (ca. 3000 BCE) was shaped by immigration and the introduction of genes by people from the Eurasian Steppe. In many areas, this demographic process has been associated with the prevalence of the Y-chromosome R1a and R1b haplogroups (Haak et al., 2015), or even with male-biased admixture (Martiniano et al., 2017; Olalde et al., 2019; Saag et al., 2017). ‘Steppe’-related ancestry (SA) was detected as south as 2200 BCE Sicily, likely following a western route from Iberia (Fernandes et al., 2020). In the Aegean, the first evidence of SA came from the southern Greek mainland ca. 1400-1200 BCE, at the time when the so-called Mycenaean culture flourished in the area (Lazaridis et al., 2017). Manuscript B increased the number of genome-wide from the Late Bronze Age Aegean from 4 to 31 and expanded the geographical range from the mainland to the Cyclades and Crete. The analyses showed that by ca. 1600 BCE -and likely not before 2800 BCE-, SA was widespread not only in the southern Greek mainland, but also the nearby islands. In the Cyclades, it was present on individuals from the early Mycenaean phase of Paros dated to 1200 BCE, when the hill of the island was fortified with a Cyclopean wall into a citadel. The exact timing of its arrival in the Aegean remains uncertain. At this stage, an eastern origin from Anatolia can be ruled out, as demonstrated by the large dataset of Manuscript A that lacks any signal of steppe-related admixture. Moreover, a recent study reported individuals from Northern Greece dating to the Middle Bronze Age (ca. 2000 BCE) that carried a higher SA proportion than the one inferred in Lazaridis et al. (2017) (Clemente et al., 2021). Overall, the genetic data seem to favor a population scenario in which SA gradually diffused into the local gene pool of the Greek mainland, likely during the earlier and middle periods of the Bronze Age; and from there, it migrated to the Aegean islands.

Human mobility and mixing of populations, however, was not a feature in the Aegean only during the Late Bronze Age period. ‘Eastern’ ancestry contributed to the gene pool of the Early Bronze Age Aegeans, both in the mainland and the islands. Adequately modeled as a source population like Chalcolithic Anatolians, the amount of eastern ancestry was estimated to be higher in individuals from Euboea, an island connected to the Cycladic world. It seems, therefore, that the Early Bronze Age ‘international spirit’ that pervaded Cyclades, and soon after Crete and the mainland, is also reflected on the genomes of the individuals from that period and as far as Middle Bronze Age Sicily (Fernandes et al., 2020).

Considering this landscape of human mobility within the Bronze Age Aegean, it comes without surprise that SA was detected in individuals from Late Bronze Age Crete (late Middle Minoan to Late Minoan IIIC). However, this finding is intriguing for two reasons: a. the inferred SA contribution in some individuals is higher than the other contemporaneous populations from the southern mainland, and b. it coincides with a ‘Mycenaean’ invasion in the island towards the 15<sup>th</sup> century, a theory that remains highly contested nowadays. Following a well-manifested horizon of destructions targeted to administrative centers and elite symbols (Late Minoan IB) (Driessen and Macdonald, 1997), Crete experienced innovations in funerary architecture and burial practices that emphasized individual aggrandizement and militarism, features traditionally ascribed to the ‘Mycenaean’. Another reason traditionally asserted to the

belief of an invasion, is the replacement of Linear A with Linear B. However, new views on how to approach identities and social interaction challenge an ethnic explanation of such innovations -and therefore their external enforcement; instead, they can serve as strategies for legitimization of power in circumstances of social unrest (Galanakis, In prep). Furthermore, the discontinuity in funerary architecture biases in archaeology, since the knowledge on burial practices from the previous Late Minoan IB is limited (Nafplioti, 2008). In this context, the genetic evidence from Manuscript B cannot settle a debate that concerns questions of political power. It does, nevertheless, inform this debate by contributing a critical social aspect, that of the biological interaction of the two populations that could be traced on the genomes of individuals from Central and Western Crete, some of which could predate the proposed 'invasion'. Overall, the increased SA within the populations from -or close to- major administrative centers during the Late Minoan period could also corroborate to the role of the island as a hub where people from the Greek mainland, but also from areas around the Aegean (e.g., Adriatic), would travel and eventually settle. Denser sampling from the eastern and inland parts of Crete would further elucidate whether this phenomenon was transient and evident only on major centers or broadly affected the demography of the island.

### **6.3 A glimpse at past social practices from aDNA**

As the big questions about past migration patterns are progressively settled for various regions of the world, archaeogenetic research has recently expanded its scope to microlevel phenomena (reviewed in Racimo et al., 2020). Marriage practices, post-marital residence, kinship, high status and social inequality can disclose biological signals. Hence, revealing such information and integrating it within theoretical frameworks from the social sciences can illuminate facets of sociocultural expressions of past societies.

Genetic evidence relevant to sociocultural practices comes from both Manuscripts, although conclusions from Manuscript A are drawn from isolated cases. This refers to the genetically outlying individual from Alalakh. With more than 300 burials identified to date at the site, the so-called 'Lady in the well' is the second known case of a non-intentional burial (the other resulted from the collapse of a building). Likely raised in Alalakh or the broader region of the Amuq Valley, she was discovered facing down at the bottom of a deep well and her extremities slayed, indicating that she was probably thrown into the well. Her skeleton also bore evidence of multiple healed traumata, while her dentition exhibited multiple episodes of enamel hypoplasia. The overall profile of this individual -reconstructed through the archaeological, paleopathological and aDNA analysis- suggests a distinct life history from the rest of the individuals found in the site. While at this stage it is not substantiated to postulate social discrimination from the 'locals' against an 'immigrant', it is more legitimate to claim that the sole analysis of the intentional burials might not entirely reflect the local population diversity.

In Manuscript B, the genealogical tree of a family was reconstructed from an intramural infant burial in the Late Bronze Age settlement at Mygdalia. The infants were placed within

the burial consecutively, and six of them belonged to the same family, related as half or full siblings and aunt-nephew/niece. This pedigree indicates a burial of a kin group with close blood ties. However, the seventh infant was second-degree relative to one of these infants through the other parental side, hence unrelated to the other five infants. Whether and to which degree the eighth infant was biologically related will stay a mystery because of the poor DNA preservation on its bones. As a matter of fact, biological kinship is a critical layer of information that is currently missing from the plethora of collective burials in the Aegean that appear since the Neolithic. In this direction, a number of comprehensive bioarchaeological studies during the last years have looked into how biological kinship and post-marital residence have structured the spatial organization of tombs in cemeteries and collective inhumations (e.g., Prevedorou, 2015; Moutafi, 2015; Prevedorou and Stojanowski, 2017). Compared to biodistances calculated from the skeletons, aDNA can give more precise estimates regarding biological relatedness. In this sense, Mygdalia provides the first solid evidence for representation of biologically kin groups into collective burials. At the same time, collective burials encompass very diverse funerary practices, from commingled secondary depositions (e.g., Hagios Charalambos cave ossuary in Lasithi) to the aforementioned infant burials within house areas, and the monumental structures such as the chamber tombs in Aidonia and Nea Styra. For none of the latter sites, though, was it possible to obtain aDNA from all the members of the burials, and therefore a proper evaluation of biological relatedness is constrained. However, the fragmentary information indicates that biological bonds existed within the chamber tombs of Aidonia. On the contrary, at Nea Styra, the five males not only were not they related, but also differed in their ancestry, with some of them carrying higher proportions of the ‘eastern’ genetic component.

Recently, aDNA studies have received critique for adhering to kinship interpretations from the inference of biological relatedness, thereby diminishing the role of ideology in shaping kin groups (Brück, 2021; Ensor, 2021). Overall, the data from Manuscript B provide evidence for biologically-based kinship within a very particular burial context (Mygdalia), whereas the opposite might be the case for another (Nea Styra). These preliminary results indicate that aDNA analysis could have its share in further elucidating collective and family identities within prehistoric Aegean societies. Reaching this point, however, would require the representation of the various burial practices, and prudent integration of the findings within the existing theoretical frameworks.

The various cases of consanguinity identified across different periods and settings in Manuscript B led to the conclusion that endogamy has been a common practice within the prehistoric Aegean. Currently, references in the literature about prehistoric endogamy in the Eastern Mediterranean are scarce. Overall, archaeogenetic studies show that, although consanguinity seemed more common within agriculturist societies than among hunter-gatherers, it was still very rare (Ceballos et al., 2021). Some studies on the concurrence and segregation of non-metric traits have postulated that consanguineous endogamy was practiced in late Pre-Pottery Neolithic Jordan before the herding and farming practices could be widely established (Alt et al., 2013), and among elite groups of predynastic Egypt (Prowse and Lovell, 1996). Exploration of the genome-wide (1240K) data from nearly 2,000 ancient humans



showed that endogamy -while practiced today by certain ethnic and religious groups- was very infrequent in prehistoric periods throughout the world (Ringbauer et al., 2021). The evidence from the Aegean suggests that certain nuances might be missing from this picture. Future aDNA datasets from more regional time-transects will greatly contribute to assess variation or convergence of marriage practices across different cultural contexts and periods. Interestingly enough, while the populations from the Aegean were shown to carry ancestry related to post-Neolithic populations from Anatolia, when the HapROH method is applied on the dataset from Manuscript A, the frequency of close-kin unions is much lower than in the Aegean (Figure 1). This striking difference might as well reflect sampling gaps from areas of the Anatolian littoral, but the (more) frequent consanguinity in the Aegean seems to be a fact, at least for the island populations. However, considering the diverse cultural contexts in which consanguineous endogamy was identified, a proposal of a universal explanation might not be mature at this point. Instead, contributing this knowledge should stimulate future archaeological and anthropological research towards holistic interpretations.

#### **6.4 Sampling limitations and future perspectives**

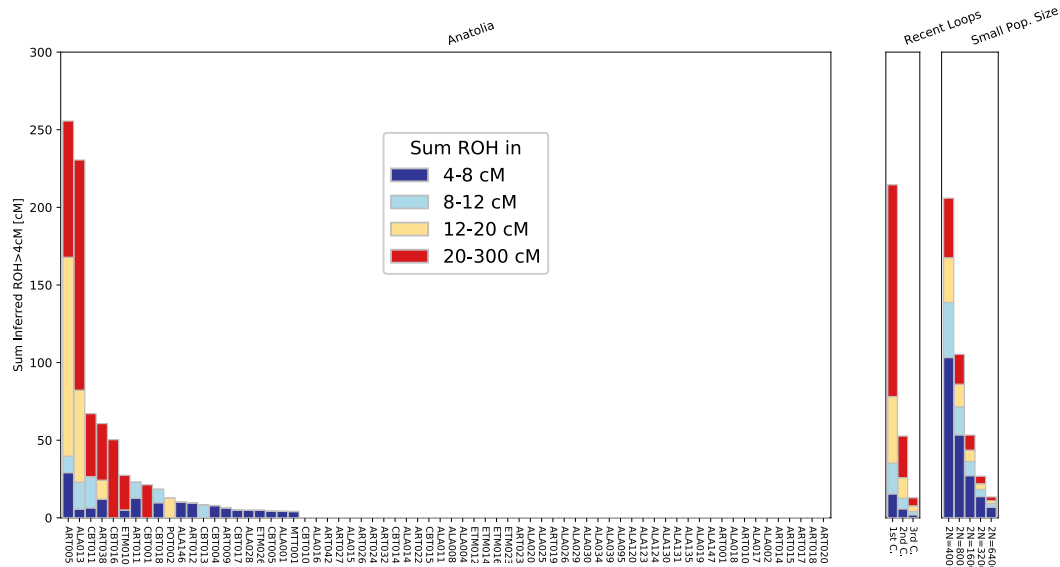
The manuscripts comprising this thesis apply state-of-the-art archaeogenomic methods, namely sampling of the *pars petrosa*, target enrichment of genome-wide polymorphic positions and a range of statistical tools that can disentangle complex patterns of population affinities even from lower-quality genetic data. On the whole, the results demonstrate that inferences about population history such as migration, individual mobility and micro-level biological interactions reflecting sociocultural features, are possible from regions in climatic zones that are typically believed to be more hostile for the preservation of aDNA. Based on the data presented here, the overall rate of Aegean, Anatolian and northern Levantine samples that yielded sufficient DNA for genome-wide analysis is approximated to 25%. Seemingly low - when compared to Northern parts of Western Eurasia- this rate is substantially higher than the <10% reported at Southern Levant, for human remains recovered from Neolithic, Bronze Age and Iron Age contexts (Feldman, 2020). This suggests that, within the Eastern Mediterranean, aDNA preservation can be variable, with areas such as Anatolia presenting more opportunities for future work. This remark is encouraging with respect to future studies on the Aegean, the Northern Levant and Anatolia, considering that, along with the novel insights brought by the two manuscripts, issues regarding the sample representativeness, as well as limitations on the resolution of methodologies were exposed. For example, with aDNA data from Northern Greece and the Balkans spanning from the Chalcolithic to the Bronze Age, the timing and mode of introduction of the steppe-related ancestry in the Aegean would be elucidated in more detail. Accordingly, the subtle genetic differences between Bronze Age Eastern Anatolia and the Northern Levant presented in Manuscript A suggest that archaeogenetic data from Mesopotamia is a critical missing link in order to delineate major trends in human mobility that brought these regions together in a period of major cultural developments. To date, no genomic data have been reported from Mesopotamia and little is known with respect to the degree of

aDNA preservation on remains from prehistoric and historic contexts. This limitation might be overcome in the near future, as the archaeogenetic community grows, thus creating more opportunities for interdisciplinary collaborations. It is nevertheless crucial that collaborations honor guidelines for ethical handling of samples that define the frame for proper communication with stakeholders, exhaustive documentation of material, application of non-invasive sampling methods, as well as joint interpretation of results and awareness about their possible political instrumentalization.

At this point it should also be acknowledged that issues concerning sample representativeness do not arise only from high aDNA degradation, limited accessibility to collections, or transdisciplinary communication, but also due to inherent constraints from the ancient burial record. One characteristic case is the Late Bronze Age in Anatolia during the Hittite influence, when a shift from inhumations to cremations has been documented, while the overall number of Hittite graves discovered thus far is very limited (Steadman and McMahon, 2011). This feature is also manifested at the site of Alalakh (Manuscript A) with a mere 10% of the total graves dating from the period of the Hittite rule on Alalakh (ca. 1400-1300 BCE), of which a third represents cremations (Ingman, 2014).

In contexts where sample preservation is less problematic, future research would benefit from a fine-grained approach of population affinities. The large number of individuals from Anatolia to the Southern Caucasus dated to the Chalcolithic and Bronze Age periods enclosed the signal of an older admixture that genetically homogenized the populations. Although fascinating in its interpretation, this genetic feature might also challenge the resolution of many analyses to infer finer structure. Indeed, *f*-statistics indicated the presence of some kind of post-Neolithic substructure between e.g., Western and Central Anatolia and within Eastern Anatolia. By applying haplotype-sharing methods, one could understand substructure in greater detail, including patterns of local human mobility reconstructed from the distribution of close and distant relatives (e.g., Cassidy et al., 2020). Gaining these insights from areas like the Aegean and the Near East would require processing of large sample assemblages in order to guarantee diachronic and spatially dense genomic datasets of certain coverage and archaeological contexts. In addition, a concern regarding the application of these methods in the ancient Near East is the imputation of missing genotypes from modern reference panels in which Near Eastern populations are underrepresented. Recently, a new method has been able to infer haplotypic information directly from genome-wide pseudo-haploid data of low coverage (i.e.,  $\geq 0.3x$  on 1240K panel) by leveraging linkage information from the reference panels of modern phased genomes (Ringbauer et al., 2021). The authors have also reported robust estimates on individuals of non-African ancestry, even with a European-only reference panel. The application of this method on the Aegean revealed runs of homozygosity equivalent to consanguinity, which would not be possible to detect with previous methods. This example showcases the growing potential of new methods in the field of ancient population genetics to gain a finer-scale genetic resolution.

**Figure 1.** Runs of Homozygosity inferred with HapROH on the data from Manuscript A. Left: Only a very small portion of individuals (coverage  $\geq 300,000$  SNPs) accumulated long ROH (20-200 cM) which are typically indicative of consanguinity. Right: expectation of ROH distribution for an individual being offspring of first, second or third cousins, or sampled from a population of a given effective size.



## 7 Summary

### 7.1 Summary (English)

Southwest Asia (Near East), as well as the Aegean, have been pivotal areas for the human sociocultural evolution. The emergence and dissemination of farming technologies and lifestyle, followed by the culmination into complex systems of urban and palatial organization, and eventually the formation of territorial states and the far-reaching networks of the Eastern Mediterranean in the 2<sup>nd</sup> mill. BCE, was a process of societal transformation over ca. 10 millennia. More than a century of intensive archaeological research in this area has probed the scope of this process providing ample evidence for intercultural encounters and exchanges that trigger questions about human mobility, its drivers, mode, scale and impact on individual lives, and essentially its role in shaping history. Ancient DNA (aDNA), as a biomolecular method applied on ancient remains, provides information about the genetic make-up of past peoples that can be used to reconstruct aspects of migration history down to micro-level social interactions. The emerging field of archaeogenetics is currently enjoying an impressive increase in data production owing to recent developments in high-throughput sequencing technology, protocol improvements and interdisciplinary collaborative programs. Following these directions, the manuscripts comprising this thesis represent a large-scale archaeogenetic approach to the Southwest Asia and the Aegean, which was not available at the time of this thesis.

In **Manuscript A**, I retrieved and analyzed genome-wide from over 100 human remains unearthed from archaeological sites in Anatolia, the Southern Caucasus and the Northern Levant, and spanning ca. 4 millennia of human history, from the Late Neolithic to the Late Bronze Age. I co-analyzed this new dataset together with available data from modern and ancient populations to set constraints to admixture models and explore as many possible alternatives that would fit the data. My main focus was to understand the process of genetic homogenization throughout this period, whether there was regional variability and how this correlates with existing archaeological evidence for networks of cultural interactions. Another focus was to gain insights into the population dynamics within the early globalized societies of the Eastern Mediterranean by recovering and analyzing dense intra-site data. The results showed that a large-scale admixture brought together people from across Anatolia to the Caucasus and Iran. Based on the methods of admixture dating, this event did not trace back neither to the beginning of the Neolithic, nor much later, to the emergence of the urban centers from Southern to Northern Mesopotamia and Eastern Anatolia, but to ca. 6500 BCE. This timing correlates with the expansion of sedentary communities in Anatolia, and suggests that this process was accompanied by gene exchange spanning a much larger area, in contrast to the earlier transition from foraging to farming. Following this population event, no major genetic shifts were shown for Anatolian populations. On the contrary, a genetic shift occurred in the Northern Levant by the early state period, and could be attributed to admixture with as-yet unsampled populations from Northern Mesopotamia. Furthermore, I was able to show that the vast majority of individuals from northern Levantine societies of the 2<sup>nd</sup> millennium BC

exhibit a very similar genetic profile. However, I could not identify the genetic origins of one individual from a non-intentional burial to the Bronze Age Eastern Iranian/Central Asia. This finding indicates that individual mobility could cross the borders of the Eastern Mediterranean globalised societies, but such individual cases are less likely to be represented in the record of formal burials.

In **Manuscript B**, I analyzed genome-wide data from 102 individuals from the Aegean spanning the same period (Neolithic – Late Bronze Age; ca. 6000-1050 BCE). Along with the available data I also included those from Manuscript A, and tried to refine the models for the admixture history of the Aegean populations during this period. The geographical scope of the sampling comprised a more restricted -but culturally diverse- area from the southern Greek mainland, to the Aegean islands and Crete. The sampling was also targeted to various types of collective burials with the goal to disentangle biological features such as relatedness or differential ancestries reflected in the burial practices. Following this research direction, I also applied newly developed methods that infer demography and inbreeding (consanguinity) from low-coverage genome-wide data. My results showed that early farmers from Crete -some of the earliest in Europe- shared the same genetic profile as contemporary populations from the Greek mainland and Anatolia. My admixture models indicated that gene-flow from Anatolia into the Aegean carried on to the Early Bronze Age, suggesting that the progressive integration of Aegean societies within the exchange networks of the Eastern Mediterranean was accompanied by population movements. Nevertheless, by the Late Bronze Age, the populations from the mainland carried additional admixture signatures related to the Bronze Age pastoralists from the Eurasian Pontic Steppe. After the Greek mainland, these signatures gradually appeared in Crete, thus providing a new angle for the long-debated hypothesis that Mycenaeans from the mainland took over the control of the island from the 15<sup>th</sup> century onwards. Furthermore, I found consanguinity among the Aegean individuals at levels unparalleled for the aDNA record of prehistoric Europe and Southwest Asia. The data suggested that these cases mostly matched with endogamy at the degree of first cousins, thus pinpointing to a social practice that was shared mainly among island populations from different cultural contexts. Finally, I reconstructed the pedigree of a Mycenaean infant burial and found that all the infants were related to some degree, and most of them shared the same two grandparents. This is the first pedigree reconstructed archaeogenetically from a collective burial in the prehistoric Aegean, and sheds a novel light on the importance of biological kinship and its emplacement within the collective memory of a Mycenaean community.

In conclusion, this thesis demonstrates the power of archaeogenomic approaches to record population history, from migration and individual mobility to micro-level biological interactions that reflect sociocultural features of past societies, such as kinship practices. In spite of the challenges in aDNA retrieval from the Aegean and the Near East, this thesis also highlights that with latest methodologies, extensive and dense sampling strategies, it is possible to recover genomic information from such contexts. Albeit the data are still far from exhaustive, their analysis and results presented in this thesis provide critical hints on questions raised through the study of material culture and physical anthropology. They have also lent new nuances to aspects of human population history that have been unattested, understudied

or very challenging to identify from the archaeological and anthropological context alone. Eventually, as one of the first large-scale archaeogenomic studies in the Near East and the Aegean, this thesis aspires to pave the way for future interdisciplinary studies on the recent prehistory of this area.

## 7.2 Zusammenfassung (Deutsch)

Südwestasien (der Nahe Osten) und die Ägäis waren für die soziokulturelle Entwicklung des Menschen von zentraler Bedeutung. Die Entstehung und Verbreitung bäuerlicher Technologien und Lebensweisen, gefolgt von der Herausbildung komplexer Systeme städtischer und palastartiger Organisation, und schließlich die Bildung von Territorialstaaten und weitreichenden Netzwerken im östlichen Mittelmeerraum im 2. Jh. v. Chr. waren Prozesse gesellschaftlichen Wandels über einen Zeitraum von ca. 10,000 Jahren. Mehr als ein Jahrhundert intensiver archäologischer Forschung auf diesem Gebiet belegen diese Prozesse und liefern zahlreiche Belege für interkulturelle Begegnungen und Austauschvorgänge, die Fragen über die menschliche Mobilität, ihre Triebkräfte, ihre Art und Weise, ihr Ausmaß und ihre Auswirkungen auf das Leben des Einzelnen und im Wesentlichen ihre Rolle bei der Gestaltung der Geschichte aufwerfen. Die Analyse alter DNA (aDNA) mit Hilfe biomolekularer Methoden, die auf antike Überreste angewandt wird, liefert Informationen über die genetische Herkunft vergangener Völker, anhand derer Aspekte der Migrationsgeschichte bis hin zu sozialen Interaktionen auf Mikroebene rekonstruiert werden können. Das aufstrebende Gebiet der Archäogenetik verzeichnet derzeit einen beeindruckenden Anstieg der Datenproduktion, was auf die jüngsten Entwicklungen in der Hochdurchsatz-Sequenzierungstechnologie, die Verbesserung von Protokollen und interdisziplinäre Kooperationsprogramme zurückzuführen ist. Diesen Richtungen folgend, repräsentieren die Manuskripte dieser Arbeit groß angelegte archäogenetische Ansätze für Südwestasien und die Ägäis, welche zum Zeitpunkt dieser Arbeit noch nicht verfügbar waren.

In **Manuskript A** habe ich genomweite Daten von über 100 menschliche Überresten von archäologischen Fundorten in Anatolien, dem südlichen Kaukasus und der nördlichen Levante, die ca. 4 Jahrtausende der Menschheitsgeschichte, vom späten Neolithikum bis zur späten Bronzezeit, umfassen, analysiert. Dieser neue Datensatz wurde zusammen mit verfügbaren Daten aus modernen und antiken Populationen ausgewertet, um Einschränkungen für Vermischungsmodelle festzulegen und möglichst viele Alternativen zu evaluieren, die zu den Daten passen würden. Mein Hauptaugenmerk lag darauf, den Prozess der genetischen Homogenisierung im genannten Zeitraum zu verstehen, d.h. ob es eine regionale Variabilität gab und wie diese mit archäologischen Befunden zu Netzwerken kultureller Interaktionen korreliert. Ein weiterer Schwerpunkt war die Gewinnung von Erkenntnissen über die Bevölkerungsdynamik in den frühen globalisierten Gesellschaften des östlichen Mittelmeerraums durch die Generierung und Analyse von Binnenanalysen (intra-group). Die Ergebnisse zeigen, dass es eine großräumige Vermischung gab, die Menschen aus ganz Anatolien, dem Kaukasus und dem heutigen Iran zusammenbrachte. Dieses

Vermischungsereignis lässt sich weder auf den Beginn des Neolithikums noch viel später, auf die Entstehung der städtischen Zentren von Süd- bis Nordmesopotamien und Ostanatolien, zurückführen, sondern auf ca. 6500 v. Chr. Dieser Zeitpunkt stimmt mit der Ausbreitung sesshafter Gemeinschaften in Anatolien überein und deutet darauf hin, dass dieser Prozess im Gegensatz zum früher datierten Übergang von der Wildbeutertum zum Ackerbau von einem Genaustausch über ein viel größeres Gebiet hinweg begleitet wurde. Nach diesem Ereignis um 6500 v. Chr. wurden für die anatolischen Populationen keine weiteren größeren genetischen Verschiebungen festgestellt. Im Gegenteil, in der nördlichen Levante kam es in der Frühzeit zu einer genetischen Verschiebung, die auf eine Vermischung mit noch nicht beprobten Populationen aus Nordmesopotamien zurückgeführt werden könnte. Darüber hinaus konnte ich zeigen, dass die überwiegende Mehrheit der Individuen aus den nordlevantinischen Gesellschaften des 2. Jahrtausends v. Chr. ein sehr ähnliches genetisches Profil ausweisen. Zudem konnte ich die genetische Herkunft eines Individuums aus einer Sonderbestattung aus dem bronzezeitlichen Ostiran/Zentralasien identifizieren. Dieser Befund deutet darauf hin, dass die Mobilität von Individuen die Grenzen der globalisierten Gesellschaften des östlichen Mittelmeerraums überschreiten konnte, solche Einzelfälle sind in den Befunden regulärer Bestattungen allerdings eher selten vertreten.

In **Manuskript B** habe ich genomweite von 102 Individuen aus der Ägäis aus demselben Zeitraum (Neolithikum - Spätbronzezeit; ca. 6000-1050 v. Chr.) analysiert. Zusammen mit den verfügbaren Daten habe ich die Daten aus Manuskript A einbezogen und versucht genetische Modelle der Herkunft ägäischer Populationen diesen Zeitraums zu verfeinern. Der geografische Umfang der Probenahme umfasste ein engeres, aber kulturell vielfältiges Gebiet vom südlichen griechischen Festland bis zu den ägäischen Inseln und Kreta. Die Probenahme wurde auch auf verschiedene Arten von Kollektivbestattungen ausgerichtet, um biologische ausgerichtete Fragen wie z.B. genetische Verwandtschaft oder unterschiedliche Abstammungsgebiete, die sich in den Bestattungspraktiken widerspiegeln, zu adressieren. Hier konnte ich auch neu entwickelte Methoden anwenden, welche es ermöglichen Aussagen zur Demografie und Inzucht (Verwandtenehe) aus genomweiten Daten mit geringer Abdeckung zu treffen. Meine Ergebnisse zeigten, dass die frühbäuerlichen Gesellschaften Kretas - einige der frühesten in Europa - das gleiche genetische Profil aufwiesen wie heutige Populationen auf dem griechischen Festland und in Anatolien. Meine genetischen Vermischungsmodelle zeigen, dass der Genfluss von Anatolien in die Ägäis bis in die frühe Bronzezeit anhielt, was darauf hindeutet, dass die fortschreitende Integration der ägäischen Gesellschaften in die Austauschnetze des östlichen Mittelmeers von Bevölkerungsbewegungen begleitet wurde. In der Spätbronzezeit zeigen die Populationen vom Festland jedoch Signaturen zusätzlicher Beimischung, die mit bronzezeitlichen Hirtenvölkern der eurasischen Steppenregionen in Zusammenhang stehen. Neben dem griechischen Festland tauchten diese Signaturen allmählich auch auf Kreta auf, was der seit langem diskutierten Hypothese, welche besagt, dass die Mykener ab dem 15. Jahrhundert v. Chr. vom Festland aus die Kontrolle über die Insel übernahmen. Darüber hinaus konnte ich enge Blutsverwandtschaft unter den ägäischen Individuen feststellen, und zwar in einem Ausmaß, welches in den aDNA-Daten des prähistorischen Westeurasiens beispiellos ist. Die genetischen Daten deuten auf

Verwandtenehen auf Ebene erster Cousins/Cousinen hin, und damit auf eine soziale Praxis, die vor allem unter Inselformationen aus verschiedenen kulturellen Kontexten verbreitet war. Zudem konnte ich einen Familienstammbaum einer mykenischen Kinderbestattung rekonstruieren und feststellen, dass alle Kinder bis zu einem gewissen Grad miteinander verwandt waren und die meisten von ihnen die gleichen zwei Großeltern hatten. Dies ist der erste archäogenetisch rekonstruierte Stammbaum aus einer Sammelbestattung in der prähistorischen Ägäis und wirft ein neues Licht auf die Bedeutung der biologischen Verwandtschaft und ihre Verankerung im kollektiven Gedächtnis einer mykenischen Gemeinschaft.

Zusammenfassend zeigt diese Arbeit, dass archäogenetische Ansätze in der Lage sind, Bevölkerungsgeschichte aufzuzeichnen, von Migration und individueller Mobilität bis hin zu biologischen Interaktionen auf Mikroebene, die soziokulturelle Merkmale vergangener Gesellschaften, wie z. B. verwandtschaftliche Praktiken, widerspiegeln. Trotz der Herausforderungen, die die Gewinnung von aDNA aus der Ägäis und dem Nahen Osten mit sich bringt, zeigt diese Arbeit auch, dass es mit den neuesten Methoden und umfangreichen und intensivierten Stichprobenstrategien möglich ist, genomische Informationen aus solchen Kontexten zu gewinnen. Auch wenn die Datenlage bei weitem noch nicht vollständig ist, liefern deren Analyse und die in dieser Arbeit vorgestellten Ergebnisse wichtige Hinweise auf Fragen, die aus Studien der materiellen Kultur und der physischen Anthropologie hervorgehen. Die neuen Daten liefern auch neue Details zu Aspekten der menschlichen Bevölkerungsgeschichte, die bisher nicht oder nur unzureichend erforscht waren oder generell nur sehr schwer aus dem archäologischen und anthropologischen Kontext zu erkennen waren. Als eine der ersten groß angelegten archäogenetischen Studien im Nahen Osten und in der Ägäis soll diese Arbeit den Weg für künftige interdisziplinäre Studien zur jüngeren Vorgeschichte dieses Gebiets ebnen.



## 8 References

Agranat-Tamir, L., Waldman, S., Martin, M. A. S., Gokhman, D., Mishol, N., Eshel, T., Cheronet, O., Rohland, N., Mallick, S., Adamski, N., et al. 2020. The Genomic History of the Bronze Age Southern Levant. *Cell*, 181, 1146-1157.e11.

Akar, M. 2013. The Late Bronze Age Fortresses at Alalakh: Architecture and Identity in Mediterranean Exchange Systems. In: Yener, K. A. (ed.) *Across the border: Late Bronze-Iron Age relations between Syria and Anatolia. Proceedings of a Symposium Held at the Research Center of Anatolian Studies, Koc University, Istanbul, May 31-June 1, 2010*. Peeters.

Akkermans, P. M. M. 1994. *Villages in the Steppe – Late Neolithic Settlement and Subsistence in the Balikh Valley, Northern Syria*, Ann Arbor, International Monographs in Prehistory.

Alcala, N. & Rosenberg, N. A. 2022. Mathematical constraints on F(ST): multiallelic markers in arbitrarily many populations. *Philos Trans R Soc Lond B Biol Sci*, 377, 20200414.

Alexander, D. H., Novembre, J. & Lange, K. 2009. Fast model-based estimation of ancestry in unrelated individuals. *Genome Res*, 19, 1655-64.

Algaze, G. 1993. *The Uruk World System: The Dynamics of Expansion of Early Mesopotamian Civilization*, Chicago, University of Chicago Press.

Algaze, G. 2008. *Ancient Mesopotamia at the Dawn of Civilization: The Evolution of an Urban Landscape*, Chicago and London, The University of Chicago Press.

Algaze, G., Brenties, B., Knapp, A. B., Kohl, P. L., Kotter, W. R., Lamberg-Karlovsky, C. C., Schwartz, G. M., Weiss, H., Wenke, R. J., Wright, R. P., et al. 1989. The Uruk Expansion: Cross-cultural Exchange in Early Mesopotamian Civilization [with Comments and Reply]. *Current Anthropology*, 30, 571-608.

Allentoft, M. E., Sikora, M., Sjogren, K. G., Rasmussen, S., Rasmussen, M., Stenderup, J., Damgaard, P. B., Schroeder, H., Ahlstrom, T., Vinner, L., et al. 2015. Population genomics of Bronze Age Eurasia. *Nature*, 522, 167-72.

Alt, K. W., Benz, M., Müller, W., Berner, M. E., Schultz, M., Schmidt-Schultz, T. H., Knipper, C., Gebel, H.-G. K., Nissen, H. J. & Vach, W. 2013. Earliest Evidence for Social Endogamy in the 9,000-Year-Old-Population of Basta, Jordan. *PLOS ONE*, 8, e65649.

Ammerman, A. J. & Cavalli-Sforza, L. L. 1973. A population model for the diffusion of early farming in Europe. In: Renfrew, C. (ed.) *The Explanation of Culture Change*. Duckworth.

Ammerman, A. J. & Cavalli-Sforza, L. L. 1984. *The Neolithic Transition and the Genetics of Populations in Europe*, Princeton University Press.

Ammerman, A. J. & Cavalli-Sforza, L. L. 2014. *The Neolithic transition and the genetics of populations in Europe*, Princeton University Press.

Amorim, C. E. G., Vai, S., Posth, C., Modi, A., Koncz, I., Hakenbeck, S., La Rocca, M. C., Mende, B., Bobo, D., Pohl, W., et al. 2018. Understanding 6th-century barbarian social organization and migration through paleogenomics. *Nature Communications*, 9, 3547.

- Anava, S., Neuhof, M., Gingold, H., Sagy, O., Munters, A., Svensson, E. M., Afshinnkoo, E., Danko, D., Foox, J., Shor, P., et al. 2020. Illuminating Genetic Mysteries of the Dead Sea Scrolls. *Cell*, 181, 1218-1231.e27.
- Andrades Valtueña, A., Mittnik, A., Key, F. M., Haak, W., Allmäe, R., Belinskij, A., Daubaras, M., Feldman, M., Jankauskas, R., Janković, I., et al. 2017. The Stone Age Plague and Its Persistence in Eurasia. *Curr Biol*, 27, 3683-3691.e8.
- Andreou, S. 2010. Northern Greece. In: Cline, E. H. (ed.) *The Oxford Handbook of the Bronze Age Aegean (ca. 3000-1000 BC)*. Oxford University Press.
- Anthony, D. W. 2010. *The Horse, the Wheel, and Language: How Bronze-Age Riders from the Eurasian Steppes Shaped the Modern World*, Princeton University Press.
- Arnaud, J. M. 1982. Néolithique ancien et processus de néolithisation dans le sud du Portugal. *Arche'ologie En Languedoc*.
- Auton, A., Abecasis, G. R., Altshuler, D. M., Durbin, R. M., Abecasis, G. R., Bentley, D. R., Chakravarti, A., Clark, A. G., Donnelly, P., Eichler, E. E., et al. 2015. A global reference for human genetic variation. *Nature*, 526, 68-74.
- Bacaër, N. 2011. *A Short History of Mathematical Population Dynamics*, London, Springer.
- Badalyan, R., Harutyunyan, A., Chataigner, C., Le Mort, F., Chabot, J., Brochier, J.-E., Balasescu, A., Radu, V. & Hovsepyann, R. 2010. The settlement of Aknashen-Khatunarkh, a Neolithic site in the Ararat plain (Armenia): excavation results 2004-2009. *TÜBA-AR*, 13, 187-220.
- Badalyan, R., Lombard, P., Avetisyan, P., Chataigner, C., Chabot, J., Vila, E., Hovsepyan, R., Willcox, G. & Pessin, H. 2007. New Data on the Late Prehistory of the Southern Caucasus. The Excavations at Aratashen (Armenia): Preliminary Report. In: Lyonnet, B. (ed.) *Les Cultures du Caucase (VIe-IIIe millénaires avant notre ère). Leurs Relations avec le Proche-Orient*. CNRS Editions.
- Badalyan, R., Lombard, P., Chataigner, C. & Avetisyan, P. 2004. The Neolithic and Chalcolithic Phases in the Ararat Plain (Armenia): The View from Aratashen. In: Sagona, A. (ed.) *A View from the Highlands. Archaeological Studies in Honour of Charles Burney*. Peeters.
- Barnett, W. K. 2000. Cardial pottery and the agricultural transition in Mediterranean Europe. In: Price, T. D. (ed.) *Europe's First Farmers*. Cambridge University Press.
- Baudouin, E. 2019. Rethinking architectural techniques of the Southern Caucasus in the 6 th millennium BC: A re-examination of former data and new insights. *Paléorient*, 45, 115-150.
- Beckman, G. 1996. *Hittite Diplomatic Texts*, Atlanta, Scholars Press.
- Betancourt, P. 2008. Minoan Trade. In: Shelmerdine, C. W. (ed.) *The Aegean Bronze Age*. Cambridge University Press.
- Bickle, P., Whittle, A., Anders, A., Arbogast, R.-M., Bentley, R. A., Blesl, C., Cramp, L., Cullen, P., Dale, C., Dočkalová, M., et al. 2013. *The First Farmers of Central Europe Diversity in LBK Lifeways*, Oxbow Books.
- Bietak, M. & Marinatos, N. 1995. The Minoan Wall Paintings from Avaris. *Ägypten und Levante*, 5, 49-62.

- Blegen, C. W. 1928. The Coming of the Greeks: II. The geographical distribution of prehistoric remains in Greece. *American Journal of Archaeology*, 32, 146-154.
- Boessenkool, S., Hanghøj, K., Nistelberger, H. M., Der Sarkissian, C., Gondek, A. T., Orlando, L., Barrett, J. H. & Star, B. 2017. Combining bleach and mild predigestion improves ancient DNA recovery from bones. *Mol Ecol Resour*, 17, 742-751.
- Bouwman, A. S., Brown, K. A., Brown, T. A., Chilvers, E. R., Arnott, R. & Prag, A. 2009. Kinship in Aegean prehistory? Ancient DNA in human bones from mainland Greece and Crete. *Annual of the British School at Athens*, 293-309.
- Boyd, M. J. 2016. Becoming Mycenaean? The Living, the Dead, and the Ancestors in the Transformation of Society in Second Millennium BC Southern Greece. In: Renfrew, C., Boyd, M. J. & Morley, I. (eds.) *Death Rituals, Social Order and the Archaeology of Immortality in the Ancient World. "Death Shall Have No Dominion"*. Cambridge University Press.
- Bramanti, B., Thomas, M. G., Haak, W., Unterlaender, M., Jores, P., Tambets, K., Antanaitis-Jacobs, I., Haidle, M. N., Jankauskas, R., Kind, C. J., et al. 2009. Genetic discontinuity between local hunter-gatherers and central Europe's first farmers. *Science*, 326, 137-40.
- Breniquet, C. 1987. *La disparition de la culture de Halaf: les origines de la culture d'Obeid dans le nord de la Mésopotamie*, Paris, Editions Recherche sur les civilisations.
- Briggs, A. W., Stenzel, U., Johnson, P. L. F., Green, R. E., Kelso, J., Prüfer, K., Meyer, M., Krause, J., Ronan, M. T., Lachmann, M., et al. 2007. Patterns of damage in genomic DNA sequences from a Neandertal. *Proceedings of the National Academy of Sciences*, 104, 14616.
- Briggs, A. W., Stenzel, U., Meyer, M., Krause, J., Kircher, M. & Pääbo, S. 2010. Removal of deaminated cytosines and detection of in vivo methylation in ancient DNA. *Nucleic Acids Research*, 38, e87-e87.
- Brogan, T. M. 2013. "Minding the Gap": Reexamining the Early Cycladic III "Gap" from the Perspective of Crete. A Regional Approach to Relative Chronology, Networks, and Complexity in the Late Prepalatial period. *Journal of Archaeology*, 117, 555-567.
- Broodbank, C. 2006. The Origins and Early Development of Mediterranean Maritime Activity. *Journal of Mediterranean Archaeology*, 19, 199-230.
- Broodbank, C. 2008. The Early Bronze Age in the Cyclades. In: Shelmerdine, C. W. (ed.) *The Aegean Bronze Age*. Cambridge University Press.
- Broodbank, C. 2013. *The Making of the Middle Sea: A History of the Mediterranean from the Beginning to the Emergence of the Classical World*, Oxford University Press.
- Brotherton, P., Endicott, P., Sanchez, J. J., Beaumont, M., Barnett, R., Austin, J. & Cooper, A. 2007. Novel high-resolution characterization of ancient DNA reveals C > U-type base modification events as the sole cause of post mortem miscoding lesions. *Nucleic Acids Res*, 35, 5717-28.
- Broushaki, F., Mark G Thomas, Vivian Link, Saioa López, Dorp, L. v., Kirsanow, K., Hofmanová, Z., Diekmann, Y., Cassidy, L. M., Díez-del-Molino, D., et al. 2016. Early Neolithic genomes from the eastern Fertile Crescent. *Science*, 353, 499-503.
- Brück, J. 2021a. Ancient DNA, kinship and relational identities in Bronze Age Britain. *Antiquity*, 95, 228-237.

- Brück, J. 2021b. Ancient DNA, kinship and relational identities in Bronze Age Britain. *Antiquity*, 1-10.
- Buikstra, J. E. & Beck, L. A. 2006. *Bioarchaeology : the contextual analysis of human remains / edited by Jane E. Buikstra and Lane A. Beck*, Amsterdam, Academic Press.
- Burbano, H. A., Hodges, E., Green, R. E., Briggs, A. W., Krause, J., Meyer, M., Good, J. M., Maricic, T., Johnson, P. L. F., Xuan, Z., et al. 2010. Targeted Investigation of the Neandertal Genome by Array-Based Sequence Capture. *Science*, 328, 723.
- Buzon, M. R. & Simonetti, A. 2013. Strontium isotope ( $^{87}\text{Sr}/^{86}\text{Sr}$ ) variability in the Nile Valley: Identifying residential mobility during ancient Egyptian and Nubian sociopolitical changes in the New Kingdom and Napatan periods. *American Journal of Physical Anthropology*, 151, 1-9.
- Campbell, J., Edward F. 1960. The Amarna Letters and the Amarna Period. *The Biblical Archaeologist*, 23, 1-22.
- Campbell, S. 2007. Rethinking Halaf Chronologies. *Paléorient*, 33, 103-136.
- Campbell, S. & Healey, E. 2016. Multiple sources: The pXRF analysis of obsidian from Kenan Tepe, S.E. Turkey. *Journal of Archaeological Science: Reports*, 10, 377-389.
- Cann, R. L., Stoneking, M. & Wilson, A. C. 1987. Mitochondrial DNA and human evolution. *Nature*, 325, 31-36.
- Carpenter, Meredith L., Buenrostro, Jason D., Valdiosera, C., Schroeder, H., Allentoft, Morten E., Sikora, M., Rasmussen, M., Gravel, S., Guillén, S., Nekhrizov, G., et al. 2013. Pulling out the 1%: Whole-Genome Capture for the Targeted Enrichment of Ancient DNA Sequencing Libraries. *The American Journal of Human Genetics*, 93, 852-864.
- Carter, R. A. & Philip, G. 2010. Deconstructing the Ubaid. In: Carter, R. A. & Philip, G. (eds.) *Beyond the Ubaid. Transformation and Integration in the Late Prehistoric Societies of the Middle East*. Chicago University press.
- Caskey, J. L. 1960. The early Helladic period in the Argoli. *The Journal of the American School of Classical Studies at Athens*, 29, 285-303.
- Cassidy, L. M., Maoldúin, R. Ó., Kador, T., Lynch, A., Jones, C., Woodman, P. C., Murphy, E., Ramsey, G., Dowd, M., Noonan, A., et al. 2020. A dynastic elite in monumental Neolithic society. *Nature*, 582, 384-388.
- Cavalli-Sforza, L. L. 1966. Population structure and human evolution. *Proceedings of the Royal Society of London. Series B. Biological Sciences*, 164, 362-379.
- Cavalli-Sforza, L. L., Menozzi, P. & Piazza, A. 1994. *The History and Geography of Human Genes*, Princeton University Press.
- Ceballos, F. C., Gürün, K., Altınışık, N. E., Gemici, H. C., Karamurat, C., Koptekin, D., Vural, K. B., Mapelli, I., Sağlıcan, E., Sürer, E., et al. 2021. Human inbreeding has decreased in time through the Holocene. *Current Biology*, 31, 3925-3934.e8.
- Cessford, C. 2005. Estimating the Neolithic population of Çatalhöyük. In: Hodder, I. (ed.) *Inhabiting Çatalhöyük: Reports from the 1995–99 Seasons*. McDonald Institute for Archaeological Research.
- Chadwick, J. 1976. *The Mycenaean World*, Cambridge University Press.

- Chataigner, C., Badalyan, R. & Arimura, M. 2014. *The Neolithic of the Caucasus*. Oxford University Press.
- Cherry, J. F. 1981. Pattern and Process in the Earliest Colonization of the Mediterranean Islands. *Proceedings of the Prehistoric Society*, 47, 41-68.
- Cherry, J. F. 1983. Evolution, Revolution, and the Origins of Complex Society in Minoan Crete. In: Krzyszkowska, O. & Nixon, L. (eds.) *Minoan Society: Proceedings of the Cambridge Colloquium 1981*. Bristol Classical Press.
- Childe, V. G. 1925. *The dawn of European civilization*, London; New York, K. Paul, Trench, Trubner & Co.; A.A. Knopf.
- Clare, L., Rohling, E. J., Weninger, B. & Hilpert, J. 2008. Warfare in Late Neolithic\Early Chalcolithic Pisidia, southwestern Turkey. Climate induced social unrest in the late 7th millennium calBC. *Documenta Praehistorica*, 35, 65-92.
- Clare, L. & Weninger, B. 2014. The Dispersal of Neolithic Lifeways: Absolute Chronology and Rapid Climate Change in Central and West Anatolia.
- Clemente, F., Unterländer, M., Dolgova, O., Amorim, C. E. G., Coroado-Santos, F., Neuenschwander, S., Ganiatsou, E., Cruz Dávalos, D. I., Anchieri, L., Michaud, F., et al. 2021. The genomic history of the Aegean palatial civilizations. *Cell*.
- Cline, E. H. (ed.) 2010. *The Oxford Handbook of the Bronze Age Aegean (ca. 3000-1000 BC)*, Oxford University Press.
- Coleman, J. 2000. An Archaeological Scenario for the "Coming of the Greeks" ca. 3200 B.C. *Journal of Indo-European Studies*, 28, 101-153.
- Cooper, A. & Poinar, H. N. 2000. Ancient DNA: Do It Right or Not at All. *Science*, 289, 1139.
- Crowley, J. 2008. The Mycenaean Art and Architecture. In: Shelmerdine, C. W. (ed.) *The Aegean Bronze Age*. Cambridge University Press.
- D'Andrea, M. 2019. The EB-MB Transition at Ebla. A State-of-the-Art Overview in the Light of the 2004–2008 Discoveries at Tell Mardikh. In: D'Andrea, M., Micale, M. G., Nadali, D., Pizzimenti, S. & Vacca, A. (eds.) *Pearls of the Past. Studies on Near Eastern Art and Archaeology in Honour of Frances Pinnock*. Zaphon.
- Dabney, J., Knapp, M., Glocke, I., Gansauge, M.-T., Weihmann, A., Nickel, B., Valdiosera, C., García, N., Pääbo, S., Arsuaga, J.-L., et al. 2013a. Complete mitochondrial genome sequence of a Middle Pleistocene cave bear reconstructed from ultrashort DNA fragments. *Proceedings of the National Academy of Sciences*, 110, 15758.
- Dabney, J. & Meyer, M. 2019. Extraction of Highly Degraded DNA from Ancient Bones and Teeth. In: Shapiro, B., Barlow, A., Heintzman, P. D., Hofreiter, M., Pajmans, J. L. A. & Soares, A. E. R. (eds.) *Ancient DNA: Methods and Protocols*. Springer New York.
- Dabney, J., Meyer, M. & Pääbo, S. 2013b. Ancient DNA damage. *Cold Spring Harbor perspectives in biology*, 5, a012567.
- Daley, T. & Smith, A. D. 2013. Predicting the molecular complexity of sequencing libraries. *Nature Methods*, 10, 325.

- Daly, K. G., Maisano Delser, P., Mullin, V. E., Scheu, A., Mattiangeli, V., Teasdale, M. D., Hare, A. J., Burger, J., Verdugo, M. P., Collins, M. J., et al. 2018. Ancient goat genomes reveal mosaic domestication in the Fertile Crescent. *Science*, 361, 85.
- Davies, W. & Charles, R. (eds.) 1999. *Dorothy Garrod and the Progress of the Palaeolithic: Studies in the Prehistoric Archaeology of the Near East and Europe*, Oxbow Books.
- Day, P. M., Wilson, D. E. & Kiriati, E. 1998. Pots, Labels, and People: Burying Ethnicity in the Cemetery of Aghia Photia, Siteias. In: Branigan, K. (ed.) *Cemetery and Society in the Aegean Bronze Age*. Sheffield Academic Press.
- de Barros Damgaard, P., Martiniano, R., Kamm, J., Moreno-Mayar, J. V., Kroonen, G., Peyrot, M., Barjamovic, G., Rasmussen, S., Zacho, C., Baimukhanov, N., et al. 2018. The first horse herders and the impact of early Bronze Age steppe expansions into Asia. *Science*, 360.
- Deger-Jalkotzy, S. & Hertel, D. 2018. *Das mykenische Griechenland: Geschichte, Kultur, Stätten*, München, CH. Beck Wissen.
- DePristo, M. A., Banks, E., Poplin, R., Garimella, K. V., Maguire, J. R., Hartl, C., Philippakis, A. A., del Angel, G., Rivas, M. A., Hanna, M., et al. 2011. A framework for variation discovery and genotyping using next-generation DNA sequencing data. *Nature Genetics*, 43, 491-498.
- Di Nocera, G. M. 2010. Metals and metallurgy: Their place in the Arslantepe society between the end of the 4th and beginning of the 3rd millennium BC. In: Frangipane, M. (ed.) *Economic Centralisation in Formative States: The Archaeological Reconstruction of the Economic System in 4th Millennium Arslantepe*. Sapienza University of Rome.
- Douka, K., Efstratiou, N., Hald, M. M., Henriksen, P. S., Karetsou, A. & (2017) "Dating Knossos and the arrival of the earliest Neolithic in the southern Aegean, A. C. U. P., 91(356), pp. 304–321. doi: 10.15184/aqy.2017.29. 2017. Dating Knossos and the arrival of the earliest Neolithic in the southern Aegean. *Antiquity*, 93, 304-321.
- Driessen, J. & Macdonald, C. F. 1997. *The troubled island: Minoan Crete before and after the Santorini eruption*, Liège, Université de Liège, Histoire de l'art et archéologie de la Grèce antique.
- Durand, E. Y., Patterson, N., Reich, D. & Slatkin, M. 2011. Testing for ancient admixture between closely related populations. *Mol Biol Evol*, 28, 2239-52.
- Düring, B. 2016. The 8.2 event and the Neolithic expansion in Western Anatolia. Climate and Cultural Change in Prehistoric Europe and the Near East. . In: Biehl, P. F. & Nieuwenhuyse, O. P. (eds.). State University of New York Press.
- Düring, B. S. 2008. The Early Holocene occupation of north-central Anatolia between 10,000 and 6,000 BC cal: investigating an archaeological terra incognita. *Anatolian Studies*, 58, 15-46.
- Düring, B. S. 2010. *The Prehistory of Asia Minor: From Complex Hunter-Gatherers to Early Urban Societies*, Cambridge, Cambridge University Press.
- Edmonson, M. S. 1961. Neolithic Diffusion Rates. *Current Anthropology*, 2, 71-102.
- Efstathiou, N., Karetsou, A., Banou, E. & Margomenou, D. 2004. The Neolithic settlement of Knossos: new light on an old picture. In: Cadogan, G., Hatzaki, E. & Vasilakis, E. (eds.) *Knossos: palace, city, state*. British School at Athens.

- Efstratiou, N., Karetsoy, A. & Ntinou, M. (eds.) 2013. *The Neolithic Settlement of Knossos in Crete: New Evidence for the Early Occupation of Crete and the Aegean Islands*, INSTAP Academic Press.
- Eisenmann, S., Bánffy, E., van Dommelen, P., Hofmann, K. P., Maran, J., Lazaridis, I., Mittnik, A., McCormick, M., Krause, J., Reich, D., et al. 2018. Reconciling material cultures in archaeology with genetic data: The nomenclature of clusters emerging from archaeogenomic analysis. *Scientific reports*, 8, 13003-13003.
- Ember, C. R., Gonzalez, B. & McCloskey, D. 2021. Marriage and Family. *Expaining Human Culture*.
- Ensor, B. E. 2021. Making aDNA useful for kinship analysis. *Antiquity*, 95, 241-243.
- Erdal, Y. S. 2012. The Population Replacement at Arslantepe: Reflections on the Human Remains. *Origini: Preistoria E Protostoria Delle Civiltà Antiche, Vol Xxxiv*, 34, 301-316.
- Evans, A. J. 1896. The 'Eastern Question' in Anthropology. *Proceedings of the British Association for the Advancement of Science*, 906–922.
- Evans, A. J. 1921. *The palace of Minos: a comparative account of the successive stages of the early Cretan civilization as illustrated by the discoveries at Knossos*, London, Macmillan and Co., Limited.
- Evans, A. J. 1935. *The palace of Minos: a comparative account of the successive stages of the early Cretan civilization as illustrated by the discoveries at Knossos*, London, Macmillan and Co., Limited.
- Evans, J. D. 1964. Excavations in the Neolithic Settlement of Knossos, 1957–60. Part I. *The Annual of the British School at Athens*. Cambridge University Press.
- Evans, J. D. 1994. The early millennia: continuity and change in a farming settlement. In: Evely, D., Hood, S., Evely, R. D. G., Hughes-Brock, H. & Momigliano, N. (eds.) *Knossos, a Labyrinth of History: Papers Presented in Honour of Sinclair Hood*. British School at Athens.
- Excoffier, L., Dupanloup, I., Huerta-Sánchez, E., Sousa, V. C. & Foll, M. 2013. Robust Demographic Inference from Genomic and SNP Data. *PLOS Genetics*, 9, e1003905.
- Falk, R. 1995. The struggle of genetics for independence. *Journal of the History of Biology*, 28, 219-246.
- Feldman, M. 2020. *Tracing past human mobility and disease in western Eurasia by the genetic analysis of ancient human remains*. Friedrich-Schiller-Universität.
- Feldman, M., Fernandez-Dominguez, E., Reynolds, L., Baird, D., Pearson, J., Herskovitz, I., May, H., Goring-Morris, N., Benz, M., Gresky, J., et al. 2019. Late Pleistocene human genome suggests a local origin for the first farmers of central Anatolia. *Nat Commun*, 10, 1218.
- Feldman, M. H. 2006. *Diplomacy by Design*, Chicago, The University of Chicago Press.
- Fernandes, D. M., Mittnik, A., Olalde, I., Lazaridis, I., Cheronet, O., Rohland, N., Mallick, S., Bernardos, R., Broomandkoshbacht, N., Carlsson, J., et al. 2020. The spread of steppe and Iranian-related ancestry in the islands of the western Mediterranean. *Nature Ecology & Evolution*, 4, 334-345.
- Forest, J.-D. 2005. The State: The Process of State Formation as Seen from Mesopotamia. In: Pollock, S. & Bernbeck, R. (eds.) *Archaeologies of the Middle East: Critical Perspectives*. Blackwell Publishing.
- Forsén, J. 1992. *The twilight of the Early Helladics: a study of the disturbances in east-central and southern Greece towards the end of the early Bronze Age*. Doctoral, University of Gothenburg.

- Frahm, E., Campbell, S. & Healey, E. 2016. Caucasus connections? New data and interpretations for Armenian obsidian in Northern Mesopotamia. *Journal of Archaeological Science: Reports*, 9, 543-564.
- Frangipane, M. 2011. Arslantepe-Malatya: A prehistoric and Early historic Center in Eastern Anatolia. In: Steadman, S. & McMahon, G. (eds.) *The Oxford Handbook of Ancient Anatolia*. Oxford University Press.
- Frangipane, M. 2012a. The Collapse of the 4th Millennium Centralised System at Arslantepe and the Far-Reaching Changes in 3rd Millennium Societies. *Origini: Preistoria E Protostoria Delle Civiltà Antiche, Vol Xxxiv*, 34, 237-260.
- Frangipane, M. 2012b. Fourth Millennium Arslantepe: The Development of a Centralised Society without Urbanisation. *Origini: Preistoria E Protostoria Delle Civiltà Antiche*, 34, 19-40.
- Frangipane, M. 2014. After collapse: Continuity and Disruption in the settlement by Kura-Araxes-linked pastoral groups at Arslantepe-Malatya (Turkey). New data. *Paléorient*, 40, 169-182.
- Frangipane, M. 2015a. Different types of multiethnic societies and different patterns of development and change in the prehistoric Near East. *Proceedings of the National Academy of Sciences*, 112, 9182.
- Frangipane, M. 2015b. Upper Euphrates Societies and Non-Sedentary Communities Linked to the Kura-Araxes World. Dynamics of Interaction, as seen from Arslantepe. In: Isikli, M. & Can, B. (eds.) *International Symposium on East Anatolia - South Caucasus Cultures: Proceedings II*. Cambridge Scholars Publishing.
- Frangipane, M. 2018. Different Trajectories in State Formation in Greater Mesopotamia: A View from Arslantepe (Turkey). *Journal of Archaeological Research*, 26, 3-63.
- Frei, K. M., Bergerbrant, S., Sjögren, K.-G., Jørkov, M. L., Lynnerup, N., Harvig, L., Allentoft, M. E., Sikora, M., Price, T. D., Frei, R., et al. 2019. Mapping human mobility during the third and second millennia BC in present-day Denmark. *PLOS ONE*, 14, e0219850.
- Freilich, S., Ringbauer, H., Los, D., Novak, M., Pavičić, D. T., Schiffels, S. & Pinhasi, R. 2021. Reconstructing genetic histories and social organisation in Neolithic and Bronze Age Croatia. *Scientific Reports*, 11, 16729.
- Fu, Q., Hajdinjak, M., Moldovan, O. T., Constantin, S., Mallick, S., Skoglund, P., Patterson, N., Rohland, N., Lazaridis, I., Nickel, B., et al. 2015. An early modern human from Romania with a recent Neanderthal ancestor. *Nature*, 524, 216.
- Fu, Q., Li, H., Moorjani, P., Jay, F., Slepchenko, S. M., Bondarev, A. A., Johnson, P. L. F., Aximu-Petri, A., Prüfer, K., de Filippo, C., et al. 2014. Genome sequence of a 45,000-year-old modern human from western Siberia. *Nature*, 514, 445-449.
- Fu, Q., Meyer, M., Gao, X., Stenzel, U., Burbano, H. A., Kelso, J. & Pääbo, S. 2013. DNA analysis of an early modern human from Tianyuan Cave, China. *Proceedings of the National Academy of Sciences*, 110, 2223.
- Fu, Q., Posth, C., Hajdinjak, M., Petr, M., Mallick, S., Fernandes, D., Furtwängler, A., Haak, W., Meyer, M., Mittnik, A., et al. 2016. The genetic history of Ice Age Europe. *Nature*, 534, 200-205.
- Fu, Q., Rudan, P., Pääbo, S. & Krause, J. 2012. Complete Mitochondrial Genomes Reveal Neolithic Expansion into Europe. *PLOS ONE*, 7, e32473.



- Furtwängler, A., Reiter, E., Neumann, G. U., Siebke, I., Steuri, N., Hafner, A., Lösch, S., Anthes, N., Schuenemann, V. J. & Krause, J. 2018. Ratio of mitochondrial to nuclear DNA affects contamination estimates in ancient DNA analysis. *Scientific Reports*, 8, 14075.
- Furtwängler, A., Rohrlach, A. B., Lamnidis, T. C., Papac, L., Neumann, G. U., Siebke, I., Reiter, E., Steuri, N., Hald, J., Denaire, A., et al. 2020. Ancient genomes reveal social and genetic structure of Late Neolithic Switzerland. *Nature Communications*, 11, 1915.
- Galanakis, Y. In prep. Neither 'Minoan' nor 'Mycenaean': The Burial Record of Knossos and the Materialisation of a New Social Order, 1600-1400 BC.
- Gamba, C., Hanghøj, K., Gaunitz, C., Alfarhan, A. H., Alquraishi, S. A., Al-Rasheid, K. A. S., Bradley, D. G. & Orlando, L. 2016. Comparing the performance of three ancient DNA extraction methods for high-throughput sequencing. *Molecular Ecology Resources*, 16, 459-469.
- Gamba, C., Jones, E. R., Teasdale, M. D., McLaughlin, R. L., Gonzalez-Fortes, G., Mattiangeli, V., Domboróczki, L., Kóvári, I., Pap, I., Anders, A., et al. 2014. Genome flux and stasis in a five millennium transect of European prehistory. *Nature Communications*, 5, 5257.
- Gansauge, M.-T., Aximu-Petri, A., Nagel, S. & Meyer, M. 2020. Manual and automated preparation of single-stranded DNA libraries for the sequencing of DNA from ancient biological remains and other sources of highly degraded DNA. *Nature Protocols*.
- Gansauge, M.-T., Gerber, T., Glocke, I., Korlević, P., Lippik, L., Nagel, S., Riehl, L. M., Schmidt, A. & Meyer, M. 2017. Single-stranded DNA library preparation from highly degraded DNA using T4 DNA ligase. *Nucleic Acids Research*, 45, e79-e79.
- Gansauge, M.-T. & Meyer, M. 2013. Single-stranded DNA library preparation for the sequencing of ancient or damaged DNA. *Nature Protocols*, 8, 737-748.
- Gibbs, R. A., Belmont, J. W., Hardenbol, P., Willis, T. D., Yu, F., Yang, H., Ch'ang, L.-Y., Huang, W., Liu, B., Shen, Y., et al. 2003. The International HapMap Project. *Nature*, 426, 789-796.
- Gilbert, M. T. P., Hansen, A. J., Willerslev, E., Turner-Walker, G. & Collins, M. 2006. Insights into the processes behind the contamination of degraded human teeth and bone samples with exogenous sources of DNA. *International Journal of Osteoarchaeology*, 16, 156-164.
- Gimbutas, M., Dexter, M. R. & Jones-Bley, K. 1997. *The Kurgan culture and the Indo-Europeanization of Europe: selected articles from 1952 to 1993*, Washington, DC, Institute for the Study of Man.
- Gkiasta, M., Russell, T., Shennan, S. & Steele, J. 2003. Neolithic transition in Europe: the radiocarbon record revisited. *Antiquity*, 77, 45-62.
- Gokcumen, O. & Frachetti, M. 2020. The Impact of Ancient Genome Studies in Archaeology. *Annual Review of Anthropology*, 49, 277-98.
- Goodman, M. 1963. SEROLOGICAL ANALYSIS OF THE SYSTEMATICS OF RECENT HOMINOIDS. *Human Biology*, 35, 377-436.
- Green, R. E., Krause, J., Briggs, A. W., Maricic, T., Stenzel, U., Kircher, M., Patterson, N., Li, H., Zhai, W., Fritz, M. H.-Y., et al. 2010. A Draft Sequence of the Neandertal Genome. *Science*, 328, 710.
- Gregoricka, L. A. 2013. Geographic origins and dietary transitions during the Bronze Age in the Oman Peninsula. *Am J Phys Anthropol*, 152, 353-69.

Günther, T., Valdiosera, C., Malmström, H., Ureña, I., Rodríguez-Varela, R., Sverrisdóttir, Ó. O., Daskalaki, E. A., Skoglund, P., Naidoo, T., Svensson, E. M., et al. 2015. Ancient genomes link early farmers from Atapuerca in Spain to modern-day Basques. *Proceedings of the National Academy of Sciences*, 112, 11917.

Gürdil, B. 2010. Exploring Social Organizational Aspects of the Ubaid Communities: a Case Study of Değirmentepe in Eastern Turkey. In: Carter, R. A. & Philip, G. (eds.) *Beyond the Ubaid. Transformation and Integration in the Late Prehistoric Societies of the Middle East*. Chicago University press.

Haak, W., Balanovsky, O., Sanchez, J. J., Koshel, S., Zaporozhchenko, V., Adler, C. J., Der Sarkissian, C. S. I., Brandt, G., Schwarz, C., Nicklisch, N., et al. 2010. Ancient DNA from European Early Neolithic Farmers Reveals Their Near Eastern Affinities. *PLOS Biology*, 8, e1000536.

Haak, W., Lazaridis, I., Patterson, N., Rohland, N., Mallick, S., Llamas, B., Brandt, G., Nordenfelt, S., Harney, E., Stewardson, K., et al. 2015. Massive migration from the steppe was a source for Indo-European languages in Europe. *Nature*, 522, 207.

Haber, M., Doumet-Serhal, C., Scheib, C., Xue, Y., Danecek, P., Mezzavilla, M., Youhanna, S., Martiniano, R., Prado-Martinez, J., Szpak, M., et al. 2017. Continuity and Admixture in the Last Five Millennia of Levantine History from Ancient Canaanite and Present-Day Lebanese Genome Sequences. *American journal of human genetics*, 101, 274-282.

Haber, M., Nassar, J., Almarri, M. A., Saupe, T., Saag, L., Griffith, S. J., Doumet-Serhal, C., Chanteau, J., Saghih-Beydoun, M., Xue, Y., et al. 2020. A Genetic History of the Near East from an aDNA Time Course Sampling Eight Points in the Past 4,000 Years. *The American Journal of Human Genetics*.

Hagan, R. W., Hofman, C. A., Hübner, A., Reinhard, K., Schnorr, S., Lewis, C. M., Jr., Sankaranarayanan, K. & Warinner, C. G. 2020. Comparison of extraction methods for recovering ancient microbial DNA from paleofeces. *Am J Phys Anthropol*, 171, 275-284.

Hajdinjak, M., Mafessoni, F., Skov, L., Vernot, B., Hübner, A., Fu, Q., Essel, E., Nagel, S., Nickel, B., Richter, J., et al. 2021. Initial Upper Palaeolithic humans in Europe had recent Neanderthal ancestry. *Nature*, 592, 253-257.

Haley, J. B. & Blegen, C. W. 1928. The Coming of the Greeks. *American Journal of Archaeology*, 32, 141-154.

Hamamy, H., Antonarakis, S. E., Cavalli-Sforza, L. L., Temtamy, S., Romeo, G., Kate, L. P. T., Bennett, R. L., Shaw, A., Megarbane, A., van Duijn, C., et al. 2011. Consanguineous marriages, pearls and perils: Geneva International Consanguinity Workshop Report. *Genetics in Medicine*, 13, 841-847.

Harney, É., Cheronet, O., Fernandes, D. M., Sirak, K., Mah, M., Bernardos, R., Adamski, N., Broomandkhoshbacht, N., Callan, K., Lawson, A. M., et al. 2021a. A minimally destructive protocol for DNA extraction from ancient teeth. *Genome Res*, 31, 472-483.

Harney, É., May, H., Shalem, D., Rohland, N., Mallick, S., Lazaridis, I., Sarig, R., Stewardson, K., Nordenfelt, S., Patterson, N., et al. 2018. Ancient DNA from Chalcolithic Israel reveals the role of population mixture in cultural transformation. *Nature Communications*, 9, 3336.

Harney, É., Patterson, N., Reich, D. & Wakeley, J. 2021b. Assessing the performance of qpAdm: a statistical tool for studying population admixture. *Genetics*.

Helwing, B. 1999. Cultural Interaction at Hassek Höyük, Turkey. New Evidence from Pottery Analysis. *Paléorient*, 25, 91-99.

- Henrickson, E. F. & Thuesen, I. 1989. Introduction: The importance of the 'Ubaid: Transition between Revolutions. *In*: Henrickson, E. F. & Thuesen, I. (eds.) *Upon this Foundation: The 'Ubaid Reconsidered (Proceedings from the 'Ubaid Symposium, Elsinore, May 30th-June 1st, 1988)*. Museum Tusulanum Press.
- Higuchi, R., Bowman, B., Freiberger, M., Ryder, O. A. & Wilson, A. C. 1984. DNA sequences from the quagga, an extinct member of the horse family. *Nature*, 312, 282-284.
- Hodos, T. (ed.) 2017. *The Routledge Handbook of Archaeology and Globalization*, Routledge
- Hofmanova, Z., Kreutzer, S., Hellenthal, G., Sell, C., Diekmann, Y., Diez-Del-Molino, D., van Dorp, L., Lopez, S., Kousathanas, A., Link, V., et al. 2016. Early farmers from across Europe directly descended from Neolithic Aegeans. *Proc Natl Acad Sci U S A*, 113, 6886-91.
- Hofmanová, Z., Kreutzer, S., Hellenthal, G., Sell, C., Diekmann, Y., Diez-Del-Molino, D., van Dorp, L., Lopez, S., Kousathanas, A., Link, V., et al. 2016. Early farmers from across Europe directly descended from Neolithic Aegeans. *Proc Natl Acad Sci U S A*, 113, 6886-91.
- Hofreiter, M., Jaenicke, V., Serre, D., von Haeseler, A. & Pääbo, S. 2001. DNA sequences from multiple amplifications reveal artifacts induced by cytosine deamination in ancient DNA. *Nucleic acids research*, 29, 4793-4799.
- Hole, F. 2000. The Prehistory of the Khabur. *In*: Rouault, O. & Wäfler, M. (eds.) *La Djéziré et l' Euphrate Syriens de la protohistoire à la fin du IIe millénaire av. J.-C.: Tendances dans l' interprétation historique des données nouvelles*. Brepols.
- Horejs, B., Milić, B., Ostmann, F., Thanheiser, U., Weninger, B. & Galik, A. 2015. The Aegean in the Early 7th Millennium BC: Maritime Networks and Colonization. *Journal of World Prehistory*, 28, 289-330.
- Horwitz, L. K. 2013. The Earliest Settlement on Crete: An Archaeozoological Perspective, Liora Kolska Horwitz. *In*: Efstratiou, N., Karetsou, A. & Ntinou, M. (eds.) *The Neolithic Settlement of Knossos in Crete: New Evidence for the Early Occupation of Crete and the Aegean Islands*. INSTAP Academic Press.
- Hughey, J. R., Paschou, P., Drineas, P., Mastropaolo, D., Lotakis, D. M., Navas, P. A., Michalodimitrakis, M., Stamatoyannopoulos, J. A. & Stamatoyannopoulos, G. 2013. A European population in Minoan Bronze Age Crete. *Nature Communications*, 4, 1861.
- Ingman, T. 2014. *Mortuary Practices at Tell Atchana, Ancient Alalakh in the Middle and Late Bronze Ages*. Koç University.
- Ingman, T., Eisenmann, S., Skourtanioti, E., Akar, M., Ilgner, J., Gnechi Ruscone, G. A., le Roux, P., Shafiq, R., Neumann, G. U., Keller, M., et al. 2021. Human mobility at Tell Atchana (Alalakh), Hatay, Turkey during the 2nd millennium BC: Integration of isotopic and genomic evidence. *PLOS ONE*, 16, e0241883.
- Jones, E. R., Gonzalez-Fortes, G., Connell, S., Siska, V., Eriksson, A., Martiniano, R., McLaughlin, R. L., Gallego Llorente, M., Cassidy, L. M., Gamba, C., et al. 2015. Upper Palaeolithic genomes reveal deep roots of modern Eurasians. *Nat Commun*, 6, 8912.
- Jónsson, H., Ginolhac, A., Schubert, M., Johnson, P. & Orlando, L. 2013. mapDamage2.0: fast approximate Bayesian estimates of ancient DNA damage parameters. *Bioinformatics (Oxford, England)*, 29, 1682–1684.

- Keller, A., Graefen, A., Ball, M., Matzas, M., Boisguerin, V., Maixner, F., Leidinger, P., Backes, C., Khairat, R., Forster, M., et al. 2012. New insights into the Tyrolean Iceman's origin and phenotype as inferred by whole-genome sequencing. *Nature Communications*, 3, 698.
- Keller, M., Spyrou, M. A., Scheib, C. L., Neumann, G. U., Kröpelin, A., Haas-Gebhard, B., Pääffgen, B., Haberstroh, J., Ribera i Lacomba, A., Raynaud, C., et al. 2019. Ancient *Yersinia pestis* genomes from across Western Europe reveal early diversification during the First Pandemic (541–750). *Proceedings of the National Academy of Sciences*, 116, 12363.
- Kendall, C., Eriksen, A. M. H., Kontopoulos, I., Collins, M. J. & Turner-Walker, G. 2018. Diagenesis of archaeological bone and tooth. *Palaeogeography, Palaeoclimatology, Palaeoecology*, 491, 21-37.
- Kılınç, G. M., Koptekin, D., Atakuman, C., Sumer, A. P., Donertas, H. M., Yaka, R., Bilgin, C. C., Buyukkarakaya, A. M., Baird, D., Altinisik, E., et al. 2017. Archaeogenomic analysis of the first steps of Neolithization in Anatolia and the Aegean. *Proc Biol Sci*, 284.
- Kılınç, G. M., Omrak, A., Ozer, F., Gunther, T., Buyukkarakaya, A. M., Bicakci, E., Baird, D., Donertas, H. M., Ghalichi, A., Yaka, R., et al. 2016. The Demographic Development of the First Farmers in Anatolia. *Curr Biol*, 26, 2659-2666.
- Killen, J. T. & Voutsaki, S. (eds.) 2001. *Economy and Politics in the Mycenaean Palace States: Proceedings of a Conference Held on 1-3 July 1999 in the Faculty of Classics, Cambridge*, Cambridge Philological Society.
- King, M. C. & Wilson, A. C. 1975. Evolution at two levels in humans and chimpanzees. *Science*, 188, 107.
- King, R. J., Özcan, S. S., Carter, T., Kalsoğlu, E., Atasoy, S., Triantaphyllidis, C., Kouvatsi, A., Lin, A. A., Chow, C. E. T., Zhivotovsky, L. A., et al. 2008. Differential Y-chromosome Anatolian Influences on the Greek and Cretan Neolithic. *Annals of Human Genetics*, 72, 205-214.
- Korneliussen, T. S., Albrechtsen, A. & Nielsen, R. 2014. ANGSD: Analysis of Next Generation Sequencing Data. *BMC Bioinformatics*, 15, 356.
- Krause, J., Fu, Q., Good, J. M., Viola, B., Shunkov, M. V., Derevianko, A. P. & Pääbo, S. 2010. The complete mitochondrial DNA genome of an unknown hominin from southern Siberia. *Nature*, 464, 894-7.
- Krauß, R., Marinova, E., De Brue, H. & Weninger, B. 2018. The rapid spread of early farming from the Aegean into the Balkans via the Sub-Mediterranean-Aegean Vegetation Zone. *Quaternary International*, 496, 24-41.
- Kuch, M. & Poinar, H. 2012. Extraction of DNA from paleofeces. *Methods Mol Biol*, 840, 37-42.
- Lander, E. S., Linton, L. M., Birren, B., Nusbaum, C., Zody, M. C., Baldwin, J., Devon, K., Dewar, K., Doyle, M., FitzHugh, W., et al. 2001. Initial sequencing and analysis of the human genome. *Nature*, 409, 860-921.
- Laneri, N. & Schwartz, M. 2011. Southeastern and Eastern Anatolia in the Middle Bronze Age. In: Steadman, S. & McMahon, G. (eds.) *The Oxford Handbook of Ancient Anatolia*. Oxford University Press.
- Lawson, D. J., Hellenthal, G., Myers, S. & Falush, D. 2012. Inference of Population Structure using Dense Haplotype Data. *PLOS Genetics*, 8, e1002453.

- Lazaridis, I., Belfer-Cohen, A., Mallick, S., Patterson, N., Cheronet, O., Rohland, N., Bar-Oz, G., Bar-Yosef, O., Jakeli, N., Kvavadze, E., et al. 2018. Paleolithic DNA from the Caucasus reveals core of West Eurasian ancestry. *bioRxiv*, 423079.
- Lazaridis, I., Mittnik, A., Patterson, N., Mallick, S., Rohland, N., Pfrengle, S., Furtwangler, A., Peltzer, A., Posth, C., Vasilakis, A., et al. 2017. Genetic origins of the Minoans and Mycenaeans. *Nature*, 548, 214-218.
- Lazaridis, I., Nadel, D., Rollefson, G., Merrett, D. C., Rohland, N., Mallick, S., Fernandes, D., Novak, M., Gamarra, B., Sirak, K., et al. 2016. Genomic insights into the origin of farming in the ancient Near East. *Nature*, 536, 419-24.
- Lazaridis, I., Patterson, N., Mittnik, A., Renaud, G., Mallick, S., Kirsanow, K., Sudmant, P. H., Schraiber, J. G., Castellano, S., Lipson, M., et al. 2014. Ancient human genomes suggest three ancestral populations for present-day Europeans. *Nature*, 513, 409-413.
- Leppard, T. P. 2021. Process and Dynamics of Mediterranean Neolithization (7000–5500 bc). *Journal of Archaeological Research*.
- Lévi-Strauss, C. 1949. *Les structures élémentaires de la parenté*. Presses Universitaires de France.
- Li, H. & Durbin, R. 2009. Fast and accurate short read alignment with Burrows-Wheeler transform. *Bioinformatics (Oxford, England)*, 25, 1754-1760.
- Librado, P., Khan, N., Fages, A., Kusliy, M. A., Suchan, T., Tonasso-Calvière, L., Schiavinato, S., Alioglu, D., Fromentier, A., Perdereau, A., et al. 2021. The origins and spread of domestic horses from the Western Eurasian steppes. *Nature*.
- Lindahl, T. 1993. Instability and decay of the primary structure of DNA. *Nature*, 362, 709-715.
- Lindahl, T. & Andersson, A. 1972. Rate of chain breakage at apurinic sites in double-stranded deoxyribonucleic acid. *Biochemistry*, 11, 3618-3623.
- Lindahl, T. & Nyberg, B. 1972. Rate of depurination of native deoxyribonucleic acid. *Biochemistry*, 11, 3610-3618.
- Lindahl, T. & Nyberg, B. 1974. Heat-induced deamination of cytosine residues in deoxyribonucleic acid. *Biochemistry*, 13, 3405-3410.
- Lindqvist, C. (ed.) 2019. *Paleogenomics: Genome-Scale Analysis of Ancient DNA*.
- Lipatov, M., Sanjeev, K., Patro, R. & Veeramah, K. R. 2015. Maximum Likelihood Estimation of Biological Relatedness from Low Coverage Sequencing Data. *bioRxiv*, 023374.
- Lipson, M., Szécsényi-Nagy, A., Mallick, S., Pósa, A., Stégmár, B., Keerl, V., Rohland, N., Stewardson, K., Ferry, M., Michel, M., et al. 2017. Parallel palaeogenomic transects reveal complex genetic history of early European farmers. *Nature*, 551, 368-372.
- Llamas, B., Valverde, G., Fehren-Schmitz, L., Weyrich, L. S., Cooper, A. & Haak, W. 2017. From the field to the laboratory: Controlling DNA contamination in human ancient DNA research in the high-throughput sequencing era. *STAR: Science & Technology of Archaeological Research*, 3, 1-14.

- Lyonnet, B., Guliyev, F., Bouquet, L., Bruley-Chabot, G., Samzun, A., Pecqueur, L., Jovenet, E., Baudouin, E., Fontugne, M., Raymond, P., et al. 2016. Mentesh Tepe, an early settlement of the Shomu-Shulaveri Culture in Azerbaijan. *Quaternary International*, 395, 170-183.
- Mallick, S., Li, H., Lipson, M., Mathieson, I., Gymrek, M., Racimo, F., Zhao, M., Chennagiri, N., Nordenfelt, S., Tandon, A., et al. 2016. The Simons Genome Diversity Project: 300 genomes from 142 diverse populations. *Nature*, 538, 201-206.
- Mann, A. E., Sabin, S., Ziesemer, K., Vågane, Å. J., Schroeder, H., Ozga, A. T., Sankaranarayanan, K., Hofman, C. A., Fellows Yates, J. A., Salazar-García, D. C., et al. 2018. Differential preservation of endogenous human and microbial DNA in dental calculus and dentin. *Scientific Reports*, 8, 9822.
- Manning, S. W. 1994. Cultural Change in the Aegean c.2200BC. In: Dalfes, N. H., Kukla, G. & Weiss, H. (eds.) *Third Millennium BC Climate Change and Old World Collapse*. Springer.
- Manning, S. W. 1995. The Absolute Chronology of the Aegean Early Bronze Age: Archaeology, Radiocarbon, and History. *Monographs in Mediterranean Archaeology*. Sheffield Academic Press.
- Manning, S. W. 2014. *Eurasian Prehistory*, 11, 9-28.
- Manning, S. W. & Knappett, C. 2008. Protopalatial Crete. In: Shelmerdine, C. W. (ed.) *The Aegean Bronze Age*. Cambridge University Press.
- Maran, J. 1998. *Kulturwandel auf dem griechischen Festland und den Kykladen im späten 3. Jahrtausend v. Chr. Studien zu den kulturellen Verhältnissen in Südosteuropa und dem zentralen sowie östlichen Mittelmeerraum i. d. späten Kupfer- und frühen Bronzezeit*, Bonn, Habelt.
- Maran, J. 2005. Late Minoan Coarse Ware Stirrup Jars on the Greek Mainland. A Postpalatial Perspective from the 12th Century BC Argolid. In: D'Agata, A. L. & Moody, J. A. (eds.) *Ariadne's Threads. Connections between Crete and the Greek Mainland in late Minoan III (LM IIIA2 to LM IIIC). Proceedings of the International Workshop held at Athens, Scuola Archeologica Italiana, 5-6 April 2003*. Scuola Archeologica Italiana di Atene.
- Maran, J. & Stockhammer, P. W. 2020. Emulation in Ceramic of a Bronze Bucket of the Kurd Type from Tiryns. *ORIGINI*, 44, 93-110.
- Maricic, T., Whitten, M. & Pääbo, S. 2010. Multiplexed DNA Sequence Capture of Mitochondrial Genomes Using PCR Products. *PLOS ONE*, 5, e14004.
- Marro, C. 2007. Continuity and Change in the Birecik Valley at the End of the Third Millennium: The Archaeological Evidence from Horum Höyük. In: Kuzucuoğlu, C. & Marro, C. (eds.) *Sociétés humaines et changement climatique à la fin du troisième millénaire: Une crise a-t-elle eu lieu en Haute Mésopotamie? Actes du Colloque de Lyon, 5-8 décembre 2005*. De Boccard.
- Martiniano, R., Cassidy, L. M., Ó'Maoldúin, R., McLaughlin, R., Silva, N. M., Manco, L., Fidalgo, D., Pereira, T., Coelho, M. J., Serra, M., et al. 2017. The population genomics of archaeological transition in west Iberia: Investigation of ancient substructure using imputation and haplotype-based methods. *PLOS Genetics*, 13, e1006852.
- Martiniano, R., Cassidy, L.M., Ó'Maoldúin, R., McLaughlin, R., Silva, N.M., Manco, L., et al. 2017. The population genomics of archaeological transition in west Iberia: Investigation of ancient substructure using imputation and haplotype-based methods. *PLoS Genet.* 13, e1006852.

- Mathieson, I., Alpaslan-Roodenberg, S., Posth, C., Szécsényi-Nagy, A., Rohland, N., Mallick, S., Olalde, I., Broomandkoshbacht, N., Candilio, F., Cheronet, O., et al. 2018. The genomic history of southeastern Europe. *Nature*, 555, 197-203.
- Mathieson, I., Lazaridis, I., Rohland, N., Mallick, S., Patterson, N., Roodenberg, S. A., Harney, E., Stewardson, K., Fernandes, D., Novak, M., et al. 2015. Genome-wide patterns of selection in 230 ancient Eurasians. *Nature*, 528, 499-503.
- Matthiae, P. 2011. Fouilles à Tell Mardikh-Ébla en 2009-2010 : les débuts de l'exploration de la citadelle paléosyrienne. *Comptes rendus des séances de l'Académie des Inscriptions et Belles-Lettres*, 155, 735-773.
- McGeorge, P. J. P. 2011. Intramural infant burials in the Aegean Bronze age: Reflections on symbolism and eschatology with particular reference to Crete. *2èmes Rencontres d'archéologie de l'IFEA: Le Mort dans la ville Pratiques, contextes et impacts des inhumations intra-muros en Anatolie, du début de l'Age du Bronze à l'époque romaine*. IFEA-Ege yayımları.
- McVean, G. A. & Cardin, N. J. 2005. Approximating the coalescent with recombination. *Philos Trans R Soc Lond B Biol Sci*, 360, 1387-93.
- Meyer, M. & Kircher, M. 2010. Illumina sequencing library preparation for highly multiplexed target capture and sequencing. *Cold Spring Harb Protoc*, 2010, pdb.prot5448.
- Michel, C. 2003. *Old Assyrian Bibliography of Cuneiform Texts, Bullae, Seals and the Results of the Excavations at Aššur, Kültepe/Kaniş, Acemhöyük, Alişar, and Boğazköy*, Leiden, Nederlands Instituut voor het Nabije Oosten.
- Milić, M. 2014. PXRF characterisation of obsidian from central Anatolia, the Aegean and central Europe. *Journal of Archaeological Science*, 41, 285-296.
- Miller, M. 2011a. *The Funerary Landscape at Knossos: A diachronic study of Minoan burial customs with special reference to the warrior graves*, Oxford, British Archaeological Reports.
- Miller, M. The Funerary Landscape at Knossos. A diachronic study of Minoan burial customs with special reference to the warrior graves. 2011b.
- Miller, M. 2016. Pottery as sign of cultural encounters: The case of Handmade Burnished and Grey Ware in Khania. In: Aslaksen, O. C. (ed.) *Local and Global Perspectives on Mobility in the Eastern Mediterranean. Workshop at NIA 11-15 nov 2011*. the Norwegian Institute at Athens.
- Mittnik, A., Massy, K., Knipper, C., Wittenborn, F., Friedrich, R., Pfrengle, S., Burri, M., Carlich-Witjes, N., Deeg, H., Furtwängler, A., et al. 2019. Kinship-based social inequality in Bronze Age Europe. *Science*, 366, 731.
- Mittnik, A., Wang, C.-C., Pfrengle, S., Daubaras, M., Zariņa, G., Hallgren, F., Allmäe, R., Khartanovich, V., Moiseyev, V., Törsv, M., et al. 2018. The genetic prehistory of the Baltic Sea region. *Nature Communications*, 9, 442.
- Monroy Kuhn, J. M., Jakobsson, M. & Gunther, T. 2018. Estimating genetic kin relationships in prehistoric populations. *PLoS One*, 13, e0195491.
- Morange, M. 2020. *The Black Box of Biology: a History of the Molecular Revolution*, Paris.

- Moutafi, I. 2015. *Towards A Social Bioarchaeology of the Mycenaean Period. A Multi-Disciplinary Analysis of Funerary Remains from the Late Helladic Chamber Tomb Cemetery of Voudeni, Achaea, Greece*. Doctoral, University of Sheffield.
- Moutafi, I. 2021. *Towards a Social Bioarchaeology of the Mycenaean Period: A biocultural analysis of human remains from the Voudeni cemetery, Achaea, Greece*, Oxford and Philadelphia, Oxbow Books.
- Nafplioti, A. 2008. "Mycenaean" political domination of Knossos following the Late Minoan IB destructions on Crete: negative evidence from strontium isotope ratio analysis (87Sr/86Sr). *Journal of Archaeological Science*, 35, 2307-2317.
- Nakatsuka, N., Harney, É., Mallick, S., Mah, M., Patterson, N. & Reich, D. 2020. ContamLD: estimation of ancient nuclear DNA contamination using breakdown of linkage disequilibrium. *Genome Biology*, 21, 199.
- Narasimhan, V. M., Patterson, N., Moorjani, P., Lazaridis, I., Lipson, M., Mallick, S., Rohland, N., Bernardos, R., Kim, A. M., Nakatsuka, N., et al. 2018. The Genomic Formation of South and Central Asia. *bioRxiv*.
- Neustupny, E. 1982. Prehistoric migrations by infiltration. *Archeologicke' Rozhledy*, 34, 278–293.
- Nichols, J. J. & Weber, J. A. 2006. Amorites, Onagers, and Social Reproduction in Middle Bronze Age Syria. In: Schwartz, G. M. & Nichols, J. J. (eds.) *After Collapse. The Regeneration of Complex Societies*. University of Arizona Press.
- Niemeier, B. & Niemeier, W. D. 2000. Aegean Frescoes in Syria-Palestine: Alalakh and Tel Kabri. *Wall paintings of Thera*. Thera Foundation.
- Niemeier, B. & Niemeier, W. D. 2002. The Frescoes in the Middle Bronze Age Palace. In: Kempinski, A., Scheftelowitz, N. m. & Oren, R. (eds.) *Tel Kabri: The 1986-1993 Excavation Seasons*. Tel Aviv University.
- Nishiaki, Y., Guliyev, F. & Kadowaki, S. 2015. Chronological Contexts of the Earliest Pottery Neolithic in the South Caucasus: Radiocarbon Dates for Goytepe and Hacı Elamxanlı Tepe, Azerbaijan. *American Journal of Archaeology*, 119, 279-294.
- Novembre, J., Johnson, T., Bryc, K., Kutalik, Z., Boyko, A. R., Auton, A., Indap, A., King, K. S., Bergmann, S., Nelson, M. R., et al. 2008. Genes mirror geography within Europe. *Nature*, 456, 98-101.
- Novembre, J. & Stephens, M. 2008. Interpreting principal component analyses of spatial population genetic variation. *Nature genetics*, 40, 646-649.
- O'Sullivan, N. J., Teasdale, M. D., Mattiangeli, V., Maixner, F., Pinhasi, R., Bradley, D. G. & Zink, A. 2016. A whole mitochondria analysis of the Tyrolean Iceman's leather provides insights into the animal sources of Copper Age clothing. *Scientific Reports*, 6, 31279.
- Olalde, I., Brace, S., Allentoft, M. E., Armit, I., Kristiansen, K., Booth, T., Rohland, N., Mallick, S., Szécsényi-Nagy, A., Mittnik, A., et al. 2018. The Beaker phenomenon and the genomic transformation of northwest Europe. *Nature*, 555, 190-196.
- Olalde, I., Mallick, S., Patterson, N., Rohland, N., Villalba-Mouco, V., Silva, M., Dulias, K., Edwards, C. J., Gandini, F., Pala, M., et al. 2019. The genomic history of the Iberian Peninsula over the past 8000 years. *Science*, 363, 1230.



- Olalde, I. & Posth, C. 2020. Latest trends in archaeogenetic research of west Eurasians. *Current Opinion in Genetics & Development*, 62, 36-43.
- Omrak, A., Gunther, T., Valdiosera, C., Svensson, E. M., Malmstrom, H., Kiesewetter, H., Aylward, W., Stora, J., Jakobsson, M. & Gotherstrom, A. 2016. Genomic Evidence Establishes Anatolia as the Source of the European Neolithic Gene Pool. *Curr Biol*, 26, 270-275.
- Orlando, L., Ginolhac, A., Zhang, G., Froese, D., Albrechtsen, A., Stiller, M., Schubert, M., Cappellini, E., Petersen, B., Moltke, I., et al. 2013. Recalibrating Equus evolution using the genome sequence of an early Middle Pleistocene horse. *Nature*, 499, 74-78.
- Özbal, R. 2011. The Chalcolithic of Southeast Anatolia. In: Steadman, S. & McMahon, G. (eds.) *The Oxford Handbook of Ancient Anatolia*. Oxford University Press.
- Özdoğan, M. 1996. Pre-Bronze Age Sequence of Central Anatolia: An Alternative Approach. In: Magen, U. & Rashad, M. (eds.) *Vom Halys zum Euphrat. Th omas Beran zu Ehren*. Ugarit-Verlag.
- Özdoğan, M. 2010. Westward Expansion of the Neolithic Way of Life: Sorting the Neolithic Package into Distinct Packages. In: Matthiae, P., Pinnock, F., Nigro, L. & Marchetti, N. (eds.) *Proceedings of the 6th International Congress on the Archaeology of the Ancient Near East*. Harrasowitz.
- Özdoğan, M. 2011. Archaeological Evidence on the Westward Expansion of Farming Communities from Eastern Anatolia to the Aegean and the Balkans. *Current Anthropology*, 52.
- Özdoğan, M. 2014. A new look at the introduction of the Neolithic way of life in Southeastern Europe. Changing paradigms of the expansion of the Neolithic way of life. *Documenta Praehistorica*, XLI.
- Özdoğan, M. 1997. The beginning of Neolithic economies in southeastern Europe: an Anatolian perspective. *Journal of European Archaeology Archive*, 5, 1-33.
- Pääbo, S. 1985. Molecular cloning of Ancient Egyptian mummy DNA. *Nature*, 314, 644-645.
- Pääbo, S. 1989. Ancient DNA: extraction, characterization, molecular cloning, and enzymatic amplification. *Proceedings of the National Academy of Sciences*, 86, 1939.
- Pääbo, S., Poinar, H., Serre, D., Jaenicke-Despres, V., Hebler, J., Rohland, N., Kuch, M., Krause, J., Vigilant, L. & Hofreiter, M. 2004. Genetic analyses from ancient DNA. *Annu Rev Genet*, 38, 645-79.
- Pääbo, S. & Wilson, A. C. 1988. Polymerase chain reaction reveals cloning artefacts. *Nature*, 334, 387-388.
- Pääbo, S. & Wilson, A. C. 1991. Miocene DNA sequences - a dream come true? *Curr Biol*, 1, 45-6.
- Pålsson Hallager, B. 1985. Crete and Italy in the Late Bronze Age III Period. *American Journal of Archaeology*, 89, 293-306.
- Palumbi, G. 2007. A Preliminary Analysis on the Prehistoric Pottery from Aratashen (Armenia). In: Lyonnet, B. (ed.) *Les Cultures du Caucase (VIe-IIIe millénaires avant notre ère). Leurs Relations avec le Proche-Orient*. CNRS Editions.
- Palumbi, G. 2010. Pastoral models and centralised animal husbandry: The case of Arslantepe. In: Frangipane, M. (ed.) *Economic Centralisation in Formative States: The Archaeological Reconstruction of the Economic System in 4th Millennium Arslantepe*. Sapienza University of Rome.

- Palumbi, G. 2011. The Chalcolithic of Eastern Anatolia. *In: Steadman, S. & McMahon, G. (eds.) The Oxford Handbook of Ancient Anatolia*. Oxford University Press.
- Palumbi, G. 2017. Push or Pull Factors? The Kura-Araxes ‘Expansion’ from a Different Perspective: the Upper Euphrates Valley. *In: Rova, E. & Tonussi, M. (eds.) At the Northern Frontier of Near Eastern Archaeology*.
- Palumbi, G. & Chataigner, C. 2014. The Kura-Araxes Culture from the Caucasus to Iran, Anatolia and the Levant: Between unity and diversity. A synthesis. *Paléorient*, 40, 247-260.
- Papathanasiou, A. 2001. *The Bioarchaeological analysis of Neolithic Alepotrypa Cave, Greece*, BAR.
- Papazoglou-Manioudaki, L. & Paschalidis, C. 2021. The Mycenaean Settlement of Mygdalia Hill near Patras. An overview. *In: Karantzali, E. (ed.) Proceedings of 3rd International Interdisciplinary Colloquium: The Periphery of the Mycenaean World, 18-21 May, Lamia 2018*. Ministry of Culture and Sports.
- Parker, B. J. 2010. Networks of Interregional Interaction during Mesopotamia’s Ubaid Period. *In: Carter, R. A. & Philip, G. (eds.) Beyond the Ubaid. Transformation and Integration in the Late Prehistoric Societies of the Middle East*. Chicago University press.
- Paschou, P., Drineas, P., Yannaki, E., Razou, A., Kanaki, K., Tsetsos, F., Padmanabhuni, S. S., Michalodimitrakis, M., Renda, M. C., Pavlovic, S., et al. 2014. Maritime route of colonization of Europe. *Proceedings of the National Academy of Sciences*, 111, 9211.
- Patterson, N., Moorjani, P., Luo, Y., Mallick, S., Rohland, N., Zhan, Y., Genschoreck, T., Webster, T. & Reich, D. 2012. Ancient Admixture in Human History. *Genetics*, 192, 1065.
- Patterson, N., Price, A. L. & Reich, D. 2006. Population Structure and Eigenanalysis. *PLOS Genetics*, 2, e190.
- Peltzer, A., Jäger, G., Herbig, A., Seitz, A., Kniep, C., Krause, J. & Nieselt, K. 2016. EAGER: efficient ancient genome reconstruction. *Genome Biology*, 17, 60.
- Perlès, C. 2003. The Mesolithic at Franchthi: an overview of the data and problems. *British School at Athens Studies*, 10, 79-87.
- Perlès, C. 2005. From the Near East to Greece: let’s reverse the focus—cultural elements that did not transfer. *In: Lichter, C. (ed.) How did farming reach Europe: anatolian-european relations from the second half of the 7th through the first half of the 6th millennium*. Byzas 2.
- Peyrégne, S. & Peter, B. M. 2020. AuthenticCT: a model of ancient DNA damage to estimate the proportion of present-day DNA contamination. *Genome Biology*, 21, 246.
- Pinhasi, R., Fernandes, D., Sirak, K., Novak, M., Connell, S., Alpaslan-Roodenberg, S., Gerritsen, F., Moiseyev, V., Gromov, A., Raczky, P., et al. 2015. Optimal Ancient DNA Yields from the Inner Ear Part of the Human Petrous Bone. *PLoS ONE*, 10.
- Pinnock, F. 2009. EB IVB–MB I in Northern Syria: Crisis and Change of a Mature Urban Civilisation. *In: Parr, P. J. (ed.) The Levant in Transition. Proceedings of a Conference Held at the British Museum on 20-21 April 2004*. The Palestine Exploration Fund.
- Prevedorou, E. & Stojanowski, C. M. 2017. Biological Kinship, Postmarital Residence and the Emergence of Cemetery Formalisation at Prehistoric Marathon. *International Journal of Osteoarchaeology*, 27, 580-597.

- Prevedorou, E.-A. 2015. *The Role of Kin Relations and Residential Mobility during the Transition from Final Neolithic to Early Bronze Age in Attica, Greece*. Ph.D. dissertation, Arizona State University.
- Price, A. L., Patterson, N. J., Plenge, R. M., Weinblatt, M. E., Shadick, N. A. & Reich, D. 2006. Principal components analysis corrects for stratification in genome-wide association studies. *Nature Genetics*, 38, 904-909.
- Prowse, T. L. & Lovell, N. C. 1996. Concordance of cranial and dental morphological traits and evidence for endogamy in ancient Egypt. *American Journal of Physical Anthropology*, 101, 237-246.
- Racimo, F., Sikora, M., Vander Linden, M., Schroeder, H. & Lalueza-Fox, C. 2020. Beyond broad strokes: sociocultural insights from the study of ancient genomes. *Nature Reviews Genetics*, 21, 355-366.
- Raghavan, M., DeGiorgio, M., Albrechtsen, A., Moltke, I., Skoglund, P., Korneliussen, T. S., Grønnow, B., Appelt, M., Gulløv, H. C., Friesen, T. M., et al. 2014a. The genetic prehistory of the New World Arctic. *Science*, 345, 1255832.
- Raghavan, M., Skoglund, P., Graf, K. E., Metspalu, M., Albrechtsen, A., Moltke, I., Rasmussen, S., Stafford, T. W., Jr., Orlando, L., Metspalu, E., et al. 2014b. Upper Palaeolithic Siberian genome reveals dual ancestry of Native Americans. *Nature*, 505, 87-91.
- Ramsey, C. B. 2009. Bayesian Analysis of Radiocarbon Dates. *Radiocarbon*, 51, 337-360.
- Rasmussen, M., Anzick, S. L., Waters, M. R., Skoglund, P., DeGiorgio, M., Stafford, T. W., Jr., Rasmussen, S., Moltke, I., Albrechtsen, A., Doyle, S. M., et al. 2014. The genome of a Late Pleistocene human from a Clovis burial site in western Montana. *Nature*, 506, 225-229.
- Rasmussen, M., Li, Y., Lindgreen, S., Pedersen, J. S., Albrechtsen, A., Moltke, I., Metspalu, M., Metspalu, E., Kivisild, T., Gupta, R., et al. 2010. Ancient human genome sequence of an extinct Palaeo-Eskimo. *Nature*, 463, 757-762.
- Reich, D. 2018. *Who we are and how we got here: Ancient DNA and the new science of the human past*, Oxford University Press.
- Reich, D., Green, R. E., Kircher, M., Krause, J., Patterson, N., Durand, E. Y., Viola, B., Briggs, A. W., Stenzel, U., Johnson, P. L. F., et al. 2010. Genetic history of an archaic hominin group from Denisova Cave in Siberia. *Nature*, 468, 1053-1060.
- Reimer, P. J., Bard, E., Bayliss, A., Beck, J. W., Blackwell, P. G., Ramsey, C. B., Buck, C. E., Cheng, H., Edwards, R. L., Friedrich, M., et al. 2013. IntCal13 and Marine13 Radiocarbon Age Calibration Curves 0–50,000 Years cal BP. *Radiocarbon*, 55, 1869-1887.
- Reingruber, A. 2011. Early Neolithic settlement patterns and exchange networks in the Aegean. *Documenta Praehistorica*, 38, 291-306.
- Renaud, G., Slon, V., Duggan, A. T. & Kelso, J. 2015. Schmutzi: estimation of contamination and endogenous mitochondrial consensus calling for ancient DNA. *Genome Biology*, 16, 224.
- Renfrew, C. 1972. *The Emergence of Civilisation: The Cyclades and The Aegean in the Third Millennium BC*, Oxford, Oxbow Books.
- Renfrew, C. 1987. *Archaeology and Language: The Puzzle of Indo-European Origins*, New York, Cambridge University Press.

- Ringbauer, H., Novembre, J. & Steinrücken, M. 2021. Parental relatedness through time revealed by runs of homozygosity in ancient DNA. *Nature Communications*, 12, 5425.
- Rivollat, M., Jeong, C., Schiffels, S., Küçükkalıpcı, İ., Pemonge, M.-H., Rohrlach, A. B., Alt, K. W., Binder, D., Friederich, S., Ghesquière, E., et al. 2020. Ancient genome-wide DNA from France highlights the complexity of interactions between Mesolithic hunter-gatherers and Neolithic farmers. *Science Advances*, 6, eaaz5344.
- Rohland, N., Glocke, I., Aximu-Petri, A. & Meyer, M. 2018. Extraction of highly degraded DNA from ancient bones, teeth and sediments for high-throughput sequencing. *Nature Protocols*, 13.
- Rohland, N., Harney, E., Mallick, S., Nordenfelt, S. & Reich, D. 2015. Partial uracil-DNA-glycosylase treatment for screening of ancient DNA. *Philosophical transactions of the Royal Society of London. Series B, Biological sciences*, 370, 20130624-20130624.
- Rohrlach, A. B., Papac, L., Childebayeva, A., Rivollat, M., Villalba-Mouco, V., Neumann, G. U., Penske, S., Skourtanioti, E., van de Loosdrecht, M., Akar, M., et al. 2021. Using Y-chromosome capture enrichment to resolve haplogroup H2 shows new evidence for a two-Path Neolithic expansion to Western Europe. *bioRxiv*, 2021.02.19.431761.
- Rosenberg, N. A., Pritchard, J. K., Weber, J. L., Cann, H. M., Kidd, K. K., Zhivotovsky, L. A. & Feldman, M. W. 2002. Genetic structure of human populations. *Science*, 298, 2381-5.
- Rothman, M. 1993. Another Look at the "Uruk Expansion" from the Tigris Piedmont. In: Frangipane, M., Hauptmann, H., Liverani, M., Matthiae, P. & Mellink, M. (eds.) *Between the Rivers and over the Mountains: Archaeologica Anatolica et Mesopotamica Alba Palmieri Dedicata*. Università di Roma "La Sapienza".
- Rothman, M. 2011a. Migration and Resettlement: Godin Period IV. In: Gopnik, H. & Rothman, M. (eds.) *On the High Road*. Mazda Publishers/ROM.
- Rothman, M. S. 2011b. Interaction of Uruk and Northern Chalcolithic Societies in Anatolia. In: Steadman, S. & McMahon, G. (eds.) *The Oxford Handbook of Ancient Anatolia*. Oxford University Press.
- Rothman, M. S. 2015. Early Bronze Age migrants and ethnicity in the Middle Eastern mountain zone. *Proceedings of the National Academy of Sciences*, 112, 9190.
- Saag, L. 2020. Human Genetics: Lactase Persistence in a Battlefield. *Current Biology*, 30, R1311-R1313.
- Saag, L., Varul, L., Scheib, C. L., Stenderup, J., Allentoft, M. E., Saag, L., Pagani, L., Reidla, M., Tambets, K., Metspalu, E., et al. 2017. Extensive Farming in Estonia Started through a Sex-Biased Migration from the Steppe. *Current Biology*, 27, 2185-2193.e6.
- Saiki, R. K., Gelfand, D. H., Stoffel, S., Scharf, S. J., Higuchi, R., Horn, G. T., Mullis, K. B. & Erlich, H. A. 1988. Primer-directed enzymatic amplification of DNA with a thermostable DNA polymerase. *Science*, 239, 487-91.
- Salo, W. L., Aufderheide, A. C., Buikstra, J. & Holcomb, T. A. 1994. Identification of *Mycobacterium tuberculosis* DNA in a pre-Columbian Peruvian mummy. *Proc Natl Acad Sci U S A*, 91, 2091-4.

- Sampson, A., Kaczanowska, M. & Kozłowski, J. K. 2010. *The prehistory of the island of Kythnos (Cyclus, Greece) and the Mesolithic settlement at Maroulas*, Krakow, Polish Academy of Arts and Sciences.
- Sankararaman, S., Mallick, S., Dannemann, M., Prüfer, K., Kelso, J., Pääbo, S., Patterson, N. & Reich, D. 2014. The genomic landscape of Neanderthal ancestry in present-day humans. *Nature*, 507, 354-357.
- Saupe, T., Montinaro, F., Scaggion, C., Carrara, N., Kivisild, T., D'Atanasio, E., Hui, R., Solnik, A., Lebrasseur, O., Larson, G., et al. 2021. Ancient genomes reveal structural shifts after the arrival of Steppe-related ancestry in the Italian Peninsula. *Current Biology*.
- Sawyer, S., Krause, J., Guschanski, K., Savolainen, V. & Pääbo, S. 2012. Temporal Patterns of Nucleotide Misincorporations and DNA Fragmentation in Ancient DNA. *PLOS ONE*, 7, e34131.
- Schepartz, L. A., Fox, S. C. & Bourbou, C. 2009. *New Directions in the Skeletal Biology of Greece*, Princeton, New Jersey, American School of Classical Studies at Athens.
- Schoep, I., Tomkins, P. & Driessen, J. M. (eds.) 2012. *Back to the Beginning: Reassessing Social and Political Complexity on Crete during the Early and Middle Bronze Age*, Oxbow Books.
- Schoop, U.-D. 2005. *Das anatolische Chalkolithikum. Eine chronologische Untersuchung zur vorbronzezeitlichen Kultursequenz im nördlichen Zentralanatolien und den angrenzenden Gebieten*, Remshalden-Grünbach, BA Greiner.
- Schoop, U.-D. 2011. The Chalcolithic on the Plateau. In: Steadman, S. & McMahon, G. (eds.) *The Oxford Handbook of Ancient Anatolia*. Oxford University Press.
- Schubert, M., Lindgreen, S. & Orlando, L. 2016. AdapterRemoval v2: rapid adapter trimming, identification, and read merging. *BMC research notes*, 9, 88-88.
- Schuenemann, V. J., Avanzi, C., Krause-Kyora, B., Seitz, A., Herbig, A., Inskip, S., Bonazzi, M., Reiter, E., Urban, C., Dangvard Pedersen, D., et al. 2018. Ancient genomes reveal a high diversity of *Mycobacterium leprae* in medieval Europe. *PLoS Pathog*, 14, e1006997.
- Schwartz, G. 1988. Excavations at Karatut Mevkii and Perspectives on the Uruk/Jemdet Nasr Expansion. *Akkadica*, 56, 1-41.
- Seeden, H. & Kaddour, M. 1983. Space, Structures and Land in Shams ed-Din Tannira on the Euphrates: An Ethnoarchaeological Perspective. In: al-Khalidi, T. (ed.) *Land Tenure and Social Transformation in the Near East*. American University of Beirut Press.
- Shapiro, B., Barlow, A., Heintzman, P. D., Hofreiter, M., Paijmans, J. L. A. & Soares, A. E. R. (eds.) 2019. *Ancient DNA: Methods and Protocols*, Springer.
- Shelmerdine, C. W. 2008. Background, Sources and Methods. In: Shelmerdine, C. W. (ed.) *The Aegean Bronze Age*. Cambridge University Press.
- Simmons, A. H. 2014. *Stone Age Sailors: Paleolithic Seafaring in the Mediterranean*, Walnut Creek, Left Coast Press.
- Siracusano, G. & Palumbi, G. 2014. "Who'd be happy, let him be so: nothing's sure about tomorrow" Discarded Bones in Early Bronze I Elite Area at Arslantepe (Malatya, Turkey): Remains of Banquets? In: Bieliński, P., Gawlikowski, M., Koliński, R., Ławecka, D., Sołtysiak, A. & Wygnańska, Z. (eds.) *Proceedings of the 8th ICAANE*. Harrassowitz Verlag.

- Skoglund, P., Mallick, S., Bortolini, M. C., Chennagiri, N., Hünemeier, T., Petzl-Erler, M. L., Salzano, F. M., Patterson, N. & Reich, D. 2015. Genetic evidence for two founding populations of the Americas. *Nature*, 525, 104-108.
- Skoglund, P., Malmström, H., Omrak, A., Raghavan, M., Valdiosera, C., Günther, T., Hall, P., Tambets, K., Parik, J., Sjögren, K.-G., et al. 2014. Genomic Diversity and Admixture Differs for Stone-Age Scandinavian Foragers and Farmers. *Science*, 344, 747.
- Skoglund, P., Malmström, H., Raghavan, M., Storå, J., Hall, P., Willerslev, E., Gilbert, M. T. P., Götherström, A. & Jakobsson, M. 2012. Origins and Genetic Legacy of Neolithic Farmers and Hunter-Gatherers in Europe. *Science*, 336, 466.
- Skoglund, P. & Mathieson, I. 2018. Ancient Genomics of Modern Humans: The First Decade. *Annu Rev Genomics Hum Genet*, 19, 381-404.
- Skourtanioti, E., Erdal, Y. S., Frangipane, M., Balossi Restelli, F., Yener, K. A., Pinnock, F., Matthiae, P., Özbal, R., Schoop, U.-D., Guliyev, F., et al. 2020. Genomic History of Neolithic to Bronze Age Anatolia, Northern Levant, and Southern Caucasus. *Cell*, 181, 1158-1175.e28.
- Slatkin, M. & Racimo, F. 2016. Ancient DNA and human history. *Proceedings of the National Academy of Sciences*, 113, 6380.
- Slon, V., Hopfe, C., Weiß, C. L., Mafessoni, F., de la Rasilla, M., Lalueza-Fox, C., Rosas, A., Soressi, M., Knul, M. V., Miller, R., et al. 2017. Neandertal and Denisovan DNA from Pleistocene sediments. *Science*, 356, 605.
- Smith, B. D. 1995. *The Emergence of Agriculture*, Scientific American Library.
- Sokal, R. R., Oden, N. L. & Thomson, B. A. 1999. A Problem with Synthetic Maps. *Human Biology*, 71, 1-13.
- Spiliopoulou, A., Colombo, M., Orchard, P., Agakov, F. & McKeigue, P. 2017. GeneImp: Fast Imputation to Large Reference Panels Using Genotype Likelihoods from Ultralow Coverage Sequencing. *Genetics*, 206, 91-104.
- Spyrou, M. A., Keller, M., Tikhbatova, R. I., Scheib, C. L., Nelson, E. A., Andrades Valtueña, A., Neumann, G. U., Walker, D., Alterauge, A., Carty, N., et al. 2019. Phylogeography of the second plague pandemic revealed through analysis of historical *Yersinia pestis* genomes. *Nature Communications*, 10, 4470.
- Spyrou, M. A., Tikhbatova, R. I., Wang, C.-C., Valtueña, A. A., Lankapalli, A. K., Kondrashin, V. V., Tsybin, V. A., Khokhlov, A., Kühnert, D., Herbig, A., et al. 2018. Analysis of 3800-year-old *Yersinia pestis* genomes suggests Bronze Age origin for bubonic plague. *Nature Communications*, 9, 2234.
- Steadman, S. & McMahon, G. 2011. *The Oxford Handbook of Ancient Anatolia*, New York, Oxford University Press.
- Stein, G. Indigenous Social Complexity at Hadınebi ( Turkey ) and the Organization of Uruk Colonial Contact. 2009.
- Stein, G. & Misir, A. 1993. Excavations at Hacinebi Tepe 1992. *Kazı Sonuçları Toplantısı*, 15, 131-152.

- Stein, G. & Özbal, R., F. 2007. A Tale of Two Oikumenai: Variation in the Expansionary Dynamics of Ubaid and Uruk Mesopotamia. In: Stone, E. C. (ed.) *Settlement and Society: Ecology, Urbanism, Trade and Technology in Mesopotamia and Beyond (Robert McC. Adams Festschrift)*. Cotsen Institute of Archaeology Press.
- Stommenger, E. 1980. *Habuba Kabira: Eine Stadt vor 5000 Jahren*, Mainz, Philipp von Zabern.
- Teasdale, M., Doorn, N. V. v., Fiddymont, S., Webb, C., O'Connor, T., Hofreiter, M., Collins, M. & Bradley, D. 2015. Paging through history: parchment as a reservoir of ancient DNA for next generation sequencing. *Philosophical Transactions of the Royal Society B: Biological Sciences*, 370.
- Thissen, L. 2010. The Neolithic–Chalcolithic sequence in the SW Anatolian Lakes Region. *Documenta Praehistorica*, 37, 269-282.
- Thuessen, I. 2000. Ubaid Expansion in the Khabur : new evidence from Tell Mashnaqa. In: Rouault, O. & Wäfler, M. (eds.) *La Djéziré et L'Euphrate syriens de la protohistoire à la fin du IIe millénaire av. J.-C.: tendances dans l'interprétation historique des données nouvelles*. Brepols
- Triantaphyllou, S. 2001. *A Bioarchaeological Approach to Prehistoric Cemetery Populations from Central and Western Greek Macedonia*, Oxford, Archaeopress.
- Tritsaroli, P. 2006. *Pratiques Funéraires en Grèce Centrale à la période Byzantine: Analyse à partir des données archéologiques et biologiques*. Muséum national d'Histoire naturelle.
- Uerpmann, H.-P. 1982. Faunal remains from Shams ed-Din Tannira, a Halafian site in Northern Syria. *Berytus*, 30, 3-52.
- Valdiosera, C., Günther, T., Vera-Rodríguez, J. C., Ureña, I., Iriarte, E., Rodríguez-Varela, R., Simões, L. G., Martínez-Sánchez, R. M., Svensson, E. M., Malmström, H., et al. 2018. Four millennia of Iberian biomolecular prehistory illustrate the impact of prehistoric migrations at the far end of Eurasia. *Proceedings of the National Academy of Sciences*, 115, 3428.
- van der Valk, T., Pečnerová, P., Díez-del-Molino, D., Bergström, A., Oppenheimer, J., Hartmann, S., Xenikoudakis, G., Thomas, J. A., Dehasque, M., Sağlıcan, E., et al. 2021. Million-year-old DNA sheds light on the genomic history of mammoths. *Nature*, 591, 265-269.
- van Driel, G. & van Driel-Murray, C. 1983. Jebel Aruda, the 1982 Season. *Akkadica*, 33, 1-26.
- Vernot, B. & Akey, J. M. 2014. Resurrecting Surviving Neandertal Lineages from Modern Human Genomes. *Science*, 343, 1017.
- Villalba-Mouco, V., van de Loosdrecht, M. S., Posth, C., Mora, R., Martínez-Moreno, J., Rojo-Guerra, M., Salazar-García, D. C., Royo-Guillén, J. I., Kunst, M., Rougier, H., et al. 2019. Survival of Late Pleistocene Hunter-Gatherer Ancestry in the Iberian Peninsula. *Current Biology*, 29, 1169-1177.e7.
- Voutsaki, S. 1999. Mortuary Display, Prestige and Identity in the Shaft Grave Era. In: Aravantinos, V. L., Barceló, J. A. & Bockisch-Bräuer, C. (eds.) *Eliten in der Bronzezeit. Ergebnisse zweier Kolloquien in Mainz und Athen*. Verl. des Römisch-Germanischen Zentralmuseums.
- Wang, C. C., Reinhold, S., Kalmykov, A., Wissgott, A., Brandt, G., Jeong, C., Cheronet, O., Ferry, M., Harney, E., Keating, D., et al. 2019. Ancient human genome-wide data from a 3000-year interval in the Caucasus corresponds with eco-geographic regions. *Nat Commun*, 10, 590.

- Warinner, C., Speller, C. & Collins, M. J. 2015. A new era in palaeomicrobiology: prospects for ancient dental calculus as a long-term record of the human oral microbiome. *Philosophical transactions of the Royal Society of London. Series B, Biological sciences*, 370, 20130376-20130376.
- Watson, P. J. 1982. The Halafian Pottery of Tilkitepe, Seen in the Hittite Museum, Ankara (Citadel). In: Korfmann, M. (ed.) *Tilkitepe*. Verlag Ernst Wasmuth.
- Weiß, C. L., Schuenemann, V. J., Devos, J., Shirsekar, G., Reiter, E., Gould, B. A., Stinchcombe, J. R., Krause, J. & Burbano, H. A. 2016. Temporal patterns of damage and decay kinetics of DNA retrieved from plant herbarium specimens. *R Soc Open Sci*, 3, 160239.
- Weiss, H. 1993. The genesis and collapse of third millennium north Mesopotamian civilization. *Science*, 261, 995-1004.
- Weiss, H. 2014a. The northern Levant during the intermediate Bronze Age: altered trajectories. In: Killebrew, A. E. (ed.) *The Oxford Handbook of the Archaeology of the Levant: c. 8000–332 BCE*. Oxford University Press.
- Weiss, H. 2014b. The northern Levant during the intermediate Bronze Age: altered trajectories. In: Killebrew, A. E. (ed.) *The Oxford Handbook of the Archaeology of the Levant: c. 8000–332 BCE*. Oxford University Press.
- Weiss, H. 2017. 4.2 ka BP megadrought and the Akkadian collapse. In: Weiss, H. (ed.) *Megadrought and Collapse: From Early Agriculture to Angkor*. Oxford University Press.
- Weissensteiner, H., Pacher, D., Kloss-Brandstätter, A., Forer, L., Specht, G., Bandelt, H. J., Kronenberg, F., Salas, A. & Schönherr, S. 2016. HaploGrep 2: mitochondrial haplogroup classification in the era of high-throughput sequencing. *Nucleic Acids Res*, 44, W58-63.
- Weninger, B., Clare, L., Gerritsen, F., Horejs, B., Krauß, R., Linstädter, J., Özbal, R. & Rohling, E. J. 2014. Neolithisation of the Aegean and Southeast Europe during the 6600–6000 calBC period of Rapid Climate Change. *Documenta Praehistorica*, 41, 1-31.
- Wiener, M. H. 2015. The Mycenaean Conquest of Minoan Crete. In: MacDonald, C. F., Hatzaki, E. M. & Andreou, S. (eds.) *The Great Islands: Studies of Crete and Cyprus Presented to Gerald Cadogan*. Kapon Editions.
- Wiersma, C. & Voutsaki, S. (eds.) 2017. *Social Change in Aegean Prehistory*, Oxbow Books.
- Willerslev, E., Cappellini, E., Boomsma, W., Nielsen, R., Hebsgaard, M. B., Brand, T. B., Hofreiter, M., Bunce, M., Poinar, H. N., Dahl-Jensen, D., et al. 2007. Ancient biomolecules from deep ice cores reveal a forested southern Greenland. *Science*, 317, 111-4.
- Willerslev, E., Hansen, A. J., Binladen, J., Brand, T. B., Gilbert, M. T. P., Shapiro, B., Bunce, M., Wiuf, C., Gilichinsky, D. A. & Cooper, A. 2003. Diverse plant and animal genetic records from Holocene and Pleistocene sediments. *Science*, 300, 791-795.
- Wilson, A. C. & Sarich, V. M. 1969. A molecular time scale for human evolution. *Proceedings of the National Academy of Sciences of the United States of America*, 63, 1088-1093.
- Wilson, D. 2008. Early Prepalatial Crete. In: Shelmerdine, C. W. (ed.) *The Aegean Bronze Age*. Cambridge University Press.
- Wright, J. C. 2008. Early Mycenaean Greece. In: Shelmerdine, C. W. (ed.) *Aegean Bronze Age*. Cambridge University Press.



Yaka, R., Mapelli, I., Kaptan, D., Doğu, A., Chyleński, M., Erdal, Ö. D., Koptekin, D., Vural, K. B., Bayliss, A., Mazzucato, C., et al. 2021. Variable kinship patterns in Neolithic Anatolia revealed by ancient genomes. *Current Biology*, 31, 2455-2468.e18.

Yakar, J. 2011. Anatolian Chronology and Terminology. *In: Steadman, S. R. & McMahon, G. (eds.) The Oxford Handbook of Ancient Anatolia*. Oxford University Press.

Yazıcıoğlu Santamaria, G. B. 2017. Locals, Immigrants, and Marriage Ties at Kültepe: Results of Strontium Isotope Analysis on Human Teeth from Lower Town Graves. *In: Kulakoğlu, F. & Barjamovic, G. (eds.) Movement, Resources, Interaction: Proceedings of the 2nd Kültepe International Meeting, Kültepe 26-30 July 2015*. Brepols.

Younger, J. G. & Rehak, P. 2008. The Material Culture of Neopalatial Crete. *In: Shelmerdine, C. W. (ed.) Aegean Bronze Age*. Cambridge University Press.

Zeberg, H. & Pääbo, S. 2020. The major genetic risk factor for severe COVID-19 is inherited from Neanderthals. *Nature*, 587, 610-612.

Zeberg, H. & Pääbo, S. 2021. A genomic region associated with protection against severe COVID-19 is inherited from Neandertals. *Proceedings of the National Academy of Sciences*, 118, e2026309118.

Zilhão, J. 1993. The Spread of Agro-Pastoral Economies across Mediterranean Europe: A View from the Far West. *Journal of Mediterranean Archaeology*, 6, 5-63.

Zvelebil, M. & Lillie, M. 2000. Transition to agriculture in eastern Europe. *In: Price, T. D. (ed.) Europe's First Farmers*. Cambridge University Press.

## 9 Eigenständigkeitserklärung

Gemäß § 5 Abs. 4 der Promotionsordnung der Fakultät für Biowissenschaften der Friedrich-Schiller-Universität Jena erkläre ich, dass mir die aktuelle Promotionsordnung der Fakultät bekannt ist. Ich bezeuge, dass ich das Dissertationsprojekt selbst erstellt habe, ohne Textpassagen Dritter oder eigene frühere Abschlussarbeiten zu verwenden, die in meiner Dissertation nicht zitiert werden. Alle statistischen Hilfsmittel, Quellen und persönlichen Mitteilungen, die für die Erstellung dieser Dissertation verwendet wurden, wurden ordnungsgemäß zitiert. Des Weiteren habe ich in der Liste der Manuskripte und den entsprechenden Danksagungen alle Personen genannt, die mich bei der Auswahl und Bewertung sowie bei der Erstellung der Manuskripte unterstützt haben. Ich versichere, dass ich keine Unterstützung durch eine/einen externen Berater/-in erhalten habe und dass Dritte weder direkt noch indirekt finanzielle Vorteile im Zusammenhang mit dieser Dissertation erhalten haben. Die vorliegende Dissertation – oder eine im Wesentlichen vergleichbare – wurde bisher an keiner anderen Hochschule oder Fakultät zu einer staatlichen oder sonstigen wissenschaftlichen Prüfung vorgelegt.

Leipzig, den 24.01.2023

---

Eirini Skourtanioti

## 10 Acknowledgments

I would like to express my deep gratitude to many people who accompanied me and supported me throughout the PhD journey.

First and foremost, my appreciation goes to my two main supervisors Johannes Krause and Wolfgang Haak who trusted me and made me part of their research group, shared their knowledge, and experience inspired me, respected me, and gave me opportunities, and space and stimulation to grow as a young researcher.

I am also equally thankful to Choongwon Jeong, my mentor throughout most of my PhD, and an exemplary scientist and person who took my training very seriously. I have learned very much from him.

With Philipp Stockhammer, from the Max Planck Harvard Center for the Archaeoscience of the Ancient Mediterranean (MHAAM), I have worked very closely over the last years; his guidance, support, and great insights he brought into my projects have been of equal importance in my intellectual development. I am grateful for this.

I have realized throughout the years how the above four people have shaped my professional path, and my personality as well. I see in them common but also different qualities which have created very high standards on how a supervisor should be and, critically, how high I should continue aiming.

I also owe a big thank you to Mehmet Somel, for being a thorough external reviewer with a critical view of my work, and a very supportive colleague.

I want to thank the lab technicians Marta Burri, Raffaella Angelina Bianco, Marta Burri, Căcilia Freund, and Nuno Filipe Gomes Martins for their excellent job and for taking a large amount of work out of my hands.

My gratitude, of course, also goes to many more people who framed my life in the warmest way and helped me make my trip through the Phd life a successful experience:

To my very dear excellent colleagues and friends Michal Feldman, Maria Spyrou, Rodrigo Barquera, Ke Wang, Anthi Tiliakou, Eleftheria Orfanou and Kathrin Nägele with whom I shared some of the most intense and joyful moments, who were an ear and hand of help, a source of courage, but mostly people to be inspired from.

To the members of the popgen and MHAAM groups for the stimulating and friendly environment they have been creating. Particular thanks go to Nada Salem, Stefanie Eisenmann, Megan Michel, Gunnar Neumann, Guido Gneccchi Ruscone, Ayshin Ghalichi, Ezgi Altınışık, Maïté Rivollat, Vanessa Villalba Mouco and Suzanne Freilich, with whom I worked closely or developed shorter but very meaningful interactions. Their drive for research and friendliness made my experience more exciting.

To my friend Anca, and the peculiar circumstances that brought her in my life, for giving another perspective to my PhD life experience.

To my flatmates during most of my stay at Jena, Thorben, Agnes, Tim and Theresa who made me feel welcome to Germany and would be a warm embrace when I would return home.

To Anna, Sophie, Christos, Kynthia, Evita, Yiannis A., Maria and Paschalia with whom I am bound with years of friendship and remained present at my good and difficult moments despite the thousand kilometres that were separating us.

To my sister Eva, and my parents Alekos and Katerina, the people I have missed the most throughout all these years, for their love and greatest support; also, for reminding that all this effort has been an act of bravery.

To my partner Arturo for being one of the greatest outcomes of my PhD life in Germany.

## 11 Appendix

### 11.1 Candidate-specific contributions to manuscripts

#### 11.1.1 Manuscript A

**Short citation:** Skourtanioti et al. (2020). *Cell*, 181, 1158-1175.e28.  
<https://doi.org/10.1016/j.cell.2020.04.044>

**Contribution of the doctoral candidate to figures reproducing experimental data (for original articles only):**

<b>*Figure #: <u>All</u></b>	<input checked="" type="checkbox"/> <b>100% (data reproduced in this figure come entirely from experimental work performed by the candidate)</b>
	<input type="checkbox"/> 0% (the data reproduced in this figure are based entirely on work performed by other co-authors)
	<input type="checkbox"/> Any contribution to the figure by the PhD candidate: _____% Brief description of the contribution: (e.g., "Figure parts a, d, and f" or "Analysis of data," etc).
*Can refer to more than one fig. if the answer is the same.	

*'Experimental data' is used here to also refer to novel scientific analysis of data produced from experimental work which includes next generation sequencing via a core facility.*

11.1.2 Manuscript B

**Short citation:** Skourtanioti et al. 2023, *Nat Ecol Evol*

(accepted on November 11 by the production editor at *Nature Ecology and Evolution*)

**Contribution of the doctoral candidate to figures reproducing experimental data (for original articles only):**

*Figure #: <u>All</u> expect from Figure S3.1	<input checked="" type="checkbox"/>	<b>100% (data reproduced in this figure come entirely from experimental work performed by the candidate)</b>
Figure S3.1	<input checked="" type="checkbox"/>	<b>0% (the data reproduced in this figure are based entirely on work performed by other co-authors)</b>
	<input type="checkbox"/>	Any contribution to the figure by the PhD candidate: _____% Brief description of the contribution: (e.g., "Figure parts a, d, and f" or "Analysis of data," etc).

\*Can refer to more than one fig. if the answer is the same.

*'Experimental data' is used here to also refer to novel scientific analysis of data produced from experimental work which includes next generation sequencing via a core facility.*

## 11.2 Table 1. Stages of cultural evolution in Anatolia from the Neolithic to the Bronze Age

*Table 1. Stages of cultural evolution in Anatolia from the Neolithic to the Bronze Age (adapted from Steadman and McMahon, 2011; pp 59-60, 68)*

Stages of cultural evolution in prehistoric Anatolia	Approximate chronology
<ul style="list-style-type: none"> <li>• Industrial specialization: decorated stone bowls; deliberate firing of clay figurines and vessels</li> <li>• Intra-/intercommunal celebrations of socioreligious nature (feasting, exchange of ornaments) to strengthen communal identity and intra- and intercommunity bonds. Special buildings for these communal activities (e.g., Göbeklitepe, Karahantepe)</li> <li>• Food procurement based on more selective hunting and gathering, requiring less mobility</li> <li>• Seasonal campsite occupation to village occupation resulting in socioeconomic changes</li> </ul>	<p><i>Early Aceramic Neolithic Stage ca. 8500 BCE</i></p>
<ul style="list-style-type: none"> <li>• Technological experimentations (lithic industry, production of native copper, floor plastering etc.)</li> <li>• Increasing community size could imply village management by councils and/or chiefs</li> <li>• Selective cultivation of wild species such as wild einkorn, emmer wheat, barley, and lentils; experimentation with sheep herding</li> <li>• Hunting and gathering-based wild resource management</li> <li>• First signs of social differentiation and economic diversification</li> <li>• Special buildings for communal gatherings and rituals of socioreligious nature</li> <li>• Larger permanent villages/houses and intramural burials under house floors</li> </ul>	<p><i>Late Aceramic Neolithic Stage ca. 7000 BCE</i></p>
<ul style="list-style-type: none"> <li>• Local changes in pottery and lithic typologies and technologies reflect changes in subsistence modes</li> <li>• Symbolisms relating to fecundity, life, and death in naturalistic human and animal forms</li> <li>• Role diversification: family lineage, age- and gender-based social ranking; village management by council and/or chiefs; pottery production</li> <li>• No identifiable community buildings</li> <li>• Partial seasonal transhumance for the pursuit of herding, hunting, and gathering activities</li> <li>• Widespread adoption of agriculture; domestication of sheep, goat, and perhaps cattle</li> </ul>	<p><i>Neolithic ca. 6000 BCE</i></p>
<ul style="list-style-type: none"> <li>• Animal husbandry and herding become more important economic component</li> <li>• Clearer manifestations of ethno/geocultural group identity in material culture</li> <li>• Intensification of interregional contacts beyond the southcentral plateau</li> </ul>	<p><i>Early Chalcolithic ca. 5000 BCE</i></p>

- New farming settlements and the consolidation of those previously established
- Small kin-related communities with more developed farming economies and fenced villages and farmsteads

- Dominance of handmade dark burnished monochrome wares in the central plateau
- Abstract artistic expressions in iconography
- Intensification of interregional interaction and acculturation

*Middle Chalcolithic*

- Consolidation of traditional agropastoral economies by village administrations
- Possible emergence of settlement hierarchies in clan-controlled/tribal territories

*Late Chalcolithic*

- Proto-urban chiefdom systems
- Early urban systems
- Emerging local seats of power, local dynasties and territorial city states

*Early Bronze Age 1 ca. 3000 BCE*

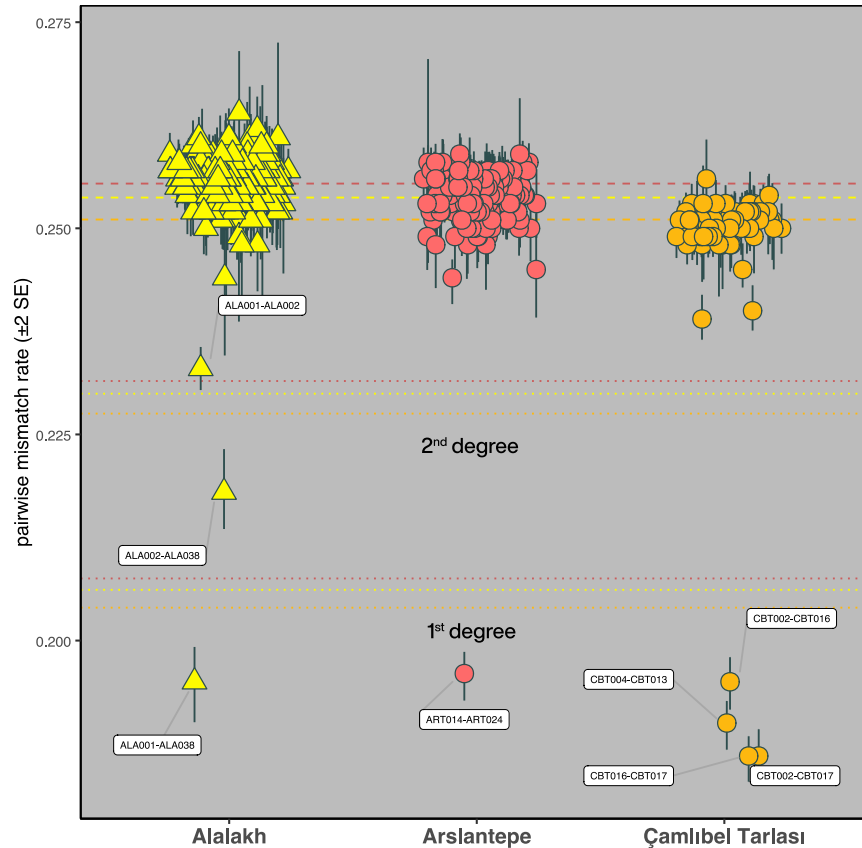
*Early Bronze Age 2*

*Early Bronze Age 3 ca. 2000 BCE*



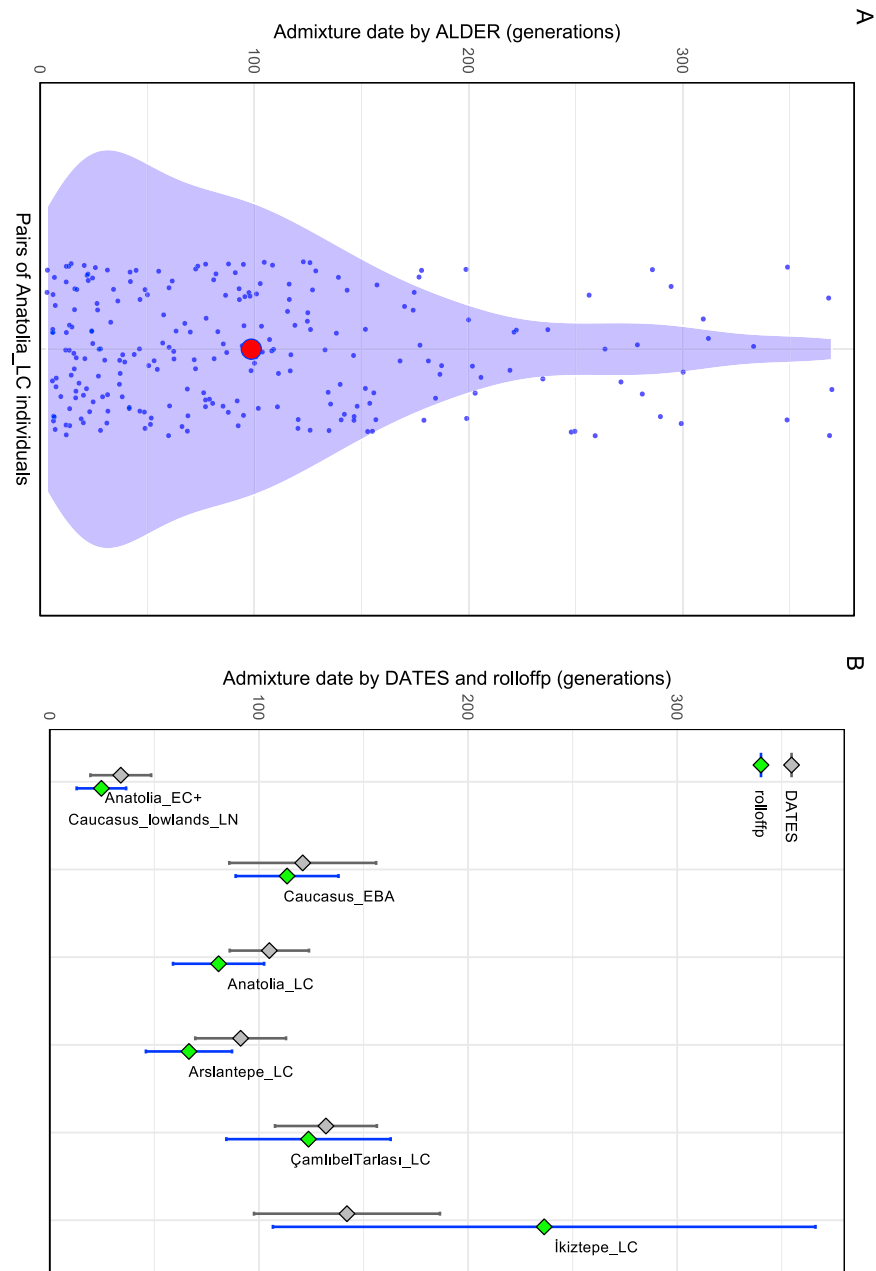
## **11.4 Supplementary Material for Manuscript A**

# Supplemental Figures



**Figure S1. Pairwise Mismatch Rate for the Three Sites with First- and Second-Degree Related Individuals, Related to Figure 2**

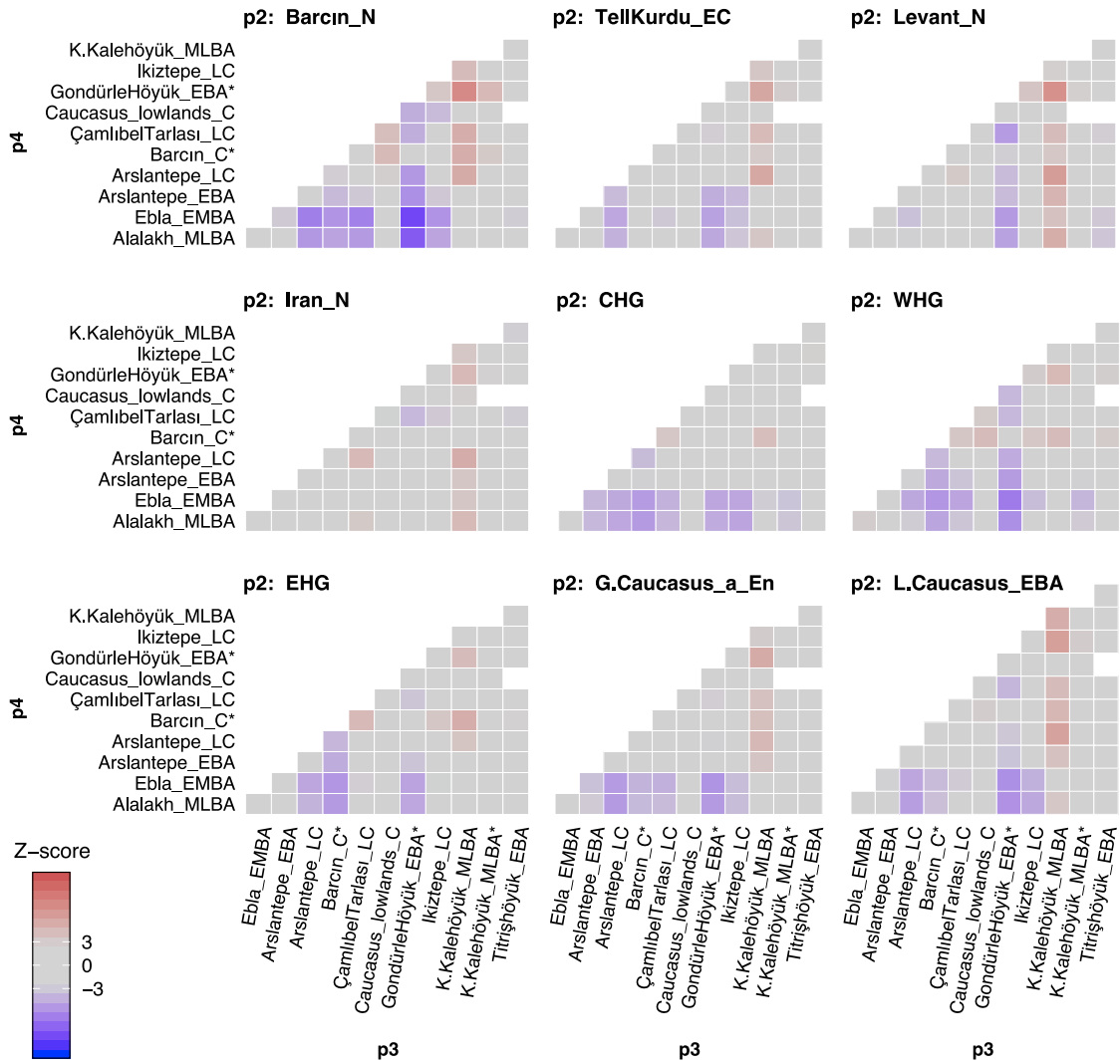
Pairwise SNP mismatch rates (pmr; the proportion of mismatching SNPs out of the total number of pairwise-overlapping SNPs) and their associated standard errors were estimated with READ (Monroy Kuhn et al., 2018). The baseline of unrelatedness ( $\geq$  third degree) in pmr was estimated as the mean of all pairwise comparisons within every site. The relatedness classification cut-offs were estimated by multiplying the baselines by 0.90625 ( $\geq$  third degree, dashed lines), 0.8125 and 0.625 for second and first degree, respectively (dotted lines).



**Figure S2. Summary of Admixture Dates Estimated with Alder and Rolloff, Related to STAR Methods (Test of Recent Admixture)**

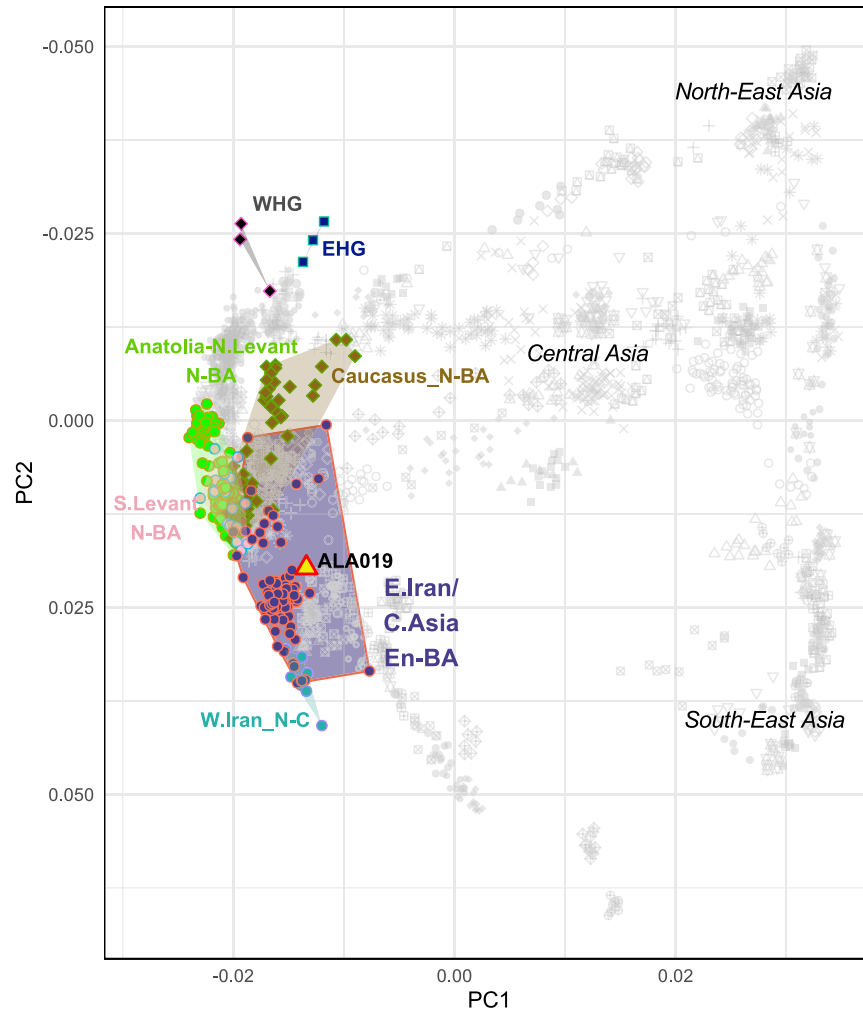
(A) Alder admixture dates on all pair combinations from 27 Anatolia\_LC individuals. Pairs include individuals from the Arslantepe\_LC and ÇamlıbelTarlası\_LC groups. Estimates for which computation of SE failed are not plotted. The average admixture date from the 241 independent tests (red dot) is very close to the estimation from DATES on Anatolia\_LC (~100 generations).

(B) rolloff estimates of admixture dates overlap with DATES within  $\pm 1$  SE.



**Figure S3. Genetic Differences among Analyzed Chalcolithic and Bronze Age Groups, Related to Figure 6**

Heatmap of  $f_4$ -statistics of the form  $f_4(Mbuti, p2; p3, p4)$ , where  $p3$  and  $p4$  are all possible pairs of LC-LBA groups from the present study and published contemporaneous (\*), and  $p2$  a selection of ancient populations from West Eurasia.  $f_4$ -statistics that do not deviate significantly from 0 (i.e.,  $|Z\text{-score}| \leq 3$ ) are represented with gray-colored tiles. Significant  $f_4$ -statistics are colored in red and blue scale according to the direction of allele sharing.  $f_4$ -statistics estimated on less than 50,000 SNPs are not plotted resulting in some missing tiles from the heatmaps.



**Figure S4. Eurasian PCA with Neolithic to Bronze Age Individuals from Iran and Turan and the Genetic Outlier Individual from Alalakh (ALA019), Related to Figure 7**

Scatter plot of PC1 and PC2 from PCA computed on modern-day Eurasian populations (gray points) shows that the Alalakh\_MLBA\_outlier (ALA019) is genetically closer to individuals from Chalcolithic and Bronze Age Iran/Turan. Colored labels and points refer to ancient populations and black labels to modern-day populations.

**Table S1** Details of AMS radiocarbon dating on selected 95 individuals after quality filtering, Related to Figure 2. (*published as excel table*)

Archaeological ID	Lab individual ID	sample ID (DNA)	skeletal sample (DNA)	14C age (BP) ±	δ13C AMS [‰]	Cal 1 sigma	Cal 2 sigma	C [‰]	C/N	Collagen (%)	skeletal material (for C14)	C14 lab number	Archaeological Site Name
45-71L, Locus 03-3017, Pall 257, Skeleton SQ4-9	ALA001	ALA001.A	petrous bone	24	-27.3	cal BCE 1487-1407	cal BCE 1496-1325	13.8	2.7	3.9	petrous bone	MAWS-33675	Alalakh
45-71L, Locus 03-3017, Pall 246, Skeleton SQ4-8	ALA002	ALA002.A	petrous bone	3158	-18.8	cal BCE 1487-1412	cal BCE 1496-1401	13.1	2.6	1.5	petrous bone	MAWS-33676	Alalakh
45-72L, Locus 03-3002	ALA004	ALA004.A	petrous bone	3507	-18.5	cal BCE 1883-1776	cal BCE 1895-1752	22.2	2.8	5.8	petrous bone	MAWS-33677	Alalakh
45-44L, Locus 133, AT 17652	ALA008.A	ALA008.A	petrous bone	3473	-17.8	cal BCE 1875-1748	cal BCE 1881-1700	15.0	2.7	4.6	petrous bone	MAWS-33678	Alalakh
45-44L, Locus 146, AT 18960	ALA011	ALA011.A	petrous bone	3382	-14.9	cal BCE 1729-1641	cal BCE 1741-1624	15.6	2.7	5.1	petrous bone	MAWS-33680	Alalakh
45-44L, Locus 152, AT 19260	ALA013	ALA013.A	petrous bone	3457	-21.5	cal BCE 1870-1698	cal BCE 1878-1693	31.6	2.9	3.9	petrous bone	MAWS-33681	Alalakh
45-45L, Locus 8, AT 8836	ALA014	ALA014.A	petrous bone	3392	-20.8	cal BCE 1737-1646	cal BCE 1749-1630	33.1	2.9	4.2	petrous bone	MAWS-33682	Alalakh
45-45L, Locus 48, AT 015741	ALA015	ALA015.A	petrous bone	3566	-19.3	cal BCE 1944-1887	cal BCE 2014-1781	7.2	2.3	2.0	petrous bone	MAWS-33683	Alalakh
32-54L, Locus 85, AT 017541	ALA016	ALA016.A	petrous bone	3284	-28.0	cal BCE 1609-1528	cal BCE 1617-1506	12.4	1.8	7.4	petrous bone	MAWS-33684	Alalakh
32-57L, Locus 164, AT 10070	ALA017.A	ALA017.A	petrous bone	3154	-23.4	cal BCE 1605-1504	cal BCE 1614-1466	23.0	2.8	1.5	petrous bone	MAWS-33685	Alalakh
42-29, 44, L. 237, AT 019127	ALA018	ALA018.A	petrous bone	3264	-20.6	cal BCE 1490-1409	cal BCE 1497-1326	22.5	2.8	1.5	petrous bone	MAWS-33686	Alalakh
32-57L, Locus 247, AT 15878	ALA019	ALA019.A	petrous bone	3298	-19.3	cal BCE 1613-1534	cal BCE 1625-1511	34.5	2.9	8.7	petrous bone	MAWS-33687	Alalakh
44-86L, Locus 22, AT 15460	ALA020	ALA020.A	petrous bone	3167	-28.5	cal BCE 1493-1415	cal BCE 1502-1395	12.2	3.3	0.3	petrous bone	MAWS-33688	Alalakh
45-44L, Locus 65, AT 6029	ALA023	ALA023.A	petrous bone	3520	-15.6	cal BCE 1892-1776	cal BCE 1921-1763	39.7	2.9	1.8	long bone	MAWS-33690	Alalakh
45-44L, Locus 68, AT 6572	ALA024	ALA024.A	petrous bone	3586	-27.7	cal BCE 2010-1891	cal BCE 2111-1779	12.0	3.4	0.2	petrous bone	MAWS-33692	Alalakh
45-44L, Locus 66, AT 6032	ALA025.A	ALA025.A	petrous bone	3443	-25	cal BCE 1862-1693	cal BCE 1877-1668	30.0	2.7	1.8	petrous bone	MAWS-33694	Alalakh
45-44L, Locus 70, AT 6931	ALA026	ALA026.A	petrous bone	3440	-23.1	cal BCE 1858-1692	cal BCE 1874-1628	33.1	2.9	3.8	petrous bone	MAWS-33693	Alalakh
45-44L, Locus 73, AT 7395	ALA028.A	ALA028.A	petrous bone	3440	-29.5	cal BCE 1858-1692	cal BCE 1877-1666	24.6	2.9	3.1	petrous bone	MAWS-33694	Alalakh
45-44L, Locus 79, AT 7695	ALA029.A	ALA029.A	petrous bone	3465	-16.7	cal BCE 1873-1702	cal BCE 1880-1695	23.1	2.8	1.3	petrous bone	MAWS-33695	Alalakh
45-44L, Locus 105, AT 10669	ALA030.A	ALA030.A	petrous bone	3256	-26.9	cal BCE 1605-1499	cal BCE 1612-1457	23.1	2.8	2.2	petrous bone	MAWS-33696	Alalakh
45-45L, Locus 6, AT 8830	ALA034.A	ALA034.A	petrous bone	3436	-11.4	cal BCE 1763-1692	cal BCE 1874-1666	30.9	3.3	1.4	petrous bone	MAWS-33696	Alalakh
45-45L, Locus 7, AT 7940	ALA035	ALA035.A	petrous bone	3543	-10.7	cal BCE 1930-1784	cal BCE 1948-1774	32.2	3.2	1.7	petrous bone	MAWS-33697	Alalakh
45-45L, Locus 30, AT 11452	ALA037.A	ALA037.A	petrous bone	3477	-12.4	cal BCE 1876-1750	cal BCE 1882-1701	19.6	3.2	1.8	petrous bone	MAWS-33698	Alalakh
45-71L, Locus 03-3017, Pall 236, Skeleton SQ4-7	ALA038	ALA038.A	petrous bone	3260	-12.4	cal BCE 1605-1501	cal BCE 1613-1461	41.8	3.2	18.0	petrous bone	MAWS-33699	Alalakh
44-85L, Locus 15, AT 14466	ALA039.A	ALA039.A	petrous bone	3125	-12.6	cal BCE 1431-1324	cal BCE 1448-1303	38.4	3.2	3.4	petrous bone	MAWS-33700	Alalakh
45-72L, Locus 03-3065, skeleton SQ4-19	ALA084	ALA084.B	tooth	3556	-16.6	cal BCE 1941-1883	cal BCE 2006-1777	3.2	33.3	2.2	tooth	MAWS-41108	Alalakh
45-72L, Locus 03-3013, Locus 03-3016, Pall 54, Skeleton SQ4-6	ALA095.A	ALA095.A	tooth	3516	-22.8	cal BCE 1889-1776	cal BCE 1913-1756	3.2	36.3	7.2	tooth	MAWS-41109	Alalakh
H156 S138	ART001	ART001.A	petrous bone	3908	-23.6	cal BCE 2465-2348	cal BCE 2470-2301	34.7	2.9	1.7	petrous bone	MAWS-33533	Arslantepe
H238 S156	ART004	ART004.A	petrous bone	4906	-19.9	cal BCE 3696-3656	cal BCE 3758-3642	25.7	2.8	1.3	petrous bone	MAWS-33534	Arslantepe
H250 S169	ART005	ART005.A	petrous bone	4934	-21.2	cal BCE 3757-3659	cal BCE 3770-3654	38.1	2.9	7.0	petrous bone	MAWS-33535	Arslantepe
H326	ART009	ART009.A	petrous bone	4069	-16.6	cal BCE 2826-2505	cal BCE 2834-2497	42.6	3.2	1.1	petrous bone	MAWS-37487	Arslantepe
H327 S220-2	ART010	ART010.A	petrous bone	4095	-20.9	cal BCE 2835-2580	cal BCE 2857-2505	37.4	2.9	7.9	petrous bone	MAWS-33537	Arslantepe
S220-1	ART011	ART011.A	petrous bone	4103	-21.6	cal BCE 2839-2581	cal BCE 2859-2575	33.7	2.9	4.6	petrous bone	MAWS-33538	Arslantepe
H331	ART012	ART012.A	petrous bone	4479	-19.0	cal BCE 3327-3098	cal BCE 3338-3031	31.5	2.9	2.6	petrous bone	MAWS-33539	Arslantepe
S216 C-2	ART014	ART014.A	petrous bone	4573	-16.8	cal BCE 3369-3140	cal BCE 3492-3119	-	3.3		petrous bone	MAWS-33540	Arslantepe
S216 C-3	ART015	ART015.A	petrous bone	4557	-19.9	cal BCE 3363-3137	cal BCE 3369-3110	31.3	2.9	2.6	petrous bone	MAWS-33541	Arslantepe
S216 C-8	ART017	ART017.A	petrous bone	4516	-18.9	cal BCE 3346-3116	cal BCE 3351-3103	35.8	2.9	2.6	petrous bone	MAWS-33542	Arslantepe
S216 C-9	ART018	ART018.A	petrous bone	4573	-13.0	cal BCE 3368-3142	cal BCE 3491-3122	28.4	3.2	0.5	petrous bone	MAWS-33543	Arslantepe
S216 C-10	ART019	ART019.A	petrous bone	4623	-1.7	cal BCE 3494-3363	cal BCE 3499-3355	33.6	3.2	0.6	petrous bone	MAWS-33544	Arslantepe
S216 C-11	ART020	ART020.A	petrous bone	4536	-18.8	cal BCE 3336-3124	cal BCE 3362-3105	34.8	2.9	6.1	petrous bone	MAWS-33545	Arslantepe
S216 C-13	ART022	ART022.A	petrous bone	4681	-10.6	cal BCE 3623-3370	cal BCE 3642-3117	38.8	2.9	3.2	petrous bone	MAWS-33546	Arslantepe
S216 C-14	ART023	ART023.A	petrous bone	4563	-15.2	cal BCE 3365-3139	cal BCE 3486-3117	35.6	2.9	3.2	petrous bone	MAWS-33547	Arslantepe
S216 Temp1	ART024	ART024.A	petrous bone	4614	-24	cal BCE 3491-3361	cal BCE 3497-3352	31.5	2.9	4.5	petrous bone	MAWS-33548	Arslantepe
S216 Temp3	ART026	ART026.A	petrous bone	4491	-28.1	cal BCE 3331-3103	cal BCE 3340-3096	38.9	3.0	3.0	petrous bone	MAWS-33549	Arslantepe
S216 Temp4	ART027	ART027.A	petrous bone	4564	-18.0	cal BCE 3360-3130	cal BCE 3365-3108	38.6	2.9	7.3	petrous bone	MAWS-33550	Arslantepe
A1335 P4 B	ART032	ART032.A	petrous bone	4588	-19.9	cal BCE 3484-3124	cal BCE 3484-3124	31.4	2.9	8.1	petrous bone	MAWS-34110	Arslantepe
S150 (H21)	ART038	ART038.B	femur bone	4534	-25.8	cal BCE 3336-3121	cal BCE 3361-3105	34.6	2.9	6.9	femur bone	MAWS-34112	Arslantepe
C7-D7 (H978)	ART039	ART039.A	tooth	4916	-17.3	cal BCE 3702-3658	cal BCE 3762-3646	29.0	2.8	5.9	tooth	MAWS-34116	Arslantepe
S254 (H882)	ART042	ART042.A	petrous bone	5014	-28.4	cal BCE 3925-3715	cal BCE 3941-3708	36.7	2.9	8.6	petrous bone	MAWS-34119	Arslantepe
Grave 1, 204-1103	CBT001	CBT001.A	petrous bone	4725	-18.4	cal BCE 3626-3384	cal BCE 3631-3379	47.1	3.2	8.0	humerus	MAWS-41627	Ganlibel Tarlasi
Grave 2, 327-921	CBT002	CBT002.A	petrous bone	4809	-22.2	cal BCE 3642-3536	cal BCE 3651-3525	3.2	37.1	14.8	tibia	MAWS-41630	Ganlibel Tarlasi
Grave 3, 80-1086	CBT003	CBT003.A	petrous bone										Ganlibel Tarlasi
Grave 4, 406-3224	CBT004	CBT004.A	petrous bone	4765	-18.8	cal BCE 3632-3526	cal BCE 3635-3521	40.1	3.2	5.8	tibia	MAWS-41628	Ganlibel Tarlasi
Grave 5, 464-4072	CBT005	CBT005.A	petrous bone	4713	-18.9	cal BCE 3622-3382	cal BCE 3628-3377	35.5	3.1	3.8	tibia	MAWS-41629	Ganlibel Tarlasi
Grave 10, 923-5423	CBT010	CBT010.A	petrous bone										Ganlibel Tarlasi
Grave 11, 970-6074	CBT011	CBT010.A	petrous bone										Ganlibel Tarlasi

Grave 13, 950-6118	CBT013 A	CBT013 A	petrous bone	4796	23	-12.2	cal BCE 3638-3536	cal BCE 3642-3526	3.3	36.0	9.2	femur bone	MAWS-41631	Garnibel Tarasi
Grave 14, 971-6144	CBT014	CBT014 A	petrous bone	4767	28	-21.7	cal BCE 3633-3525	cal BCE 3639-3385	3.2	36.7	14.9	femur bone	MAWS-41632	Garnibel Tarasi
Grave 15, 978-6140	CBT015 A	CBT015 A	petrous bone	4787	28	-17.6	cal BCE 3637-3533	cal BCE 3642-3522	3.2	33.3	2.5	femur bone	MAWS-41633	Garnibel Tarasi
Grave 16, 894-5819	CBT016	CBT016 A	petrous bone	4828	29	-21.7	cal BCE 3651-3539	cal BCE 3691-3528	3.2	38.1	14.2	femur bone	MAWS-41634	Garnibel Tarasi
Grave 17, 1010-5876	CBT017	CBT017 A	petrous bone				not dated due to sample preservation restrictions							
347/410-315	CBT018	CBT018 A	petrous bone	6635	30	-18.3	cal BCE 5617-5546	cal BCE 5626-5515	-	-	-	clay/cle bone (not dated by WPI-SHH)	SUFER C. East Kilbride, UK	Blyukakaya
TM.82/79-G.400	ETM001	ETM001 A	petrous bone				No collagen preservation							
TM.98.V.538 (Cranio A)	ETM004	ETM004 A	petrous bone				No collagen preservation							
TM.98.V.538 (Cranio C)	ETM005	ETM005 A	petrous bone				No collagen preservation							
TM.98.V.538 (Cranio B)	ETM006	ETM006 A	petrous bone				No collagen preservation							
TM.98.CC.113	ETM010	ETM010 A	petrous bone				No collagen preservation							
TM.91.P.653/2 (P4)	ETM012	ETM012 A	petrous bone	3997	25	-21.2	cal BCE 2565-2476	cal BCE 2572-2470	3.2	31.6	2.0	bone	MAWS-41114	
TM.95.V.491	ETM014	ETM014 A	petrous bone				No collagen preservation							
TM.95.V.497	ETM016	ETM016 A	petrous bone	3605	25	-18.0	cal BCE 2015-1925	cal BCE 2026-1896	3.2	39.7	0.5	bone	MAWS-41116	
TM.98.AA.310	ETM018	ETM018 A	tooth	3667	26	-26.0	cal BCE 2129-1981	cal BCE 2135-1964	3.2	27.8	3.1	tooth	MAWS-41635	
TM.82.G.438	ETM023	ETM023 A	petrous bone				No collagen preservation							
TM.83.G	ETM026	ETM026 A	petrous bone				No collagen preservation							
SK 528	IK002	IK002 A	tooth	4488	22	-22.2	cal BCE 3329-3102	cal BCE 3338-3095	3.2	37.5	4.7	tooth	MAWS-40673	
SK 552	IK009	IK009 A	tooth	4552	22	-18.9	cal BCE 3361-3137	cal BCE 3366-3115	3.2	40.8	3.9	tooth	MAWS-40674	
SK 567	IK012	IK012 A	tooth	4557	22	-22.5	cal BCE 3362-3139	cal BCE 3368-3118	3.2	43.5	6.1	tooth	MAWS-40675	
SK 581	IK016	IK016 A	tooth	4671	22	-21.2	cal BCE 3512-3374	cal BCE 3518-3371	3.2	42.2	6.3	tooth	MAWS-40676	
SK 593	IK017	IK017 A	tooth	4580	26	-20.2	cal BCE 3484-3198	cal BCE 3494-3124	2.9	37.2	4.0	tooth	MAWS-40677	
SK 635	IK024	IK024 A	tooth	5080	27	-20.0	cal BCE 3950-3806	cal BCE 3958-3799	2.9	33.2	4.2	tooth	MAWS-40678	
SK 652	IK030	IK030 A	tooth	4635	26	-21.9	cal BCE 3497-3365	cal BCE 3512-3357	3.0	41.5	2.5	tooth	MAWS-40679	
SK 665	IK034	IK034 A	tooth	4623	26	-21.2	cal BCE 3494-3362	cal BCE 3500-3352	2.9	45.2	8.2	tooth	MAWS-40680	
SK 668	IK036	IK036 A	tooth	4700	26	-22.6	cal BCE 3619-3378	cal BCE 3627-3374	2.9	37.8	4.7	tooth	MAWS-40681	
SK 675	IK037	IK037 A	tooth	4748	29	-30.7	cal BCE 3631-3520	cal BCE 3635-3382	2.9	35.8	5.5	tooth	MAWS-40682	
SK 677	IK038	IK038 A	tooth	4738	26	-21.9	cal BCE 3631-3386	cal BCE 3633-3381	2.9	39.3	5.7	tooth	MAWS-40683	
TK_12_81	KRD001	KRD001 A	petrous bone	6783	23	-18.8	cal BCE 5710-5662	cal BCE 5720-5640	2.9	33.2	3.1	petrous bone	MAWS-40663	Tell Kurdu
TK_24_3	KRD002	KRD002 A	petrous bone	6044	22	-20.8	cal BCE 4991-4911	cal BCE 5005-4849	2.7	28.6	3.9	petrous bone	MAWS-40664	Tell Kurdu
TK_22_2	KRD003	KRD003 A	petrous bone	6739	23	-15.6	cal BCE 5661-5630	cal BCE 5706-5622	2.9	33.5	1.4	petrous bone	MAWS-40665	Tell Kurdu
TK_25_80	KRD004	KRD004 A	petrous bone	6766	25	-22.1	cal BCE 5703-5639	cal BCE 5714-5632	3.2	35.6	0.5	petrous bone	MAWS-40666	Tell Kurdu
TK_25_89	KRD005	KRD005 A	petrous bone	6838	24	-14.1	cal BCE 5739-5676	cal BCE 5756-5664	3.2	37.7	0.8	petrous bone	MAWS-40667	Tell Kurdu
TK_26_12	KRD006	KRD006 A	petrous bone				No collagen preservation							
987H.80084	TTT021	TTT021 A	tooth	3799	25	-19.6	cal BCE 2285-2156	cal BCE 2331-2141	3.3	41.0	0.7	tooth	MAWS-40684	Ttrig-Heyuk
Polutepe Burial 2	POT002	POT002 A	tooth	6491	26	-19.0	cal BCE 5486-5386	cal BCE 5508-5376	38.9	2.9	6.6	tooth	MAWS-40331	Polutepe
Grave 342.20.7.12: individual 1	MTT001	MTT001 A	tooth	6802	27	-25.9	cal BCE 5717-5670	cal BCE 5729-5644	32.1	3.2	0.4	tooth	MAWS-40333	Mentesh Tepe
Alkantepe Burial 2	ALX002	ALX002 A	tooth	4950	23	-16.9	cal BCE 3785-3696	cal BCE 3776-3661	24.0	2.4	1.1	tooth	MAWS-40330	Alkantepe

**Table S2. Coverage on 1240K SNPs, genetic sex, terminal C-T damage, nuclear and mitochondrial contamination estimates, Related to Figure 2.** For newly reported individuals, mitochondrial contamination estimates calculated with Schmutzi (STAR Methods) are given. For genetic males the nuclear contamination estimate (STAR Methods) is provided. The levels of DNA damage for every halfUDG-treated library are given as the deamination level at the 1<sup>st</sup> and 2<sup>nd</sup> 5' terminal position of the mapped reads. Annotated in bold letters are samples for which quality requirements were not fulfilled (e.g., SNP coverage, sex determination, damage patterns, contamination; in bold *Italics*), and therefore were excluded from downstream genetic analyses.

Genomic Library ID	Nº SNPs covered	sex	group label in genetic study	dmg 1st 5'	dmg 2nd 5'	mito contam.	Xchr contam.
ALA001.A0101.TF1	752723	M	Alalakh_MLBA	0.16	0.02	0.02	0.018
ALA002.A0101.TF1	787174	M	Alalakh_MLBA	0.14	0.02	0.02	0.010
ALA004.A0101.TF1	751616	M	Alalakh_MLBA	0.16	0.02	0.02	0.009
ALA008.A0101.TF1	777877	M	Alalakh_MLBA	0.15	0.02	0.02	0.013
<b>ALA009.A0101.TF2.1</b>	108037	F	<i>not included (genetic outlier-contam.)</i>	<b>0.01</b>	0.00	0.03	
ALA011.A0101.TF1.1	715222	M	Alalakh_MLBA	0.13	0.02	0.04	0.009
ALA013.A0101.TF1	1020648	F	Alalakh_MLBA	0.12	0.02	0.02	
ALA014.A0101.TF2	662161	M	Alalakh_MLBA	0.14	0.02	0.02	0.026
ALA015.A0102.TF2	436587	M	Alalakh_MLBA	0.15	0.02	0.02	0.010
ALA016.A0101-2.TF1.1	381000	F	Alalakh_MLBA	0.16	0.02	0.05	
ALA017.A0101.TF1	546325	F	Alalakh_MLBA	0.14	0.02	0.02	
ALA018.A0102.TF2	702586	M	Alalakh_MLBA	0.13	0.02	0.02	0.015
ALA019.A0101.TF1	759728	F	Alalakh_MLBA_outlier	0.12	0.02	0.02	
ALA020.A0101.TF1	697240	F	Alalakh_MLBA	0.17	0.02	0.02	
ALA023.A0101.TF2.1	141680	F	Alalakh_MLBA	0.14	0.02	0.02	
ALA024.A0101.TF2.1	68573	F	Alalakh_MLBA	0.12	0.01	0.02	
ALA025.A0101.TF1	726597	F	Alalakh_MLBA	0.14	0.02	0.02	
ALA026.A0101.TF1	1010397	M	Alalakh_MLBA	0.12	0.02	0.02	0.010
ALA028.A0101.TF1	894015	F	Alalakh_MLBA	0.15	0.02	0.02	
ALA029.A0102.TF1	717237	F	Alalakh_MLBA	0.17	0.02	0.02	
ALA030.A0102.TF1	818001	F	Alalakh_MLBA	0.14	0.02	0.02	
ALA034.A0102.TF1	856852	F	Alalakh_MLBA	0.17	0.02	0.02	
ALA035.A0101.TF2.1	230762	M	Alalakh_MLBA	0.16	0.02	0.02	0.008
ALA037.A0101.TF2.1	231078	F	Alalakh_MLBA	0.17	0.02	0.02	
ALA038.A0101.TF2.1	60744	F	Alalakh_MLBA_rel.of.ALA001-002	0.16	0.02	0.03	
ALA039-040.A0101.TF1	774537	F	Alalakh_MLBA	0.14	0.02	0.02	
ALA084.B0102.TF1	120240	M	Alalakh_MLBA	0.21	0.03	0.02	0.094*
ALA095.A0102.TF1	592843	M	Alalakh_MLBA	0.27	0.04	0.01	0.016
ALX002.A0101.TF1	226260	M	Caucasus_lowlands_LC	0.24	0.02	0.01	0.007
ART001.A0101.TF1	815007	M	Arslantepe_EBA	0.02	0.15	0.02	0.008
ART004.A0101.TF1	79693	M	Arslantepe_LC	0.01	0.12	NA	-0.002*
ART005.A0101.TF1	485318	F	Arslantepe_LC	0.02	0.14	0.02	
ART009.A0201.TF1	1037836	F	Arslantepe_EBA	0.09	0.01	0.01	
ART010.A0101.TF1	805342	F	Arslantepe_EBA	0.02	0.10	0.02	
ART011.A0101.TF1	661840	M	Arslantepe_EBA	0.02	0.12	0.02	0.011
ART012.A0101.TF1	911305	F	Arslantepe_LC	0.02	0.12	0.02	
ART014.A0101.TF1	789681	M	Arslantepe_LC	0.02	0.13	0.02	0.012
ART015-028.A0101.TF1	1061958	M	Arslantepe_LC	0.02	0.12	0.02	0.010



Genomic Library ID	No SNPs covered	sex	group label in genetic study	dmg 1st 5'	dmg 2nd 5'	mito contam.	Xchr contam.
ART017.A0101.TF1	758458	M	Arslantepe_LC	0.02	0.13	0.02	0.009
ART018.A0101.TF1	881362	M	Arslantepe_LC	0.02	0.13	0.02	0.007
ART019.A0101.TF1	463307	M	Arslantepe_LC	0.02	0.13	0.02	0.015
ART020-025.A0101.TF1	941359	M	Arslantepe_LC	0.02	0.13	0.02	0.016
ART021-027.A0101.TF1	857755	M	Arslantepe_LC	0.02	0.10	0.02	0.015
ART022.A0101.TF1	840434	M	Arslantepe_LC	0.02	0.11	0.02	0.009
ART023.A0101.TF1	315329	M	Arslantepe_LC	0.01	0.11	0.02	0.004
ART024.A0101.TF1	741741	M	Arslantepe_LC_rel.of.ART014	0.02	0.14	0.02	0.014
ART026.A0101.TF1	818210	F	Arslantepe_LC	0.01	0.10	0.02	
ART032.A0101.TF1	921538	M	Arslantepe_LC	0.11	0.02	0.01	0.007
ART038.B0101.TF1.1	327016	M	Arslantepe_LC	0.13	0.01	0.02	0.005
ART039.A0101.TF1.1	96306	F	Arslantepe_LC	0.08	0.01	0.01	
ART042.A0101.TF1	990692	M	Arslantepe_LC	0.14	0.02	0.01	0.009
CBT001.A0101.TF1.1	634502	F	ÇamlıbelTarlasi_LC	0.09	0.01	0.01	
CBT002.A0101.TF2.1	308452	F	ÇamlıbelTarlasi_LC_rel.of.CBT016	0.16	0.02	0.01	
CBT003.A0101.TF2.1	66204	F	ÇamlıbelTarlasi_LC	0.21	0.02	0.01	
CBT004.A0101.TF1.1	641838	F	ÇamlıbelTarlasi_LC	0.09	0.01	0.01	
CBT005.A0101.TF1.1	533913	M	ÇamlıbelTarlasi_LC	0.09	0.01	0.01	0.001
CBT010.A0101.TF1.1	552349	F	ÇamlıbelTarlasi_LC	0.14	0.02	0.01	
CBT011.A0101.TF1.1	698605	F	ÇamlıbelTarlasi_LC	0.09	0.01	0.01	
CBT013.A0101.TF1.1	552046	M	ÇamlıbelTarlasi_LC_rel.of.CBT004	0.10	0.01	0.01	0.004
CBT014.A0101.TF1.1	740725	M	ÇamlıbelTarlasi_LC	0.08	0.01	0.01	0.006
CBT015.A0101.TF1.1	662844	M	ÇamlıbelTarlasi_LC	0.12	0.02	0.01	0.010
CBT016.A0101.TF1.1	745307	F	ÇamlıbelTarlasi_LC	0.10	0.01	0.01	
CBT017.A0101.TF1.1	715320	F	ÇamlıbelTarlasi_LC_rel.of.CBT016	0.07	0.01	0.01	
CBT018.A0101.TF1.1	629214	F	Büyükkaya_EC	0.14	0.02	0.01	
ETM001.A0101.TF1.1	114546	M	Ebla_EMBA	0.07	0.01	0.1	NA
<b>ETM003.B0101.TF1.1</b>	<b>654</b>	<b>U</b>	<i>not included</i>	<b>0.01</b>	0.01	<i>NA</i>	
ETM004.A0101.TF1.1	70124	F	Ebla_EMBA	0.10	0.02	0.01	
ETM005.A0101.TF1	167423	M	Ebla_EMBA	0.13	0.02	0.04	0.012*
ETM006.A0101.TF1	280452	F	Ebla_EMBA	0.14	0.02	0.02	
ETM010.B0101.TF1	607763	M	Ebla_EMBA	0.43	0.24	0.02	0.016
ETM012.A0101.TF1	736311	M	Ebla_EMBA	0.14	0.02	0.01	0.007
ETM014.A0101.TF1	628579	F	Ebla_EMBA	0.15	0.02	0.01	
<b>ETM015.A0101.TF1.1</b>	<b>9592</b>	<b>U</b>	<i>not included</i>	0.09	0.02	<i>NA</i>	
ETM016.A0101.TF1.1	425797	F	Ebla_EMBA	0.13	0.02	0.01	
<b>ETM017.A0101.TF1.1</b>	<b>893</b>	<b>U</b>	<i>not included</i>	<b>0.03</b>	0.01	<i>NA</i>	
ETM018.A0101.TF1.1	66794	M	Ebla_EMBA	0.30	0.16	0.03	NA
<b>ETM021.A0101.TF1.1</b>	<b>3028</b>	<b>U</b>	<i>not included</i>	<b>0.04</b>	0.01	<i>NA</i>	
ETM023.A0101.TF1	709632	F	Ebla_EMBA	0.16	0.02	0.02	
<b>ETM025.B0101.TF1.1</b>	<b>862</b>	<b>U</b>	<i>not included</i>	<b>0.01</b>	0.01	<i>NA</i>	
ETM026.A0101.TF1.1	329463	M	Ebla_EMBA	0.13	0.02	0.01	0.008
IKI002.A0102.TF1.1	75526	F	İkiztepe_LC	0.12	0.02	0.01	
<b>IKI006.A0102.TF1.1</b>	<b>24959</b>	<b>M</b>	<i>not included</i>	0.11	0.02	<i>NA</i>	<i>NA</i>
IKI009.A0102.TF1.1	83716	F	İkiztepe_LC	0.10	0.01	0.01	
IKI012.A0102.TF1.1	122036	F	İkiztepe_LC	0.11	0.02	0.01	
IKI016.A0102.TF1.1	196479	F	İkiztepe_LC	0.08	0.01	0.03	
IKI017.A0102.TF1.1	60871	F	İkiztepe_LC	0.11	0.02	0.01	

Genomic Library ID	№ SNPs covered	sex	group label in genetic study	dmg 1st 5'	dmg 2nd 5'	mito contam.	Xchr contam.
<b>IKI019.A0102.TF1.1</b>	<b>28387</b>	M	<i>not included</i>	0.11	0.02	0.01	NA
<b>IKI020.A0102.TF1.1</b>	<b>31159</b>	F	<i>not included</i>	0.14	0.03	0.01	
IKI024.A0102.TF1.1	110561	M	İkiztepe_LC	0.17	0.02	0.01	NA
IKI030.A0102.TF1.1	43569	F	İkiztepe_LC	0.10	0.02	0.01	
<b>IKI032.A0102.TF1.1</b>	<b>2055</b>	<i>U</i>	<i>not included</i>	0.06	0.00	0	NA
IKI034.A0102.TF1.1	144778	F	İkiztepe_LC	0.08	0.01	0.01	
IKI036.A0102.TF1.1	69048	F	İkiztepe_LC	0.09	0.01	0.01	
IKI037.A0102.TF1.1	104170	M	İkiztepe_LC	0.11	0.02	0.02	-0.002*
IKI038.A0102.TF1.1	44399	F	İkiztepe_LC	0.12	0.02	0.01	
KRD001.A0101.TF	248595	M	TellKurdu_EC	0.22	0.02	0.01	-0.002*
KRD002.A0101.TF	181778	M	TellKurdu_MC	0.27	0.03	0.01	-0.004*
KRD003.A0101.TF	432714	M	TellKurdu_EC	0.26	0.03	0.03	0.010
KRD004.A0101.TF	72302	F	TellKurdu_EC	0.21	0.02	0.02	
KRD005.A0101.TF	42470	M	TellKurdu_EC	0.18	0.02	0.01	NA
KRD006.B0101.TF	264754	F	TellKurdu_EC	0.19	0.02	0.01	
MTT001.A0101.TF1	683441	F	Caucasus_lowlands_LN	0.21	0.02	0.03	
POT002.A0101.TF1	503982	F	Caucasus_lowlands_LN	0.31	0.03	0.02	
<b>TIT003.A0102.TF1.1</b>	<b>3496</b>	M	<i>not included</i>	0.11	0.02	<i>NA</i>	<i>NA</i>
<b>TIT012.A0102.TF1.1</b>	<b>30190</b>	<i>U</i>	<i>not included</i>	0.11	0.02	<i>NA</i>	<i>NA</i>
<b>TIT014.A0102.TF1.1</b>	<b>8534</b>	<i>U</i>	<i>not included</i>	0.11	0.02	<i>NA</i>	<i>NA</i>
<b>TIT015.A0102.TF1.1</b>	<b>3250</b>	<i>U</i>	<i>not included</i>	0.05	0.02	<i>NA</i>	<i>NA</i>
<b>TIT019.A0102.TF1.1</b>	<b>1958</b>	<i>U</i>	<i>not included</i>	0.09	0.03	<i>NA</i>	<i>NA</i>
TIT021.A0102.TF1	104493	M	TitrişHöyük_EBA	0.22	0.03	0.01	-0.010*
<b>TIT025.A0102.TF1.1</b>	<b>20129</b>	<i>U</i>	<i>not included</i>	0.14	0.05	<i>NA</i>	<i>NA</i>

\* Contamination estimates on less than 200 polymorphic sites on X chromosome

**Table S3.** List of ancient populations published by previous studies which are used in our analyses, Related to STAR Methods (Grouping of individuals and nomenclature; Dataset). (*published as excel table*)

Groups/populations and labels used in present study	previous grouping/label (only if different)	Date	Publication
G.Caucasus_b_EMBA	Catacomb	ancient	C. C. Wang et al., Ancient human genome-wide data from a 3000-year interval in the Caucasus corresponds with eco-geographic regions. <i>Nat Commun</i> 10, 590 (2019)
G.Caucasus_a_EBA	Dolmen LBA	ancient	C. C. Wang et al., Ancient human genome-wide data from a 3000-year interval in the Caucasus corresponds with eco-geographic regions. <i>Nat Commun</i> 10, 590 (2019)
G.Caucasus_a_MLBA	MBA_North_Caucas	ancient	C. C. Wang et al., Ancient human genome-wide data from a 3000-year interval in the Caucasus corresponds with eco-geographic regions. <i>Nat Commun</i> 10, 590 (2019)
G.Caucasus_a_En	Neolithic Caucasus	ancient	C. C. Wang et al., Ancient human genome-wide data from a 3000-year interval in the Caucasus corresponds with eco-geographic regions. <i>Nat Commun</i> 10, 590 (2019)
G.Caucasus_b_En	Neolithic steppe	ancient	C. C. Wang et al., Ancient human genome-wide data from a 3000-year interval in the Caucasus corresponds with eco-geographic regions. <i>Nat Commun</i> 10, 590 (2019)
L.Caucasus_EBA	Kura-Araxes	ancient	C. C. Wang et al., Ancient human genome-wide data from a 3000-year interval in the Caucasus corresponds with eco-geographic regions. <i>Nat Commun</i> 10, 590 (2019)
G.Caucasus_a_EBA	Kura-Araxes	ancient	C. C. Wang et al., Ancient human genome-wide data from a 3000-year interval in the Caucasus corresponds with eco-geographic regions. <i>Nat Commun</i> 10, 590 (2019)
G.Caucasus_a_EBA	Late Maykop	ancient	C. C. Wang et al., Ancient human genome-wide data from a 3000-year interval in the Caucasus corresponds with eco-geographic regions. <i>Nat Commun</i> 10, 590 (2019)
G.Caucasus_c_EMBA	Lola	ancient	C. C. Wang et al., Ancient human genome-wide data from a 3000-year interval in the Caucasus corresponds with eco-geographic regions. <i>Nat Commun</i> 10, 590 (2019)
G.Caucasus_a_EBA	Maykop	ancient	C. C. Wang et al., Ancient human genome-wide data from a 3000-year interval in the Caucasus corresponds with eco-geographic regions. <i>Nat Commun</i> 10, 590 (2019)
G.Caucasus_a_EBA	Maykop Novosvobk	ancient	C. C. Wang et al., Ancient human genome-wide data from a 3000-year interval in the Caucasus corresponds with eco-geographic regions. <i>Nat Commun</i> 10, 590 (2019)
G.Caucasus_b_EMBA	North Caucasus	ancient	C. C. Wang et al., Ancient human genome-wide data from a 3000-year interval in the Caucasus corresponds with eco-geographic regions. <i>Nat Commun</i> 10, 590 (2019)
G.Caucasus_c_EMBA	Steppe Maykop	ancient	C. C. Wang et al., Ancient human genome-wide data from a 3000-year interval in the Caucasus corresponds with eco-geographic regions. <i>Nat Commun</i> 10, 590 (2019)
G.Caucasus_b_EMBA	Yamaya Caucasus	ancient	C. C. Wang et al., Ancient human genome-wide data from a 3000-year interval in the Caucasus corresponds with eco-geographic regions. <i>Nat Commun</i> 10, 590 (2019)
L.Caucasus_EBA	Armenia_EBA	ancient	I. Lazaridis et al., Genomic insights into the origin of farming in the ancient Near East. <i>Nature</i> 536, 419-424 (2016)
L.Caucasus_MBA	Armenia_MBA	ancient	I. Lazaridis et al., Genomic insights into the origin of farming in the ancient Near East. <i>Nature</i> 536, 419-424 (2016)
L.Caucasus_C	Armenia_Chalcolit	ancient	I. Lazaridis et al., Genomic insights into the origin of farming in the ancient Near East. <i>Nature</i> 536, 419-424 (2016)
L.Caucasus_LBA_SG	Armenia_LBA_SG	ancient	M. E. Allentoft et al., Population genomics of Bronze Age Eurasia. <i>Nature</i> 522, 167-172 (2015)
Barcin_N	Anatolia	ancient	I. Mathieson et al., Genome-wide patterns of selection in 230 ancient Eurasians. <i>Nature</i> 528, 499-503 (2015)
Barcin_C	Anatolia_Chalcolit	ancient	I. Lazaridis et al., Genomic insights into the origin of farming in the ancient Near East. <i>Nature</i> 536, 419-424 (2016)
Topakhöyük_EBA	Anatolia_EBA	ancient	P. de Barros Dangaard et al., The first horse herders and the impact of early Bronze Age steppe expansions into Asia. <i>Science</i> 360 (2018)
K.Kalehöyük_MLBA	Anatolia_MLBA	ancient	P. de Barros Dangaard et al., The first horse herders and the impact of early Bronze Age steppe expansions into Asia. <i>Science</i> 360 (2018)
Gondürle Höyük_EBA	Anatolia_BA	ancient	I. Lazaridis et al., Genetic origins of the Minoans and Mycenaeans. <i>Nature</i> 548, 214-218 (2017)
Levant_N	PPNB	ancient	I. Lazaridis et al., Genomic insights into the origin of farming in the ancient Near East. <i>Nature</i> 536, 419-424 (2016)
Levant_N	PPNC	ancient	I. Lazaridis et al., Genomic insights into the origin of farming in the ancient Near East. <i>Nature</i> 536, 419-424 (2016)
Minoan_Oidigitria / Aegean_MMinoan (PCA)	Minoan_Oidigitria	ancient	I. Lazaridis et al., Genetic origins of the Minoans and Mycenaeans. <i>Nature</i> 548, 214-218 (2017)
Minoan_Lasitthi / Aegean_MMinoan (PCA)	Minoan_Lasitthi	ancient	I. Lazaridis et al., Genetic origins of the Minoans and Mycenaeans. <i>Nature</i> 548, 214-218 (2017)
Late_Helladic	Mycenaean	ancient	I. Lazaridis et al., Genetic origins of the Minoans and Mycenaeans. <i>Nature</i> 548, 214-218 (2017)
Levant_MBA_SG	Sidon_BA	ancient	M. Haber et al., Continuity and Admixture in the Last Five Millennia of Levantine History from Ancient Canaanite and Present-Day Lebanese Genome Sequences. <i>Am J Hum Genet</i> 101, 274-282 (2017)
Levant_EP		ancient	I. Lazaridis et al., Genomic insights into the origin of farming in the ancient Near East. <i>Nature</i> 536, 419-424 (2016)
Levant_EBA		ancient	I. Lazaridis et al., Genomic insights into the origin of farming in the ancient Near East. <i>Nature</i> 536, 419-424 (2016)
Iran_N		ancient	I. Lazaridis et al., Genomic insights into the origin of farming in the ancient Near East. <i>Nature</i> 536, 419-424 (2016)
Iran_EP		ancient	I. Lazaridis et al., Genetic origins of the Minoans and Mycenaeans. <i>Nature</i> 548, 214-218 (2017)
Iran_N_SG		ancient	F. Broushaki et al., Early Neolithic genomes from the eastern Fertile Crescent. <i>Science</i> 353, 499-503 (2016)
Iran_LN		ancient	I. Lazaridis et al., Genomic insights into the origin of farming in the ancient Near East. <i>Nature</i> 536, 419-424 (2016)
Iran_C		ancient	I. Lazaridis et al., Genomic insights into the origin of farming in the ancient Near East. <i>Nature</i> 536, 419-424 (2016)
Levant_C		ancient	É. Harney et al., Ancient DNA from Chalcolithic Israel reveals the role of population mixture in cultural transformation. <i>Nature Communications</i> 9, 3336 (2018)
Balkans_N_SG		ancient	Z. Hofmanova et al., Early farmers from across Europe directly descended from Neolithic Aegeans. <i>Proc Natl Acad Sci U S A</i> 113, 6886-6891 (2016)
Barcin_N_SG		ancient	Z. Hofmanova et al., Early farmers from across Europe directly descended from Neolithic Aegeans. <i>Proc Natl Acad Sci U S A</i> 113, 6886-6891 (2016)
CHG (Caucasus hunter-gatherers)		ancient	E. R. Jones et al., Upper Palaeolithic genomes reveal deep roots of modern Eurasians. <i>Nat Commun</i> 6, 8912 (2015)
Boncuclu_N_SG		ancient	G. M. Kilinc et al., The Demographic Development of the First Farmers in Anatolia. <i>Curr Biol</i> 26, 2659-2666 (2016)
WHG (Western European hunter-gatherers)		ancient	I. Lazaridis et al., Ancient human genomes suggest three ancestral populations for present-day Europeans. <i>Nature</i> 513, 409-413 (2014); I. Mathieson et al., Genome-wide patterns of selection in 230 ancient Eurasians. <i>Nature</i> 528, 499-503 (2015)
Boncuclu_N		ancient	M. Feldman et al., Late Pleistocene human genome suggests a local origin for the first farmers of central Anatolia. <i>Nat Commun</i> 10, 1218 (2019)
Levant_N_KFH		ancient	M. Feldman et al., Late Pleistocene human genome suggests a local origin for the first farmers of central Anatolia. <i>Nat Commun</i> 10, 1218 (2019)
Pınarbaşı_EP		ancient	M. Feldman et al., Late Pleistocene human genome suggests a local origin for the first farmers of central Anatolia. <i>Nat Commun</i> 10, 1218 (2019)
ElMiron		ancient	Q. Fu et al., The genetic history of Ice Age Europe. <i>Nature</i> 534, 200-205 (2016)
Kostenki12		ancient	Q. Fu et al., The genetic history of Ice Age Europe. <i>Nature</i> 534, 200-205 (2016)
Kostenki14		ancient	Q. Fu et al., The genetic history of Ice Age Europe. <i>Nature</i> 534, 200-205 (2016)
Vestonice13		ancient	Q. Fu et al., The genetic history of Ice Age Europe. <i>Nature</i> 534, 200-205 (2016)
Fillifurca		ancient	Q. Fu et al., The genetic history of Ice Age Europe. <i>Nature</i> 534, 200-205 (2016)
Hungary_LBA_SG		ancient	C. Gamba et al., Genome flux and stasis in a five millennium transect of European prehistory. <i>Nature Communications</i> 5, 5257 (2014)
Iron_Gates_HG_SG		ancient	G. González-Forbes et al., Paleogenomic Evidence for Multi-generational Mixing between Neolithic Farmers and Mesolithic Hunter-Gatherers in the Lower Danube Basin. <i>Current Biology</i> 27, 1801-1810.e1810 (2017)
Romania_EN_SG		ancient	G. González-Forbes et al., Paleogenomic Evidence for Multi-generational Mixing between Neolithic Farmers and Mesolithic Hunter-Gatherers in the Lower Danube Basin. <i>Current Biology</i> 27, 1801-1810.e1810 (2017)
Iberia_CSG		ancient	T. Günther et al., Ancient genomes link early farmers from Atapuerca in Spain to modern-day Basques. <i>Proceedings of the National Academy of Sciences</i> 112, 11917 (2015)
Iberia_C		ancient	M. Lipson et al., Parallel palaeogenomic transects reveal complex genetic history of early European farmers. <i>Nature</i> 551, 368-372 (2017)
Iberia_EN		ancient	M. Lipson et al., Parallel palaeogenomic transects reveal complex genetic history of early European farmers. <i>Nature</i> 551, 368-372 (2017)
Koros_EN		ancient	M. Lipson et al., Parallel palaeogenomic transects reveal complex genetic history of early European farmers. <i>Nature</i> 551, 368-372 (2017)
Koros_EN_HG		ancient	M. Lipson et al., Parallel palaeogenomic transects reveal complex genetic history of early European farmers. <i>Nature</i> 551, 368-372 (2017)
LBK_EN		ancient	M. Lipson et al., Parallel palaeogenomic transects reveal complex genetic history of early European farmers. <i>Nature</i> 551, 368-372 (2017)
LBK_EN_outlier		ancient	M. Lipson et al., Parallel palaeogenomic transects reveal complex genetic history of early European farmers. <i>Nature</i> 551, 368-372 (2017)
Starcevo_EN		ancient	M. Lipson et al., Parallel palaeogenomic transects reveal complex genetic history of early European farmers. <i>Nature</i> 551, 368-372 (2017)
Portugal_MBA		ancient	R. Martiniano et al., The population genomics of archaeological transition in west Iberia: Investigation of ancient substructure using imputation and haplotype-based methods. <i>PLoS Genet</i> 13, e1006852 (2017)
Portugal_MN		ancient	R. Martiniano et al., The population genomics of archaeological transition in west Iberia: Investigation of ancient substructure using imputation and haplotype-based methods. <i>PLoS Genet</i> 13, e1006852 (2017)
Bell_Beaker_Germany		ancient	I. Mathieson et al., Genome-wide patterns of selection in 230 ancient Eurasians. <i>Nature</i> 528, 499-503 (2015)
Corded_Ware_Germany		ancient	I. Mathieson et al., Genome-wide patterns of selection in 230 ancient Eurasians. <i>Nature</i> 528, 499-503 (2015)
EHG (Easter European hunter-gatherers)		ancient	I. Mathieson et al., Genome-wide patterns of selection in 230 ancient Eurasians. <i>Nature</i> 528, 499-503 (2015)
Hungary_LBA		ancient	I. Mathieson et al., Genome-wide patterns of selection in 230 ancient Eurasians. <i>Nature</i> 528, 499-503 (2015)
Iberia_C		ancient	I. Mathieson et al., Genome-wide patterns of selection in 230 ancient Eurasians. <i>Nature</i> 528, 499-503 (2015)
Iberia_EN		ancient	I. Mathieson et al., Genome-wide patterns of selection in 230 ancient Eurasians. <i>Nature</i> 528, 499-503 (2015)
Koros_EN		ancient	I. Mathieson et al., Genome-wide patterns of selection in 230 ancient Eurasians. <i>Nature</i> 528, 499-503 (2015)
LBK_EN		ancient	I. Mathieson et al., Genome-wide patterns of selection in 230 ancient Eurasians. <i>Nature</i> 528, 499-503 (2015)
Potapovka		ancient	I. Mathieson et al., Genome-wide patterns of selection in 230 ancient Eurasians. <i>Nature</i> 528, 499-503 (2015)
Samara_EN		ancient	I. Mathieson et al., Genome-wide patterns of selection in 230 ancient Eurasians. <i>Nature</i> 528, 499-503 (2015)
Starcevo_EN		ancient	I. Mathieson et al., Genome-wide patterns of selection in 230 ancient Eurasians. <i>Nature</i> 528, 499-503 (2015)
Ureitic_EBA		ancient	I. Mathieson et al., Genome-wide patterns of selection in 230 ancient Eurasians. <i>Nature</i> 528, 499-503 (2015)
Yamaya_Samara		ancient	I. Mathieson et al., Genome-wide patterns of selection in 230 ancient Eurasians. <i>Nature</i> 528, 499-503 (2015)
Balkans_C		ancient	I. Mathieson et al., The genomic history of southeastern Europe. <i>Nature</i> 555, 197-203 (2018)
Balkans_N		ancient	I. Mathieson et al., The genomic history of southeastern Europe. <i>Nature</i> 555, 197-203 (2018)
Bulgaria_BA/Balkans_BA (PCA)		ancient	I. Mathieson et al., The genomic history of southeastern Europe. <i>Nature</i> 555, 197-203 (2018)
Bulgaria_C		ancient	I. Mathieson et al., The genomic history of southeastern Europe. <i>Nature</i> 555, 197-203 (2018)
Bulgaria_EBA/Balkans_BA (PCA)		ancient	I. Mathieson et al., The genomic history of southeastern Europe. <i>Nature</i> 555, 197-203 (2018)
Bulgaria_EN		ancient	I. Mathieson et al., The genomic history of southeastern Europe. <i>Nature</i> 555, 197-203 (2018)
Bulgaria_Ezero_EBA/Balkans_BA (PCA)		ancient	I. Mathieson et al., The genomic history of southeastern Europe. <i>Nature</i> 555, 197-203 (2018)
Bulgaria_IA		ancient	I. Mathieson et al., The genomic history of southeastern Europe. <i>Nature</i> 555, 197-203 (2018)
Bulgaria_Late_C/Balkans_C (PCA)		ancient	I. Mathieson et al., The genomic history of southeastern Europe. <i>Nature</i> 555, 197-203 (2018)
Bulgaria_Late_C1/Balkans_C (PCA)		ancient	I. Mathieson et al., The genomic history of southeastern Europe. <i>Nature</i> 555, 197-203 (2018)
Bulgaria_Late_C2/Balkans_C (PCA)		ancient	I. Mathieson et al., The genomic history of southeastern Europe. <i>Nature</i> 555, 197-203 (2018)
Bulgaria_MLBA/Balkans_BA (PCA)		ancient	I. Mathieson et al., The genomic history of southeastern Europe. <i>Nature</i> 555, 197-203 (2018)
Bulgaria_N/Balkans_N (PCA)		ancient	I. Mathieson et al., The genomic history of southeastern Europe. <i>Nature</i> 555, 197-203 (2018)
Balkans_MP_Neolithic/Balkans_N (PCA)		ancient	I. Mathieson et al., The genomic history of southeastern Europe. <i>Nature</i> 555, 197-203 (2018)
Croatia_Cardial_N		ancient	I. Mathieson et al., The genomic history of southeastern Europe. <i>Nature</i> 555, 197-203 (2018)
Croatia_EMBA		ancient	I. Mathieson et al., The genomic history of southeastern Europe. <i>Nature</i> 555, 197-203 (2018)
Croatia_impresna_EN		ancient	I. Mathieson et al., The genomic history of southeastern Europe. <i>Nature</i> 555, 197-203 (2018)
Croatia_EBA		ancient	I. Mathieson et al., The genomic history of southeastern Europe. <i>Nature</i> 555, 197-203 (2018)
Globular_Amphora		ancient	I. Mathieson et al., The genomic history of southeastern Europe. <i>Nature</i> 555, 197-203 (2018)
Globular_Amphora_Ukraine		ancient	I. Mathieson et al., The genomic history of southeastern Europe. <i>Nature</i> 555, 197-203 (2018)
Greece_N		ancient	I. Mathieson et al., The genomic history of southeastern Europe. <i>Nature</i> 555, 197-203 (2018)
Iberia_C		ancient	I. Mathieson et al., The genomic history of southeastern Europe. <i>Nature</i> 555, 197-203 (2018)
Iron_Gates_EN		ancient	I. Mathieson et al., The genomic history of southeastern Europe. <i>Nature</i> 555, 197-203 (2018)
Iron_Gates_HG		ancient	I. Mathieson et al., The genomic history of southeastern Europe. <i>Nature</i> 555, 197-203 (2018)
LBK_EN		ancient	I. Mathieson et al., The genomic history of southeastern Europe. <i>Nature</i> 555, 197-203 (2018)
Peloponnese_N		ancient	I. Mathieson et al., The genomic history of southeastern Europe. <i>Nature</i> 555, 197-203 (2018)
Romania_EN		ancient	I. Mathieson et al., The genomic history of southeastern Europe. <i>Nature</i> 555, 197-203 (2018)
Serbia_N/Balkans_N (PCA)		ancient	I. Mathieson et al., The genomic history of southeastern Europe. <i>Nature</i> 555, 197-203 (2018)
Starcevo_EN		ancient	I. Mathieson et al., The genomic history of southeastern Europe. <i>Nature</i> 555, 197-203 (2018)
Starcevo_EN_outlier		ancient	I. Mathieson et al., The genomic history of southeastern Europe. <i>Nature</i> 555, 197-203 (2018)
Ukraine_Mesolithic		ancient	I. Mathieson et al., The genomic history of southeastern Europe. <i>Nature</i> 555, 197-203 (2018)
Ukraine_N		ancient	I. Mathieson et al., The genomic history of southeastern Europe. <i>Nature</i> 555, 197-203 (2018)
Yamaya_Ukraine		ancient	I. Mathieson et al., The genomic history of southeastern Europe. <i>Nature</i> 555, 197-203 (2018)
Yamaya_Ukraine_Ozera		ancient	I. Mathieson et al., The genomic history of southeastern Europe. <i>Nature</i> 555, 197-203 (2018)
Karfišana.DG		ancient	M. Meyer et al., A high-coverage genome sequence from an archaic Denisovan individual. <i>Science</i> (New York, N.Y.) 338, 222-226 (2012)
Mbuti.DG		ancient	M. Meyer et al., A high-coverage genome sequence from an archaic Denisovan individual. <i>Science</i> (New York, N.Y.) 338, 222-226 (2012)
Russia_HG		ancient	A. Mittnik et al., The genetic prehistory of the Baltic Sea region. <i>Nature Communications</i> 9, 442 (2018)
Iberia_EN_SG		ancient	I. Olalde et al., A Common Genetic Origin for Early Farmers from Mediterranean Cardial and Central European LBK Cultures. <i>Molecular Biology and Evolution</i> 32, 3132-3142 (2015)









**Table S4.** Outgroup f3-statistics, Related to Figure 6. Shared genetic drift between each of the Late Chalcolithic/Bronze Age (LC-LBA) groups of the present study and a panel of Test populations compared to the distal population Mbuti. Test populations consist of 300 ancient and modern worldwide populations. f3-statistics were estimated on autosomal portion of the Human Origins (HO) SNPs with a minimum total Ne SNP per test of 50,000. The highest 40 f3-statistics are presented per LC-LBA group. (published as excel table)

Outgroup	LC-LBA group	Test	f3-statistic	SE	z-score	Ne SNPs
Mbuti	Alalakh_MLBA	Romania_EN	0.258139	0.002106	122.596	381056
Mbuti	Alalakh_MLBA	Croatia_Cardial_N	0.258134	0.002127	121.339	415956
Mbuti	Alalakh_MLBA	Bulgaria_Late_C	0.258133	0.002073	124.511	400382
Mbuti	Alalakh_MLBA	Greece_N	0.258088	0.002296	112.403	335431
Mbuti	Alalakh_MLBA	Czech_N	0.257748	0.002152	119.765	409900
Mbuti	Alalakh_MLBA	Bulgaria_EN	0.257734	0.002478	103.998	182304
Mbuti	Alalakh_MLBA	Peloponnese_N	0.257653	0.002009	128.23	462779
Mbuti	Alalakh_MLBA	Koros_EN	0.257407	0.002151	119.667	439820
Mbuti	Alalakh_MLBA	Balkans_N	0.257372	0.002014	127.803	468868
Mbuti	Alalakh_MLBA	Croatia_Impressa_EN	0.257318	0.002175	118.28	338907
Mbuti	Alalakh_MLBA	Barcin_N	0.257169	0.001968	130.666	487206
Mbuti	Alalakh_MLBA	Bulgaria_C	0.257064	0.002206	116.508	406723
Mbuti	Alalakh_MLBA	LBK_EN	0.256998	0.001989	129.218	488840
Mbuti	Alalakh_MLBA	Bulgaria_IA	0.256969	0.002348	109.463	314977
Mbuti	Alalakh_MLBA	Starcevo_EN	0.256926	0.002032	126.457	461204
Mbuti	Alalakh_MLBA	Bulgaria_N	0.256776	0.002101	122.227	366550
Mbuti	Alalakh_MLBA	TellKurdu_EC	0.25635	0.002201	116.466	294730
Mbuti	Alalakh_MLBA	Lasithi_MMinoan	0.256005	0.001992	128.527	456051
Mbuti	Alalakh_MLBA	Bulgaria_BA	0.255916	0.002087	122.648	398250
Mbuti	Alalakh_MLBA	GondürleHöyük_EBA	0.255504	0.002078	122.973	448974
Mbuti	Alalakh_MLBA	Balkans_C	0.25482	0.002278	111.862	232352
Mbuti	Alalakh_MLBA	Bell_Beaker_Italy	0.254728	0.002121	120.073	400296
Mbuti	Alalakh_MLBA	Arslantepe_LC	0.254563	0.001968	129.328	480042
Mbuti	Alalakh_MLBA	Globular_Amphora	0.254498	0.002101	121.153	339355
Mbuti	Alalakh_MLBA	İkiztepe_LC	0.254386	0.002152	118.194	266680
Mbuti	Alalakh_MLBA	Portugal_N_EBA	0.254314	0.00256	99.323	170657
Mbuti	Alalakh_MLBA	Iberia_EN	0.254258	0.002051	123.963	463062
Mbuti	Alalakh_MLBA	Iberia_C	0.254188	0.00199	127.701	480507
Mbuti	Alalakh_MLBA	Boncuklu_N	0.254147	0.002043	124.381	461450
Mbuti	Alalakh_MLBA	Croatia_EMBA	0.253993	0.002148	118.27	379148
Mbuti	Alalakh_MLBA	Barcin_C	0.253857	0.002208	114.951	420056
Mbuti	Alalakh_MLBA	Levant_C	0.253854	0.001985	127.859	463661
Mbuti	Alalakh_MLBA	Bell_Beaker_Hungary	0.2536	0.002026	125.151	432154
Mbuti	Alalakh_MLBA	Arslantepe_EBA	0.253519	0.002014	125.901	438433
Mbuti	Alalakh_MLBA	Iberia_EBA	0.253465	0.002461	102.982	211831
Mbuti	Alalakh_MLBA	Büyükkaya_EC	0.253408	0.002395	105.827	262912
Mbuti	Alalakh_MLBA	Tepecik_N	0.253402	0.002214	114.443	314930
Mbuti	Alalakh_MLBA	Bell_Beaker_Iberia	0.253354	0.002029	124.841	469288
Mbuti	Alalakh_MLBA	Pınarbaşı	0.253254	0.002333	108.564	380965
Mbuti	Alalakh_MLBA	Croatia_LBA	0.253044	0.002312	109.46	354752
Mbuti	Arslantepe_EBA	Bulgaria_Late_C	0.260163	0.002143	121.413	369096
Mbuti	Arslantepe_EBA	Croatia_Impressa_EN	0.260115	0.002322	112.029	307126
Mbuti	Arslantepe_EBA	Bulgaria_IA	0.260001	0.002595	100.191	290111
Mbuti	Arslantepe_EBA	Greece_N	0.259922	0.002454	105.936	304824
Mbuti	Arslantepe_EBA	Bulgaria_EN	0.259798	0.002658	97.745	169535
Mbuti	Arslantepe_EBA	Croatia_Cardial_N	0.259777	0.002258	115.047	380474
Mbuti	Arslantepe_EBA	Romania_EN	0.259152	0.00224	115.715	350863
Mbuti	Arslantepe_EBA	Starcevo_EN	0.259015	0.002161	119.844	413735
Mbuti	Arslantepe_EBA	Koros_EN	0.258781	0.002203	117.442	394785
Mbuti	Arslantepe_EBA	Peloponnese_N	0.258699	0.002114	122.365	414851
Mbuti	Arslantepe_EBA	Czech_N	0.258647	0.002266	114.163	373733
Mbuti	Arslantepe_EBA	Bulgaria_BA	0.258617	0.002159	119.799	365083
Mbuti	Arslantepe_EBA	Barcin_N	0.258491	0.002072	124.758	439812
Mbuti	Arslantepe_EBA	Balkans_N	0.258434	0.002079	124.33	418826
Mbuti	Arslantepe_EBA	LBK_EN	0.258123	0.002043	126.348	442214
Mbuti	Arslantepe_EBA	Bulgaria_C	0.257855	0.002338	110.311	372198
Mbuti	Arslantepe_EBA	Bulgaria_N	0.257589	0.002209	116.599	335855
Mbuti	Arslantepe_EBA	GondürleHöyük_EBA	0.257412	0.002167	118.79	403926
Mbuti	Arslantepe_EBA	İkiztepe_LC	0.257394	0.002353	109.405	245359
Mbuti	Arslantepe_EBA	Barcin_C	0.257129	0.002353	109.267	377013
Mbuti	Arslantepe_EBA	Lasithi_MMinoan	0.257107	0.002112	121.749	406333
Mbuti	Arslantepe_EBA	TellKurdu_EC	0.256722	0.002356	108.975	270883
Mbuti	Arslantepe_EBA	Balkans_C	0.256613	0.002527	101.533	209527
Mbuti	Arslantepe_EBA	Portugal_N_EBA	0.256567	0.002846	90.155	156350
Mbuti	Arslantepe_EBA	Bell_Beaker_Italy	0.25647	0.002243	114.361	365369
Mbuti	Arslantepe_EBA	Croatia_EMBA	0.256302	0.002339	109.573	347924
Mbuti	Arslantepe_EBA	Croatia_LBA	0.256115	0.00251	102.045	325048
Mbuti	Arslantepe_EBA	Arslantepe_LC	0.256037	0.002046	125.135	435061
Mbuti	Arslantepe_EBA	Bell_Beaker_Hungary	0.255839	0.002131	120.054	394665
Mbuti	Arslantepe_EBA	Globular_Amphora	0.255528	0.002246	113.786	315185
Mbuti	Arslantepe_EBA	Iberia_EN	0.255351	0.002156	118.424	413653
Mbuti	Arslantepe_EBA	Boncuklu_N	0.25534	0.002111	120.942	409764
Mbuti	Arslantepe_EBA	Tepecik_N	0.255261	0.002381	107.197	276191
Mbuti	Arslantepe_EBA	Hungary_EMBA	0.255251	0.002373	107.581	296083
Mbuti	Arslantepe_EBA	Levant_C	0.25512	0.002073	123.061	421711
Mbuti	Arslantepe_EBA	Iberia_C	0.255078	0.00204	125.063	432880
Mbuti	Arslantepe_EBA	Bulgaria_EBA	0.255007	0.002192	116.331	369432
Mbuti	Arslantepe_EBA	Bell_Beaker_Iberia	0.254341	0.002082	122.147	422227
Mbuti	Arslantepe_EBA	MBA_North_Caucasus	0.254177	0.002248	113.053	347607
Mbuti	Arslantepe_EBA	Pınarbaşı	0.254124	0.002553	99.557	340645
Mbuti	Arslantepe_EBA	ÇamlıbelTarlası_LC	0.254075	0.002068	122.887	417632
Mbuti	Arslantepe_LC	Bulgaria_EN	0.261499	0.002511	104.15	180514
Mbuti	Arslantepe_LC	Croatia_Cardial_N	0.26111	0.002151	121.404	412808
Mbuti	Arslantepe_LC	Greece_N	0.260764	0.002313	112.715	332073
Mbuti	Arslantepe_LC	Czech_N	0.26055	0.002184	119.307	406530



Mbuti	Arslantepe_LC	Romania_EN	0.26043	0.002088	124.727	377998
Mbuti	Arslantepe_LC	Croatia_Impressa_EN	0.260098	0.002216	117.368	335590
Mbuti	Arslantepe_LC	Bulgaria_Late_C	0.259964	0.002092	124.291	397367
Mbuti	Arslantepe_LC	Koros_EN	0.259964	0.002156	120.601	435998
Mbuti	Arslantepe_LC	Bulgaria_C	0.259742	0.002219	117.065	403506
Mbuti	Arslantepe_LC	Peloponnese_N	0.259713	0.002034	127.668	458718
Mbuti	Arslantepe_LC	Bulgaria_N	0.259703	0.002127	122.125	363479
Mbuti	Arslantepe_LC	LBK_EN	0.259687	0.002022	128.413	485479
Mbuti	Arslantepe_LC	Barcin_N	0.259548	0.002005	129.433	483697
Mbuti	Arslantepe_LC	Starcevo_EN	0.259453	0.002077	124.923	457157
Mbuti	Arslantepe_LC	Bulgaria_JA	0.259374	0.002405	107.846	312177
Mbuti	Arslantepe_LC	Balkans_N	0.259224	0.002023	128.123	464575
Mbuti	Arslantepe_LC	TellKurdu_EC	0.258967	0.00223	116.117	291924
Mbuti	Arslantepe_LC	Bulgaria_BA	0.258316	0.002097	123.159	395003
Mbuti	Arslantepe_LC	Lasithi_MMinoan	0.257887	0.002032	126.918	451891
Mbuti	Arslantepe_LC	GondürleHöyük_EBA	0.25783	0.002078	124.08	445247
Mbuti	Arslantepe_LC	Bell_Beaker_Italy	0.257388	0.002125	121.146	396979
Mbuti	Arslantepe_LC	Balkans_C	0.257338	0.002296	112.058	230035
Mbuti	Arslantepe_LC	İkitzepe_LC	0.257229	0.00219	117.439	264219
Mbuti	Arslantepe_LC	Globular_Amphora	0.256814	0.002121	121.09	336741
Mbuti	Arslantepe_LC	Büyükaya_EC	0.256733	0.002421	106.04	260477
Mbuti	Arslantepe_LC	Boncuklu_N	0.256706	0.002083	123.23	456757
Mbuti	Arslantepe_LC	Iberia_EN	0.256679	0.002094	122.584	459033
Mbuti	Arslantepe_LC	Croatia_EMBA	0.256547	0.002203	116.468	375985
Mbuti	Arslantepe_LC	Barcin_C	0.256529	0.002243	114.371	416019
Mbuti	Arslantepe_LC	Bell_Beaker_Hungary	0.256425	0.00205	125.059	428943
Mbuti	Arslantepe_LC	Iberia_EBA	0.256236	0.00253	101.275	210036
Mbuti	Arslantepe_LC	Arslantepe_EBA	0.256037	0.002046	125.135	435061
Mbuti	Arslantepe_LC	Iberia_C	0.256001	0.002005	127.711	476721
Mbuti	Arslantepe_LC	Pınarbaşı	0.255871	0.002384	107.333	377191
Mbuti	Arslantepe_LC	Levant_C	0.255702	0.002021	126.509	460729
Mbuti	Arslantepe_LC	Croatia_LBA	0.255608	0.002315	110.423	351553
Mbuti	Arslantepe_LC	Portugal_N_EBA	0.255496	0.002579	99.056	169109
Mbuti	Arslantepe_LC	Bulgaria_EBA	0.255432	0.002093	122.038	400420
Mbuti	Arslantepe_LC	ÇamlıbelTarlası_LC	0.255012	0.002026	125.899	461041
Mbuti	Arslantepe_LC	Tepecik_N	0.254992	0.002225	114.612	311318
Mbuti	Barcin_C	Bulgaria_EN	0.266483	0.003315	80.387	161266
Mbuti	Barcin_C	Balkans_N	0.263996	0.00238	110.943	396937
Mbuti	Barcin_C	Croatia_Impressa_EN	0.263854	0.002745	96.113	291817
Mbuti	Barcin_C	Romania_EN	0.263635	0.002636	100.031	332307
Mbuti	Barcin_C	Bulgaria_JA	0.263606	0.003101	85.009	273239
Mbuti	Barcin_C	Starcevo_EN	0.262915	0.002426	108.365	392545
Mbuti	Barcin_C	Peloponnese_N	0.262847	0.00242	108.623	393433
Mbuti	Barcin_C	Barcin_N	0.262726	0.002314	113.545	421266
Mbuti	Barcin_C	Bulgaria_Late_C	0.262698	0.002461	106.748	351417
Mbuti	Barcin_C	Bulgaria_BA	0.262588	0.00262	100.216	345294
Mbuti	Barcin_C	Iberia_EBA	0.262474	0.00325	80.763	184580
Mbuti	Barcin_C	Greece_N	0.262411	0.002973	88.275	288598
Mbuti	Barcin_C	LBK_EN	0.262291	0.00232	113.04	423896
Mbuti	Barcin_C	Bulgaria_N	0.262037	0.002598	100.867	318107
Mbuti	Barcin_C	Czech_N	0.261869	0.002644	99.049	353288
Mbuti	Barcin_C	Croatia_Cardial_N	0.261801	0.002546	102.847	360826
Mbuti	Barcin_C	Koros_EN	0.261784	0.00267	98.05	372202
Mbuti	Barcin_C	Portugal_N_EBA	0.261645	0.003373	77.573	147596
Mbuti	Barcin_C	Boncuklu_N	0.261536	0.002526	103.55	386882
Mbuti	Barcin_C	Globular_Amphora	0.261126	0.002622	99.606	300579
Mbuti	Barcin_C	Bell_Beaker_Italy	0.260793	0.002647	98.514	346113
Mbuti	Barcin_C	Büyükaya_EC	0.260734	0.00305	85.478	225990
Mbuti	Barcin_C	Bulgaria_C	0.260492	0.002728	95.5	351824
Mbuti	Barcin_C	Pınarbaşı	0.260463	0.003029	85.979	318963
Mbuti	Barcin_C	Iberia_EN	0.260249	0.002399	108.464	390822
Mbuti	Barcin_C	Bell_Beaker_Hungary	0.260155	0.002428	107.162	374382
Mbuti	Barcin_C	Boncuklu_N_SG	0.260062	0.002809	92.597	357203
Mbuti	Barcin_C	Lasithi_MMinoan	0.259906	0.002416	107.59	383949
Mbuti	Barcin_C	Iberia_C	0.259577	0.002332	111.288	413440
Mbuti	Barcin_C	TellKurdu_EC	0.259474	0.002757	94.121	256585
Mbuti	Barcin_C	İkitzepe_LC	0.259336	0.002773	93.517	232461
Mbuti	Barcin_C	GondürleHöyük_EBA	0.259139	0.002512	103.181	380666
Mbuti	Barcin_C	Bell_Beaker_Iberia	0.259103	0.00237	109.342	401876
Mbuti	Barcin_C	Yamnaya_LCA_EBA	0.258319	0.002463	104.893	373771
Mbuti	Barcin_C	Caucasus_lowlands_LC	0.258292	0.004046	63.837	87817
Mbuti	Barcin_C	Croatia_EMBA	0.258094	0.002675	96.491	329821
Mbuti	Barcin_C	Croatia_LBA	0.257951	0.003033	85.05	306808
Mbuti	Barcin_C	Hungary_LBA	0.257934	0.002974	86.728	261412
Mbuti	Barcin_C	Balkans_C	0.257642	0.002939	87.652	197561
Mbuti	Barcin_C	ÇamlıbelTarlası_LC	0.257416	0.002366	108.777	396761
Mbuti	ÇamlıbelTarlası_LC	Bulgaria_EN	0.261298	0.00265	98.612	173959
Mbuti	ÇamlıbelTarlası_LC	Romania_EN	0.260795	0.002192	118.995	362978
Mbuti	ÇamlıbelTarlası_LC	Croatia_Impressa_EN	0.260501	0.002267	114.914	321253
Mbuti	ÇamlıbelTarlası_LC	Croatia_Cardial_N	0.260438	0.002241	116.221	396438
Mbuti	ÇamlıbelTarlası_LC	Balkans_N	0.260414	0.002079	125.256	445158
Mbuti	ÇamlıbelTarlası_LC	Barcin_N	0.260053	0.002059	126.311	468101
Mbuti	ÇamlıbelTarlası_LC	Greece_N	0.260018	0.002456	105.882	317653
Mbuti	ÇamlıbelTarlası_LC	LBK_EN	0.260009	0.002057	126.379	470311
Mbuti	ÇamlıbelTarlası_LC	Czech_N	0.259914	0.002261	114.937	389679
Mbuti	ÇamlıbelTarlası_LC	Bulgaria_C	0.259886	0.002327	111.702	386982
Mbuti	ÇamlıbelTarlası_LC	Peloponnese_N	0.259862	0.002125	122.305	439459
Mbuti	ÇamlıbelTarlası_LC	Starcevo_EN	0.259825	0.002133	121.816	438260
Mbuti	ÇamlıbelTarlası_LC	Bulgaria_JA	0.259157	0.002488	104.144	299553
Mbuti	ÇamlıbelTarlası_LC	Koros_EN	0.259147	0.002216	116.942	416398
Mbuti	ÇamlıbelTarlası_LC	Bulgaria_BA	0.258795	0.002164	119.588	379176
Mbuti	ÇamlıbelTarlası_LC	Lasithi_MMinoan	0.258683	0.002099	123.251	431859
Mbuti	ÇamlıbelTarlası_LC	Bulgaria_Late_C	0.25865	0.0022	117.591	382442
Mbuti	ÇamlıbelTarlası_LC	Boncuklu_N	0.258422	0.002135	121.051	436461

Mbuti	ÇamlıbelTarlası_LC	İkiztepe_LC	0.258404	0.002287	112.982	254041
Mbuti	ÇamlıbelTarlası_LC	Balkans_C	0.258106	0.002436	105.968	219826
Mbuti	ÇamlıbelTarlası_LC	Bulgaria_N	0.257867	0.00218	118.297	348509
Mbuti	ÇamlıbelTarlası_LC	GondürleHöyük_EBA	0.257755	0.002193	117.559	425402
Mbuti	ÇamlıbelTarlası_LC	TellKurdu_EC	0.257578	0.002338	110.159	280518
Mbuti	ÇamlıbelTarlası_LC	Pınarbaşı	0.257452	0.002513	102.438	359449
Mbuti	ÇamlıbelTarlası_LC	Barcin_C	0.257416	0.002366	108.777	396761
Mbuti	ÇamlıbelTarlası_LC	Tepecik_N	0.257007	0.002283	112.575	295843
Mbuti	ÇamlıbelTarlası_LC	Iberia_EN	0.256471	0.002149	119.34	439154
Mbuti	ÇamlıbelTarlası_LC	Globular_Amphora	0.25633	0.002216	115.696	324310
Mbuti	ÇamlıbelTarlası_LC	Bell_Beaker_Hungary	0.2561	0.002086	122.796	412355
Mbuti	ÇamlıbelTarlası_LC	Büyükkaya_EC	0.255962	0.002524	101.43	249625
Mbuti	ÇamlıbelTarlası_LC	Iberia_C	0.255956	0.002072	123.521	459790
Mbuti	ÇamlıbelTarlası_LC	Croatia_EMBA	0.255839	0.002266	112.898	361047
Mbuti	ÇamlıbelTarlası_LC	Boncuklu_N.SG	0.255764	0.002318	110.318	410788
Mbuti	ÇamlıbelTarlası_LC	Bell_Beaker_Italy	0.255667	0.002181	117.21	380885
Mbuti	ÇamlıbelTarlası_LC	Croatia_LBA	0.255648	0.002404	106.349	337072
Mbuti	ÇamlıbelTarlası_LC	Bell_Beaker_Iberia	0.255066	0.002076	122.842	447525
Mbuti	ÇamlıbelTarlası_LC	Arslantepe_LC	0.255012	0.002026	125.899	461041
Mbuti	ÇamlıbelTarlası_LC	Portugal_N_EBA	0.254485	0.002666	95.458	161929
Mbuti	ÇamlıbelTarlası_LC	Arslantepe_EBA	0.254075	0.002068	122.887	417632
Mbuti	ÇamlıbelTarlası_LC	Bulgaria_EBA	0.254072	0.002162	117.506	384261
Mbuti	Caucasus_lowlands_LC	Balkans_C	0.260881	0.004467	58.398	52948
Mbuti	Caucasus_lowlands_LC	Barcin_C	0.258292	0.004046	63.837	87817
Mbuti	Caucasus_lowlands_LC	Bulgaria_EN	0.257947	0.004461	57.827	50652
Mbuti	Caucasus_lowlands_LC	TellKurdu_EC	0.257579	0.003724	69.176	72633
Mbuti	Caucasus_lowlands_LC	Büyükkaya_EC	0.2575	0.004334	59.418	64136
Mbuti	Caucasus_lowlands_LC	Czech_N	0.257463	0.003541	72.708	88669
Mbuti	Caucasus_lowlands_LC	Caucasus_lowlands_LN	0.257202	0.003545	72.562	81411
Mbuti	Caucasus_lowlands_LC	Croatia_Impressa_EN	0.25667	0.003718	69.035	77504
Mbuti	Caucasus_lowlands_LC	Balkans_N	0.256574	0.003025	84.817	94751
Mbuti	Caucasus_lowlands_LC	Bulgaria_Late_C	0.256212	0.003253	78.771	89641
Mbuti	Caucasus_lowlands_LC	Croatia_Cardial_N	0.255906	0.003236	79.076	90164
Mbuti	Caucasus_lowlands_LC	Barcin_N	0.255887	0.002905	88.09	99978
Mbuti	Caucasus_lowlands_LC	Tepecik_N	0.255353	0.004214	60.59	63197
Mbuti	Caucasus_lowlands_LC	Lasithi_MMinoan	0.2552	0.003217	79.339	92228
Mbuti	Caucasus_lowlands_LC	Bulgaria_IA	0.255192	0.004091	62.372	75583
Mbuti	Caucasus_lowlands_LC	Peloponnese_N	0.255145	0.003132	81.468	94374
Mbuti	Caucasus_lowlands_LC	Starcevo_EN	0.255051	0.003195	79.83	94272
Mbuti	Caucasus_lowlands_LC	LBK_EN	0.254971	0.002907	87.724	100596
Mbuti	Caucasus_lowlands_LC	GondürleHöyük_EBA	0.25488	0.003304	77.14	91956
Mbuti	Caucasus_lowlands_LC	Bulgaria_C	0.254643	0.003385	75.216	88566
Mbuti	Caucasus_lowlands_LC	Romania_EN	0.254526	0.003453	73.709	86231
Mbuti	Caucasus_lowlands_LC	Ebla_EMBA	0.25432	0.003073	82.754	91945
Mbuti	Caucasus_lowlands_LC	L.Caucasus_MBA	0.254029	0.003977	63.881	80961
Mbuti	Caucasus_lowlands_LC	Topakhöyük_EBA	0.253973	0.003551	71.528	83903
Mbuti	Caucasus_lowlands_LC	Bell_Beaker_Hungary	0.253968	0.003209	79.15	92261
Mbuti	Caucasus_lowlands_LC	Levant_C	0.253841	0.002882	88.089	97077
Mbuti	Caucasus_lowlands_LC	Koros_EN	0.2537	0.003504	72.405	90732
Mbuti	Caucasus_lowlands_LC	Bell_Beaker_Italy	0.253185	0.003326	76.125	87960
Mbuti	Caucasus_lowlands_LC	Bulgaria_N	0.253148	0.003546	71.397	83967
Mbuti	Caucasus_lowlands_LC	G.Caucasus_a_EBA	0.253136	0.003018	83.871	93628
Mbuti	Caucasus_lowlands_LC	MBA_North_Caucasus	0.252914	0.003376	74.918	85516
Mbuti	Caucasus_lowlands_LC	Greece_N	0.252775	0.003892	64.952	77877
Mbuti	Caucasus_lowlands_LC	Croatia_EMBA	0.252735	0.003578	70.628	85620
Mbuti	Caucasus_lowlands_LC	Arslantepe_LC	0.252361	0.002881	87.585	99201
Mbuti	Caucasus_lowlands_LC	Croatia_LBA	0.252295	0.004053	62.241	81615
Mbuti	Caucasus_lowlands_LC	Hungary_EBA	0.25229	0.003627	69.562	88745
Mbuti	Caucasus_lowlands_LC	Boncuklu_N	0.252251	0.003233	78.017	92644
Mbuti	Caucasus_lowlands_LC	Bulgaria_BA	0.252236	0.003365	74.964	87563
Mbuti	Caucasus_lowlands_LC	Hungary_EMBA	0.251916	0.003758	67.032	74172
Mbuti	Caucasus_lowlands_LC	Arslantepe_EBA	0.251896	0.003154	79.867	92542
Mbuti	Ebla_EMBA	Greece_N	0.257262	0.00246	104.565	299329
Mbuti	Ebla_EMBA	Bulgaria_EN	0.257112	0.002648	97.079	167043
Mbuti	Ebla_EMBA	Romania_EN	0.256873	0.002177	117.993	340350
Mbuti	Ebla_EMBA	Bulgaria_C	0.25637	0.002289	112.021	360024
Mbuti	Ebla_EMBA	Croatia_Cardial_N	0.256188	0.002245	114.113	367786
Mbuti	Ebla_EMBA	Croatia_Impressa_EN	0.256118	0.002334	109.753	301475
Mbuti	Ebla_EMBA	Bulgaria_Late_C	0.255963	0.002151	118.975	357764
Mbuti	Ebla_EMBA	Barcin_N	0.255933	0.002052	124.707	425828
Mbuti	Ebla_EMBA	Peloponnese_N	0.255884	0.002096	122.082	402173
Mbuti	Ebla_EMBA	TellKurdu_EC	0.255747	0.002307	110.872	266663
Mbuti	Ebla_EMBA	Bulgaria_N	0.255689	0.002184	117.093	327787
Mbuti	Ebla_EMBA	Bulgaria_IA	0.255624	0.002501	102.218	281695
Mbuti	Ebla_EMBA	Bulgaria_BA	0.255575	0.00217	117.764	353126
Mbuti	Ebla_EMBA	Koros_EN	0.255481	0.002231	114.506	382456
Mbuti	Ebla_EMBA	Balkans_N	0.255465	0.002126	120.177	405149
Mbuti	Ebla_EMBA	LBK_EN	0.255448	0.002059	124.051	428068
Mbuti	Ebla_EMBA	İkiztepe_LC	0.255281	0.002321	109.988	241024
Mbuti	Ebla_EMBA	Starcevo_EN	0.255193	0.002105	121.23	400632
Mbuti	Ebla_EMBA	GondürleHöyük_EBA	0.254898	0.002206	115.565	390321
Mbuti	Ebla_EMBA	Lasithi_MMinoan	0.254603	0.002113	120.486	393136
Mbuti	Ebla_EMBA	Czech_N	0.254509	0.002243	113.459	361696
Mbuti	Ebla_EMBA	Caucasus_lowlands_LC	0.25432	0.003073	82.754	91945
Mbuti	Ebla_EMBA	Balkans_C	0.25419	0.002474	102.731	204812
Mbuti	Ebla_EMBA	Levant_C	0.253692	0.002069	122.634	407243
Mbuti	Ebla_EMBA	Croatia_EMBA	0.253361	0.002303	109.995	337347
Mbuti	Ebla_EMBA	Bell_Beaker_Italy	0.253322	0.002192	115.586	354984
Mbuti	Ebla_EMBA	Arslantepe_LC	0.253286	0.002042	124.012	420664
Mbuti	Ebla_EMBA	Barcin_C	0.253077	0.002374	106.583	366685
Mbuti	Ebla_EMBA	Tepecik_N	0.252971	0.002335	108.317	268729
Mbuti	Ebla_EMBA	Boncuklu_N	0.252603	0.002099	120.364	397857
Mbuti	Ebla_EMBA	Portugal_N_EBA	0.252521	0.00285	88.606	153232
Mbuti	Ebla_EMBA	Büyükkaya_EC	0.252328	0.002539	99.392	235361

Mbuti	Ebla_EMBA	Arslantepe_EBA	0.252273	0.002094	120.453	385958
Mbuti	Ebla_EMBA	Iberia_C	0.252107	0.002051	122.907	418720
Mbuti	Ebla_EMBA	Iberia_EBA	0.252043	0.002623	96.072	191429
Mbuti	Ebla_EMBA	Bulgaria_EBA	0.251991	0.002256	111.687	358336
Mbuti	Ebla_EMBA	Caucasus_lowlands_LN	0.251942	0.002262	111.364	308124
Mbuti	Ebla_EMBA	Iberia_EN	0.251919	0.002156	116.83	399672
Mbuti	Ebla_EMBA	Bell_Beaker_Hungary	0.251801	0.002089	120.565	381046
Mbuti	Ebla_EMBA	Globular_Amphora	0.251729	0.002243	112.225	306715
Mbuti	GondürleHöyük_EBA	Czech_N	0.266004	0.002391	111.242	377958
Mbuti	GondürleHöyük_EBA	Bulgaria_EN	0.265523	0.002845	93.334	168714
Mbuti	GondürleHöyük_EBA	Romania_EN	0.265181	0.002363	112.231	353570
Mbuti	GondürleHöyük_EBA	Bulgaria_Late_C	0.265025	0.002244	118.094	373184
Mbuti	GondürleHöyük_EBA	Croatia_Impressa_EN	0.264551	0.002448	108.072	309058
Mbuti	GondürleHöyük_EBA	Croatia_Cardial_N	0.264061	0.002372	111.334	385391
Mbuti	GondürleHöyük_EBA	Starcevo_EN	0.263913	0.002257	116.946	421569
Mbuti	GondürleHöyük_EBA	Koros_EN	0.263783	0.002346	112.421	400440
Mbuti	GondürleHöyük_EBA	Bulgaria_C	0.263761	0.002422	108.917	376448
Mbuti	GondürleHöyük_EBA	Bulgaria_IA	0.263638	0.002736	96.371	290698
Mbuti	GondürleHöyük_EBA	LBK_EN	0.263586	0.002169	121.504	453111
Mbuti	GondürleHöyük_EBA	Barcin_N	0.263443	0.002154	122.284	450666
Mbuti	GondürleHöyük_EBA	Peloponnese_N	0.263022	0.002243	117.288	422474
Mbuti	GondürleHöyük_EBA	Bulgaria_N	0.262863	0.002282	115.195	337993
Mbuti	GondürleHöyük_EBA	Greece_N	0.262823	0.002661	98.78	306034
Mbuti	GondürleHöyük_EBA	Bulgaria_BA	0.262707	0.002285	114.995	368782
Mbuti	GondürleHöyük_EBA	Lasithi_MMinoan	0.262668	0.002197	119.543	412944
Mbuti	GondürleHöyük_EBA	Balkans_N	0.26256	0.002211	118.752	426679
Mbuti	GondürleHöyük_EBA	Boncuklu_N	0.262449	0.002243	117.003	416606
Mbuti	GondürleHöyük_EBA	Globular_Amphora	0.262185	0.002348	111.687	316709
Mbuti	GondürleHöyük_EBA	Balkans_C	0.261809	0.002652	98.707	210547
Mbuti	GondürleHöyük_EBA	Bell_Beaker_Italy	0.261498	0.002358	110.888	369066
Mbuti	GondürleHöyük_EBA	Bell_Beaker_Hungary	0.261135	0.002244	116.351	401046
Mbuti	GondürleHöyük_EBA	Croatia_EMBA	0.261133	0.002438	107.111	350907
Mbuti	GondürleHöyük_EBA	Iberia_C	0.261118	0.002182	119.649	442717
Mbuti	GondürleHöyük_EBA	TellKurdu_EC	0.26106	0.002468	105.77	270831
Mbuti	GondürleHöyük_EBA	Iberia_EN	0.260789	0.002252	115.798	420851
Mbuti	GondürleHöyük_EBA	Portugal_N_EBA	0.260292	0.002917	89.239	156621
Mbuti	GondürleHöyük_EBA	Pınarbaşı	0.260257	0.002697	96.509	343639
Mbuti	GondürleHöyük_EBA	Iberia_EBA	0.260042	0.002839	91.591	195081
Mbuti	GondürleHöyük_EBA	Bulgaria_EBA	0.259469	0.002258	114.927	373596
Mbuti	GondürleHöyük_EBA	Barcin_C	0.259139	0.002512	103.181	380666
Mbuti	GondürleHöyük_EBA	Bell_Beaker_Iberia	0.259012	0.002181	118.744	430530
Mbuti	GondürleHöyük_EBA	İkiztepe_LC	0.25891	0.002393	108.192	245309
Mbuti	GondürleHöyük_EBA	Hungary_LBA	0.258478	0.002571	100.541	276979
Mbuti	GondürleHöyük_EBA	Tepecik_N	0.258334	0.002487	103.87	280680
Mbuti	GondürleHöyük_EBA	Croatia_LBA	0.257982	0.002598	99.319	326375
Mbuti	GondürleHöyük_EBA	Arslantepe_LC	0.25783	0.002078	124.08	445247
Mbuti	GondürleHöyük_EBA	ÇamlibelTarlası_LC	0.257755	0.002193	117.559	425402
Mbuti	GondürleHöyük_EBA	Hungary_EMBA	0.257582	0.002555	100.797	298276
Mbuti	İkiztepe_LC	Bulgaria_Late_C	0.262322	0.002415	108.626	233168
Mbuti	İkiztepe_LC	Croatia_Impressa_EN	0.261901	0.002682	97.637	197487
Mbuti	İkiztepe_LC	Croatia_Cardial_N	0.261798	0.002442	107.204	237161
Mbuti	İkiztepe_LC	Greece_N	0.261738	0.002899	90.288	197219
Mbuti	İkiztepe_LC	Boncuklu_N	0.261659	0.002344	111.626	248039
Mbuti	İkiztepe_LC	Balkans_N	0.261434	0.002301	113.63	253468
Mbuti	İkiztepe_LC	Koros_EN	0.261421	0.002496	104.746	241226
Mbuti	İkiztepe_LC	Czech_N	0.261209	0.00254	102.839	233023
Mbuti	İkiztepe_LC	Bulgaria_C	0.260969	0.002578	101.227	232415
Mbuti	İkiztepe_LC	Barcin_N	0.260962	0.002219	117.62	266709
Mbuti	İkiztepe_LC	Romania_EN	0.260868	0.00249	104.764	223272
Mbuti	İkiztepe_LC	Bulgaria_EN	0.260739	0.002987	87.288	119018
Mbuti	İkiztepe_LC	Lasithi_MMinoan	0.260531	0.002328	111.917	246284
Mbuti	İkiztepe_LC	Büyükkaya_EC	0.260231	0.002927	88.894	158779
Mbuti	İkiztepe_LC	TellKurdu_EC	0.26021	0.002691	96.688	179844
Mbuti	İkiztepe_LC	LBK_EN	0.26011	0.002237	116.297	268341
Mbuti	İkiztepe_LC	Bulgaria_N	0.259902	0.002431	106.892	215231
Mbuti	İkiztepe_LC	Peloponnese_N	0.259849	0.002275	114.231	251865
Mbuti	İkiztepe_LC	Bulgaria_IA	0.259835	0.002846	91.294	190210
Mbuti	İkiztepe_LC	Starcevo_EN	0.25956	0.002378	109.13	251494
Mbuti	İkiztepe_LC	Barcin_C	0.259336	0.002773	93.517	232461
Mbuti	İkiztepe_LC	Pınarbaşı	0.259096	0.002819	91.902	210921
Mbuti	İkiztepe_LC	Tepecik_N	0.258965	0.002709	95.602	167683
Mbuti	İkiztepe_LC	GondürleHöyük_EBA	0.25891	0.002393	108.192	245309
Mbuti	İkiztepe_LC	Bulgaria_BA	0.258715	0.002418	106.993	229165
Mbuti	İkiztepe_LC	ÇamlibelTarlası_LC	0.258404	0.002287	112.982	254041
Mbuti	İkiztepe_LC	Portugal_N_EBA	0.258272	0.00337	76.639	103670
Mbuti	İkiztepe_LC	Boncuklu_N.SG	0.25799	0.002668	96.68	229585
Mbuti	İkiztepe_LC	Croatia_EMBA	0.257798	0.002534	101.721	221224
Mbuti	İkiztepe_LC	Balkans_C	0.257754	0.002912	88.5	134264
Mbuti	İkiztepe_LC	Iberia_EN	0.257735	0.002345	109.928	250214
Mbuti	İkiztepe_LC	Bell_Beaker_Italy	0.257633	0.002385	108.003	229886
Mbuti	İkiztepe_LC	Arslantepe_EBA	0.257394	0.002353	109.405	245359
Mbuti	İkiztepe_LC	Arslantepe_LC	0.257229	0.00219	117.439	264219
Mbuti	İkiztepe_LC	Croatia_LBA	0.257034	0.00274	93.794	209432
Mbuti	İkiztepe_LC	Bell_Beaker_Hungary	0.257029	0.002329	110.358	243828
Mbuti	İkiztepe_LC	Iberia_C	0.25702	0.002212	116.174	263049
Mbuti	İkiztepe_LC	Globular_Amphora	0.256603	0.002522	101.747	206365
Mbuti	İkiztepe_LC	Bell_Beaker_Iberia	0.256517	0.002258	113.597	256948
Mbuti	İkiztepe_LC	Bulgaria_EBA	0.256191	0.00241	106.292	232128
Mbuti	K.Kalehöyük_MLBA	Czech_N	0.258187	0.002349	109.898	373762
Mbuti	K.Kalehöyük_MLBA	Greece_N	0.258119	0.002579	100.09	303076
Mbuti	K.Kalehöyük_MLBA	Croatia_Cardial_N	0.25774	0.002361	109.184	381585
Mbuti	K.Kalehöyük_MLBA	LBK_EN	0.257349	0.002105	122.227	469922
Mbuti	K.Kalehöyük_MLBA	Croatia_Impressa_EN	0.257339	0.002461	104.586	308131
Mbuti	K.Kalehöyük_MLBA	Balkans_C	0.257274	0.002578	99.784	211224

Mbuti	K.Kalehöyük_MLBA	Bulgaria_EN	0.257243	0.002797	91.972	163196
Mbuti	K.Kalehöyük_MLBA	Balkans_N	0.257193	0.002149	119.671	438121
Mbuti	K.Kalehöyük_MLBA	Lasithi_MMinoan	0.257177	0.002142	120.071	423763
Mbuti	K.Kalehöyük_MLBA	Starcevo_EN	0.257112	0.002199	116.936	428879
Mbuti	K.Kalehöyük_MLBA	Koros_EN	0.257024	0.002333	110.161	402391
Mbuti	K.Kalehöyük_MLBA	Barcin_N	0.256896	0.002113	121.603	467253
Mbuti	K.Kalehöyük_MLBA	Bulgaria_Late_C	0.256761	0.002246	114.298	367851
Mbuti	K.Kalehöyük_MLBA	Bulgaria_C	0.256539	0.002386	107.499	370548
Mbuti	K.Kalehöyük_MLBA	Peloponnese_N	0.256164	0.002135	119.981	430558
Mbuti	K.Kalehöyük_MLBA	Romania_EN	0.256033	0.002295	111.554	346263
Mbuti	K.Kalehöyük_MLBA	Boncuklu_N	0.255868	0.002195	116.558	427638
Mbuti	K.Kalehöyük_MLBA	Bulgaria_N	0.255762	0.0023	111.184	333052
Mbuti	K.Kalehöyük_MLBA	Bulgaria_BA	0.255141	0.002325	109.752	362461
Mbuti	K.Kalehöyük_MLBA	Iberia_EBA	0.254881	0.002827	90.17	190068
Mbuti	K.Kalehöyük_MLBA	Bell_Beaker_Italy	0.25479	0.002346	108.615	365382
Mbuti	K.Kalehöyük_MLBA	Tepecik_N	0.254607	0.002414	105.488	289943
Mbuti	K.Kalehöyük_MLBA	Portugal_MN	0.254033	0.00225	112.915	444885
Mbuti	K.Kalehöyük_MLBA	Boncuklu_N.SG	0.253955	0.00242	104.934	402014
Mbuti	K.Kalehöyük_MLBA	Barcin_C	0.253922	0.00245	103.638	380540
Mbuti	K.Kalehöyük_MLBA	Croatia_EMBA	0.253845	0.002398	105.871	344727
Mbuti	K.Kalehöyük_MLBA	Büyükkaya_EC	0.253797	0.002692	94.291	236801
Mbuti	K.Kalehöyük_MLBA	Topakhöyük_EBA	0.253775	0.002271	111.735	399949
Mbuti	K.Kalehöyük_MLBA	Pınarbaşı	0.253674	0.002672	94.953	345538
Mbuti	K.Kalehöyük_MLBA	Bulgaria_IA	0.253645	0.002629	96.469	282670
Mbuti	K.Kalehöyük_MLBA	Iberia_EN	0.253434	0.002262	112.038	430465
Mbuti	K.Kalehöyük_MLBA	Sardinian	0.253368	0.002088	121.33	479702
Mbuti	K.Kalehöyük_MLBA	Globular_Amphora	0.253212	0.002311	109.565	308714
Mbuti	K.Kalehöyük_MLBA	Iberia_C	0.253077	0.002144	118.013	456600
Mbuti	K.Kalehöyük_MLBA	Bell_Beaker_Iberia	0.25307	0.002162	117.079	440921
Mbuti	K.Kalehöyük_MLBA	Croatia_LBA	0.253023	0.002578	98.147	319286
Mbuti	K.Kalehöyük_MLBA	GondürleHöyük_EBA	0.25298	0.002267	111.578	412619
Mbuti	K.Kalehöyük_MLBA	İkiztepe_LC	0.252695	0.002417	104.538	241863
Mbuti	K.Kalehöyük_MLBA	Bell_Beaker_Hungary	0.25259	0.002202	114.693	399511
Mbuti	K.Kalehöyük_MLBA	ÇamlıbelTarlası_LC	0.252525	0.002162	116.825	435197
Mbuti	TitrişHöyük_EBA	French	0.252323	0.003347	75.671	50308
Mbuti	TitrişHöyük_EBA	Spanish	0.251391	0.003312	75.908	50336
Mbuti	TitrişHöyük_EBA	Russian	0.251112	0.003308	75.92	50458
Mbuti	TitrişHöyük_EBA	Turkish	0.249581	0.003288	75.918	50462
Mbuti	TitrişHöyük_EBA	Tajik	0.242249	0.003279	73.873	50128
Mbuti	TitrişHöyük_EBA	Bashkir	0.239667	0.003278	73.109	50552
Mbuti	TitrişHöyük_EBA	Palestinian	0.239429	0.003262	73.39	50451
Mbuti	TitrişHöyük_EBA	Nogai	0.237333	0.003318	71.539	50107
Mbuti	TitrişHöyük_EBA	Uzbek	0.236201	0.003292	71.74	50308
Mbuti	TitrişHöyük_EBA	BedouinA	0.234164	0.003198	73.232	50102
Mbuti	TitrişHöyük_EBA	Kazakh	0.229956	0.003287	69.949	50640
Mbuti	TitrişHöyük_EBA	Mongol	0.22125	0.003338	66.29	50547
Mbuti	Topakhöyük_EBA	Greece_N	0.259021	0.002616	99.01	282457
Mbuti	Topakhöyük_EBA	Croatia_Cardial_N	0.258046	0.002338	110.362	356221
Mbuti	Topakhöyük_EBA	Romania_EN	0.25727	0.002392	107.575	323209
Mbuti	Topakhöyük_EBA	Czech_N	0.257204	0.002425	106.056	348581
Mbuti	Topakhöyük_EBA	Balkans_N	0.256771	0.002204	116.497	408901
Mbuti	Topakhöyük_EBA	Bulgaria_EN	0.256587	0.002988	85.881	152576
Mbuti	Topakhöyük_EBA	LBK_EN	0.256415	0.002168	118.284	439748
Mbuti	Topakhöyük_EBA	Barcin_N	0.255956	0.00215	119.037	437126
Mbuti	Topakhöyük_EBA	Tepecik_N	0.255914	0.002433	105.187	270322
Mbuti	Topakhöyük_EBA	Croatia_Impressa_EN	0.255654	0.002467	103.626	287357
Mbuti	Topakhöyük_EBA	Starcevo_EN	0.255641	0.002266	112.798	400185
Mbuti	Topakhöyük_EBA	Bulgaria_Late_C	0.25555	0.002364	108.122	343599
Mbuti	Topakhöyük_EBA	Koros_EN	0.255322	0.002395	106.627	375036
Mbuti	Topakhöyük_EBA	Peloponnese_N	0.255312	0.002231	114.452	401757
Mbuti	Topakhöyük_EBA	Bulgaria_IA	0.254947	0.00272	93.719	263971
Mbuti	Topakhöyük_EBA	Balkans_C	0.254943	0.00275	92.697	196678
Mbuti	Topakhöyük_EBA	Lasithi_MMinoan	0.254828	0.00216	117.969	395178
Mbuti	Topakhöyük_EBA	Bulgaria_C	0.254801	0.002486	102.48	345715
Mbuti	Topakhöyük_EBA	Bulgaria_N	0.254579	0.002362	107.795	310922
Mbuti	Topakhöyük_EBA	Boncuklu_N	0.25455	0.002295	110.908	398710
Mbuti	Topakhöyük_EBA	Caucasus_lowlands_LC	0.253973	0.003551	71.528	83903
Mbuti	Topakhöyük_EBA	K.Kalehöyük_MLBA	0.253775	0.002271	111.735	399949
Mbuti	Topakhöyük_EBA	Croatia_LBA	0.253609	0.002607	97.27	297803
Mbuti	Topakhöyük_EBA	Portugal_MN	0.2536	0.002322	109.217	414535
Mbuti	Topakhöyük_EBA	Bell_Beaker_Italy	0.253498	0.002361	107.365	341080
Mbuti	Topakhöyük_EBA	Iberia_EN	0.253439	0.002264	111.927	401638
Mbuti	Topakhöyük_EBA	Bulgaria_BA	0.253262	0.002297	110.25	338386
Mbuti	Topakhöyük_EBA	TellKurdu_EC	0.253104	0.002499	101.277	250228
Mbuti	Topakhöyük_EBA	Boncuklu_N.SG	0.253094	0.002475	102.253	374313
Mbuti	Topakhöyük_EBA	Büyükkaya_EC	0.253054	0.002746	92.158	221186
Mbuti	Topakhöyük_EBA	Iberia_C	0.252887	0.002168	116.656	426913
Mbuti	Topakhöyük_EBA	Iberia_EBA	0.252836	0.002834	89.207	177611
Mbuti	Topakhöyük_EBA	ÇamlıbelTarlası_LC	0.252793	0.002198	115.004	406417
Mbuti	Topakhöyük_EBA	Bulgaria_EBA	0.252712	0.002311	109.363	343851
Mbuti	Topakhöyük_EBA	GondürleHöyük_EBA	0.252567	0.002292	110.195	384789
Mbuti	Topakhöyük_EBA	Globular_Amphora	0.25242	0.002467	102.303	288250
Mbuti	Topakhöyük_EBA	Barcin_C	0.252346	0.002595	97.226	354371
Mbuti	Topakhöyük_EBA	Croatia_EMBA	0.252264	0.002505	100.707	321987
Mbuti	Topakhöyük_EBA	Sardinian	0.252218	0.002118	119.11	449241
Mbuti	Topakhöyük_EBA	Bell_Beaker_Hungary	0.251953	0.002244	112.265	373219

**Table S5** Genetic differences between Neolithic-Early Chalcolithic (N-EC) populations and the Late Chalcolithic-Late Bronze Age (LC-LBA) with respect to a Test population measured by f4(Mbuti;Test;Barcin\_N/Büyükaya\_EC/TellKurdu\_EC, LC-LBA), Related to Figure 6. Test populations include European and West Asians ancient populations. f4-statistics were estimated on the on the autosomal portion of the 1240K SNP panel and standard errors were estimated by 5 cM block jack-knifing. Significant values ( $|z\text{-score}| \geq 3$ ) indicate that Test shares more alleles with the LC-LBA than N-EC (positive sign) or vice versa (negative sign) and are annotated in bold. Results important for our interpretations are annotated in Italics. (*published as excel table*)

Outgroup	Test	N-EC group	LC-LBA group	f4-statistic	z-score	SE	№ BABA SNPs	№ ABBA SNP	№ SNPs	sign of f4 result
Mbuti.DG	<b>Iran_N.SG</b>	<b>Barcin_N</b>	<b>Alalakh_MLBA</b>	<b>0.001238</b>	<b>9.282</b>	0.000133	58695	57331	1101912	pos
Mbuti.DG	<b>Iran_N</b>	<b>Barcin_N</b>	<b>Alalakh_MLBA</b>	<b>0.001321</b>	<b>7.878</b>	0.000168	45054	43936	846334	pos
Mbuti.DG	CHG	Barcin_N	Alalakh_MLBA	0.000379	2.362	0.000160	58882	58465	1101782	pos
Mbuti.DG	G.Caucasus_c_EMBA	Barcin_N	Alalakh_MLBA	0.000056	0.305	0.000184	42219	42174	793747	pos
Mbuti.DG	<b>Iran_N.SG</b>	<b>Barcin_N</b>	<b>Arslantepe_EBA</b>	<b>0.001195</b>	<b>6.201</b>	0.000193	55341	54095	1042818	pos
Mbuti.DG	<b>CHG</b>	<b>Barcin_N</b>	<b>Arslantepe_EBA</b>	<b>0.001238</b>	<b>5.404</b>	0.000229	56038	54747	1042696	pos
Mbuti.DG	<b>Iran_N</b>	<b>Barcin_N</b>	<b>Arslantepe_EBA</b>	<b>0.001218</b>	<b>5.296</b>	0.000230	43962	42952	829094	pos
Mbuti.DG	G.Caucasus_c_EMBA	Barcin_N	Arslantepe_EBA	0.000585	2.243	0.000261	41845	41386	784338	pos
Mbuti.DG	G.Caucasus_b_En	Barcin_N	Arslantepe_EBA	0.000398	1.941	0.000205	51997	51610	972423	pos
Mbuti.DG	G.Caucasus_b_EMBA	Barcin_N	Arslantepe_EBA	0.000057	0.318	0.000179	51764	51708	970497	pos
Mbuti.DG	G.Caucasus_a_En	Barcin_N	Arslantepe_EBA	0.000002	0.008	0.000250	39739	39738	744235	pos
Mbuti.DG	<b>Iran_N.SG</b>	<b>Barcin_N</b>	<b>Arslantepe_LC</b>	<b>0.001526</b>	<b>11.305</b>	0.000135	58385	56709	1098437	pos
Mbuti.DG	<b>Iran_N</b>	<b>Barcin_N</b>	<b>Arslantepe_LC</b>	<b>0.001529</b>	<b>9.268</b>	0.000165	44902	43608	845902	pos
Mbuti.DG	<b>CHG</b>	<b>Barcin_N</b>	<b>Arslantepe_LC</b>	<b>0.001104</b>	<b>7.041</b>	0.000157	58840	57627	1098309	pos
Mbuti.DG	<b>G.Caucasus_b_En</b>	<b>Barcin_N</b>	<b>Arslantepe_LC</b>	<b>0.000464</b>	<b>3.287</b>	0.000141	53305	52841	998233	pos
Mbuti.DG	G.Caucasus_c_EMBA	Barcin_N	Arslantepe_LC	0.000544	2.978	0.000183	42226	41795	793594	pos
Mbuti.DG	G.Caucasus_b_EMBA	Barcin_N	Arslantepe_LC	0.000219	1.917	0.000114	53115	52897	995848	pos
Mbuti.DG	Iran_C	Barcin_N	Arslantepe_LC	0.000209	1.657	0.000126	53597	53387	1004460	pos
Mbuti.DG	G.Caucasus_a_En	Barcin_N	Arslantepe_LC	0.000159	0.88	0.000181	40207	40088	753643	pos
Mbuti.DG	G.Caucasus_a_MLBA	Barcin_N	Arslantepe_LC	0.000088	0.57	0.000154	44825	44751	840066	pos
Mbuti.DG	G.Caucasus_a_EBA	Barcin_N	Arslantepe_LC	0.000023	0.195	0.000118	53142	53119	996358	pos
Mbuti.DG	<b>CHG</b>	<b>Barcin_N</b>	<b>Barcin_C</b>	<b>0.002462</b>	<b>6.84</b>	0.000360	51526	49181	952368	pos
Mbuti.DG	<b>Iran_N.SG</b>	<b>Barcin_N</b>	<b>Barcin_C</b>	<b>0.00154</b>	<b>4.776</b>	0.000322	50424	48957	952513	pos
Mbuti.DG	<b>G.Caucasus_b_En</b>	<b>Barcin_N</b>	<b>Barcin_C</b>	<b>0.001437</b>	<b>4.163</b>	0.000345	48571	47272	903539	pos
Mbuti.DG	<b>G.Caucasus_b_EMBA</b>	<b>Barcin_N</b>	<b>Barcin_C</b>	<b>0.001038</b>	<b>3.563</b>	0.000291	48363	47426	902339	pos
Mbuti.DG	Samara_En	Barcin_N	Barcin_C	0.00114	2.97	0.000384	36467	35689	682752	pos
Mbuti.DG	Iran_N	Barcin_N	Barcin_C	0.001167	2.938	0.000397	41398	40481	785465	pos
Mbuti.DG	EHG	Barcin_N	Barcin_C	0.00108	2.691	0.000401	47922	46953	896772	pos
Mbuti.DG	G.Caucasus_c_EMBA	Barcin_N	Barcin_C	0.00111	2.559	0.000434	39942	39111	748913	pos
Mbuti.DG	G.Caucasus_a_En	Barcin_N	Barcin_C	0.000843	2.039	0.000413	38254	37652	714143	pos
Mbuti.DG	G.Caucasus_a_EBA	Barcin_N	Barcin_C	0.00046	1.543	0.000298	48181	47766	902717	pos
Mbuti.DG	Iran_C	Barcin_N	Barcin_C	0.000365	1.181	0.000309	48220	47890	905496	pos
Mbuti.DG	L.Caucasus_EBA	Barcin_N	Barcin_C	0.000299	0.967	0.000309	49114	48838	920091	pos
Mbuti.DG	G.Caucasus_a_MLBA	Barcin_N	Barcin_C	0.000285	0.817	0.000349	41981	41756	787430	pos
Mbuti.DG	L.Caucasus_LBA.SG	Barcin_N	Barcin_C	0.000239	0.632	0.000378	25051	24936	480803	pos
Mbuti.DG	<b>Iran_N.SG</b>	<b>Barcin_N</b>	<b>ÇamlıbelTarlasi_LC</b>	<b>0.00106</b>	<b>6.808</b>	0.000156	56248	55119	1064878	pos
Mbuti.DG	<b>CHG</b>	<b>Barcin_N</b>	<b>ÇamlıbelTarlasi_LC</b>	<b>0.001113</b>	<b>5.787</b>	0.000192	56986	55801	1064763	pos
Mbuti.DG	<b>Iran_N</b>	<b>Barcin_N</b>	<b>ÇamlıbelTarlasi_LC</b>	<b>0.000674</b>	<b>3.403</b>	0.000198	43790	43228	833709	pos
Mbuti.DG	G.Caucasus_b_En	Barcin_N	ÇamlıbelTarlasi_LC	0.000067	0.409	0.000164	51974	51908	979969	pos
Mbuti.DG	G.Caucasus_a_En	Barcin_N	ÇamlıbelTarlasi_LC	0.000049	0.224	0.000219	39672	39635	746497	pos
Mbuti.DG	<b>Iran_N.SG</b>	<b>Barcin_N</b>	<b>Caucasus_lowlands_LI</b>	<b>0.001759</b>	<b>4.121</b>	0.000427	11438	11059	215706	pos
Mbuti.DG	<b>Iran_N</b>	<b>Barcin_N</b>	<b>Caucasus_lowlands_LI</b>	<b>0.002277</b>	<b>4.118</b>	0.000553	10532	10085	192616	pos
Mbuti.DG	CHG	Barcin_N	Caucasus_lowlands_LC	0.001464	2.949	0.000496	11515	11199	215697	pos
Mbuti.DG	G.Caucasus_b_En	Barcin_N	Caucasus_lowlands_LC	0.000712	1.664	0.000428	11352	11201	212381	pos
Mbuti.DG	Iran_C	Barcin_N	Caucasus_lowlands_LC	0.000218	0.511	0.000427	11288	11242	211572	pos
Mbuti.DG	G.Caucasus_c_EMBA	Barcin_N	Caucasus_lowlands_LC	0.000148	0.259	0.000571	10323	10294	194996	pos
Mbuti.DG	<b>Iran_N.SG</b>	<b>Barcin_N</b>	<b>Ebla_EMBA</b>	<b>0.001289</b>	<b>7.471</b>	0.000173	54331	53015	1021024	pos
Mbuti.DG	<b>Iran_N</b>	<b>Barcin_N</b>	<b>Ebla_EMBA</b>	<b>0.00116</b>	<b>5.492</b>	0.000211	43374	42427	816001	pos
Mbuti.DG	CHG	Barcin_N	Ebla_EMBA	0.000233	1.17	0.000199	54358	54120	1020913	pos
Mbuti.DG	<b>Iran_N</b>	<b>Barcin_N</b>	<b>GondürleHöyük_EBA</b>	<b>0.001797</b>	<b>7.118</b>	0.000252	43518	42038	823475	pos
Mbuti.DG	<b>CHG</b>	<b>Barcin_N</b>	<b>GondürleHöyük_EBA</b>	<b>0.001569</b>	<b>5.943</b>	0.000264	54463	52862	1020285	pos
Mbuti.DG	<b>Iran_N.SG</b>	<b>Barcin_N</b>	<b>GondürleHöyük_EBA</b>	<b>0.00125</b>	<b>5.872</b>	0.000213	53598	52322	1020493	pos
Mbuti.DG	<b>G.Caucasus_b_En</b>	<b>Barcin_N</b>	<b>GondürleHöyük_EBA</b>	<b>0.001088</b>	<b>4.962</b>	0.000219	51177	50132	959823	pos
Mbuti.DG	<b>G.Caucasus_b_EMBA</b>	<b>Barcin_N</b>	<b>GondürleHöyük_EBA</b>	<b>0.000954</b>	<b>4.949</b>	0.000193	51166	50251	958965	pos
Mbuti.DG	<b>G.Caucasus_a_En</b>	<b>Barcin_N</b>	<b>GondürleHöyük_EBA</b>	<b>0.000935</b>	<b>3.076</b>	0.000304	39616	38922	741955	pos
Mbuti.DG	G.Caucasus_a_EBA	Barcin_N	GondürleHöyük_EBA	0.000582	2.806	0.000207	51067	50509	959058	pos
Mbuti.DG	G.Caucasus_a_MLBA	Barcin_N	GondürleHöyük_EBA	0.000711	2.701	0.000263	43895	43309	822678	pos
Mbuti.DG	L.Caucasus_EBA	Barcin_N	GondürleHöyük_EBA	0.000489	2.415	0.000202	52040	51562	976907	pos
Mbuti.DG	G.Caucasus_c_EMBA	Barcin_N	GondürleHöyük_EBA	0.000688	2.391	0.000288	41202	40666	779320	pos
Mbuti.DG	Iran_C	Barcin_N	GondürleHöyük_EBA	0.000479	2.28	0.000210	50827	50369	957883	pos
Mbuti.DG	L.Caucasus_MBA	Barcin_N	GondürleHöyük_EBA	0.000455	1.479	0.000308	42309	41947	794972	pos
Mbuti.DG	Samara_En	Barcin_N	GondürleHöyük_EBA	0.000235	0.897	0.000262	37701	37532	716244	pos
Mbuti.DG	EHG	Barcin_N	GondürleHöyük_EBA	0.000088	0.334	0.000263	50044	49960	950800	pos
Mbuti.DG	<b>CHG</b>	<b>Barcin_N</b>	<b>İkiztepe_LC</b>	<b>0.001753</b>	<b>7.088</b>	0.000247	31967	30924	594839	pos
Mbuti.DG	<b>Iran_N.SG</b>	<b>Barcin_N</b>	<b>İkiztepe_LC</b>	<b>0.001266</b>	<b>5.797</b>	0.000218	31407	30654	594920	pos
Mbuti.DG	<b>Iran_N</b>	<b>Barcin_N</b>	<b>İkiztepe_LC</b>	<b>0.001581</b>	<b>5.641</b>	0.000280	27469	26650	517767	pos
Mbuti.DG	G.Caucasus_b_En	Barcin_N	İkiztepe_LC	0.000533	2.366	0.000225	30816	30508	578469	pos
Mbuti.DG	G.Caucasus_b_EMBA	Barcin_N	İkiztepe_LC	0.000455	2.346	0.000194	30814	30551	577929	pos
Mbuti.DG	G.Caucasus_c_EMBA	Barcin_N	İkiztepe_LC	0.000676	2.182	0.000310	27011	26667	507750	pos
Mbuti.DG	Iran_C	Barcin_N	İkiztepe_LC	0.000242	1.146	0.000211	30634	30495	575826	pos
Mbuti.DG	G.Caucasus_a_En	Barcin_N	İkiztepe_LC	0.000228	0.809	0.000282	25691	25581	482184	pos
Mbuti.DG	L.Caucasus_EBA	Barcin_N	İkiztepe_LC	0.000154	0.749	0.000206	31118	31028	583136	pos
Mbuti.DG	G.Caucasus_a_MLBA	Barcin_N	İkiztepe_LC	0.000188	0.726	0.000259	28186	28087	527095	pos
Mbuti.DG	G.Caucasus_a_EBA	Barcin_N	İkiztepe_LC	0.000081	0.404	0.000200	30780	30733	577786	pos
Mbuti.DG	<b>Iran_N.SG</b>	<b>Barcin_N</b>	<b>K.Kalehöyük_MLBA</b>	<b>0.001625</b>	<b>5.345</b>	0.000304	10981	10645	207100	pos
Mbuti.DG	<b>CHG</b>	<b>Barcin_N</b>	<b>K.Kalehöyük_MLBA</b>	<b>0.001868</b>	<b>5.336</b>	0.000350	11196	10809	207109	pos
Mbuti.DG	Iran_N	Barcin_N	K.Kalehöyük_MLBA	0.000706	1.633	0.000432	8104	7995	154468	pos
Mbuti.DG	G.Caucasus_c_EMBA	Barcin_N	K.Kalehöyük_MLBA	0.000596	1.313	0.000454	7645	7559	144096	pos
Mbuti.DG	G.Caucasus_b_En	Barcin_N	K.Kalehöyük_MLBA	0.000006	0.019	0.000316	9721	9720	183535	pos
Mbuti.DG	G.Caucasus_b_EMBA	Barcin_N	TitrişHöyük_EBA	0.0059	0.841	0.007015	2743	2711	50939	pos
Mbuti.DG	Iran_N.SG	Barcin_N	TitrişHöyük_EBA	0.0015	0.227	0.006608	2695	2687	51391	pos
Mbuti.DG	<b>CHG</b>	<b>Barcin_N</b>	<b>Topakhöyük_EBA</b>	<b>0.001889</b>	<b>5.091</b>	0.000371	10737	10358	200285	pos
Mbuti.DG	<b>Iran_N.SG</b>	<b>Barcin_N</b>	<b>Topakhöyük_EBA</b>	<b>0.001514</b>	<b>4.684</b>	0.000323	10513	10210	200279	pos

Mbuti.DG	Iran_N	Barcin_N	Topakhöyük_EBA	0.000487	1.079	0.000451	7760	7687	149929	pos
Mbuti.DG	L.Caucasus_LBA.SG	Barcin_N	Topakhöyük_EBA	0.000024	0.047	0.000511	4823	4821	93943	pos
Mbuti.DG	Iran_N.SG	Büyükkaya_EC	Alalakh_MLBA	0.0041	1.302	0.003149	31767	31507	599806	pos
Mbuti.DG	Levant_EBA	Büyükkaya_EC	Alalakh_MLBA	0.0023	0.690	0.003333	29014	28881	540151	pos
Mbuti.DG	G.Caucasus_c_EMBA	Büyükkaya_EC	Alalakh_MLBA	0.002	0.468	0.004274	27154	27046	508951	pos
Mbuti.DG	Iran_N	Büyükkaya_EC	Alalakh_MLBA	0.0012	0.287	0.004181	27466	27401	519577	pos
Mbuti.DG	G.Caucasus_c_EMBA	Büyükkaya_EC	Arslantepe_EBA	0.0067	1.422	0.004712	27267	26904	506874	pos
Mbuti.DG	Iran_N.SG	Büyükkaya_EC	Arslantepe_EBA	0.0039	1.105	0.003529	31292	31049	590347	pos
Mbuti.DG	L.Caucasus_MBA	Büyükkaya_EC	Arslantepe_EBA	0.0047	1.056	0.004451	27213	26958	503468	pos
Mbuti.DG	G.Caucasus_b_EMBA	Büyükkaya_EC	Arslantepe_EBA	0.0028	0.913	0.003067	30877	30704	575602	pos
Mbuti.DG	G.Caucasus_b_En	Büyükkaya_EC	Arslantepe_EBA	0.0032	0.878	0.003645	30978	30781	575997	pos
Mbuti.DG	G.Caucasus_a_MLBA	Büyükkaya_EC	Arslantepe_EBA	0.0034	0.865	0.003931	28360	28171	526072	pos
Mbuti.DG	Bulgaria_Varna_En3	Büyükkaya_EC	Arslantepe_EBA	0.0045	0.833	0.005402	15220	15083	281570	pos
Mbuti.DG	CHG	Büyükkaya_EC	Arslantepe_EBA	0.0034	0.819	0.004151	31664	31449	590283	pos
Mbuti.DG	Levant_EBA	Büyükkaya_EC	Arslantepe_EBA	0.0021	0.567	0.003704	28894	28776	537456	pos
Mbuti.DG	G.Caucasus_a_EBA	Büyükkaya_EC	Arslantepe_EBA	0.0009	0.309	0.002913	30902	30844	575394	pos
Mbuti.DG	L.Caucasus_LBA.SG	Büyükkaya_EC	Arslantepe_EBA	0.0013	0.308	0.004221	16719	16675	317917	pos
Mbuti.DG	L.Caucasus_EBA	Büyükkaya_EC	Arslantepe_EBA	0.0006	0.177	0.003390	31198	31163	579700	pos
Mbuti.DG	Iran_C	Büyükkaya_EC	Arslantepe_EBA	0.0003	0.079	0.003797	30630	30614	572322	pos
Mbuti.DG	Levant_N	Büyükkaya_EC	Arslantepe_EBA	0.0001	0.037	0.002703	27713	27705	517384	pos
Mbuti.DG	L.Caucasus_MBA	Büyükkaya_EC	Arslantepe_LC	0.0058	1.429	0.004059	27208	26892	506512	pos
Mbuti.DG	G.Caucasus_b_EMBA	Büyükkaya_EC	Arslantepe_LC	0.0039	1.420	0.002746	31027	30785	580761	pos
Mbuti.DG	Levant_EBA	Büyükkaya_EC	Arslantepe_LC	0.004	1.247	0.003208	28949	28716	540156	pos
Mbuti.DG	G.Caucasus_b_En	Büyükkaya_EC	Arslantepe_LC	0.004	1.224	0.003268	31105	30858	581177	pos
Mbuti.DG	Iran_C	Büyükkaya_EC	Arslantepe_LC	0.0032	1.102	0.002904	30911	30711	578364	pos
Mbuti.DG	G.Caucasus_a_En	Büyükkaya_EC	Arslantepe_LC	0.0037	0.905	0.004088	25964	25772	484871	pos
Mbuti.DG	L.Caucasus_EBA	Büyükkaya_EC	Arslantepe_LC	0.0024	0.802	0.002993	31437	31284	586001	pos
Mbuti.DG	Iran_N	Büyükkaya_EC	Arslantepe_LC	0.0029	0.707	0.004102	27379	27220	519509	pos
Mbuti.DG	G.Caucasus_a_EBA	Büyükkaya_EC	Arslantepe_LC	0.0017	0.628	0.002707	31054	30948	580718	pos
Mbuti.DG	L.Caucasus_LBA.SG	Büyükkaya_EC	Arslantepe_LC	0.0019	0.474	0.004008	16781	16718	320810	pos
Mbuti.DG	Levant_N	Büyükkaya_EC	Arslantepe_LC	0.0012	0.347	0.003458	27802	27735	520336	pos
Mbuti.DG	Balkans_C	Büyükkaya_EC	Arslantepe_LC	0.001	0.218	0.004587	16377	16343	305495	pos
Mbuti.DG	<b>G.Caucasus_b_EMBA</b>	<b>Büyükkaya_EC</b>	<b>Barcin_C</b>	<b>0.0115</b>	<b>3.020</b>	0.003808	29716	29042	553198	pos
Mbuti.DG	CHG	Büyükkaya_EC	Barcin_C	0.0146	2.862	0.005101	30354	29483	563754	pos
Mbuti.DG	G.Caucasus_b_En	Büyükkaya_EC	Barcin_C	0.0129	2.831	0.004557	29819	29062	553429	pos
Mbuti.DG	G.Caucasus_a_En	Büyükkaya_EC	Barcin_C	0.0116	2.124	0.005461	25423	24839	471703	pos
Mbuti.DG	EHG	Büyükkaya_EC	Barcin_C	0.0103	2.004	0.005140	29089	28497	543018	pos
Mbuti.DG	L.Caucasus_LBA.SG	Büyükkaya_EC	Barcin_C	0.0109	1.979	0.005508	16205	15857	306871	pos
Mbuti.DG	G.Caucasus_c_EMBA	Büyükkaya_EC	Barcin_C	0.0103	1.814	0.005678	26467	25926	493911	pos
Mbuti.DG	Bulgaria_Varna_En3	Büyükkaya_EC	Barcin_C	0.0121	1.784	0.006783	14929	14573	276787	pos
Mbuti.DG	L.Caucasus_EBA	Büyükkaya_EC	Barcin_C	0.0058	1.460	0.003973	29852	29506	556742	pos
Mbuti.DG	G.Caucasus_a_MLBA	Büyükkaya_EC	Barcin_C	0.0065	1.408	0.004616	27582	27223	511273	pos
Mbuti.DG	Iberia_C	Büyükkaya_EC	Barcin_C	0.0038	1.011	0.003759	30362	30131	562272	pos
Mbuti.DG	Levant_EP	Büyükkaya_EC	Barcin_C	0.0054	0.914	0.005908	17577	17389	333668	pos
Mbuti.DG	Iran_C	Büyükkaya_EC	Barcin_C	0.0023	0.560	0.004107	29364	29230	550932	pos
Mbuti.DG	Levant_MBA.SG	Büyükkaya_EC	Barcin_C	0.0021	0.513	0.004094	29924	29798	559722	pos
Mbuti.DG	Levant_EBA	Büyükkaya_EC	Barcin_C	0.0016	0.369	0.004336	27842	27751	522163	pos
Mbuti.DG	Iran_N	Büyükkaya_EC	Barcin_C	0.0002	0.038	0.005263	26253	26242	500997	pos
Mbuti.DG	Levant_C	Büyükkaya_EC	Barcin_C	0	0.011	0.000000	29960	29957	559738	pos
Mbuti.DG	L.Caucasus_MBA	Büyükkaya_EC	ÇamlıbelTarlasi_LC	0.0071	1.738	0.004085	27062	26678	504010	pos
Mbuti.DG	Bulgaria_Varna_En3	Büyükkaya_EC	ÇamlıbelTarlasi_LC	0.0062	1.178	0.005263	15110	14924	281644	pos
Mbuti.DG	L.Caucasus_LBA.SG	Büyükkaya_EC	ÇamlıbelTarlasi_LC	0.0041	0.988	0.004150	16672	16536	318659	pos
Mbuti.DG	Iran_N.SG	Büyükkaya_EC	ÇamlıbelTarlasi_LC	0.003	0.893	0.003359	31193	31007	593221	pos
Mbuti.DG	G.Caucasus_a_MLBA	Büyükkaya_EC	ÇamlıbelTarlasi_LC	0.0028	0.781	0.003585	28221	28061	526396	pos
Mbuti.DG	Iran_C	Büyükkaya_EC	ÇamlıbelTarlasi_LC	0.0018	0.574	0.003136	30565	30458	573768	pos
Mbuti.DG	CHG	Büyükkaya_EC	ÇamlıbelTarlasi_LC	0.0022	0.542	0.004059	31572	31435	593160	pos
Mbuti.DG	G.Caucasus_c_EMBA	Büyükkaya_EC	ÇamlıbelTarlasi_LC	0.0017	0.386	0.004404	26884	26791	507085	pos
Mbuti.DG	L.Caucasus_EBA	Büyükkaya_EC	ÇamlıbelTarlasi_LC	0.0009	0.278	0.003237	31089	31036	581302	pos
Mbuti.DG	Levant_MBA.SG	Büyükkaya_EC	ÇamlıbelTarlasi_LC	0.0007	0.241	0.002905	31471	31427	588770	pos
Mbuti.DG	G.Caucasus_b_EMBA	Büyükkaya_EC	ÇamlıbelTarlasi_LC	0.0005	0.180	0.002778	30653	30622	576655	pos
Mbuti.DG	CHG	Büyükkaya_EC	Caucasus_lowlands_LC.0101	0.0101	1.416	0.007133	8287	8122	155921	pos
Mbuti.DG	Iran_N.SG	Büyükkaya_EC	Caucasus_lowlands_LC.0068	0.0068	1.102	0.006171	8161	8050	155921	pos
Mbuti.DG	Iran_C	Büyükkaya_EC	Caucasus_lowlands_LC.0061	0.0061	1.068	0.005712	8229	8130	154557	pos
Mbuti.DG	G.Caucasus_a_En	Büyükkaya_EC	Caucasus_lowlands_LC.0012	0.0012	0.159	0.007547	7535	7517	141736	pos
Mbuti.DG	<b>Levant_EBA</b>	<b>Büyükkaya_EC</b>	<b>GondürleHöyük_EBA</b>	<b>0.0122</b>	<b>3.123</b>	0.003907	28999	28300	536649	pos
Mbuti.DG	G.Caucasus_b_EMBA	Büyükkaya_EC	GondürleHöyük_EBA	0.0096	2.931	0.003275	30710	30126	572517	pos
Mbuti.DG	Bulgaria_Varna_En3	Büyükkaya_EC	GondürleHöyük_EBA	0.0152	2.605	0.005835	15294	14836	281120	pos
Mbuti.DG	G.Caucasus_a_MLBA	Büyükkaya_EC	GondürleHöyük_EBA	0.01	2.379	0.004203	28312	27751	524426	pos
Mbuti.DG	G.Caucasus_a_En	Büyükkaya_EC	GondürleHöyük_EBA	0.0104	2.100	0.004952	25986	25452	482051	pos
Mbuti.DG	Iberia_C	Büyükkaya_EC	GondürleHöyük_EBA	0.0063	1.926	0.003271	31625	31227	583453	pos
Mbuti.DG	Levant_N	Büyükkaya_EC	GondürleHöyük_EBA	0.0078	1.913	0.004077	27680	27253	516239	pos
Mbuti.DG	Levant_MBA.SG	Büyükkaya_EC	GondürleHöyük_EBA	0.0058	1.752	0.003311	31230	30873	580955	pos
Mbuti.DG	Iran_N	Büyükkaya_EC	GondürleHöyük_EBA	0.007	1.486	0.004711	27105	26729	514529	pos
Mbuti.DG	CHG	Büyükkaya_EC	GondürleHöyük_EBA	0.0056	1.287	0.004351	31242	30894	585280	pos
Mbuti.DG	Late_Helladic	Büyükkaya_EC	GondürleHöyük_EBA	0.0057	1.186	0.004806	11452	11322	232759	pos
Mbuti.DG	Iran_N.SG	Büyükkaya_EC	GondürleHöyük_EBA	0.0043	1.164	0.003694	30810	30546	585350	pos
Mbuti.DG	Levant_C	Büyükkaya_EC	GondürleHöyük_EBA	0.0037	1.144	0.003234	31240	31010	580277	pos
Mbuti.DG	L.Caucasus_LBA.SG	Büyükkaya_EC	GondürleHöyük_EBA	0.005	1.075	0.004651	16692	16657	316523	pos
Mbuti.DG	Bulgaria_Varna_En2	Büyükkaya_EC	GondürleHöyük_EBA	0.0048	0.892	0.005381	16109	15957	299264	pos
Mbuti.DG	L.Caucasus_C	Büyükkaya_EC	GondürleHöyük_EBA	0.0016	0.463	0.003456	30686	30585	571994	pos
Mbuti.DG	Lasithi_MMinoan	Büyükkaya_EC	GondürleHöyük_EBA	0.0018	0.461	0.003905	30048	29942	558563	pos
Mbuti.DG	LBK_EN	Büyükkaya_EC	GondürleHöyük_EBA	0.0008	0.240	0.003333	31724	31675	585362	pos
Mbuti.DG	G.Caucasus_b_EMBA	Büyükkaya_EC	İkiztepe_LC	0.0079	2.328	0.003393	20667	20341	387374	pos
Mbuti.DG	G.Caucasus_a_En	Büyükkaya_EC	İkiztepe_LC	0.0102	2.052	0.004971	18396	18025	341798	pos
Mbuti.DG	Iran_N.SG	Büyükkaya_EC	İkiztepe_LC	0.0078	1.965	0.003969	20597	20280	391307	pos
Mbuti.DG	L.Caucasus_EBA	Büyükkaya_EC	İkiztepe_LC	0.0071	1.950	0.003641	20814	20521	388451	pos
Mbuti.DG	Iran_C	Büyükkaya_EC	İkiztepe_LC	0.0059	1.644	0.003589	20514	20273	385447	pos
Mbuti.DG	G.Caucasus_c_EMBA	Büyükkaya_EC	İkiztepe_LC	0.0079	1.475	0.005356	19073	18773	358060	pos
Mbuti.DG	G.Caucasus_a_EBA	Büyükkaya_EC	İkiztepe_LC	0.0043	1.267	0.003394	20692	20516	387336	pos
Mbuti.DG	L.Caucasus_MBA	Büyükkaya_EC	İkiztepe_LC	0.0057	1.124	0.005071	18799	18587	352099	pos
Mbuti.DG	Levant_MBA.SG	Büyükkaya_EC	İkiztepe_LC	0.0029	0.818	0.003545	20738	20619	388589	pos
Mbuti.DG	Balkans_C	Büyükkaya_EC	İkiztepe_LC	0.0033	0.550	0.006000	11562	11486	215846	pos

Mbuti.DG	Late_Helladic	Büyükkaya_EC	İkiztepe_LC	0.0029	0.496	0.005847	7566	7523	155431	pos
Mbuti.DG	Levant_EBA	Büyükkaya_EC	İkiztepe_LC	0.0018	0.448	0.004018	19784	19713	372202	pos
Mbuti.DG	G.Caucasus_a_MLBA	Büyükkaya_EC	K.Kalehöyük_MLBA	0.0042	0.646	0.006502	5157	5114	96583	pos
Mbuti.DG	Iran_N.SG	Büyükkaya_EC	K.Kalehöyük_MLBA	0.0027	0.447	0.006040	5764	5733	110998	pos
Mbuti.DG	G.Caucasus_b_En	Büyükkaya_EC	K.Kalehöyük_MLBA	0.0018	0.306	0.005882	5652	5632	106924	pos
Mbuti.DG	L.Caucasus_LBA.SG	Büyükkaya_EC	K.Kalehöyük_MLBA	0.0017	0.193	0.008808	2998	2988	57943	pos
Mbuti.DG	CHG	Büyükkaya_EC	Topakhöyük_EBA	0.0041	0.576	0.007118	5697	5650	107763	pos
Mbuti.DG	Iran_N.SG	TellKurdu_EC	Alalakh_MLBA	0.0098	4.426	0.002214	33631	32976	637395	pos
Mbuti.DG	CHG	TellKurdu_EC	Alalakh_MLBA	0.0081	3.302	0.002453	33946	33398	637359	pos
Mbuti.DG	Iran_N	TellKurdu_EC	Alalakh_MLBA	0.0077	2.707	0.002844	29352	28906	555239	pos
Mbuti.DG	G.Caucasus_b_En	TellKurdu_EC	Alalakh_MLBA	0.0005	2.230	0.002242	32967	32636	618265	pos
Mbuti.DG	G.Caucasus_c_EMBA	TellKurdu_EC	Alalakh_MLBA	0.0004	1.344	0.002976	28783	28555	541961	pos
Mbuti.DG	EHG	TellKurdu_EC	Alalakh_MLBA	0.0011	0.425	0.002588	32246	32174	608983	pos
Mbuti.DG	G.Caucasus_b_En	TellKurdu_EC	Arslantepe_EBA	0.0085	3.056	0.002781	32863	32310	613038	pos
Mbuti.DG	G.Caucasus_c_EMBA	TellKurdu_EC	Arslantepe_EBA	0.0097	2.669	0.003634	28916	28363	539854	pos
Mbuti.DG	Iran_N	TellKurdu_EC	Arslantepe_EBA	0.0076	2.313	0.003286	29166	28726	551703	pos
Mbuti.DG	G.Caucasus_b_EMBA	TellKurdu_EC	Arslantepe_EBA	0.0032	1.317	0.002430	32704	32495	612826	pos
Mbuti.DG	EHG	TellKurdu_EC	Arslantepe_EBA	0.0024	0.719	0.003338	32041	31888	602551	pos
Mbuti.DG	CHG	TellKurdu_EC	Arslantepe_LC	0.0143	5.498	0.002601	34044	33086	636987	pos
Mbuti.DG	Iran_N.SG	TellKurdu_EC	Arslantepe_LC	0.0117	5.143	0.002275	33536	32763	637022	pos
Mbuti.DG	G.Caucasus_b_En	TellKurdu_EC	Arslantepe_LC	0.0094	4.091	0.002298	33008	32391	618164	pos
Mbuti.DG	Iran_N	TellKurdu_EC	Arslantepe_LC	0.0102	3.506	0.002909	29307	28713	555186	pos
Mbuti.DG	EHG	TellKurdu_EC	Arslantepe_LC	0.0068	2.538	0.002679	32335	31895	608824	pos
Mbuti.DG	G.Caucasus_b_EMBA	TellKurdu_EC	Arslantepe_LC	0.0037	1.864	0.001985	32842	32599	617992	pos
Mbuti.DG	L.Caucasus_EBA	TellKurdu_EC	Arslantepe_LC	0.0001	0.494	0.002024	33172	33104	623165	pos
Mbuti.DG	Iran_C	TellKurdu_EC	Arslantepe_LC	0.0007	0.309	0.002265	32650	32607	615543	pos
Mbuti.DG	CHG	TellKurdu_EC	Barcin_C	0.0278	6.346	0.004381	32661	30893	600871	pos
Mbuti.DG	EHG	TellKurdu_EC	Barcin_C	0.0231	5.011	0.004610	31490	30069	579870	pos
Mbuti.DG	G.Caucasus_b_EMBA	TellKurdu_EC	Barcin_C	0.0123	3.629	0.003389	31723	30953	589888	pos
Mbuti.DG	Iran_N.SG	TellKurdu_EC	Barcin_C	0.0119	3.121	0.003813	31755	31009	600920	pos
Mbuti.DG	L.Caucasus_EBA	TellKurdu_EC	Barcin_C	0.0065	1.799	0.003613	31879	31466	593531	pos
Mbuti.DG	G.Caucasus_a_En	TellKurdu_EC	Barcin_C	0.0066	1.349	0.004893	26851	26497	499992	pos
Mbuti.DG	L.Caucasus_LBA.SG	TellKurdu_EC	Barcin_C	0.0059	1.189	0.004962	16987	16787	323806	pos
Mbuti.DG	G.Caucasus_a_EBA	TellKurdu_EC	Barcin_C	0.0003	0.887	0.003382	31527	31340	598657	pos
Mbuti.DG	G.Caucasus_a_MLBA	TellKurdu_EC	Barcin_C	0.0003	0.732	0.004098	29133	28957	544336	pos
Mbuti.DG	Bulgaria_Varna_En3	TellKurdu_EC	Barcin_C	0.0026	0.450	0.005778	15514	15433	289342	pos
Mbuti.DG	Iran_C	TellKurdu_EC	Barcin_C	0.0014	0.382	0.003665	31283	31198	587453	pos
Mbuti.DG	CHG	TellKurdu_EC	ÇamlıbelTarlası_LC	0.0161	5.952	0.002705	33806	32735	630436	pos
Mbuti.DG	G.Caucasus_b_En	TellKurdu_EC	ÇamlıbelTarlası_LC	0.0072	2.930	0.002457	32708	32242	613847	pos
Mbuti.DG	G.Caucasus_c_EMBA	TellKurdu_EC	ÇamlıbelTarlası_LC	0.0058	1.822	0.003183	28661	28328	539932	pos
Mbuti.DG	Iran_N	TellKurdu_EC	ÇamlıbelTarlası_LC	0.0032	1.031	0.003104	28948	28764	552150	pos
Mbuti.DG	L.Caucasus_EBA	TellKurdu_EC	ÇamlıbelTarlası_LC	0.0009	0.383	0.002350	32940	32883	618231	pos
Mbuti.DG	CHG	TellKurdu_EC	Caucasus_lowlands_LC 0.0164		2.718	0.006034	8909	8622	166803	pos
Mbuti.DG	G.Caucasus_b_En	TellKurdu_EC	Caucasus_lowlands_LC 0.0141		2.705	0.005213	8886	8639	165921	pos
Mbuti.DG	Iran_N.SG	TellKurdu_EC	Caucasus_lowlands_LC 0.011		2.118	0.005194	8734	8544	166803	pos
Mbuti.DG	EHG	TellKurdu_EC	Caucasus_lowlands_LC 0.0013		0.213	0.006103	8621	8598	163453	pos
Mbuti.DG	Iran_N.SG	TellKurdu_EC	Ebla_EMBA	0.0103	4.177	0.002466	32799	32130	621668	pos
Mbuti.DG	Iran_N	TellKurdu_EC	Ebla_EMBA	0.0069	2.208	0.003125	28963	28569	547558	pos
Mbuti.DG	G.Caucasus_c_EMBA	TellKurdu_EC	Ebla_EMBA	0.0018	0.546	0.003297	28399	28298	535989	pos
Mbuti.DG	CHG	TellKurdu_EC	GondürleHöyük_EBA	0.0198	5.849	0.003385	32376	31984	622129	pos
Mbuti.DG	G.Caucasus_b_En	TellKurdu_EC	GondürleHöyük_EBA	0.0161	5.403	0.002980	32654	31617	609109	pos
Mbuti.DG	G.Caucasus_b_EMBA	TellKurdu_EC	GondürleHöyük_EBA	0.0103	3.872	0.002660	32464	31802	609020	pos
Mbuti.DG	Iran_N.SG	TellKurdu_EC	GondürleHöyük_EBA	0.0098	3.353	0.002923	32546	31916	622183	pos
Mbuti.DG	G.Caucasus_c_EMBA	TellKurdu_EC	GondürleHöyük_EBA	0.0116	2.924	0.003967	28577	27924	538153	pos
Mbuti.DG	G.Caucasus_a_EBA	TellKurdu_EC	GondürleHöyük_EBA	0.0005	1.955	0.002558	32354	32030	608809	pos
Mbuti.DG	Bulgaria_Varna_En3	TellKurdu_EC	GondürleHöyük_EBA	0.0072	1.582	0.004551	15768	15542	293590	pos
Mbuti.DG	G.Caucasus_a_En	TellKurdu_EC	GondürleHöyük_EBA	0.0056	1.512	0.003704	27155	26850	510342	pos
Mbuti.DG	L.Caucasus_MBA	TellKurdu_EC	GondürleHöyük_EBA	0.0032	0.828	0.003865	28307	28125	533416	pos
Mbuti.DG	L.Caucasus_LBA.SG	TellKurdu_EC	GondürleHöyük_EBA	0.0012	0.295	0.004068	17260	17219	333028	pos
Mbuti.DG	CHG	TellKurdu_EC	İkiztepe_LC	0.0212	5.804	0.003653	22486	21553	418777	pos
Mbuti.DG	Iran_N.SG	TellKurdu_EC	İkiztepe_LC	0.0108	3.501	0.003085	22021	21552	418817	pos
Mbuti.DG	G.Caucasus_b_En	TellKurdu_EC	İkiztepe_LC	0.0101	3.326	0.003037	22162	21717	414757	pos
Mbuti.DG	G.Caucasus_c_EMBA	TellKurdu_EC	İkiztepe_LC	0.0113	2.743	0.004120	20448	19991	382891	pos
Mbuti.DG	Iran_N	TellKurdu_EC	İkiztepe_LC	0.0077	1.954	0.003941	20159	19852	384053	pos
Mbuti.DG	L.Caucasus_EBA	TellKurdu_EC	İkiztepe_LC	0.0056	1.945	0.002879	22231	21985	415747	pos
Mbuti.DG	Iran_C	TellKurdu_EC	İkiztepe_LC	0.0011	0.360	0.003056	21844	21797	412507	pos
Mbuti.DG	G.Caucasus_a_EBA	TellKurdu_EC	İkiztepe_LC	0.0006	0.237	0.002532	22012	21985	414501	pos
Mbuti.DG	L.Caucasus_MBA	TellKurdu_EC	İkiztepe_LC	0.0005	0.115	0.004348	19971	19953	375986	pos
Mbuti.DG	Iran_N.SG	TellKurdu_EC	K.Kalehöyük_MLBA	0.0144	2.806	0.005132	6180	6005	118398	pos
Mbuti.DG	G.Caucasus_b_En	TellKurdu_EC	K.Kalehöyük_MLBA	0.0105	2.050	0.005122	6075	5949	114231	pos
Mbuti.DG	G.Caucasus_c_EMBA	TellKurdu_EC	K.Kalehöyük_MLBA	0.0008	1.160	0.006897	5270	5186	99145	pos
Mbuti.DG	L.Caucasus_LBA.SG	TellKurdu_EC	K.Kalehöyük_MLBA	0.0071	0.927	0.007659	3171	3126	61221	pos
Mbuti.DG	EHG	TellKurdu_EC	K.Kalehöyük_MLBA	0.0051	0.855	0.005965	5901	5841	112590	pos
Mbuti.DG	Bulgaria_Varna_En3	TellKurdu_EC	K.Kalehöyük_MLBA	0.0003	0.033	0.009091	2778	2777	53117	pos
Mbuti.DG	CHG	TellKurdu_EC	Topakhöyük_EBA	0.0191	3.107	0.006147	6120	5890	114803	pos
Mbuti.DG	G.Caucasus_c_EMBA	TellKurdu_EC	Topakhöyük_EBA	0.0037	0.514	0.007198	5069	5032	96305	pos
Mbuti.DG	L.Caucasus_LBA.SG	TellKurdu_EC	Topakhöyük_EBA	0.0039	0.466	0.008369	3079	3055	59582	pos
Mbuti.DG	G.Caucasus_b_En	Barcin_N	Alalakh_MLBA	-0.000052	-0.366	0.000142	53292	53344	998728	neg
Mbuti.DG	G.Caucasus_b_EMBA	Barcin_N	Alalakh_MLBA	-0.000277	-2.318	0.000119	53133	53409	996413	neg
Mbuti.DG	Iran_C	Barcin_N	Alalakh_MLBA	-0.000331	-2.568	0.000129	53611	53944	1005536	neg
Mbuti.DG	G.Caucasus_a_En	Barcin_N	Alalakh_MLBA	-0.000675	-3.710	0.000182	40020	40529	753671	neg
Mbuti.DG	G.Caucasus_a_MLBA	Barcin_N	Alalakh_MLBA	-0.000586	-3.869	0.000151	44726	45218	840209	neg
Mbuti.DG	Samara_En	Barcin_N	Alalakh_MLBA	-0.000636	-4.175	0.000152	39362	39836	745485	neg
Mbuti.DG	L.Caucasus_MBA	Barcin_N	Alalakh_MLBA	-0.00075	-4.262	0.000176	43527	44140	817229	neg
Mbuti.DG	G.Caucasus_a_EBA	Barcin_N	Alalakh_MLBA	-0.000571	-4.663	0.000122	53089	53658	996869	neg
Mbuti.DG	L.Caucasus_LBA.SG	Barcin_N	Alalakh_MLBA	-0.000822	-5.295	0.000155	27552	27989	531212	neg
Mbuti.DG	L.Caucasus_EBA	Barcin_N	Alalakh_MLBA	-0.000748	-5.959	0.000126	54637	55404	1025853	neg
Mbuti.DG	EHG	Barcin_N	Alalakh_MLBA	-0.001182	-7.470	0.000158	52784	53972	1004586	neg
Mbuti.DG	Levant_EBA	Barcin_N	Alalakh_MLBA	-0.001178	-8.702	0.000135	45911	46934	867966	neg
Mbuti.DG	Bulgaria_Varna_En3	Barcin_N	Alalakh_MLBA	-0.001784	-9.413	0.000190	21379	22102	405260	neg
Mbuti.DG	L.Caucasus_C	Barcin_N	Alalakh_MLBA	-0.001322	-10.190	0.000130	53729	55067	1012860	neg
Mbuti.DG	Levant_MBA.SG	Barcin_N	Alalakh_MLBA	-0.001352	-10.771	0.000126	58038	59514	1092574	neg

Mbuti.DG	Srubnaya	Barcin_N	Alalakh_MLBA	-0.001486	-11.644	0.000128	57721	59334	1085367	neg
Mbuti.DG	Levant_EP	Barcin_N	Alalakh_MLBA	-0.00201	-11.647	0.000173	27358	28419	528047	neg
Mbuti.DG	Late_Helladic	Barcin_N	Alalakh_MLBA	-0.001878	-12.147	0.000155	21087	21906	436014	neg
Mbuti.DG	SHG	Barcin_N	Alalakh_MLBA	-0.001914	-12.473	0.000153	53372	55318	1016685	neg
Mbuti.DG	Levant_N	Barcin_N	Alalakh_MLBA	-0.002359	-16.031	0.000147	43846	45819	836748	neg
Mbuti.DG	WHG	Barcin_N	Alalakh_MLBA	-0.002494	-16.419	0.000152	57857	60605	1101873	neg
Mbuti.DG	Bulgaria_Varna_En2	Barcin_N	Alalakh_MLBA	-0.003163	-16.473	0.000192	22940	24324	437849	neg
Mbuti.DG	Levant_C	Barcin_N	Alalakh_MLBA	-0.00217	-18.453	0.000118	54975	57232	1040166	neg
Mbuti.DG	Tepecik_N	Barcin_N	Alalakh_MLBA	-0.003162	-19.186	0.000165	37686	39977	724699	neg
Mbuti.DG	Balkans_C	Barcin_N	Alalakh_MLBA	-0.003807	-19.675	0.000193	25454	27322	490758	neg
Mbuti.DG	Greece_N	Barcin_N	Alalakh_MLBA	-0.004274	-22.077	0.000194	39837	43088	760720	neg
Mbuti.DG	Lasithi_MMinoan	Barcin_N	Alalakh_MLBA	-0.0292	-23.010	0.001269	51699	54811	989968	neg
Mbuti.DG	Boncuklu_N.SG	Barcin_N	Alalakh_MLBA	-0.004755	-24.706	0.000192	52107	56895	1007057	neg
Mbuti.DG	Iberia_C	Barcin_N	Alalakh_MLBA	-0.003715	-30.378	0.000122	56264	60254	1074255	neg
Mbuti.DG	Balkans_N	Barcin_N	Alalakh_MLBA	-0.004282	-30.416	0.000141	53891	58319	1034044	neg
Mbuti.DG	Boncuklu_N	Barcin_N	Alalakh_MLBA	-0.004959	-33.515	0.000148	55549	60853	1069643	neg
Mbuti.DG	LBK_EN	Barcin_N	Alalakh_MLBA	-0.004279	-34.251	0.000125	57689	62395	1099789	neg
Mbuti.DG	G.Caucasus_a_MLBA	Barcin_N	Arslantepe_EBA	-0.000084	-0.375	0.000224	44230	44300	828603	neg
Mbuti.DG	L.Caucasus_MBA	Barcin_N	Arslantepe_EBA	-0.000105	-0.394	0.000266	42859	42943	801656	neg
Mbuti.DG	Iran_C	Barcin_N	Arslantepe_EBA	-0.000162	-0.901	0.000180	51730	51887	971749	neg
Mbuti.DG	G.Caucasus_a_EBA	Barcin_N	Arslantepe_EBA	-0.000239	-1.300	0.000184	51701	51933	970046	neg
Mbuti.DG	Samara_En	Barcin_N	Arslantepe_EBA	-0.000385	-1.647	0.000234	38338	38617	725623	neg
Mbuti.DG	L.Caucasus_EBA	Barcin_N	Arslantepe_EBA	-0.00036	-1.953	0.000184	52840	53197	991413	neg
Mbuti.DG	L.Caucasus_LBA.SG	Barcin_N	Arslantepe_EBA	-0.000546	-2.441	0.000224	26720	27000	514487	neg
Mbuti.DG	EHG	Barcin_N	Arslantepe_EBA	-0.000985	-4.203	0.000234	50824	51777	967983	neg
Mbuti.DG	Bulgaria_Varna_En3	Barcin_N	Arslantepe_EBA	-0.001415	-4.671	0.000303	21230	21799	402323	neg
Mbuti.DG	Levant_EBA	Barcin_N	Arslantepe_EBA	-0.001151	-5.821	0.000198	45149	46133	855028	neg
Mbuti.DG	L.Caucasus_C	Barcin_N	Arslantepe_EBA	-0.001157	-5.843	0.000198	51891	53024	978994	neg
Mbuti.DG	Levant_MBA.SG	Barcin_N	Arslantepe_EBA	-0.001225	-7.075	0.000173	54736	56003	1034328	neg
Mbuti.DG	Late_Helladic	Barcin_N	Arslantepe_EBA	-0.001691	-7.290	0.000232	20387	21100	421741	neg
Mbuti.DG	Srubnaya	Barcin_N	Arslantepe_EBA	-0.001432	-7.918	0.000181	54819	56300	1034191	neg
Mbuti.DG	Levant_EP	Barcin_N	Arslantepe_EBA	-0.002263	-8.592	0.000263	26819	27995	519873	neg
Mbuti.DG	SHG	Barcin_N	Arslantepe_EBA	-0.002006	-9.403	0.000213	51247	53212	979871	neg
Mbuti.DG	Levant_N	Barcin_N	Arslantepe_EBA	-0.00218	-10.352	0.000211	43051	44843	822002	neg
Mbuti.DG	Bulgaria_Varna_En2	Barcin_N	Arslantepe_EBA	-0.003252	-11.637	0.000279	22652	24063	433973	neg
Mbuti.DG	WHG	Barcin_N	Arslantepe_EBA	-0.00269	-11.901	0.000226	54381	57186	1042783	neg
Mbuti.DG	Levant_C	Barcin_N	Arslantepe_EBA	-0.002159	-12.492	0.000173	52880	55049	1004487	neg
Mbuti.DG	Tepecik_N	Barcin_N	Arslantepe_EBA	-0.002944	-12.582	0.000234	35815	37847	690138	neg
Mbuti.DG	Balkans_C	Barcin_N	Arslantepe_EBA	-0.003723	-13.177	0.000283	24856	26642	479846	neg
Mbuti.DG	Greece_N	Barcin_N	Arslantepe_EBA	-0.004001	-14.960	0.000267	39113	42100	746697	neg
Mbuti.DG	Lasithi_MMinoan	Barcin_N	Arslantepe_EBA	-0.0285	-15.171	0.001879	49816	52734	955782	neg
Mbuti.DG	Boncuklu_N.SG	Barcin_N	Arslantepe_EBA	-0.004298	-16.295	0.000264	49505	53615	956288	neg
Mbuti.DG	Iberia_C	Barcin_N	Arslantepe_EBA	-0.003602	-19.333	0.000186	53721	57423	1027831	neg
Mbuti.DG	Balkans_N	Barcin_N	Arslantepe_EBA	-0.003974	-20.577	0.000193	52012	55976	997588	neg
Mbuti.DG	LBK_EN	Barcin_N	Arslantepe_EBA	-0.004058	-22.334	0.000182	54554	58783	1042100	neg
Mbuti.DG	Boncuklu_N	Barcin_N	Arslantepe_EBA	-0.004804	-22.685	0.000212	52889	57792	1020484	neg
Mbuti.DG	L.Caucasus_MBA	Barcin_N	Arslantepe_LC	-0.00004	-0.214	0.000187	43595	43627	816848	neg
Mbuti.DG	L.Caucasus_EBA	Barcin_N	Arslantepe_LC	-0.000109	-0.839	0.000130	54669	54780	1024750	neg
Mbuti.DG	Samara_En	Barcin_N	Arslantepe_LC	-0.000254	-1.651	0.000154	39280	39469	744782	neg
Mbuti.DG	L.Caucasus_LBA.SG	Barcin_N	Arslantepe_LC	-0.000458	-2.950	0.000155	27524	27767	530601	neg
Mbuti.DG	EHG	Barcin_N	Arslantepe_LC	-0.000508	-3.169	0.000160	52808	53318	1003277	neg
Mbuti.DG	L.Caucasus_C	Barcin_N	Arslantepe_LC	-0.000792	-6.035	0.000131	53730	54531	1011836	neg
Mbuti.DG	Bulgaria_Varna_En3	Barcin_N	Arslantepe_LC	-0.001438	-7.032	0.000204	21326	21909	405250	neg
Mbuti.DG	Levant_EBA	Barcin_N	Arslantepe_LC	-0.000979	-7.157	0.000137	45785	46634	867905	neg
Mbuti.DG	Levant_MBA.SG	Barcin_N	Arslantepe_LC	-0.000998	-7.678	0.000130	57760	58846	1089120	neg
Mbuti.DG	Srubnaya	Barcin_N	Arslantepe_LC	-0.001053	-8.610	0.000122	57594	58735	1083132	neg
Mbuti.DG	Late_Helladic	Barcin_N	Arslantepe_LC	-0.00147	-9.440	0.000156	21081	21722	435901	neg
Mbuti.DG	SHG	Barcin_N	Arslantepe_LC	-0.001431	-9.899	0.000145	53300	54752	1015368	neg
Mbuti.DG	Levant_EP	Barcin_N	Arslantepe_LC	-0.002065	-11.581	0.000178	27185	28275	527825	neg
Mbuti.DG	Bulgaria_Varna_En2	Barcin_N	Arslantepe_LC	-0.002573	-13.438	0.000191	22966	24092	437822	neg
Mbuti.DG	Levant_C	Barcin_N	Arslantepe_LC	-0.001611	-13.470	0.000120	54975	56649	1039492	neg
Mbuti.DG	Levant_N	Barcin_N	Arslantepe_LC	-0.002009	-13.531	0.000148	43793	45474	836447	neg
Mbuti.DG	WHG	Barcin_N	Arslantepe_LC	-0.002092	-13.634	0.000153	57627	59925	1098405	neg
Mbuti.DG	Tepecik_N	Barcin_N	Arslantepe_LC	-0.002578	-15.161	0.000170	37622	39485	722658	neg
Mbuti.DG	Balkans_C	Barcin_N	Arslantepe_LC	-0.003129	-15.979	0.000196	25506	27041	494056	neg
Mbuti.DG	Greece_N	Barcin_N	Arslantepe_LC	-0.003484	-17.958	0.000194	39971	42619	760199	neg
Mbuti.DG	Lasithi_MMinoan	Barcin_N	Arslantepe_LC	-0.0243	-18.768	0.001295	51659	54236	988795	neg
Mbuti.DG	Boncuklu_N.SG	Barcin_N	Arslantepe_LC	-0.003986	-21.549	0.000185	52123	56125	1004063	neg
Mbuti.DG	Iberia_C	Barcin_N	Arslantepe_LC	-0.003164	-25.295	0.000125	56253	59647	1072624	neg
Mbuti.DG	Balkans_N	Barcin_N	Arslantepe_LC	-0.003703	-26.399	0.000140	53892	57718	1033051	neg
Mbuti.DG	Boncuklu_N	Barcin_N	Arslantepe_LC	-0.004304	-29.181	0.000147	55525	60117	1066989	neg
Mbuti.DG	LBK_EN	Barcin_N	Arslantepe_LC	-0.00358	-29.245	0.000122	57666	61591	1096636	neg
Mbuti.DG	Srubnaya	Barcin_N	Barcin_C	-0.000048	-0.162	0.000296	50699	50744	947463	neg
Mbuti.DG	SHG	Barcin_N	Barcin_C	-0.00013	-0.374	0.000348	48152	48270	906607	neg
Mbuti.DG	L.Caucasus_MBA	Barcin_N	Barcin_C	-0.000231	-0.544	0.000425	40533	40710	764398	neg
Mbuti.DG	L.Caucasus_C	Barcin_N	Barcin_C	-0.000223	-0.719	0.000310	48517	48720	911384	neg
Mbuti.DG	Bulgaria_Varna_En3	Barcin_N	Barcin_C	-0.000659	-1.350	0.000488	20688	20945	390048	neg
Mbuti.DG	WHG	Barcin_N	Barcin_C	-0.000628	-1.696	0.000370	50526	51125	952486	neg
Mbuti.DG	Levant_MBA.SG	Barcin_N	Barcin_C	-0.000883	-2.831	0.000312	49946	50781	945075	neg
Mbuti.DG	Levant_EP	Barcin_N	Barcin_C	-0.001402	-3.321	0.000422	25699	26397	498381	neg
Mbuti.DG	Levant_EBA	Barcin_N	Barcin_C	-0.001189	-3.497	0.000340	42685	43652	813023	neg
Mbuti.DG	Late_Helladic	Barcin_N	Barcin_C	-0.001533	-4.093	0.000375	18362	18947	381976	neg
Mbuti.DG	Bulgaria_Varna_En2	Barcin_N	Barcin_C	-0.002203	-4.772	0.000462	21967	22890	419121	neg
Mbuti.DG	Tepecik_N	Barcin_N	Barcin_C	-0.001996	-5.367	0.000372	33104	34372	635370	neg
Mbuti.DG	Levant_C	Barcin_N	Barcin_C	-0.001644	-5.696	0.000289	48911	50437	928839	neg
Mbuti.DG	Balkans_C	Barcin_N	Barcin_C	-0.002738	-5.916	0.000463	23644	24889	454896	neg
Mbuti.DG	Levant_N	Barcin_N	Barcin_C	-0.002305	-6.580	0.000350	40636	42436	781172	neg
Mbuti.DG	Lasithi_MMinoan	Barcin_N	Barcin_C	-0.0209	-6.587	0.003173	46369	48351	886787	neg
Mbuti.DG	Boncuklu_N.SG	Barcin_N	Barcin_C	-0.002863	-6.628	0.000432	45866	48377	877115	neg
Mbuti.DG	Greece_N	Barcin_N	Barcin_C	-0.00316	-6.804	0.000464	37459	39714	713633	neg
Mbuti.DG	Iberia_C	Barcin_N	Barcin_C	-0.002156	-7.253	0.000297	49776	51809	943081	neg
Mbuti.DG	Balkans_N	Barcin_N	Barcin_C	-0.002605	-7.825	0.000333	48583	50987	922846	neg



Mbuti.DG	Boncuklu_N	Barcin_N	Barcin_C	-0.003125	-8.980	0.000348	49159	52086	936655	neg
Mbuti.DG	LBK_EN	Barcin_N	Barcin_C	-0.002747	-9.128	0.000301	50244	52859	952168	neg
Mbuti.DG	G.Caucasus_c_EMBA	Barcin_N	ÇamlıbelTarlası_LC	-0.000038	-0.185	0.000205	41485	41515	786200	neg
Mbuti.DG	L.Caucasus_MBA	Barcin_N	ÇamlıbelTarlası_LC	-0.000007	-0.346	0.000202	42928	42984	806176	neg
Mbuti.DG	Iran_C	Barcin_N	ÇamlıbelTarlası_LC	-0.000097	-0.649	0.000149	52190	52286	983004	neg
Mbuti.DG	G.Caucasus_a_MLBA	Barcin_N	ÇamlıbelTarlası_LC	-0.000163	-0.931	0.000175	44173	44308	831403	neg
Mbuti.DG	L.Caucasus_LBA.SG	Barcin_N	ÇamlıbelTarlası_LC	-0.000291	-1.593	0.000183	26945	27096	520559	neg
Mbuti.DG	G.Caucasus_b_EMBA	Barcin_N	ÇamlıbelTarlası_LC	-0.000353	-2.563	0.000138	51734	52079	977807	neg
Mbuti.DG	G.Caucasus_a_EBA	Barcin_N	ÇamlıbelTarlası_LC	-0.000391	-2.747	0.000142	51858	52240	977907	neg
Mbuti.DG	L.Caucasus_EBA	Barcin_N	ÇamlıbelTarlası_LC	-0.000421	-2.891	0.000146	53223	53645	1002786	neg
Mbuti.DG	Samara_En	Barcin_N	ÇamlıbelTarlası_LC	-0.000619	-3.213	0.000193	38394	38847	731832	neg
Mbuti.DG	EHG	Barcin_N	ÇamlıbelTarlası_LC	-0.000839	-4.530	0.000185	51273	52095	979831	neg
Mbuti.DG	Bulgaria_Varna_En3	Barcin_N	ÇamlıbelTarlası_LC	-0.001141	-5.086	0.000224	21239	21699	403034	neg
Mbuti.DG	Srubnaya	Barcin_N	ÇamlıbelTarlası_LC	-0.00095	-6.650	0.000143	55905	56905	1052592	neg
Mbuti.DG	L.Caucasus_C	Barcin_N	ÇamlıbelTarlası_LC	-0.001071	-6.813	0.000157	52331	53391	990350	neg
Mbuti.DG	Levant_MBA.SG	Barcin_N	ÇamlıbelTarlası_LC	-0.001141	-8.113	0.000141	55779	56984	1056042	neg
Mbuti.DG	Levant_EBA	Barcin_N	ÇamlıbelTarlası_LC	-0.001539	-9.622	0.000160	44921	46241	857888	neg
Mbuti.DG	Late_Helladic	Barcin_N	ÇamlıbelTarlası_LC	-0.00174	-9.723	0.000179	20447	21185	424338	neg
Mbuti.DG	SHG	Barcin_N	ÇamlıbelTarlası_LC	-0.00175	-10.479	0.000167	51818	53553	991809	neg
Mbuti.DG	WHG	Barcin_N	ÇamlıbelTarlası_LC	-0.001888	-10.644	0.000177	55849	57859	1064834	neg
Mbuti.DG	Tepecik_N	Barcin_N	ÇamlıbelTarlası_LC	-0.002106	-10.644	0.000198	36726	38207	703134	neg
Mbuti.DG	Levant_EP	Barcin_N	ÇamlıbelTarlası_LC	-0.002351	-11.756	0.000200	26734	27961	521999	neg
Mbuti.DG	Bulgaria_Varna_En2	Barcin_N	ÇamlıbelTarlası_LC	-0.002838	-12.452	0.000228	22708	23942	434760	neg
Mbuti.DG	Balkans_C	Barcin_N	ÇamlıbelTarlası_LC	-0.002984	-12.765	0.000234	25126	26567	482882	neg
Mbuti.DG	Lasithi_MMinoan	Barcin_N	ÇamlıbelTarlası_LC	-0.00218	-14.002	0.001557	50597	52853	966701	neg
Mbuti.DG	Levant_N	Barcin_N	ÇamlıbelTarlası_LC	-0.002551	-14.907	0.000171	42876	44982	825696	neg
Mbuti.DG	Greece_N	Barcin_N	ÇamlıbelTarlası_LC	-0.003523	-15.412	0.000229	39376	42021	750573	neg
Mbuti.DG	Levant_C	Barcin_N	ÇamlıbelTarlası_LC	-0.002116	-15.946	0.000133	53329	55479	1015793	neg
Mbuti.DG	Boncuklu_N.SG	Barcin_N	ÇamlıbelTarlası_LC	-0.003803	-17.069	0.000223	50643	54352	975306	neg
Mbuti.DG	Balkans_N	Barcin_N	ÇamlıbelTarlası_LC	-0.003431	-21.339	0.000161	52727	56190	1009310	neg
Mbuti.DG	Iberia_C	Barcin_N	ÇamlıbelTarlası_LC	-0.003125	-21.813	0.000143	54654	57916	1043879	neg
Mbuti.DG	Boncuklu_N	Barcin_N	ÇamlıbelTarlası_LC	-0.003843	-22.974	0.000167	54236	58225	1038060	neg
Mbuti.DG	LBK_EN	Barcin_N	ÇamlıbelTarlası_LC	-0.003374	-24.953	0.000135	55919	59507	1063419	neg
Mbuti.DG	G.Caucasus_b_EMBA	Barcin_N	Caucasus_lowlands_LC	-0.000132	-0.339	0.000389	11256	11284	212361	neg
Mbuti.DG	G.Caucasus_a_En	Barcin_N	Caucasus_lowlands_LC	-0.000206	-0.349	0.000590	9895	9933	186437	neg
Mbuti.DG	L.Caucasus_LBA.SG	Barcin_N	Caucasus_lowlands_LC	-0.000265	-0.448	0.000592	6276	6308	121361	neg
Mbuti.DG	L.Caucasus_MBA	Barcin_N	Caucasus_lowlands_LC	-0.000431	-0.740	0.000582	10236	10319	192517	neg
Mbuti.DG	Samara_En	Barcin_N	Caucasus_lowlands_LC	-0.000429	-0.800	0.000536	8931	9004	169721	neg
Mbuti.DG	EHG	Barcin_N	Caucasus_lowlands_LC	-0.000454	-0.895	0.000507	11034	11129	209139	neg
Mbuti.DG	G.Caucasus_a_EBA	Barcin_N	Caucasus_lowlands_LC	-0.000392	-0.990	0.000396	11246	11330	212254	neg
Mbuti.DG	G.Caucasus_a_MLBA	Barcin_N	Caucasus_lowlands_LC	-0.00052	-1.051	0.000495	10608	10712	199951	neg
Mbuti.DG	L.Caucasus_EBA	Barcin_N	Caucasus_lowlands_LC	-0.000899	-2.282	0.000394	11265	11457	213265	neg
Mbuti.DG	L.Caucasus_C	Barcin_N	Caucasus_lowlands_LC	-0.001141	-2.686	0.000425	11207	11449	212316	neg
Mbuti.DG	Srubnaya	Barcin_N	Caucasus_lowlands_LC	-0.001525	-3.808	0.000400	11360	11688	215362	neg
Mbuti.DG	Late_Helladic	Barcin_N	Caucasus_lowlands_LC	-0.002243	-3.880	0.000578	4206	4403	87802	neg
Mbuti.DG	Bulgaria_Varna_En3	Barcin_N	Caucasus_lowlands_LC	-0.002757	-3.906	0.000706	5898	6213	113964	neg
Mbuti.DG	Levant_EP	Barcin_N	Caucasus_lowlands_LC	-0.002394	-4.094	0.000585	6941	7268	136210	neg
Mbuti.DG	Levant_MBA.SG	Barcin_N	Caucasus_lowlands_LC	-0.001818	-4.247	0.000428	11239	11629	214345	neg
Mbuti.DG	Levant_EBA	Barcin_N	Caucasus_lowlands_LC	-0.00192	-4.323	0.000444	10589	10978	202932	neg
Mbuti.DG	Tepecik_N	Barcin_N	Caucasus_lowlands_LC	-0.002937	-4.863	0.000604	7741	8181	149889	neg
Mbuti.DG	Bulgaria_Varna_En2	Barcin_N	Caucasus_lowlands_LC	-0.003207	-4.916	0.000652	6380	6774	122955	neg
Mbuti.DG	SHG	Barcin_N	Caucasus_lowlands_LC	-0.002243	-5.040	0.000445	10989	11463	211100	neg
Mbuti.DG	Levant_N	Barcin_N	Caucasus_lowlands_LC	-0.002808	-5.719	0.000491	10249	10804	197470	neg
Mbuti.DG	Balkans_C	Barcin_N	Caucasus_lowlands_LC	-0.004042	-6.158	0.000656	6215	6701	120296	neg
Mbuti.DG	WHG	Barcin_N	Caucasus_lowlands_LC	-0.003322	-7.143	0.000465	11121	11838	215706	neg
Mbuti.DG	Levant_C	Barcin_N	Caucasus_lowlands_LC	-0.002727	-7.148	0.000382	11166	11750	214122	neg
Mbuti.DG	Boncuklu_N.SG	Barcin_N	Caucasus_lowlands_LC	-0.005102	-8.902	0.000573	10392	11426	202686	neg
Mbuti.DG	Greece_N	Barcin_N	Caucasus_lowlands_LC	-0.005789	-9.927	0.000583	9510	10585	185741	neg
Mbuti.DG	Iberia_C	Barcin_N	Caucasus_lowlands_LC	-0.004308	-10.954	0.000393	11100	12026	215130	neg
Mbuti.DG	Balkans_N	Barcin_N	Caucasus_lowlands_LC	-0.004867	-11.287	0.000431	11004	12043	213436	neg
Mbuti.DG	Boncuklu_N	Barcin_N	Caucasus_lowlands_LC	-0.005313	-11.847	0.000448	11012	12151	214386	neg
Mbuti.DG	LBK_EN	Barcin_N	Caucasus_lowlands_LC	-0.0048	-12.129	0.000396	11149	12184	215704	neg
Mbuti.DG	G.Caucasus_c_EMBA	Barcin_N	Ebla_EMBA	-0.000362	-1.645	0.000220	40878	41158	772471	neg
Mbuti.DG	Iran_C	Barcin_N	Ebla_EMBA	-0.000418	-2.601	0.000161	50711	51109	952843	neg
Mbuti.DG	G.Caucasus_b_En	Barcin_N	Ebla_EMBA	-0.000561	-3.088	0.000182	50398	50931	950872	neg
Mbuti.DG	G.Caucasus_a_MLBA	Barcin_N	Ebla_EMBA	-0.000695	-3.431	0.000203	43325	43891	814397	neg
Mbuti.DG	L.Caucasus_MBA	Barcin_N	Ebla_EMBA	-0.000914	-3.822	0.000239	41906	42626	788253	neg
Mbuti.DG	G.Caucasus_a_En	Barcin_N	Ebla_EMBA	-0.000958	-4.083	0.000235	38765	39467	732495	neg
Mbuti.DG	Samara_En	Barcin_N	Ebla_EMBA	-0.001005	-4.518	0.000222	37495	38212	713122	neg
Mbuti.DG	G.Caucasus_b_EMBA	Barcin_N	Ebla_EMBA	-0.000722	-4.643	0.000156	50369	51054	949561	neg
Mbuti.DG	L.Caucasus_EBA	Barcin_N	Ebla_EMBA	-0.000885	-5.534	0.000160	51552	52411	970334	neg
Mbuti.DG	L.Caucasus_LBA.SG	Barcin_N	Ebla_EMBA	-0.001183	-5.643	0.000210	26068	26666	504873	neg
Mbuti.DG	G.Caucasus_a_EBA	Barcin_N	Ebla_EMBA	-0.000973	-6.010	0.000162	50288	51212	949225	neg
Mbuti.DG	EHG	Barcin_N	Ebla_EMBA	-0.001456	-7.079	0.000206	49556	50936	947293	neg
Mbuti.DG	Levant_EBA	Barcin_N	Ebla_EMBA	-0.001491	-8.240	0.000181	44266	45518	839447	neg
Mbuti.DG	Levant_EP	Barcin_N	Ebla_EMBA	-0.002013	-8.621	0.000233	26654	27690	514535	neg
Mbuti.DG	Levant_MBA.SG	Barcin_N	Ebla_EMBA	-0.001376	-8.633	0.000159	53708	55102	1013121	neg
Mbuti.DG	Bulgaria_Varna_En3	Barcin_N	Ebla_EMBA	-0.002334	-9.231	0.000253	20824	21752	397334	neg
Mbuti.DG	L.Caucasus_C	Barcin_N	Ebla_EMBA	-0.001649	-9.602	0.000172	50695	52276	959181	neg
Mbuti.DG	Late_Helladic	Barcin_N	Ebla_EMBA	-0.002219	-10.506	0.000211	19712	20621	409525	neg
Mbuti.DG	SHG	Barcin_N	Ebla_EMBA	-0.002406	-11.995	0.000201	50012	52318	958524	neg
Mbuti.DG	Srubnaya	Barcin_N	Ebla_EMBA	-0.00197	-12.805	0.000154	53441	55434	1011560	neg
Mbuti.DG	Levant_N	Barcin_N	Ebla_EMBA	-0.002605	-13.906	0.000187	42341	44450	809880	neg
Mbuti.DG	Bulgaria_Varna_En2	Barcin_N	Ebla_EMBA	-0.003621	-14.511	0.000250	22361	23915	429237	neg
Mbuti.DG	WHG	Barcin_N	Ebla_EMBA	-0.003032	-15.010	0.000202	53202	56298	1020996	neg
Mbuti.DG	Levant_C	Barcin_N	Ebla_EMBA	-0.002403	-15.541	0.000155	51735	54094	981907	neg
Mbuti.DG	Balkans_C	Barcin_N	Ebla_EMBA	-0.004215	-16.477	0.000256	24379	26371	472499	neg
Mbuti.DG	Tepecik_N	Barcin_N	Ebla_EMBA	-0.003512	-16.503	0.000213	35055	37434	677429	neg
Mbuti.DG	Greece_N	Barcin_N	Ebla_EMBA	-0.004404	-17.315	0.000254	38544	41794	737829	neg
Mbuti.DG	Lasithi_MMinoan	Barcin_N	Ebla_EMBA	-0.00329	-19.742	0.001666	48626	51937	935542	neg
Mbuti.DG	Boncuklu_N.SG	Barcin_N	Ebla_EMBA	-0.005311	-22.398	0.000237	48179	53160	937653	neg
Mbuti.DG	Iberia_C	Barcin_N	Ebla_EMBA	-0.004211	-26.329	0.000160	52275	56505	1004546	neg

Mbuti.DG	Balkans_N	Barcin_N	Ebla_EMBA	-0.004883	-27.398	0.000178	50539	55302	975410	neg
Mbuti.DG	Boncuklu_N	Barcin_N	Ebla_EMBA	-0.005406	-29.209	0.000185	51631	57038	1000258	neg
Mbuti.DG	LBK_EN	Barcin_N	Ebla_EMBA	-0.004706	-29.882	0.000157	53165	57966	1020082	neg
Mbuti.DG	Levant_EBA	Barcin_N	GondürleHöyük_EBA	-0.000055	-0.243	0.000226	45123	45170	852809	neg
Mbuti.DG	L.Caucasus_LBA.SG	Barcin_N	GondürleHöyük_EBA	-0.000071	-0.273	0.000260	26309	26345	508854	neg
Mbuti.DG	L.Caucasus_C	Barcin_N	GondürleHöyük_EBA	-0.000145	-0.628	0.000231	51276	51416	965754	neg
Mbuti.DG	Bulgaria_Varna_En3	Barcin_N	GondürleHöyük_EBA	-0.000227	-0.672	0.000338	21270	21361	400884	neg
Mbuti.DG	Srubnaya	Barcin_N	GondürleHöyük_EBA	-0.000167	-0.823	0.000203	53945	54114	1013215	neg
Mbuti.DG	SHG	Barcin_N	GondürleHöyük_EBA	-0.000551	-2.268	0.000243	50605	51135	962556	neg
Mbuti.DG	Levant_MBA.SG	Barcin_N	GondürleHöyük_EBA	-0.000593	-2.992	0.000198	53443	54043	1012089	neg
Mbuti.DG	Late_Helladic	Barcin_N	GondürleHöyük_EBA	-0.000861	-3.353	0.000257	19836	20189	410328	neg
Mbuti.DG	WHG	Barcin_N	GondürleHöyük_EBA	-0.000901	-3.402	0.000265	53750	54670	1020454	neg
Mbuti.DG	Bulgaria_Varna_En2	Barcin_N	GondürleHöyük_EBA	-0.001472	-4.530	0.000325	22801	23438	432451	neg
Mbuti.DG	Levant_N	Barcin_N	GondürleHöyük_EBA	-0.001129	-4.735	0.000238	42901	43825	818426	neg
Mbuti.DG	Levant_EP	Barcin_N	GondürleHöyük_EBA	-0.001669	-5.704	0.000293	26587	27451	517693	neg
Mbuti.DG	Levant_C	Barcin_N	GondürleHöyük_EBA	-0.001155	-5.818	0.000199	52270	53416	991707	neg
Mbuti.DG	Lasithi_MMinoan	Barcin_N	GondürleHöyük_EBA	-0.0138	-6.260	0.002204	49348	50725	939477	neg
Mbuti.DG	Balkans_C	Barcin_N	GondürleHöyük_EBA	-0.002335	-7.189	0.000325	24706	25813	474075	neg
Mbuti.DG	Tepecik_N	Barcin_N	GondürleHöyük_EBA	-0.00195	-7.264	0.000268	35202	36522	677203	neg
Mbuti.DG	Greece_N	Barcin_N	GondürleHöyük_EBA	-0.002621	-8.249	0.000318	39016	40958	740672	neg
Mbuti.DG	Iberia_C	Barcin_N	GondürleHöyük_EBA	-0.001756	-8.259	0.000213	53274	55045	1008745	neg
Mbuti.DG	Boncuklu_N.SG	Barcin_N	GondürleHöyük_EBA	-0.003182	-10.492	0.000303	48682	51664	937195	neg
Mbuti.DG	Boncuklu_N	Barcin_N	GondürleHöyük_EBA	-0.002751	-11.896	0.000231	52475	55225	999646	neg
Mbuti.DG	Balkans_N	Barcin_N	GondürleHöyük_EBA	-0.002724	-12.009	0.000227	51426	54100	981681	neg
Mbuti.DG	LBK_EN	Barcin_N	GondürleHöyük_EBA	-0.002455	-12.660	0.000194	53809	56313	1020024	neg
Mbuti.DG	L.Caucasus_MBA	Barcin_N	İkiztepe_LC	-0.000059	-0.197	0.000299	26975	27005	506050	neg
Mbuti.DG	L.Caucasus_LBA.SG	Barcin_N	İkiztepe_LC	-0.000203	-0.661	0.000307	16424	16488	316265	neg
Mbuti.DG	Samara_En	Barcin_N	İkiztepe_LC	-0.000487	-1.718	0.000283	23568	23787	448285	neg
Mbuti.DG	EHG	Barcin_N	İkiztepe_LC	-0.000507	-2.026	0.000250	29999	30288	569996	neg
Mbuti.DG	Bulgaria_Varna_En3	Barcin_N	İkiztepe_LC	-0.001017	-2.789	0.000365	14785	15069	279274	neg
Mbuti.DG	Srubnaya	Barcin_N	İkiztepe_LC	-0.000719	-3.693	0.000195	31539	31965	593233	neg
Mbuti.DG	L.Caucasus_C	Barcin_N	İkiztepe_LC	-0.000786	-3.707	0.000212	30649	31104	578640	neg
Mbuti.DG	Levant_MBA.SG	Barcin_N	İkiztepe_LC	-0.000951	-4.463	0.000213	31195	31757	590642	neg
Mbuti.DG	Late_Helladic	Barcin_N	İkiztepe_LC	-0.001466	-4.918	0.000298	11618	11972	241194	neg
Mbuti.DG	Levant_EBA	Barcin_N	İkiztepe_LC	-0.001201	-5.338	0.000225	28177	28822	536928	neg
Mbuti.DG	SHG	Barcin_N	İkiztepe_LC	-0.001443	-6.345	0.000227	30189	31019	575916	neg
Mbuti.DG	Bulgaria_Varna_En2	Barcin_N	İkiztepe_LC	-0.00236	-6.550	0.000360	15671	16376	298841	neg
Mbuti.DG	Levant_EP	Barcin_N	İkiztepe_LC	-0.002438	-7.503	0.000325	17528	18364	343015	neg
Mbuti.DG	Balkans_C	Barcin_N	İkiztepe_LC	-0.002826	-8.335	0.000339	16003	16870	306515	neg
Mbuti.DG	WHG	Barcin_N	İkiztepe_LC	-0.001998	-8.670	0.000230	31152	32341	594937	neg
Mbuti.DG	Tepecik_N	Barcin_N	İkiztepe_LC	-0.002542	-8.864	0.000287	20997	22025	404533	neg
Mbuti.DG	Lasithi_MMinoan	Barcin_N	İkiztepe_LC	-0.0196	-9.211	0.002128	29797	30987	566700	neg
Mbuti.DG	Levant_N	Barcin_N	İkiztepe_LC	-0.002438	-9.375	0.000260	26999	28263	518709	neg
Mbuti.DG	Levant_C	Barcin_N	İkiztepe_LC	-0.001946	-10.051	0.000194	30816	31957	586739	neg
Mbuti.DG	Boncuklu_N.SG	Barcin_N	İkiztepe_LC	-0.003233	-10.831	0.000298	28897	30687	553514	neg
Mbuti.DG	Greece_N	Barcin_N	İkiztepe_LC	-0.003453	-11.104	0.000311	25143	26800	479975	neg
Mbuti.DG	Boncuklu_N	Barcin_N	İkiztepe_LC	-0.003609	-15.662	0.000230	30794	32920	588966	neg
Mbuti.DG	Balkans_N	Barcin_N	İkiztepe_LC	-0.003489	-15.849	0.000220	30554	32592	584073	neg
Mbuti.DG	Iberia_C	Barcin_N	İkiztepe_LC	-0.003165	-16.475	0.000192	30942	32815	591888	neg
Mbuti.DG	LBK_EN	Barcin_N	İkiztepe_LC	-0.003531	-18.565	0.000190	31143	33243	594896	neg
Mbuti.DG	L.Caucasus_LBA.SG	Barcin_N	K.Kalehöyük_MLBA	-0.000192	-0.399	0.000481	4999	5018	96674	neg
Mbuti.DG	L.Caucasus_MBA	Barcin_N	K.Kalehöyük_MLBA	-0.000187	-0.405	0.000462	7903	7931	148966	neg
Mbuti.DG	G.Caucasus_a_En	Barcin_N	K.Kalehöyük_MLBA	-0.000206	-0.465	0.000443	7163	7191	136138	neg
Mbuti.DG	EHG	Barcin_N	K.Kalehöyük_MLBA	-0.000276	-0.736	0.000375	9733	9784	185832	neg
Mbuti.DG	Samara_En	Barcin_N	K.Kalehöyük_MLBA	-0.000412	-0.971	0.000424	7216	7273	137277	neg
Mbuti.DG	G.Caucasus_a_MLBA	Barcin_N	K.Kalehöyük_MLBA	-0.000425	-1.096	0.000388	8073	8138	152815	neg
Mbuti.DG	G.Caucasus_a_EBA	Barcin_N	K.Kalehöyük_MLBA	-0.000359	-1.188	0.000302	9685	9751	183326	neg
Mbuti.DG	L.Caucasus_EBA	Barcin_N	K.Kalehöyük_MLBA	-0.000425	-1.368	0.000311	10035	10116	189283	neg
Mbuti.DG	G.Caucasus_b_EMBA	Barcin_N	K.Kalehöyük_MLBA	-0.000409	-1.415	0.000289	9646	9721	182991	neg
Mbuti.DG	Bulgaria_Varna_En3	Barcin_N	K.Kalehöyük_MLBA	-0.001092	-1.799	0.000607	3790	3869	72412	neg
Mbuti.DG	Iran_C	Barcin_N	K.Kalehöyük_MLBA	-0.000689	-2.149	0.000321	9797	9925	185958	neg
Mbuti.DG	Levant_MBA.SG	Barcin_N	K.Kalehöyük_MLBA	-0.000704	-2.368	0.000297	10853	10997	205205	neg
Mbuti.DG	L.Caucasus_C	Barcin_N	K.Kalehöyük_MLBA	-0.000774	-2.494	0.000310	9876	10021	186887	neg
Mbuti.DG	Srubnaya	Barcin_N	K.Kalehöyük_MLBA	-0.000917	-3.003	0.000305	10760	10946	202500	neg
Mbuti.DG	Late_Helladic	Barcin_N	K.Kalehöyük_MLBA	-0.00137	-3.287	0.000417	3865	3975	80861	neg
Mbuti.DG	SHG	Barcin_N	K.Kalehöyük_MLBA	-0.001288	-3.662	0.000352	9847	10089	188093	neg
Mbuti.DG	WHG	Barcin_N	K.Kalehöyük_MLBA	-0.001439	-4.316	0.000333	10939	11238	207144	neg
Mbuti.DG	Levant_EP	Barcin_N	K.Kalehöyük_MLBA	-0.002126	-4.382	0.000485	4933	5137	95857	neg
Mbuti.DG	Balkans_C	Barcin_N	K.Kalehöyük_MLBA	-0.002369	-4.621	0.000513	4666	4879	89800	neg
Mbuti.DG	Tepecik_N	Barcin_N	K.Kalehöyük_MLBA	-0.001985	-5.075	0.000391	7981	8284	152594	neg
Mbuti.DG	Bulgaria_Varna_En2	Barcin_N	K.Kalehöyük_MLBA	-0.003344	-6.028	0.000555	4100	4363	78694	neg
Mbuti.DG	Levant_EBA	Barcin_N	K.Kalehöyük_MLBA	-0.002238	-6.228	0.000359	8177	8530	157979	neg
Mbuti.DG	Levant_N	Barcin_N	K.Kalehöyük_MLBA	-0.002391	-6.479	0.000369	7916	8281	152577	neg
Mbuti.DG	Lasithi_MMinoan	Barcin_N	K.Kalehöyük_MLBA	-0.0204	-6.577	0.003102	9588	9987	183070	neg
Mbuti.DG	Greece_N	Barcin_N	K.Kalehöyük_MLBA	-0.003686	-7.739	0.000476	7269	7781	138885	neg
Mbuti.DG	Boncuklu_N.SG	Barcin_N	K.Kalehöyük_MLBA	-0.003546	-8.481	0.000418	10170	10862	195352	neg
Mbuti.DG	Levant_C	Barcin_N	K.Kalehöyük_MLBA	-0.002419	-8.575	0.000282	10020	10485	192070	neg
Mbuti.DG	Balkans_N	Barcin_N	K.Kalehöyük_MLBA	-0.003519	-11.181	0.000315	9938	10610	191129	neg
Mbuti.DG	Boncuklu_N	Barcin_N	K.Kalehöyük_MLBA	-0.004109	-12.482	0.000329	10369	11187	199260	neg
Mbuti.DG	Iberia_C	Barcin_N	K.Kalehöyük_MLBA	-0.003654	-12.586	0.000290	10409	11139	199914	neg
Mbuti.DG	LBK_EN	Barcin_N	K.Kalehöyük_MLBA	-0.003734	-14.076	0.000265	10815	11585	206278	neg
Mbuti.DG	CHG	Barcin_N	TitrişHöyük_EBA	-0.0011	-0.142	0.007746	2717	2723	51387	neg
Mbuti.DG	Iran_C	Barcin_N	TitrişHöyük_EBA	-0.002	-0.312	0.006410	2721	2732	50789	neg
Mbuti.DG	G.Caucasus_a_EBA	Barcin_N	TitrişHöyük_EBA	-0.0041	-0.682	0.006012	2717	2740	50923	neg
Mbuti.DG	G.Caucasus_b_EMBA	Barcin_N	TitrişHöyük_EBA	-0.0046	-0.790	0.005823	2717	2742	50935	neg
Mbuti.DG	L.Caucasus_EBA	Barcin_N	TitrişHöyük_EBA	-0.005	-0.815	0.006135	2727	2755	51064	neg
Mbuti.DG	L.Caucasus_C	Barcin_N	TitrişHöyük_EBA	-0.0111	-1.695	0.006549	2721	2782	50911	neg
Mbuti.DG	EHG	Barcin_N	TitrişHöyük_EBA	-0.0145	-1.938	0.007482	2653	2731	50169	neg
Mbuti.DG	Levant_MBA.SG	Barcin_N	TitrişHöyük_EBA	-0.0154	-2.385	0.006457	2695	2780	50996	neg
Mbuti.DG	Srubnaya	Barcin_N	TitrişHöyük_EBA	-0.0173	-2.899	0.005968	2726	2822	51346	neg
Mbuti.DG	Levant_C	Barcin_N	TitrişHöyük_EBA	-0.0184	-3.425	0.005372	2706	2808	51211	neg
Mbuti.DG	SHG	Barcin_N	TitrişHöyük_EBA	-0.0241	-3.529	0.006829	2659	2790	50523	neg

Mbuti.DG	WHG	Barcin_N	TitrişHöyük_EBA	-0.0289	-4.194	0.006891	2684	2844	51387	neg
Mbuti.DG	Iberia_C	Barcin_N	TitrişHöyük_EBA	-0.0335	-6.178	0.005422	2684	2871	51324	neg
Mbuti.DG	Boncuklu_N	Barcin_N	TitrişHöyük_EBA	-0.0421	-6.489	0.006488	2678	2913	51158	neg
Mbuti.DG	Balkans_N	Barcin_N	TitrişHöyük_EBA	-0.0402	-6.527	0.006159	2657	2880	51070	neg
Mbuti.DG	LBK_EN	Barcin_N	TitrişHöyük_EBA	-0.0378	-7.043	0.005367	2702	2914	51392	neg
Mbuti.DG	G.Caucasus_a_En	Barcin_N	Topakhöyük_EBA	-0.000022	-0.050	0.000440	6917	6920	132167	neg
Mbuti.DG	G.Caucasus_c_EMBA	Barcin_N	Topakhöyük_EBA	-0.000196	-0.407	0.000482	7295	7322	139889	neg
Mbuti.DG	Samara_En	Barcin_N	Topakhöyük_EBA	-0.000352	-0.767	0.000459	6959	7006	133135	neg
Mbuti.DG	Iran_C	Barcin_N	Topakhöyük_EBA	-0.000318	-0.922	0.000345	9460	9517	180104	neg
Mbuti.DG	G.Caucasus_b_En	Barcin_N	Topakhöyük_EBA	-0.000799	-2.178	0.000367	9286	9428	177814	neg
Mbuti.DG	G.Caucasus_a_MLBA	Barcin_N	Topakhöyük_EBA	-0.000971	-2.348	0.000414	7728	7873	148335	neg
Mbuti.DG	EHG	Barcin_N	Topakhöyük_EBA	-0.001054	-2.575	0.000409	9282	9472	179974	neg
Mbuti.DG	L.Caucasus_MBA	Barcin_N	Topakhöyük_EBA	-0.001389	-2.916	0.000476	7513	7713	144440	neg
Mbuti.DG	Levant_MBA.SG	Barcin_N	Topakhöyük_EBA	-0.000879	-2.921	0.000301	10376	10550	198487	neg
Mbuti.DG	G.Caucasus_b_EMBA	Barcin_N	Topakhöyük_EBA	-0.001014	-3.215	0.000315	9215	9395	177367	neg
Mbuti.DG	L.Caucasus_EBA	Barcin_N	Topakhöyük_EBA	-0.001111	-3.288	0.000338	9585	9789	183353	neg
Mbuti.DG	Late_Helladic	Barcin_N	Topakhöyük_EBA	-0.001599	-3.405	0.000470	3709	3834	78500	neg
Mbuti.DG	G.Caucasus_a_EBA	Barcin_N	Topakhöyük_EBA	-0.001069	-3.420	0.000313	9239	9429	177658	neg
Mbuti.DG	L.Caucasus_C	Barcin_N	Topakhöyük_EBA	-0.00136	-4.052	0.000336	9449	9696	181045	neg
Mbuti.DG	Bulgaria_Varna_En2	Barcin_N	Topakhöyük_EBA	-0.002495	-4.171	0.000598	3973	4164	76540	neg
Mbuti.DG	Bulgaria_Varna_En3	Barcin_N	Topakhöyük_EBA	-0.002594	-4.255	0.000610	3582	3764	70336	neg
Mbuti.DG	SHG	Barcin_N	Topakhöyük_EBA	-0.001738	-4.755	0.000366	9408	9725	182063	neg
Mbuti.DG	Levant_EBA	Barcin_N	Topakhöyük_EBA	-0.002132	-5.577	0.000382	7879	8206	153325	neg
Mbuti.DG	Levant_EP	Barcin_N	Topakhöyük_EBA	-0.003134	-5.631	0.000557	4721	5014	93211	neg
Mbuti.DG	Srubnaya	Barcin_N	Topakhöyük_EBA	-0.001765	-5.754	0.000307	10241	10587	195959	neg
Mbuti.DG	Tepecik_N	Barcin_N	Topakhöyük_EBA	-0.002617	-6.061	0.000432	7590	7977	147707	neg
Mbuti.DG	Balkans_C	Barcin_N	Topakhöyük_EBA	-0.003545	-6.485	0.000547	4428	4737	87164	neg
Mbuti.DG	WHG	Barcin_N	Topakhöyük_EBA	-0.00238	-6.498	0.000366	10400	10877	200310	neg
Mbuti.DG	Greece_N	Barcin_N	Topakhöyük_EBA	-0.003315	-6.577	0.000504	7026	7473	134791	neg
Mbuti.DG	Levant_N	Barcin_N	Topakhöyük_EBA	-0.002689	-6.583	0.000408	7584	7983	148079	neg
Mbuti.DG	Lasithi_MMinoan	Barcin_N	Topakhöyük_EBA	-0.0301	-8.748	0.003441	9106	9670	177335	neg
Mbuti.DG	Boncuklu_N.SG	Barcin_N	Topakhöyük_EBA	-0.004127	-9.578	0.000431	9686	10466	189027	neg
Mbuti.DG	Levant_C	Barcin_N	Topakhöyük_EBA	-0.003035	-10.238	0.000296	9570	10134	186020	neg
Mbuti.DG	Balkans_N	Barcin_N	Topakhöyük_EBA	-0.003803	-11.157	0.000341	9515	10220	185171	neg
Mbuti.DG	Boncuklu_N	Barcin_N	Topakhöyük_EBA	-0.00428	-12.249	0.000349	9937	10762	192847	neg
Mbuti.DG	Iberia_C	Barcin_N	Topakhöyük_EBA	-0.003962	-12.967	0.000306	9968	10735	193510	neg
Mbuti.DG	LBK_EN	Barcin_N	Topakhöyük_EBA	-0.004101	-14.435	0.000284	10336	11154	199511	neg
Mbuti.DG	Levant_EP	Büyükkaya_EC	Alalakh_MLBA	-0.0007	-0.166	0.004217	18113	18140	343194	neg
Mbuti.DG	L.Caucasus_MBA	Büyükkaya_EC	Alalakh_MLBA	-0.0009	-0.212	0.004245	27161	27208	506550	neg
Mbuti.DG	G.Caucasus_b_En	Büyükkaya_EC	Alalakh_MLBA	-0.0009	-0.268	0.003358	31064	31119	581215	neg
Mbuti.DG	L.Caucasus_LBA.SG	Büyükkaya_EC	Alalakh_MLBA	-0.0013	-0.318	0.004088	16792	16835	320857	neg
Mbuti.DG	G.Caucasus_a_MLBA	Büyükkaya_EC	Alalakh_MLBA	-0.0016	-0.461	0.003471	28348	28441	528566	neg
Mbuti.DG	Levant_MBA.SG	Büyükkaya_EC	Alalakh_MLBA	-0.0014	-0.476	0.002941	31918	32005	595283	neg
Mbuti.DG	G.Caucasus_a_EBA	Büyükkaya_EC	Alalakh_MLBA	-0.003	-1.079	0.002780	31028	31212	580758	neg
Mbuti.DG	Balkans_C	Büyükkaya_EC	Alalakh_MLBA	-0.0053	-1.115	0.004753	16309	16481	305526	neg
Mbuti.DG	Iberia_C	Büyükkaya_EC	Alalakh_MLBA	-0.0102	-3.685	0.002768	31877	32536	595968	neg
Mbuti.DG	Balkans_N	Büyükkaya_EC	Alalakh_MLBA	-0.0163	-5.289	0.003082	31353	32389	587206	neg
Mbuti.DG	Barcin_N	Büyükkaya_EC	Alalakh_MLBA	-0.015	-5.331	0.002814	32027	33002	599345	neg
Mbuti.DG	Boncuklu_N	Büyükkaya_EC	Alalakh_MLBA	-0.0187	-5.874	0.003184	31516	32719	592975	neg
Mbuti.DG	Iran_N	Büyükkaya_EC	Arslantepe_EBA	0	-0.009	0.000000	27248	27251	516066	neg
Mbuti.DG	Levant_MBA.SG	Büyükkaya_EC	Arslantepe_EBA	-0.0005	-0.159	0.003145	31494	31526	585922	neg
Mbuti.DG	Late_Helladic	Büyükkaya_EC	Arslantepe_EBA	-0.003	-0.655	0.004580	11554	11623	235531	neg
Mbuti.DG	Balkans_C	Büyükkaya_EC	Arslantepe_EBA	-0.0038	-0.732	0.005191	16234	16357	303460	neg
Mbuti.DG	Levant_EP	Büyükkaya_EC	Arslantepe_EBA	-0.0042	-0.904	0.004646	18010	18164	341490	neg
Mbuti.DG	Levant_C	Büyükkaya_EC	Arslantepe_EBA	-0.0032	-1.039	0.003080	31380	31579	583747	neg
Mbuti.DG	EHG	Büyükkaya_EC	Arslantepe_EBA	-0.0074	-1.796	0.004120	29881	30326	565045	neg
Mbuti.DG	Bulgaria_Varna_En2	Büyükkaya_EC	Arslantepe_EBA	-0.0101	-1.974	0.005117	15986	16311	299753	neg
Mbuti.DG	L.Caucasus_C	Büyükkaya_EC	Arslantepe_EBA	-0.0068	-2.077	0.003274	30779	31201	575373	neg
Mbuti.DG	Greece_N	Büyükkaya_EC	Arslantepe_EBA	-0.0118	-2.364	0.004992	25675	26287	476373	neg
Mbuti.DG	LBK_EN	Büyükkaya_EC	Arslantepe_EBA	-0.0118	-3.806	0.003100	31767	32523	590340	neg
Mbuti.DG	Lasithi_MMinoan	Büyükkaya_EC	Arslantepe_EBA	-0.0136	-3.820	0.003560	29915	30743	562468	neg
Mbuti.DG	Barcin_N	Büyükkaya_EC	Arslantepe_EBA	-0.0124	-4.040	0.003069	31664	32462	590161	neg
Mbuti.DG	Balkans_N	Büyükkaya_EC	Arslantepe_EBA	-0.0136	-4.042	0.003365	31138	31997	580688	neg
Mbuti.DG	Boncuklu_N.SG	Büyükkaya_EC	Arslantepe_EBA	-0.0206	-4.398	0.004684	29127	30355	549652	neg
Mbuti.DG	Late_Helladic	Büyükkaya_EC	Arslantepe_LC	-0.0011	-0.255	0.004314	11598	11623	237856	neg
Mbuti.DG	Levant_EP	Büyükkaya_EC	Arslantepe_LC	-0.0025	-0.581	0.004303	18022	18113	343174	neg
Mbuti.DG	Bulgaria_Varna_En2	Büyükkaya_EC	Arslantepe_LC	-0.0046	-1.029	0.004470	16072	16222	300594	neg
Mbuti.DG	EHG	Büyükkaya_EC	Arslantepe_LC	-0.004	-1.094	0.003656	30195	30440	571274	neg
Mbuti.DG	L.Caucasus_C	Büyükkaya_EC	Arslantepe_LC	-0.0036	-1.201	0.002998	31012	31239	581517	neg
Mbuti.DG	Greece_N	Büyükkaya_EC	Arslantepe_LC	-0.0081	-1.816	0.004460	25784	26206	479145	neg
Mbuti.DG	LBK_EN	Büyükkaya_EC	Arslantepe_LC	-0.0083	-2.999	0.002768	32198	32737	599400	neg
Mbuti.DG	Lasithi_MMinoan	Büyükkaya_EC	Arslantepe_LC	-0.0105	-3.238	0.003243	30156	30796	568382	neg
Mbuti.DG	Barcin_N	Büyükkaya_EC	Arslantepe_LC	-0.0092	-3.290	0.002796	32099	32694	599079	neg
Mbuti.DG	Boncuklu_N.SG	Büyükkaya_EC	Arslantepe_LC	-0.0195	-4.752	0.004104	29401	30572	557526	neg
Mbuti.DG	Boncuklu_N	Büyükkaya_EC	Barcin_C	-0.0021	-0.498	0.004217	30085	30213	559319	neg
Mbuti.DG	Balkans_N	Büyükkaya_EC	Barcin_C	-0.0023	-0.554	0.004152	30035	30175	557226	neg
Mbuti.DG	Boncuklu_N.SG	Büyükkaya_EC	Barcin_C	-0.0077	-1.349	0.005708	27984	28416	525916	neg
Mbuti.DG	Levant_EBA	Büyükkaya_EC	ÇamlıbelTarlasi_LC	-0.0002	-0.059	0.003390	28643	28655	537719	neg
Mbuti.DG	Late_Helladic	Büyükkaya_EC	ÇamlıbelTarlasi_LC	-0.0018	-0.399	0.004511	11484	11524	235550	neg
Mbuti.DG	Levant_C	Büyükkaya_EC	ÇamlıbelTarlasi_LC	-0.0022	-0.794	0.002771	31310	31447	585390	neg
Mbuti.DG	Iberia_C	Büyükkaya_EC	ÇamlıbelTarlasi_LC	-0.0036	-1.275	0.002824	31647	31876	590101	neg
Mbuti.DG	Levant_N	Büyükkaya_EC	ÇamlıbelTarlasi_LC	-0.0046	-1.294	0.003555	27424	27676	517780	neg
Mbuti.DG	L.Caucasus_C	Büyükkaya_EC	ÇamlıbelTarlasi_LC	-0.0044	-1.345	0.003271	30747	31016	576936	neg
Mbuti.DG	EHG	Büyükkaya_EC	ÇamlıbelTarlasi_LC	-0.006	-1.548	0.003876	29828	30186	566507	neg
Mbuti.DG	Greece_N	Büyükkaya_EC	ÇamlıbelTarlasi_LC	-0.0072	-1.572	0.004580	25649	26018	476905	neg
Mbuti.DG	Barcin_N	Büyükkaya_EC	ÇamlıbelTarlasi_LC	-0.0062	-2.180	0.002844	31859	32257	592890	neg
Mbuti.DG	Lasithi_MMinoan	Büyükkaya_EC	ÇamlıbelTarlasi_LC	-0.0079	-2.330	0.003391	29996	30475	563840	neg
Mbuti.DG	Balkans_N	Büyükkaya_EC	ÇamlıbelTarlasi_LC	-0.0079	-2.472	0.003196	31220	31715	582202	neg
Mbuti.DG	Boncuklu_N	Büyükkaya_EC	ÇamlıbelTarlasi_LC	-0.0086	-2.645	0.003251	31387	31932	587003	neg
Mbuti.DG	Boncuklu_N.SG	Büyükkaya_EC	ÇamlıbelTarlasi_LC	-0.0165	-3.769	0.004378	29217	30197	552093	neg
Mbuti.DG	L.Caucasus_MBA	Büyükkaya_EC	Caucasus_lowlands_LC	-0.0016	-0.197	0.008122	7650	7674	144597	neg
Mbuti.DG	G.Caucasus_b_En	Büyükkaya_EC	Caucasus_lowlands_LC	-0.0031	-0.514	0.006031	8148	8198	155109	neg

Mbuti.DG	G.Caucasus_a_MLBA	Büyükkaya_EC	Caucasus_lowlands_LC -0.0067	-0.958	0.006994	7935	8042	149971	neg
Mbuti.DG	G.Caucasus_b_EMBA	Büyükkaya_EC	Caucasus_lowlands_LC -0.0053	-1.017	0.005211	8137	8224	155100	neg
Mbuti.DG	Levant_EP	Büyükkaya_EC	Caucasus_lowlands_LC -0.0094	-1.121	0.008385	5401	5504	104896	neg
Mbuti.DG	Balkans_C	Büyükkaya_EC	Caucasus_lowlands_LC -0.0123	-1.244	0.009887	4804	4923	91722	neg
Mbuti.DG	Bulgaria_Varna_En2	Büyükkaya_EC	Caucasus_lowlands_LC -0.011	-1.262	0.008716	5093	5207	97369	neg
Mbuti.DG	G.Caucasus_a_EBA	Büyükkaya_EC	Caucasus_lowlands_LC -0.0067	-1.265	0.005296	8163	8273	155113	neg
Mbuti.DG	Levant_EBA	Büyükkaya_EC	Caucasus_lowlands_LC -0.0087	-1.438	0.006050	7949	8089	151314	neg
Mbuti.DG	EHG	Büyükkaya_EC	Caucasus_lowlands_LC -0.0107	-1.512	0.007077	7928	8099	152689	neg
Mbuti.DG	L.Caucasus_EBA	Büyükkaya_EC	Caucasus_lowlands_LC -0.0085	-1.568	0.005421	8177	8317	155326	neg
Mbuti.DG	Bulgaria_Varna_En3	Büyükkaya_EC	Caucasus_lowlands_LC -0.0165	-1.680	0.009821	4709	4867	91013	neg
Mbuti.DG	Late_Helladic	Büyükkaya_EC	Caucasus_lowlands_LC -0.018	-1.932	0.009317	2949	3058	62196	neg
Mbuti.DG	L.Caucasus_C	Büyükkaya_EC	Caucasus_lowlands_LC -0.0123	-2.145	0.005734	8110	8312	154868	neg
Mbuti.DG	Levant_C	Büyükkaya_EC	Caucasus_lowlands_LC -0.0128	-2.564	0.004992	8174	8386	155616	neg
Mbuti.DG	Iberia_C	<b>Büyükkaya_EC</b>	<b>Caucasus_lowlands_LC -0.0191</b>	<b>-3.693</b>	0.005172	8148	8465	155826	neg
Mbuti.DG	<b>Balkans_N</b>	<b>Büyükkaya_EC</b>	<b>Caucasus_lowlands_LC -0.0219</b>	<b>-3.986</b>	0.005494	8166	8532	155325	neg
Mbuti.DG	<b>Boncuklu_N.SG</b>	<b>Büyükkaya_EC</b>	<b>Caucasus_lowlands_LC -0.0318</b>	<b>-4.082</b>	0.007790	7609	8110	147634	neg
Mbuti.DG	<b>LBK_EN</b>	<b>Büyükkaya_EC</b>	<b>Caucasus_lowlands_LC -0.0225</b>	<b>-4.373</b>	0.005145	8185	8561	155935	neg
Mbuti.DG	Iran_N	Büyükkaya_EC	Ebla_EMBA -0.0004	-0.088	0.004545	27058	27079	511281	neg
Mbuti.DG	G.Caucasus_c_EMBA	Büyükkaya_EC	Ebla_EMBA -0.0009	-0.200	0.004500	26745	26792	502541	neg
Mbuti.DG	G.Caucasus_a_MLBA	Büyükkaya_EC	Ebla_EMBA -0.0002	-0.530	0.003774	27944	28056	520953	neg
Mbuti.DG	L.Caucasus_LBA.SG	Büyükkaya_EC	Ebla_EMBA -0.0037	-0.833	0.004442	16467	16590	314479	neg
Mbuti.DG	Levant_EP	Büyükkaya_EC	Ebla_EMBA -0.0041	-0.870	0.004713	17875	18022	339326	neg
Mbuti.DG	Bulgaria_Varna_En3	Büyükkaya_EC	Ebla_EMBA -0.0053	-1.016	0.005217	14959	15118	279629	neg
Mbuti.DG	G.Caucasus_b_En	Büyükkaya_EC	Ebla_EMBA -0.0043	-1.234	0.003485	30314	30574	568679	neg
Mbuti.DG	Levant_N	Büyükkaya_EC	Ebla_EMBA -0.0049	-1.343	0.003649	27372	27644	512774	neg
Mbuti.DG	G.Caucasus_a_En	Büyükkaya_EC	Ebla_EMBA -0.0061	-1.409	0.004329	25492	25802	478431	neg
Mbuti.DG	CHG	Büyükkaya_EC	Ebla_EMBA -0.0065	-1.648	0.003944	30908	31314	582629	neg
Mbuti.DG	Late_Helladic	Büyükkaya_EC	Ebla_EMBA -0.0082	-1.822	0.004501	11287	11474	231931	neg
Mbuti.DG	L.Caucasus_EBA	Büyükkaya_EC	Ebla_EMBA -0.0059	-1.859	0.003174	30580	30946	572424	neg
Mbuti.DG	Balkans_C	Büyükkaya_EC	Ebla_EMBA -0.0106	-2.057	0.005153	16005	16348	300901	neg
Mbuti.DG	Levant_C	Büyükkaya_EC	Ebla_EMBA -0.0061	-2.097	0.002909	30877	31256	576141	neg
Mbuti.DG	G.Caucasus_a_EBA	Büyükkaya_EC	Ebla_EMBA -0.0067	-2.284	0.002933	30237	30647	568278	neg
Mbuti.DG	Bulgaria_Varna_En2	Büyükkaya_EC	Ebla_EMBA -0.0138	-2.877	0.004797	15846	16289	297986	neg
Mbuti.DG	<b>Greece_N</b>	<b>Büyükkaya_EC</b>	<b>Ebla_EMBA -0.0156</b>	<b>-3.342</b>	0.004668	25336	26138	472971	neg
Mbuti.DG	<b>L.Caucasus_C</b>	<b>Büyükkaya_EC</b>	<b>Ebla_EMBA -0.0113</b>	<b>-3.477</b>	0.003250	30219	30908	568374	neg
Mbuti.DG	<b>Iberia_C</b>	<b>Büyükkaya_EC</b>	<b>Ebla_EMBA -0.0157</b>	<b>-5.348</b>	0.002936	30868	31851	580157	neg
Mbuti.DG	<b>Lasithi_MMinoan</b>	<b>Büyükkaya_EC</b>	<b>Ebla_EMBA -0.0187</b>	<b>-5.416</b>	0.003453	29394	30516	555672	neg
Mbuti.DG	<b>LBK_EN</b>	<b>Büyükkaya_EC</b>	<b>Ebla_EMBA -0.0184</b>	<b>-6.242</b>	0.002948	31105	32270	582665	neg
Mbuti.DG	<b>Barcin_N</b>	<b>Büyükkaya_EC</b>	<b>Ebla_EMBA -0.0186</b>	<b>-6.282</b>	0.002961	31045	32221	582488	neg
Mbuti.DG	<b>Balkans_N</b>	<b>Büyükkaya_EC</b>	<b>Ebla_EMBA -0.0214</b>	<b>-6.594</b>	0.003245	30473	31804	573184	neg
Mbuti.DG	<b>Boncuklu_N</b>	<b>Büyükkaya_EC</b>	<b>Ebla_EMBA -0.0244</b>	<b>-7.288</b>	0.003348	30499	32027	577410	neg
Mbuti.DG	Greece_N	Büyükkaya_EC	GondürleHöyük_EBA -0.0005	-0.107	0.004673	25739	25767	474716	neg
Mbuti.DG	Boncuklu_N	Büyükkaya_EC	GondürleHöyük_EBA -0.0013	-0.351	0.003704	31267	31348	579853	neg
Mbuti.DG	Balkans_N	Büyükkaya_EC	GondürleHöyük_EBA -0.0021	-0.599	0.003506	31131	31265	576762	neg
Mbuti.DG	Boncuklu_N.SG	Büyükkaya_EC	GondürleHöyük_EBA -0.0125	-2.549	0.004904	28945	29680	545219	neg
Mbuti.DG	Bulgaria_Varna_En2	Büyükkaya_EC	İkiztepe_LC -0.0012	-0.206	0.005825	11803	11831	222284	neg
Mbuti.DG	Levant_N	Büyükkaya_EC	İkiztepe_LC -0.0009	-0.214	0.004206	19134	19168	360754	neg
Mbuti.DG	L.Caucasus_C	Büyükkaya_EC	İkiztepe_LC -0.0018	-0.480	0.003750	20587	20663	386656	neg
Mbuti.DG	EHG	Büyükkaya_EC	İkiztepe_LC -0.0029	-0.637	0.004553	20072	20189	380444	neg
Mbuti.DG	Boncuklu_N	Büyükkaya_EC	İkiztepe_LC -0.0036	-0.927	0.003883	20840	20989	389200	neg
Mbuti.DG	Lasithi_MMinoan	Büyükkaya_EC	İkiztepe_LC -0.0046	-1.153	0.003990	20219	20404	379859	neg
Mbuti.DG	Greece_N	Büyükkaya_EC	İkiztepe_LC -0.0087	-1.615	0.005387	18081	18399	337473	neg
Mbuti.DG	LBK_EN	Büyükkaya_EC	İkiztepe_LC -0.0054	-1.689	0.003197	20964	21193	391337	neg
Mbuti.DG	Barcin_N	Büyükkaya_EC	İkiztepe_LC -0.0057	-1.748	0.003261	20922	21162	391300	neg
Mbuti.DG	Iran_C	Büyükkaya_EC	K.Kalehöyük_MLBA -0.0002	-0.031	0.006452	5604	5606	106626	neg
Mbuti.DG	Balkans_C	Büyükkaya_EC	K.Kalehöyük_MLBA -0.0007	-0.069	0.010145	2959	2963	55930	neg
Mbuti.DG	Levant_MBA.SG	Büyükkaya_EC	K.Kalehöyük_MLBA -0.0012	-0.216	0.005556	5798	5812	110072	neg
Mbuti.DG	L.Caucasus_MBA	Büyükkaya_EC	K.Kalehöyük_MLBA -0.0032	-0.385	0.008312	4867	4898	92493	neg
Mbuti.DG	G.Caucasus_c_EMBA	Büyükkaya_EC	K.Kalehöyük_MLBA -0.0003	-0.387	0.007752	4856	4885	92646	neg
Mbuti.DG	EHG	Büyükkaya_EC	K.Kalehöyük_MLBA -0.0029	-0.417	0.006954	5503	5535	105270	neg
Mbuti.DG	G.Caucasus_a_En	Büyükkaya_EC	K.Kalehöyük_MLBA -0.0039	-0.489	0.007975	4622	4657	87921	neg
Mbuti.DG	Levant_EP	Büyükkaya_EC	K.Kalehöyük_MLBA -0.0046	-0.498	0.009237	3242	3273	62336	neg
Mbuti.DG	Iran_N	Büyükkaya_EC	K.Kalehöyük_MLBA -0.0054	-0.674	0.008012	4941	4994	94865	neg
Mbuti.DG	Lasithi_MMinoan	Büyükkaya_EC	K.Kalehöyük_MLBA -0.0041	-0.678	0.006047	5526	5572	104691	neg
Mbuti.DG	Levant_EBA	Büyükkaya_EC	K.Kalehöyük_MLBA -0.0045	-0.726	0.006198	5165	5212	98633	neg
Mbuti.DG	G.Caucasus_a_EBA	Büyükkaya_EC	K.Kalehöyük_MLBA -0.0042	-0.806	0.005211	5623	5670	106838	neg
Mbuti.DG	Levant_N	Büyükkaya_EC	K.Kalehöyük_MLBA -0.0062	-0.951	0.006519	4970	5032	95041	neg
Mbuti.DG	Boncuklu_N	Büyükkaya_EC	K.Kalehöyük_MLBA -0.0058	-1.002	0.005788	5818	5886	109505	neg
Mbuti.DG	L.Caucasus_EBA	Büyükkaya_EC	K.Kalehöyük_MLBA -0.0055	-1.009	0.005451	5688	5751	107908	neg
Mbuti.DG	Greece_N	Büyükkaya_EC	K.Kalehöyük_MLBA -0.0096	-1.174	0.008177	4672	4763	87561	neg
Mbuti.DG	Bulgaria_Varna_En2	Büyükkaya_EC	K.Kalehöyük_MLBA -0.0231	-2.366	0.009763	2837	2972	54212	neg
Mbuti.DG	LBK_EN	Büyükkaya_EC	K.Kalehöyük_MLBA -0.012	-2.466	0.004866	5884	6027	110956	neg
Mbuti.DG	Balkans_N	Büyükkaya_EC	K.Kalehöyük_MLBA -0.0135	-2.541	0.005313	5709	5865	108155	neg
Mbuti.DG	Barcin_N	Büyükkaya_EC	K.Kalehöyük_MLBA -0.0142	-2.975	0.004773	5846	6014	110846	neg
Mbuti.DG	G.Caucasus_a_MLBA	Büyükkaya_EC	Topakhöyük_EBA -0.0005	-0.073	0.006849	4975	4981	93884	neg
Mbuti.DG	Iran_N.SG	Büyükkaya_EC	Topakhöyük_EBA -0.0028	-0.453	0.006181	5572	5603	107770	neg
Mbuti.DG	Balkans_C	Büyükkaya_EC	Topakhöyük_EBA -0.0009	-0.855	0.010526	2848	2900	54424	neg
Mbuti.DG	Greece_N	Büyükkaya_EC	Topakhöyük_EBA -0.0076	-0.880	0.008636	4548	4617	85133	neg
Mbuti.DG	Levant_EBA	Büyükkaya_EC	Topakhöyük_EBA -0.0059	-0.917	0.006434	5022	5081	95904	neg
Mbuti.DG	Levant_MBA.SG	Büyükkaya_EC	Topakhöyük_EBA -0.0056	-0.981	0.005708	5599	5662	106895	neg
Mbuti.DG	G.Caucasus_b_En	Büyükkaya_EC	Topakhöyük_EBA -0.0063	-0.997	0.006319	5444	5513	103862	neg
Mbuti.DG	Iran_N	Büyükkaya_EC	Topakhöyük_EBA -0.0106	-1.292	0.008204	4739	4841	92250	neg
Mbuti.DG	G.Caucasus_c_EMBA	Büyükkaya_EC	Topakhöyük_EBA -0.0103	-1.304	0.007899	4721	4819	90093	neg
Mbuti.DG	Levant_EP	Büyükkaya_EC	Topakhöyük_EBA -0.0155	-1.539	0.010071	3119	3217	60747	neg
Mbuti.DG	G.Caucasus_a_EBA	Büyükkaya_EC	Topakhöyük_EBA -0.0087	-1.610	0.005404	5436	5532	103790	neg
Mbuti.DG	Levant_C	Büyükkaya_EC	Topakhöyük_EBA -0.0009	-1.685	0.005341	5570	5671	105725	neg
Mbuti.DG	L.Caucasus_MBA	Büyükkaya_EC	Topakhöyük_EBA -0.0156	-1.760	0.008864	4652	4800	89895	neg
Mbuti.DG	Levant_N	Büyükkaya_EC	Topakhöyük_EBA -0.0136	-1.928	0.007054	4795	4927	92418	neg
Mbuti.DG	L.Caucasus_C	Büyükkaya_EC	Topakhöyük_EBA -0.0119	-1.964	0.006059	5452	5583	104060	neg
Mbuti.DG	Boncuklu_N	Büyükkaya_EC	Topakhöyük_EBA -0.0135	-2.132	0.006332	5598	5751	106329	neg
Mbuti.DG	Lasithi_MMinoan	Büyükkaya_EC	Topakhöyük_EBA -0.0144	-2.236	0.006440	5317	5473	101684	neg
Mbuti.DG	Iberia_C	Büyükkaya_EC	Topakhöyük_EBA -0.0121	-2.298	0.005265	5632	5771	106865	neg

Mbuti.DG	Barcin_N	Büyükkaya_EC	Topakhöyük_EBA	-0.0157	-3.085	0.005089	5657	5837	107621	neg
Mbuti.DG	Boncuklu_N.SG	Büyükkaya_EC	Topakhöyük_EBA	-0.0277	-3.556	0.007790	5345	5650	102925	neg
Mbuti.DG	G.Caucasus_b_EMBA	TellKurdu_EC	Alalakh_MLBA	-0.0008	-0.414	0.001932	32797	32852	618044	neg
Mbuti.DG	L.Caucasus_LBA.SG	TellKurdu_EC	Alalakh_MLBA	-0.0052	-1.643	0.003165	17471	17653	637445	neg
Mbuti.DG	L.Caucasus_EBA	TellKurdu_EC	Alalakh_MLBA	-0.0041	-2.012	0.002038	33115	33387	623331	neg
Mbuti.DG	Iran_C	TellKurdu_EC	Alalakh_MLBA	-0.0045	-2.069	0.002175	32596	32890	615713	neg
Mbuti.DG	Bulgaria_Varna_En3	TellKurdu_EC	Alalakh_MLBA	-0.0076	-2.146	0.003541	15632	15870	294716	neg
Mbuti.DG	L.Caucasus_MBA	TellKurdu_EC	Alalakh_MLBA	-0.0071	-2.419	0.002935	28562	28973	538686	neg
Mbuti.DG	G.Caucasus_a_EBA	TellKurdu_EC	Alalakh_MLBA	-0.0053	-2.643	0.002005	32720	33069	617721	neg
Mbuti.DG	G.Caucasus_a_En	TellKurdu_EC	Alalakh_MLBA	-0.0092	-3.150	0.002921	27052	27552	513229	neg
Mbuti.DG	Late_Helladic	TellKurdu_EC	Alalakh_MLBA	-0.0128	-4.284	0.002988	12454	12777	257922	neg
Mbuti.DG	L.Caucasus_C	TellKurdu_EC	Alalakh_MLBA	-0.01	-4.633	0.002158	32711	33373	618618	neg
Mbuti.DG	Levant_EP	TellKurdu_EC	Alalakh_MLBA	-0.0211	-6.909	0.003054	19055	19875	370935	neg
Mbuti.DG	Boncuklu_N.SG	TellKurdu_EC	Alalakh_MLBA	-0.0202	-6.972	0.002897	31201	32488	593436	neg
Mbuti.DG	Levant_EBA	TellKurdu_EC	Alalakh_MLBA	-0.0169	-7.345	0.002301	30067	31097	573556	neg
Mbuti.DG	Levant_MBA.SG	TellKurdu_EC	Alalakh_MLBA	-0.0149	-7.468	0.001995	33329	34340	633337	neg
Mbuti.DG	Balkans_C	TellKurdu_EC	Alalakh_MLBA	-0.0277	-8.090	0.003424	17049	18019	327521	neg
Mbuti.DG	Levant_C	TellKurdu_EC	Alalakh_MLBA	-0.0218	-11.579	0.001883	32912	34381	627679	neg
Mbuti.DG	Iberia_C	TellKurdu_EC	Alalakh_MLBA	-0.0219	-11.749	0.001864	33333	34828	635324	neg
Mbuti.DG	Balkans_N	TellKurdu_EC	Alalakh_MLBA	-0.0269	-12.624	0.002131	32766	34580	624205	neg
Mbuti.DG	G.Caucasus_a_En	TellKurdu_EC	Arslantepe_EBA	-0.0024	-0.705	0.003404	27203	27333	511213	neg
Mbuti.DG	G.Caucasus_a_MLBA	TellKurdu_EC	Arslantepe_EBA	-0.0022	-0.731	0.003010	29812	29943	559514	neg
Mbuti.DG	L.Caucasus_MBA	TellKurdu_EC	Arslantepe_EBA	-0.0032	-0.899	0.003560	28619	28804	535614	neg
Mbuti.DG	Iran_C	TellKurdu_EC	Arslantepe_EBA	-0.0024	-0.942	0.002548	32392	32551	609506	neg
Mbuti.DG	L.Caucasus_LBA.SG	TellKurdu_EC	Arslantepe_EBA	-0.0035	-0.966	0.003623	17398	17518	334558	neg
Mbuti.DG	G.Caucasus_a_EBA	TellKurdu_EC	Arslantepe_EBA	-0.0029	-1.212	0.002393	32572	32763	612370	neg
Mbuti.DG	Bulgaria_Varna_En3	TellKurdu_EC	Arslantepe_EBA	-0.0053	-1.256	0.004220	15680	15846	294143	neg
Mbuti.DG	Boncuklu_N.SG	TellKurdu_EC	Arslantepe_EBA	-0.0154	-4.276	0.003601	30968	31938	585221	neg
Mbuti.DG	Levant_EBA	TellKurdu_EC	Arslantepe_EBA	-0.0167	-5.873	0.002844	30016	31035	570856	neg
Mbuti.DG	Balkans_C	TellKurdu_EC	Arslantepe_EBA	-0.0255	-6.085	0.004191	17003	17895	325468	neg
Mbuti.DG	Bulgaria_Varna_En2	TellKurdu_EC	Arslantepe_EBA	-0.0255	-6.435	0.003963	16664	17536	318334	neg
Mbuti.DG	Levant_EP	TellKurdu_EC	Arslantepe_EBA	-0.0254	-6.878	0.003693	18886	19869	369176	neg
Mbuti.DG	Boncuklu_N	TellKurdu_EC	Arslantepe_EBA	-0.0192	-6.929	0.002771	32971	34265	622760	neg
Mbuti.DG	Lasithi_MMinoan	TellKurdu_EC	Arslantepe_EBA	-0.0206	-7.395	0.002786	31536	32862	599438	neg
Mbuti.DG	LBK_EN	TellKurdu_EC	Arslantepe_EBA	-0.0249	-10.689	0.002329	33192	34885	628014	neg
Mbuti.DG	L.Caucasus_LBA.SG	TellKurdu_EC	Arslantepe_LC	-0.0025	-0.775	0.003226	17463	17549	337372	neg
Mbuti.DG	Late_Helladic	TellKurdu_EC	Arslantepe_LC	-0.0086	-2.801	0.003070	12468	12684	257919	neg
Mbuti.DG	Boncuklu_N.SG	TellKurdu_EC	Arslantepe_LC	-0.0131	-4.400	0.002977	31331	32163	593108	neg
Mbuti.DG	Bulgaria_Varna_En2	TellKurdu_EC	Arslantepe_LC	-0.0194	-5.790	0.003351	16776	17441	319166	neg
Mbuti.DG	Levant_EBA	TellKurdu_EC	Arslantepe_LC	-0.0152	-6.407	0.002372	30019	30945	573538	neg
Mbuti.DG	Levant_EP	TellKurdu_EC	Arslantepe_LC	-0.0209	-6.849	0.003052	18970	19780	370903	neg
Mbuti.DG	Greece_N	TellKurdu_EC	Arslantepe_LC	-0.022	-6.972	0.003155	27218	28442	515383	neg
Mbuti.DG	Lasithi_MMinoan	TellKurdu_EC	Arslantepe_LC	-0.0172	-7.674	0.002241	31798	32912	605280	neg
Mbuti.DG	Iberia_C	TellKurdu_EC	Arslantepe_LC	-0.0177	-9.162	0.001932	33355	34554	633328	neg
Mbuti.DG	Levant_C	TellKurdu_EC	Arslantepe_LC	-0.0179	-9.174	0.001951	32950	34150	627585	neg
Mbuti.DG	Balkans_N	TellKurdu_EC	Arslantepe_LC	-0.0224	-10.488	0.002136	32815	34321	624113	neg
Mbuti.DG	Levant_N	TellKurdu_EC	Arslantepe_LC	-0.0274	-10.658	0.002571	28806	30428	556865	neg
Mbuti.DG	LBK_EN	TellKurdu_EC	Arslantepe_LC	-0.0206	-11.194	0.001840	33656	35075	636945	neg
Mbuti.DG	L.Caucasus_C	TellKurdu_EC	Barcin_C	-0.0014	-0.396	0.003535	31469	31557	590090	neg
Mbuti.DG	Late_Helladic	TellKurdu_EC	Barcin_C	-0.0102	-2.009	0.005077	11729	11970	243123	neg
Mbuti.DG	Iberia_C	TellKurdu_EC	Barcin_C	-0.0077	-2.315	0.003326	32023	32522	599385	neg
Mbuti.DG	Balkans_N	TellKurdu_EC	Barcin_C	-0.0103	-2.806	0.003671	31731	32391	593717	neg
Mbuti.DG	Levant_MBA.SG	TellKurdu_EC	Barcin_C	-0.0109	-3.070	0.003550	31566	32261	597210	neg
Mbuti.DG	Balkans_C	TellKurdu_EC	Barcin_C	-0.0179	-3.140	0.005701	16664	17271	316711	neg
Mbuti.DG	Greece_N	TellKurdu_EC	Barcin_C	-0.0191	-3.774	0.005061	26564	27599	500104	neg
Mbuti.DG	Levant_EBA	TellKurdu_EC	Barcin_C	-0.016	-3.963	0.004037	29129	30074	555326	neg
Mbuti.DG	Levant_C	TellKurdu_EC	Barcin_C	-0.0171	-5.246	0.003260	31422	32514	596543	neg
Mbuti.DG	Levant_N	TellKurdu_EC	Barcin_C	-0.028	-6.959	0.004024	27893	29497	538549	neg
Mbuti.DG	L.Caucasus_MBA	TellKurdu_EC	ÇamlıbelTarlasi_LC	-0.0002	-0.064	0.003125	28581	28593	536013	neg
Mbuti.DG	G.Caucasus_a_En	TellKurdu_EC	ÇamlıbelTarlasi_LC	-0.0005	-0.156	0.003205	27132	27159	511378	neg
Mbuti.DG	Bulgaria_Varna_En3	TellKurdu_EC	ÇamlıbelTarlasi_LC	-0.0016	-0.439	0.003645	15653	15705	294111	neg
Mbuti.DG	G.Caucasus_a_MLBA	TellKurdu_EC	ÇamlıbelTarlasi_LC	-0.0017	-0.670	0.002537	29698	29802	559703	neg
Mbuti.DG	L.Caucasus_C	TellKurdu_EC	ÇamlıbelTarlasi_LC	-0.0064	-2.753	0.002325	32485	32907	613714	neg
Mbuti.DG	Late_Helladic	TellKurdu_EC	ÇamlıbelTarlasi_LC	-0.0091	-2.775	0.003279	12393	12620	255438	neg
Mbuti.DG	Boncuklu_N.SG	TellKurdu_EC	ÇamlıbelTarlasi_LC	-0.0092	-2.910	0.003162	31203	31780	587400	neg
Mbuti.DG	Boncuklu_N	TellKurdu_EC	ÇamlıbelTarlasi_LC	-0.0096	-4.029	0.002383	33335	33982	624824	neg
Mbuti.DG	Bulgaria_Varna_En2	TellKurdu_EC	ÇamlıbelTarlasi_LC	-0.0181	-5.047	0.003586	16758	17376	318321	neg
Mbuti.DG	Lasithi_MMinoan	TellKurdu_EC	ÇamlıbelTarlasi_LC	-0.0127	-5.147	0.002467	31754	32570	600513	neg
Mbuti.DG	Greece_N	TellKurdu_EC	ÇamlıbelTarlasi_LC	-0.0203	-6.228	0.003259	27118	28243	512839	neg
Mbuti.DG	Levant_EP	TellKurdu_EC	ÇamlıbelTarlasi_LC	-0.0236	-7.033	0.003356	18866	19779	369364	neg
Mbuti.DG	Iberia_C	TellKurdu_EC	ÇamlıbelTarlasi_LC	-0.015	-7.316	0.002050	33198	34211	627401	neg
Mbuti.DG	Balkans_N	TellKurdu_EC	ÇamlıbelTarlasi_LC	-0.0187	-8.164	0.002291	32718	33963	618962	neg
Mbuti.DG	LBK_EN	TellKurdu_EC	ÇamlıbelTarlasi_LC	-0.017	-8.537	0.001991	33487	34648	630427	neg
Mbuti.DG	Levant_C	TellKurdu_EC	ÇamlıbelTarlasi_LC	-0.0198	-9.666	0.002048	32616	33935	622378	neg
Mbuti.DG	Levant_N	TellKurdu_EC	ÇamlıbelTarlasi_LC	-0.0304	-11.102	0.002738	28587	30381	554063	neg
Mbuti.DG	Iran_C	TellKurdu_EC	Caucasus_lowlands_LC	-0.0002	-0.031	0.006452	8748	8750	165308	neg
Mbuti.DG	G.Caucasus_a_En	TellKurdu_EC	Caucasus_lowlands_LC	-0.0079	-1.096	0.007208	7924	8051	150883	neg
Mbuti.DG	G.Caucasus_a_MLBA	TellKurdu_EC	Caucasus_lowlands_LC	-0.0094	-1.604	0.005860	8396	8555	160143	neg
Mbuti.DG	L.Caucasus_EBA	TellKurdu_EC	Caucasus_lowlands_LC	-0.0085	-1.809	0.004699	8720	8870	166132	neg
Mbuti.DG	Bulgaria_Varna_En3	TellKurdu_EC	Caucasus_lowlands_LC	-0.0181	-2.174	0.008326	4943	5125	95497	neg
Mbuti.DG	L.Caucasus_C	TellKurdu_EC	Caucasus_lowlands_LC	-0.0116	-2.346	0.004945	8670	8873	165642	neg
Mbuti.DG	Bulgaria_Varna_En2	TellKurdu_EC	Caucasus_lowlands_LC	-0.0274	-3.411	0.008033	5344	5645	103170	neg
Mbuti.DG	Levant_EP	TellKurdu_EC	Caucasus_lowlands_LC	-0.0269	-3.687	0.007296	5689	6004	112943	neg
Mbuti.DG	Levant_MBA.SG	TellKurdu_EC	Caucasus_lowlands_LC	-0.0221	-4.442	0.004975	8607	8997	165872	neg
Mbuti.DG	Balkans_C	TellKurdu_EC	Caucasus_lowlands_LC	-0.0422	-5.203	0.008111	5011	5453	97955	neg
Mbuti.DG	Boncuklu_N	TellKurdu_EC	Caucasus_lowlands_LC	-0.029	-5.620	0.005160	8652	9168	166309	neg
Mbuti.DG	Levant_N	TellKurdu_EC	Caucasus_lowlands_LC	-0.0385	-6.506	0.005918	8081	8728	158406	neg
Mbuti.DG	Iberia_C	TellKurdu_EC	Caucasus_lowlands_LC	-0.0294	-6.566	0.004478	8615	9137	166709	neg
Mbuti.DG	Greece_N	TellKurdu_EC	Caucasus_lowlands_LC	-0.0479	-6.626	0.007229	7695	8469	150514	neg
Mbuti.DG	Levant_C	TellKurdu_EC	Caucasus_lowlands_LC	-0.0308	-7.007	0.004396	8593	9139	166469	neg
Mbuti.DG	LBK_EN	TellKurdu_EC	Caucasus_lowlands_LC	-0.034	-7.858	0.004327	8648	9257	166817	neg
Mbuti.DG	EHG	TellKurdu_EC	Ebla_EMBA	-0.0013	-0.422	0.003081	31468	31548	596574	neg

Mbuti.DG	L.Caucasus_LBA.SG	TellKurdu_EC	Ebla_EMBA	-0.0065	-1.851	0.003512	17132	17355	331791	neg
Mbuti.DG	G.Caucasus_b_EMBA	TellKurdu_EC	Ebla_EMBA	-0.0042	-1.859	0.002259	32078	32348	606719	neg
Mbuti.DG	Iran_C	TellKurdu_EC	Ebla_EMBA	-0.005	-2.134	0.002343	31928	32250	603825	neg
Mbuti.DG	L.Caucasus_MBA	TellKurdu_EC	Ebla_EMBA	-0.0084	-2.457	0.003419	28166	28643	531477	neg
Mbuti.DG	G.Caucasus_a_MLBA	TellKurdu_EC	Ebla_EMBA	-0.008	-2.910	0.002749	29391	29864	555025	neg
Mbuti.DG	<b>Bulgaria_Varna_En3</b>	<b>TellKurdu_EC</b>	<b>Ebla_EMBA</b>	<b>-0.0121</b>	<b>-3.040</b>	0.003980	15422	15800	292438	neg
Mbuti.DG	<b>G.Caucasus_a_En</b>	<b>TellKurdu_EC</b>	<b>Ebla_EMBA</b>	<b>-0.0103</b>	<b>-3.081</b>	0.003343	26688	27245	507510	neg
Mbuti.DG	<b>G.Caucasus_a_EBA</b>	<b>TellKurdu_EC</b>	<b>Ebla_EMBA</b>	<b>-0.0087</b>	<b>-3.867</b>	0.002250	31953	32515	606236	neg
Mbuti.DG	<b>Late_Helladic</b>	<b>TellKurdu_EC</b>	<b>Ebla_EMBA</b>	<b>-0.0156</b>	<b>-4.475</b>	0.003486	12178	12564	252434	neg
Mbuti.DG	<b>L.Caucasus_C</b>	<b>TellKurdu_EC</b>	<b>Ebla_EMBA</b>	<b>-0.0126</b>	<b>-5.115</b>	0.002463	31952	32768	606558	neg
Mbuti.DG	<b>Levant_MBA.SG</b>	<b>TellKurdu_EC</b>	<b>Ebla_EMBA</b>	<b>-0.0151</b>	<b>-6.499</b>	0.002323	32471	33469	617830	neg
Mbuti.DG	<b>Levant_EBA</b>	<b>TellKurdu_EC</b>	<b>Ebla_EMBA</b>	<b>-0.0189</b>	<b>-7.250</b>	0.002607	29625	30766	565984	neg
Mbuti.DG	<b>Bulgaria_Varna_En2</b>	<b>TellKurdu_EC</b>	<b>Ebla_EMBA</b>	<b>-0.0268</b>	<b>-7.482</b>	0.003582	16572	17483	316752	neg
Mbuti.DG	<b>Boncklu_N.SG</b>	<b>TellKurdu_EC</b>	<b>Ebla_EMBA</b>	<b>-0.0259</b>	<b>-8.062</b>	0.003213	30258	31864	579673	neg
Mbuti.DG	<b>Balkans_C</b>	<b>TellKurdu_EC</b>	<b>Ebla_EMBA</b>	<b>-0.0319</b>	<b>-8.318</b>	0.003835	16734	17838	323220	neg
Mbuti.DG	<b>Greece_N</b>	<b>TellKurdu_EC</b>	<b>Ebla_EMBA</b>	<b>-0.0302</b>	<b>-8.944</b>	0.003377	26722	28386	509470	neg
Mbuti.DG	<b>Lasithi_MMinoan</b>	<b>TellKurdu_EC</b>	<b>Ebla_EMBA</b>	<b>-0.0241</b>	<b>-9.356</b>	0.002576	31021	32552	593594	neg
Mbuti.DG	<b>Boncklu_N</b>	<b>TellKurdu_EC</b>	<b>Ebla_EMBA</b>	<b>-0.0249</b>	<b>-9.830</b>	0.002533	32390	34044	616687	neg
Mbuti.DG	<b>Levant_N</b>	<b>TellKurdu_EC</b>	<b>Ebla_EMBA</b>	<b>-0.0331</b>	<b>-11.750</b>	0.002817	28383	30329	549785	neg
Mbuti.DG	<b>LBK_EN</b>	<b>TellKurdu_EC</b>	<b>Ebla_EMBA</b>	<b>-0.0301</b>	<b>-14.221</b>	0.002117	32575	34598	621650	neg
Mbuti.DG	Late_Helladic	TellKurdu_EC	GondürleHöyük_EBA	-0.0027	-0.701	0.003852	12218	12284	252308	neg
Mbuti.DG	Boncklu_N.SG	TellKurdu_EC	GondürleHöyük_EBA	-0.0047	-1.179	0.003986	30788	31078	580094	neg
Mbuti.DG	Bulgaria_Varna_En2	TellKurdu_EC	GondürleHöyük_EBA	-0.0077	-1.843	0.004178	16880	17143	317733	neg
Mbuti.DG	Lasithi_MMinoan	TellKurdu_EC	GondürleHöyük_EBA	-0.0062	-2.108	0.002941	31511	31906	594814	neg
Mbuti.DG	Iberia_C	TellKurdu_EC	GondürleHöyük_EBA	-0.0059	-2.250	0.002622	32958	33347	620264	neg
Mbuti.DG	Levant_EBA	TellKurdu_EC	GondürleHöyük_EBA	-0.0078	-2.569	0.003036	29946	30416	569813	neg
Mbuti.DG	Levant_MBA.SG	TellKurdu_EC	GondürleHöyük_EBA	-0.0071	-2.714	0.002616	32573	33035	618268	neg
Mbuti.DG	<b>Greece_N</b>	<b>TellKurdu_EC</b>	<b>GondürleHöyük_EBA</b>	<b>-0.0139</b>	<b>-3.343</b>	0.004158	27121	27885	510441	neg
Mbuti.DG	<b>Balkans_C</b>	<b>TellKurdu_EC</b>	<b>GondürleHöyük_EBA</b>	<b>-0.0151</b>	<b>-3.579</b>	0.004219	17006	17527	323773	neg
Mbuti.DG	<b>LBK_EN</b>	<b>TellKurdu_EC</b>	<b>GondürleHöyük_EBA</b>	<b>-0.0106</b>	<b>-4.391</b>	0.002414	33123	33830	622204	neg
Mbuti.DG	<b>Balkans_N</b>	<b>TellKurdu_EC</b>	<b>GondürleHöyük_EBA</b>	<b>-0.0134</b>	<b>-4.818</b>	0.002781	32450	33329	613110	neg
Mbuti.DG	<b>Levant_EP</b>	<b>TellKurdu_EC</b>	<b>GondürleHöyük_EBA</b>	<b>-0.0205</b>	<b>-5.243</b>	0.003910	18809	19598	368313	neg
Mbuti.DG	<b>Levant_C</b>	<b>TellKurdu_EC</b>	<b>GondürleHöyük_EBA</b>	<b>-0.013</b>	<b>-5.258</b>	0.002472	32429	33281	616999	neg
Mbuti.DG	<b>Levant_N</b>	<b>TellKurdu_EC</b>	<b>GondürleHöyük_EBA</b>	<b>-0.0184</b>	<b>-5.604</b>	0.003283	28721	29800	552249	neg
Mbuti.DG	G.Caucasus_a_En	TellKurdu_EC	İkiztepe_LC	-0.0008	-0.194	0.004124	19282	19312	363958	neg
Mbuti.DG	Boncklu_N.SG	TellKurdu_EC	İkiztepe_LC	-0.0049	-1.227	0.003993	20947	21153	393629	neg
Mbuti.DG	Lasithi_MMinoan	TellKurdu_EC	İkiztepe_LC	-0.0101	-3.276	0.003083	21595	22037	407124	neg
Mbuti.DG	Levant_MBA.SG	TellKurdu_EC	İkiztepe_LC	-0.011	-3.849	0.002858	21874	22360	416313	neg
Mbuti.DG	<b>Balkans_C</b>	<b>TellKurdu_EC</b>	<b>İkiztepe_LC</b>	<b>-0.0228</b>	<b>-4.821</b>	0.004729	12096	12661	231765	neg
Mbuti.DG	<b>Greece_N</b>	<b>TellKurdu_EC</b>	<b>İkiztepe_LC</b>	<b>-0.0244</b>	<b>-5.944</b>	0.004105	19060	20012	363104	neg
Mbuti.DG	<b>Iberia_C</b>	<b>TellKurdu_EC</b>	<b>İkiztepe_LC</b>	<b>-0.0172</b>	<b>-6.583</b>	0.002613	22004	22776	418229	neg
Mbuti.DG	<b>Levant_EP</b>	<b>TellKurdu_EC</b>	<b>İkiztepe_LC</b>	<b>-0.0291</b>	<b>-6.658</b>	0.004371	13470	14277	266456	neg
Mbuti.DG	<b>Levant_C</b>	<b>TellKurdu_EC</b>	<b>İkiztepe_LC</b>	<b>-0.0207</b>	<b>-8.305</b>	0.002492	21790	22712	417090	neg
Mbuti.DG	<b>Levant_N</b>	<b>TellKurdu_EC</b>	<b>İkiztepe_LC</b>	<b>-0.0307</b>	<b>-9.283</b>	0.003307	19937	21199	387190	neg
Mbuti.DG	Iran_N	TellKurdu_EC	K.Kalehöyük_MLBA	-0.0002	-0.026	0.007692	5289	5291	101910	neg
Mbuti.DG	L.Caucasus_EBA	TellKurdu_EC	K.Kalehöyük_MLBA	-0.0003	-0.057	0.005263	6091	6094	115320	neg
Mbuti.DG	G.Caucasus_b_EMBA	TellKurdu_EC	K.Kalehöyük_MLBA	-0.0026	-0.547	0.004753	5970	6001	114129	neg
Mbuti.DG	L.Caucasus_MBA	TellKurdu_EC	K.Kalehöyük_MLBA	-0.0042	-0.601	0.006988	5190	5234	98733	neg
Mbuti.DG	G.Caucasus_a_EBA	TellKurdu_EC	K.Kalehöyük_MLBA	-0.003	-0.625	0.004800	6013	6049	114160	neg
Mbuti.DG	L.Caucasus_C	TellKurdu_EC	K.Kalehöyük_MLBA	-0.0061	-1.259	0.004845	6006	6080	114449	neg
Mbuti.DG	G.Caucasus_a_MLBA	TellKurdu_EC	K.Kalehöyük_MLBA	-0.0076	-1.307	0.005815	5398	5481	103070	neg
Mbuti.DG	Boncklu_N.SG	TellKurdu_EC	K.Kalehöyük_MLBA	-0.0138	-2.231	0.006186	5939	6105	113053	neg
Mbuti.DG	Levant_MBA.SG	TellKurdu_EC	K.Kalehöyük_MLBA	-0.0128	-2.591	0.004940	6110	6269	117527	neg
Mbuti.DG	Boncklu_N	TellKurdu_EC	K.Kalehöyük_MLBA	-0.0132	-2.664	0.004955	6174	6339	117047	neg
Mbuti.DG	Lasithi_MMinoan	TellKurdu_EC	K.Kalehöyük_MLBA	-0.014	-2.670	0.005243	5869	6036	111877	neg
Mbuti.DG	Levant_EP	TellKurdu_EC	K.Kalehöyük_MLBA	-0.022	-2.813	0.007821	3435	3590	67588	neg
Mbuti.DG	<b>Bulgaria_Varna_En2</b>	<b>TellKurdu_EC</b>	<b>K.Kalehöyük_MLBA</b>	<b>-0.0342</b>	<b>-3.891</b>	0.008790	2969	3179	57658	neg
Mbuti.DG	<b>Levant_EBA</b>	<b>TellKurdu_EC</b>	<b>K.Kalehöyük_MLBA</b>	<b>-0.0239</b>	<b>-4.248</b>	0.005626	5395	5659	105230	neg
Mbuti.DG	<b>Balkans_N</b>	<b>TellKurdu_EC</b>	<b>K.Kalehöyük_MLBA</b>	<b>-0.0232</b>	<b>-4.748</b>	0.004886	6010	6295	115477	neg
Mbuti.DG	<b>Levant_N</b>	<b>TellKurdu_EC</b>	<b>K.Kalehöyük_MLBA</b>	<b>-0.0289</b>	<b>-4.959</b>	0.005828	5261	5573	102257	neg
Mbuti.DG	<b>LBK_EN</b>	<b>TellKurdu_EC</b>	<b>K.Kalehöyük_MLBA</b>	<b>-0.0211</b>	<b>-5.021</b>	0.004202	6208	6476	118353	neg
Mbuti.DG	Iran_N	TellKurdu_EC	Topakhöyük_EBA	-0.0025	-0.348	0.007184	5087	5112	98960	neg
Mbuti.DG	G.Caucasus_b_En	TellKurdu_EC	Topakhöyük_EBA	-0.0025	-0.451	0.005543	5805	5834	110825	neg
Mbuti.DG	Greece_N	TellKurdu_EC	Topakhöyük_EBA	-0.0036	-0.471	0.007643	4927	4962	91759	neg
Mbuti.DG	EHG	TellKurdu_EC	Topakhöyük_EBA	-0.0047	-0.776	0.006057	5639	5692	109221	neg
Mbuti.DG	Iran_C	TellKurdu_EC	Topakhöyük_EBA	-0.0067	-1.289	0.005198	5774	5852	110496	neg
Mbuti.DG	G.Caucasus_b_EMBA	TellKurdu_EC	Topakhöyük_EBA	-0.0074	-1.534	0.004824	5751	5837	110757	neg
Mbuti.DG	Bulgaria_Varna_En3	TellKurdu_EC	Topakhöyük_EBA	-0.0147	-1.537	0.009564	2661	2740	51628	neg
Mbuti.DG	G.Caucasus_a_MLBA	TellKurdu_EC	Topakhöyük_EBA	-0.0115	-1.869	0.006153	5208	5329	100112	neg
Mbuti.DG	Bulgaria_Varna_En2	TellKurdu_EC	Topakhöyük_EBA	-0.0195	-2.155	0.009049	2928	3044	56078	neg
Mbuti.DG	L.Caucasus_MBA	TellKurdu_EC	Topakhöyük_EBA	-0.0154	-2.168	0.007103	4954	5109	95849	neg
Mbuti.DG	G.Caucasus_a_EBA	TellKurdu_EC	Topakhöyük_EBA	-0.0116	-2.316	0.005009	5751	5886	110751	neg
Mbuti.DG	L.Caucasus_C	TellKurdu_EC	Topakhöyük_EBA	-0.0128	-2.639	0.004850	5778	5928	111029	neg
Mbuti.DG	Boncklu_N.SG	TellKurdu_EC	Topakhöyük_EBA	-0.0188	-2.974	0.006321	5705	5923	109667	neg
Mbuti.DG	<b>Levant_EP</b>	<b>TellKurdu_EC</b>	<b>Topakhöyük_EBA</b>	<b>-0.0274</b>	<b>-3.314</b>	0.008268	3312	3499	65729	neg
Mbuti.DG	<b>Levant_MBA.SG</b>	<b>TellKurdu_EC</b>	<b>Topakhöyük_EBA</b>	<b>-0.0173</b>	<b>-3.428</b>	0.005047	5877	6084	113980	neg
Mbuti.DG	<b>Boncklu_N</b>	<b>TellKurdu_EC</b>	<b>Topakhöyük_EBA</b>	<b>-0.0183</b>	<b>-3.598</b>	0.005086	5941	6163	113504	neg
Mbuti.DG	<b>Levant_EBA</b>	<b>TellKurdu_EC</b>	<b>Topakhöyük_EBA</b>	<b>-0.0267</b>	<b>-4.528</b>	0.005897	5223	5509	102192	neg
Mbuti.DG	<b>Iberia_C</b>	<b>TellKurdu_EC</b>	<b>Topakhöyük_EBA</b>	<b>-0.0224</b>	<b>-4.958</b>	0.004518	5926	6198	113914	neg
Mbuti.DG	<b>Balkans_N</b>	<b>TellKurdu_EC</b>	<b>Topakhöyük_EBA</b>	<b>-0.0248</b>	<b>-4.987</b>	0.004973	5800	6095	112026	neg
Mbuti.DG	<b>LBK_EN</b>	<b>TellKurdu_EC</b>	<b>Topakhöyük_EBA</b>	<b>-0.025</b>	<b>-5.906</b>	0.004233	5972	6279	114765	neg

**Table S6. *qpAdm* results for Late Chalcolithic – Late Bronze Age groups with Barcin\_N or TellKurdu\_EC as Reference (source) 1 and various populations from Iran and Caucasus as Reference 2, Related to Figure 6. *P-values*, admixture proportions and their  $\pm 1$  SE for every admixture model are presented. Right populations: Mbuti.DG, Ami.DG, Mixe.DG, Kostenki14, EHG, Villabruna and Levant\_EP. Fitting models ( $p\text{-value} \geq 0.05$ ) are annotated with bold letters and bold *Italics* when  $0.01 \leq p\text{-value} < 0.05$ . Published contemporaneous Anatolian groups are annotated with asterisk.**

Target	Reference 2	Reference 1: Barcin_N				Reference 1: TellKurdu_EC			
		<i>P-value</i>	Coef <sub>1</sub> (%)	Coef <sub>2</sub> (%)	SE (%)	<i>P-value</i>	Coef <sub>1</sub> (%)	Coef <sub>2</sub> (%)	SE (%)
Alalakh_MLBA	Iran_N	4.50E-05	72.8	27.2	1.8	<b>4.75E-01</b>	74.8	25.2	2.8
Arslantepe_EBA		<b>8.94E-02</b>	68.8	31.2	2.6	<b>3.38E-01</b>	68.2	31.8	3.5
Arslantepe_LC		3.93E-03	71.6	28.4	1.8	1.11E-03	73.6	26.4	3.1
Barcin_C*		1.14E-03	78.6	21.4	4.4	2.09E-06	76.7	23.3	5.6
ÇamlıbelTarlasi_LC		<b>6.46E-01</b>	70.1	29.9	2.3	4.95E-03	72	28	3.6
Caucasus_lowlands_LC		<b>1.35E-02</b>	69.2	30.8	7.4	<b>2.33E-01</b>	74.7	25.3	8
Ebla_EMBA		1.60E-04	73.3	26.7	2.6	<b>7.45E-01</b>	74.8	25.2	3.3
GondürleHöyük_EBA*		<b>1.25E-01</b>	77.8	22.2	2.9	1.30E-04	76.5	23.5	4.4
İkiztepe_LC		<b>6.27E-01</b>	68.5	31.5	3.3	7.96E-03	68.2	31.8	4.5
K.Kalehöyük_MLBA*		<b>7.87E-01</b>	68.8	31.2	5.4	<b>5.60E-01</b>	67.8	32.2	7.5
TitrişHöyük_EBA		<b>1.08E-01</b>	79.1	20.9	9.1	<b>5.76E-01</b>	93.7	6.3	13.8
Topakhöyük_EBA*		<b>5.07E-01</b>	62.1	37.9	6.1	<b>2.01E-01</b>	65.6	34.4	8.1
Alalakh_MLBA	CHG	5.96E-18	70.4	29.6	2.4	<b>7.26E-01</b>	71.9	28.1	2.8
Arslantepe_EBA		2.81E-05	66	34	3.2	<b>8.58E-01</b>	64.2	35.8	3.7
Arslantepe_LC		2.07E-06	67.3	32.7	2.2	<b>9.69E-01</b>	67.5	32.5	2.9
Barcin_C*		<b>2.52E-02</b>	72.6	27.4	4.9	1.63E-03	67	33	5.7
ÇamlıbelTarlasi_LC		2.68E-04	66.1	33.9	2.6	<b>4.10E-01</b>	66.2	33.8	3.5
Caucasus_lowlands_LC		7.99E-03	63.3	36.7	8.1	<b>3.49E-01</b>	67.3	32.7	8.8
Ebla_EMBA		3.68E-12	72.9	27.1	3.3	<b>3.82E-01</b>	72.2	27.8	3.5
GondürleHöyük_EBA*		<b>4.05E-01</b>	74	26	3.3	<b>3.86E-01</b>	67.4	32.6	4.2
İkiztepe_LC		<b>1.49E-01</b>	63.3	36.7	4	<b>8.45E-01</b>	60.6	39.4	4.4
K.Kalehöyük_MLBA*		<b>6.86E-01</b>	62.6	37.4	6	<b>6.90E-01</b>	61.4	38.6	7.9
TitrişHöyük_EBA		<b>9.87E-02</b>	73.5	26.5	12.8	<b>5.95E-01</b>	86.7	13.3	19
Topakhöyük_EBA*		<b>1.15E-01</b>	59	41	7.2	<b>3.47E-01</b>	60.4	39.6	9.2
Alalakh_MLBA	Iran_C	3.79E-05	57.6	42.4	2.5	<b>8.40E-01</b>	60.4	39.6	3.7
Arslantepe_EBA		<b>2.63E-01</b>	51.3	48.7	3.9	<b>8.46E-01</b>	49.7	50.3	5
Arslantepe_LC		<b>2.95E-01</b>	54.7	45.3	2.6	<b>5.02E-02</b>	57.1	42.9	4
Barcin_C*		2.56E-03	66	34	6.6	9.91E-06	61.8	38.2	8.6
ÇamlıbelTarlasi_LC		<b>8.90E-01</b>	54.1	45.9	3.3	6.42E-03	55.1	44.9	5.1
Caucasus_lowlands_LC		<b>2.33E-02</b>	47.1	52.9	11.2	<b>1.90E-01</b>	56.5	43.5	14.6
Ebla_EMBA		6.78E-05	58.4	41.6	3.8	<b>8.51E-01</b>	58.7	41.3	4.6
GondürleHöyük_EBA*		<b>6.54E-01</b>	64.8	35.2	4.4	2.36E-03	61.3	38.7	6.5
İkiztepe_LC		<b>9.97E-01</b>	51.4	48.6	4.8	<b>1.26E-01</b>	48.8	51.2	6.1
K.Kalehöyük_MLBA*		<b>8.52E-01</b>	57.2	42.8	7	<b>2.14E-01</b>	55.3	44.7	11.6
TitrişHöyük_EBA		<b>2.59E-01</b>	63.7	36.3	13.1	<b>5.40E-01</b>	83	17	22.4
Topakhöyük_EBA*		<b>1.56E-01</b>	53.8	46.2	7.9	<b>8.00E-02</b>	58.9	41.1	12.7
Alalakh_MLBA	G.Caucasus_a_En	1.36E-11	43.7	56.3	6.5	<b>1.35E-01</b>	59	41	5.1
Arslantepe_EBA		1.07E-05	41.1	58.9	7.2	<b>1.54E-01</b>	49.3	50.7	6.5
Arslantepe_LC		3.45E-06	42.1	57.9	5.6	<b>4.36E-01</b>	51.9	48.1	5.2

Target	Reference 2	Reference 1: Barcın_N				Reference 1: TellKurdu_EC			
		<i>P-value</i>	Coef <sub>1</sub> (%)	Coef <sub>2</sub> (%)	SE (%)	<i>P-value</i>	Coef <sub>1</sub> (%)	Coef <sub>2</sub> (%)	SE (%)
Barcın_C*		<b>1.18E-01</b>	51.7	48.3	8.5	<b>3.75E-02</b>	44.6	55.4	9.4
ÇamlıbelTarlasi_LC		5.96E-04	43	57	6	<b>5.17E-01</b>	48.8	51.2	6.2
Caucasus_lowlands_LC		<b>1.45E-02</b>	42.6	57.4	15.2	<b>2.57E-01</b>	55.9	44.1	14.2
Ebla_EMBA		5.05E-09	48.4	51.6	7.9	<b>6.93E-02</b>	59.6	40.4	6.1
GondürleHöyük_EBA*		<b>1.64E-01</b>	54.8	45.2	6.2	<b>9.15E-01</b>	49.9	50.1	6.5
İkiztepe_LC		<b>3.39E-02</b>	35.9	64.1	7.9	<b>8.15E-01</b>	41	59	7.2
K.Kalehöyük_MLBA*		<b>5.36E-01</b>	43.3	56.7	12.2	<b>6.70E-01</b>	36.4	63.6	14.6
TitrişHöyük_EBA		<b>1.46E-02</b>	78	22	18.8	<i>3.77E-01</i>	<i>104.1</i>	<i>-4.1</i>	<i>25.7</i>
Topakhöyük_EBA*		<b>1.18E-01</b>	24.3	75.7	17.6	<b>2.79E-01</b>	32.9	67.1	19.6
Alalakh_MLBA	G.Caucasus _b_En	1.68E-56	94.9	5.1	2	1.71E-06	87.8	12.2	2.2
Arslantepe_EBA		4.36E-25	90.3	9.7	2.4	5.05E-06	83.8	16.2	2.7
Arslantepe_LC		7.59E-46	89.8	10.2	1.9	5.56E-05	83.3	16.7	2.1
Barcın_C*		<b>4.08E-02</b>	80.1	19.9	3.4	<b>6.12E-01</b>	73.9	26.1	3.5
ÇamlıbelTarlasi_LC		2.06E-32	88.7	11.3	2	1.19E-05	83.8	16.2	2.4
Caucasus_lowlands_LC		5.78E-05	84.9	15.1	4.7	<b>9.63E-02</b>	84.6	15.4	5.4
Ebla_EMBA		1.12E-27	95.7	4.3	2.1	2.41E-05	88.2	11.8	2.4
GondürleHöyük_EBA*		7.47E-07	87.6	12.4	2.4	<b>8.95E-02</b>	80.3	19.7	2.8
İkiztepe_LC		2.79E-15	88.4	11.6	2.8	2.30E-04	80.8	19.2	3
K.Kalehöyük_MLBA*		9.31E-05	83.1	16.9	4.3	<b>1.90E-01</b>	79.9	20.1	5.3
TitrişHöyük_EBA		<b>1.55E-02</b>	94.9	5.1	7	<b>5.04E-01</b>	97.9	2.1	9.3
Topakhöyük_EBA*		1.16E-07	85.4	14.6	5.2	<b>3.28E-02</b>	79.9	20.1	6.2
Alalakh_MLBA	G.Caucasus _c_EMBA	8.02E-56	95.7	4.3	1.3	2.23E-06	89.7	10.3	1.8
Arslantepe_EBA		6.71E-25	91.9	8.1	1.8	4.68E-06	86.4	13.6	2.2
Arslantepe_LC		2.75E-44	91.9	8.1	1.3	5.87E-05	86	14	1.8
Barcın_C*		<b>7.29E-02</b>	83.9	16.1	2.7	<b>6.42E-01</b>	78.4	21.6	2.9
ÇamlıbelTarlasi_LC		7.08E-33	91.9	8.1	1.4	1.71E-06	87.1	12.9	2
Caucasus_lowlands_LC		1.19E-05	88.6	11.4	4	<b>5.11E-02</b>	87.6	12.4	4.7
Ebla_EMBA		1.95E-27	95.9	4.1	1.5	3.45E-05	89.9	10.1	2
GondürleHöyük_EBA*		1.65E-06	90.3	9.7	1.8	<b>3.59E-02</b>	83.9	16.1	2.4
İkiztepe_LC		4.20E-15	91.1	8.9	2	8.07E-05	84.7	15.3	2.5
K.Kalehöyük_MLBA*		4.29E-04	86.3	13.7	3	<b>1.75E-01</b>	83.8	16.2	4.2
TitrişHöyük_EBA		<b>1.78E-02</b>	96.4	3.6	5.2	<b>5.44E-01</b>	96.6	3.4	6.7
Topakhöyük_EBA*		1.04E-06	87.8	12.2	3.5	<b>8.77E-02</b>	82.7	17.3	4.6
Alalakh_MLBA	L.Caucasus _C	6.27E-41	42	58	14.8	6.60E-07	69	31	5.4
Arslantepe_EBA		4.37E-14	44.8	55.2	8	1.70E-05	55.2	44.8	7.1
Arslantepe_LC		5.06E-23	38	62	7.6	1.67E-04	56.9	43.1	5
Barcın_C*		<b>4.06E-01</b>	45.2	54.8	8.9	<b>5.37E-01</b>	35.6	64.4	8.6
ÇamlıbelTarlasi_LC		9.97E-19	43.5	56.5	7.7	7.92E-06	57.1	42.9	6.5
Caucasus_lowlands_LC		3.79E-04	48.1	51.9	15.4	<b>5.94E-02</b>	60.4	39.6	16.1
Ebla_EMBA		6.27E-22	65.4	34.6	9.4	1.13E-04	68.4	31.6	6.3
GondürleHöyük_EBA*		3.42E-03	59.4	40.6	6.4	<b>2.39E-01</b>	50.1	49.9	6.3
İkiztepe_LC		2.08E-07	45.3	54.7	8.6	1.05E-03	46.9	53.1	8
K.Kalehöyük_MLBA*		<b>6.07E-02</b>	42.8	57.2	11.4	<b>5.77E-01</b>	46.1	53.9	12.1
TitrişHöyük_EBA		<b>2.64E-02</b>	77.3	22.7	21.5	<b>5.33E-01</b>	96	4	26.3
Topakhöyük_EBA*		8.68E-04	36.3	63.7	14.4	<b>2.54E-01</b>	41.3	58.7	14.2



Target	Reference 2	Reference 1: Barcın_N				Reference 1: TellKurdu_EC			
		<i>P-value</i>	Coef <sub>1</sub> (%)	Coef <sub>2</sub> (%)	SE (%)	<i>P-value</i>	Coef <sub>1</sub> (%)	Coef <sub>2</sub> (%)	SE (%)
Alalakh_MLBA	L.Caucasus _EBA	6.73E-23	50.9	49.1	4.1	<b>1.38E-02</b>	58.5	41.5	4
Arslantepe_EBA		7.33E-06	43.4	56.6	5.1	<b>9.79E-02</b>	45.3	54.7	5.4
Arslantepe_LC		1.16E-06	43.4	56.6	3.8	<b>7.05E-01</b>	48.4	51.6	4.1
Barcın_C*		<b>1.49E-01</b>	50.8	49.2	8.1	<b>3.63E-02</b>	40.6	59.4	8.6
ÇamlıbelTarlası_LC		7.70E-06	43.6	56.4	4.5	<b>1.83E-02</b>	48.1	51.9	5.4
Caucasus_lowlands_LC		<b>2.28E-02</b>	37.7	62.3	13.2	<b>2.54E-01</b>	48.6	51.4	14.6
Ebla_EMBA		2.96E-13	54.4	45.6	5.6	<b>1.72E-02</b>	59.2	40.8	5.1
GondürleHöyük_EBA*		<b>7.07E-01</b>	55.2	44.8	5.6	<b>6.23E-01</b>	46.4	53.6	6.1
İkiztepe_LC		<b>7.25E-02</b>	40.7	59.3	6.6	<b>4.05E-01</b>	39.9	60.1	6.4
K.Kalehöyük_MLBA*		<b>8.85E-01</b>	39.3	60.7	9.4	<b>8.93E-01</b>	41.4	58.6	11
TitrişHöyük_EBA		<b>7.43E-02</b>	65.3	34.7	18.1	<b>5.33E-01</b>	87.7	12.3	29.2
Topakhöyük_EBA*		<b>7.28E-02</b>	33.9	66.1	11.1	<b>4.18E-01</b>	39.2	60.8	13

**Table S7. qpAdm results for Late Chalcolithic – Late Bronze Age groups with TellKurdu\_EC or Büyükkaya\_EC as Reference (source) 1 and various populations from Iran and Caucasus as Reference 2, Related to Figure 6. P-values, admixture proportions and their  $\pm 1$  SE for every admixture model are presented. Right populations: Mbuti.DG, Ami.DG, Mixe.DG, Kostenki14, EHG, Villabruna, Levant\_EP and Barcin\_N. Fitting models ( $p\text{-value} \geq 0.05$ ) are annotated with bold letters and bold *Italics* when  $0.01 \leq p\text{-value} < 0.05$ . Published contemporaneous Anatolian groups are annotated with asterisk.**

Target	Reference 2	Reference 1: TellKurdu_EC				Reference 1: Büyükkaya_EC			
		<i>P-value</i>	Coef <sub>1</sub> (%)	Coef <sub>2</sub> (%)	SE (%)	<i>P-value</i>	Coef <sub>1</sub> (%)	Coef <sub>2</sub> (%)	SE (%)
Alalakh_MLBA	Iran_N	<b>3.87E-02</b>	68.2	31.8	1.6	2.40E-04	80.7	19.3	2.9
Arslantepe_EBA		<b>4.44E-01</b>	68.8	31.2	2	<b>9.25E-02</b>	81.4	18.6	3.1
Arslantepe_LC		2.15E-03	72.5	27.5	1.7	<b>6.13E-02</b>	84.4	15.6	2.8
Barcin_C*		5.42E-06	75.9	24.1	3.2	<b>2.04E-02</b>	89.6	10.4	4.2
ÇamlıbelTarlası_LC		5.07E-03	75.6	24.4	2	<b>2.33E-01</b>	88.7	11.3	3
Caucasus_lowlands_LC		<b>1.55E-01</b>	64.7	35.3	4.4	<b>7.27E-02</b>	72.6	27.4	5.3
Ebla_EMBA		<b>8.44E-02</b>	66.8	33.2	1.9	2.28E-04	79	21	3.2
GondürleHöyük_EBA*		1.43E-04	81	19	2.4	<b>3.34E-01</b>	94.3	5.7	3.5
İkiztepe_LC		3.05E-03	75.5	24.5	2.5	<b>1.82E-01</b>	88.3	11.7	3.5
K.Kalehöyük_MLBA*		<b>6.76E-01</b>	67.5	32.5	4.1	<b>4.82E-01</b>	78.7	21.3	5.2
TitrişHöyük_EBA		<b>4.90E-01</b>	79.4	20.6	5.8	<b>3.27E-01</b>	88.3	11.7	7.4
Topakhöyük_EBA*		<b>2.89E-01</b>	65	35	4.3	<b>8.02E-01</b>	76.7	23.3	5.7
Alalakh_MLBA	CHG	<b>1.52E-02</b>	64	36	1.7	2.55E-06	81.5	18.5	3.6
Arslantepe_EBA		<b>9.19E-01</b>	63.9	36.1	2.2	5.87E-03	80.6	19.4	3.9
Arslantepe_LC		<b>9.87E-01</b>	67.4	32.6	1.7	<b>3.11E-02</b>	82.2	17.8	3.4
Barcin_C*		3.16E-03	68.8	31.2	3.5	<b>3.75E-02</b>	84.2	15.8	4.8
ÇamlıbelTarlası_LC		<b>2.19E-01</b>	71.3	28.7	2.1	<b>8.17E-02</b>	87.8	12.2	3.6
Caucasus_lowlands_LC		<b>3.23E-01</b>	59.2	40.8	4.7	<b>2.16E-02</b>	66	34	6.6
Ebla_EMBA		7.15E-03	62.7	37.3	2	1.68E-06	79.3	20.7	4
GondürleHöyük_EBA*		<b>9.19E-02</b>	75.7	24.3	2.5	<b>3.98E-01</b>	93.2	6.8	4.2
İkiztepe_LC		<b>2.66E-01</b>	69.4	30.6	2.6	<b>1.59E-01</b>	87.1	12.9	4.1
K.Kalehöyük_MLBA*		<b>7.89E-01</b>	60.3	39.7	4.3	<b>4.36E-01</b>	74	26	5.9
TitrişHöyük_EBA		<b>5.74E-01</b>	71.1	28.9	7	<b>2.71E-01</b>	85.9	14.1	10.4
Topakhöyük_EBA*		<b>4.60E-01</b>	60.8	39.2	4.6	<b>8.09E-01</b>	72.1	27.9	6.2
Alalakh_MLBA	Iran_C	7.57E-05	47.1	52.9	2.4	3.35E-06	68.1	31.9	5.1
Arslantepe_EBA		<b>8.74E-01</b>	47.2	52.8	2.9	<b>2.60E-02</b>	65.1	34.9	5.2
Arslantepe_LC		<b>5.08E-02</b>	53.6	46.4	2.4	<b>3.33E-02</b>	70.4	29.6	4.7
Barcin_C*		2.22E-05	58.6	41.4	5.1	7.48E-03	80.5	19.5	7.8
ÇamlıbelTarlası_LC		8.39E-03	59	41	2.9	<b>1.15E-01</b>	78.7	21.3	5.3
Caucasus_lowlands_LC		<b>1.18E-01</b>	38.7	61.3	7.8	<b>2.12E-02</b>	45.4	54.6	10.8
Ebla_EMBA		3.71E-03	44.1	55.9	2.7	5.09E-06	63	37	5.7
GondürleHöyük_EBA*		2.97E-03	66.7	33.3	3.7	<b>2.65E-01</b>	89.5	10.5	6.6
İkiztepe_LC		<b>8.89E-02</b>	56	44	3.6	<b>2.62E-01</b>	76.7	23.3	6.2
K.Kalehöyük_MLBA*		<b>1.68E-01</b>	43.9	56.1	6.6	<b>3.23E-01</b>	61.6	38.4	8.7
TitrişHöyük_EBA		<b>4.05E-01</b>	58.7	41.3	9.9	<b>4.25E-01</b>	71	29	14.3
Topakhöyük_EBA*		<b>5.75E-02</b>	45.3	54.7	6.9	<b>4.32E-01</b>	59.5	40.5	9.1
Alalakh_MLBA	G.Caucasus_a_En	<b>2.58E-02</b>	48.6	51.4	2.8	5.42E-06	70.1	29.9	6.3
Arslantepe_EBA		<b>2.24E-01</b>	50.5	49.5	3.3	9.92E-03	70.8	29.2	5.9

Target	Reference 2	Reference 1: TellKurdu_EC				Reference 1: Büyükkaya_EC			
		<i>P-value</i>	Coef <sub>1</sub> (%)	Coef <sub>2</sub> (%)	SE (%)	<i>P-value</i>	Coef <sub>1</sub> (%)	Coef <sub>2</sub> (%)	SE (%)
Arslantepe_LC		<b>5.33E-01</b>	53.6	46.4	2.8	<b>2.33E-02</b>	72.5	27.5	5.2
Barcın_C*		<b>3.55E-02</b>	53.4	46.6	5.5	<b>8.11E-02</b>	73.2	26.8	7.3
ÇamlıbelTarlası_LC		<b>1.34E-01</b>	60.9	39.1	3.2	<b>1.08E-01</b>	81.5	18.5	5.4
Caucasus_lowlands_LC		<b>2.35E-01</b>	42.8	57.2	7.6	<b>7.09E-02</b>	52.6	47.4	10.1
Ebla_EMBA		9.86E-03	46.2	53.8	3.3	9.93E-06	64	36	6.8
GondürleHöyük_EBA*		<b>1.81E-01</b>	65.4	34.6	3.8	<b>4.90E-01</b>	89.4	10.6	6.3
İkiztepe_LC		<b>2.68E-01</b>	54.4	45.6	4.1	<b>2.08E-01</b>	78.5	21.5	6.7
K.Kalehöyük_MLBA*		<b>6.94E-01</b>	45.4	54.6	7	<b>8.38E-01</b>	64.5	35.5	8.5
TitrişHöyük_EBA		<b>1.11E-01</b>	67.3	32.7	10.7	<b>1.33E-01</b>	86.9	13.1	17.7
Topakhöyük_EBA*		<b>3.45E-01</b>	41.7	58.3	7.3	<b>5.86E-01</b>	60.6	39.4	10
Arslantepe_EBA	G.Caucasus _b_En	5.77E-16	77.7	22.3	1.3	1.44E-08	92.3	7.7	2.5
Arslantepe_LC		1.23E-07	77.7	22.3	1.6	6.41E-05	91.8	8.2	2.7
Barcın_C*		2.76E-06	78.8	21.2	1.3	8.24E-04	91.4	8.6	2.4
ÇamlıbelTarlası_LC		<b>6.78E-01</b>	75.4	24.6	2.5	<b>2.22E-01</b>	86.8	13.2	3.2
Caucasus_lowlands_LC		1.84E-05	81.9	18.1	1.5	<b>1.90E-02</b>	94.4	5.6	2.5
Ebla_EMBA		9.71E-03	73.9	26.1	3.3	3.96E-04	82.2	17.8	4.5
Ebla_EMBA		5.66E-14	77.1	22.9	1.5	3.80E-09	91.9	8.1	2.6
GondürleHöyük_EBA*		<b>7.78E-02</b>	83.3	16.7	1.8	<b>3.72E-01</b>	95.9	4.1	2.9
İkiztepe_LC		5.14E-04	80.4	19.6	1.9	<b>3.36E-02</b>	94.5	5.5	3
K.Kalehöyük_MLBA*		<b>1.14E-01</b>	73.3	26.7	3.3	<b>2.68E-01</b>	84.3	15.7	4.3
TitrişHöyük_EBA		<b>2.02E-01</b>	83.3	16.7	4.8	<b>1.68E-01</b>	99.2	0.8	7.1
Topakhöyük_EBA*		<b>2.51E-02</b>	72.9	27.1	3.4	<b>2.31E-01</b>	85.4	14.6	4.7
Alalakh_MLBA	G.Caucasus _c_EMBA	3.25E-15	81.5	18.5	1.1	1.65E-08	93.4	6.6	1.9
Arslantepe_EBA		1.75E-07	81.5	18.5	1.4	5.25E-05	92.9	7.1	2.1
Arslantepe_LC		5.12E-06	82.5	17.5	1.1	7.92E-04	92.9	7.1	1.9
Barcın_C*		<b>6.98E-01</b>	79.8	20.2	2	<b>2.60E-01</b>	89.2	10.8	2.6
ÇamlıbelTarlası_LC		2.21E-06	85.3	14.7	1.2	<b>1.26E-02</b>	95.3	4.7	1.9
Caucasus_lowlands_LC		6.29E-03	78.5	21.5	2.8	4.15E-04	86.2	13.8	3.6
Ebla_EMBA		5.07E-13	81	19	1.2	5.06E-09	93	7	2
GondürleHöyük_EBA*		<b>3.44E-02</b>	86.3	13.7	1.5	<b>3.20E-01</b>	96.7	3.3	2.3
İkiztepe_LC		1.83E-04	84.2	15.8	1.6	<b>2.81E-02</b>	95.4	4.6	2.3
K.Kalehöyük_MLBA*		<b>1.23E-01</b>	79	21	2.6	<b>2.04E-01</b>	87	13	3.3
TitrişHöyük_EBA		<b>2.58E-01</b>	86.4	13.6	3.7	<b>1.58E-01</b>	99.6	0.4	5.1
Topakhöyük_EBA*		<b>8.52E-02</b>	78.5	21.5	2.7	<b>2.26E-01</b>	88	12	3.6
Alalakh_MLBA	L.Caucasus _C	4.23E-16	46	54	3.1	7.62E-10	83.9	16.1	8.5
Arslantepe_EBA		7.51E-06	45.6	54.4	3.8	6.24E-05	73	27	8.3
Arslantepe_LC		7.04E-05	50	50	2.9	8.22E-04	73.6	26.4	6.6
Barcın_C*		<b>4.82E-01</b>	43.2	56.8	5.5	<b>3.30E-01</b>	60.9	39.1	9
ÇamlıbelTarlası_LC		2.01E-05	56.5	43.5	3.3	<b>2.12E-02</b>	82.7	17.3	6.6
Caucasus_lowlands_LC		<b>2.74E-02</b>	38.3	61.7	7.7	2.10E-03	44.5	55.5	13
Ebla_EMBA		3.63E-11	43.1	56.9	3.5	2.06E-10	81.1	18.9	10.8
GondürleHöyük_EBA*		<b>7.45E-02</b>	61.4	38.6	4	<b>4.04E-01</b>	86.7	13.3	7.7
İkiztepe_LC		1.49E-03	52.6	47.4	4.4	<b>2.97E-02</b>	81.8	18.2	8.8
K.Kalehöyük_MLBA*		<b>5.76E-01</b>	37.4	62.6	6.9	<b>3.29E-01</b>	55.2	44.8	10.4
TitrişHöyük_EBA		<b>2.26E-01</b>	59.8	40.2	11.6	<b>1.29E-01</b>	99	1	29.4

Target	Reference 2	Reference 1: TellKurdu_EC				Reference 1: Büyükkaya_EC			
		<i>P-value</i>	Coef <sub>1</sub> (%)	Coef <sub>2</sub> (%)	SE (%)	<i>P-value</i>	Coef <sub>1</sub> (%)	Coef <sub>2</sub> (%)	SE (%)
Topakhöyük_EBA*		<b>3.34E-01</b>	36.7	63.3	7.2	<b>1.33E-01</b>	59.8	40.2	13
Alalakh_MLBA	L.Caucasus_EBA	4.11E-07	44.4	55.6	2.2	2.87E-08	72.7	27.3	7
Arslantepe_EBA		<b>1.44E-01</b>	43.6	56.4	3.1	1.85E-03	65.9	34.1	6.8
Arslantepe_LC		<b>8.04E-01</b>	48.3	51.7	2.4	<b>1.77E-02</b>	67.6	32.4	5.7
Barcın_C*		<b>4.18E-02</b>	47.4	52.6	5.3	<b>7.41E-02</b>	67.6	32.4	8.8
ÇamlıbelTarlası_LC		<b>1.12E-02</b>	55.2	44.8	3	<b>5.23E-02</b>	79.3	20.7	6.3
Caucasus_lowlands_LC		<b>2.08E-01</b>	33.5	66.5	7.7	<b>1.17E-02</b>	34.6	65.4	13.6
Ebla_EMBA		3.94E-06	42.2	57.8	2.8	1.38E-08	67.5	32.5	8.7
GondürleHöyük_EBA*		<b>7.85E-02</b>	61.7	38.3	3.7	<b>4.46E-01</b>	87.1	12.9	7.6
İkiztepe_LC		<b>1.17E-01</b>	52.1	47.9	3.8	<b>1.03E-01</b>	77.8	22.2	7.6
K.Kalehöyük_MLBA*		<b>9.30E-01</b>	37.7	62.3	6.2	<b>6.02E-01</b>	48.3	51.7	10.3
TitrişHöyük_EBA		<b>3.76E-01</b>	55.8	44.2	11	<b>1.96E-01</b>	84	16	23.1
Topakhöyük_EBA*		<b>5.36E-01</b>	38.4	61.6	6.8	<b>4.64E-01</b>	49.7	50.3	12.1
Alalakh_MLBA	(1-way)					5.37E-10			
Arslantepe_EBA						2.70E-06			
Arslantepe_LC						1.57E-05			
Barcın_C*						1.70E-03			
ÇamlıbelTarlası_LC						4.33E-03			
Caucasus_lowlands_LC						3.27E-06			
Ebla_EMBA						1.61E-10			
GondürleHöyük_EBA*						<b>2.88E-01</b>			
İkiztepe_LC						<b>1.59E-02</b>			
K.Kalehöyük_MLBA*						5.70E-03			
TitrişHöyük_EBA						<b>2.25E-01</b>			
Topakhöyük_EBA*						<b>1.86E-02</b>			

**Table S8. *qpAdm* results for modeling of Bronze Age Northern Levant with TellKurdu\_EC as Reference (source) 1, Related to Figure 6.** *P-values*, admixture proportions and their  $\pm 1$ SE for two-way (+Reference 2) and three-way (+Reference 2 +Reference 3) models are given. Admixture models with positive coefficients and  $p\text{-value} \geq 0.05$  are annotated in bold letters and those with  $0.01 \leq p\text{-value} < 0.05$  in bold *Italics*. Right populations: Mbuti.DG, Ami.DG, Mixe.DG, Kostenki14, EHG, Villabruna, Levant\_EP and Barcin\_N.

Target	Reference 2	Reference 3	<i>P-value</i>	Coef <sub>1</sub> (%)	Coef <sub>2</sub> (%)	Coef <sub>3</sub> (%)	SE <sub>1</sub> (%)	SE <sub>2</sub> (%)	SE <sub>3</sub> (%)
Alalakh_MLBA	Arslantepe_LC		5.31E-07	-19	119		4.9	4.9	
	G.Caucasus_a_En		<b>2.58E-02</b>	48.6	51.4		2.8	2.8	
	Iran_C		7.57E-05	47.1	52.9		2.4	2.4	
	L.Caucasus_EBA		4.11E-07	44.4	55.6		2.2	2.2	
	Arslantepe_LC	Levant_EBA	3.40E-02	-13.1	80.7	32.4	4.1	4.1	6.2
	<b>G.Caucasus_a_En</b>	<b>Levant_EBA</b>	<b>4.92E-01</b>	<b>33.5</b>	<b>38.3</b>	<b>28.2</b>	<b>4.8</b>	<b>4.8</b>	<b>7.7</b>
	Iran_C	Levant_EBA	<b>1.92E-02</b>	33.9	41.3	24.8	4.2	4.2	7.2
	L.Caucasus_EBA	Levant_EBA	<b>1.75E-02</b>	26.4	40	33.6	3.9	3.9	6.5
Ebla_EMBA	Arslantepe_LC		1.33E-05	-22.7	122.7		6.8	2.8	
	G.Caucasus_a_En		9.86E-03	46.2	53.8		3.3	3.3	
	Iran_C		3.71E-03	44.1	55.9		2.7	2.7	
	L.Caucasus_EBA		3.94E-06	42.2	57.8		2.8	2.8	
	Arslantepe_LC	Levant_EBA	4.27E-01	-14.8	74.6	40.2	5.2	5.2	7.9
	<b>G.Caucasus_a_En</b>	<b>Levant_EBA</b>	<b>5.83E-01</b>	<b>26.8</b>	<b>35.5</b>	<b>37.7</b>	<b>5.4</b>	<b>5.4</b>	<b>8.9</b>
	<b>Iran_C</b>	<b>Levant_EBA</b>	<b>5.22E-01</b>	<b>28.1</b>	<b>39.9</b>	<b>32</b>	<b>5</b>	<b>5</b>	<b>8.6</b>
	<b>L.Caucasus_EBA</b>	<b>Levant_EBA</b>	<b>2.90E-01</b>	<b>20.8</b>	<b>37</b>	<b>42.1</b>	<b>4.8</b>	<b>4.8</b>	<b>7.9</b>

**Table S9. Assignment of Y-chromosome and mitochondrial haplogroups, Related to STAR methods (Sex determination and uniparental haplotypes). (published as excel table)**

Individual ID	Y-Chromosome coverage and haplogroup assignment			mitochondrial coverage and haplogroup assignment						
	Library treatment	coverage on Y-Chromosome	Y-Haplogroup	Library treatment	total mitochondrial reads	coverage on mitochondrial mtDNA	Haplogroup	Overall Rank	Sex	Found Polymorphisms
AAU001	1240K capture	0.131	J1a2a1a2b2b2b2~ CT511741/Pf-4847	mtlo capture	29955	87.82	X2	0.9794	16223T	73G 153G 199C 263G 750G 1438G 1719A 2706G 4769G 6221C 6371T 7028T 8860G 11719A 12705T 13966G 14470C 14766T 15326G 16189C 16278T
AAU002	1240K capture	0.143	J1a2a1a2b2b2b2~ CT511741/Pf-4847	mtlo capture	29953	99.47	N1a3a2	0.9519	195C 204C 207A 270G	73G 188G 263G 750G 1438G 1719A 2706G 4769G 5981C 7028T 822C 8860G 10238C 11025C 11437G 11719A 11914A 12501A 12705T 13637G 13780G 14361G 15326G 16111T 16201T 16231T 16265G
AAU004	1240K capture	0.158	J1a2a1a2b2a1b~ Pf-4848/27234	mtlo capture	29977	94.04	X2a2a	0.9837		73G 153G 199C 263G 750G 1438G 1719A 2706G 3948G 4769G 6221C 6371T 7028T 8860G 11719A 12084T 12705T 13966G 14470C 14766T 15310C 15326G 16189C 16223T 16278T
AAU008	1240K capture	0.158	H2	mtlo capture	29988	94.29	H6a1b	0.9727		239C 263G 750G 1438G 3915A 4775G 4769G 8860G 9380A 10589A 15366G 16362C 16482G
AAU009	1240K capture	0.166	Pf5126/271847	mtlo capture	4188	13.36	I1c3	0.917	188A 228A 295T	73G 263G 462T 489C 750G 1438G 1719A 2706G 3010A 4216C 4769G 7028T 8860G 10398G 11251G 11719A 12612G 13708A 13934T 14766T 14798C 15326G 16452A 16069T 16126C
AAU011	1240K capture	0.166	J2a1a1a2b2a	mtlo capture	30094	98.70	X2d	0.9551		73G 153G 199C 263G 750G 1438G 1719A 2706G 4769G 6221C 6371T 6919G 7028T 8503C 8860G 11719A 12705T 13708A 13966G 14470C 14766T 15326G 16189C 16231T 16278T
AAU013	1240K capture	0.111	M205	mtlo capture	29784	111.51	H47	0.9572		263G 750G 1438G 4769G 8860G 9320C 12635T 15326G
AAU014	1240K capture	0.058	M205	mtlo capture	30110	93.96	H14b	0.9587	150C	73G 263G 497T 750G 1189C 1438G 1811G 2706G 3480G 4769G 7028T 8860G 9075A 9698C 10398G 10550G 11299G 11467G 11719A 12308G 12372A 14167T 14766T 14798C 15326G 16224C 16311C
AAU015	1240K capture	0.058	CT511451	mtlo capture	30033	91.43	K1a	0.9306	16093C	73G 153C 199C 263G 750G 1438G 1719A 2706G 4529T 4769G 7028T 8251A 8860G 10034C 10238C 10398G 11719A 12501A 12705T 13708G 14766T 15043A 15326G 15758G 15924G 16129A 16231T 16391A
AAU016	1240K capture	0.126	Pf5126/271847	mtlo capture	16985	48.75	I2	0.9386	204C 207A 250C 573XC	13780G 14766T 15043A 15326G 15758G 15924G 16129A 16231T 16391A
AAU017	1240K capture	0.126	J1a2a1a2b2b2b2~ CT511741/Pf-4847	mtlo capture	30004	73.36	U1a1d	0.9399	285T	73G 263G 750G 1438G 2218T 2706G 4769G 4991A 6026A 7028T 7581C 8860G 11467G 11719A 12308G 12372A 12879C 13104G 14070G 14664A 14766T 15148A 15326G 15954C 16189C 16242T 16249C 16362C
AAU018	1240K capture	0.126	J1a2a1a2b2b2b2~ CT511741/Pf-4847	mtlo capture	29828	94.08	HV1b3b	0.9158	14161G 16311C	152C 195C 263G 750G 1438G 2706G 4769G 5250C 7028T 8014T 8860G 10295G 10750G 12696C 15218G 15326G 16067T
AAU020	1240K capture	0.126	J1a2a1a2b2b2b2~ CT511741/Pf-4847	mtlo capture	29927	85.54	H23	1		263G 750G 1438G 8860G 10810C 15326G 16274A
AAU023	1240K capture	0.126	J1a2a1a2b2b2b2~ CT511741/Pf-4847	mtlo capture	29948	89.53	H6a	0.9137	16482G	239C 263G 750G 1438G 3915A 4769G 8860G 9380A 15326G 16362C
AAU024	1240K capture	0.361	J1a2a1a2b2b2b2~ CT511741/Pf-4847	mtlo capture	23420	55.53	N1b1a	0.9939	1719A 8472T	73G 153C 263G 750G 1438G 1598A 1703T 2639T 2921A 4769G 4960T 5471A 7028T 8251A 8836G 8860G 9335T 10238C 11362G 11719A 12501A 12705T 12822C 14766T 15326G 16145A 16176G 16223T 16390A
AAU025	1240K capture	0.361	J1a2a1a2b2b2b2~ CT511741/Pf-4847	mtlo capture	6401	15.08	U3b	0.9125	150T 4769G 14766T	73G 263G 750G 1438G 1811G 2706G 4188G 4604A 7028T 8860G 9566C 11467G 11719A 12308G 12372A 13749C 14130G 15326G 15454C 16348G
AAU026	1240K capture	0.361	J1a2a1a2b2b2b2~ CT511741/Pf-4847	mtlo capture	30095	87.38	H	0.7525	263G	750G 1438G 4769G 8860G 15326G
AAU028	1240K capture	0.024	J1a2a1a2b2b2b2~ CT511741/Pf-4847	mtlo capture	29828	104.36	T1a	0.955		73G 263G 750G 1438G 15267G 15928A 16126C 16163G 16181T 16189C 16294T
AAU029	1240K capture	0.024	J1a2a1a2b2b2b2~ CT511741/Pf-4847	mtlo capture	30054	92.95	K1a17	0.9311	15670C 16093C	73G 247A 263G 497T 750G 1189C 1438G 1811G 2706G 3480G 4561C 4769G 7028T 8860G 9055A 9698C 10398G 10550G 11299C 11467G 11719A 12308G 12372A 14167T 14766T 14798C 15326G 16224C 16311C
AAU030	1240K capture	0.024	J1a2a1a2b2b2b2~ CT511741/Pf-4847	mtlo capture	29811	93.06	H2	0.967	16296T	73G 263G 709A 750G 1438G 1888A 2706G 4216C 4769G 4917G 7028T 8692A 8860G 10463C 11251G 11719A 11812G 13368A 14236G 14664A 14766T 14995A 15326G 15452A 15675G 15928A 16126C 16294T
AAU031	1240K capture	0.024	J1a2a1a2b2b2b2~ CT511741/Pf-4847	mtlo capture	30058	104.90	H5a11	0.95		14664A 14766T 15148A 15326G 15954C 16189C 16242T 16249C 16362C
AAU032	1240K capture	0.024	J1a2a1a2b2b2b2~ CT511741/Pf-4847	mtlo capture	29832	94.70	H13a2b2	0.9724		263G 750G 1438G 4769G 8860G 10463C 15371T 15782G 14872T 15326G
AAU033	1240K capture	0.024	J1a2a1a2b2b2b2~ CT511741/Pf-4847	mtlo capture	19174	57.68	H2a	0.9001		73G 188G 263G 709A 750G 1231C 1406C 1438G 2706G 3505G 4769G 5046A 5460A 7028T 8251A 8860G 8994A 11674T 11719A 11947G 12414C 12705T 12923T 14766T 15326G 15888C 16223T 16292T
AAU037	1240K capture	0.011	G	mtlo capture	25431	74.61	W3b	0.918	194T 195C 199C 204C 207A	73G 263G 462T 489C 750G 1438G 2706G 3010A 4769G 7028T 8860G 10398G 11251G 11719A 12612G 13708A 15172T 15326G 15452A 15490T 15530C 16069T 16126C 16227T 16235C 16261T
AAU038	1240K capture	0.010	L2	mtlo capture	5560	15.16	J1b3b1	0.9111	285T 4216C 8216A 8460G 14766T 16145A	73G 150T 363G 497T 750G 1189C 1438G 1811G 2706G 3480G 4769G 7028T 8860G 9055A 9698C 10398G 10550G 11299C 11467G 11719A 12308G 12372A 14167T 14766T 14798C 15326G 16093C 16224C 16311C
AAU039	1240K capture	0.010	L2	mtlo capture	30134	90.13	K1a+150	0.9403	16093C	73G 263G 750G 1438G 2706G 4769G 8860G 15326G
AAU044	1240K capture	0.078	J2b2~	mtlo capture	964	2.74	HV	0.94	7028T	14766T 14798C 15326G 15452A 16069T 16126C
AAU055	1240K capture	0.048	M342	mtlo capture	2550	6.39	HV	0.94	7028T	263G 750G 1438G 4769G 8860G 10217G 15326G 16260T
AAU002	1240K capture	0.048	M342	mtlo capture	3635	12.36	K1a12a1a	0.97		73G 188A 228A 295G 295T 462T 489C 750G 1438G 2706G 3010A 4216C 4769G 7028T 8860G 10398G 11251G 11719A 12612G 13708A 14766T 14798C 15326G 15452A 15675G 15928A 16126C 16294T
AAU001	1240K capture	0.196	Pf5132	mtlo capture	30043	90.06	H4b3	0.929	150C	73G 263G 497T 750G 1189C 1438G 1811G 2706G 3480G 4769G 6071C 7028T 8860G 9055A 9698C 10398G 10550G 11299C 11467G 11719A 12308G 12372A 14167T 14766T 14798C 15326G 16093C 16224C 16311C
AAU004	1240K capture	0.011	M201/Pf-2957	mtlo capture	4068	13.79	H	1		263G 750G 1438G 4769G 8860G 15326G
AAU005	1240K capture	0.103	Pf5126/271847	mtlo capture	29988	89.12	I1c	0.9775		73G 153C 263G 669C 750G 1438G 1719A 2702A 2706G 339C 4769G 5315G 7028T 8860G 8801G 10238C 10398G 11719A 12501A 12705T 13708A 13966G 14470C 14766T 15326G 16189C 16231T 16278T
AAU009	1240K capture	0.175	M406/Pf-3285	mtlo capture	29894	92.66	N1a1a1a	0.9112	199C 204C 573XC 16147G 16147T	73G 153G 199C 263G 750G 1438G 1719A 2706G 4769G 6221C 6371T 7028T 8860G 11719A 12705T 13966G 14470C 14766T 15326G 16189C 16231T 16278T
AAU014	1240K capture	0.743	E1b1b1b2a1a1~	mtlo capture	29870	92.70	X21@225	0.9834	466C	73G 153G 199C 263G 750G 1438G 1719A 2706G 4769G 6221C 6371T 7028T 8860G 11719A 12705T 13966G 14470C 14766T 15326G 16189C 16231T 16278T
AAU015	1240K capture	0.142	Pf5126/271847	mtlo capture	29986	105.78	U1a1d	0.9686	285T	73G 263G 750G 1438G 2218T 2706G 4769G 4991A 6026A 7028T 7581C 8860G 11467G 11719A 12308G 12372A 12879C 13104G 14070G 14664A 14766T 15148A 15326G 15954C 16189C 16242T 16249C 16362C
AAU017	1240K capture	0.221	J1a2b1~	mtlo capture	30041	90.30	H1a1d	0.9542		73G 146C 263G 709A 750G 1438G 1888A 2706G 4216C 4769G 4917G 6516A 7028T 8860G 10463C 10827T 16294T 16296T
AAU018	1240K capture	0.221	Z1842	mtlo capture	30024	90.24	H1a4+146	0.9667		14664A 14766T 15148A 15326G 15954C 16189C 16242T 16249C 16362C

ART019	1240K capture	0.051	12a1a2b2a1	Pf5132	milo capture	30115	83.17	K1a3	0.9371	73G 263G 497T 750G 1189C 1438G 1811G 2706G 3480G 4789G 7028T 8880G 9055A 9698C 10398G 10550G 11299C 11467G 11719A 12308G 12372A 1317G 14167T 14766T 14798C 15326G 16093C 16224C 16311C
ART020	1240K capture	0.379	12a1a	F4286/L2/PF5111	milo capture	29868	92.11	K1c6	0.9198	73G 153C 185A 263G 295T 462T 489C 750G 1438G 2706G 3010A 4216C 4769G 7028T 8880G 10398G 11251G 11719A 12123T 12612G 13708A 14766T 14798C 15326G 15452A 16069T 16126C 16218T
ART022	1240K capture	0.237	12a1a2b2a	Pf5126/2/1847	milo capture	30009	102.45	J1c	0.9497	73G 185A 228A 263G 462T 489C 750G 1438G 2706G 3010A 4216C 4769G 7028T 8880G 10398G 11251G 11719A 12612G 13708A 14766T 14798C 15326G 15452A 16069T 16126C
ART023	1240K capture	0.050	12a1a	F4286/L2/PF5111	milo capture	11681	31.92	U3b1	0.8857	73G 150T 263G 750G 1438G 1811G 2706G 3480G 4789G 7028T 8880G 9656C 11467G 11719A 12308G 12372A 13743C 14139G 14766T 15326G 15452C 16343G
ART024	1240K capture	0.127	G2a2b1	M466/Pf3285	milo capture	29746	90.68	X2a@225	0.9834	73G 153G 195C 225A1 263G 750G 1438G 1719A 2706G 4789G 6221C 6317T 7028T 8880G 11719A 12308G 12372A 13708G 14766T 15326G 16189C 16221T 16248T 16278T
ART026	1240K capture	0.187	12a1a2b2b	M319	milo capture	29920	106.73	K1a8b	0.9935	73G 263G 295A 497T 750G 1189C 1438G 1811G 2706G 3480G 4789G 7028T 8880G 9055A 9698C 10398G 10550G 11299C 11467G 11719A 11818G 12308G 12372A 14167T 14766T 14798C 15326G 16224C 16311C 1679G
ART027	1240K capture	0.271	H2	M319	milo capture	29677	90.48	T1	0.9809	11719A 11818G 12308G 12372A 14167T 14766T 14798C 15326G 16224C 16311C 1679G
ART028	1240K capture	0.032	H2	P96	milo capture	48632	142.85	N1b1a2	0.97	73G 263G 709A 750G 1438G 1888A 2706G 4216C 4769G 4917G 7028T 8697A 8880G 10463C 11251G 11719A 12612G 13688A 14766T 14805A 15326G 15452A 15607G 15928A 16126C 16163G 16294T
ART032	1240K capture	0.032	R1b1a2	V1836	milo capture	2555	7.07	K1a17a	0.95	73G 153C 263G 750G 1438G 1908A 1703T 1719A 2639T 2706G 3921A 4789G 4904T 4960T 5471A 7028T 8251A 8472T 8836G 8860G 9351T 10298C 11565G 11719A 12501A 12705T 12822G 14766T 15326G 16145A 16176G 16221T 16237T 16990A
ART039	1240K capture	0.427	H2	P96	milo capture	33596	90.39	I5a	0.91	12372A 14167T 14766T 14798C 15326G 15670C 16093C 16224C 16311C
ART042	1240K capture	0.427	H2	P96	milo capture	48570	144.94	T1b	1.00	73G 263G 750G 1438G 1719A 2706G 4529T 4789G 5074C 7028T 8251A 8880G 1034C 10238C 10398G 11719A 12501A 12705T 13708G 14336G 14766T 15094A 15326G 15924G 16126A 16148T 16223T 16391A
GR1001	1240K capture	0.079	G2a2b1	M466/Pf3285	milo capture	10100	35.63	K1a	0.95	73G 263G 709A 750G 1438G 1888A 2706G 4216C 4769G 4917G 5147A 7028T 8697A 8860G 10463C 11251G 11719A 11818G 13688A 14233G 14766T 14905A 15326G 15452A 15607G 15928A 16126C 16179C 16294T 16304C
GR1002	1240K capture	0.091	G2a2b1a	FG5089/7279	milo capture	44372	151.73	K1a	0.96	73G 263G 497T 750G 1189C 1438G 1811G 2706G 3480G 4789G 7028T 8880G 9055A 9698C 10398G 10550G 11299C 11467G 11719A 12308G 12372A 1317G 14167T 14766T 14798C 15326G 16224C 16311C
GR1003	1240K capture	0.183	G2a2b1a	FG5089/7279	milo capture	10454	35.25	HV1	0.92	263G 750G 1438G 2706G 4769G 7028T 801T 8860G 15326G 16067T
GR1004	1240K capture	0.121	G2a2b1a	FG5089/7279	milo capture	71878	236.82	H5	0.94	73G 263G 497T 750G 1189C 1438G 1811G 2706G 3480G 4789G 7028T 8880G 9055A 9698C 10398G 10550G 11299C 11467G 11719A 12308G 12372A 1317G 14167T 14766T 14798C 15326G 16093C 16224C 16311C
GR1010	1240K capture	0.079	G2a2b1	M466/Pf3285	milo capture	10100	35.63	K1a	0.95	73G 263G 497T 750G 1189C 1438G 1811G 2706G 3480G 4789G 7028T 8880G 9055A 9698C 10398G 10550G 11299C 11467G 11719A 12308G 12372A 1317G 14167T 14766T 14798C 15326G 16093C 16224C 16311C
GR1011	1240K capture	0.091	G2a2b1a	FG5089/7279	milo capture	44372	151.73	K1a	0.96	73G 263G 497T 750G 1189C 1438G 1811G 2706G 3480G 4789G 7028T 8880G 9055A 9698C 10398G 10550G 11299C 11467G 11719A 12308G 12372A 1317G 14167T 14766T 14798C 15326G 16093C 16224C 16311C
GR1013	1240K capture	0.183	G2a2b1a	FG5089/7279	milo capture	10454	35.25	HV1	0.92	263G 750G 1438G 2706G 4769G 7028T 801T 8860G 15326G 16067T
GR1014	1240K capture	0.121	G2a2b1a	FG5089/7279	milo capture	71878	236.82	H5	0.94	73G 263G 497T 750G 1189C 1438G 1811G 2706G 3480G 4789G 7028T 8880G 9055A 9698C 10398G 10550G 11299C 11467G 11719A 12308G 12372A 1317G 14167T 14766T 14798C 15326G 16093C 16224C 16311C
GR1015	1240K capture	0.143	G2a2b1a	FG5089/7279	milo capture	61224	195.54	U3a2	0.96	73G 263G 497T 750G 1189C 1438G 1811G 2706G 3480G 4789G 7028T 8880G 9055A 9698C 10398G 10550G 11299C 11467G 11719A 12308G 12372A 1317G 14167T 14766T 14798C 15326G 16093C 16224C 16311C
GR1016	1240K capture	0.165	E1b1b1b2a1a1*	CT54483/1795	milo capture	114816	368.39	K1a3	0.96	73G 263G 497T 750G 1189C 1438G 1811G 2706G 3480G 4789G 7028T 8880G 9055A 9698C 10398G 10550G 11299C 11467G 11719A 12308G 12372A 1317G 14167T 14766T 14798C 15326G 16093C 16224C 16311C
GR1017	1240K capture	0.013	J1a2a1a2	PSG/Pf868/Pf4698	milo capture	57118	197.03	K1a3	0.96	12308G 12372A 1317G 14167T 14766T 14798C 15326G 16093C 16224C 16311C
GR1018	1240K capture	0.015	J1a2a1a2	PSG/Pf868/Pf4698	milo capture	21172	67.83	X2	0.96	73G 263G 497T 750G 1189C 1438G 1811G 2706G 3480G 4789G 7028T 8880G 9055A 9698C 10398G 10550G 11299C 11467G 11719A 12308G 12372A 1317G 14167T 14766T 14798C 15326G 16093C 16224C 16311C
ETM004	1240K capture	0.015	J1a2a1a2	PSG/Pf868/Pf4698	milo capture	721	2.09	K1a	0.92	73G 263G 497T 750G 1189C 1438G 1811G 2706G 3480G 4789G 7028T 8880G 9055A 9698C 10398G 10550G 11299C 11467G 11719A 12308G 12372A 1317G 14167T 14766T 14798C 15326G 16093C 16224C 16311C
ETM005	1240K capture	0.015	J1a2a1a2	PSG/Pf868/Pf4698	milo capture	902	2.46	H5	0.94	73G 263G 497T 750G 1189C 1438G 1811G 2706G 3480G 4789G 7028T 8880G 9055A 9698C 10398G 10550G 11299C 11467G 11719A 12308G 12372A 1317G 14167T 14766T 14798C 15326G 16093C 16224C 16311C
ETM006	1240K capture	0.143	E1b1b1b2a1a1*	CT54483/1795	milo capture	1903	5.17	U3a3	0.84	73G 263G 497T 750G 1189C 1438G 1811G 2706G 3480G 4789G 7028T 8880G 9055A 9698C 10398G 10550G 11299C 11467G 11719A 12308G 12372A 1317G 14167T 14766T 14798C 15326G 16093C 16224C 16311C
ETM010	1240K capture	0.143	E1b1b1b2a1a1*	CT54483/1795	milo capture	17548	40.68	K1a3	0.85	73G 263G 497T 750G 1189C 1438G 1811G 2706G 3480G 4789G 7028T 8880G 9055A 9698C 10398G 10550G 11299C 11467G 11719A 12308G 12372A 1317G 14167T 14766T 14798C 15326G 16093C 16224C 16311C
ETM012	1240K capture	0.165	J1a2a1a2b2b*	CT52566/Pf4870/	milo capture	9604	31.15	T2c1446	0.98	150T 11467G 12372A 14766T 15452C 16343C
ETM014	1240K capture	0.008	J1a1	Pf4610	milo capture	19943	53.76	U3b2a1	0.98	263G 271T 295T 16222T 16241T
ETM016	1240K capture	0.009	G2a	P287/Pf3140	milo capture	14438	38.23	U8b1a2b	0.97	15944d
ETM018	1240K capture	0.009	G2a	P287/Pf3140	milo capture	3660	10.72	J1b1b1	0.88	195C 16234T
ETM023	1240K capture	0.035	T1a1	L162/Pf8621	milo capture	14329	38.53	H14a	0.89	73G 462T 489C 750G 1438G 2706G 3010A 4216C 4769G 5460A 7028T 8269A 8860G 10398G 10410A 11251G 11719A 12612G 13708A 13879C 14766T 15326G 15452A 16069T 16145A 16216T
ETM026	1240K capture	0.035	T1a1	L162/Pf8621	milo capture	5159	15.00	K1a4	0.98	263G 271T 295T 16126C 16222T
IK002	1240K capture	0.008	J1a1	L162/Pf8621	milo capture	6412	19.60	J1c16	0.95	73G 263G 497T 750G 1189C 1438G 1811G 2706G 3480G 4789G 7028T 8880G 9055A 9698C 10398G 10550G 11299C 11467G 11719A 12308G 12372A 14167T 14766T 14798C 15326G 15452A 16069T 16126C 16218T
IK009	1240K capture	0.008	J1a1	L162/Pf8621	milo capture	2754	8.81	K1a1	0.88	185A 228A 295T 16256T
IK012	1240K capture	0.008	J1a1	L162/Pf8621	milo capture	783	2.56	J2a1	0.88	150T 152C 195C 295T 10499G 12612G
IK016	1240K capture	0.008	J1a1	L162/Pf8621	milo capture	3673	11.40	I5	0.87	73G 750G 1438G 1719A 2706G 4529T 4789G 7028T 8251A 8860G 10034C 10238C 10398G 11719A 12501A 12705T 13708G 14233G
IK017	1240K capture	0.008	J1a1	L162/Pf8621	milo capture	1368	3.84	J1b1	0.92	199C 204C 250C 263G 573XC 16129A 16199T 14766T 15043A 15326G 15924G 16223T
IK024	1240K capture	0.008	J1a1	L162/Pf8621	milo capture	8707	25.58	U1b1	0.92	73G 146C 263G 750G 1438G 2387C 2706G 4769G 7028T 8395T 8860G 10885C 11467G 11566G 11719A 12308G 12372A 12879C 13104G
IK030	1240K capture	0.008	J1a1	L162/Pf8621	milo capture	1485	4.47	U1b1	0.92	14706G 14766T 1510A 15164A 15172A 15326G 15954C 16249C 16327T
IK034	1240K capture	0.008	J1a1	L162/Pf8621	milo capture	8187	28.37	K1a17	0.97	73G 263G 497T 750G 1189C 1438G 1811G 2706G 3480G 4789G 7028T 8880G 9055A 9698C 10398G 10550G 11299C 11467G 11719A 12308G 12372A 1317G 14167T 14766T 14798C 15326G 15670C 16093C 16224C 16311C

KR036	1240K capture	0.011	G2a2b1	MA66PF3285	mito capture	8700	27.53	12D1C	0.99	150T 152C	73G 263G 295T 489C 750G 1438G 1438G 2706G 4215C 4769G 5633T 7028T 7475T 8860G 10172A 10398G 11251G 11719A 12612G 13708A
KR037	1240K capture	0.018	H2	P9G	mito capture	2376	7.29	X173	0.87	7028T 14770C 14766T	13899C 14766T 15257A 15326G 15452A 15812A 16069T 16126C 16193T
KR001	1240K capture	0.012	G2a2	CT3436/11259M	mito capture	338	0.87				73G 153G 263G 750G 1438G 2706G 4769G 621C 6371T 8860G 11719A 12705T 13866G 15326G 16189C 16223T 16278T
KR002	1240K capture	0.037	J1a2a*	AM01306/CT5179	mito capture	665	1.72				
KR003	1240K capture	0.003	CT	-NA - low coverage	mito capture	173	0.50				
KR004	1240K capture				mito capture	519	1.72				
KR005	1240K capture				mito capture	1022	3.13				
KR006	1240K capture				mito capture	6516	17.21	U7	0.91	1811G 47769G 16309G	73G 152C 263G 750G 980C 1438G 1438G 2706G 3741T 5360T 7028T 8137T 8684T 8860G 10142T 11467G 11719A 12308G 12372A 1390C
MTT001					mito capture	3221	8.06	H13a2b	0.91	4769G	14659A 14766T 15326G 16318T
POT002					mito capture	947	2.41				263G 709A 750G 1438G 2259T 8860G 13762G 14872T 15326G
TI1021	1240K capture	0.007	12b	M12	mito capture						



**Table S10. Significant  $f_4$ -statistics ( $|z\text{-score}|\geq 3$ ) for ART018 and ART027 and other Arslantepe (ART) individuals, Related to STAR methods (Grouping of individuals and nomenclature).** We performed  $f_4$ -statistics of the form  $f_4(\text{Outgroup}, \text{Test}; \text{ART}_x, \text{ART}_y)$  that measure excess of allele sharing of one individual from Arslantepe with a *Test* population compared to another individual from the site. Two male individuals ART018 (3491-3122 cal BCE) and ART027 (3365-3108 cal BCE) appear to systematically share more alleles with ancient populations from the Caucasus or less alleles with ancient Levantine, Aegean and European populations compared to other individuals from Arslantepe.

Outgroup	Test	ART <sub>x</sub>	ART <sub>y</sub>	$f_4$	z-score	BABA SNPs	ABBA SNPs	Total SNPs
Mbuti	Serbia_N	ART018	ART042	0.003	3.80	4632	4308	93145
Mbuti	Late_North_Caucasus	ART018	ART042	-0.002	-3.19	15225	15832	320993
Mbuti	G.Caucasus_b_En	ART018	ART042	-0.002	-3.79	15751	16381	332304
Mbuti	G.Caucasus_b_EMBA	ART018	ART042	-0.002	-3.85	15770	16279	332411
Mbuti	CHG	ART018	ART042	-0.002	-3.26	15874	16467	336147
Mbuti	Yamnaya_Samara	ART018	ART012	-0.001	-3.16	19629	19101	398453
Mbuti	Topakhoyuk_EBA	ART018	ART009	0.002	3.12	15011	15516	320326
Mbuti	Serbia_N	ART018	ART010	0.003	3.33	4681	4983	99308
Mbuti	Serbia_N	ART018	ART011	0.003	3.16	3955	4209	85021
Mbuti	Serbia_N	ART018	ART009	0.003	3.11	4515	4791	96187
Mbuti	Serbia_N	ART018	ART012	0.003	3.54	5057	5379	105846
Mbuti	Serbia_N	ART018	ART020	0.003	3.47	5377	5046	107407
Mbuti	Romania_EN	ART018	ART005	0.002	3.77	10159	10652	213039
Mbuti	Levant_N	ART018	ART011	0.002	3.02	13080	13538	278122
Mbuti	Levant_N	ART018	ART014	0.002	3.46	15192	15760	319619
Mbuti	Levant_N	ART018	ART017	0.002	3.06	14617	15107	307136
Mbuti	Levant_ChI	ART018	ART012	0.001	3.02	19092	19542	397003
Mbuti	LBKT_MN	ART018	ART005	0.002	3.48	10679	11101	222603
Mbuti	LBKT_MN	ART018	ART017	0.002	3.26	16130	16665	335040
Mbuti	G.Caucasus_b_En	ART018	ART005	-0.002	-3.29	11017	10601	222746
Mbuti	G.Caucasus_b_En	ART018	ART012	-0.001	-3.19	19390	18806	392901
Mbuti	G.Caucasus_b_En	ART018	ART015	-0.001	-3.03	21051	20443	426754
Mbuti	G.Caucasus_b_EMBA	ART018	ART012	-0.001	-3.52	19320	18794	393152
Mbuti	CHG	ART018	ART015	-0.002	-3.62	21570	20731	436146
Mbuti	CHG	ART018	ART017	-0.002	-3.13	16696	16104	339063
Mbuti	Bulgaria_C	ART018	ART023	0.002	3.02	6791	7096	141545
Mbuti	Barcin_N	ART018	ART005	0.001	3.12	10826	11157	224465
Mbuti	Balkans_N	ART018	ART005	0.002	3.13	10810	11178	223994
Mbuti	Balkans_C	ART018	ART017	0.002	3.02	8922	9319	188477
Mbuti	Yamnaya_Samara	ART027	ART042	-0.001	-3.36	15759	16249	332320
Mbuti	Late_North_Caucasus	ART027	ART042	-0.002	-3.20	15030	15680	318245
Mbuti	G.Caucasus_b_En	ART027	ART042	-0.002	-3.70	15480	16088	329157
Mbuti	G.Caucasus_b_EMBA	ART027	ART042	-0.001	-3.30	15587	16029	329131
Mbuti	Atayal	ART027	ART042	-0.002	-3.35	15314	15841	332616
Mbuti	Anatolia_Ottoman	ART027	ART042	-0.002	-3.52	9038	9490	197515
Mbuti	Yamnaya_Samara	ART027	ART012	-0.002	-4.19	19224	18547	392098
Mbuti	Yamnaya_Samara	ART027	ART017	-0.001	-3.07	16284	15835	334940
Mbuti	Mongola	ART027	ART017	-0.001	-3.17	15945	15468	335268
Mbuti	Miao	ART027	ART017	-0.001	-3.19	15934	15458	335268
Mbuti	Lahu	ART027	ART017	-0.001	-3.11	15919	15443	335268
Mbuti	Hezhen	ART027	ART012	-0.001	-3.51	18678	18098	392601
Mbuti	Han	ART027	ART012	-0.001	-3.25	18636	18125	392601
Mbuti	G.Caucasus_c_EMBA	ART027	ART012	-0.002	-3.69	18901	18288	388642
Mbuti	G.Caucasus_c_EMBA	ART027	ART014	-0.002	-3.36	16949	16409	346474
Mbuti	G.Caucasus_b_En	ART027	ART005	-0.002	-3.47	10848	10408	221198
Mbuti	Even	ART027	ART017	-0.001	-3.17	16062	15625	335268
Mbuti	Eskimo_Naukan	ART027	ART012	-0.001	-3.01	18720	18195	392601
Mbuti	Dolgan	ART027	ART012	-0.002	-3.85	18823	18175	392601
Mbuti	Dai	ART027	ART012	-0.001	-3.36	18644	18109	392601

Outgroup	Test	ART <sub>x</sub>	ART <sub>y</sub>	$f_4$	z-score	BABA SNPs	ABBA SNPs	Total SNPs
Mbuti	Chukchi1	ART027	ART012	-0.002	-3.22	18786	18167	392601
Mbuti	Chukchi	ART027	ART012	-0.001	-3.28	18726	18182	392601
Mbuti	Borneo	ART027	ART026	-0.001	-3.32	17219	16712	362850
Mbuti	Borneo	ART027	ART012	-0.001	-3.58	18637	18062	392601
Mbuti	Atayal	ART027	ART026	-0.001	-3.05	17253	16756	362850
Mbuti	Atayal	ART027	ART012	-0.002	-3.41	18708	18104	392601
Mbuti	Atayal	ART027	ART018	-0.001	-3.01	17724	17191	373258
Mbuti	Ami	ART027	ART012	-0.002	-3.69	18677	18059	392601
Mbuti	Altaian	ART027	ART012	-0.001	-3.35	18778	18293	392601
Mbuti	Aleut	ART027	ART012	-0.001	-3.76	19005	18427	392601
Mbuti	Adygei	ART027	ART012	-0.001	-3.01	19073	18662	392601

## **11.5 Supplementary Material for Manuscript B**



---

# Ancient DNA reveals admixture history and endogamy in the prehistoric Aegean

---

In the format provided by the authors and unedited

## **SUPPLEMENTARY NOTE 1**

### **Details on the archaeological background of the human skeletal material analysed for DNA.**

In this section, we present extended information regarding the archaeological context from which the human skeletal remains mentioned in this study were recovered. New data from direct radiocarbon dates on selected human skeletal elements are included, as well.

## **CRETE**

### **The Neolithic period in Crete**

The Neolithic period in Crete has not received the attention that other periods of prehistoric Crete have to date. The reason for this is the lack of full publication of newly excavated sites. There are, however, several publications presenting material from surveys or sites which are partly excavated and published in preliminary reports. In addition, a number of papers concentrate on theoretical interpretations of existing data. Well-stratified evidence from settlements is not plentiful. Most of the existing settlement material comes from the sites of Knossos and Phaistos.

Currently, the earliest known Neolithic settlement in Crete was discovered at Knossos during the excavations of Sir Arthur Evans and later in the excavations of John D. Evans. This old material has been only partially published. A re-appraisal of the Evans material and its relation to finds from the rest of Crete has been published (Tomkins, 2018), taking into account previous publications (Evans, 1901; Evans, 1921; Evans, 1928; Evans, 1964; Mackenzie, 1903; Warren et al., 1968; Tomkins, 2007).

More recently, stratigraphic tests in the Neolithic levels of Knossos have produced stratified archaeological and palaeoenvironmental material (Efstratiou et al., 2013). A series of C14 dates, together with the dates from John D. Evans' excavations, give us a chronological framework into which pottery, architecture and artifact typology can be fitted, starting ca. 7000 BC. Recently, the C14 dates from Knossos have been re-evaluated, and the implications for their relation to other Neolithic sites have been studied (Douka et al., 2017).

The second main Cretan site which has produced Neolithic material, though of a late date, is that of Phaistos, excavated by the Italian School of Archaeology at Athens and later studied by Lucia Vagnetti (Vagnetti, 1972-1973). Neolithic material has also been found in later stratigraphic tests. In a recent appraisal of the Phaistos evidence (Todaro and Di Tonto, 2008), the Phaistos material is dated at present to two stratigraphic phases, Final Neolithic III and Final Neolithic IV (but see also (Tomkins, 2018)).

At Katsambas, not far from the northern coast, Stylianos Alexiou has excavated an important Neolithic house, at present dated to Early Neolithic I and II or alternatively to Late Neolithic I and II, with burials in cave-like tombs (Alexiou, 1953; Galanidou and Manteli, 2008). In recent years, Neolithic material and human bones have been found in a building plot at Katsambas not far from the house excavated by Alexiou (Serpetsidaki, 2011; Tomkins, 2012). Several underground cavities containing human bones and pottery were excavated. They were independent of excavated houses. A preliminary dating to Early Neolithic I and Early Neolithic II is given by the excavator. The material found in these cavities is very similar to that discovered near the Kastambas house (Galanidou and Manteli, 2008). Architectural remnants also came to light (Serpetsidaki, 2011). Comparable underground cavities have been found at Kannia near Gortys (Kontopodi, forthcoming). Part of a Neolithic settlement has been excavated at Nerokourou, on the plain, in the area of Souda Bay (Istituto per gli studi micenei ed, 1989). Lucia Vagnetti, who has studied this material, dates it to the Final Neolithic IV [e.g., see Tomkins (2007)]. A site considered as roughly contemporary was found in a totally different landscape: remnants of a settlement were found on the defensible site of the Acropolis of Gortys (Vagnetti, 1973). If this date is correct, the difference in the location chosen for the last two sites suggests that different needs and/or conditions were operative in different parts of Crete.

Neolithic houses have been excavated at Magasa near Palaikastro (Dawkins et al., 1904-1905) and at Kaloi Limenes in eastern Messara (Vassilakis, 1987). A partly-investigated settlement dating to the end of the Final Neolithic and continuing into Early Minoan I has been unearthed at Petras in eastern Crete (Papadatos, 2008). Another Neolithic settlement site with good stratification and paleoenvironmental remains has been excavated by Athanasia Kanta in the village of Kardoulianos near Kasteli Pediada, central Crete. The material from this site is presently under study. A different type of site which has produced Final Neolithic pottery is a well at Phourni, eastern Crete. The complete or almost complete vases provide a good idea of the shapes of the period (Manteli, 1992).

Cretan caves have produced Neolithic material, but few of them have been excavated exhaustively. It has been suggested that some of them were used for habitation, burial and cult practices. Most are known from preliminary reports. The cave of Gerani near Rethymnon on the northern coast is prominent among them. The Gerani cave material possibly dates from the Middle Neolithic and may continue later in the Neolithic period (Tomkins, 2009; Tomkins, 2012; Tzedakis, 1970). Extensive excavations have taken place in the cave of Pelekita, Kato Zakros. They have produced large quantities of paleoenvironmental material and C14 dates. Only preliminary reports have been published so far (Kanta et al., 2016; Bonga and Ferrence, 2016; Bonga, 2016), and the final publication is under preparation. Neolithic burials are not plentiful, though human bones and complete skeletons are known from Cretan caves (Tomkins, 2012). They all, however, have a problem of a lack of exact dating. Intramural burials are also known from Knossos (Evans, 1964; Triantaphyllou, 2008).

### **Aposelemis (Neolithic), Heraklion, Greece**

Coordinates: 35.245350, 25.403200

Excavation: Antiquities for the Heraklion Prefecture, Hellenic Ministry of Culture and Sports, 2011-2012, directed by Dr. Athanasia Kanta (Director Emerita) and, for bioanthropological research, by Prof. Anagnostis P. Agelarakis.

Organized Neolithic cemeteries were unknown in Crete until recently. A Neolithic cemetery at Kephali in the Aposelemis Valley, central Crete, was partly located well below a large Minoan Neopalatial building and extended beyond it (Agelarakis and Kanta, 2016; Agelarakis and Kanta 2020). The cemetery was mostly comprised of graves dug into the natural soft bedrock. They varied in dimensions from ca. 1.30 by 1.20m and had a depth of ca. 0.50 to 0.65m, although there were graves of even smaller dimensions. Stones (and possibly earth) were placed on top of the bodies and covered the graves. There were also indications of burial customs, as some graves contained charcoal and animal bones, as well as small vases and some stone tools. All skeletons were placed in tightly flexed positions. There were also hearths and pits containing pottery. It seems, at present, that the pits did not contain human bones, but they had pottery, artifacts and animal bones and seem to have been related to burial ceremonies. No clear evidence of a Neolithic settlement has been found on Kephali hill. The duration of the cemetery is under consideration at present, but it does not seem to have lasted for centuries. A final answer to this will have to await the completion of the study of the material. The collagen

C14 dates from four Aposelemis skeletons are of particular importance because they provide crucial information about Crete at this time. For views on the beginning of the Neolithic in Crete, see Tomkins (2018); Douka et al. (2017).

Dento-skeletal specimens for archaeogenetic analyses were collected through random and selective sampling techniques which based on a project protocol were aiming to target a representation of different aspects of archaeological/funerary data, combined with assessments derived from the demographic/palaeopathological profiles of the skeletal population involved. Therefore, emphasis was placed on matters of: 1. the construction, spatial distribution and axonometric contextual relations of burial features, between the tightly clustered and among the relatively adjacently or peripherally positioned interments, 2. their respective relatedness to associated features of ritual function, 3. the presence or lack of associated burial artifacts, ecofacts, and manuports, 4. the age subgroups and biological sex categories, 5. the documented discrete non-metric traits of dental and skeletal variability, 6. the assessed skeleto-anatomic manifestations of developmental growth, along with acquired markers of habitual and/or occupational stress, and 7. the diagnosed dento-skeletal changes afforded by a gamut of pathological and traumatic conditions. An inherent rule of the sampling protocol dictated the absolute care and most careful handling and preservation of the archaeo-anthropological record (Agelarakis, 1996; Agelarakis, 2014); hence, no dental or relative skeletal samples were extracted which would have caused anatomic or similar structural damage to the human remains. The entirety of the materials retrieved through the random and selective sampling of specimens were already anatomically disarticulated and taphonomically, yet carefully, identified as mending components of the specific parent skeletons involved.

In total, 41 individuals from the Neolithic cemetery of Aposelemis were sampled for aDNA. Samples from the following six individuals produced genome-wide data that are presented in the genetic analyses. In addition, we present direct radiocarbon dates for four of them:

- APO004 (Grave 55-Burial 67; Lab 2014-2) is a female individual of estimated age ca. 65 years buried in a simple pit grave in a flexed position, lying on the left body side and in an east-northeast to west-northwest orientation (Supplementary Figures 1, 2). One small stone axe was found in the burial. In addition, the burial is also associated with seven stone querns. The skeleton was completely preserved but partially fragmented. The individual had a gracile morphoanatomy and exhibited significant dental



pathologies and a significant cranial vault compressed fracture in an advanced stage of healing.

- APO028 (Grave 26-Burial 30; Lab 2018-1) is a female individual of estimated age range 35-50 years who was buried in a circular-like pit (maximum diameter 0.9m; depth 0.3m) in a contracted position with the skull oriented to the south. Various limited morphological manifestations suggested a female biological sex, an estimation confirmed by the DNA analysis. One open clay vase and one stone tool were also recovered from the burial. The individual had a rather gracile morphoanatomy. Due to prevalent *ante-mortem* bio-mechanical stresses on her skeleto-muscular system, the upper extremities manifested bone changes indicative of specialized kinetics associated with heavy utility of hand flexing. She also exhibited ectocranial hyperporosis with some manifestations of healing. Radiocarbon-dating of a tooth (APO028.B): 7134±25 BP, 6059-5934 cal BC (2-sigma) (ID: MAMS-45082).
- APO029 (Grave 8-Burial 16; Lab 2018-10a) is a male individual of estimated age range 31-45 years who was buried in a contracted position with the skull oriented to the west (Supplementary Figure 3). The interment was in an ovoid pit with a maximum diameter of 1.33m. Burial goods included one clay bowl with horizontal handles, two obsidian chippings, one flint chipping and two stone axes. The individual displayed a very robust morphoanatomy both on the axial skeleton and the upper/lower extremities. Some dental pathologies and a regional ectocranial hyperporosity were also identified.
- APO037 (Burial 60; Lab 2013-23) is a male individual of estimated age range 35-50 years and was probably part of a double burial (Supplementary Figure 4). The skeleton was in a contracted position with the skull oriented southwest and was possibly covered by stones. One stone tool was included. The individual had a robust morphoanatomy and exhibited dental pathologies and mandibular superficial trauma in advanced healing and ectocranial porosity. In addition, evidence of specialized kinetics in the upper extremities was identified.  
Radiocarbon-dating of a tooth (APO037.A): 7168±32 BP, 6075-5986 cal BC (95% probability), (ID: MAMS-49519, AMS, IntCal20).
- APO043 (Grave 54-Burial 66; Lab 2014-4) is a female individual of estimated age range 35-45 years buried in a shallow circular pit of 0.85m diameter, dug on the bedrock and covered by stones (Supplementary Figure 5). The skeleton was in a contracted position with the skull oriented to the west. Three stone tools were found in the burial.

The individual had a gracile morphoanatomy and displayed cranial artificial deformation. Dental pathologies and ecto-endocranial pathological changes were identified. In addition, she exhibited specialized upper-extremity kinetics. Radiocarbon-dating of a bone (APO043.A): 7012±32 BP, 5984-5803 cal BC (95% probability, 0.4% collagen) (ID: MAMS-49520, AMS, IntCal20).

- APO044 (Grave 49-Burial 62; Lab 2014-26) is a male individual of estimated age range 25-35 years buried in a shallow circular pit of 0.85m diameter, dug on the bedrock and covered by stones (Supplementary Figure 6). The skeleton was in a contracted position, and the skull was oriented to the south. One clay vase was found in the burial. The individual had a robust morphoanatomy and presented dental pathologies and a healed superficial ectocranial compressed fracture, as well as regional ectocranial hyperporosity. Radiocarbon-dating of a bone (APO044.A): 7125±33 BP, 6065-5919 cal BC (95% probability, 0.3% collagen) (ID: MAMS-49521, AMS, IntCal20).



**Supplementary Figure 1.** Grave 55 in the Neolithic cemetery of Aposelemis.



**Supplementary Figure 2.** Individual APO004 (Grave 55-Burial 67; Lab 2014-2): A left mandibular *corpus* fragment with the M<sub>2</sub> and M<sub>3</sub> *in situ* showing bifurcations due to alveolar bone resorption caused by advanced periodontal disease and severe, oblique wear patterns on the dental platforms. There is a nearly complete obliteration of the M<sub>2</sub> crown except for a remaining disto-lingual/disto-interdental enamel ring component, while the M<sub>3</sub> retains the periphery of its enamel ring surface where focally, buccal, supra-gingival, calculus deposits were preserved. Both masticatory platforms reveal traces of the *in vivo* reparative processes by tertiary dentin; for the M<sub>2</sub>, nearly within the roof of the pulp chamber.



**Supplementary Figure 3.** Grave 8-Burial 16 in the Neolithic cemetery of Aposelemis.



**Supplementary Figure 4.** Burial 60 (Northern sector; Cut B) in the Neolithic cemetery of Aposelemis.



**Supplementary Figure 5.** Grave 54-Burial 66 in the Neolithic cemetery of Aposelemis.



**Supplementary Figure 6.** Grave 49-Burial 62 in the Neolithic cemetery of Aposelemis.

**Aposelemis-Ornias (Late Minoan), Heraklion, Greece**

Coordinates: 35.28016123, 25.34358724

Excavation: Antiquities for the Heraklion Prefecture, Hellenic Ministry of Culture and Sports, 2007, directed by Dr. Calliope E. Galanaki; study team: Dr. Athanasia Kanta (Director Emerita), Danae Kontopodi and, for bioanthropological research, Prof. Anagnostis P. Agelarakis.

The burial cave at Ornias lies in the wider Aposelemis area. The archaeological context of this site is not very exact, as the material was collected by the Heraklion Ephorate after illicit looting activities. The site has not been published yet. Re-evaluation of the excavation data and the pottery material found in the cave suggest that the human bones collected from the cave do not belong to primary burials but represent a secondary disposal of skeletal material after a clearing of the cave for re-use. They were mostly found in a pit near the entrance of the cave. This pit contained only bones and no pottery, and direct radiocarbon dating on the skeletons (see below) produced Neopalatial dates. In addition, among the sherds collected from the cave, there were distinct Neopalatial sherds. It seems that the cave was cleared for re-use during the Late Minoan IIIA2 period and most specifically from 1350-1300 BC. Probably, the secondary disposal of skeletal material happened at this time. After the recent re-study of the pottery, the above date was confirmed. Burial caves of the rock shelter type in Crete have a long history which extends from the Early Bronze Age to the Geometric and possibly beyond. Many of these caves were used multiple times.

Following the same method for sample collection described for the Neolithic human skeletal remains from Aposelemis, samples from six individuals from the secondary burial pit were analyzed for aDNA. We present genome-wide data and direct radiocarbon dates for three of them:

- APO022 (Pit of bones at entrance of cave; Lab 2015-Dental Homo 1) is an individual of estimated age range 17-25 years. The limited skeletal preservation indicated a female, an estimation confirmed by the DNA analysis. One linear enamel hypoplastic (LEH) defect, as well as other dentoalveolar pathologies, was detected. Radiocarbon-dating of a tooth (APO022.A): 3286±21 BP, 1612-1506 cal BC (95% probability), (ID: MAMS-47520, AMS, IntCal20).

- APO023 (Pit of bones at entrance of cave; Lab 2015-Dental Homo 2) is an individual of estimated age range 35-55 years. The limited skeletal preservation indicated a female, an estimation confirmed by the DNA analysis. Advanced periodontal disease and other dentoalveolar pathologies were detected. Radiocarbon-dating of a tooth (APO023.A):  $3287 \pm 21$  BP, 1612-1506 cal BC (95% probability), (ID: MAMS-47521, AMS, IntCal20).
- APO025 (Pit of bones at entrance of cave; Lab 2015-Dental Homo 3) is an individual of estimated age range 35-45 years. The limited skeletal preservation indicated a female, an estimation confirmed by the DNA analysis. Very advanced periodontal disease, linear enamel hypoplastic (LEH) defect and other dentoalveolar pathologies were detected. Radiocarbon-dating of a tooth (APO025.A):  $3315 \pm 24$  BP, 1627-1509 cal BC (95% probability), (ID: MAMS-47522, AMS, IntCal20).



**Supplementary Figure 7.** Five proximal ulnar components of right forearms, identifying five individuals, within the ossuary at Aposelemis-Ornias.

**Chania/Khania (ancient Kydonia), Chania/Khania, Greece**

Coordinates: 35.5172563, 24.0149291 (Supplementary Figure 8)

Excavations: 25<sup>th</sup> Ephorate of Prehistoric and Classical Antiquities (-2014) and Ephorate of Khania Antiquities (2015-present), directed by Dr. Maria Andreadaki-Vlazaki (except for Palama Street: co-directed by Dr. Elpida Hadjidaki; Malefakis plot: co-directed by Ms

Efthymia Kataki; Tsapakis plot: directed by Ms Eftychia Protopapadaki). Bioanthropological research: Dr. P.J.P. McGeorge

In the 4<sup>th</sup> millennium BC, Kastelli hill in Khania (Kydonia), which dominates a natural harbour, was chosen as the most advantageous location for the first organized settlement in the area. A Minoan palace was later founded on the same site overlooking the harbour, which favoured contacts with the mainland. Contacts with the Peloponnese began in the Early Minoan period, if not earlier, and continued throughout Antiquity. A reciprocal flow of influence and merging of Minoan and Mycenaean cultural elements is evident in Khania in the Neopalatial period (ca. 1700-1450 BC).

After the palatial complex at Kydonia was destroyed in 1450 BC, a new palace was erected in LM IIIA1/A2 (ca. 1370/1350 BC) and a Linear B-based administration was established at Khania, which seems to imply the presence of Greek speakers. Khania was a vibrant centre of commerce, evidently with a multi-lingual, multi-ethnic urban population in contact with many different areas of the Mediterranean including Sardinia, Italy, Cyprus, Syria, the Levant and Egypt. In the Final Palatial period (ca. 14<sup>th</sup>-13<sup>th</sup> BC), Kydonia, based on recent finds, appears to have been a Mycenaean palatial stronghold with hints of a military capability to defend the interests of its administration. This is suggested by spectacular weapons in the “warrior tombs” discovered in the Kouklakis plot, while the position of Khania as the Cretan port closest to the Mycenaean centres of the Peloponnese and Mainland was clearly a factor that would have facilitated immigration. The simultaneous appearance in central and western Crete of new material culture and social practices characteristic of the southern Greek Mainland raises the issue of immigration on a significant scale. Mainland influence permeated many aspects of life at this time, from writing systems and trade to palatial, residential and funerary architecture.

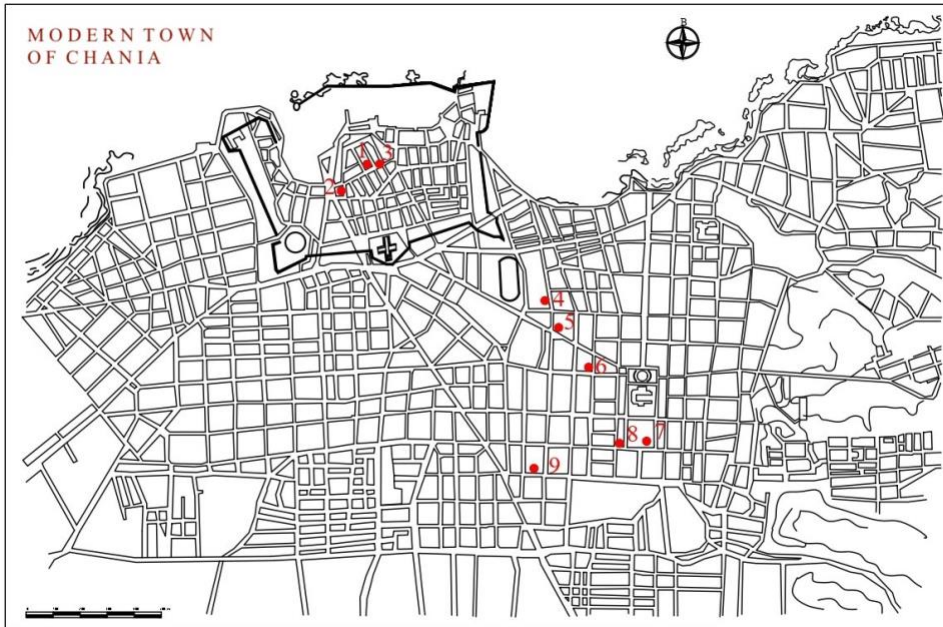
The foundation of a new cemetery at Kydonia in this period, in LMII-LMIII, and the adoption of new burial practices and customs reflects remarkable social change and presented the opportunity to use aDNA to substantiate whether or not the theory of immigration holds true. The extramural cemetery, 800m to the southeast of the settlement, spread over an area 2km<sup>2</sup> to the southeast of the settlement, now lies under the expanding modern suburbs of the town and so has been excavated piecemeal as opportunities for research arose due to building permits required by private individuals (Andreadaki-Vlazaki, 1997; Andreadaki-Vlazaki, 2010; Andreadaki-Vlazaki, 2011; Protopapadaki, 2021). Two hundred tombs, isolated or arranged in groups, have been uncovered thus far. They belong mainly to three discrete

architectural types, previously unknown in Crete: chamber tombs of Mycenaean type (which replaced the multi-chambered Neopalatial tombs), pit-caves and shaft graves. This admixture of funerary architecture suggests the presence of people from different regions. Marked on the map (Supplementary Figure 8) are 9 sites from which the samples submitted for aDNA analysis derive.

The recently discovered Kouklakis plot (no. 7) is very significant for the history of Khania at the transition from the 15<sup>th</sup> to the 14<sup>th</sup> century BC, because a number of “warrior graves” furnished with bronze weapons were discovered there. Most of the burials are in “pit-caves,” consisting of a narrow trench about 3m deep with a cave-like opening in one long side to house a single burial. There are three exceptional cases with side chambers that face each other. In Crete, pit-caves had previously only been found at Zafer Papoura near Knossos, the island’s dominant Minoan palatial centre. Among the Kouklakis tombs, two examples stand out: the LM II pit-cave no. 40 and the LM IIIA1 Mainland-type shaft grave no. 46. The swords of Type C1 and D found in the tombs, suggestive of high-ranking warriors, are closely comparable with tombs at Knossos and the Argolid, and support the hypothesis of Mycenaean domination of the island during the second half of the 15<sup>th</sup> century. The new architectural tomb types, mortuary practices and grave furnishings (the weapons, clay alabastra and the three-handled piriform jars or amphoriskoi), as well as the overt warlike character of the tombs, suggest Mycenaean elements (Andreadaki-Vlazaki, 2022b).

In the Postpalatial period, after 1200 BC, following disturbances and destructions, the town was abandoned. However, the evidence provided by the cemetery indicates that some inhabitants remained in this location, implying uninterrupted occupation on Kastelli hill.





**Supplementary Figure 8. Google map view of modern city of Khania with the locations of mentioned excavations.** 1. Agia Aikaterini Square, 2. Katre Street, 3. Kanevaro Street, 4. Palama Street, 5. Lentaris Plot, 6. Malefakis Plot, 7. Kouklakis Plot, 8. Tsapakis Plot, 9. Rovithakis Plot.

A total of 61 samples representing 53 individuals were analysed for aDNA. These individuals come from 3 different locations on Kastelli Hill and 6 locations under the suburbs of Khania.

## **Kastelli Hill (Kydonia Palatial Centre)**

### **1. Agia Aikaterini Square**

The collaborative Greek-Swedish-Danish systematic excavation (Hallager and Hallager, 2003, 2011 and 2016) of Agia Aikaterini Square on Kastelli Hill has unearthed a Neopalatial two-storey building and part of four others. In this building complex, a baby burial (**XAN035**) without grave offerings came to light in 2014 (McGeorge, 2017; Hallager and Andreadaki-Vlazaki, 2017) buried in a shallow oval pit, 50cm long by 30cm wide and 9 to 14cm deep, covered by three stone slabs, below the LM IIIA2/B1 building 2, which in this part of the excavation was constructed deep into the Neopalatial layers. It is securely dated stratigraphically to the MM III/LM I (ca. 1700-1450 BC) and at present is the earliest

occurrence of an intramural subfloor pit burial in western Crete. Another sub-floor pit burial of a premature infant was previously discovered under an LM IIIB2 floor near the hearth in Room E used for the preparation of food (McGeorge 2003; Persson 2003). Numerous infant burials of this type have been also found at Knossos, where 16 in the Stratigraphical Museum excavation were similarly dated to MM IIIB/LM IA. Intramural burial of infants is not a typical Minoan burial custom; it was practised on the Greek Mainland throughout the Bronze Age. For example, at Asine in the Argolid, there were 57 intramural infant or child burials, 45 of them in pits (Nordquist, 1987; McGeorge, 2011; McGeorge, 2012).

In conclusion, considering the geographic proximity of western Crete to the Peloponnese, the introduction of this burial rite in Crete could be related to a subtle migration process at the height of the island's prestige and prosperity, which initiated a gradual transformation of the local population's social and genetic matrix earlier than was previously expected.

- XAN035 is a full-term infant consisting of cranial fragments including the petrous bones, long bones, ribs, metacarpals, metatarsals, manual and pedal phalanges and 12 partially-formed, unerupted deciduous teeth, which appear malformed. Since enamel hypoplasia is a correlate of low-birth-weight infants, this was probably a low birth weight, full-term infant. Lesions on the internal surfaces of the parietal and occipital bone may have been caused by bacterial infection or foetal distress due to poor maternal nutrition. These indications suggest that perinatal death may have been caused by poor maternal nutrition, poor hygiene or neonatal infection.

## **2. Katre Street**

The ongoing Greek systematic excavation at Number 1, Katre Street on Kastelli Hill, has attracted much attention. The site lies on top of an active seismic fault, where a space of more than 140m<sup>2</sup>, covered by a roof supported by wooden pillars in two rows, was discovered (Supplementary Figure 9). In the northern and northeastern end of the area, the lower parts of walls were covered with wall paintings preserved up to 0.65m in height (Andreadaki-Vlazaki, 2022a), reinforcing the view that the structure is part of the Mycenaean palatial building complex.

In the LM IIIB1 period (ca. 1300-1250 BC), following a catastrophic earthquake (6.5/7.5 Richter), a huge sacrifice took place in the plaster floor, part of which had been intentionally removed. The dismembered remains of a young woman (XAN036) (Supplementary Figure 10) were found mingled with a mass of similarly dismembered remains of various animals (43 sheep and wild goats, 4 pigs and 2 cattle) (Supplementary Figure 11). Her body had been treated in precisely the same manner as the animal carcasses. There was no evidence of burning (Andreadaki-Vlazaki, 2015; McGeorge, 2015; Mylona, 2015; Andreadaki-Vlazaki, 2018). The deposit was demarcated and sealed by a deposition of stones and slabs. This unique discovery of a human sacrificed in a ritual context should not come as a surprise, since Greek mythology presents numerous examples of virgins offered in purification sacrifices in exceptional circumstances. The sacrifice enacted here appears to have been intended to appease chthonic deities after the emotionally shocking devastation caused by the earthquake.

- XAN036 is a young female, whose skeletal remains had similar breakages and cut marks to the animal bones, sustained on ‘green’ or fresh bone. All the parts of the skeleton, which is far from complete (Supplementary Figure 12), clearly belonged to a single female individual of small, slight build.



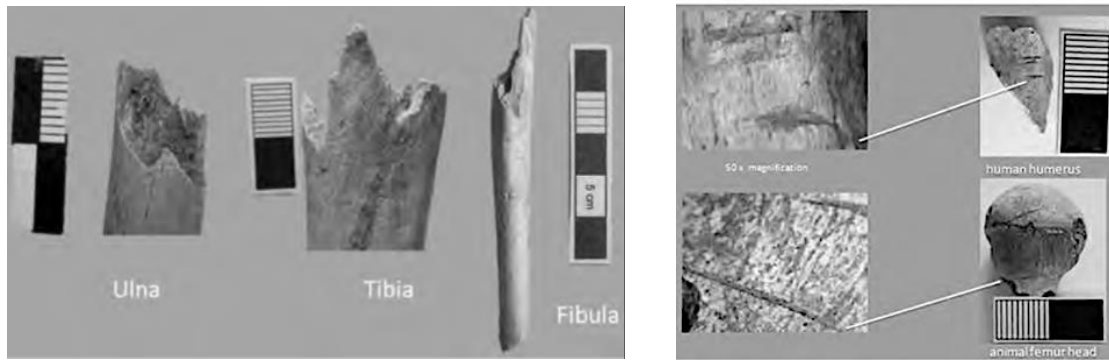
**Supplementary Figure 9. Katre Street N°1. Part of the Column Space with plaster floor.**



**Supplementary Figure 10. Katre Street N° 1 (XAN036).** The human skull reconstituted.



**Supplementary Figure 11. Katre Street N° 1.** Detail of the deposit of bones found *in situ* on the destroyed plaster floor.



**Supplementary Figure 12. Katre Street N° 1 (XAN036).** Left: W-shaped fractures, with sharp, bevelled edges. Right: Cut marks on human humerus and animal femur.

### 3. Kanevaro Street

In 1998, the paving of Kanevaro Street, the main road that crosses Kastelli hill from west to east, revealed building remains of various phases of the Minoan palatial settlement (Andreadaki-Vlazaki, 2004). The remains of three human skeletons, two women and a man (XAN013, XAN014, XAN015), were found at different levels in a deep narrow well carved into the bedrock. The well was filled with many stones, slabs, parts of pithoid and cylindrical vessels, an *asaminthos* and a painted stirrup jar. The pottery from the well dates to the LM IIIB1 period (ca. 1300-1250 BC).

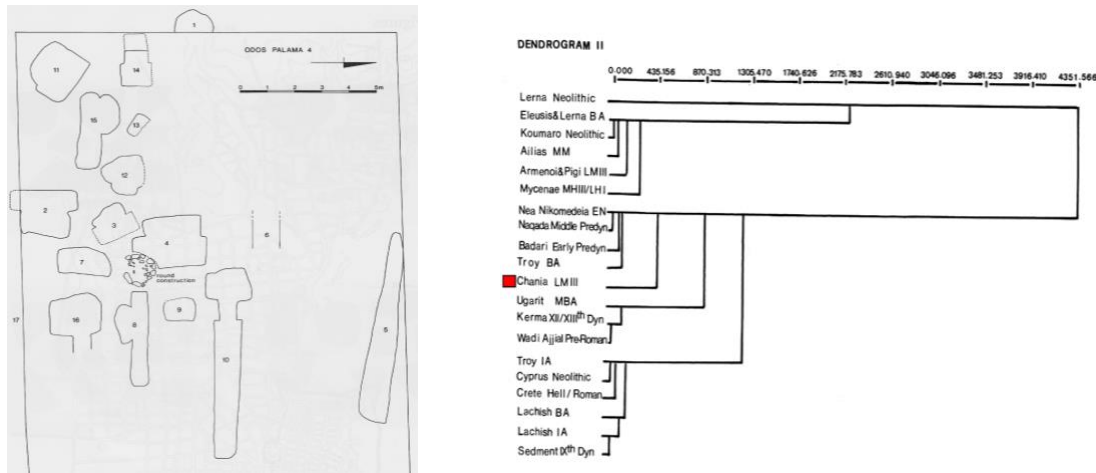
- XAN013
- XAN014
- XAN015

### Kydonian Cemetery

#### 4. Palama Street

A building plot at No. 4 Palama Street is 800m from the excavated area of the Bronze Age settlement on Kastelli Hill. A dense cluster of 17 rock-cut tombs of three different types was excavated (Supplementary Figure 13). Eleven were pit-caves (: 1-4, 8,9 and 11-15); four were

chamber tombs (: 5, 10, 16 and 17); one was a mere ‘cavity’ (:6); and, one was a simple pit grave (:7). A circular stone structure in the midst of the tombs is thought to have served some practical or ritual purpose in funeral ceremonies.



**Supplementary Figure 13. Left: The Palama St. tombs; Right: Cluster analysis**

The 17 tombs from Palama St. yielded a total of 29 inhumation burials, 16 adults and 13 children, of which one was an embryo and seven were under 5 years old. The remaining five children in pit cave 11 were between 6 and 11 years old and appeared to have died in a short space of time, perhaps victims of an epidemic, such as cholera, typhus, measles, plague, or of an accident or natural disaster. Two children with *cribra orbitalia* may have suffered from iron deficiency anaemia or a heavy parasite load. The mean age at death of males (n=7) was 34.14 years and of females (n=9) 25.6 years. Caries in females was 10% higher, and the incidence of abscesses and the rate of tooth loss twice as high as in males. The abnormal difference in mean stature of males (164.54 cm) and females (148.83) reflects a difference in the status of men and women. Stature correlates directly with nutritional status and access to food resources, which is in turn linked to susceptibility to disease and to factors such as population density, hygiene and medicine.

The Palama Street tombs all date to the LM IIIA2-LM IIIB1 period (ca. 1350-1250 BC) (Hallager and McGeorge, 1992). None had been robbed or re-used, probably because they are not high-status and contained only modest grave gifts. Most of the 14 clay vases were locally made, but there was one imported Mycenaean piriform jar.

The most exotic and precious finds from amongst the tombs in this plot were the three “un-Aegean” silver signet rings that were found in tomb 8: one in the cave with the pregnant

female 8C (XAN007) and another two in the earth fill of the rectangular pit, together with the bones of a man and a woman. All three signet rings are similar in size and design and probably originated from the same geographical source. The seal devices of the two best-preserved rings present a rather crude quadruped and a human figure. A close parallel to the latter is found in a silver signet ring with the figure of the Egyptian god Bes, guardian of pregnant women and children, found at Ras Ibn Hani, the harbour town of Ugarit (Bunni et al., 1998). Although this parallel was not known at the time of the 1992 publication, the cluster analysis of morphometric cranial measurements on 20 female populations from Mainland Greece, Crete, Cyprus and the Levant had previously clustered the females from pit-caves 3 and 8 between Bronze Age Troy and Middle Bronze Age Ugarit (Supplementary Figure 13).

- XAN003 is a young adult female interred in chamber Tomb 10A with two children accompanied by a steatite and two carnelian beads, a bone pendant and a crab's claw. Fusion of the basilar suture and tooth wear place this individual within the 17–25-year age range. Her cranium was stippled with coarse porotic lesions, the aetiology of which could be thalassaemia, a quantitative disorder of the haemoglobin, or some other form of anaemia, such as anaemia associated with chronic infections. Her dental health was poor: 70% of her teeth had caries. Enamel hypoplasia indicates episodes of ill-health or poor nutrition in childhood. Pronounced development of the right humerus' deltoid muscle contrasted noticeably with the left arm, indicating right hand dominance.
- XAN007 is an undisturbed male burial without grave gifts in the pit cave Tomb 15C. He was a mature male, aged between 30-40 years of age. In the shaft, 15kg of broken pottery dated to LM IIIB1 allows a terminus *ante quem* for the burial. Like XAN003, this cranium also bore porotic lesions. Thirteen teeth had been lost *ante-mortem* and three *post-mortem*. The remaining 16 teeth exhibited fairly severe dental attrition, and 10 had caries. Hypoplastic lines were observed on most teeth. There were traces of plaque and evidence of alveolar recession caused by periodontal disease. The teeth of the lower dental arch were crowded and misaligned. The enamel of the lower left 1st molar was fractured, probably when biting on some hard substance; over time, with usage, the damage became worn and shiny. Herniation of the discs of the mirror surfaces of thoracics 8 and 9 and severe degenerative changes in the lower thoracic and lumbar sections (Th10 to L3), rarely seen in the modern era in patients under 60, may

be linked with bending, turning or pivoting movements putting a strain on the spinal column.

## 5. Lentaris Plot

The E. Lentari - Ch. Manolikaki plot, in A. Papandreou Street, was excavated in 1987 (Andreadaki-Vlazaki, 1992; Preve, 2009a). Five tombs came to light: four chamber tombs and one pit cave, which was found empty. The chamber tomb burials had been disturbed by looters. The few offerings, mainly clay vessels, that were left date to the LM IIIB period (ca. 1300-1200 BC). Tomb 3 is a chamber tomb (1.70 X 2.10, ca. 1.50m with a dromos 5.50m long and 2.70m deep. In the centre of the chamber, there was a male burial in situ (**XAN016**) and the bones of at least seven other individuals in heaps and in a deep pit carved into the floor (**XAN017**, **XAN018**). The material is being prepared for a detailed publication.

- XAN016 (Lentaris plot – Tomb 3 – Individual 1) was found in a crouched position in the centre of the tomb, with its head towards the entrance, and covered in debris from the roof collapse. Its damaged cranium and pelvic bones were diagnostically male. All of the molars had been lost ante-mortem. Some severely worn anterior mandibular teeth, with their pulp chambers exposed, suggest an age of 40-45 years. Linear enamel hypoplasia seen on the lateral incisors and premolars and Harris lines seen on the x-rays of the fibulae and tibia with marked periostitis indicate growth arrests. Calcified tendons were present on a right patella and left calcaneum. A mean stature of 169.77cm was estimated from the right femur and tibiae.
- XAN017 (Lentaris plot Tomb 3 – Skull 2) is the well-preserved secondary burial of a young adult female. She presents porotic hyperostosis on the parietals and squamous, wormian ossicles on the left branch of lambda and a unilateral occurrence of the left parietal notch bone. She shares these hereditary traits with 3B, to whom she is very probably related. Her dental health was very poor, having lost 10 teeth ante-mortem (including all the mandibular molars and premolars, apart from the RM<sub>3</sub>, and pm<sub>1</sub>). Three sockets (RM<sup>2</sup>, Rpm<sub>1</sub>, LI<sup>2</sup>) had abscess infections, and there was an abscess sinus on the right cheek bone. All the teeth had significant amounts of root exposure, ranging from 3.5 to 1.8mm, indicating serious periodontal disease with inflamed gingiva.



Calculus adheres to the buccal and distal surfaces of upper RM<sup>1</sup>. The basilar suture was fused. Clearly visible vault sutures and dental attrition indicate an age of 17-25 years. Almost the entire vertebral column is present, but only the first element of the sacrum. S1-2 centra had not fused, confirming this individual was < 27 years old. Prominent intertrochanteric lines for the ilio-femoral ligament, a well-developed deltoid ridge on the right humerus and radius pronator teres insertion indicate a physically active individual. Post-bregmatic flattening of the parietals might be due to carrying weights on the head. A mean stature of 159.93 cm was estimated from 8 long bones.

- XAN018 (Lentaris plot. Tomb 3 Skull 3C) is the well-preserved secondary burial of another young adult female, aged between 17-25 years based on suture synostosis and tooth wear and pubic symphysis morphology. Four molars had been shed ante-mortem (both lower M<sub>1S</sub> and RM<sub>3</sub> and upper LM<sup>2</sup>). There are deposits of calculus on the upper molars and premolars, with evidence of periodontal disease. RM<sub>2</sub> had an abscess infection. Nearly all teeth had dental hypoplasia. There is a unilateral, left side, occurrence of the epipteric bone. A small osteoma on the occipital bone near lambda, 4-5mm in diameter, about 2 mm above the vault surface. The post cranium shows a strong, young individual actively involved in manual labour. The medial surface of the tibiae presents periostitis, and the left fibula below the distal third of the shaft has a sinus for the evacuation of pus. Stature, estimated from 10 long bones, was 157.60cm.

## 6. Malefakis Plot

Two LM III chamber tombs, 1 and 3, and the dromos of a third, tomb 2, were excavated in 2008 in the Malefakis plot at the junction of I. Sphakianakis and Platon streets in the heart of the cemetery of ancient Kydonia (Kataki 2014). Tomb 1 is a subterranean, rock-cut chamber tomb (Supplementary Figure 14). The dromos is 15m long and 6.90m deep. The dimensions of the chamber are 2.90 x 3.50 x 2m. It was plundered in antiquity, like the majority of similar tombs in Khania. Bones of four skeletons were interred in the dromos (**XAN022**, **XAN023**, **XAN024**: two women and a man) (Supplementary Figure 15), covered with huge stones, while another skeleton of a child lay on the wall blocking the entrance, together with two LM IIIB conical cups (**XAN021**). The chamber had traces of extensive fire and the remains of at least

one burial accompanied by four clay vases dated to the LM IIIB period, an agate sealstone and two stone conical button beads.

Tomb 3 is also a chamber tomb, plundered in antiquity. The dromos is 10m long and 6.13m deep. The dimensions of the chamber are 2.80 x 2.50 x 1.70m. The skeletal remains of a man (XAN027) were found in the dromos. At a depth of 4.50m, in front of the entrance to the chamber, a rectangular stone (0.56 x 0.25m) may have been a grave marker. The upper part of the blocking wall of the chamber had been removed by looters. A small part of the roof had collapsed into the chamber, and bones from at least four skeletons were found around its rectangular perimeter, though none was in situ (Supplementary Figure 16). Female skeleton 2 (XAN025) was found in a rectangular niche in the northwestern corner of the chamber. In addition to the niche, there are two other shallow pits in the southeastern part of the chamber. The bones of skeleton 3 (XAN026) were piled, together with the bones of the fourth skeleton, along the western side of the chamber. Owing to the looting, only sherds dated to LM IIIB, a sealstone and two steatite beads were found. The material is being prepared for a detailed publication.

- XAN021 (Malefakis plot – Tomb 1 – Individual 1) is a female child aged between 8 and 10 years old represented by a fragmented cranium, mixed dentition (Supplementary Figure 14) and incomplete postcranial remains. The child's unerupted RC<sup>1</sup> and RM<sup>2</sup> exhibit linear enamel hypoplasia, evidence of stress possibly due to malnutrition or childhood illness.
- XAN022 (Malefakis plot – Tomb 1 – Individual 2; Supplementary Figure 15) is the young adult female skeleton uncovered in the dromos at a depth of 3.05 - 3.16m, about 50 cm below burial 1, with sherds from an amphoroid krater, a kylix and the shaft of a bronze needle. She lay supine, arms by her sides, head to the southwest, towards the chamber, facing west where a boulder was positioned. Her cranial table, in numerous pieces, was thin. There were 28 teeth with maxilla and mandible fragments. Both mandibular 2<sup>nd</sup> molars appear to have been lost not long before death, as the alveoli had just begun to heal. The upper lateral incisors were lost *post-mortem*. There were 5 cavities. The upper right M<sup>1</sup> had a large interdental cavity, while the upper left pm<sup>2</sup>, M<sup>2</sup>, M<sup>3</sup> and RM<sub>3</sub> all had occlusal cavities. Wear, correlating with age, had exposed dentine on the incisive surfaces of upper central incisors, on the anterior cusps of the

maxillary 1<sup>st</sup> molars and on the buccal and palato-distal cusps of the mandibular 1<sup>st</sup> molars.

- XAN023 (Malefakis plot – Tomb 1 – Individual 3) is an adult female of ca. 25-35 years, burial 3, found below burial 2 (XAN022) at a depth of 3.30 / 3.70m, under a huge stone with some plain sherds. Represented by a few long bones and a damaged skull, she also lay supine with her head southwest towards the chamber. Mandibular and maxillary teeth with cavities and ante-mortem tooth loss (Supplementary Figure 17), indicate poor dental health.
- XAN024 (Malefakis plot – Tomb 1 – Individual 4) is the fourth burial in the dromos, a young adult male found at a depth of 4.00-4.10m in front of the entrance to the chamber. Positioned in an east-west orientation with head to the east, enclosed in an irregular pit cut into the rock, lined with many small stones. There was a large slab in front of the knees and the posture of the body seemed peculiar placed face down: the upper spine was twisted, and the arms appeared to be behind the back.
- XAN025 (Malefakis plot – Tomb 3 – Individual 2) is a young adult female in a secondary burial in a rectangular niche in the northwestern corner of the chamber. Her cranium exhibited remarkable metopism and multiple wormian ossicles on both branches of the lambdoid suture. Two loose maxillary teeth, identified as RI<sup>1</sup> and a LC presented linear enamel hypoplasia. There were four fragments of a mandible and 9 mandibular teeth, five of them with cavities and most with substantial deposits of calculus. A left femur<sub>r</sub> gave a stature estimate of  $143.267 \pm 3.72\text{cm}$  Supernumerary body parts, indicated the presence of a second, taller most probably a female individual. A stature of 156.603cm was estimated from a right radius.
- XAN026 (Tomb 3 – Individual 3) are the skeletal remains of a young adult female individual commingled with a second female, a male skeleton and animal remains found piled along the western side of the chamber. This anatomically female cranium presented external auditory exostoses (EAE), more pronounced on the left than the right. EAEs are associated with prolonged exposure of the auditory canal to cold water.

They have been reported extensively in Holocene skeletal samples where people engaged in exploiting aquatic resources, which seems plausible since the site is close to the sea. A stature of  $150.677 \pm 3.72$  cm was estimated from a complete left femur.

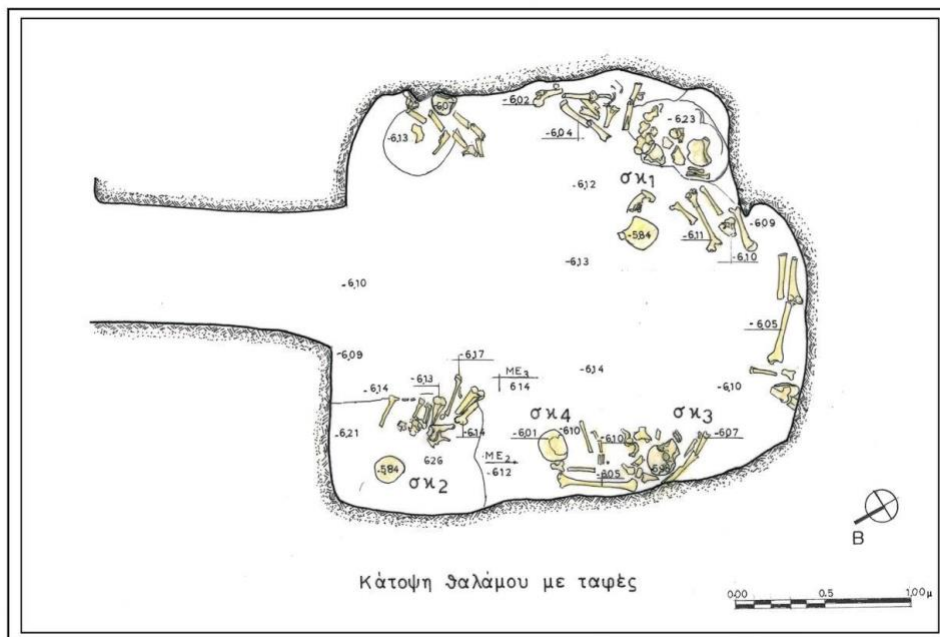
- XAN027 (Malefakis plot – Tomb 3 – Individual 1) belongs to a poorly preserved adult male skeleton found in the dromos in front of the entrance to the tomb resting in a foetal position and surrounded by stones and covered with slabs. The aperture used to plunder the tomb was just to the south of the burial. This material included 5 femurs representing a minimum of 3 people, as well as 3 tibias (two left and one right).



**Supplementary Figure 14.** Malefakis Plot, Tomb 1.



**Supplementary Figure 15.** Malefakis Plot, Tomb 1. Individual 2.



**Supplementary Figure 16.** Malefakis Plot; Tomb 3. Plan of the chamber (‘σκ’: skeleton).



**Supplementary Figure 17.** Malefakis plot, XAN023: mandible, maxillary teeth  $M^1$ ,  $Pm^{1-2}$ ,  $C^1$ ,  $I^2$  with cavities and wear

## 7. Kouklakis Plot

Sixty tombs dating to LM II-LM IIIA2 (ca. 1450-1300 BC) were excavated in 2004 in the Kouklakis plot (Andreadaki-Vlazaki and Protopapadaki, 2009; Andreadaki-Vlazaki, 2010) (Supplementary Figure 18). Apart from chamber tombs, the majority were pit-caves and graves, dating to LM II and IIIA1 (about 1450-1370/1350 BC). Most pit-caves consist of a ca. 3m deep narrow trench with a cave-like opening, a chamber or niche, in one long side of the pit, intended for a single burial (Supplementary Figure 19). A rough-and-ready dry-stone blocking sealed the opening.

Among the tombs, two examples stand out: the LM II pit-cave no. 40 and the LM IIIA1 mainland-type shaft grave no. 46. Their weapons were symbols of warrior superiority and status. The admixture of funerary architectural types: of chamber tombs, pit caves, shaft and pit graves, suggests the advent of peoples from different regions. This extraordinary combination of tomb types and burial customs, practised by people springing perhaps from different tribal and cultural origins, apparently flourished in this new setting.

Samples for aDNA analysis were taken from 12 tombs, but there was no ancient DNA preservation from the warrior tombs. The only results came from individuals in tombs N° 25 and 36, which are dated to LM IIIA1 and A2 (ca. 1400-1300 BC).

Tomb 25 is a chamber tomb. The dromos is 8.66m long and 3.00m deep. The dimensions of the chamber are 2.40 x 2.10 x 2.15m. A deceased was placed in a rectangular pit in the floor of the dromos. In the chamber, two burials were found in situ (**XAN042**) accompanied by a single clay vase. On the east side of the chamber, the bones of two more individuals, a man and a woman (**XAN040**, **XAN041**), were placed in heaps, also accompanied by only one clay vase.

Tomb 36 is a pit grave that received successive burials of children (**XAN051**, **XAN053**), two males and a female. The three children were covered by a ritual deposit with an abundance of domestic pottery, prominent among them cooking utensils. The excavation as a whole is not yet published.

- XAN040 (Kouklakis plot - Tomb 25 – Skull 1) is a secondary burial with a well-preserved cranium and rugged skeleton of a young adult male, in the 17–25-year age range. The young man had an apical abscess above upper Lpm<sup>1</sup> and traces of calculus on right and left pm<sup>2</sup>, M<sup>1</sup> and M<sup>2</sup> were noted. The medial right tibia presented periostitis. Mean stature was 166.62cm.

- XAN041 (Kouklakis plot - Tomb 25 – Skull 2), also a secondary burial (buried with XAN040), includes the partially preserved cranium and completely edentulous mandible of an elderly female, ca. 50-60 years old. The cranial sutures were entirely obliterated on the endocranium and, except for coronal 1-2 and lambdoid 2-3, were barely visible on the exocranium. Of the post-cranial remains, only the right clavicle and right femur were complete, the latter providing a stature estimate of 147.59cm.
- XAN042 – The material is being prepared for a detailed publication.
- XAN051 - The material is being prepared for a detailed publication.
- XAN053 - The material is being prepared for a detailed publication.



**Supplementary Figure 18. Kouklakis Plot.** General view of the excavation.



**Supplementary Figure 19. Kouklakis Plot.** A pit cave.

## **8. Tsapakis plot**

Between 2010 and 2018, eight tombs were excavated in the Tsapakis plot, located to the west of the Kouklakis plot. Six date back to the early Hellenistic period. The other two tombs are chamber tombs that date to LM IIIB1 (ca. 1300-1250 BC: tomb 5) and LM IIIC1 (ca. 1200-1150 BC: tomb 1). Sample **XAN028** comes from tomb 5 (Supplementary Figure 20), with a spacious chamber of 11m<sup>2</sup>, approached by a 7.50m long and 3.70m deep dromos (Supplementary Figure 21). The chamber had collapsed to half its height. Although there were no signs of looting, the fill was very disturbed. Fragmented clay offerings were found on all sides of the tomb.

- XAN028 (Tsapakis plot – Tomb 5 - Individual) is a female skeleton, represented by a mandible. She was accompanied by grave gifts including a bronze knife, a carnelian sealstone and nine clay vases: a small piriform jar, a mug, the lid of an incense burner, a kylix, and two one-handed cups. The most interesting offerings in the ensemble are two hybrid types of ritual vessels made in the local pottery workshop of Kydonia. The first is an incense burner with four ventilation holes, the second a triple ritual vessel with two plastic female heads, whose elaborate ritual headdress, a rendering of divine figures characteristic in Aegean iconography, affirms the religious character of the vase.





**Supplementary Figure 20. Tsapakis Plot. Tomb 5. Dromos.**



**Supplementary Figure 21. Tsapakis Plot. Tomb 5. Chamber.**

## **9. Rovithakis plot**

A cluster of five chamber tombs was excavated in 1996 in the Rovithakis plot in the western part of the cemetery (Andreadaki-Vlazaki, 2003; Preve, 2009b). Tombs 1 and 2 are impressive examples of underground rock-cut subterranean burial monuments of prehistoric Kydonia. Tomb 1 has a dromos 14.40m long and 5.80m deep and a chamber measuring 2.95 x 3.55 x 2.10m. It was plundered in antiquity. Three stirrup jars were found by the entrance to the chamber, and nearby was the burial of a dog. Part of the walls and ceiling of the chamber had collapsed. Two disturbed burials were lying on the floor (one of which belonged to the male **XAN029**), and bones of a third skeleton had been placed in a heap. Fragments of decorated plaster testify to the presence of wooden coffins for the dead. Objects that escaped the looters are a stirrup jar, a one-handed cup, a censer, a glass bead and a rock crystal pendant that date to the LM IIIB1 period (ca. 1300-1250 BC).

Only the eastern part of the dromos of the tomb 4 (maximum dimensions: length 3.60m, width 1.85m, depth 6.85m) could be explored. Some quite bulky, worked stones probably belong to a grave marker. Male skulls 3 and 4 (**XAN030** and **XAN031**, respectively) were uncovered in the thick layer of fallen stones. Two more skulls were collected from the fill in front of the chamber, along with a small bowl. Two burials had been placed on the blocking wall of the entrance to the chamber in the Subminoan period (ca. 1100-1000 BC). They were accompanied by two pieces of sealstones, a bronze fibula, two bronze rings and a glass bead and had been partly damaged during the looting of the tomb. The plundered chamber was

square, measuring approximately 3.00 x 3.05 x 2.75m. Five skulls (one of which belongs to the female **XAN034**; N° 8) and scattered bones were left on the floor. Among the grave offerings are vases (a spouted cup, a kalathos, another double one, a stirrup jar and pieces of a kylix and an amphoroid krater), stone spindle whorls and a bronze utensil that date the burials to the LM IIIB1 period (ca. 1300-1250 BC). A few bones of a dog and a sheep were also collected from the chamber. The material is being prepared for a detailed publication.

### **Hagios Charalambos, Lasithi, Greece**

Coordinates: 35.1772505, longitude 25.4410963

Excavation(s): Ephorate of Antiquities 1976 and 1982-1983, directed by Prof. Costis Davaras; The American School of Classical Studies at Athens, 2002-2003, directed by Prof. Philip Betancourt and Prof. Costis Davaras. Bioanthropological research: Dr. P.J.P. McGeorge

The Hagios Charalambos Cave (also known as Gerontomouri), on the Lasithi Plain in the mountains of central Crete, was discovered by chance in 1976. During the construction of a road that passed in front of the cave, dynamiting operations destroyed the roof of two outer chambers of the original seven, brimming with human remains. A spectacular volume of human and animal skeletal remains was recovered during the excavations of 1976, 1982-83 (Davaras, 1983; Davaras, 1986; Davaras, 1989b; Davaras, 1989a; Davaras, 2015; Davaras, 1976) and 2002-2003 (Betancourt, 2014; Betancourt et al., 2008). The bones are amazingly well-preserved because of the low temperatures in the cave. With only minor temperature fluctuations, it was a natural refrigerator and contributed to unprecedented standards of preservation for human remains of this early date, making them ideal specimens for aDNA analysis (McGeorge, 1988).

The Lasithi Plain has a microclimate and in harsh winters is often cut off by snow for months. This must have been the case in the past so that the people of this relatively remote region were isolated for periods, though not totally, since the study of the pottery from the cave indicated that in successive periods, people came under alternate, competing spheres of external influence. This is relevant for an understanding of the genomic data, which suggests a significant degree of endogamy.

In the Neolithic and Early Minoan periods, caves were often used for primary burial, but the Hagios Charalambos cave was used as an ossuary in the Middle Minoan IIB for the secondary burial of human remains originally interred elsewhere. This is evident from the many

bones that are “etched” with root impressions, although the cave itself had virtually no soil other than sediment washed into it. The pottery provides the best dates for the material placed in the ossuary (Langford-Verstegen, 2015). Although it was all placed in the cave in a single episode, the pottery shows that it consisted of burials that had been made over a long period of time, from Late Neolithic II (4<sup>th</sup> millennium BC) to Middle Minoan IIB (18<sup>th</sup> century BC). Neolithic pottery was scattered throughout from the modern surface to the floor of the cave. These remains can only have come from a long series of burials that were removed from their original place of deposition and placed in the cave without concern for their original contexts. Along with the bones, those who moved the remains brought objects that had been placed in the original graves, including jewellery, tools, pieces of pottery, seals, and other items. Joins of pottery fragments found in different rooms help attest to the random nature of the collection and deposition. Stones intrusive to the context of the cave suggested a possible origin from built tombs, but no trace of tombs has yet been found. An alternative, elegantly-reasoned hypothesis (Davaras, 2015) proposes that the Psychro Cave, only 1km away, could have been the original location of the primary burials, which had to be removed to purify it when Psychro became the focus of cult worship in the Middle Minoan period.

The remains under study, derived from all campaigns, constitute perhaps the largest and best-preserved corpus of human material from such an early period. These commingled burials, mixed with grave goods that range in date from the Neolithic to Middle Minoan, with some Late Minoan offerings, remained undisturbed following the Bronze Age. The placing of all the human remains together makes us reflect on a different sense of individuality in that period. Mindful, however, of rapid progress in archaeological techniques, a large volume of material was left behind for future researchers, and the cave was sealed in 2003 to protect it from potential looters.

The transfer of the primary burials to their new location was clearly a major undertaking, but the care with which the bones were collected is revealed by the fact that virtually every part of the anatomy is represented in the burial corpus, although in varying frequencies. As there are no discrete burials, each bone is treated as a separate individual, and so far, 32,000 records have been made. The chances of identifying bones that belong to the same individual are slim indeed. However, there are some exceptions. For example, the limb bones of a pituitary dwarf, fused vertebrae, and some articulated vertebrae suggest incomplete decomposition at the time of the transfer from the primary burial site.

As illustrated in Supplementary Figueres 22 and 23, there is little actual soil deposit in the cave. Post-excavation, it was determined that the secondary deposition was a single short

event, apparently without meaningful stratigraphy. Nonetheless, when the human remains were sorted into anatomical elements, the provenance of each bone continued to be recorded in case this information should turn out to be useful. Printed provenance labels have been attached to every bone or fragment. Where broken fragments of a single bone united, there can be several provenance labels for the same bone.

The size of the sample is still not yet reliably calculable, and there are many, many fragments of skulls still to be restored and examined. Almost 5000 tarsals, metatarsals and pedal phalanges have been studied. Of the latter, the 1109 calcaneus and talus bones, which are fairly dense and durable bones, are the most numerous. The right calcaneus has given a minimum number of individuals (MNI) of 292. Sorting the bones into anatomical elements allows one to group and seriate them, enabling one to study and observe variations in comparative morphology and size. This facilitates differentiation of sex and age in the population and permits one to assess the burden of pathology affecting particular areas of the anatomy and the differences in the distribution of pathology between the sexes. Surprisingly, no more than 10-12% of the material appears to be immature. The percentage of immature individuals may be low due to the greater fragility of subadult remains, although perhaps that is not the entire explanation. In addition, the immature individuals are affected by pathology which reveals their participation in arduous chores causing repetitive injury to the articulations of very young limbs (Supplementary Figure 24).

There is evidence that life was not always peaceful and that it could be “nasty, brutish and short”, but there were skilled medical practitioners who could prolong life. The study has provided amazing examples of audacious surgical interventions (McGeorge, 2006) which patients survived. Trephination seems to follow Hippocratic procedure long before the Hippocratic treatises were written. There is also evidence for a range of pathologies: traumas, arthropathies, spondyloarthropathies, neoplasm (McGeorge, 2019), endocrine and genetic disorders.

All of the teeth that have been analysed for DNA come from Room 5, which was excavated in 2002 and 2003. The room was a roughly elliptical space ca. 4 x 6m in size at the base, oriented with the long dimension east-west. It could be entered in antiquity either from Room 4 in the south or from Room 3 in the east, but at the time of excavation, the deposit of bones inside the room was so deep that less than a meter of space existed at the entrances. In the west, a hole led down to Room 7. The eastern end of the room was filled with stones that had fallen from the highly cracked ceiling, and the fallen blocks supported the ceiling at the northeast of the room.

The teeth for DNA analysis were collected by a staff member (Louise Langford-Verstegen) at one time in the centre of Room 5 several centimetres below the surface of the deposit. The deposit of Room 5 consisted of mixed human bones, animal bones, stones, soil, pottery, and a number of other artifacts. It had no internal stratigraphy except for the human skulls placed on top of the deposit. The room had been prepared for the deposition of the human remains by the construction of two rubble walls oriented north-south, one at the west beside the hole leading down to Room 7 and one near the centre of the room. These walls helped retain the deposit because the floor sloped down toward the west. At its deepest, the top was ca. 1.6m above the floor. Like most other items in this deposit, they were not associated with any specific artifacts or other human bones. In the aDNA lab (MPI-SHH), a minimum number of unique individuals was defined, and 42 well-preserved teeth were selected for aDNA analysis. After merging data from samples determined after analysis to be from the same individuals and excluding those of poor quality (Methods), genome-wide data from a total of 28 individuals were assembled (21 males/7 females). Radiocarbon-dating analyses on eight samples suggest that they fall mainly within the Early Minoan II and III periods (second half of the third millennium BC). This date is compatible with some of the pottery found in Room 5 (Langford-Verstegen, 2015). The teeth would have been old when they were deposited in the cave, which may help explain why they were loose within the deposit.

- Radiocarbon-dating on human tooth HGC001.A: 3732±19 BP, 2200-2041 cal BC (95% probability), (ID: MAMS-37426, AMS, IntCal13).
- Radiocarbon-dating on human tooth HGC002.B: 3777±19 BP, 2283-2139 cal BC (95% probability), (ID: MAMS-37427, AMS, IntCal13).
- Radiocarbon-dating on human tooth HGC003.A: 3648±19 BP, 2125-1948 cal BC (95% probability), (ID: MAMS-37428, AMS, IntCal13).
- Radiocarbon-dating on human tooth HGC004.A (*no genome-wide data reported*): 3716±22 BP, 2196-2034 cal BC (95% probability), (ID: MAMS-37429, AMS, IntCal13).
- Radiocarbon-dating on human tooth HGC005.A: 3757±19 BP, 2276-2059 cal BC (95% probability), (ID: MAMS-37430, AMS, IntCal13).
- Radiocarbon-dating on human tooth HGC006.A: 3764±19 BP, 2279-2063 cal BC (95% probability), (ID: MAMS-37431, AMS, IntCal13).

- Radiocarbon-dating on human tooth HGC007.A (*no genome-wide data reported*): 3725±19 BP, 2198-2038 cal BC (95% probability), (ID: MAMS-37432, AMS, IntCal13).
- Radiocarbon-dating on human tooth HGC008.A: 3795±19 BP, 2290-2146 cal BC (95% probability), (ID: MAMS-37433, AMS, IntCal13).
- Radiocarbon-dating on human tooth HGC026.A: 3751±25 BP, 2280-2039 cal BC (95% probability), (ID: MAMS-49762, AMS IntCal20).

This assemblage of human teeth provides an examination of Minoan DNA from an early phase of Minoan culture. It comes from an interior part of the island of Crete, from a period well before the increased trade and travel that characterizes the island in the Late Bronze Age (after 1500 BC). The radiocarbon analysis indicates a date before the major palaces were built at Knossos and elsewhere early in the Middle Bronze Age.



**Supplementary Figure 22.** Hagios Charalambos outer chamber, 1983.



**Supplementary Figure 23.** Hagios Charalambos chamber 5, 2002.



**Supplementary Figure 24.** Radii of a child and an adult with epiphyseal lesions.

### **Krousonas, Heraklion, Greece**

Coordinates: 35.2394569205021, 24.9883048004559

Excavation: Antiquities for the Heraklion Prefecture, 2011, directed by Dr. Athanasia Kanta (Director Emerita) and for bioanthropological research by Prof. Anagnostis P. Agelarakis.

The built, square tholos tomb of Krousonas (Supplementary Figures 25 and 26) came to light during work operations for a road leading to the village. In the interior of the tomb were a sarcophagus, vases, other burial gifts and skeletons. A preliminary report of the excavation is available (Kanta and Serpetsidaki, 2013). The tomb contained at least ten burials. It produced pottery and artefacts dating to the 12<sup>th</sup> and the first half of the 11<sup>th</sup> century BC (Supplementary Figure 27). Such tombs in Crete are usually family tombs and elite burial places.

Following the same method for sample collection described for the human skeletal remains from Aposelemis, samples from twelve individuals from the tholos tomb at Krousonas were sampled for DNA. We present genome-wide data and direct radiocarbon dates for two of them:

- KRO008 (Square A1: Stratigraphic Layer 1; Lab 2016-4) is an individual of estimated age range 35-55 years, tentatively assigned to female. No apparent skeletal pathologies were identified. Radiocarbon-dating on human bone (KRO008.A):  $2975 \pm 24$  BP, 1365-1114 cal BC (95% probability), (ID: MAMS-49524, AMS, IntCal20).
- KRO009 (Square A1: Stratigraphic Layer 1; Lab 2016-6-a) is an individual of estimated age range 35-50 years, tentatively assigned by limited morphoanatomic loci to female. Palaeopathological changes caused by spondyloarthropathies were identified (Supplementary Figure 28). Radiocarbon-dating on human bone (KRO009.A):

2970±22 BP, 1268-1060 cal BC (95% probability), (ID: MAMS-49525, AMS, IntCal20).

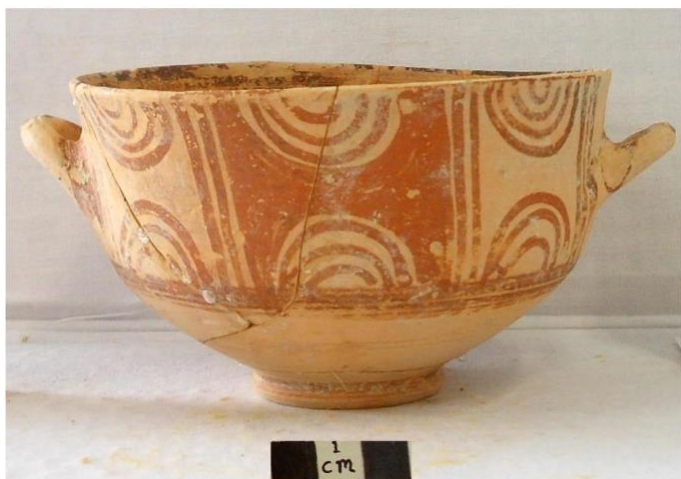


**Supplementary Figure 25.** The exterior of the Krousonas tholos tomb.



**Supplementary Figure 26.** The interior of the Krousonas tholos tomb.





**Supplementary Figure 27.** Typical Late Minoan IIIIC deep bowl.



**Supplementary Figure 28.** A superior view of the first two cervical vertebrae, the atlas (top) and axis (bottom) preserved in an incomplete and fragmentary state due to taphonomic effects, recovered anatomically disassociated, yet morpho-anatomically belonging to the parent skeleton of an older female individual, revealing palaeopathological changes caused by spondyloarthropathies. On the atlas, they were recorded as manifestations of marginal lipping on both the fovea articularis superior and inferior bilaterally, as well as at the fovea dentis, while marginal osteophytic growths were documented peripherally to the fovea dentis, on the region of arcus anterior and inferiorly towards the basal adjacency of *tuberculum anterius*. On the axis, incipient marginal lipping manifestations were observed on the *facies articularis anterior dentis*, yet more derived marginal lipping was observed on the preserved, right side, *facies articularis superior* and *processus articularis inferior*. Due to taphonomic disturbances, the vertebrae can only be tentatively assigned to individual KRO009.

## MAINLAND GREECE

### Aidonia, Corinthia, Greece

Coordinates: 37.84083, 22.5832

Excavation(s): 4<sup>th</sup> Ephorate of Antiquities (Nafplion), 1978-1980 and 1986, directed by Kalliope Krystalli-Votsi and Konstantina Kaza-Papageorgiou; 37<sup>th</sup> Ephorate of Antiquities (Corinth), 2002, directed by Panagiota Kasimi; TAPHOS (Corinthian Ephorate of Antiquities and the Nemea Center for Classical Archaeology, UC Berkeley), 2014-present, directed by Konstantinos Kissas and Kim Shelton. Bioanthropological study: Dr. Gypsy Price.

The site of Aidonia is situated on the slopes of the northeastern Phlious Valley in southwestern Corinthia. Today located in olive groves, during the Late Bronze Age, the hillside was used as an extramural cemetery with at least three *systades* of chamber tombs (upper, middle, and lower) and associated mortuary features. The site was discovered through looting in the late 1970s, followed by rescue and systematic excavations (Krystalli-Votsi, 1998; Krystalli-Votsi and Kaza-Papageorgiou, 2013). The settlement was located by the Phlious Valley Survey in the early 2000s (Casselmann et al., 2004; Hachtmann, 2013) and remains unexcavated.

Most of the tombs excavated in the late 1970s and early 1980s had been disturbed and looted, and precious material from them came onto the antiquities market during the early 1990s. These multi-burial and multi-generational tombs contained material dating to the Late Helladic (LH) period, from the 15<sup>th</sup> to early 13<sup>th</sup> centuries BC (LH II-III B1) and an unknown number of burials. The Middle Cemetery, centrally located on the hillside, is the location of the original cemetery known since the 1970s, and the focus of the TAPHOS excavations in 2015-2019, along with three chamber tombs in the Lower Cemetery in 2016-2018. Our project has produced evidence of burials from the late 16<sup>th</sup> to early 12<sup>th</sup> centuries BC (LH I-III C Early) based on a broad range of grave gifts and burial materials. The TAPHOS project has also found evidence of use in the area during the Geometric, Archaic-Classical, Late Roman, and Medieval periods.

To date, the TAPHOS project has excavated eight chamber tombs in the Middle and Lower Cemeteries with a MNI of 97 from primary and secondary burials. Primary burials were placed on the chamber floors and in cists under the floors, while a variety of burial rituals are exhibited through disarticulated secondary burials individually placed in cists and on the

chamber floor or commingled in piles or cists, some quite organized and others very mixed (Kvapil and Shelton, 2019).

Samples for this study were taken from 17 individuals from three chamber tombs excavated by TAPHOS in 2015-2016. Tombs 100 and 101 were adjacent to each other in the southeastern part of the Middle Cemetery. Both contained multiple individuals, with 100 in use ca. 1500-1375 BC (LH IIA-III A1) and 101 in use ca. 1375-1200 BC (LH IIIA-III B). Tomb 103 was one of two early and large chamber tombs located in the Lower Cemetery. It contained at least 12 individuals, several of which were primary burials in a central shaft-like cist, while others were secondary burials placed in a variety of deposit types. Sampling preference was largely based on preservation (individuals with preserved petrous portions, associated teeth - preferably with dental calculus). In addition, we focused on individuals from discrete contexts, but both primary and secondary burials were chosen.

Nine individuals from Aidonia produced genome-wide data that are presented in the genetic analyses:

- AID001 ([1] 15/100064) is an adult female in a primary burial context in the centre cist under the chamber floor of Tomb 100, which dates to LH IIIA1. The skeleton exhibits significant attrition but no apparent pathologies.
- AID002 (15/100028 skull A) is an adult (middle-aged) male in a secondary burial deposit from the Western Burial Platform of Tomb 100. This skull was one of the four that were arranged at the bottom of the deposit on the burial platform. It has no definitively associated skeletal elements; however, the upper left third molar was inverted and partially erupted well above the typical location, with no apparent associated abscess or lesion. The burial likely dates to LH II.
- AID007 ([3] 16/101132) is a young adult male, one of two primary burials at the bottom of Tomb 101's SW Cist. The burial dates broadly to LH IIIA-III B. It had no pathologies aside from a couple carious lesions.
- AID008 ([4] 16/101132), the second of two primary burials (with AID007 [3] above) at the bottom of Tomb 101's SW Cist, is also a young adult male with no apparent pathologies. The burial also dates broadly to LH IIIA-III B.
- AID009 ([6] 16/101133) is a young adult male from a secondary burial which overlay the primary burial ([7] 16/101133) in the West Cist of Tomb 101. This burial had no apparent pathologies and dates broadly to LH IIIA-III B.

- AID010 (16/101123 skull K) is an adult female. This individual is one of at least three fragmentary secondary burials scattered throughout the eastern half of Tomb 101 near the original floor surface. The deposit dates to LH IIIB.
- AID012 ([3] 16/103058) is a middle-aged female in a primary burial context within the Centre Cist of Tomb 103 dating to Late Helladic IIA. This is one of several primary burials placed on top of and alongside each other on the floor of the deep shaft-like cist in the centre of the large chamber. Burial [3] immediately preceded in death/burial the final primary burial in the cist ([2]). It exhibited no apparent pathologies or trauma.
- AID014 (16/103056 skull A) is a young adult female. This individual is one of at least three likely female individuals from a secondary commingled deposit in a shallow oval cist located in the northeastern portion of Tomb 103's Dromos. There are no apparent pathologies. The deposit has a *terminus ante quem* of LH IIB but contains earlier material as well, including sherds that join vases from the Centre Cist (see contexts of AID012 and AID017).
- AID017 (16/103058 skull) is an adult female from a secondary burial of fragmentary and commingled remains of two individuals at the northern end of Tomb 103's Centre Cist. Preservation and the dissociation of elements prevents any further biological profiles, while associated ceramic material suggests a date of Late Helladic I-IIA.

### **Glyka Nera, Attica, Greece**

Coordinates: 37.9901700, 23.8499070

Excavation(s): B' Ephorate of Prehistoric and Classical Antiquities, 1991-2002, directed by E. Kakavogiannis and O. Kakavogianni (Honorary Director).

Bioanthropological study: Dr. Anastasia Papathanasiou.

The cemetery of Glyka Nera is a rich and extensive Mycenaean, Late Helladic chamber tomb cemetery, radiocarbon-dated around 1400-1325 BC. The site is situated in eastern Attica on a plain not far from the Aegean coast. Salvage excavations started in 1991 (Kakavoyannis, 1999-2001), and no settlement or palatial centre has yet been located. The cemetery consists of 22 unlooted chamber tombs and a number of pit burials. Notable is a considerably larger square chamber tomb with exceptional, valuable, symbolic, imported offerings, some of clear Minoan

origin. All tombs were reused for multiple inhumations, representing 102 partial individuals, including a variety of pottery, seals, beads, and a number of terracotta or lead figurines (Polychronakou-Sgouritsa and Kakavogiannis, 2020).

The study of the human assemblage from Glyka Nera confirmed trends of social and gender differentiations (Papathanasiou et al., 2020), compared to other Mycenaean sites or within the same site, between the Large Chamber and the rest of the tombs. Subadult underrepresentation, pointing towards differential burial treatment of these age groups and preferential access to the chamber tomb cemeteries, is observed in Glyka Nera, as in all Mycenaean chamber tomb and tholos cemeteries, but Glyka Nera is differentiated from other Mycenaean cemeteries in resembling more peripheral regions of the Peloponnese and less those of the palatial centres of southern Greece, as there is a presence, though modest, of subadults and especially of individuals under the age of four. Statistical analysis of the prevalence of dental pathological conditions showed that ante-mortem tooth loss (AMTL), linear enamel hypoplasia (LEH), and caries are significantly higher in females, implying that females in Glyka Nera, both in childhood and in adult life, may have experienced a lower health status, parallel to similar observations in the chamber and tholos tomb burials in the Athenian Agora and Pylos.

Bone collagen samples from 40 individuals were analysed for stable carbon and nitrogen isotopes, showing a primarily C<sub>3</sub> terrestrial, plant-based diet. Compared to other Bronze Age sites, Glyka Nera individuals have high  $\delta^{15}\text{N}$  values, similar to individuals from the royal tholoi of the palatial centers of Pylos, Kazanaki, and Grave Circles A and B in Mycenae, and comparatively higher than the observed values in individuals buried in chamber tombs at those and other Late Helladic sites. Differential access to animal protein resources in the Mycenaean world has been documented, with individuals buried in richer tombs showing better, protein-rich diets, reflecting consistent status differences. The diet at Glyka Nera, as a whole group, conforms with one similar to the richer and higher status Mycenaean tombs.

An intra-site statistically significant difference was observed in the mean  $\delta^{15}\text{N}$  values between individuals who were buried in the Large Chamber tomb and those who were interred in the other graves, implying that individuals in the Large Chamber tomb at Glyka Nera were consuming more animal protein in the form of meat and/or dairy products than those in the other tombs. Since the Large Chamber tomb is also differentiated in its material culture, being richer in offerings of special importance and Minoan origin, and is more prominent architecturally, the isotopic data corroborate possible status differences within this community.

In the case of Glyka Nera, questions about the origin of the prominent individuals of the Large Chamber are raised by the presence of exquisite ritual artefacts which were most probably of Minoan provenience. Finally, the possibility of genetic affinities within the entire group should be investigated, as the prevalence of certain cranial non-metric traits is relatively high.

Three individuals from Glyka Nera were sampled for DNA. We present genome-wide data and direct radiocarbon dates for two of them:

- GLI002 (K2) is a male individual of 30-40 years of age at death represented by a partial cranium and mandible. He was one of the individuals buried in the Large Chamber in the Vorylla plot. A number of pathological conditions were observed on these cranial remains, including porotic hyperostosis on the left parietal, LEH on the lower canines, and an abscess on a right first molar. The burial is dated to the LH IIA-B (ca. 1400-1325 BC). Radiocarbon-dating on human bone (GLI002.A):  $3103 \pm 22$  BP, 1429-1293 cal BC (95% probability), (ID: MAMS-49522, AMS, IntCal20).
- GLI003 (Individual 3) is a male individual of 40-50 years of age at death represented by an almost complete cranium, the right innominate, and partial long bones. He was found in Chamber 5 of the Krystalli plot, a small chamber tomb containing the highest number of individuals and common offerings. Ante-mortem tooth loss of all right mandibular teeth was observed. The burial is dated to the Late Helladic IIA-B (ca. 1400-1325 BC). Radiocarbon-dating on human bone (GLI003.A):  $3110 \pm 27$  BP, 1421-1313 cal BC (95% probability), (ID: MAMS-49523, AMS, IntCal20).

### **Mygdalia, Achaea, Greece**

Coordinates: 38.186889, 21.776528

Excavation: Ephorate of Antiquities of Achaea, 2008-present, directed by Dr. Lena Papazoglou-Manioudaki, co-directed by Dr. Constantinos Paschalidis.

Bioanthropological study: Dr. Olivia A. Jones.

The excavation on Mygdalia hill (Papazoglou-Manioudaki and Paschalidis, 2017) provides a unique opportunity to investigate the life ways of a local Mycenaean society in the Patras region of Achaea, the settlement, the cemeteries, and the resources available (arable land, areas for herding, water supply).

Mygdalia belongs to the group of Mycenaean settlements that were founded in the transitional period of Middle Helladic III/Late Helladic I (Mygdalia I) and rose to local prominence in the Early Mycenaean period (Mygdalia II). Substantial architectural remains, floor deposits and a tholos tomb furnished with pottery, that now finds parallels in settlement strata, will help define this important period in western Achaea. Its floruit came to an abrupt end at the beginning of the Palatial period, and continuation of full-scale habitation on the hill remains ambiguous (Mygdalia III) until its new floruit in the 12<sup>th</sup> century BC (Mygdalia IV). The mansion on top of Mygdalia hill (Terrace 1) and a large storeroom (Terrace 2) provide evidence for social organization in the Postpalatial period, the time of chamber tomb cemetery reuse and the warrior graves in Achaea.

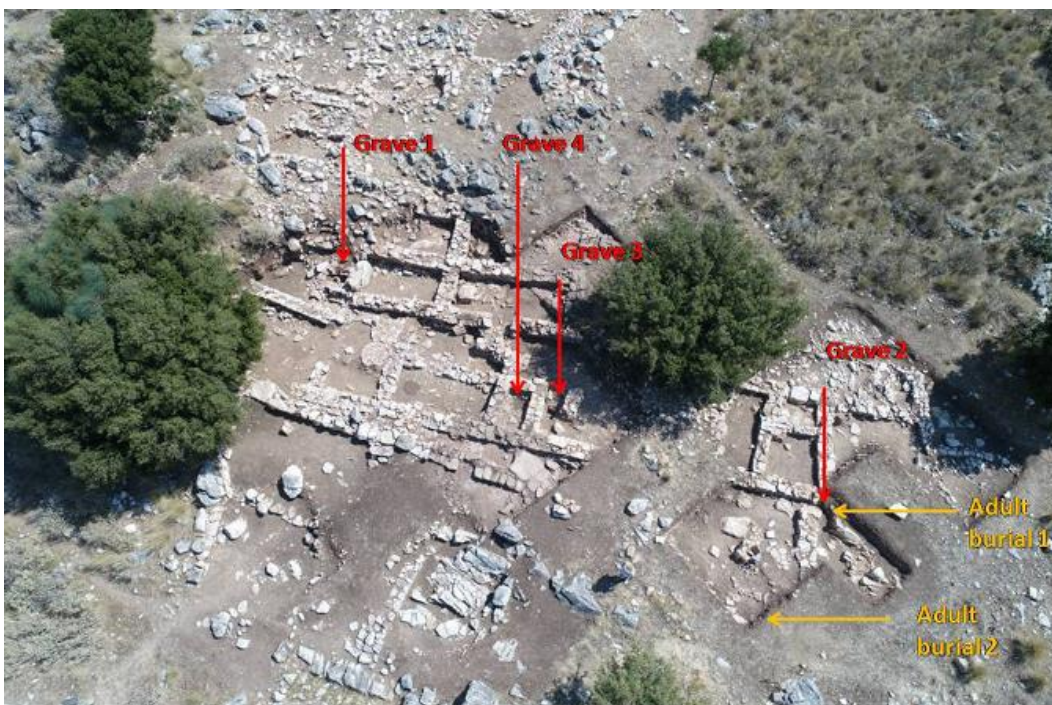
The primary domestic space at Mygdalia was found on Terrace 2 (Supplementary Figure 29). The area consists of densely built houses with rectangular rooms, semi open spaces and courtyards. Also found on Terrace 2 were four Mycenaean intramural children's graves (Supplementary Figure 29), containing the remains of multiple infant and child inhumations interred in stone cists without grave goods, and two Archaic adult burials containing single primary inhumations (Papazoglou-Manioudaki et al., 2019) dating from the onset of the 7<sup>th</sup> century BC (Mygdalia V) when the area was transformed into an early Greek temple.

Intramuros Child Grave 3 is a stone slab cist grave with cover stone that is located just outside of the settlement's wall (Papazoglou-Manioudaki et al., 2019) (Supplementary Figure 30). A minimum of eight individuals could be identified, and the completeness of the skeletons suggest primary burials with secondary manipulation likely occurring when subsequent individuals were added to the grave. No grave goods were included. Despite the good preservation of the skeletons, the body positions, orientations and the temporal sequence of the interments could not be easily reconstructed due to the disarticulation and commingling of the bones. In total, eight petrous portions from the left temporal bones were sampled for DNA. We present genome-wide data and direct radiocarbon dates for seven of them:

- MYG001 (Intramuros Child Grave3.A) is a perinatal infant of 30-40 weeks in utero with no apparent pathologies. Radiocarbon-dating on human bone (MYG001.A): 3265±21 BP, 1611-1457 cal BC (95% probability), (ID: MAMS-47527, AMS, IntCal20).
- MYG002 (Intramuros Child Grave3.B) is a perinatal infant of 30-40 weeks in utero with no apparent pathologies. Radiocarbon-dating on human bone (MYG002.A):

3318±21 BP, 1626-1518 cal BC (95% probability), (ID: MAMS-47528, AMS, IntCal20).

- MYG003 (Intramuros Child Grave3.C) is an infant of 30-40 weeks in utero with no apparent pathologies. Radiocarbon-dating on human bone (MYG003.A): 3318±21 BP, 1596-1438 cal BC (95% probability), (ID: MAMS-47529, AMS, IntCal20).
- MYG004 (Intramuros Child Grave3.D) is a perinatal infant of 30-40 weeks in utero with no apparent pathologies. Radiocarbon-dating on human bone (MYG004.A): 3318±21 BP, 1609-1446 cal BC (95% probability), (ID: MAMS-47530, AMS, IntCal20).
- MYG005 (Intramuros Child Grave3.E) is a perinatal infant of 30-40 weeks in utero with no apparent pathologies. Radiocarbon-dating on human bone (MYG005.A): 3198±23 BP, 1504-1425 cal BC (95% probability), (ID: MAMS-47531, AMS, IntCal20).
- MYG006 (Intramuros Child Grave3.F) is a perinatal infant of 30-40 weeks in utero with no apparent pathologies. Radiocarbon-dating on human bone (MYG006.A): 3262±29 BP, 1612-1452 cal BC (95% probability), (ID: MAMS-47532, AMS, IntCal20).
- MYG008 (Intramuros Child Grave3.H) is an infant one-three months old with no apparent pathologies. Radiocarbon-dating on human bone (MYG008.A): 3262±29 BP, 1611-1452 cal B-(95% probability), (ID: MAMS-47533, AMS, IntCal20).





**Supplementary Figure 29.** Plan view of the Terrace 2 in Mygdalia. The locations of the four infant graves are marked.



**Supplementary Figure 30.** Intramuros Child Grave 3 at Mygdalia.

### **Nea Styra, Euboea, Greece**

Coordinates: 38.17975, 24.207417

Excavation: 11<sup>th</sup> Ephorate of Prehistoric and Classical Antiquities (currently Ephorate of Antiquities of Euboea), 2009, directed by Maria Kosma (rescue excavation). The excavation of Graves 2 and 3 was completed in 2013, directed by Maria Kosma and funded by the Phycha Foundation. Bioanthropological study: Eleni-Anna Prevedorou.

The town and harbour of Nea Styra is located on the western coast of southern Euboea in the sheltered Nea Styra Bay. The site lies at a strategic location on a narrow strait along the north-south and east-west axes of the maritime routes along the Euboean Gulf. The presence of a flourishing Early Bronze Age site on the coast of the Bay of Nea Styra has been known since the accidental discovery of three marble Early Cycladic figurines in the late 19<sup>th</sup> century (Kosma, 2010; Wolters, 1891) and detailed by field surveys in the area during the 20<sup>th</sup> century [e.g., see Sackett et al. (1966); Sampson (1980); Theocharis (1959)]. In 2009, three monumental built shaft graves of the Early Bronze Age were recovered during salvage excavations on the low hill of Gkisouri to the east of the modern settlement [see Kosma (2010)]. Thus, the recent excavations have marked Nea Styra as an important node in the southern

Euboean Gulf, right across from the roughly contemporaneous cemetery of Tsepi at Marathon in eastern Attica. The coexistence of both Helladic (mainland) and Cycladic features and influences in the burial practices at Nea Styra raise significant questions regarding its people and may suggest a regional network (Kosma, 2020b; Kosma, 2020a).

The extent of the cemetery is not known, though there was evidence for two more graves on the slopes, completely or partially destroyed by the construction of the road (Kosma, 2020b). The excavated graves were of monumental construction, all oriented differently. Grave 1 (Kosma, 2020b; Kosma, 2019) was lined with square schist slabs and consisted of a trapezoidal chamber and a short passage with three stone-paved steps leading to it (*dromos* or *prothyron*). The entrance was blocked by a schist slab and preserved two schist slabs as antae (pilasters) and a threshold. No covering or roof was preserved, though there was evidence for the presence of a large lintel made out of schist. Grave 3 was similar in construction, and both of these differ significantly from contemporaneous graves in Euboea and Boeotia, as well as from the cist graves observed in the Cyclades (Kosma, 2020b). Grave 2, however, shared more similarities with the rock-cut tombs in the Cyclades and Crete (Kosma, 2019). Overall, the Nea Styra graves showed great similarities with Early Helladic cemeteries in Attica, specifically with Tsepi at Marathon (Pantelidou-Gofa, 2005), Asteria at Glyfada (Kaza-Papageorgiou, 2019; Kaza-Papageorgiou, 2018) and Hagios Kosmas (Mylonas, 1959). A ritual deposit pit was discovered to the southeast of the complex of Graves 2 and 3 containing a large number of broken vessels (Kosma, 2020b). Analogous special deposits areas have been found at the Early Helladic cemetery of Tsepi in Marathon (Pantelidou-Gofa, 2005; Pantelidou-Gofa, 2008; Pantelidou-Gofa, 2016), as well as Asteria in Glyfada (Kaza-Papageorgiou, 2019; Kaza-Papageorgiou, 2018).

The material culture recovered in the three graves showed close stylistic affinities with the Cyclades, including a plethora of fragmented marble bowls and *pyxides*, marble palettes, bone tubes, obsidian blades, and figurines (Kosma, 2019). Specifically, a total of 16 specimens of marble Cycladic figurines were recovered (Kosma, 2019). Artifact typologies were representative of the “Keros-Syros culture,” dating the assemblage to the Early Helladic II (ca. 2700-2300 BC) (Kosma, 2019; Kosma, 2010; Kosma, 2020a).

The Nea Styra graves were used for the burial of multiple individuals. No articulated and/or *in situ* skeletons were recovered, suggesting their use as ossuaries. Skeletal remains, as well as artifacts were found fragmented, and at different depths. Skeletal elements, mainly skulls, from earlier burials were sometimes covered by schist slabs and/or layers of pebbles (Kosma, 2019). The specimens included in this study were recovered from Grave 1, which

produced the largest number of skeletal remains: an estimated number of 50 skulls, commingled with postcranial elements, according to the excavation notes.

Conservation completion of the skeletal remains was supported by the Institute for Aegean Prehistory. Final bioarchaeological analysis and publication are in progress. All of our work is a tribute to the late Maria Kosma and her untimely loss in 2015.

A total of 26 individuals from Grave 1 were sampled for DNA. We present genome-wide data and direct radiocarbon dates for the following five:

- NST001 (NST-1; Cranium 5, Layer 3, Tomb 1) is an adult individual represented by cranial and dental elements. Radiocarbon-dating on human bone (NST001.A): 3956±27 BP, 2568-2348 cal BC (95% probability), (ID: MAMS-41246, AMS, IntCal13).
- NST004 (NST-5; Cranium 18, Layer 4, Tomb 1) is an adult individual represented by cranial elements. Radiocarbon-dating on human bone (NST004.A): 3974±28 BP, 2574-2371 cal BC (95% probability), (ID: MAMS-41247, AMS, IntCal13).
- NST005 (NST-7; Cranium 25, Layer 4, Tomb 1) is an adult individual represented by cranial elements. Radiocarbon-dating on human bone (NST005.A): 3886±28 BP, 2465-2292 cal BC (95% probability), (ID: MAMS-41248, AMS, IntCal13).
- NST010 (NST-12; Cranium 41, Layer 5, Tomb 1) is an adult individual represented by cranial elements. Radiocarbon-dating on human bone (NST010.A): 4075±28 BP, 2851-2495 cal BC (95% probability), (ID: MAMS-41249, AMS, IntCal13).
- NST012 (NST-14; Skeletal Group 18, Layer 5, Tomb 1) is an individual represented by an isolated temporal bone. Radiocarbon-dating on human bone (NST012.A): 3933±28 BP, 2475-2350 cal BC (95% probability), (ID: MAMS-41250, AMS, IntCal13).

### **Tiryns, Argolid, Greece**

Coordinates: 37.5995263, 22.7995951

Excavation(s): First excavation by the German Archaeological Institute, 1876-1929; latest excavation by the German Archaeological Institute and the Greek Archaeological Service, 2013-2018, directed by Prof. Joseph Maran and Dr. Alkestis Papadimitriou. A detailed history of the excavations is provided in Table 1. Bioanthropological research: Prof. Michael Schultz, Dr. Tyede Schmidt-Schultz.

1876 – 1929	German Archaeological Institute, excavations directed by Heinrich Schliemann, Wilhelm Dörpfeld, Georg Karo and Kurt Müller in the Upper, Middle and Lower Citadel, the Lower Town and the chamber tomb necropolis, as well as the first tholos tomb at the Prophitis Elias hill.
1957 – 1963	Greek Archaeological Service, excavations directed by Nikolaos Verdelis in the Lower Citadel
1957 – today	Greek Archaeological Service rescue excavations in the Lower Town
1965	Greek Archaeological Service and German Archaeological Institute, excavations directed by Nikolaos Verdelis in the Lower Citadel
1967 – 1974	German Archaeological Institute, excavations directed by Ulf Jantzen in the Lower Citadel and Western Lower Town
1976 – 1985	German Archaeological Institute, excavations directed by Klaus Kilian in the Northwestern Lower Town, Lower and Upper Citadel
1985	Greek Archaeological Service, excavations directed by Eleni Palaiologou in the second tholos tomb at the Prophitis Elias hill
1997 – 1998	German Archaeological Institute, excavations directed by Joseph Maran in the Upper Citadel
1999 – 2000	German Archaeological Institute and Greek Archaeological Service, excavations directed by Joseph Maran and Alkestis Papadimitriou in the Northeastern Lower Town
2000 – 2003	German Archaeological Institute, excavations directed by Joseph Maran in the Lower Citadel

2006 – 2010	German Archaeological Institute, excavations directed by Joseph Maran in the Western Lower Town
2013 – 2018	German Archaeological Institute and Greek Archaeological Service, excavations directed by Joseph Maran and Alkestis Papadimitriou in the Northwestern Lower Town

**Table 1.** History of excavations at the site of Tiryns.

The strongly fortified Mycenaean acropolis and palatial centre of Tiryns is situated about 1.5km from the present coast of the Bay of Nafplion (but only about 500m in the Early Bronze Age and 1km in the Late Bronze Age), where it perches on a narrow, rocky outcrop that reaches a height of up to 28m above sea level. The acropolis hill slopes from south to north, a topographic feature used during the Mycenaean palatial period (1400–1200 BC) to create a division into an Upper Citadel, a Middle Citadel, and a Lower Citadel by demarcating the limits of the different parts of the hill with strong, supporting walls built in so-called Cyclopean masonry. The acropolis was surrounded by an extensive settlement, the Lower Town, whose size during the different phases of occupation of the site is still difficult to determine.

During the Mycenaean period, extramural cemeteries used by inhabitants of Tiryns are attested by two tholos tombs and a chamber tomb necropolis (Rudolph, 1973; Müller, 1975) cut into the slopes of the Prophitis Elias hill, situated at a distance of about 1km to the east of the acropolis. In addition, an unusually high number of intramural burials without grave offerings dating to the Late Palatial and Postpalatial Mycenaean period (ca. 1300–1050 BC) was uncovered in the Lower Citadel (see below). Burials of the Early Iron Age (ca. 1050–700 BC) were encountered in different parts of the Lower Town next to house remains of that period, with the highest concentration of such burials having been found in the Western and Southwestern Lower Town. In the Byzantine period, burials are attested in the acropolis and different parts of the Lower Town.

Inhabited intermittently from the Middle Neolithic (ca. 5900–5400 BC), Tiryns became in the mid-3<sup>rd</sup> millennium BC an extensive and important Early Helladic settlement. Between ca. 1400 and 1200 BC, Tiryns was one of the major palatial centres of the Mycenaean palatial period in Greece and the most important harbour of the Peloponnesian Argolid region (Maran, 2010). The first palace built on the Upper Citadel in the course of the 14<sup>th</sup> century BC was replaced around 1250 BC by a second palace that was destroyed around 1200 BC in a major

conflagration (Kilian, 1988b). During the palatial period, the Lower Citadel was densely occupied, and its inhabitants were closely tied to the palace as administrators, artisans, workers or warriors. After the palatial period, Tiryns recovered much more rapidly than other sites from the setback caused by the destruction of the palace around 1200 BC and rose to the status of one of the foremost centres of the ensuing Postpalatial Aegean (ca. 1200–1050 BC) (Maran, 2016; Maran, 2015). After the Bronze Age, Tiryns remained continuously inhabited between the Early Iron Age and the early Classical period (ca. 1050–450 BC), but the focus of occupation shifted to the Lower Town, while the acropolis remained, at most, sparsely inhabited, with the Upper Citadel serving as a cult focus for the community of Tiryns. Little is known about Tiryns during the Byzantine period (ca. 7<sup>th</sup> – 14<sup>th</sup> cent CE), during which the occupation of the site seems to have been concentrated on the acropolis.

Based on the most recent anthropological-paleopathological analysis, at least 150 skeletal individuals buried without grave goods dating to the Late Palatial (ca. 1300–1200 BC; Late Helladic IIIB) or Postpalatial period (ca. 1200–1050 BC; Late Helladic IIIC) have been uncovered since the 1960s in open spaces or in ruins of former buildings of the Lower Citadel (Maran, 2008; Kilian, 1980). Despite the lack of grave goods, the burials do not have an irregular or haphazard appearance, since the deceased were carefully deposited on their backs in an extended position or lying on their side in a crouched (i.e., ‘foetal’) position in shallow pits. The burials without grave goods in the Lower Citadel markedly deviate from the Palatial and Postpalatial period burial tradition of interring the dead with grave goods in extramural chamber tombs dug into the slopes of hills around a settlement, such as the chamber tomb necropolis at the nearby Prophetis Elias hill. Kilian (1980) (Kilian, 1980) interpreted such Mycenaean intramural burials of the Late Palatial period as those of members of low social status groups within the palatial society to whom the right was denied to be buried with grave goods in such chamber tombs. This interpretation may very well be correct, but fact is that the practice of depositing the dead without grave goods continued after the destruction of the palace, when the social conditions must have been considerably different to those from the Palatial period. In the early 12<sup>th</sup> century BC, it seems that the entire northernmost part of the Lower Citadel was even temporarily transformed into a burial ground for such burials (Maran, 2008). Therefore, we may be dealing with funerary traditions linking the Palatial and Postpalatial period that were not only practiced because burial in chamber tombs was prohibited, but because there were social groups that did not identify with the normative funeral traditions and wanted to bury their dead differently.

In contrast to these Mycenaean burials, the ones of the Early Iron Age were usually placed in stone cists, storage vessels or in pits and were usually furnished with grave offerings (Papadimitriou, 2003). Single burials or groups of burials of the Byzantine period, some of them with grave offerings, were found in grave pits and rarely in stone cists in the Lower Citadel and different parts of the Lower Town.

The ongoing anthropological-paleopathological study by Michael Schultz and Tyede H. Schmidt-Schultz began in 2011 and focuses on the human skeletal remains from burials dating between the Mycenaean and the Byzantine period that have been uncovered since the 1960s in different parts of the acropolis and Lower Town. Unfortunately, due to a lack of available human skeletal remains from earlier excavations, it was not possible to include any of the burials in the extramural chamber tomb necropolis and tholos tombs at Prophitis Elias hill in the study. The anthropological-paleopathological study aims to determine the sex, age, height, type of constitution and handedness, as well as finding evidence of the living conditions, diseases and, when possible, the cause of death, in order to demographically characterize this segment of the population of Tiryns (Schultz and Schmidt-Schultz, 2015). The identified skeletal individuals were differentiated by the anthropologists through a numbering system consisting of the name of the excavator and a consecutive number starting with “1” for each excavator (cf. “Kilian 035”).

Of the 16 individuals from the Mycenaean contexts sampled for this study, only three produced genome-wide data that are included in the genetic analyses. All of them were directly radiocarbon-dated:

- TIR001 (Burial 5/03; LXIII35/03, VIF/VIG; Maran 010) is a male individual approximately 26-30 years old. The skeleton was found in 2003 in the Northwestern Lower Citadel lying on its back in an extended position and without grave offerings in an archaeological context dating to the Late Palatial period (Maran, 2008). The individual had a normally developed musculoskeletal system and suffered from chronic diseases of the upper and the lower respiratory tract. Radiocarbon-dating of human bone:  $3053 \pm 24$  BP, 1403–1229 cal BC (95% probability), (ID: MAMS-47534, AMS, IntCal20).
- TIR002 (Grave 7/1; LXII37/8 Nr.3; Nr. 1015; Kilian 024) is an individual ca. 40-55 years old represented by the partially preserved upper body of the skeleton found in 1977 in the Northwestern Lower Citadel. It was part of a group of burials without grave offerings in an archaeological context dating either to the Late Palatial period (LH IIIB

Developed or Final) or the early Postpalatial period (Kilian, 1979; Damm-Meinhardt, 2015) (LH IIIC Early). The individual had a very well-developed musculoskeletal system and suffered from chronic diseases of the upper respiratory tract. Despite the absence of important diagnostic features (e.g., the pelvis, femur, tibia, radius and ulna), a morphological sex diagnosis could be established based on the very pronounced male features of the skull (i.e., muscle marks on the occipital bone) and the humerus. Interestingly though, genetic sexing conducted on a tooth sample determined it was a female. Radiocarbon-dating of human tooth (TIR002.A):  $3044 \pm 23$  BP, 1394-1222 cal BC (95% probability), (ID: MAMS-47535, AMS, IntCal20).

- TIR010 (Grave 18; LXII44/29.30, XVIIa Nr.1048; Kilian 032) is a male individual approximately 45-50 years old. The skeleton was found in 1982/1983 lying on its back in an extended position in the Southwestern Lower Citadel as part of a group of burials without grave offerings in an archaeological context dating to the Late Palatial period (Kilian, 1988a) (LH IIIB Middle or Developed). The individual had a very well-developed musculoskeletal system and suffered from chronic diseases of the upper respiratory tract. Radiocarbon-dating of human bone:  $3116 \pm 26$  BP, 1440-1299 cal BC (95% probability), (ID: MAMS-42114, AMS, IntCal13).

Of the five individuals from the Iron Age (Protogeometric and Geometric) contexts sampled for this study, only one produced genome-wide data.

- TIR008 (Burial 1/14, Individual 1; LII25/58 II/II A & Of. II in. Nr. 134/14 and LII 25/58 I A; Maran 067) is represented by a well-preserved skeleton of a male who died at the age of 25-30 years, possibly as late as 35 years. This young male was of average height and had a medium physical constitution. The bones of this individual were found in 2014 in the Northwestern Lower Town in a concentration of redeposited human bones and three miniature vessels of the Geometric period immediately to the west of the covering slabs of Grave 2/14 containing burials of the Geometric period (Maran and Papadimitriou, 2016). The redeposited bones are likely to represent the collected remains of earlier, removed internments that dated to the Geometric period and possibly also the Protogeometric period, since the latter is represented by pottery also found in the vicinity of the same grave. Radiocarbon-dating of human bone:  $2765 \pm 26$  BP, 991-835 cal BC (95% probability), (ID: MAMS-42113, AMS, IntCal13).



## **AEGEAN ISLANDS**

### **Koukounaries, Paros, Greece**

Coordinates: 37.126595, 25.208784

Excavation: Archaeological Society at Athens, 1976-1992, directed by Prof. Demetrius U. Schilardi. Excavations by the “Paros Excavations” team were carried out under the auspices of the Archaeological Society at Athens, and subsequent studies and research on Koukounaries were supported by the Institute for Aegean Prehistory, the A.G. Leventis Foundation, the National Geographic Society and private donors (see acknowledgements in Schilardi, 2016). Bioanthropological study: Eleni-Anna Prevedorou.

The study and final publication of Koukounaries were interrupted by the sudden death of Dimitrius Schilardi in 2020. We are all making efforts to continue his devoted work. The volume on the Mycenaean pottery is now in press with Archaeopress by Robert Koehl. The publication of the Koukounaries excavations and related materials is currently coordinated by Prof. Alexandros Mazarakis Ainian under the auspices of the Archaeological Society at Athens.

The site of Koukounaries is located on a rocky hill (about 75m above sea level) by the Naoussa Bay, on the northern coast of Paros Island. The panoramic view over the bay and the sea, combined with the difficult access to the summit of the hill, offer strategic advantages. The site forms a palimpsest of occupation phases ranging from the Late Neolithic to Hellenistic times (Schilardi, 2016; Schilardi, 1999).

Late Neolithic (5<sup>th</sup> millennium BC) and successive Early Cycladic II finds (ca. 2700-2300 BC) were recovered on the Lower Plateau. In the early 12<sup>th</sup> century BC, the hill was fortified with a Cyclopean wall, transforming it into a citadel, including a Mycenaean palatial “mansion” and numerous artifacts of wealth and prestige; this citadel was destroyed in ca. 1150 BC. This destruction did not mark the end of habitation at the settlement, though, and both cult and domestic buildings are present from the Protogeometric through the early Archaic periods, with a temple of Athena continuing in use until the 3rd century BC.

The Mycenaean phase of Koukounaries Hill is of great importance. The primary Mycenaean phase dates to the LH IIIC – Middle (around 1175-1150 BC) (Schilardi, 2016). The mansion was built in LH IIIC Middle Developed, i.e., after the destruction of the mainland Mycenaean citadels, and destroyed in LH IIIC Middle Advanced, perhaps as the result of a siege, as suggested by the piles of sling bullets, arrowheads and pikes found in the destruction

level. A siege might thus explain the circumstances of the intramural burial in storeroom 2 (E 1; see below). The building, which was originally two-storied, collapsed, thus preserving a large number of storage areas filled with everyday vessels and storage jars (*pithoi*), as well as prestigious artifacts and metal finds. A layer of ash, in places reaching over 1m in thickness, covered the floors of the mansion. Skeletal human and faunal remains (including horse remains) were identified in the lower stories (basement and ground floor) of the building. This led to the hypothesis that the skeletal remains recovered belonged to people who sought refuge in the citadel along with animals during a siege and probably died in the collapse of the building during the conflagration (Schilardi, 2016). After the destruction of the mansion, small areas of the building were cleared and re-occupied in LH IIIC Late. Additionally, a small cave located on the upper slope of the hill, just outside the mansion, contained the skeletal remains of a male, probably dated to LH IIIC Middle.

The nature of the destruction, population mobility and the role of Koukounaries during late Mycenaean times remain important archaeological questions under investigation. We should note that a Mycenaean cemetery with chamber tombs was identified in the nearby narrow valley to the west called Loggos, associated with the acropolis (Schilardi, 2016). However, the tombs were completely emptied, and no skeletal or other remains were recovered. Thus, all skeletal material discussed here comes from the citadel. A subset of the human skeletal remains from the Koukounaries acropolis were studied by Sara Bisel in 1981 but were not published [see Schilardi (1999)]. Bioarchaeological and biogeochemical analyses and the publication of the human skeletal assemblage recovered at Koukounaries are in progress. The skeletal information reported here is based only on preliminary observations. Sampling and isotopic analyses are funded by the M. H. Wiener Foundation.

Of the seven individuals from Koukounaries sampled for this study, four produced genome-wide data and are included in the genetic analyses:

- KUK001 (KOU-1) is a middle adult female represented by a nearly complete skeleton whose burial was dug into the floor of the second storeroom (Schilardi, 2016). The skeleton was found in a tightly contracted position, lying on the right side. An engraved, discoid sealstone worn as a pendant was recovered with the skeleton (Schilardi, 2016). Preliminary skeletal evidence includes sharp-force cranial trauma, antemortem tooth loss and extensive osteoarthritic changes.
- KUK002 (KOU-3) is a young adult male represented by a nearly complete skeleton, buried in the cave at the northeastern edge of the Upper Plateau, accessed by a stone

staircase (Schilardi, 1999; Schilardi, 2016). The skeleton was placed in a supine position, with the lower legs bent, possibly due to a lack of space (Schilardi, 1999). It was accompanied by the ceramic figurine of a small horse. Sara Biesel reported hypertrophy of the adductor tubercles (and thus of the muscles) of the femora and attributed this to habitual horse-back riding (Schilardi, 1999).

- KUK005 (KOU-B) is an infant, approximately 3 years old, represented by an incomplete skeleton (Plateau, D2, Layer 8, 1982).
- KUK006 (KOU-D) is an infant, approximately 2 years old, represented by an incomplete skeleton (Plateau, D5, 1981).

### **Lazarides, Aegina, Greece**

Coordinates: 37.721203, 23.505420

Excavation(s): B' Ephorate of Antiquities, 1979-1980, directed by Cl. Eustratiou; Department of Archaeology and History of Art of the University of Athens, 2002-present, directed by Prof. Naya Polychronakou-Sgouritsa. Bioanthropological study: Eleni-Anna Prevedorou.

The Mycenaean settlement at Lazarides, in the neighbourhood of the homonymous semi-mountainous modern village, is located on a high plateau on eastern Aegina, 10km from Kolonna and an hour's walk from the the bay of Kyllindras, where finds suggest another Mycenaean community (Supplementary Figure 31). Although not visible from the sea, it had an excellent view of the Saronic Gulf and the adjacent areas of Attica and the northwestern Peloponnese (Sgouritsa and Salavoura, 2014). Research started in 1979 as a salvage excavation of the built chamber tomb cemetery and of the settlement in 1980, continuing to the present day. In 2002, the Department of Archaeology and History of Art of the University of Athens undertook a field survey and the systematic excavation of this site. Since then, a great part of the settlement has been discovered (Supplementary Figure 32), and the material, old and recent, from the cemetery has been published (Eustratiou and Polychronakou-Sgouritsa, 2016).

The site thrived during the period from LH IIIA2 to the end of LH IIIB/beginning of LH IIIC, judging by the pottery from the settlement and the neighbouring cemetery about 200m away. The earliest evidence dates to the Middle Helladic (MH) III/LH I period (Sgouritsa, 2010; Sgouritsa, 2021b), and it is highly probable that people from Kolonna founded the community at Lazarides. Besides agro-pastoral activities, the inhabitants of the site maintained

contacts with Attica, the northwestern Peloponnese (Sgouritsa, 2015), the Cyclades, the southeastern Aegean and Crete (Eustratiou and Polychronakou-Sgouritsa, 2016): they participated in exchange networks involving, among other goods (Sgouritsa and Salavoura, 2014; Sgouritsa, 2021b), storage and, mostly, cooking vessels, that reached to Thessaly (Sgouritsa, 2021b; Lis, 2012), while metal artifacts of bronze, lead, silver and iron (Tselios, 2016; Eustratiou and Polychronakou-Sgouritsa, 2016), as well as jewellery (Sgouritsa, 2012), point to an unexpected affluence. Moreover, weights found in the settlement imply relations with foreign traders, possibly Cypriots (Sgouritsa, 2021a).

Human remains come from both the cemetery, with male, female and infant interments, and the settlement (Prevedorou, 2016), where infant burials were discovered in several rooms of different uses. The latter were either simply deposited in the corners of rooms (Supplementary Figure 33), wherein one burial was enclosed by a wall (Supplementary Figure 34), or in small cist graves (Supplementary Figure 35). Sometimes they were supplied with offerings, such as a necklace, a figurine or even miniature bronze tools (probably toys?). Besides the intramural infant burials, very few adults seem to have been buried in the settlement during the last phase of its inhabitation, although the cemetery was still in use at this time.

The human skeletal remains included in this study have been published with the remains excavated before 2013 (Prevedorou, 2016). The bioarchaeological, biogeochemical, and radiocarbon analyses of the Lazarides skeletal assemblage are in progress by Eleni-Anna Prevedorou, funded by the Institute for Aegean Prehistory (INSTAP). Of the 22 individuals from Lazarides sampled for this study, five produced genome-wide data and are included in the genetic analyses. All of them were directly radiocarbon-dated, and all come from within the settlement (Supplementary Figure 32).

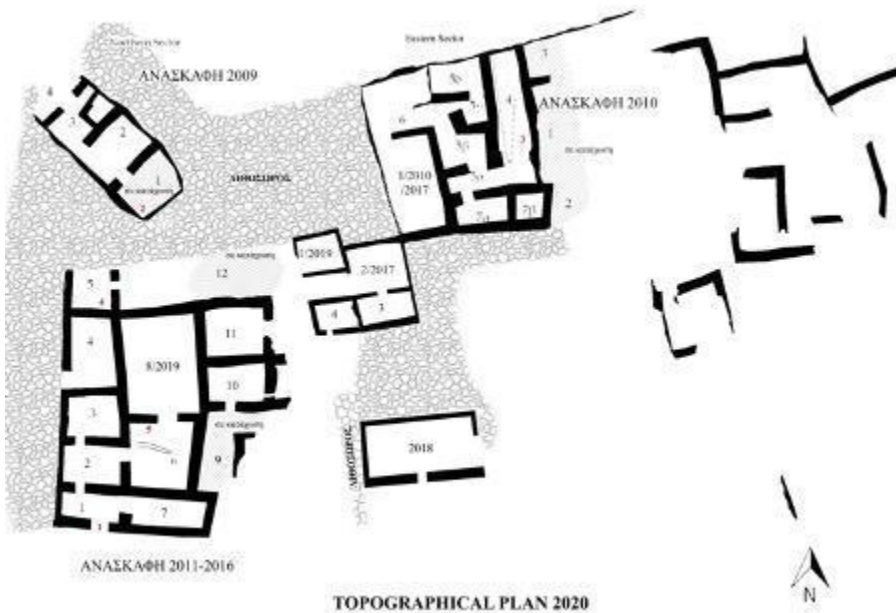
- LAZ017 (LZR-23) is probably an adult individual represented by a fragmented petrous bone. It was found in a bone concentration at the southern wall/entrance of room 1 of the complex located in the Papadimitris Plot. In total, the remains of at least three mature individuals and one young child approximately 3 years old ( $\pm 1$  year) could be identified in a pile of mingled bones and teeth. The early date of LAZ017 suggests this was likely a secondary treatment of earlier burials, a relocation carried out for unknown reasons or a burial of several persons. Radiocarbon-dating of human bone (LAZ017.A):  $4171 \pm 25$  BP, 2881-2635 cal BC (95% probability), (ID: MAMS-47523, AMS, IntCal20).

- LAZ018 (LZR-24) is a neonate, represented by cranial and postcranial elements found in Room 1 of the complex, used for storage and dated to the LH IIIA2/B1 period. The burial was deposited in the southwestern corner without offerings (Supplementary Figure 31) and with the head to the east. Radiocarbon-dating of human bone (LAZ018.A): 3097±21 BP, 1424-1293 cal BC (95% probability), (ID: MAMS-47524, AMS, IntCal20).
- LAZ019 (LZR-25) is an infant approximately 1 year old (12-16 months). The relatively complete skeleton was found in a cist tomb without a slab cover (0.6m E-W x 0.35m N-S) in space 5a, which was probably an open area, in 2010. It was provided with a necklace (Supplementary Figure 33). It may be dated to the LH IIIB period, as it was discovered in close proximity to a wall reconstructed at that time. Cranial and postcranial involvement suggest severe, prolonged symptoms of genetic anemia. The co-presence of infectious processes (e.g., parasitic) is also possible. The skeletal evidence and the clinical literature indicate that the infant had been severely ill for several months, if not all, of his young life [see Prevedorou (2016)]. Radiocarbon-dating of human bone (LAZ019.A): 3045±27 BP, 1398-1221 cal BC (95% probability), (ID: MAMS-47525, AMS, IntCal20).
- LAZ020 (LZR-26) is an infant approximately 12-16 months old represented by cranial and postcranial elements. It was found in a bone concentration in the southeastern corner of Room 5 of the Papadimitris Plot excavated in 2011 and contained the remains of at least five more individuals: one preterm, three perinates, and an infant about 6-9 months old, along with a few faunal remains. It was provided with a typical Psi- type figurine, dated to the LH IIIB1 period. Radiocarbon-dating of human bone (LAZ020.A): 3055±21 BP, 1403-1233 cal BC (95% probability), (ID: MAMS-47526, AMS, IntCal20).
- LAZ021 (LZR-27) is a perinatal infant (ca. 36-38 weeks old) represented mainly by cranial elements. It was found in Room 6 of the Papadimitris Plot, excavated in 2013, under a platform built in the northwestern corner during its final reorganization in the LH IIIB2 period. It may be dated to the LH IIIA2/B1 period. Radiocarbon-dating of human tooth (LAZ021.A): 3311±26 BP, 1626-1508 cal BC (95% probability), (ID: MAMS-49526, AMS, IntCal20).



- LH sites
- ▲ possible LH sites

**Supplementary Figure 31.** Map of Aegina with the location of Lazarides and other Late Helladic (LH) sites.



**Supplementary Figure 32.** Topographic plan of Lazarides with the locations of the individuals presented in this study marked in red.



**Supplementary Figure 33.** Infant burial in the southwestern corner of Room 1 (excavation 2009).



**Supplementary Figure 34.** Infant burial in the southwestern corner of Room 7 (2013).



**Supplementary Figure 35.** Infant burial in a cist grave (excavation 2010) provided with a necklace.

## References

Agelarakis, A. P. 1996. A Field and Laboratory Manual for Archaeologists, for the Excavation, Documentation, and Preservation of Human Osseous Remains. *Ariadne*, 189-247.

Agelarakis, A. P. 2014. On the Preservation and Conservation of Archaeologically Recovered Anthropological Remains: A Brief Communication to Younger Colleagues. In: Korika, E. (ed.) *The Protection of Archaeological Heritage in Times of Economic Crisis*. Cambridge Scholars Publishing.

Agelarakis, A. P. & Kanta, A. 2019. Intra-group dynamics, glimpses of labor diversity and specialization, and evidence of incipient social stratification in Neolithic Crete: Reflections from the Aposelemis Burial Ground. 12th International Congress of Cretan Studies, 21-25 September 2016 Heraklion. 1-17.

Agelarakis, A. P. & Kanta, A. 2020. The Neolithic Cemetery of Aposelemis. In: Karanastasi, P., Tsigounaki, A. & Tsigonaki, C. (eds.) *Proceedings 4th Archaeological Work in Crete Congress*. Hellenic Ministry of Culture & Athletics, Antiquities Authority of Rethymnon, University of Crete.

Alexiou, S. 1953. *Anaskafai en Katsamba* [Ανασκαφαί εν Κατσαμπά; Excavations at Katsambas]. ΠΑΕ / Prakt

Andreadaki-Vlazaki, M. 1992. Oikopedo Emm. Lentari - H. Manolakaki [Οικόπεδο Εμμ. Λεντάρη – Χ. Μανωλικάκη]. *ArchDelt* (Αρχαιολογικόν Δελτίον), 42 (1987), 556-557.



Andreadaki-Vlazaki, M. 1997. La nécropole du Minoen Récent III de la ville de La Canée. In: Driessen, J. & Farnoux, A. (eds.) *La Crète mycénienne*.

Andreadaki-Vlazaki, M. 2003. Odos Malinou kai Kritovoulidou (oikopedo K. Rovithaki) [Οδός Μαλινού και Κριτοβουλίδου (οικόπεδο Κ. Ροβιθάκη)]. *ArchDelt (Αρχαιολογικόν Δελτίον)*, 52 (1997), 1003-1042.

Andreadaki-Vlazaki, M. 2004. Odos Kanevaro [Οδός Κανέβαρο]. *ArchDelt (Αρχαιολογικόν Δελτίον)*, 53 (1998), 856-858.

Andreadaki-Vlazaki, M. 2010. Khandia (Kydonia). In: Cline, E. H. (ed.) *The Oxford Handbook of the Bronze Age Aegean (ca. 3000-1000 BC)*. Oxford University Press.

Andreadaki-Vlazaki, M. 2011. To palimpsiston tis arhais Kydonias [Το «παλίμψηστον» της αρχαίας Κυδωνίας]. *Proceedings of 10th International Congress of Cretan Studies (Chania 1-8 October 2006)* [Πεπραγμένα του 10ου Διεθνούς Κρητολογικού Συνεδρίου (Χανιά, Οκτ. 1-8, 2006)]. The Philological Association "Chrysostomos".

Andreadaki-Vlazaki, M. 2015. Sacrifices in LMIIIB: Early Kydonia Palatial Centre. *Pasiphae*, 9, 27-40.

Andreadaki-Vlazaki, M. 2018. Das Menschenopfer von Kydonia. Besanftigung zorniger Gotter? Mykene. Die sagenhafte Welt des Agamemnon. wbg Philipp von Zabern.

Andreadaki-Vlazaki, M. 2022a. Recent Evidence from the ‘Katre 1’ Excavation, Kastelli Hill, Khandia. *Pasiphae*, 14, 25-36.

Andreadaki-Vlazaki, M. 2022b. The Arrival of the Mycenaeans at Kydonia: Ancient Tradition and Archaeological Evidence. In: D’Agata, A. L., Girella, L., Papadopoulou, E. & Aquini, D. G. (eds.) *Supplemento 2 - One State, Many Worlds. Crete in the Late Minoan II-III A2 Early Period*. Edizioni Quasar.

Andreadaki-Vlazaki, M. & Protopapadaki, E. 2009. “Kouklaki” excavation (73-77 Igoumenou Gabriel St. In: Andreadaki-Vlazaki, M. (ed.) *A Tour to Sites of Ancient Memory*. Ministry of Culture and Tourism – 25th Ephorate of Prehistoric and Classical Antiquities.

Betancourt, P. P. 2014. *Hagios Charalambos: A Minoan Burial Cave in Crete: I. Excavation and Portable Objects*, Philadelphia, INSTAP Academic Press.

Betancourt, P. P., Davaras, C., Stravopodi, E., Karkanias, P., Langford-Verstegen, L., Mubly, J. M., Hickman, J., Dierckx, H. M. C., Ferrence, S. C., Reese, D. S., et al. 2008. Excavations in the Hagios Charalambos Cave, a Preliminary Report. *Hesperia*, 77, 539-605.

Bonga, L. 2019. Neolithiki keramiki apo to spilaio Pelekiton [Νεολιθική κεραμική από το σπήλαιο Πελεκητών; Neolithic ceramics from the Pelekita cave]. In: Mitsotaki, C. & Tzedaki-Apostolaki, L., eds. Proceedings of 12th International Congress of Cretan Studies, 2016 Heraklion. Heraklion: Εταιρία Κρητικών Ιστορικών Μελετών - Ιστορικό Μουσείο Κρήτης.

Bonga, L. & Ferrence, S. In press. Pelekita Cave, Kato Zakros, Crete: Late Neolithic and Minoan Interactions with the Dodecanese. Southeast Aegean / Southwest Coastal Anatolian Region International Conference (SASCAR). Material Evidence and Cultural Identity: 1. Early and Middle Bronze Age, 12-14 May 2016 Italian Archaeological School at Athens.

Bunni, A., Lagarce, J., Lagarce, E., Saliby, N., J., L. & P., B. 1998. Ras Ibn Hani, fouilles 1979-1995. Synthèse préliminaire I. Le palais nord du bronze récent., Beyrouth, Institut français d'archéologie du Proche-Orient.

Casselmann, C., Fuchs, M., Ittameier, D., Maran, J. & Wagner, G. A. 2004. Interdisziplinäre landschaftsarchäologische Forschungen im Becken von Phlious, 1998-2002. Archäologischer Anzeiger, 1, 1-58.

Damm-Meinhardt, U. 2015. Baubefunde und Stratigraphie der Unterburg (Kampagnen 1976-1983). Die mykenische Palastzeit (SH III B2) und beginnende Nachpalastzeit (Beginn SH III C), Dr. Ludwig Reichert Verlag.

Davaras, C. 1976. Guide to Cretan Antiquities, New Jersey, Park Ridge.

Davaras, C. 1983. Hagios Charalambos (Getontomouri) Lasithiou [Άγιος Χαράλαμπος (Γεροντομουρί) Λασιθίου]. ArchDelt (Αρχαιολογικόν Δελτίον), 31, 379-380.

Davaras, C. 1986. Proimes minoikes sfragistikoi daktylioi apo to spilaio Gerontomouri Lasithiou [Πρώιμες μινωικές σφραγιστικοί δακτύλοι από το σπήλαιο Γεροντομουρί Λασιθίου]. ArchEph (Αρχαιολογική Εφημερίς), 9-48.

Davaras, C. 1989a. Spilaio Gerontomouri [Σπήλαιο Γεροντομουρί; Gerontomouri Cave]. ArchDelt (Αρχαιολογικόν Δελτίον), 38, 375.

Davaras, C. 1989b. Spilaio Hagiou Charalambous [Σπήλαιο Αγίου Χαράλαμπος; Hagios Charalambos Cave]. ArchDelt (Αρχαιολογικόν Δελτίον), 37, 387-388.

Davaras, C. 2015. The Elusive site of the Primary Burials of the Hagios Charalambos Cave: A Speculative Scenario. In: Betancourt, P. P., Davaras, C. & Stravopodi, E. (eds.) Hagios Charalambos. A Minoan Burial Cave in Crete II, The Pottery. INSTAP Academic Press.

Dawkins, R. M., Hawes, C. H. & C., B. R. 1904-1905. Excavations at Palaikastro. IV.

Douka, K., Efstratiou, N., Hald, M. M., Henriksen, P. S., Karetsou, A. & (2017) “Dating Knossos and the arrival of the earliest Neolithic in the southern Aegean, *A. C. U. P.*, 91(356), pp. 304–321. doi: 10.15184/aqy.2017.29. 2017. Dating Knossos and the arrival of the earliest Neolithic in the southern Aegean. *Antiquity*, 93, 304-321.

Efstratiou, N., Karetsou, A. & Ntinou, M. (eds.) 2013. *The Neolithic Settlement of Knossos in Crete: New Evidence for the Early Occupation of Crete and the Aegean Islands*, INSTAP Academic Press.

Eustratiou, K. & Polychronakou-Sgouritsa, N. 2016. Το Μυκηναϊκό νεκροταφείο στους Λαζάρηδες Αίγινας [To Μυκηναϊκό νεκροταφείο στους Λαζάρηδες Αίγινας; The Mycenaean cemetery at Lazarides, Aegina]. *ArchDelt (Αρχαιολογικόν Δελτίον)*, 65-66, 2010-2011, 1-162.

Evans, A. J. 1901. *The Neolithic Settlement at Knossos and its Place in the History of Early Aegean Culture*, London, Royal Anthropological Institute of Great Britain and Ireland.

Evans, A. J. 1921. *The Palace of Minos at Knossos: The Neolithic and Early and Middle Minoan Ages*, London, Macmillan and Co., Limited.

Evans, A. J. 1928. *The Palace of Minos at Knossos: A comparative account of the successive stages of the early Cretan civilization as illustrated by the discoveries*, London, Macmillan and Co., Limited.

Evans, J. D. 1964. *Excavations in the Neolithic Settlement of Knossos, 1957–60. Part I. The Annual of the British School at Athens*. Cambridge University Press.

Galanidou, N. & Manteli, K. 2008. *Neolithic Katsambas Revisited: the Evidence from the House*. In: Isaakidou, V. & Tomkins, P. D. (eds.) *Escaping the Labyrinth: The Cretan Neolithic in Context*. Oxbow Books.

Hachtmann, V. 2013. *The Bronze Age settlement at Aidonia*. In: Kissas, K. & Niemeier, W.-D. (eds.) *The Corinthia and the Northeast Peloponnese. Topography and History from Prehistoric Times until the End of Antiquity*.

Hallager, B. P. & McGeorge, P. J. P. 1992. *Late Minoan III burials at Khania. The tombs, finds and deceased in Odos Palama*, Göteborg, Åström.

Hallager, E. & Andreadaki-Vlazaki, M. 2017. *The Greek-Swedish-Danish Excavations 2014: A short preliminary report*. *Proceedings of the Danish Institute at Athens*, 8, 280-292.

Hallager, E. & Hallager, B. P. (eds.) 2003, 2011 and 2016. *The Greek-Swedish Excavations at the Agia Aikaterini Square, Kastelli, Khania 1970-1987 and 2001*.

Istituto per gli studi micenei ed, e.-a. 1989. Scavi a Nerokourou, Kydonias, Roma, Edizioni dell'Ateneo.

Kakavoyannis, E. 1999-2001. Mykinaiko nekrotafeio sto lofo Fouresi tou Dimou ton Glykon Neron Attikis [Μυκηναϊκό νεκροταφείο στο λόφο Φούρεσι του Δήμου των Γλυκών Νερών Αττικής; Mycenaen cemetery at the Fouresi hill of Glyka Nera in Attica]. *Athens Annals of Archaeology*, 32-34, 55-70.

Kanta, A., Ferrence, S. & Bonga, L. in press. Spilaio Pelekiton Zaktou 2014, 2015. Prokatartiki Ekthesi ton ergasion. [Σπήλαιο Πελεκητών Ζάκρου 2014, 2015. Προκαταρκτική Έκθεση των εργασιών; Pelekita Cave at Zakros 2014, 2015. A preliminary report]. 4th Meeting for the Archaeological Work in Crete, 2016 Rethymnon.

Kanta, A. & Serpetsidaki, I. To ergo tis 23 Ephoreias Proistorion kai Klassikon Arhaiotiton kata ta eti 2011-2013 [Το έργο της ΚΓ΄ Εφορείας Προϊστορικών και Κλασικών Αρχαιοτήτων κατά τα έτη 2011 – 2013; The work of the 23st Ephorate of Prehistoric and Classical Antiquities between 2011 and 2013]. In: Karanastasi, P., Tzigoudaki, A. & Tsigonaki, C., eds. 3rd Meeting for the Archaeological Work in Crete, 2013 Rethymnon. 53-68.

Kataki, E. 2014. Symvoli ton odon I. Sfakianaki 27 kai Platonos (oikopedo Melefaki) [Συμβολή των οδών Ι. Σφακιανάκη 27 και Πλάτωνος (οικόπεδο Μαλεφάκη)]. *ArchDelt (Αρχαιολογικών Δελτίων)*, 63 (2008), 1154-1155.

Kaza-Papageorgiou, K. 2018. Asteria Glyfadas. Anthropini Parousia stin proistoriki epohi [Asteria at Glyfada. Human presence at prehistoric times]. *Arhaiologia kai Tehnes*, 128, 30-41.

Kaza-Papageorgiou, K. 2019. Cycladic-type figurines from the Early Helladic cemetery of Asteria at Glyfada, Attica. In: Marthari, M., Renfrew, C. & Boyd, M. J. (eds.) *Beyond the Cyclades. Early Cycladic Sculpture in Context from Mainland Greece, the North and East Aegean*. Oxbow Books.

Kilian, K. 1979. Ausgrabungen in Tiryns 1977. Bericht zu den Ausgrabungen. *Archäologischer Anzeiger*, 379–411.

Kilian, K. 1980. Zum Ende der mykenischen Epoche in der Argolis. *Jahrbuch des Römisch-Germanischen Zentralmuseums Mainz*, 27, 166–195.

Kilian, K. 1988a. Ausgrabungen in Tiryns 1982/83. Bericht zu den Ausgrabungen. *Archäologischer Anzeiger*, 105–151.

Kilian, K. 1988b. Mycenaens up to Date: Trends and Changes in Recent Research. In: French, E. B. & Wardle, K. A. (eds.) *Problems in Greek Prehistory: Papers Presented at the Centenary*

Conference of the British School of Archaeology at Athens, Manchester, April 1986. Bristol Classical Press.

Kontopodi, D. forthcoming. Kannia Gortys. ArchDelt (Αρχαιολογικόν Δελτίον).

Kosma, M. 2010. New Early Cycladic figurine at Nea Styra. *Mediterranean Archaeology and Archaeometry*, 10, 29-36.

Kosma, M. 2019. Cycladic Marble Figurines from the Early Bronze Age Cemetery at Nea Styra, Euboea. In: Marthari, M., Renfrew, C. & Boyd, M. J. (eds.) *Beyond the Cyclades. Early Cycladic Sculpture in Context from Mainland Greece, the North and East Aegean*. Oxbow Books.

Kosma, M. 2020a. Nea stoiheia gia tis sheseis Attikis kai Euboias kata tin Proimi Epohi tou Halkou, mesa apo ta dedomena tou protoelladikou nekrotafeiou sta Nea Styra Euboias [Νέα στοιχεία για τις σχέσεις Αττικής και Εύβοιας κατά την Πρώιμη Εποχή του Χαλκού, μέσα από τα δεδομένα του πρωτοελλαδικού νεκροταφείου στα Νέα Στύρα Ευβοίας; New insights for the relations between Attica and Euboea during the Early Bronze Age via the evidence from the Early Helladic cemetery at Nea Styra in Euboea]. In: Papadimitriou, N., Wright, J. C., Fachard, S., Polychronakou-Sgouritsa, N. & Andriku, E. (eds.) *Athens and Attica in Prehistory: Proceedings of the International Conference*. Athens, 27-31 May 2015. Archaeopress.

Kosma, M. 2020b. To protoelladiko nekrotafeio sti thesi Gkisouri sta Nea Styra Euboias [Το πρωτοελλαδικό νεκροταφείο στη θέση Γκισούρι στα Νέα Στύρα Εύβοιας; The Early Helladic Cemetery at Gkisouri in Nea Styra of Euboea]. In: Mazarakis Ainian, A. (ed.) *Archaiologiko Ergo Thessalias kai Stereas Elladas*, 5 (2015): *Praktika Epistimonikis Synantisis*, Volos, 26 Fevrouariou – 1 Martiou 2015. Ypourgeio Politismou kai Athlitismou, Tameio Arhaiologikon Poron kai Apallotrioseon, Ergastirio Arhaiologias Panepistimiou Thessalias.

Krystalli-Votsi, K. 1998. The Excavation of the Mycenaean Cemetery at Aidonia. In: Demakopoulou, K. (ed.) *The Aidonia Treasure. Seals and Jewelry of the Aegean Late Bronze Age*.

Krystalli-Votsi, K. & Kaza-Papageorgiou, K. 2013. To mykinaiko nekrotafeio ton Aidionion (Το μυκηναϊκό νεκροταφείο των Αηδονιών; The mycenaen cemetery at Aidonia). In: Kissas, K. & Niemeier, W.-D. (eds.) *The Corinthia and the Northeast Peloponnese. Topography and History from Prehistoric Times until the End of Antiquity*.

Kvapil, L. & Shelton, K. 2019. Among the Ancestors at Aidonia. In: Borgna, E., Caloi, I., Carinci, F. M. & Laffineur, R. (eds.) *Μνήμη/Mneme: Past and Memory in the Aegean Bronze Age*. Proceedings of the 17th International Aegean Conference, University of Udine, Department of Humanities and Cultural Heritage, and the Ca' Foscari University of Venice, Department of Humanities. Peeters Publishers & Booksellers.

- Langford-Verstegen, L. 2015. Hagios Charalambos. A Minoan Burial Cave in Crete II, The Pottery, Philadelphia, INSTAP Academic Press.
- Lis, B. 2012. Aeginetan pottery in Central Greece and its wider perspective. *Arhailogiko Ergo Thessalias kai Stereas Elladas*, 3 (2009): Praktika Epistimonikis Synantisis, Volos, 12 – 15 Martiou, Volos.
- Mackenzie, D. 1903. The Pottery of Knossos. *Journal of Hellenic Studies*, 23, 157–205.
- Manteli, K. 1992. The Neolithic Well at Kastelli Phournis in Eastern Crete. *Annual of the British School at Athens*, 87, 103-120.
- Maran, J. 2008. Forschungen in der Unterburg von Tiryns 2000–2003. *Archäologischer Anzeiger*, 35–111.
- Maran, J. 2010. Tiryns. In: Cline, E. H. (ed.) *The Oxford Handbook of the Bronze Age Aegean (ca. 3000-1000 BC)*. Oxford University Press.
- Maran, J. 2015. Tiryns and the Argolid in Mycenaean Times: New Clues and Interpretations. In: Schallin, A.-L. & Tournavitou, I. (eds.) *Mycenaeans Up to Date: The Archaeology of the North-Eastern Peloponnese. Current Concepts and New Directions*. Swedish Institute at Athens.
- Maran, J. 2016. Against the Currents of History: The Early 12th-Century BCE Resurgence of Tiryns. In: Driessen, J. (ed.) *RA-PI-NE-U. Studies on the Mycenaean world offered to Robert Laffineur for his 70th Birthday*. UCL Presses Universitaires de Louvain.
- Maran, J. & Papadimitriou, A. 2016. Gegen den Strom der Geschichte - Die nördliche Unterstadt von Tiryns: Ein gescheitertes Urbanisierungsprojekt der mykenischen Nachpalastzeit. *Archäologischer Anzeiger*, 19–118.
- McGeorge, P. J. P. 1988. Health and Diet in Minoan Times. In: Jones, R. E. & Catling, H. W. (eds.) *New Aspects of Archaeological Science in Greece: Proceedings of a Meeting held at the British School at Athens January 1987 BSA Occ. Paper 3 of the Fitch Laboratory*.
- McGeorge, P. J. P. 2003. Appendix 2 : Intramural Infant Burials in the Aegean. In: Hallager, E. & Hallager, B. P. (eds.) *The Greek-Swedish Excavations at the Agia Aikaterini Square Kastelli, Khania 1970-1987 and 2001*. Astrom Editions.
- McGeorge, P. J. P. 2011. Trauma, surgery and prehistoric events. *Proceedings of the 10th International Congress of Cretan Studies*, 1-8 October 2006 Khania. 347-361.
- McGeorge, P. J. P. 2011. Intramural infant burials in the Aegean Bronze age: Reflections on symbolism and eschatology with particular reference to Crete. *2èmes Rencontres d'archéologie*

de l'IFEA: Le Mort dans la ville Pratiques, contextes et impacts des inhumations intra-muros en Anatolie, du début de l'Age du Bronze à l'époque romaine. IFEA-Ege yayınları.

McGeorge, P. J. P. 2012. The Petras intramural infant jar burial: context, symbolism, eschatology. In: Tsipopoulou, M. (ed.) Petras, Siteia – 25 years of excavations and studies. The Danish Institute at Athens.

McGeorge, P. J. P. 2015. The Earliest Archaeological Evidence for a Mycenaean Greek Ritual Form of Human Sacrifice. *Pasiphae*, 9, 43-52.

McGeorge, P. J. P. 2017. The Pit L Baby Burial – Hermeneutics: Implications for immigration into Kydonia in MMIII/LMI. *Proceedings of the Danish Institute at Athens*, 8, 293-302.

McGeorge, P. J. P. 2020. Palaeo-Oncological Findings from Prehistoric Crete. In: Γραμματείας, Κ. Ε. τ. Ε. κ. Λ., ed. *Proceedings of the 2nd International Symposium of the European Society for the History of Oncology, 2019 Athens*. Athens: Academy of Athens, 81-91.

Morris, M. W. 2002. *Soil Science and Archaeology: Three Test Cases from Minoan Crete*, Philadelphia, INSTAP Academic Press.

Müller, K. 1975. Das Kuppelgrab von Tiryns. In: Jantzen, U. (ed.) *Tiryns: Forschungen und Berichte*. Philipp von Zabern.

Mylona, D. 2015. Sacrifices in LM IIIB: Early Kydonia Palatial Centre. *The Animal Remains*. 9, 53-58.

Mylonas, G. E. 1959. *Aghios Kosmas: an Early Bronze Age settlement and cemetery in Attica*, Princeton University Press.

Nordquist, G. C. 1987. A Middle Helladic village: Asine in the Argolid. *Academia Ubsalaliens*.

Pantelidou-Gofa, M. 2005. Tsepi Marathonos: to protoelladiko nekrotafeio [Τσέπι Μαραθώνος: το πρωτοελλαδικό νεκροταφείο; Tsepi at Marathon: the Early Helladic cemetery], Athens, Archaeological Society at Athens.

Pantelidou-Gofa, M. 2008. The EHI deposit pit at Tsepi, Marathon: features, formation and the breakage of finds. In: Brodie, N., Doole, J., Gavalas, G. & Renfrew, C. (eds.) *Horizon: a colloquium on the prehistory of the Cyclades*. McDonald Institute for Archaeological Research/Stavros Niarchos Foundation.

Pantelidou-Gofa, M. 2016. Tsepi Marathonos: o apothetis 39 tou protoelladikou nekrotafeiou [Τσέπι Μαραθώνος: ο αποθέτης 39 του πρωτοελλαδικού νεκροταφείου; Tsepi at Marathon: the deposit 39 of the Early Helladic cemetery], Athens, Archaeological Society at Athens.

Papadatos, Y. 2008. The Neolithic-Early Bronze Age Transition in Crete: New Evidence from the Settlement at Petras Kephala, Siteia. In: Isaakidou, V. & Tomkins, P. D. (eds.) *Escaping the Labyrinth: The Cretan Neolithic in Context*. Oxbow Books.

Papadimitriou, A. 2003. Οι υπομυκηναϊκοί και πρωτογεωμετρικοί τάφοι της Τίρυνθας. *Ανάλυση και ερμηνεία*. In: Vlachopoulos, A. & Birtacha, K. (eds.) *Argonautis. Timitikos tomos gia ton kathigiti Christo G. Douma apo tous mathites tou sto Panepistimio Athinon (1980-2000)* [Αργοναύτης. Τιμητικός τόμος για τον καθηγητή Χρίστο Γ. Ντούμα από τους μαθητές του στο Πανεπιστήμιο Αθηνών (1980–2000)]. Kathimerini.

Papathanasiou, A., Tiliakou, A., Kwok, C. S., Moutafi, I. & Kakavogianni, O. 2020. The human remains of the Late Bronze Age cemetery of Glyka Nera. In: Papadimitriou, N., Wright, J., Fachard, S., Polychronakou-Sgouritsa, N. & Andrikou, E. (eds.) *Athens and Attica in Prehistory. Proceedings of the International Conference, Athens, 27-31 May 2015*. Archaeopress.

Papazoglou-Manioudaki, L. & Paschalidis, C. 2017. A Society of Merchants and Warriors to the East of the West. The Case of the Mycenaean Settlement on Mygdalia Hill, near Patras, in Achaea. In: Fotiadis, M., Laffineur, R., Lolos, Y. & Vlachopoulos, A. (eds.) *Ἑσπερος/Hesperos. The Aegean seen from the West*. Peeters.

Papazoglou-Manioudaki, L., Paschalidis, C. & Jones, O. A. 2019. Community and Memory in the Periphery of the Mycenaean World: Incidents in the Life of the Mygdalia Settlement Near Patras, in Achaea. In: Borgna, E., Caloi, I., Carinci, F. M. & Laffineur, R. (eds.) *MNHMH/MNEME: Past and Memory in the Aegean Bronze Age. Proceedings of the 17th International Aegean Conference, University of Udine, Department of Humanities and Cultural Heritage, and the Ca' Foscari University of Venice, Department of Humanities*. Peeters.

Persson, P. Å. 2003. A Note on the Foetus. In: Hallager, E. & Hallager, B. P. (eds.) *The Greek-Swedish Excavations at the Agia Aikaterini Square Kastelli, Khania 1970-1987 and 2001*. Astrom Editions.

Polychronakou-Sgouritsa, N. & Kakavogiannis, E. 2020. Minoans in Mesogaia? In: Papadimitriou, N., Wright, J., Fachard, S., Polychronakou-Sgouritsa, N. & Andrikou, E. (eds.) *Athens and Attica in Prehistory Proceedings of the International Conference, Athens, 27-31 May 2015*. Archaeopress.

Preve, S. 2009a. “Lendari” excavation (83 A. Papandreou St.). In: Andreadaki-Vlazaki, M. (ed.) *Khania (Kydonia). A Tour to Sites of Ancient Memory*. Ministry of Culture and Tourism – 25th Ephorate of Prehistoric and Classical Antiquities.



Preve, S. 2009b. "Rovithaki" excavation (11 Malinou St.). In: Andreadaki-Vlazaki, M. (ed.) Khandia (Kydonia). A Tour to Sites of Ancient Memory. Ministry of Culture and Tourism – 25th Ephorate of Prehistoric and Classical Antiquities.

Prevedorou, E. 2016. A bioarchaeological perspective on the human skeletal remains from the Mycenaean settlement and cemetery at Lazarides. To Mykinaiko nekrotafeio stous Lazarides Aiginas [To Μυκηναϊκό νεκροταφείο στους Λαζάρηδες Αίγινας; The Mycenaean cemetery at Lazarides, Aegina].

Protopapadaki, E. 2021. I poli pano sti nekropoli: I nekropoli tis arhais Kydonias sti xoriki egrafi tis syghronis polis ton Hanion [Η πόλη πάνω στη νεκρόπολη: Η νεκρόπολη της αρχαίας Κυδωνίας στη χωρική εγγραφή της σύγχρονης πόλης των Χανίων]. Masters, Technical University of Crete.

Rudolph, W. 1973. Die Nekropole am Prophitis Elias bei Tiryns. In: Jantzen, U. (ed.) Tiryns: Forschungen und Berichte. Verlag Philipp von Zabern.

Sackett, L. H., Hankey, V., Howell, R. J., Jacobsen, T. W. & Popham, M. R. 1966. Prehistoric Euboea: Contributions toward a survey. Annual of the British School at Athens, 61, 33-112.

Sampson, A. 1980. Proistorikes theseis kai oikismoι stin Euboiα [Προϊστορικές θέσεις και οικισμοί στην Εύβοια; Prehistoric sites and settlements in Euboea]. Arheio Euboikon Meleton (Αρχείο Ευβοϊκών Μελετών), 23, 91-249.

Schilardi, D. U. 1999. The Mycenaean horseman (?) of Koukounaries. In: Betancourt, P. P., Karageorghis, V., Laffineur, R. & Niemeier, W.-D. (eds.) Meletemata: Studies Presented to Malcolm H. Wiener as He Enters his 65th Year.

Schilardi, D. U. 2016. Koukounaries, Paros: the excavations and history of a most ancient Aegean acropolis (version in Greek), Athens, Paros excavations, Center of Historical and Archaeological Studies.

Schultz, M. & Schmidt-Schultz, T. 2015. Anthropologie. In: Maran, J. & Papadimitriou, A. (eds.) Tiryns, Griechenland: Die Arbeiten der Jahre 2012 bis 2014.

Serpetsidaki, I. Neoteri anaskafiki ereuna sto neolithiko Katsamba [Νεότερη ανασκαφική έρευνα στο νεολιθικό Κατσαμπά; Latest excavation survey at Neolithic Katsambas]. 11th International Congress of Cretan Studies, 21-27 October 2011 Rethymnon. 2011.

Sgouritsa, N. 2010. Lazarides on Aegina: Another prehistoric site. In: Touchais, G., Philippa-Touchais, A., Voutsaki, S. & J. Wright, J. (eds.) Mesohelladica. The Greek Mainland in the Middle Bronze Age. De Boccard.

Sgouritsa, N. 2012. Remarks on jewels from the Mycenaean Settlement and Cemetery at Lazarides on eastern Aegina. In: Nosch, M.-L. & Laffineur, R. (eds.) *Kosmos. Jewellery, Adornment and Textiles in the Aegean Bronze Age*. Peeters.

Sgouritsa, N. 2015. Lazarides on eastern Aegina: The relationships with the NE Peloponnese. In: Schallin, A.-L. & Tournavitou, I. (eds.) *Mycenaeans Up to Date: The Archaeology of the NE Peloponnese—Current Concepts and New Directions*. Proceedings of the Conference held 10-16 November 2010, Swedish Institute at Athens. The Editorial Committee of the Swedish Institutes at Athens and Rome.

Sgouritsa, N. 2021a. Animal-shaped standard-weights in the Aegean of the Mycenaean Era. In: Lambrinoudakis, V., Mendoni, L., Koutsoubou, M., Panagou, T., Sfiroera, A. & Charalampidou, X. (eds.) *Έξοχος άλλων. Τιμητικός Τόμος για την Ε. Σημαντώνη –Μπουρνιά*.

Sgouritsa, N. 2021b. Ο Μυκηναϊκός οικισμός στους Λαζάρηδες Αίγινας: δέκα χρόνια έρευνας. Ερωτήματα που ζητούν ακόμη απάντηση]. In: Karantzali, E. (ed.) *Praktika tou C' diethnous diepistimonikou symposiou, I Perifereia tou Mykinaikou Kosμου. Prosfata eurimata kai porismata tis ereunas, Lamia 18-21 Μαΐου [Πρακτικά του Γ' διεθνούς διεπιστημονικού συμποσίου, Η Περιφέρεια του Μυκηναϊκού Κόσμου. Πρόσφατα ευρήματα και πορίσματα της έρευνας, Λαμία 18-21 Μαΐου 2018; Proceedings of the third interdisciplinary symposium, The periphery of the Mycenaean Word]*.

Sgouritsa, N. & Salavoura, E. 2014. The Exploitation of Inland Natural Resources on an Island Environment: The Case of the Mycenaean Settlement at Lazarides and the south/southeast Aegina. In: Touchais, G., Laffineur, R. & Rougemont, F. (eds.) *PHYSIS. L'environnement naturel et la relation home-milieu dans le monde égéen protohistorique*. Leuven

Theocharis, D. 1959. Ek tis proistorias Euboias kai Skyrou [Εκ της προϊστορίας Ευβοίας και Σκύρου; From the prehistory of Euboea and Skyros]. *Arheio Euboikon Meleton (Αρχείο Ευβοϊκών Μελετών)*, 6, 279-328.

Todaro, S. & Di Tonto, S. 2008. The Neolithic Settlement of Phaistos Revisited: Evidence for Ceremonial Activity on the Eve of the Bronze Age. In: Isaakidou, V. & Tomkins, P. D. (eds.) *Escaping the Labyrinth: The Cretan Neolithic in Context*. Oxbow Books.

Tomkins, P. D. 2007. Neolithic: Strata IX-VIII, VII-VIB, VIA-V, IV, IIIB, IIIA, IIB, IIA and IC Groups. In: Momigliano, N. (ed.) *Knossos Pottery Handbook: Neolithic and Bronze Age (Minoan)*. The British School at Athens.

Tomkins, P. D. 2009. Domesticity by default. Ritual, ritualization and cave-use in the Neolithic Aegean. *Oxford Journal of Archaeology*, 28, 125-153.

Tomkins, P. D. 2012. Landscapes of Ritual, Identity, and Memory: Reconsidering Neolithic and Bronze Age Cave Use in Crete, Greece. In: Holley, M. (ed.) *Sacred Darkness: A Global Perspective on the Ritual Use of Caves*. University Press of Colorado.

Tomkins, P. D. 2018. About Time. Rehabilitating chronology in the interpretation of settlement in east Crete between the Neolithic and Early Minoan I. *Creta Antica*, 19, 45-92.

Triantaphyllou, S. 2008. Living with the Dead: a Re-Consideration of Mortuary Practices in the Greek Neolithic. In: Isaakidou, V. & Tomkins, P. D. (eds.) *Escaping the Labyrinth: The Cretan Neolithic in Context*. Oxbow Books.

Trotter, M. 1970. Estimation of stature from intact long limb bones. Personal identification in mass disasters, 71-83.

Tselios, C. 2016. Ergastiriaki Eksetasi ton metallikon eurimatou tou mykinaikou oikismou kai nekrotafeiou ton Lazaridon Aiginas (Εργαστηριακή εξέταση μεταλλικών ευρημάτων του μυκηναϊκού οικισμού και του νεκροταφείου των Λαζάρηδων Αίγινας). *To Mykinaiko nekrotafeio stous Lazarides Aiginas [Το Μυκηναϊκό νεκροταφείο στους Λαζάρηδες Αίγινας; The Mycenaean cemetery at Lazarides, Aegina]*.

Tzedakis, Y. 1970. Anaskafi tou spilaiou Genariou [Ανασκαφή σπηλαίου Γερανίου; Excavation at Gerani Cave]. *ArchDelt (Αρχαιολογικόν Δελτίον)*, 25, 474-476.

Vagnetti, L. 1972-1973. L'insediamento neolitico di Festos. *Annuario della Scuola archeologica di Atene e delle Missioni italiane in Oriente*, 50-51, 7-138.

Vagnetti, L. 1973. Tracce di due insediamenti neolitici nel territorio dell'antica Gortina, Catania, Università di Catania, Istituto di Archaeologia.

Vassilakis, A. 1987. Anaskafi Neolithikou Spitiou stous Kalous Limenes Kritis [Ανασκαφή Νεολιθικού Σπιτιού στους Καλούς Λιμένες της Νότιας Κρήτης; Excavation of the Neolithic House at Kaloi Limenes, Crete]. In: Platon, N., Kastrinakis, L., Orphanou, G. & Giannadakis, N. (eds.) *Eilapini: Tomos timitikos gia ton kathigiti N. Platona (Είλαπινή: Τόμος Τιμητικός για τον καθηγητή Ν. Πλάτωνα)*. Δήμος Ηρακλείου.

Warren, P., Jarman, M. R., Jarman, H. N., Shackleton, N. J. & Evans, J. D. 1968. Knossos Neolithic, Part II. *Annual of the British School at Athens*, 63, 239 – 276.

Wolters, P. 1891. Marmorkopf aus Amorgos. *Athenische Mitteilungen*, 16, 46-58.

## SUPPLEMENTARY NOTE 2

### Modeling and dating of genetic admixture

In this section we provide details on allele frequency-based methods that were applied in order to quantify gene-flow into the Aegean populations, infer ancestry mixture models and estimate the dates of the admixture events.

To avoid biases in allele frequencies caused by genetic relatedness, we removed first and second-degree relatives from group-based analyses. For the sites of Mygdalia and Hagios Charalambos, where a high rate of relatedness is observed among the individuals (Extended Data Fig. 4), we also excluded individuals related at the third degree. On the other hand, given the high rate of genotype missingness in Aposelemis individuals, we included both individuals from a second-degree related pair (APO004 and APO028), but we also estimated and compared  $f_4$ -statistics and significance levels from APO004 alone (highest SNP coverage).

Individual and group IDs are reported as in <https://reich.hms.harvard.edu/allen-ancient-dna-resource-aadr-downloadable-genotypes-present-day-and-ancient-dna-data>, and whenever another grouping label was employed, we specify which individual were included.

The following abbreviations are applied on the nomenclature E: Early, M: Middle, L: Late, N: Neolithic, En: Eneolithic, C: Chalcolithic, BA: Bronze Age, W.: Western, S.: Southern, N.: Northern, E.: Eastern, C.: Central, .sg/.SG: pulldown to 1240K SNPs from shotgun sequencing data. We use these abbreviations across the text compositely (e.g., EMBA: Early Middle Bronze Age, or SE: Southeastern).

#### **$f_4$ -statistics**

We computed a 4-population test (qpDstat) from ADMIXTOOLS [v57.1] (Patterson et al., 2012) with default parameters and `f4mode:YES`. qpDstat (or here  $f_4$ -statistic) is a formal test of admixture based on the allele-frequency correlation patterns among the four populations of the test. Under a null hypothesis of an unrooted topology of the populations ((A,B),(C,D)), the test  $f_4(A, B; C, D)$  calculates  $(p_A - p_B)(p_C - p_D)$ , which is expected to be zero as the allele differences within these two pairs should not be correlated. The calculation of the summary statistic includes a weighted block jackknife method for the calculation of the standard error (SE). A  $f_4$ -statistic that differs from 0 (conventionally beyond  $\pm 3SE$  or  $|Z| > 3$ ) is interpreted as a rejection of the null topology for a different one, or as gene-flow between A/B and C/D after their divergence. Hence, in order to use the method as a formal test of admixture prior knowledge about the divergence of the four populations is necessary. The sign of the statistic

is also informative about the direction of the allele sharing. A negative statistic means asymmetric allele sharing between A and D or B and C, while an asymmetric allele sharing between A and C or B and D results in a positive value. Another important implication derived from the formula of the 4-population test is that it harnesses information from the internal branches of the topology and therefore, it is insensitive to post gene-flow genetic drift on the branches leading to populations A, B, C and D.

We performed  $f_4$ -statistics of the form  $f_4(\text{Mbuti, Test; Anatolian farmer group, Aegean groups})$  (Supplementary Table 4). By placing in the position of ‘A’ an African population who is a common outgroup to the others, we could directly test for populations who -compared to the Anatolian farmers- share excessive alleles with Neolithic and Bronze Age Aegean groups. As ‘Test’ we run a battery of populations, earlier or coeval to the Aegean groups, who represent ancestries present in West Eurasia since the Early Holocene. Positive results ( $Z \geq 3$ ) were obtained in the majority for the Late Bronze Age (LBA) Aegean groups and suggest affinity of the latter with populations from East Europe and Central Asia [e.g., Eastern European hunter-gatherers (EEHG)] and West Asia [e.g., Caucasus hunter-gatherers (CHG)], or younger populations related to the pastoralists from the Eurasian Steppe (e.g., Russia\_Smara\_EBA\_Yamnaya, Poland\_Globular\_Amphora, Italy\_Sardinia\_LBA, Germany\_CordedWare) who in turn derive their ancestry from these earlier groups. Among the preceding Aegean groups (Early and Middle Bronze Age), Nea Styra EBA, Hagios (Hg.) Charalambos EMBA and published Odigitria EMBA from Crete displayed evidence of excessive allele sharing that is specific to earlier/contemporaneous West Eurasian groups from Iran and the Caucasus, and occasionally groups affiliated to the BA Eurasian Steppe. Strongly positive results (i.e.,  $Z \geq 2.5$  but no more than 4) for the Cretan Neolithic population Aposelemis\_N indicate that the groups likely harbors some extra affinity with some Iranian/Levantine populations. Because such affinities are not visible in the PCA, and Aposelemis\_N as a group has low heterozygosity (i.e., pairwise mismatch rate is equivalent to second-third degree relatives for the rest of the Aegean dataset - see also Extended Data Fig. 4), we also provide the same  $f_4$  tests but only on APO004, the individual with the highest SNP coverage. By doing so, we can test for overestimation of the significance of the allele frequency differences between Aposelemis and W.Anatolia\_N/Mainland\_Greece\_N, owing to long-term inbreeding at Aposelemis. We note that the most positive Z scores decreased (now  $< 2$ , with the exception of Iran\_C\_TepeHissar, ANE and Levant\_C with  $3 < Z \leq 2$ ), while for some test the sign became negative or more negative (i.e., WEHG, BalkanHG) making the tests more consistent with those from  $f_4(\text{Mbuti, Test; W.Anatolia_N, Mainland_Greece_N})$ .

### Admixture $f_3$ -test

We performed a test of admixture  $f_3(A,B;C)$  from ADMIXTOOLS [v57.1] (Patterson et al., 2012) which essentially tests whether allele frequencies in the target population C are intermediate between those of the source populations A and B, in which case the statistic becomes negative. However, high rate of data missingness or post-admixture drift on the branch of ‘C’ can hinder the power of the test to detect admixture. To enhance the statistical power of the test, we used merged meta-populations. For population A, we used Early European-Anatolian farmers (EEAF) that include Anatolia\_N (Barcın, Menteşe and Bocuklu), Germany\_EN\_LBK (associated with the Early Neolithic Linear Pottery archeological horizon in Central Europe). For population B, we iterated over Anatolia\_LC-EBA (sites Arslantepe, İkiztepe, Çamlıbel Tarlası, Harmanören-Göndürle Höyük), mCaucasus\_En-BA (mountain Caucasus Eneolithic-Bronze Age: I1635, I1633, I1658, I1656, RISE396.SG, RISE397.SG, RISE407.SG, RISE408.SG, RISE412.SG, RISE413.SG, RISE416.SG, RISE423.SG, DA31.SG, DA35.SG, ARM001, ARM002, I1720, I2051, I2056, I6266, I6267, I6268, I6272, KDC001, KDC002, MK5004, MK5008, OSS001, SA6002, VEK007, and the lowland ALX002), W. Eurasian Steppe En-BA (‘WES’ ancestry, i.e., Yamnaya pastoralists from the Caucasus, Eastern Russia and Ukraine: I0370, I0441, I0444, I0439, I0357, I0429, I0438\_published, RISE240.SG, RISE546.SG, RISE547.SG, RISE548.SG, RISE550.SG, RISE552.SG, I0443, I2105, I3141\_published, I7489, BU2001, GW1001, I1723, KBD001, LYG001, MK3003, MK5009, PG2001, PG2002, PG2004, RK1001, RK1003, RK1007, RK4001, RK4002, SA6003, VJ1001, ZO2002, I0231\_published), CHG (Caucasus hunter-gatherers: Kottias KK1.SG and Satsurlbia SATP.SG), Eastern European hunter-gatherers (EEHG: I0124, I0211, I0061, Popovo2, UzOO77\_new), and W. Iran N (Iran\_GanjDareh\_N). We chose these groups according to the  $f_4$ -statistics and their PCA coordinates (Fig. 2). We run the admixture  $f_3$ -test with the option inbreed:YES, which is recommended by the authors of the method when the target population is pseudo-diploid data. We present evidence of admixture detected with the test ( $< -3$  SE) (Supplementary Table 5). Among the M/LBA groups, Chania LBA is the largest group ( $n=27$ ) and exhibits the strongest signals of admixture between a population like EEAF and a population related to East Europe, the Caucasus and Iran, but not with Anatolia LC-EBA. Aidonia LBA, Glyka Nera LBA, Krousonas LBA, Logkas MBA, Mygdalia LBA and Tiryns LBA also display admixture signals from one or more distal sources (CHG, EEHG or W. Iran N), but always from W. Eurasian Steppe En-BA. On the contrary, for the earlier Nea Styra EBA admixture source include the proximal mount. Caucasus En-BA,

and -more weakly- Anatolia LC-EBA ( $Z = 1.14$ ). Notably, no admixture evidence is obtained for Hg. Charalambos EMBA or Odigitria EMBA from Crete despite the evidence from PCA and  $f_4$ -statistics, which could be attributed to private drift on the lineage leading to these groups.

### Dating of recent admixture

Using the same setting of source and target populations, we tested for a signal of recent admixture with DATES (<https://github.com/priyamoorejani/DATES>) (Methods). The method effectively estimates local ancestry within the target individual/population -that is, whether a genomic segment descends from either of the two sources. The size of these segments is expected to decay across genetic distance at a rate that depends on the time since admixture.

To minimize standard errors for the admixture dates, we compiled five Late Neolithic-Bronze Age supergroups as targets based on geography and archeological periodization: 1. Crete LBA [Chania, Krousonas, Aposelemis and published Armenoi (Lazaridis et al., 2017)], 2. Crete EMBA [Hagios Charalambos from this study, Hagios Charalambos and (Moni) Odigitria previously published (Lazaridis et al., 2017), and Kephala (Clemente et al., 2021)], 3. S. Mainland-Islands LN-EBA [LN I3708, I3709, I2318 and I3920 from Peloponnese (Mathieson et al., 2018), Kou01.SG, Kou03.SG Koufonisia and Euboea (Clemente et al., 2021), and Nea Styra and Lazarides], 4. S. Mainland-Islands LBA [Aidonia, Glyka Nera, Mygdalia, Tiryns, Lazarides, Koukounaries and previously published Apatheia, Pylos and Salamis (Lazaridis et al., 2017)] and 5. N. Mainland MBA [two Logkas individuals (Clemente et al., 2021)]. In addition, we dated admixture separately on Chania LBA and Nea Styra EBA to test whether the variation in the PCA is consistent with more recent admixture. We also merged W. Eurasian Steppe En-BA with ‘Germany\_CordedWare’ into the supergroup source 2 ‘Steppe-Corded Ware En-BA’. We present the results and mark the tests for which a recent date was inferred and an exponential decay curve against the genetic distance was fitted (Supplementary Table 6). We also present the admixture dates in BC format. On average, earlier groups (i.e., S. Mainland-Islands LN-EBA and Crete EMBA) are consistent with older admixture dates (ca. 5000 BC), while the succeeding LBA groups with earlier ones (ca. 3000 BC). Admixture on the group Nea Styra is younger than the average on all LN-EBA individuals combined, but for Chania LBA the admixture date matches the average from the group Crete LBA. In addition, for the two supergroups S. Mainland-Islands LBA and N. Mainland MBA, the more recent admixture is inferred only with either EEHG or Steppe-CordedWare En-BA as sources. On the contrary, more genetically distinct sources produce similar decay and date estimation for the earlier groups, which might point to a reduced resolution of the method to

distinguish between these sources for older admixture events. Furthermore, these results corroborate a multi-phased genetic admixture in the Aegean between the 6<sup>th</sup> and 2<sup>nd</sup> millennia BC, also shown with the *f*-statistics and the *qpAdm* modeling (see below). We acknowledge though that contextualization of the aforementioned dates with archeological evidence comes with certain limitations as the method cannot distinguish between one-pulse and continuous admixture. In particular, this hinders robust signals of very recent admixture in Crete\_LBA as the incoming source(s) were also most likely very recently admixed.

### **Ancestry deconvolution with *qpWave/qpAdm***

To better understand the interplay of the various ancestry components that formed the gene-pool of the Aegean populations since the Neolithic until the end of the Bronze Age, we performed analyses with the *qpWave/qpAdm* tools from ADMIXTOOLS [v7.1] (Patterson et al., 2012) (see also Methods). A critical parameter when using these tools is the choice of reference (outgroup or ‘right’) populations. While explicit knowledge of the phylogeny relating those populations is not necessary, the method behind these tools relies on some assumptions in order to infer meaningful models. For *qpWave*, which is usually used to estimate the minimum number of independent gene pools that explain a set of targets from the references, it is important that the references are chosen such that the target populations are differentially related to them because of their deeper or more recent evolutionary history. For *qpAdm*, which is used to fit ancestries on a target from a set of source populations and estimate mixture coefficients, two more criteria need to be fulfilled. First, the references should be related with the target through the source populations and second, there should be no subsequent direct gene flow between the references and the target.

We first run *qpWave* under default parameters in order to cluster individuals within and/or across sites that are genetically indistinguishable compared to the set of reference (right) populations. We set the following set of eleven ancient reference populations (R11) from published studies (Methods): Ethiopia\_4500BP\_published.SG (Mota.SG), Russia\_Ust\_Ishim\_HG\_published.SG, Russia\_Kostenki\_14, Balkan\_HG (hunter-gatherers from the Iron Gates in Serbia), Western European hunter gatherers (WEHG; Loschbour\_published.DG, Iboussieres25-1, Iboussieres31-2, Rochedane, BerryAuBac, I1507, Villabruna, I2158, Bichon.SG, I1875, I4971, Falkenstein, Chaudardes1\_published, Ranchot88\_published), CHG, EEHG, Israel\_Natufian\_published, Ancestral North Eurasians (ANE; MA1.SG and AfontovoGora2.SG), ‘W. Iran N’ (Iran\_GanjDareh\_N) and ‘W. Anatolia N’ (individuals from sites Barcın and Menteşe in the Marmara Sea). With the exception of



Mota.SG who is an outgroup, the remaining populations represent Upper Pleistocene and Early Holocene lineages present in West Eurasia and beyond.

We summarise the results from the pairwise *qpWave* models in the form of a heatmap (Extended Data Fig. 1). Grey tiles correspond to rejected models (p-values < 0.01), which suggests that more than one stream of ancestry from the references are necessary to explain the given pair of individuals. Subsequently, grouping such individuals for downstream analyses (i.e., *qpAdm*) can underestimate genetic complexity. The highest rate of p-values < 0.01 is observed for pairs including an individual from the Late Bronze Age and an individual from a previous period (Neolithic or Early-Middle Bronze Age) (upper left or lower right corner of heatmap). Within sites of the same period (black-outlined squares), individuals are clustering together and the rate of rejected models (e.g., individuals HGCXXX, I071, I073, I074 and I9005 from Hagios Charalambos) is the expected for true models to be rejected with a cut-off of 1% given a uniform distribution of the p-values. However, a high rate of rejected models is observed among individuals from Chania LBA (XANXXX), and the islands of Euboea, Koufonisia and Aegina [Nea Styra EBA (NSTXXX), Mik15, Kou001/3, and Lazarides (LAZ0017)].

We repeated the same analysis on the MBA and LBA individuals adding ‘W. Eurasian Steppe En-BA’ to R11 (Extended Data Fig. 2.A). With this setting we wanted to test whether this metapopulation can pull additional differences among the LBA individuals, implying that their affinity to WES-related ancestry shown with  $f_4$ -statistics was diverse within the Greek mainland, Crete and the other islands. Within sites of the same period, the new set of references increased the number of non-cladal pairs in Chania from 56 to 65 (p-value  $\geq$  0.01), or from 14 to 27 (p-value  $\geq$  0.05). Overall though, the *qpWave* analysis under the two setting supported the ‘Site\_period’ grouping with the exception of the published individuals from Logkas and Koufonisia, as well as Nea Styra and Chania.

We performed *qpAdm* modeling both per individual, as well as on groups. Besides the ‘Site\_period’ groups, we split Chania in ‘Chania LBA (a)’, ‘Chania LBA (b)’ and ‘Chania (XAN030)’ and , and grouped Hg. Charalambos, Odigitria and Kephala from Early/Middle Bronze Age (Minoan) Crete as ‘Crete EMBA’. By applying this mixed approach of grouping, we reconcile the need to maintain geographical and chronological designations for testing of archeological hypotheses with the need to reduce redundancy on a genetic level, and thereby increase the resolution of admixture inferences based of allele-frequencies (i.e., *qpAdm*) (Eisenmann et al., 2018). Accordingly, we also tested *qpAdm* models with proximal sources on the group of all LN-EBA individuals from Euboea, other islands as well as Peloponnese (‘S.

Mainland-Islands LNEBA’). Despite the differences among these individuals indicated by *qpWave* and the per-individual *qpAdm* models, we tested whether this group was on average consistent with admixture from some proximal sources rather than others, a difference that might not be captured when the targets are single individuals with low SNP coverage.

*‘Crete N’ (Aposelemis): One-way qpAdm models from Anatolia*

We carried out *qpAdm* analysis (default parameters) on ‘Crete Aposelemis N’ initially by testing the scenario that the group is a sister clade of Neolithic Anatolian groups of farmers. As a set of reference populations, we applied R11b: Ethiopia\_4500BP\_published.SG, Russia\_Ust\_Ishim\_HG\_published.DG, Russia\_Kostenki14, BalkanHG, EEHG, ANE, Israel\_Natufian\_published, WEHG, CHG, W. Iran N and ‘S. Levant N’. ‘S. Levant N’ which consists of ten Pre-Pottery Neolithic individuals from Israel and Jordan. The two 7<sup>th</sup> millennium BC ceramic farming groups from Çatalhöyük in Central Anatolia and the Marmara Sea region (‘W. Anatolia N’) could model ‘Crete Aposelemis N’ (p-value of one-way model = 0.2 and 0.58, respectively). On the contrary, Aposelemis was not cladal to either the Central Anatolian aceramic farmers from Boncuklu (9<sup>th</sup> millennium BC), or the 7<sup>th</sup> millennium BC Tepecik Ciftlik -located more to the east and harboring additional ancestry related to W. Iran N (p-value =  $9.3 \times 10^{-5}$  and  $2.5 \times 10^{-3}$ , respectively). This stark difference between the fit of the ceramic and aceramic farmers for Aposelemis was also noted for many of the other Neolithic individuals from the Greek mainland (e.g., Rev05, I2937, I2318, I3708), excluding those later who were shown to require additional contribution from a CHG/W. Iran N-related source (e.g., I3920) (Fig. 3).

We also checked whether the inclusion of the Boncuklu group in the references [R11b + Turkey\_Boncuklu\_N(.SG)] influenced the fit of the one-way model from W. Anatolia N. We found that although the p-value decreased, the model for Aposelemis N as cladal to W. Anatolia N remained adequate (p-value = 0.08). We also checked the one-way model from the three earliest Aegean Neolithic individuals in the Greek mainland ‘Mainland\_Greece\_N’ (Rev5.SG, I5427 and I2937), which was also adequate (p-value=0.8). Overall, these analyses support a shared genetic pool within the Aegean as far as the inner part of the Anatolian littoral, without further contribution from populations related to the Levant and/or Iran.

*Ancestry modelling for the Early/ Middle Bronze Age Aegean populations*

We implement a framework for *qpAdm* in which we explore two-way admixture models by fixing the first source to be either W. Anatolia N or Crete Aposelemis N. The plausible

populations serving as second sources were chosen based on insights provided by the PCA and  $f_4$ -statistics. We assess the fit of the models by rotating the second source, that is by moving the remaining candidate sources 2 in the reference (right) populations. This ‘competing’ approach was shown to enable *qpAdm* to differentiate between genetically similar sources that would otherwise result in equally fitting models if tested independently (Harney et al., 2021). For the Late Neolithic and Early/Middle Bronze Age groups (‘Crete EMBA’, ‘S. Mainland-Islands LN-EBA’), we rotated among the distal CHG, EEHG, W. Iran N, S. Levant N, and proximal Iran C (from She Gabi), Anatolia LC-EBA, (mountain) Caucasus En-BA and W. Eurasian Steppe En-BA. These temporally proximal metapopulations can be modelled as a linear combination from the temporally distal sources. The fixed references included Ethiopia\_4500BP\_published.SG, Russia\_Ust\_Ishim\_HG\_published.DG, Russia\_Kostenki14, BalkanHG, ANE, Turkey\_Boncuklu\_N, Israel\_Natufian\_published, WEHG (R8) (Supplementary Table 7). Models with ‘Crete Aposelemis N’ as source 1 became adequate for the majority of the rotating sources 2. On the contrary, models with ‘W. Anatolia N’ as source 1 were estimated on ca. twice as many SNPs and were deemed inadequate besides source 2 being mount. Caucasus En-BA for S. Mainland-Islands LN-EBA. For Crete EMBA the less strongly rejected model included Anatolia LC-EBA (p-value =  $1.5 \cdot 10^{-3}$ ), which lead us to explore possible tree-way admixture models with W. Anatolia N and Anatolia LC-EBA as fixed sources. By rotation of the remaining candidate sources, only the three-way W. Anatolia N + ‘Anatolia LC-EBA’ + (5.4 + 2.9%) ‘W. Iran N’ became adequate, but notably, it did not serve as an alternative model for ‘S. Mainland LN-EBA’ (p-value =  $8.91 \cdot 10^{-3}$ ). Only when this model was substituted with ca. 10% from CHG it fitted the data from S. Mainland LN-EBA (p-value = 0.48). These results suggest that in the central Aegean (e.g., Euboea, Cyclades, Peloponnese) gene-flow could have been directly associated with populations from the Caucasus (the mountain area and to the south), whereas in Crete with Anatolia, precisely to populations likely lying on the W/C. Anatolian-Caucasian genetic cline.

#### *Ancestry modelling for the Middle/Late Bronze Age Aegean populations*

Multiple analyses ( $f_4$ -statistics, admixture  $f_3$ , PCA and DATES) point to a substantial change in the ancestry profile of the Aegean populations towards the Late Bronze Age. In fact, most all the LBA groups including those from Crete exhibit affinities with ancient Eastern European populations that are not observed in the preceding populations. Archeological evidence suggests that movements of people from Northern Greece and the Balkans (currently underrepresented in the aDNA record) towards southern parts of the Greek mainland were a

regular feature that started already in the 4<sup>th</sup> millennium BC (Maran, 1998). Therefore, gene-flow from northern populations could be taking place at the time of the EBA individuals of this study. However, confined to Euboea -an island adjacent to the west with the central Greek mainland, the EBA individuals of this study might not serve as a surrogate of the biological relations between the mainland and these northern populations.

We first modelled the genetic shift from EBA/EMBA to M/LBA by trying exploratively two-way models for LBA groups from the corresponding local source ('Crete EMBA', 'S. Mainland-Islands\_LN-EBA', or 'N. Mainland LN' consisting of individuals Klei10 and Pal07), and selected representative sources from a set of Late Neolithic-Bronze Age European populations from published datasets (Supplementary Table 8). We applied R11. We also tested one-way models from these local sources as well as non-local but genetically similar groups like 'Italy-Sicily LBA', 'Croatia MBA', and 'Italy BA (WES)'. The latter group consists of individuals from the N. and C. Italy (Regina Margherita and Broion) that represent the earliest presence of WES-related ancestry in the peninsula (Saupe et al., 2021). Some groups showed continuity from their local baseline (i.e., 'Aposelemis LBA', 'Chania LBA (a)' and 'Salamis LBA'), but the remaining 'Site/Individual\_MBA/LBA' required additional contribution from one of these external sources: Serbia EBA (Mokrin Necropolis - Maros culture), W. Eurasian Steppe En-BA, Czech EBA 'Bell Beaker', Czech Bohemia EBA 'Unetice', Croatia MBA or Italy BA (WES). Individuals XAN030, Pylos LBA, Logkas2 MBA, Logkas4 MBA and the small groups (n=2) Glyka Nera LBA and Apatheia LBA could also be modelled as cladal from Croatia MBA or Italy BA (WES). To overcome model discrepancies owing to variable group sizes and SNP coverage among the target groups, we grouped them in six supergroups based on geography and their overlapping coefficients of WES-related source (Fig. 4A): 'Mainland LBA' (southern), 'Mainland MBA' (northern), 'Islands LBA', and 'Crete LBA' altogether, or split in 'Crete LBA (Group A)', 'Crete LBA (Group B)' and 'Crete LBA (Group C)'. We tested whether some of the candidate sources fit better in the models than others by rotating them: Germany LN-EBA 'Corded Ware' (C. Europe), W. Eurasian Steppe En-BA (E. Europe), Serbia EBA and Croatia MBA (SE. Europe), and Italy BA (WES) (W. Europe). Notably, models with the most spatially proximal sources like Serbia EBA, Croatia MBA and Italy BA (WES) failed for the Islands and the Mainland ( $p\text{-value} \leq 2.3 \cdot 10^{-3}$ ). On the contrary, two-way models with any of these sources were adequate for all Crete LBA or the two groups (B and C) separately (Fig. 4B, Supplementary Table 9). Alternatively, Group C could be modelled as cladal to (S.) Mainland LBA, which is counterintuitive to the WES ancestry (modeled with Germany LN-EBA 'Corded Ware') being significantly higher in Chania Group C (i.e.,  $32 \pm 2.7\%$ ; 1SE) than

in (S.) Mainland LBA (i.e.,  $24 \pm 1$  %; 1SE). As this inconsistency could reflect a lack of resolution of *qpAdm* to distinguish between these two genetically very similar groups, we do not interpret this result as direct evidence of immigrants from the S. Mainland in Chania, but equally consider the broader Aegean region as well as admixture from less proximal sources similar to Italy BA (WES).

## References

Clemente, F., Unterländer, M., Dolgova, O., Amorim, C. E. G., Coroado-Santos, F., Neuenschwander, S., Ganiatsou, E., Cruz Dávalos, D. I., Anchieri, L., Michaud, F., et al. 2021. The genomic history of the Aegean palatial civilizations. *Cell*.

Eisenmann, S., Bánffy, E., van Dommelen, P., Hofmann, K. P., Maran, J., Lazaridis, I., Mittnik, A., McCormick, M., Krause, J., Reich, D., et al. 2018. Reconciling material cultures in archaeology with genetic data: The nomenclature of clusters emerging from archaeogenomic analysis. *Scientific reports*, 8, 13003-13003.

Harney, É., Patterson, N., Reich, D. & Wakeley, J. 2021. Assessing the performance of *qpAdm*: a statistical tool for studying population admixture. *Genetics*.

Lazaridis, I., Mittnik, A., Patterson, N., Mallick, S., Rohland, N., Pfrengle, S., Furtwangler, A., Peltzer, A., Posth, C., Vasilakis, A., et al. 2017. Genetic origins of the Minoans and Mycenaeans. *Nature*, 548, 214-218.

Maran, J. 1998. *Kulturwandel auf dem griechischen Festland und den Kykladen im späten 3. Jahrtausend v. Chr. Studien zu den kulturellen Verhältnissen in Südosteuropa und dem zentralen sowie östlichen Mittelmeerraum i. d. späten Kupfer- und frühen Bronzezeit*, Bonn, Habelt.

Mathieson, I., Alpaslan-Roodenberg, S., Posth, C., Szécsényi-Nagy, A., Rohland, N., Mallick, S., Olalde, I., Broomandkoshbacht, N., Candilio, F., Cheronet, O., et al. 2018. The genomic history of southeastern Europe. *Nature*, 555, 197-203.

Patterson, N., Moorjani, P., Luo, Y., Mallick, S., Rohland, N., Zhan, Y., Genschoreck, T., Webster, T. & Reich, D. 2012. Ancient Admixture in Human History. *Genetics*, 192, 1065.

Saupe, T., Montinaro, F., Scaggion, C., Carrara, N., Kivisild, T., D'Atanasio, E., Hui, R., Solnik, A., Lebrasseur, O., Larson, G., et al. 2021. Ancient genomes reveal structural shifts after the arrival of Steppe-related ancestry in the Italian Peninsula. *Current Biology*.

### SUPPLEMENTARY NOTE 3

#### Genotype imputation and pedigree reconstruction for Mygdalia individuals

In this section we describe additional analyses to resolve the pedigree among the three infants from the burial at Mygdalia.

The pair of infant males MYG001 and MYG008 are inferred to be full siblings, and both of them are inferred to be second degree-related with the infant male MYG006 (using READ and *lcMLkin*, see Methods; Fig. 5, Extended Data Fig. 4). The full siblings MYG001 and MYG008 have the same mtDNA and Y-chr haplogroup. Their second-degree relative MYG006 has the same Y-chr haplogroup as well, but a different *mtDNA* haplogroup. In addition, all three individuals are related to three more infant individuals at Mygdalia (see Fig. 5; e.g., all three are second degree relatives of MYG002). These lines of evidence limit the possible pedigrees to two: 1. MYG001/MYG008 are double first cousins with MYG006, so they share all four grandparents, or 2. MYG001/MYG008 are half-siblings with MYG006 sharing the same father (same Y-chr but different *mtDNA* haplogroup).

To distinguish between these two scenarios, we use the fact that scenarios 1 and 2 differ in  $k_2$ , the probability that a pair of individuals shares both alleles at a locus as identical by descent (IBD), which is expected to be 0.0625 and 0, respectively. While *lcMLkin* estimates  $k_0$ ,  $k_1$  and  $k_2$  and can successfully distinguish between parent-offspring and full siblings, however  $k_2$  estimates can become too noisy for more distantly related pairs, especially when coverage on 1240K positions is low (<1x).

Therefore, we decided to directly assess identical diploid genotypes along the genome. For this analysis, we computed genotype imputations using a reference panel as described below. The pair of full siblings MYG001 and MYG008 have long stretches of identical diploid markers on several chromosomes, as expected for a pair of full siblings (Supplementary Figure 36). However, both pairs MYG001-MYG008 and MYG001-MYG006 lack any such stretches of fully identical genotypes (Supplementary Figure 36), which would be expected for double first cousins (in ca. 6.25% of the genome), thereby pointing toward both pairs being paternal half-siblings.

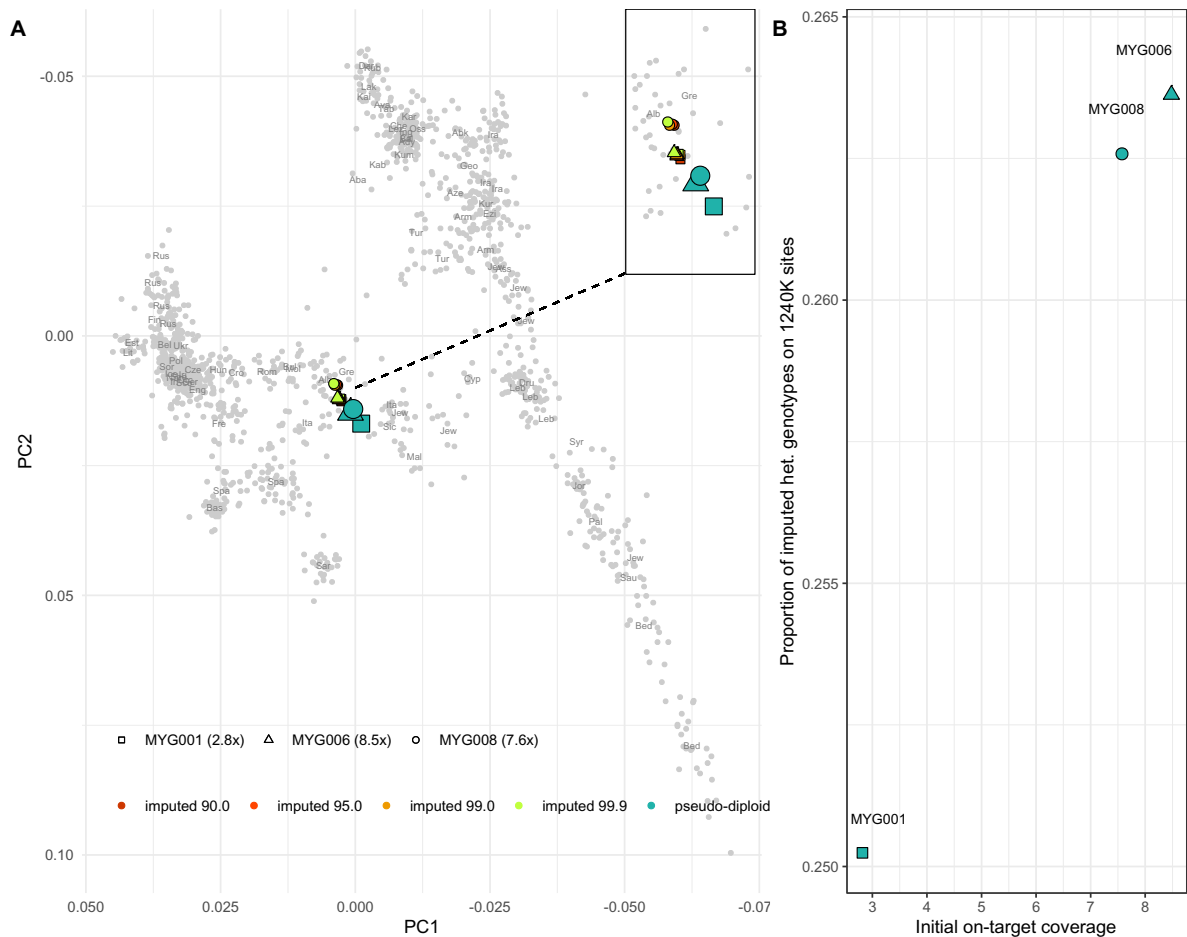
For the genotype imputations, we used the 2bp-masked  $q30$ -filtered reads of the three Mygdalia individuals' ds-libraries and called genotype likelihoods (GL) through GATK [v3.5]

(DePristo et al., 2011). We called GL for all 29,083,171 diallelic positions with a minor allele count 5 or higher contained in the 1000 Genomes Phase 3 release (Auton et al., 2015), using the “UnifiedGenotyper” module with a mean base quality score higher than 30 “-mbq 30”. We then provided these likelihoods to GeneImp [v1.3] software (Spiliopoulou et al., 2017) for the statistical imputation of all the 1KG SNPs, using all the 2,504 individuals of the 1KG statistically phased genomes as reference dataset. The imputation was run independently using three different window lengths “kl” {15, 20, 25}, following the developers’ instructions (Spiliopoulou et al., 2017). For each imputed SNP the average genotype call probability (GP) across the three different runs was considered. GeneImp also assigns a posterior probability (PP) for each diploid call. For the evaluation of the performance of the imputation, we considered only the SNPs overlapping with the 1240K panel by extracting these specific genotypes and then merged them with the HO dataset (Methods) by keeping the intersection of the two panels. We computed PCA with smartpca in EIGENSOFT [v6.01] package (Patterson et al., 2006; Price et al., 2006) and projected the imputed data for four PP thresholds (0.9, 0.95, 0.99, 0.999) (Supplementary Figure 37A). All imputed versions were shifted in PC1 and PC2 towards modern European populations who are included in the reference panel, but this deviation from the original pseudo-diploid counterparts is very subtle. To further quantify the performance of imputations and the possible introduction of reference bias, we calculated heterozygosity from the imputed data applying the stringiest PP cut-off (0.999) (Supplementary Figure 37B) and computed outgroup  $f_3$ -statistics (Supplementary Figure 38). For the individuals with high initial coverage (MYG006 and MYG008, ca. 7-8x coverage), the proportions of heterozygous calls matched those calculated with pmr among non-related pairs from Mygdalia and other BA sites (ca. 0.26). For the lower-coverage individual MYG001 (3x) the heterozygosity was slightly lower (ca. 0.25). No reference bias could be detected with  $f_3$ -statistics (Supplementary Figure 38).



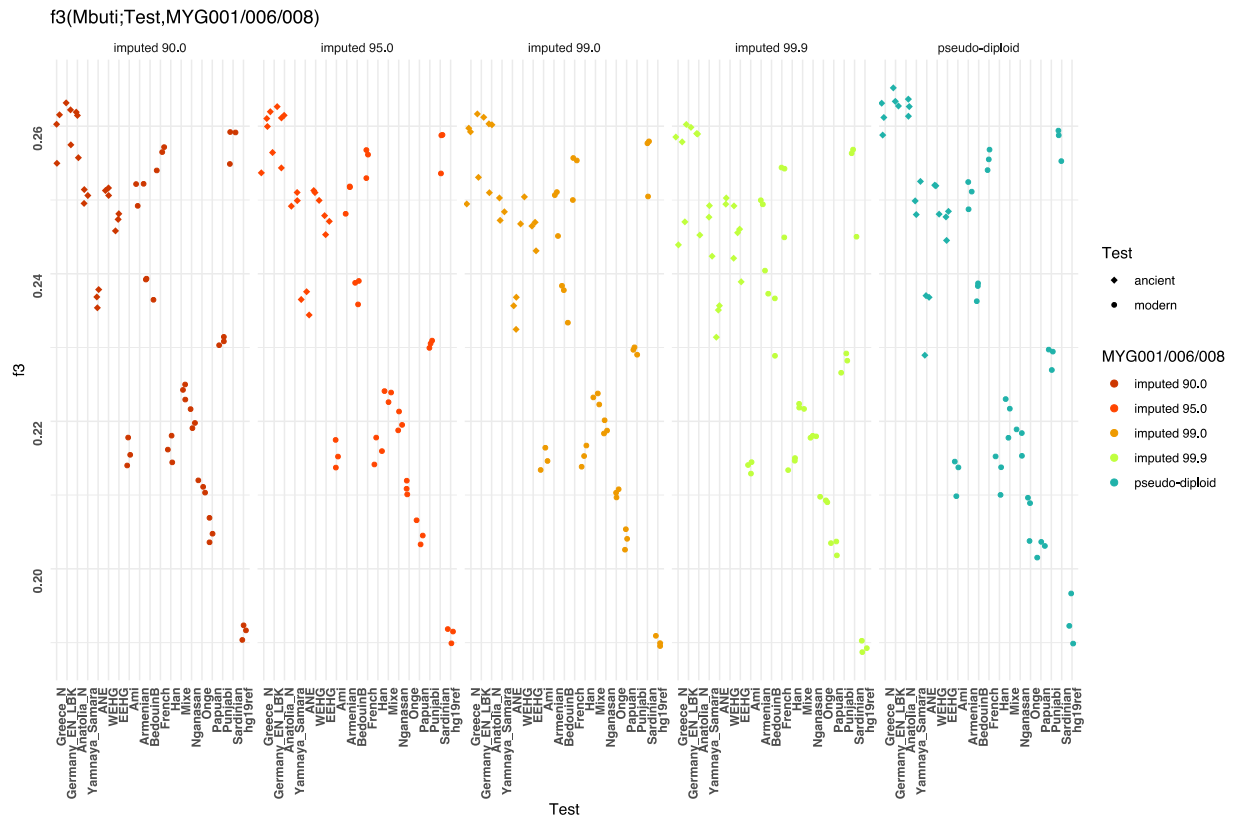
**Supplementary Figure 36.** Opposing genotypes along the 22 autosomes for the three pairs of infants from Mydgalia. For each of the three possible pairs between MYG001, MYG006 and MYG008, a subfigure shows identical and differing diploid imputed genotype status along the autosomes (raised and lowered points, respectively). The figures are restricted to SNPs from the 1240K panel with reported probability of the imputed diploid genotype at least 0.999. The pair of full siblings MYG001 and MYG008 have long stretches of identical diploid markers on several chromosomes. In contrast, the two other pairs of individuals do not have such stretches. But such identical stretches would be expected for double first cousins (in expectation 6.25% of the genome).





**Supplementary Figure 37. A.** West-Eurasian PCA with modern individuals plotted as individuals and as mean of within-population PC1 and PC2 coordinates. The pseudo-diploid and imputed genotypes for different PP thresholds (in %) of the three Mygdalia individuals are projected.

**B.** Heterozygosity calculated as the proportion of imputed (0.99 PP) heterozygous over all imputed genotypes against initial coverage on 1240K positions.



**Supplementary Figure 38.** Genetic drift measures with  $f_3(\text{Mubti}; \text{Test}, \text{MYG001}/\text{006}/\text{008})$  with Test being non-African modern populations and some representative ancient groups.

## References

Auton, A., Abecasis, G. R., Altshuler, D. M., Durbin, R. M., Abecasis, G. R., Bentley, D. R., Chakravarti, A., Clark, A. G., Donnelly, P., Eichler, E. E., et al. 2015. A global reference for human genetic variation. *Nature*, 526, 68-74.

DePristo, M. A., Banks, E., Poplin, R., Garimella, K. V., Maguire, J. R., Hartl, C., Philippakis, A. A., del Angel, G., Rivas, M. A., Hanna, M., et al. 2011. A framework for variation discovery and genotyping using next-generation DNA sequencing data. *Nature Genetics*, 43, 491-498.

Patterson, N., Price, A. L. & Reich, D. 2006. Population Structure and Eigenanalysis. *PLOS Genetics*, 2, e190.

Price, A. L., Patterson, N. J., Plenge, R. M., Weinblatt, M. E., Shadick, N. A. & Reich, D. 2006. Principal components analysis corrects for stratification in genome-wide association studies. *Nature Genetics*, 38, 904-909.

Spiliopoulou, A., Colombo, M., Orchard, P., Agakov, F. & McKeigue, P. 2017. GeneImp: Fast Imputation to Large Reference Panels Using Genotype Likelihoods from Ultralow Coverage Sequencing. *Genetics*, 206, 91-104.